



Virginia Commonwealth University
VCU Scholars Compass

Theses and Dissertations

Graduate School

2017

Computational All Atom Energy Density Landscape Mappings of Intra-protein Interactions from Static and Dynamic Ensemble Structure Data

Oscar H. Bastidas
Virginia Commonwealth University

Follow this and additional works at: <https://scholarscompass.vcu.edu/etd>

 Part of the [Biochemical and Biomolecular Engineering Commons](#)

© The Author

Downloaded from

<https://scholarscompass.vcu.edu/etd/4955>

This Dissertation is brought to you for free and open access by the Graduate School at VCU Scholars Compass. It has been accepted for inclusion in Theses and Dissertations by an authorized administrator of VCU Scholars Compass. For more information, please contact libcompass@vcu.edu.

© Oscar H. Bastidas 2017
All rights reserved

Computational All Atom Energy Density Landscape Mappings of Intra-protein Interactions from Static and Dynamic Ensemble Structure Data

A thesis submitted in partial fulfillment of the requirements for the degree of Doctor of Philosophy at
Virginia Commonwealth University

by

Oscar H. Bastidas

Master of Science in Chemical Engineering-Virginia Commonwealth University, 2014
Bachelor of Science in Chemical Engineering-Virginia Commonwealth University, 2011

Director: Dr. Michael H. Peters
Professor, Chemical and Life Science Engineering

Virginia Commonwealth University
Richmond, Virginia
June, 2017

Acknowledgement

The author wishes to thank several people. I would like to thank my family for the unending love, support and patience I have received throughout the five or so years it has taken me to graduate. I would also like to thank Dr. Michael Peters for his help and for his direction with this project.

TABLE OF CONTENTS

Table of Contents.....	iii
Abstract.....	v
I. Introduction and Background.....	1
A. Overall Objectives, Aims and Goals of this Thesis	1
B. Background on Protein Structure and Function.....	5
C. Background on Experimental Dynamic Methods for Protein Fluctuations	12
D. Background on Computational Approaches to Protein Fluctuations.....	18
E. References.....	20
II. Aim 1: Informatics Ensemble Mappings	25
A. Introduction.....	25
B. Materials and Methods.....	29
C. Results and Discussion	34
D. Conclusions	55
E. References	57
III. Aim 2: Static Mapping of Amyloid Systems	59
A. Introduction	59
B. Results and Discussion	61
C. Conclusions	79
D. References	81
IV. Aim 3: Long-Time Dynamic Simulations of Protein Fluctuation States.....	85
A. Introduction.....	85
B. Materials and Methods.....	91
C. Results and Discussion.....	97
D. Conclusions.....	117
E. References.....	118
V. Aim 4: Inhibitor Design.....	123
A. Introduction.....	123

TABLE OF CONTENTS (CONTINUED)

B. Materials and Methods.....	126
C. Results and Discussion.....	132
D. Conclusions.....	137
E. References.....	138
VI. Future Work.....	143
A. References.....	144
VII. Thesis Summary.....	144
Appendix A.....	147
Appendix B.....	152
Appendix C.....	160
Appendix D.....	196
Appendix E.....	320
Appendix F.....	327
Appendix G.....	330
Vita.....	333
Publications and Intellectual Properties.....	334

Abstract:

COMPUTATIONAL ALL ATOM ENERGY DENSITY LANDSCAPE MAPPINGS OF
INTRA-PROTEIN INTERACTIONS FROM STATIC AND DYNAMIC ENSEMBLE
STRUCTURE DATA

By Oscar Herminio Bastidas, Ph.D.

A thesis submitted in partial fulfillment of the requirements for the degree of Doctor of
Philosophy at Virginia Commonwealth University

Virginia Commonwealth University, 2017.

Director: Dr. Michael H. Peters, Professor, Chemical and Life Science Engineering

Understanding the energetic and dynamic behavior of natural protein fluctuations is critical to elucidating important information associated with a multitude of protein functions including signaling processes, enzyme behavior, aggregation pathways etc... This information is also critically important in the development of novel and effective strategies aimed at target proteins associated with pathologies and disease. In order to obtain such useful information, tools and techniques are lacking that: 1) permit the efficient quantitative analysis of fluctuation behavior of existing protein structure ensembles and 2) permit computationally generated natural fluctuation states of proteins at relatively large timescales demanded by the need for biologically relevant results. This thesis presents such methods as well as the results of their application to a case study of A β 40 and pathogenic A β 42 where we identify key differences in energy interactions between those two isoforms. Additionally, our detailed atom-level analysis, was able to identify very minute differences in Ramachandran angles between the two strains as the cause for these interaction energy differences. We also demonstrate the efficacy of our implicit

solvent algorithm in recovering independently, experimentally identified domain motion over a variety of protein systems. Such a system that is medically significant is the HIV-1 protease for which we identified significant motion of a flap domain known to be pharmaceutically important to the protease's active site in drug targeting strategies. Lastly, we employ the insights thus acquired from the A β 40/42 case study to see if A β 42 aggregation inhibitors can be rationally developed and then tested *in vitro* for their efficacy. Results were very promising with A β 42 aggregate sizes being significantly reduced by statistically significant margins by the inhibitor compounds. Due to these encouraging results, we have consequently obtained a provisional patent application for our inhibitors.

I. Introduction and Background:¹

IA. Overall Objectives, Aims and Goals of this Thesis

The overall objective of this thesis is to investigate intra-protein interactions and their effects on natural protein fluctuation states. Specifically, this thesis involves the development of novel methods to efficiently carry out energy mappings ensemble structure data, the computational generation of dynamic structure ensembles, and the applications of these methods to specific, contemporary systems.

In general, this thesis will focus on the characterization and generation of natural fluctuation states of proteins about an average equilibrium structure. Characterization and generation of natural protein fluctuation states is critical, for example, to drug design aimed at providing inhibitors (antagonists) and enhancers (agonists) to protein functions, enzyme function, aggregation phenomena, including fibril formation, and many other protein functions, discussed more fully below. An important part of this characterization is a local, atomic level intra-protein energy landscape mapping, which is ultimately critical to protein function. As will be discussed in detail shortly, certain regions in the protein structure are stabilized by non-covalent atom-atom interactions known as energy “hot-spots” which are not entirely persistent throughout an ensemble. Hot-spots may be short-lived (non-persistent) or persistent across natural fluctuation states of proteins and are the result of different types of forces associated with

¹ Since the following discussion will address more advanced and specialized topics associated with protein behavior, an extended literature review of more basic information such as amino acid architecture and protein structure is provided in Appendix A.

intra-protein interactions. Currently there exists a void in the methods of processing protein structural ensembles to reveal these critical energetic details.

Another fundamental concern this thesis addresses is the generation of “dynamic” ensembles that faithfully capture actual protein motion. As will be explained in greater detail later, NMR ensembles have proven useful in drug design applications, but their ensembles are not always guaranteed to capture true fluctuations as they are generated from model fits of one set of nuclear spin data. Although computational dynamic simulations (MD) are able to generate such ensembles of true protein motion, MD is often computationally prohibitive, particularly for relatively large proteins, and is not readily extendable to the wider range of time scales associated with protein dynamics in general. Thus, generating protein structure ensembles whose statistical variations in atomic positions reflect actual protein fluctuations over biologically relevant time scales fills yet another void where such ensembles can now yield accurate insight into a dynamic protein’s potential energy landscape over meaningful timescales. Such ensemble energetic information is furthermore preferable since fluctuating regions potentially important to drug targeting efforts can be identified in contrast to using purely single structures (as obtained from X-ray crystallography experiments) whose energy mappings may not discriminate between persistent hot-spots and short-lived ones (Figure 1).

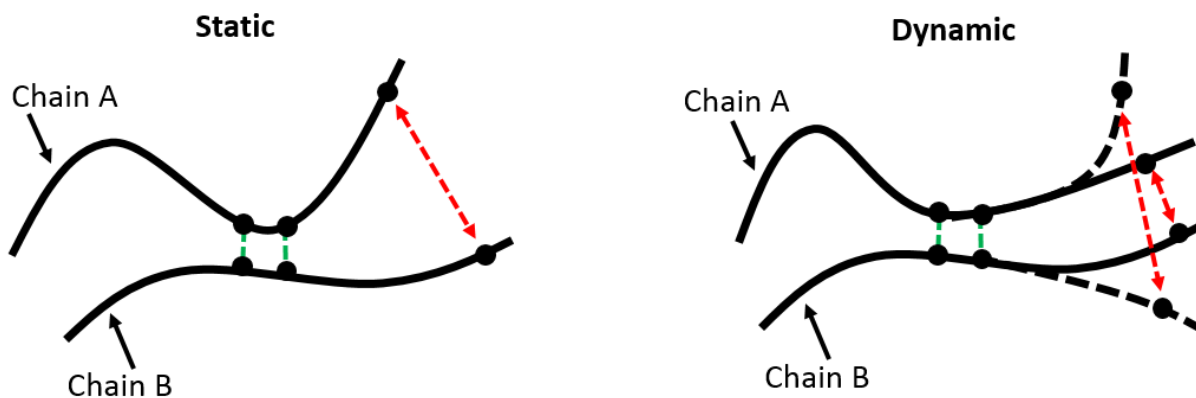


Figure 1: Illustration of protein conformation aspects probed by static vs. dynamic studies. Hot-spot atom-atom interaction contact points between 2 chains of a protein that do not vary despite intra-protein fluctuations are represented by green dashed lines versus short-lived hot-spot interactions unique to individual conformations observed during fluctuations as seen by red dashed lines.

To address these needs, the work of this project has been divided into four major aims as summarized in Table 1. This subdivision of our research goals and objectives specifically details the topics, or aims, that constitute the basis of our research plan as well as their relevant outstanding research questions, novel contributions and methods of investigation.

Table 1: Framework for Research Aims

Aims	Outstanding Questions	Novel Contributions	Methods
Aim 1: Informatics Ensemble Mappings (Intra-protein or inter-chain interactions)	<ol style="list-style-type: none"> 1) How to map across an ensemble of structures? 2) Statistically how many ensembles are needed? 3) Are there persistent dominant atom-atom interactions across ensembles? 4) Can we acquire insights on mutations by static mappings alone? 	<ol style="list-style-type: none"> 1) Ensemble energy mapping results organizing algorithm 2) 10 structure models are statistically sufficient 3) There is a large persistent core 4) There are insights into WT vs. mutant functional differences 	<ol style="list-style-type: none"> 1) Protein energy mapping algorithm 1) Ensemble energy mapping results organizing algorithm
Aim 2: Static mapping of amyloid systems	<ol style="list-style-type: none"> 1) Can mappings offer insight into fibril state of wild-type vs. mutant? 	<ol style="list-style-type: none"> 1) Found long-range interactions in mutant strain not present in wild-type 2) Identified differences in peptide plane Ramachandran angle values as cause for inter-strain interaction energy differences 	<ol style="list-style-type: none"> 1) Protein energy mapping algorithm 2) Ensemble energy mapping results organizing algorithm
Aim 3: Long-time dynamic simulations of protein fluctuation states	<ol style="list-style-type: none"> 1) Can we recover fluctuation data identified by previous computational and experimental studies? 2) Are fluctuation states captured in NMR ensembles? 	<ol style="list-style-type: none"> 1) Able to recover experimental data on fluctuation states 2) NMR ensembles capture some true fluctuations, miss others and predict some where none exist 	<ol style="list-style-type: none"> 1) Implicit solvent 2) Protein energy mapping algorithm 3) Ensemble energy mapping results organizing algorithm
Aim 4: Inhibitor Design	<ol style="list-style-type: none"> 1) Can we use <i>ab initio</i> methods (energetic mappings and dynamic computations) to rationally design an effective Aβ42 oligomer inhibitor? 2) Verify experiments 	<ol style="list-style-type: none"> 1) Analyzed certain regions which could be important in aggregation inhibitor design 2) Provisional patent for intellectual property protection 	<ol style="list-style-type: none"> 1) Implicit solvent dynamics on Aβ42 dimer stability at nsec timescale 2) Atomic force microscopy (AFM)

In Aim 1, we seek to develop a general tool to map dominant atomistic energy landscapes across an arbitrarily generated ensemble of protein structures, about some equilibrium structure, expressing statistical variation in the position of each ensemble members' constituent atoms. These dominant "hot-spot" locations of non-covalent atom-atom interactions act as "glue points" and are therefore a critical consideration in the detailed analysis of protein fluctuations and dynamics. There currently is lacking an open-source, user-friendly tool to provide and interpret such mapping data. Aim 2 applies the tools developed in Aim 1 to a case study of the A β 40 and A β 42 peptides which are responsible for the etiology of Alzheimer's disease. Such a characterization is undertaken in order to identify any inter-chain energy interaction differences between these two strains. Although the literature presently acknowledges aggregation

propensity differences between these two isoforms (with the pathogenic A β 42 being more aggregation prone), there has, heretofore, been a void discussing potential reasons as to why these aggregation propensities exist which Aim 2 strives to address. Ultimately the differences in these two strains are shown to be traceable to specific changes in the inter-chain “hot-spots.” In Aim 3 we then seek to apply potentially long-time implicit solvent (IS) dynamic simulations to a variety of protein systems to verify IS capability to recover known fluctuations independently obtained in the literature. Additionally, Aim 3 hopes to address whether statistical variations observed in NMR structure ensembles correlate with the aforementioned fluctuations known to actually occur in the proteins analyzed as this question remains unanswered for many systems. Lastly, in Aim 4, we hope to apply the techniques and insight gained from the methods described to see if an effective aggregation inhibitor, based on hot-spot disruption, for the pathogenic A β 42 peptide can be rationally developed and then subsequently tested *in vitro* for its aggregation inhibition efficacy.²

IB. Background on Protein Structure and Function

An important starting consideration of this work is the recognition of the variety of timescales of protein functions that are of biological interest (Figure 2). As broader scientific impact, part of our goal is to develop novel techniques to investigate protein and peptide fluctuations, dynamics and energetics that can be applied to a wide variety of systems that may function over a variety of time-scales. When considering internal protein dynamics, it is important to bear in mind the wide range of time-scales associated with the motions of interest

² Because these computational studies rely heavily on the description of covalent and non-covalent interactions in proteins, an extended literature review of this topic is provided in Appendix B.

(Figure 2). Allosteric transitions, for example, occupy a time regime spanning hundreds of nanoseconds to seconds (10^{-5} - 10^0 seconds) and rotations of side chains at the surface of a protein are known to reside within the picosecond to nanosecond time window (10^{-11} - 10^{-10} seconds) [1]. Figure 2 below summarizes a variety of time-dependent protein fluctuation phenomena with their associated relative time-scales.

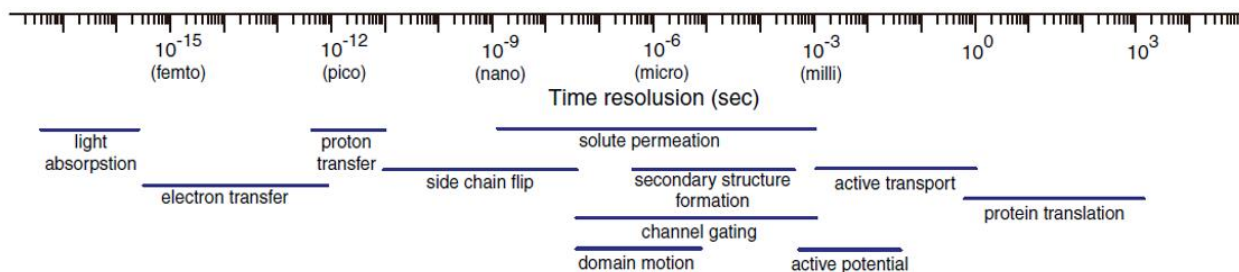


Figure 2: Time scales associated with various aspects of protein dynamics. Adapted from Ode, Nakashima, Kitamura, Sugiura and Sato [2].

More dramatic conformational changes associated with domain motion that might lead to aggregation phenomena can also occur between tens of nanoseconds and microseconds (10^{-8} - 10^{-6} seconds) [2].

Peptides and proteins can then affect biological changes owing to their participation in bio-chemical reactions either as reactants, transporters of other chemical species, catalysts (i.e. enzymes) or even providing structural support to the organism [3]. Table 2 provides a brief outline of different protein families and some representative proteins belonging to those families.

Table 2: Protein classifications by function [3].

Protein Functional Classifications	Example Proteins
Enzymes	lactase, DNA polymerase, alcohol dehydrogenase
Hormones	adiponectin, vasopressin, insulin
Transport Proteins	transferrin, S100A1, hemoglobin
Immunization	defensin-5, toll-like receptor 3, interleukin
Membrane Proteins	amyloid precursor protein, potassium channel, aquaporins
Transcription Factors	p53, HEXIM-1, TFIIA
Structural	collagen, keratin, HIV capsid protein

Understanding the relationship involved between protein structure and function can naturally lead the curious to query the nature of the internal status of proteins in their appropriate three-dimensional conformations. Indeed when we speak of a protein's structure, it is important to consider that this structure has an associated internal free energy landscape that is responsible for the associated structure and therefore function of the protein [4-9]. One can therefore reasonably state that the physical form and pragmatism of a protein is a function of the protein's energy landscape of internal interactions which encourages the endeavor of approaching the study of proteins through the lens of energetic analyses.

Our studies in this thesis focus specifically on strong intra-protein atom-atom interactions that impart internal structural inter-chain stability within multi-chain proteins as well as peptide aggregate species.

In general, inter-atomic energy mappings between specific atoms of specific residues in proteins demonstrate conspicuous “hot-spots” or regions of dominant non-covalent interactions rather than a more uniform distribution across the protein [10]. Hot-spots are responsible for

protein stability and the creation of overall structure that is conducive to protein function. Identifying these regions is therefore the goal of protein energy mappings due to the potential use of this information in applications pertinent to the identification of possible therapeutic agents. These energy hot-spots are due to relatively larger partial atomic charge and van der Waals type interactions that may not necessarily correlate with inter-atomic separations and ultimately require force field models for their quantitative analysis. The starting point for such an analysis, however, is the actual atomic structural information of the protein, which may be experimentally acquired through nuclear magnetic resonance spectroscopy or X-ray crystallography. These structures may then be obtained from structure databases such as the Protein Data Bank [11] as was done for this thesis. For example, Krall et al. [10] studied the energetic hot-spots in proteins using an all-atom force field model with structural information provided by X-ray crystallography. This study thus led to the rapid identification of hot-spots within proteins associated with specific disease states and potential peptide mimetics aimed at their disruption [10]. Thus, static all-atom energy mapping studies alone show potential in providing more rational approaches to analyze the stability of proteins and possible therapeutic interventions to aberrant states.

In addition to static mappings, dynamic structural information on natural changes in the energy states of proteins communicate how these atomic hot-spots can change as a function of protein molecular fluctuations. As seen above, Figure 1 schematically details the concepts behind such dynamic energy mappings as they pertain to atom-atom hot-spot regions between two protein chains where dynamic fluctuations can incur changes in the hot-spot location landscape. This scenario is juxtaposed with the concept of the static single structure mapping

analysis carried out by Krall et al [10]. The implication that one can derive from Figure 1 is that the use of a single structure in energy mappings, although informative, has the potential to provide extraneous artifacts communicating persistent hot-spot regions/locations where none exist. This is depicted as the atom-atom interactions conjoined by the red dashed lines which may exist during a particular “snapshot” of when the crystallographic single structure was specifically determined as an example. On the other hand, mappings on an ensemble of structures, as may be provided by computational simulation experiments (ideally) or nuclear magnetic resonance experiments (there are caveats with this technique however, more on this later), may provide a more realistic energy portrait of the protein or protein domain structure under study specifically in regards to these fluctuation hot-spots. In either case, long-lived, or dominant atom-atom interactions that persist across the range of protein molecular motions are represented with the green dashed lines in Figure 1 and they correspond to the interaction atomistic hot spots that energy mappings hope to identify. Specific processes such as catalytic turnover of enzymes, signal transduction/regulation, transcription, thermal stability, etc. are all heavily influenced by the fundamental relation of protein structure and these inter-atomic interactions [12-17]. Indeed, given the relationship that these fluctuations have on important biological systems such as enzymes whose function and performance are intimately tethered to dynamic fluctuations [18-22], a compelling case may be made for the study and the development of novel protocols that seek to elucidate internal protein or peptide energetics and dynamics as a function of their motion.

With these considerations in mind, it becomes possible to appreciate the role that atom-atom interaction energetics can play not only in normal protein behavior, but also in pathogenic

states possibly incurred by mutations. For example, missense genetic mutations can lead to a plethora of altered folded states of proteins (“misfolded states”) that radically change their functional behavior and result in the cancerous states of cells [23-28]. Missense genetic mutations can alter both the structure and the inter-atomic energy landscape of proteins that result in this loss or gain of functionality associated with the specific disease state. Certain mutations can also indirectly result in disease as is the case with Alzheimer’s disease where a mutation can result in an incorrect proteolysis location in the Alzheimer precursor protein (APP) resulting in peptide fragments possessing an aberrant amino acid sequence which then aggregate together into toxic species. In such aggregation events, natural energy fluctuations associated with conformational changes in proteins have been shown to be important in pathogenic plaque formations where such aggregates form from opportunistic conformations that the peptide may assume wherein the energetics to conjoin in non-covalently held structures are favorable [29-33]. Figure 3 below conceptually shows how these opportunistic conformations may lead to aggregation states. Thus the interplay between shifts in internal protein energy landscapes and structural changes are therefore ultimately discernable through the study of the interactions of all of the constituent atoms of the protein.

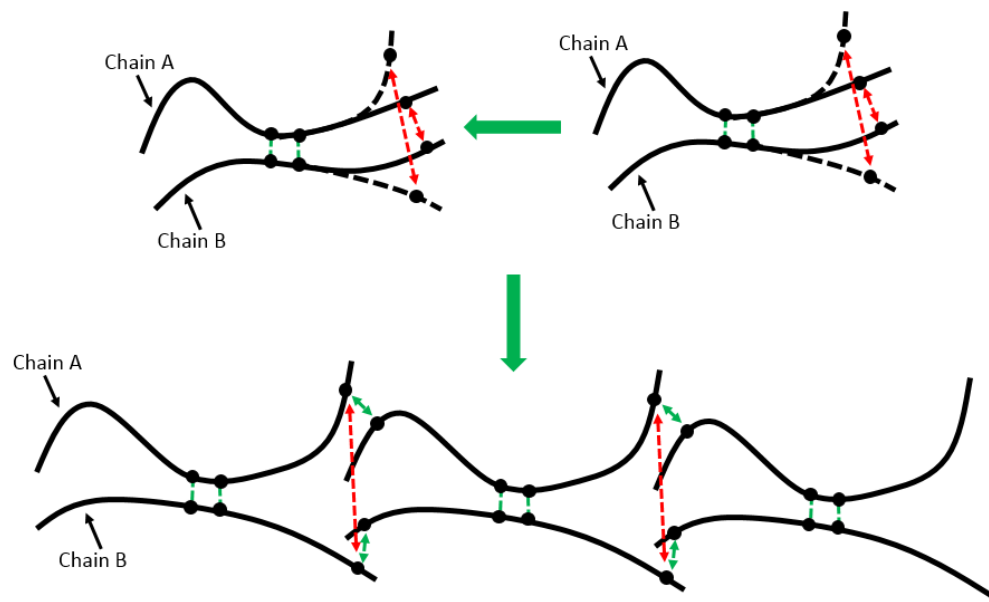


Figure 3: Illustration of how certain short-lived conformations within a protein (or peptide in the case of Alzheimer’s disease) can lead to opportunistic atom-atom interaction contact points conducive to the growth of aggregation states (lower panel).

We note that in the interest of investigating the phenomena addressed thus far as well as other relevant questions for other protein systems, the work in this thesis covers a wide range of proteins that have a variety of functions. Table 3 shows a variety of protein families (though by no means exhaustive) as classified according to function originally presented in Table 2 with specific systems hi-lighted in Table 3 that have been employed in our studies which shall be described in greater detail later.

Table 3: Protein classifications by function [4]. Bold and italicized proteins were explicitly analyzed in the thesis.

Protein Functional Classifications	Example Proteins
Enzymes	lactase, DNA polymerase, alcohol dehydrogenase
Hormones	adiponectin, vasopressin, <i>insulin</i>
Transport Proteins	transferrin, <i>S100A1</i> , hemoglobin
Immunization	<i>defensin-5</i> , <i>toll-like receptor 3</i> , interleukin
Membrane Proteins	<i>amyloid precursor protein</i> , potassium channel, aquaporins
Transcription Factors	<i>p53</i> , <i>HEXIM-1</i> , TFIIA
Structural	collagen, keratin, <i>HIV capsid protein</i>

IC. Background on Experimental Dynamic Methods for Protein Fluctuations

We now turn to various experimental techniques that can be employed to study protein dynamics although we are careful to note that this list is not exhaustive. One such technique recently developed (circa 2010) by Dhar and Gruebele [34] is known as fast relaxation imaging which hybridizes fluorescence microscopy and fast, laser-induced temperature jumps. This technique is powerful insofar as it permits the observation and study of protein dynamics inside a living cell [34]. The obvious benefits of this technique are that protein behavior can be observed under the sphere of influence of co-existent chemical species such as ions and any co-factors *in vivo* and that protein dynamics can be observed in different areas of the cell as well where differences in dynamics may exist for the same protein species [34]. Additionally, it is worth noting that all these observations can be observed in real-time with fast relaxation imaging. There are limitations to this technique, however, that may hinder the study of protein dynamics for certain scenarios. Some of these disadvantages are that proteins in cells can only be imaged over a narrow temperature range of 25° to 45°C (processes of interest outside this temperature

window are therefore inaccessible) and proteins need to be fluorescently labeled so that their dynamics can be detected which has the potential to perturb the dynamics being studied [34].

Another experimental technique that has classically been used for studying protein dynamics and motion is fluorescence anisotropy decay. This technique is able to provide information on both mobility and dynamics of a fluorophore, which is covalently bound to a residue in a protein [35]. The properties of mobility and dynamics can be probed by measuring/quantifying the polarized light of the fluorescence emission. By measuring the fluorescence through the same polarization as the excitation (known as parallel polarization) and then subtracting the fluorescence recorded using a perpendicular polarizer, the investigator can obtain a precise measure of the rotational correlation time that the protein or protein domain is undergoing as the fluorescence probe usually emits with a transition dipole moment nearly parallel to the excitation transition moment [36]. Motion of the tagged protein or protein domain therefore results in a change in polarization that can be observed [36]. Advantages of fluorescence anisotropy decay are that it is fast, it uses low concentration of the protein, and it offers high sensitivity and specificity [36]. Limitations to this technique, however, are that the extraction of structural information from the anisotropy decay curves is not straightforward [35]. Empirical models have been proposed to facilitate interpretation but the fallback of this paradigm is that many results obtained from these experiments depend on the particular choice of model used which are in turn contingent on certain assumptions that are not always easy to verify [35].

Hole burning spectroscopy is another experimental technique that has been used to study protein dynamics and fluctuations. Similar to the fluorescence techniques heretofore described,

hole burning spectroscopy makes use of molecules known as chromophores which are attached to the protein under study and which emit electromagnetic radiation upon relaxation of their electronic state from photonic excitation [37, 38]. Unlike the aforementioned fluorescence techniques, however, the chromophore's wavelength absorption bandwidth/spectrum is directly influenced by the conformational fluctuations of the protein and thus the absorption spectrum changes with those fluctuations [37, 38]. These wavelength absorption spectra are in turn directly correlated with the free energy landscape of the protein and so the overall absorption spectrum reflects the conformational variability of the conformational free energy landscape of the protein [37, 38]. Thus by irradiating the sample with very intense light in a very narrow wavelength bandwidth, the chromophores are selectively excited and accumulated in a long-living state around the laser frequency. This excitation also induces protein conformational changes given the connection between chromophore electronic state and protein conformational states. This results in a "hole" in the entire absorption spectrum around the laser frequency which will equilibrate back to the original absorption spectrum thus eliminating the hole [37, 38]. Thus by monitoring the rate (read time dependence) with which the hole disappears, it is possible to elucidate the distribution of the heights of the energy barriers that separate all of the conformational states of the protein and also elucidate the relevant time dynamics [37, 38]. An advantage of hole-burning spectroscopy is that it is a technique that offers the time-domain observation of the equilibrium fluctuation of a protein over a wide temporal region [37]. This is due to the temporal evolution of the hole that is induced by the transition-energy fluctuation of the unexcited molecules that do not suffer from the perturbation by the exciting laser pulse and consequently continue the equilibrium fluctuation even after the burning. Disadvantages to this technique are that hole-burning systems undergo a single photon process and the signal-to-noise

ratio degrades in each reading scan due to simultaneous burning in addition to signal interference resulting from the fluctuations of scattered laser light intensity [37].

Another important static and dynamic experimental method to study protein structure and motion is nuclear magnetic resonance, or NMR, spectroscopy which can provide structural information on proteins in their natural aqueous environment. The basis of NMR relies on the physical phenomenon where atomic nuclei in a magnetic field can absorb and re-emit electromagnetic radiation as they relax from being released from the magnetic field [12]. This phenomenon is known as spin. The energy of the emitted electromagnetic radiation is in turn at a specific resonance frequency, and it depends on the strength of the magnetic field and the magnetic properties of the isotopes of the affected atoms [12]. For proteins, the NMR-active nuclei are the isotopes ^1H , ^2H , ^{13}C , ^{15}N and ^{31}P [12]. These isotopic probes can be introduced at desired locations within the protein rendering many site-specific probes of local structure and dynamics. The protein is thus placed in a strong magnetic field where the magnetic moment for each set of isotopes will align with the magnetic field until it is released resulting in a relaxation of the isotopic nuclei back to their ground state [12]. This data is what is processed resulting in the structural and dynamic information of the protein. Although crystallography diffraction studies provide structures that are accepted as correct in spite of the non-physiological environment of the crystal packing, certain protein surface structural details may be modified due to the dense packing of protein molecules in the crystal lattice [39]. Thus the utility of using NMR-derived structures lies in that a potentially more accurate protein structure can be better observed and appreciated in an aqueous environment that may better mimic the *in vivo* environment.

The structural output of NMR spectroscopy comes in the form of structure ensembles that are based on data fitting models with the restraint set used [40]. In the NMR data, regions of the protein that are experimentally highly restrained (well-defined regions) overlap significantly across the ensembles, whereas regions that have less experimental restraints (ill-defined regions) have variable positions across each model [41]. Limitations of protein NMR spectroscopy as they relate to protein dynamics are that observable metrics, which report on the dynamics as an exchange between multiple states, may not observe differences between truly exchanging states even though there may be dynamically-driven state exchanges taking place [42]. Conversely, metrics for detecting and quantifying dynamics may pick up on fluctuations where there are none. An example of such phenomena is when there are rigid backbones with an adjacent and mobile side chain group which results in the entire region appearing dynamic when in truth it is not (observable metrics employed by protein NMR to probe protein dynamics are chemical shifts, relaxation rates, paramagnetic relaxation enhancement and residual dipolar couplings) [42]. Other limitations include the upper size of the proteins being investigated where proteins larger than 50-100 kDa cannot be quantified by NMR (the limit may be up to 1MDa for specialized studies) and the poor sensitivity of signal detection due to the low characteristic energy of magnetic spin transitions which results in the necessity of large quantities of sample to study [42]. Financially, protein NMR can also be costly in the procurement of isotopically labeled samples [42]. Due to the aqueous solvent environment inherent with NMR spectroscopy, however, this technique provides a unique opportunity to experimentally observe energy hot-spots in the structural states of proteins as given by the set of ensembles.

Outstanding questions arise, however, as to the incorporation of the various NMR ensemble members in energy mapping algorithms and energy differences between individual NMR structure models.

Thus part of the objectives of the proposed study is to develop a method to rigorously handle ensemble structures, to extract meaningful energetic data.

For completeness, we note that several studies have identified the ill-defined regions of NMR ensembles as associated with flexible domains of proteins [43-45]. For example, Bertini et al. [43] state that in their structure determination of a matrix metalloproteinase 12 by NMR, loop regions with reduced Nuclear Overhauser Effect, or NOE, interactions (thus showing greater variability in the superimposed ensembles) are linked to local protein motion whereas superimposed regions with little variability are associated with static protein regions. However, those authors also note that regions with such reduced NOE interactions may likewise be due to low data quality and/or severe overlap of NOESY cross peaks and are not necessarily due to local motion strictly speaking; although for their study, motion proved to be the predominant reason for structural variability. We, therefore, note that due to the fact that the NMR structure ensembles are based on various model fittings of the same data, the association of ill-defined regions or uncommon energy interactions with flexible protein domains, and likewise, common interactions with more rigid domains is questionable. In addition, it is not clear how NMR ensembles can be effectively used to provide electrostatic mappings due to variation in output.

ID. Background on Computational Approaches to Protein Fluctuations

An alternative approach to obtain dynamics is to turn to all-atom molecular dynamics, or alternatively, all-atom implicit solvent methods that can provide a time-dependent ensemble of structures at the atomic level which can truly be considered time-dependent snapshots of protein motion. Both all-atom molecular dynamics and all-atom implicit solvent models are based on simulating the atomic motions from classical mechanics laws (i.e. Newton's laws of motions) using interaction parameters to model the potential energy experienced by interacting atoms [46, 47]. Differences between these two techniques are that molecular dynamics simulations model the molecules of the protein's solvent, usually water, explicitly as opposed to implicit solvent simulations where the properties of the solvent are instead averaged [48]. This is accomplished by the implicit solvent algorithm carrying out a short time averaging of the host solvent dynamics. This is in turn coupled to a relatively longer-time, macromolecule dynamics step. The macromolecular dynamics step itself requires Brownian particle diffusion terms and implicit solvent force terms determined via the short-time behavior. On a practical level, the diffusion and implicit fluid force terms can be approximated via separate analytical or computational studies for any given system as demonstrated in [49-52]. Therefore, implicit solvent methods have demonstrated the potential to greatly reduce the computational work load for protein dynamic simulations by reducing both the total atom-atom force computations load and increasing the integration time steps required.

Considering the limitations that can be expected from these two computational techniques, one of the weaknesses of molecular dynamics methods lies in that the time scales that can be explored are on the order of tens to hundreds of nanoseconds; however, many

energetic changes of interest occur on longer timescales of up to milliseconds or more [53, 54] as illustrated in Figure 4. Structures thus acquired solely by molecular dynamics might therefore risk omission of certain additional conformations that may be critical in an analysis, in particular, the fluctuation dynamics inherent in protein interactions. Although molecular dynamic simulations are more precise due to their treatment of individual atoms in the solvent, time scales are generally limited to the nanosecond time scale. Larger time scales can be addressed with all-atom molecular dynamics algorithms, but generally require specialized supercomputing resources [55, 56]. Since computing times have been a traditional bottleneck in molecular dynamics simulations, all-atom implicit solvent methods can be used to cut down on this time and are capable of achieving millisecond timescales or longer [57]. In this method the proteins are treated on an all-atom basis, but the solvent behavior is averaged over the so-called solvent relaxation time as just described. Limitations that implicit solvent methods might face include scenarios where the host solvent is unable to respond quickly enough to adjust to any new configuration of the protein [54-57]. Such a situation arises when there are significant heterogeneities in the host fluid and results in so-called rarefied gas flows [49-52]. As the name implies, this scenario is of concern to gas phase systems, which is not a pertinent concern to our studies considering that our studies take place in the liquid phase. For the dynamic simulations proposed here, the rarefaction issue is not important and all-atom implicit solvent methods may provide a critical tool for analyzing protein fluctuation behavior and its associated dynamics at longer time scales of interest. We note that that there are a multitude of alternative computational techniques bearing names similarly known as coarse-grained, implicit solvent, Brownian dynamics, or stochastic dynamics that have been developed and applied to biological macromolecules. Unfortunately, many of the published methods are incomplete and certain

fluctuation phenomena such as rotational motions and important coupled translational-rotational motions are not accounted for in these other computational techniques. Additionally, many of these computational methods often include empirical additions such as empirically-based force potentials (and other “fudging” methods) in order to achieve “good” results that are unfortunately restricted to the empirical conditions from which such empiricisms arose. We note that no attempt is made here to review this myriad of methods.

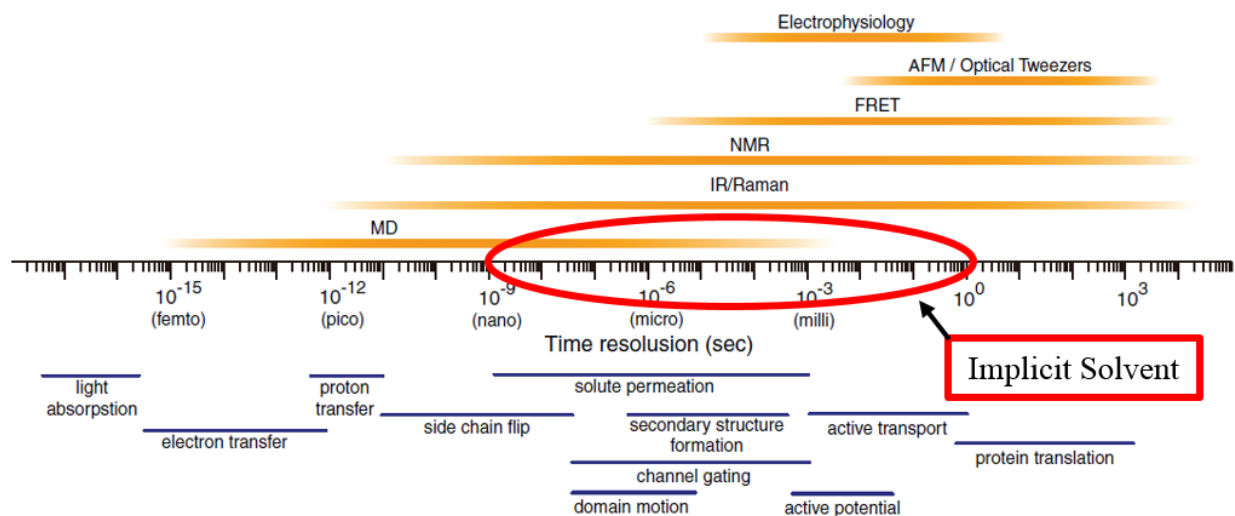


Figure 4: Fluctuation phenomena addressed by molecular dynamics and implicit solvent methods. Adapted from Ode, Nakashima, Kitamura, Sugiura and Sato [2].

At this time, we now shift our discussion to the results for each of this thesis’ four aims.

IE. References:

- (1) McCammon JA, Harvey CS. Protein Dynamics. Dynamics of proteins and Nucleic Acids Cambridge, UK: Cambridge University Press; 1987. p. 28-30.
- (2) Ode H, Nakashima M, Kitamura S, Sugiura W, Sato H. Molecular dynamics simulation in virus research. Frontiers in microbiology 2012 July;3(258):1-9.

- (3) Creighton TE. *Proteins: Structures and Molecular Properties*. 2nd ed. New York: W.H. Freeman and Company; 1993.
- (4) Alm E, Baker D. Prediction of protein-folding mechanisms from free-energy landscapes derived from native structures. *Proc Natl Acad Sci U S A* 1999 Sep 28;96(20):11305-11310.
- (5) Banushkina PV, Krivov SV. High-resolution free energy landscape analysis of protein folding. *Biochem Soc Trans* 2015 Apr;43(2):157-161.
- (6) Dinner AR, Šali A, Smith LJ, Dobson CM, Karplus M. Understanding protein folding via free-energy surfaces from theory and experiment. *Trends Biochem Sci* 2000;25(7):331-339.
- (7) Karplus M. How does a protein fold? *Nature* 1994;369:19.
- (8) Bryngelson JD, Onuchic JN, Socci ND, Wolynes PG. Funnels, pathways, and the energy landscape of protein folding: a synthesis. *Proteins: Structure, Function, and Bioinformatics* 1995;21(3):167-195.
- (9) Low Energy Conformations of a Three-Helix Peptide in a All-Atom Biomolecular Forcefield. *Technical Proceedings of the 2003 Nanotechnology Conference and Trade Show, Volume 1*; 2003; 2003.
- (10) Krall A, Brunn J, Kankanala S, Peters MH. A simple contact mapping algorithm for identifying potential peptide mimetics in protein–protein interaction partners. *Proteins: Structure, Function, and Bioinformatics* 2014;82(9):2253-2262.
- (11) Berman, H. M., et al. "The Protein Data Bank." *Nucleic acids research* 28.1 (2000): 235-42.
- (12) Kleckner IR, Foster MP. An introduction to NMR-based approaches for measuring protein dynamics. *Biochimica et Biophysica Acta* 2011;1814(8):942-968.
- (13) Boehr DD, Dyson HJ, Wright PE. An NMR perspective on enzyme dynamics. *Chem Rev* 2006;106(8):3055-3079.
- (14) Namanja AT, Wang XJ, Xu B, Mercedes-Camacho AY, Wilson BD, Wilson KA, et al. Toward Flexibility– Activity Relationships by NMR Spectroscopy: Dynamics of Pin1 Ligands. *J Am Chem Soc* 2010;132(16):5607-5609.
- (15) Loria JP, Berlow RB, Watt ED. Characterization of enzyme motions by solution NMR relaxation dispersion. *Acc Chem Res* 2008;41(2):214-221.
- (16) Smock RG, Gierasch LM. Sending signals dynamically. *Science* 2009 Apr 10;324(5924):198-203.
- (17) Kamerzell TJ, Middaugh CR. The complex inter-relationships between protein flexibility and stability. *J Pharm Sci* 2008;97(9):3494-3517.

- (18) Eisenmesser EZ, Bosco DA, Akke M, Kern D. Enzyme dynamics during catalysis. *Science* 2002 Feb 22;295(5559):1520-1523.
- (19) Xie XS. Single-molecule approach to dispersed kinetics and dynamic disorder: Probing conformational fluctuation and enzymatic dynamics. *J Chem Phys* 2002;117(24):11024-11032.
- (20) Henzler-Wildman KA, Lei M, Thai V, Kerns SJ, Karplus M, Kern D. A hierarchy of timescales in protein dynamics is linked to enzyme catalysis. *Nature* 2007;450(7171):913-916.
- (21) Eisenmesser EZ, Millet O, Labeikovsky W, Korzhnev DM, Wolf-Watz M, Bosco DA, et al. Intrinsic dynamics of an enzyme underlies catalysis. *Nature* 2005;438(7064):117-121.
- (22) Hammes-Schiffer S, Benkovic SJ. Relating protein motion to catalysis. *Annu Rev Biochem* 2006;75:519-541.
- (23) Kato S, Han SY, Liu W, Otsuka K, Shibata H, Kanamaru R, et al. Understanding the function-structure and function-mutation relationships of p53 tumor suppressor protein by high-resolution missense mutation analysis. *Proc Natl Acad Sci U S A* 2003 Jul 8;100(14):8424-8429.
- (24) Paez JG, Janne PA, Lee JC, Tracy S, Greulich H, Gabriel S, et al. EGFR mutations in lung cancer: correlation with clinical response to gefitinib therapy. *Science* 2004 Jun 4;304(5676):1497-1500.
- (25) Samuels Y, Wang Z, Bardelli A, Silliman N, Ptak J, Szabo S, et al. High frequency of mutations of the PIK3CA gene in human cancers. *Science* 2004 Apr 23;304(5670):554.
- (26) Davies H, Bignell GR, Cox C, Stephens P, Edkins S, Clegg S, et al. Mutations of the BRAF gene in human cancer. *Nature* 2002;417(6892):949-954.
- (27) Ellison DW, Onilude OE, Lindsey JC, Lusher ME, Weston CL, Taylor RE, et al. beta-Catenin status predicts a favorable outcome in childhood medulloblastoma: the United Kingdom Children's Cancer Study Group Brain Tumour Committee. *J Clin Oncol* 2005 Nov 1;23(31):7951-7957.
- (28) Riely GJ, Marks J, Pao W. KRAS mutations in non-small cell lung cancer. *Proceedings of the American Thoracic Society* 2009;6(2):201-205.
- (29) Zhuravlev PI, Reddy G, Straub JE, Thirumalai D. Propensity to form amyloid fibrils is encoded as excitations in the free energy landscape of monomeric proteins. *J Mol Biol* 2014;426(14):2653-2666.
- (30) Thirumalai D, Klimov D, Dima R. Emerging ideas on the molecular basis of protein and peptide aggregation. *Peptides* 2003;16:22.
- (31) Hammarstrom P, Wiseman RL, Powers ET, Kelly JW. Prevention of transthyretin amyloid disease by changing protein misfolding energetics. *Science* 2003 Jan 31;299(5607):713-716.

- (32) Hammarstrom P, Jiang X, Hurshman AR, Powers ET, Kelly JW. Sequence-dependent denaturation energetics: A major determinant in amyloid disease diversity. *Proc Natl Acad Sci U S A* 2002 Dec 10;99 Suppl 4:16427-16432.
- (33) Tsemekhman K, Goldschmidt L, Eisenberg D, Baker D. Cooperative hydrogen bonding in amyloid formation. *Protein Science* 2007;16(4):761-764.
- (34) Dhar A, Gruebele M. Fast relaxation imaging in living cells. *Current Protocols in Protein Science* 2011;28.1. 1-28.1. 19.
- (35) Schröder GF, Alexiev U, Grubmüller H. Simulation of fluorescence anisotropy experiments: probing protein dynamics. *Biophys J* 2005;89(6):3757-3770.
- (36) Otzen DE editor. *Amyloid Fibrils and Prefibrillar Aggregates*. Germany: Wiley-VCH; 2013.
- (37) Shibata Y, Kurita A, Kushida T. Solvent effects on conformational dynamics of Zn-substituted myoglobin observed by time-resolved hole-burning spectroscopy. *Biochemistry (N Y)* 1999;38(6):1789-1801.
- (38) Shibata Y. Time-domain observation of conformational fluctuation of protein by time-resolved hole-burning spectroscopy. *Sci Prog* 1999;83(2):193-208.
- (39) Billeter M. Comparison of protein structures determined by NMR in solution and by X-ray diffraction in single crystals. *Q Rev Biophys* 1992;25(03):325-377.
- (40) Berndt KD, Güntert P, Orbons LP, Wüthrich K. Determination of a high-quality nuclear magnetic resonance solution structure of the bovine pancreatic trypsin inhibitor and comparison with three crystal structures. *J Mol Biol* 1992;227(3):757-775.
- (41) Knegt RM, Kuntz ID, Oshiro C. Molecular docking to ensembles of protein structures. *J Mol Biol* 1997;266(2):424-440.
- (42) Young TS, Schultz PG. Beyond the canonical 20 amino acids: expanding the genetic lexicon. *J Biol Chem* 2010 Apr 9;285(15):11039-11044.
- (43) Bertini I, Calderone V, Cosenza M, Fragai M, Lee YM, Luchinat C, et al. Conformational variability of matrix metalloproteinases: beyond a single 3D structure. *Proc Natl Acad Sci U S A* 2005 Apr 12;102(15):5334-5339.
- (44) Chalaoux F, O'Donoghue SI, Nilges M. Molecular dynamics and accuracy of NMR structures: effects of error bounds and data removal. *Proteins: Structure, Function, and Bioinformatics* 1999;34(4):453-463.
- (45) Andersen CA, Palmer AG, Brunak S, Rost B. Continuum secondary structure captures protein flexibility. *Structure* 2002;10(2):175-184.

- (46) Karplus M, Petsko GA. Molecular dynamics simulations in biology. *Nature* 1990 Oct 18;347(6294):631-639.
- (47) MacKerell AD, Feig M, Brooks CL. Extending the treatment of backbone energetics in protein force fields: Limitations of gas-phase quantum mechanics in reproducing protein conformational distributions in molecular dynamics simulations. *Journal of computational chemistry* 2004;25(11):1400-1415.
- (48) Anandakrishnan R, Drozdetski A, Walker RC, Onufriev AV. Speed of conformational change: comparing explicit and implicit solvent molecular dynamics simulations. *Biophys J* 2015;108(5):1153-1164.
- (49) Peters MH. The Smoluchowski diffusion equation for structured macromolecules near structured surfaces. *J Chem Phys* 2000;112(12):5488-5498.
- (50) Zhang Y, Peters MH, Li Y. Nonequilibrium, multiple-timescale simulations of ligand-receptor interactions in structured protein systems. *Proteins: Structure, Function, and Bioinformatics* 2003;52(3):339-348.
- (51) Peters MH. Langevin dynamics for the transport of flexible biological macromolecules in confined geometries. *J Chem Phys* 2011;134(025105):1-11.
- (52) Peters MH. Fokker-Planck equation and the grand molecular friction tensor for coupled rotational and translational motions of structured Brownian particles near structured surfaces. *J Chem Phys* 1999;110(1):528-538.
- (53) Pierce LC, Salomon-Ferrer R, Augusto F. de Oliveira, Cesar, McCammon JA, Walker RC. Routine access to millisecond time scale events with accelerated molecular dynamics. *Journal of chemical theory and computation* 2012;8(9):2997-3002.
- (54) Tozzini V. Coarse-grained models for proteins. *Curr Opin Struct Biol* 2005;15(2):144-150.
- (55) Osuna S, Jiménez-Osés G, Noey EL, Houk K. Molecular Dynamics Explorations of Active Site Structure in Designed and Evolved Enzymes. *Acc Chem Res* 2015;48(4):1080-1089.
- (56) Shaw DE, Deneroff MM, Dror RO, Kuskin JS, Larson RH, Salmon JK, et al. Anton, a special-purpose machine for molecular dynamics simulation. *Commun ACM* 2008;51(7):91-97.
- (57) Ingólfsson HI, Lopez CA, Uusitalo JJ, de Jong DH, Gopal SM, Periole X, et al. The power of coarse graining in biomolecular simulations. *Wiley Interdisciplinary Reviews: Computational Molecular Science* 2014;4(3):225-248.

II. Aim 1: Informatics Ensemble Mappings³

Abstract:

Previously, it has been demonstrated that an ensemble of protein structures, such as those generated experimentally and computationally, may provide improved insight into the functional role of proteins over a single structure representation. In this study, we develop an efficient sorting and parsing algorithm to identify critical adhesion sites or “hot spots” associated with intra-protein interactions, where an ensemble of structures is available. We determined an approximate minimum number of ensemble members required for statistically meaningful results across a broad range of protein functions using ensembles of structural data. In addition, we demonstrated the utility of the method by examining the structural and functional differences between wild-type versus mutant proteins where an ensemble of structures was available for each strain.

IIA. Introduction:

The use of protein structure representations plays a critical role in the study of protein function and behavior. Specifically, in the quest for developing pharmaceutical compounds for the treatment of disease, using a target protein's structure, known as structure-based drug design (SBDD), has facilitated the engineering and design of many life-saving pharmaceutical agents. SBDD uses a variety of computational tools in drug discovery efforts along with an a priori knowledge of protein structures to rationally identify possible agonistic and antagonistic compounds that may have biological relevance as pharmaceutical agents. Notably, SBDD has made possible the development of some "firsts," such as the first topical treatment of glaucoma (dorzolamide) and the first oral anti-influenza drug (oseltamivir) [1]. Structure-based all-atom

³ Submitted for publication to ACS Omega

energy mappings of intra-protein interactions such as those carried out by Krall et al. [2] have similarly yielded very promising results in rapidly identifying bio-mimetic peptide drug compounds previously identified by more laborious methods, thus illustrating the utility of employing protein structures beyond small molecule identification. The use of such structure-based energy mapping techniques has also resulted in the identification of critical non-covalent protein-protein interaction “hot-spots” in the Alzheimer's disease A β peptide that may be responsible for explaining the causes of the different aggregation tendencies between pathogenic and non-pathogenic strains of the A β peptide [3]. For all these different endeavors, computational methods to critically analyze structure information is extremely important in order to obtain meaningful results that may translate into potential drug candidates in drug discovery programs and even aid in the understanding of disease mechanisms at the molecular level.

For these different applications, and particularly for drug design efforts, X-ray crystallography has been the classic experimental means for generating protein structures [1, 4, 5, 6]. Although generally accepted as depicting biologically relevant conformations, legitimate concerns do arise with regards to the non-physiological crystallization conditions (i.e., pH and temperature) of the experiment that may affect certain conformations in the crystal packing and may not otherwise be observed in vivo [7]. Additionally, certain residues with inherent flexibility diffract poorly during the X-ray diffraction experiments and so the final conformations of their side-chains is often the result of approximations and assumptions and may likewise fail to reflect protein conformations actually assumed in vivo [1]. This problem is particularly exacerbated for the side-chains of surface residues, but may also be an issue for some active sites, particularly with the flexible side-chains of lysine and glutamate [1]. Examples of residues

whose observed positions in X-ray crystal structures should be accepted with some skepticism for these reasons are (in increasing order of improving resolution) Lys < Glu < Arg, Gln < Asp, Asn [1]. Lastly, an important consideration in the characteristics of proteins is their available range of natural motion. This consideration becomes particularly important in research endeavors that seek to exploit domains such as allosteric and active sites where this flexibility is crucial to the protein's function [8, 9]. Given that crystal structures reported on databases are an average of the various conformations observed during data acquisition of the X-ray diffraction experiment [10], crystal protein structures provide only one explicit structure conformation of the protein for structural analysis (although inherent dynamics may be inferred from the so-called thermal or B factors in the protein *.pdb structure file). Recognition of these considerations has consequently resulted in efforts to use structure ensembles instead, which may communicate a better statistical and physical representation of protein structure and, in turn, may result in more accurate functional analyses.

Indeed, Carlson et al. [11] successfully developed the first receptor-based pharmacophore model of HIV-1 integrase using an ensemble of unbound structures derived from molecular dynamics (MD) simulations to account for the inherent flexibility of the active site thus overcoming the limitation of an incomplete crystal structure of the target protein. Through this novel structure ensemble-based drug discovery method, several small molecule compounds were identified that have been validated by experiment to be successful HIV-1 integrase inhibitors. The success of this structure ensemble-based paradigm was enough to further apply it to the search for HIV-1 protease inhibitors which likewise successfully identified known small molecule inhibitor candidates [10, 12]. Similarly, studies involving ensembles derived

experimentally from nuclear magnetic resonance experiments, which are conducted in solution and may therefore yield structures closer to the actual *in vivo* native state, have also yielded impressive results. For example, pharmacophore models using the experimental nuclear magnetic resonance generated ensembles discriminated between known HIV-1 protease inhibitors and decoy molecules much more effectively compared to those pharmacophore models created from a collection of crystal structure conformations of the protein [13]. It is worth noting that in that study, the pharmacophore model using the experimental ensemble appeared to provide the most accurate representation of the active site and revealed only the most essential features of the protein's binding site. These findings were in turn tied to the observation that the nuclear magnetic resonance experimental ensemble consisting of 28 individual structures exhibited greater structural variation compared to 90 crystal structures [13]. Those authors lastly noted the additional appeal of using readily available experimental ensemble structures over ensembles derived from MD simulations as use of the former significantly helps in reducing the time to develop such pharmacophore models, time that MD simulations would otherwise consume in generating their ensembles. Even so, in another study by Carlson, Musukawa & McCammon [8], the use of even as little as 2 crystal structures has likewise been shown to yield better results in identifying HIV-1 integrase inhibitors compared to the use of simply one crystal structure. In all, it can thus be concluded that the "hierarchy" of ensemble structures that may provide improved results over single structure models in structure-based drug design efforts are: nuclear magnetic resonance derived experimental structure ensembles, ensembles derived from MD simulations, and an ensemble of experimental crystal structures obtained from multiple diffraction experiments. Regardless of their origin, however, the aforementioned studies show that all three structure types, when used as an ensemble cast, may, in some cases, out-perform the

use of a single structure in the search for pharmaceutically relevant small molecule ligands. These precedents hopefully illustrate the promising potential of employing ensembles, or collections, of structures regardless of their origin (simulations or experimental), in SBDD and other related drug discovery efforts.

For this study, we present a computational method to robustly process ensemble structure data in order to identify non-covalent protein interaction hot-spots across a range of protein structure data for further use in applications and analysis. Previous computational energy mappings to identify critical intra-protein interaction hot-spots such as those carried out by Krall et al. [2], used single structure conformations as the starting protein structures and so no consideration was given on how an ensemble of structures, derived from simulation or experimentally, would be processed using this energy mapping method. We therefore provide here a detailed description on how an ensemble of structures may be processed in order to identify potentially more accurate energetic hot-spots. This data may in turn be used for biomimetic peptide drug design, characterization of pathological versus non-pathological protein strains, or other protein function characteristics.

IIB. Materials and Methods:

Input Structure Data: For the selection of protein structural ensemble data, we sought a broad range of proteins (predominantly from *Homo sapiens*) whose biological functions vary significantly being involved in diverse roles such as calcium ion transportation, hormonal function and immunization, to name a few as summarized in Table 1. Proteins from other

organisms such as the rat (*Rattus norvegicus*) and the viral capsid protein of HIV are also included in the forthcoming results. All identified atoms in the *.pdb files as well as the results are according to the IUPAC naming convention for amino acids [14]. Additional criteria for selecting the structures analyzed in this study include selecting multi-chain protein systems, so that explicit chains could be mapped, as well as selecting systems with both wild-type and mutant ensemble structure data to see if any functional differences could be identified between the two strains. Furthermore, the wild-type and mutant proteins analyzed for this portion of the study were selected according to the following criteria: structure data had to exist as an ensemble of structures and both wild-type and mutant structures had to span the same residues. In all, 14 different protein structure ensembles were analyzed which are subsequently shown to provide a consistent set of unique inter-chain hot-spots which in some cases, can be traced back to known functionality.

Protein Mapping Algorithm: The method used to initially carry out the computational intra-protein potential energy analysis on individual structures of an ensemble was the energy mapping algorithm previously developed by Krall et al. [2]. This algorithm carries out an all-atom energy mapping of the non-covalent atom-atom interactions (partial charge and van der Waals forces) in a protein *.pdb structure file based on the AMBER 03 force field model parameters. The energy mapping algorithm efficiently parses the strongest non-covalent atom-atom energetic interactions and their inter-atomic distances from structure file data according to empirically established criteria to ensure that all dominant interactions are accounted for [2, 15, 16]. Those parsing criteria were taken as the upper limit of $-0.1 kT$ units for Lennard-Jones interactions and $-0.3 kT$ units for Coulombic interactions [2] which are associated with relatively

strong hydrophobic and hydrophilic interactions, respectively, in the internal non-covalent atom-atom interactions of proteins. Thus, the mapping algorithm is applied over one static protein structure model where two chains or segments are specified for analysis in order to then identify the most energetically favorable atom-atom interaction regions, or hot-spots, for non-covalent interactions (see Figure 1).

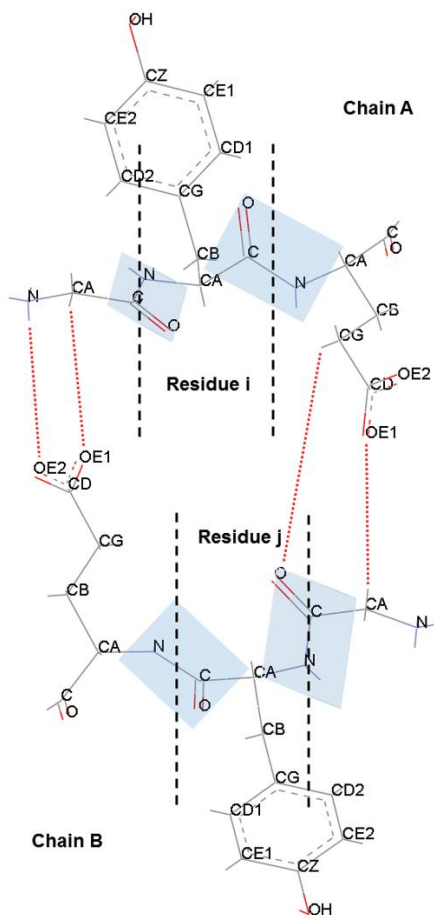


Figure 1: Illustration of energy mapping algorithm's atom-atom interaction mapping targets for a series of hydrogen bonds (interactions indicated by red dashed lines). Peptide planes are shown in blue.

The output, thus provided, is ultimately the identification of the intra-protein/inter-chain atoms which are strongest in exerting attractive Lennard-Jones and Coulombic (charge) forces on their partner atoms on the opposite sub-unit chain. Individual quantitative values for the magnitude of these atom-atom interactions according to the Lennard-Jones and Coulombic parameters are also part of the energy mapping algorithm output.

Since the fundamental objective of this investigation was to develop a method to obtain the regions of strong non-covalent interactions persistent across various structure models in an ensemble of structure conformations for a given protein, an organizing algorithm was developed to analyze and compare the energy mapping algorithm's results for each individual structure model analyzed. This algorithm organizes the data by first separating Lennard-Jones from Coulombic values for each ensemble model and then reporting, for each energy type, which atom-atom interaction pairs survived across the mappings for all ensemble models employed according to the empirical parsing criteria mentioned earlier. Un-common/un-persistent interactions obtained for certain members of the ensemble but that were not observed throughout all the structures in an ensemble are also identified and compiled as part of the results provided by the organizing algorithm. Lastly, in reporting the results, a statistical analysis was carried out consisting of averages and 95% confidence interval margins of error over the persistent/common atom-atom interactions of the ensemble models utilized for each protein/protein domain system. The organizing algorithm's function is schematically represented in the flow diagram in Figure 2.

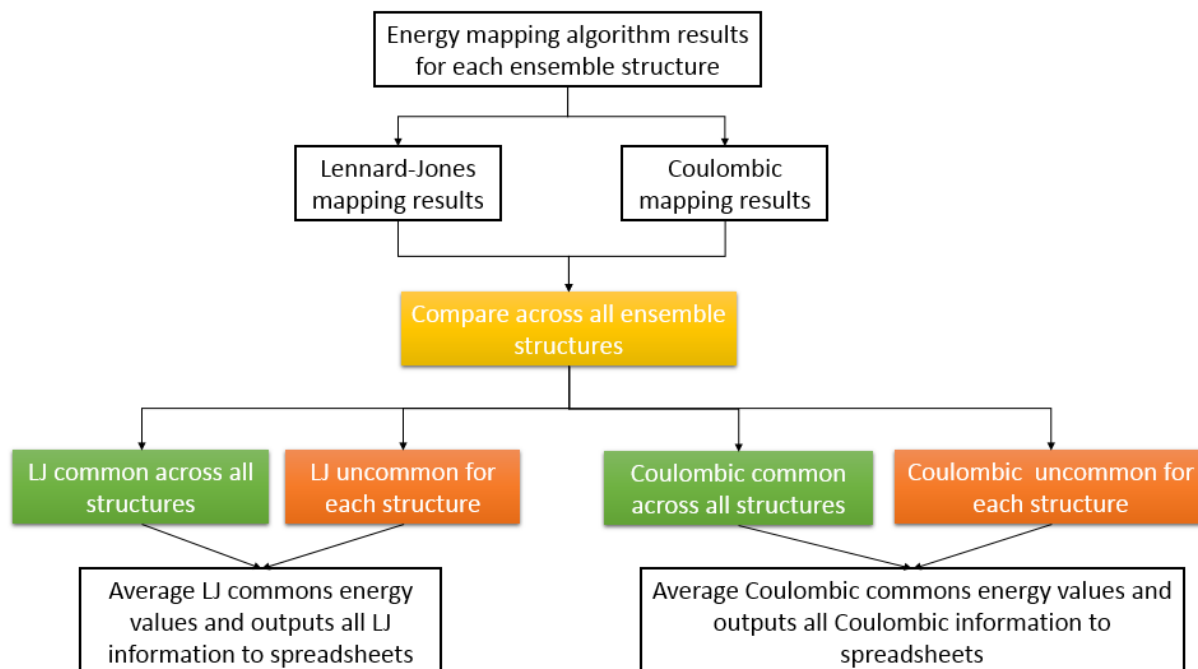


Figure 2: Flow diagram showing the organizing algorithm's function.

The whole protocol, thus, involved mapping multiple ensemble member structures one at a time for a given protein or protein domain followed by feeding these results into the organizing algorithm to obtain those non-covalent atom-atom interactions that persist across all ensemble structure conformations. This process is schematically summarized in Figure 3 below.

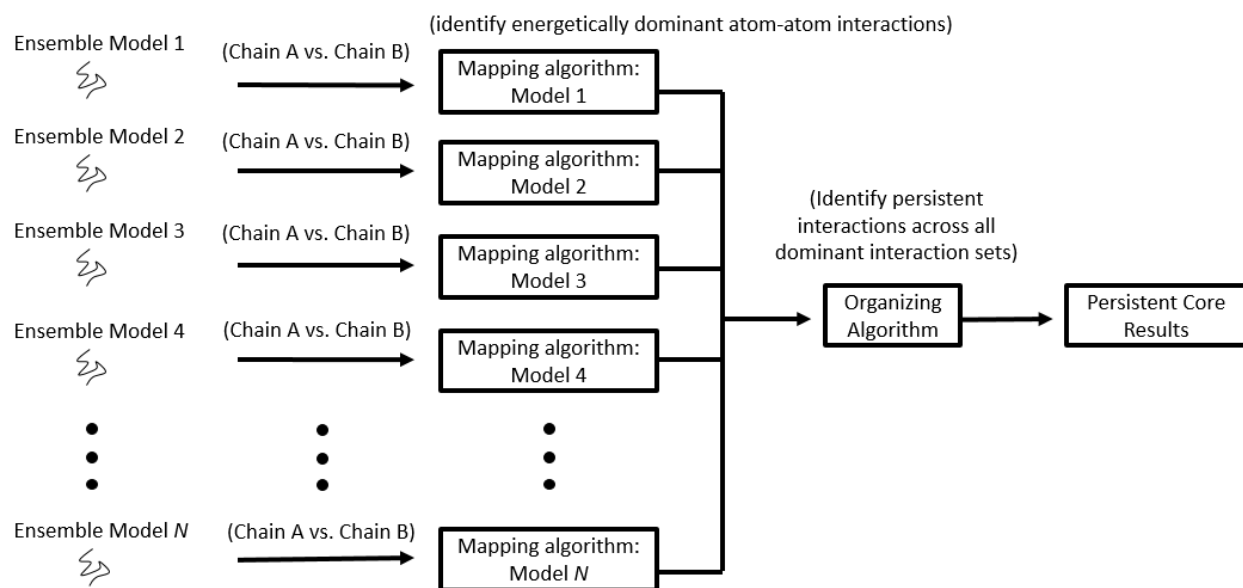


Figure 3: Method process flow diagram.

IIC. Results and Discussion:

Since the aim of this study was to identify energetically dominant atom-atom interaction pairs from structure data expressing structural variation across an ensemble of structures, the first goal of the study was to determine how many ensemble members would be sufficient for a meaningful analysis. It is worth noting that some *.pdb files possessed a minimum of 10 ensemble structures and so it was first necessary to determine if this could provide a statistically meaningful minimum data set. This analysis proceeded by determining the margin of error (MOE) for a 95% confidence interval for a total of 20 ensemble members (from ensembles that had more than 10 models) starting first with a MOE calculation for the energy mapping results of only 2 structures and then increasing the number of structures by increments of 1 for each MOE calculation until reaching the aforementioned 20 structures. For this exercise, MOE values were calculated from the sums/totals of the common/persistent core energy mapping data of the

individual structure models since, for each protein/protein domain system, each structure model yielded slightly different energy totals owing to slight variations in their conformations (separate MOE analyses were dedicated to Coulombic and Lennard-Jones interactions). The different MOE values were then plotted as a function of the quantity of the structure set that produced them to observe their profile and trend. It was determined that the behavior/profile of the MOEs for each protein/protein domain system initially decreased dramatically before stabilizing asymptotically to a given MOE value unique to the data set. The minimum quantity of structures that heralded the profile regions of MOE stabilization to a constant value was found to be around approximately 10 structures which incidentally coincides with the minimum number of ensemble structures observed for some *.pdb structure files. Thus, the analysis for every protein/protein domain system examined below employed 10 ensemble structures starting with the first structure in the *.pdb file. An example of a typical MOE profile is shown below in Figure 4 for the Coulombic and Lennard-Jones interactions for the A-B chains of the tetramerization domain of wild-type human p53 (*pdb accession: 2J0Z). Data for the MOE analysis for all proteins analyzed in this study (10 and 20 ensemble members) are in Appendix C.

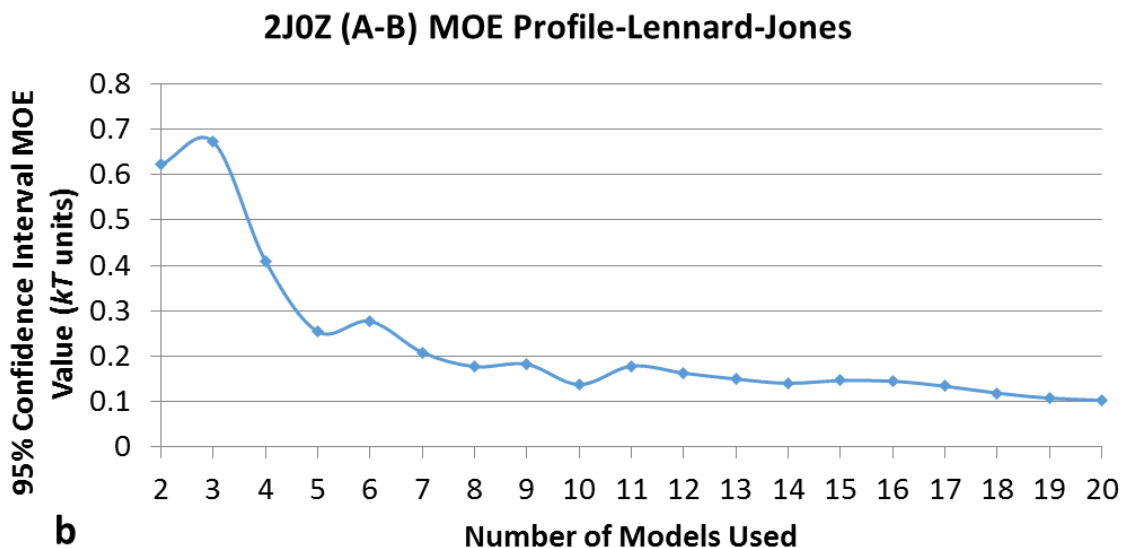
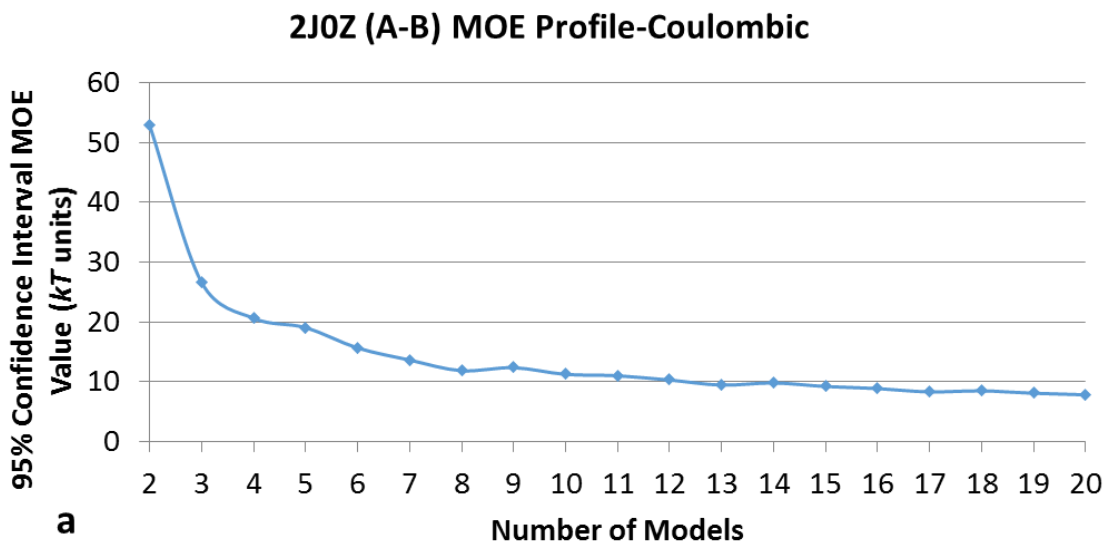


Figure 4. (a, b): 2J0Z A-B chain interaction MOE Coulombic (a) and Lennard-Jones (b) profiles. 95% Confidence MOE interval values (in kT units) plotted as a function of the number of structure models used.

As shown in Table 1, the energetic mapping results indicated that across all 14 proteins and protein domains analyzed, there was a large set of persistent atom-atom interactions common to all ensemble members. In Table 1, for each protein, the quantity of common atom-atom

interactions in the persistent core across all models used as well as the energetic sum values for both Coulombic and Lennard-Jones interactions are reported with their respective MOE values that correspond to using the first 10 structures from their respective ensembles. The energetic total/sum values reported in Table 1 for these common/persistent interactions were obtained by averaging together the individual energetic total values for each individual model, as provided by the organizing algorithm, since each protein/protein domain system employed 10 models and each model yielded slightly different totals for the common results (although the *identity* and *quantity* of those atom-atom interactions were constant throughout all models for the common interaction sets). 95% confidence intervals are also reported for each protein as part of the statistical analysis in tandem with the aforementioned averages. Table 1 also features energetic total/sum data for those atom-atom interactions that did not survive across every single ensemble structure employed in the mapping. These interactions are thus referred to as un-common interactions in Table 1. It is important to note that the nature of these un-common interactions is that they are representative of relatively strong atom-atom interactions that may appear in one or some individual structures in the mapped ensemble, but not across all the mapped ensemble structures. Thus, including these interactions as hot-spots in a study of protein interactions could be potentially misleading.

Table 1: Quantity of persistent atom-atom interactions and averages of their energy totals (kT units) across the 10 structures used per system analyzed. Total average energies are presented as 95% confidence intervals. “LJ” and “Coul” stand for Lennard-Jones and Coulombic respectively. Asterisked entry is a thionylated protein.

PDB ID	Protein	Species	Mutation	95% ^{Coul} , Common	95% ^{LJ} , Common	Number of Coulombic Common	Number of LJ Common	95% ^{Coul} , Un-Common	95% ^{LJ} , Un-Common
2LP3	S100A1 (<i>wild-type</i>)	H. sapiens	-	-264.9 ± 15.2	-8.6 ± 0.2	444	47	-129.2 ± 13.3	-22.7 ± 1.9
2LP2	S100A1* (<i>wild-type</i>)	H. sapiens	-	-386.6 ± 7.8	-31.1 ± 0.2	622	197	-183.8 ± 14.6	-23.8 ± 1.5
2LUX	S100A1 (<i>mutant</i>)	H. sapiens	C85M	-198.1 ± 13.1	-5.1 ± 0.1	320	30	-160.9 ± 18.7	-25.5 ± 2.5
1B4C	S100B	R. norvegicus	-	-173.3 ± 18.0	-0.6 ± 0.0	253	4	-228.9 ± 34.7	-24.8 ± 3.8
2GD7	Hexim-1	H. sapiens	-	-848.7 ± 33.0	-34.8 ± 0.3	1024	217	-971.5 ± 176.6	-86.6 ± 10.1
2KM2	Galectin-1	H. sapiens	-	-169.7 ± 8.1	-6.9 ± 0.2	231	37	-72.5 ± 8.8	-17.8 ± 1.7
2MK9	Toll-like receptor-3	H. sapiens	-	-22.2 ± 4.2	-2.8 ± 0.1	42	18	-34.2 ± 16.3	-7.3 ± 1.7
2LZ3	Amyloid precursor protein (<i>wild-type</i>)	H. sapiens	-	-45.0 ± 0.7	-2.8 ± 0.0	104	19	-24.1 ± 6.9	-5.2 ± 0.8
2LZ4	Amyloid precursor protein (<i>mutant</i>)	H. sapiens	V21M	-50.9 ± 6.3	-3.1 ± 0.1	108	19	-27.3 ± 10.2	-7.8 ± 2.3
2M8L	HIV capsid protein	HIV	-	-103.7 ± 1.2	-10.6 ± 0.0	191	72	-54.0 ± 24.7	-3.3 ± 0.4
2MIT	Defensin-5	H. sapiens	-	-175.5 ± 3.3	-17.6 ± 0.1	290	101	-46.1 ± 4.5	-10.9 ± 0.6
2MLI	Insulin	H. sapiens	-	-234.8 ± 6.0	-33.4 ± 0.1	414	207	-28.2 ± 7.9	-2.9 ± 0.7
2J0Z:	p53 (<i>wild-type</i>) (chains A, B, C & D)	H. sapiens	-						
A-B				-260.4 ± 11.2	-6.6 ± 0.1	353	38	-293.5 ± 20.4	-43.1 ± 2.1
A-C				-2.0 ± 0.2	0	3	0	-18.4 ± 7.3	-1.1 ± 0.3
A-D				-37.4 ± 3.2	0	62	0	-71.7 ± 14.0	-6.0 ± 0.7
B-C				-34.3 ± 5.1	0	52	0	-68.9 ± 6.4	-5.7 ± 0.9
B-D				-0.6 ± 0.1	0	1	0	-25.2 ± 9.2	-1.0 ± 0.4
C-D				-249.7 ± 10.0	-6.5 ± 0.1	337	39	-283.6 ± 24.5	-41.1 ± 2.7
2J11:	p53 (<i>mutant</i>) (chains A, B, C & D)	H. sapiens	Y327S, T329G, Q331G						
A-B				-198.9 ± 5.3	-3.6 ± 0.1	263	20	-290.4 ± 30.6	-40.6 ± 2.8
A-C				0	0	0	0	-22.5 ± 4.9	-1.3 ± 0.3
A-D				-24.6 ± 3.6	0	39	0	-62.8 ± 7.3	-4.5 ± 0.6
B-C				-38.2 ± 3.6	0	53	0	-55.7 ± 9.3	-4.9 ± 0.9
B-D				-2.4 ± 0.7	0	3	0	-27.5 ± 10.3	-1.5 ± 0.4
C-D				-209.5 ± 5.8	-4.1 ± 0.1	284	22	-254.3 ± 35.6	-37.7 ± 2.8

To further illustrate the utility of the method, an analysis of the results was carried out to examine whether these ensemble mappings could provide any functional insight between wild-type and mutant strains for the species selected. The outcome of this inquiry was that correlations were indeed found between the energetic mappings and known functional differences between the wild-type and mutant strains, as summarized in Table 1. For completeness, we further sought to verify whether the mutant residues were observed to participate in the atom-atom interactions persistent across the ensemble structures and so this information is thus catalogued in Table 2 for all mutant species, whether or not the mutations were found in the common/persistent core and un-common atom-atom interaction sets.

Wild-type vs. mutant APP: The first system to have wild-type and mutant structures analyzed was the amyloid precursor protein, or, APP. It is noted that for the transmembrane domain region of the alpha-helical homo-dimer APP, there is a key protease binding site demarcated by the *.pdb file's residue leucine 26/L26 [17] (residue L49, in the wider Alzheimer's literature) that does not yield the precursor to cytotoxic aggregates (*.pdb file residue naming shall be used henceforth). In the presence of mutations such as V21M, which is the mutation analyzed here, the protease binding site shifts to the previous residue, T25 [17]. Protease binding to T25 is thus implicated in the formation of cytotoxic aggregate species following enzymatic proteolysis of APP at this position particularly for this mutant strain. Results of the structure ensemble mapping method indeed showed that the non-pathogenic L26 binding site was identified for the wild-type strain (*.pdb accession: 2LZ3) as this residue was seen to engage in interactions that persisted across its ensemble of structures. The mutant strain (*.pdb accession: 2LZ4), on the other hand, did not show its T25 to engage in any persistent interactions across its ensemble

structures. These mappings further characterized the interactions involving wild-type's L26 residue as van der Waals-type Lennard-Jones interactions. It is worth noting that the mutation (V21M) is located upstream from either wild-type or mutant binding site thus implying that the mutation may contribute indirectly to the downstream destabilization of the intra-protein electrostatic cohesion naturally present in the wild-type. It may therefore be possible that the destabilization of the inter-chain electrostatics in this region in the mutant strain might contribute to the protease's inability to bind at its proper non-pathogenic location on APP (L26) thereby resulting in proteolysis at aberrant locations (such as T25) and resulting in anomalous peptide fragments that aggregate into the fibrillar structures seen in Alzheimer's disease. Figure 5 shows plots of the energy values in kT units for those Lennard-Jones interactions that persisted across the ensemble of 10 structures for both the wild-type and mutant strains of APP. The strongest interactions have the more negative energy interaction values. Figure 6 then shows on molecular representations five of the strongest Lennard-Jones atom-atom interactions for the comparison of wild-type and mutant APP which includes residue L26 for the wild-type strain's dominant binding site. We note that the curve profiles of Figure 5 and others like it are not meant to be compared according to superficial shape but should instead be viewed and considered in light of the local minima kT energy magnitude values and the atom-atom interaction identities that correspond to those local minima

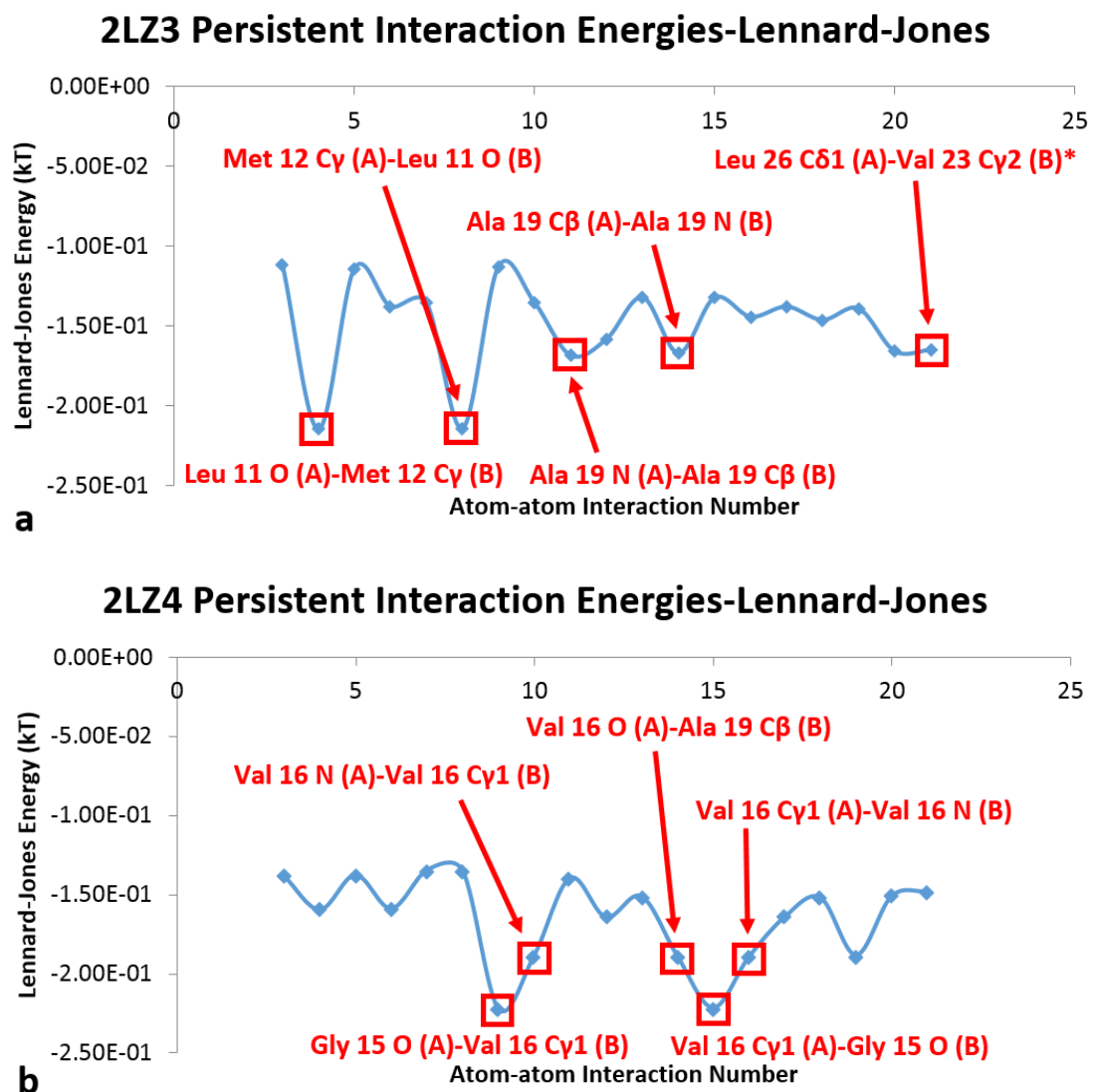


Figure 5: Plots of the Lennard-Jones atom-atom interactions' energies that survived across the energy mapping of 10 ensemble structures for wild-type (a) and mutant (b) APP. Asterisked interaction corresponds to unique surviving interaction in the wild-type that incorporates the APP protease binding site residue discussed in the results. Five of the strongest atom-atom interactions are boxed for each respective set with the interacting atoms identified as follows: [residue name] [*].pdb residue number] [atomic element] (chain A)- [residue name] [*].pdb residue number] [atomic element] (chain B).

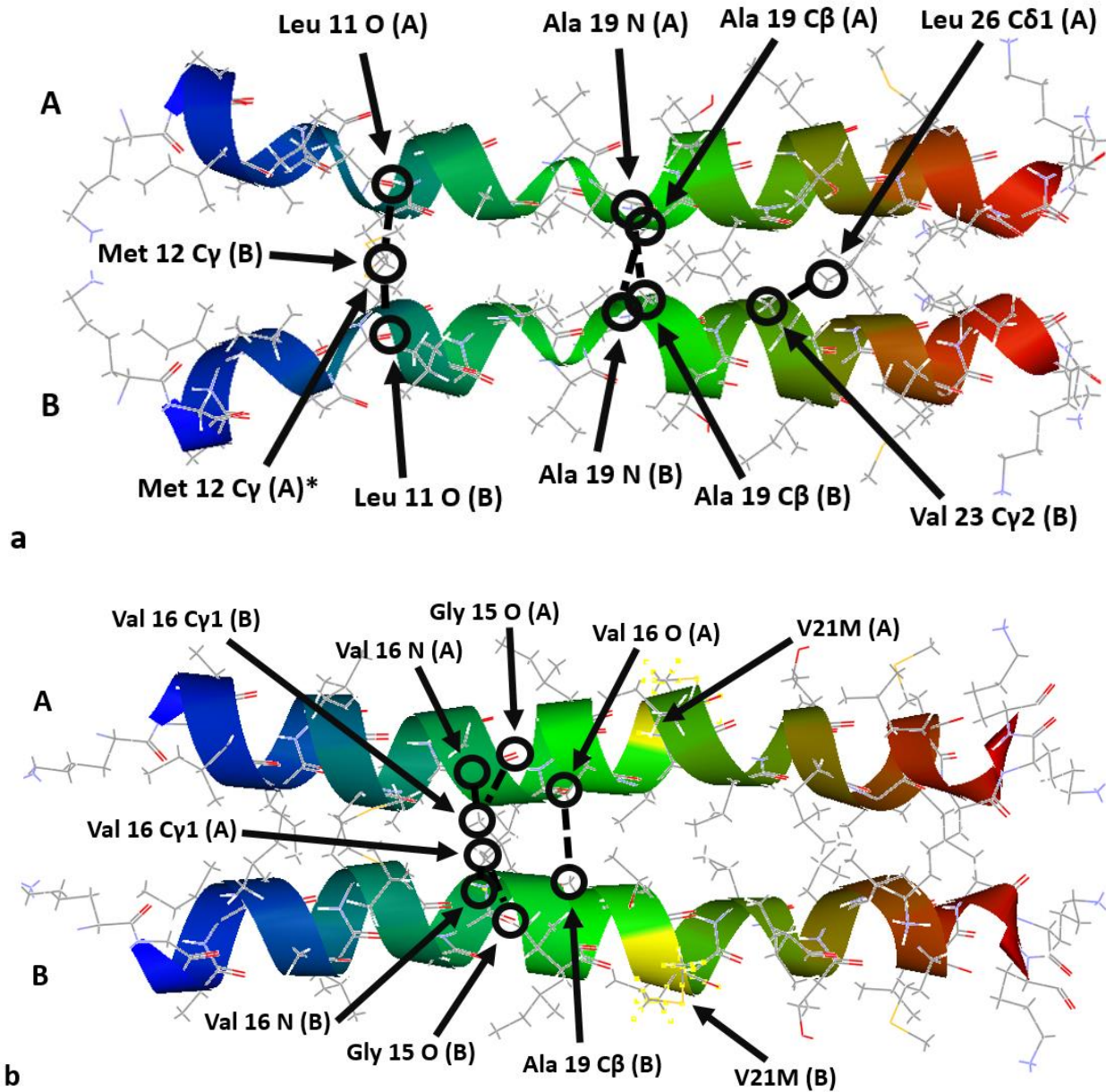


Figure 6 (a, b): Five strongest persistent core Lennard-Jones atom-atom interactions (from Figure 5) between APP chains A and B for wild-type (a) and mutant (b) strains. Individual atom-atom interaction energy values across all 10 structure models were averaged to identify the four strongest for both strains. Asterisked atom corresponds to it being obscured behind another atom. Mutant residue, V21M, is hi-lighted in yellow and labeled in the mutant structure.

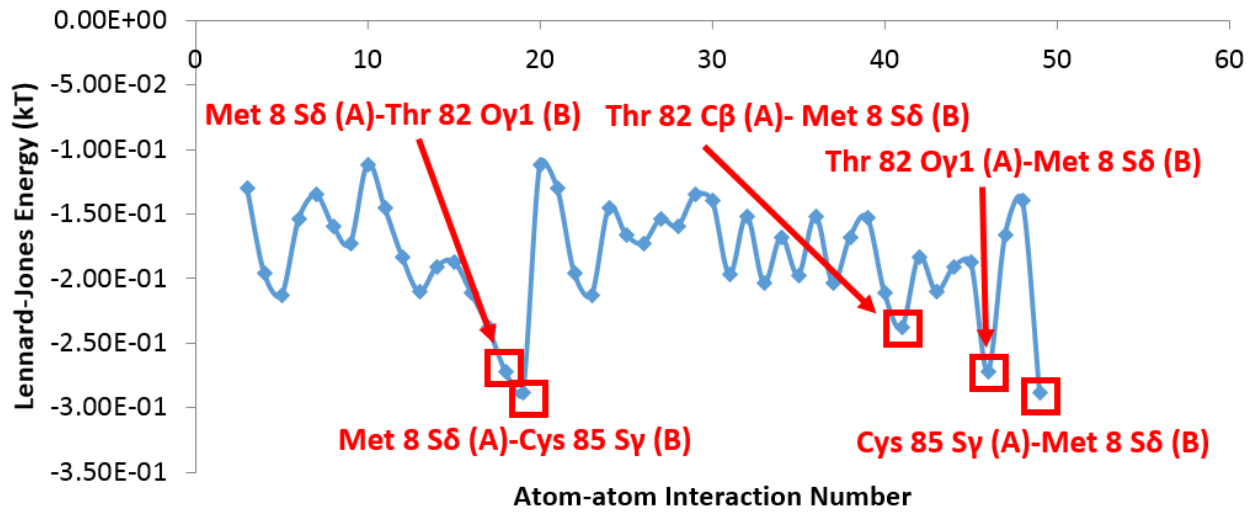
Table 2: Results for mutant residue presence in mutant persistent cores and un-common atom-atom interaction sets. “LJ” and “Coul” stand for Lennard-Jones and Coulombic respectively. Asterisked entries correspond to no persistent cores identified. †: *.pdb accession 2J11 is a four-chain triple mutant.

PDB ID:	Mutation	Mutation(s) in Coul Persistent Core?	Mutation(s) in LJ Persistent Core?	Mutation(s) in Coul Un-Common Interactions?	Mutation(s) in LJ Un-Common Interactions?
2LUX (<i>mutant</i>)	C85M	Yes	No	Yes	Yes
2LZ4 (<i>mutant</i>)	V21M	No	No	Yes	No
2J11 (<i>mutant</i>)†:	Y327S, T329G, Q331G				
A-B		Yes (Y327S, T329G, Q331G)	Yes (Y327S, T329G)	Yes (Y327S, T329G, Q331G)	Yes (Y327S, T329G, Q331G)
A-C		No*	No*	No	No
A-D		No	No*	No	No
B-C		No	No*	No	No
B-D		No	No*	No	No
C-D		Yes (Y327S, T329G, Q331G)	Yes (Y327S, T329G, Q331G)	Yes (Y327S, T329G, Q331G)	Yes (Y327S, T329G, Q331G)

Wild-type vs. mutant S100A1: The next wild-type/mutant system analyzed was the S100A1 protein in the holo state for 3 distinct species: wild-type (*.pdb accession: 2LP3), homocysteine thionylated wild-type (*.pdb accession: 2LP2) and the C85M mutant to 2LP3 (*.pdb accession: 2LUX). Only atom-atom interactions pertinent to the actual protein itself were mapped and analyzed and so holo state metal ions and homocysteine were not considered in this study. Results from the ensemble energy mapping for this system indicated that the homocysteine thionylated species had a greater quantity of intra-protein/inter-chain atom-atom interactions as well as stronger interactions than the other 2 species (Table 1). By contrast, the mutant experienced the fewest quantity of atom-atom interactions as well as the weakest interaction strength of all three species (Table 1). Our findings thus appear to corroborate known experimental characterization information regarding the internal binding affinities of the

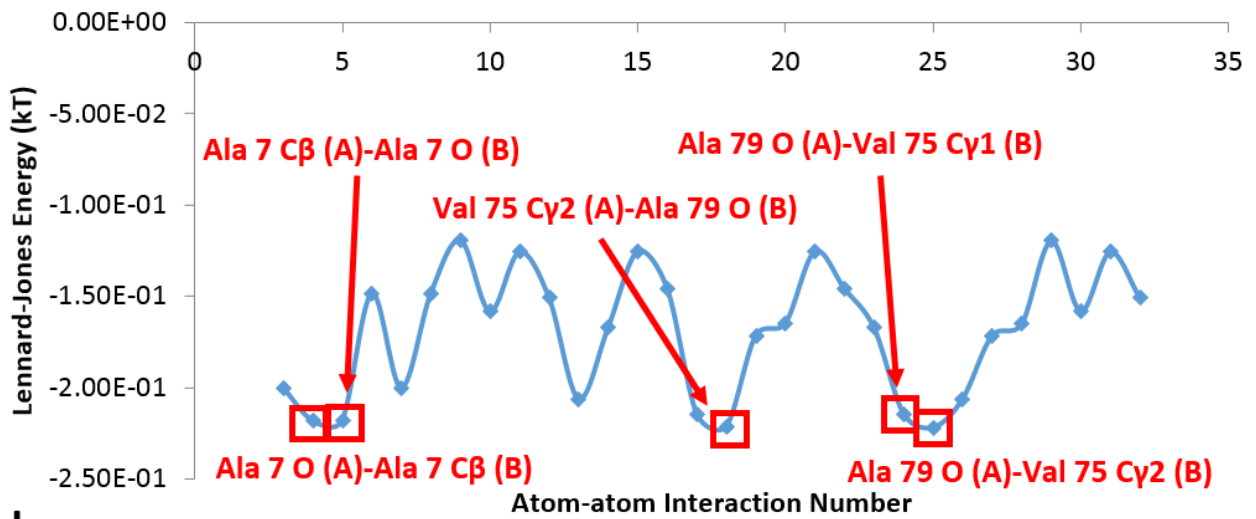
thionylated species. In this regard, Nowakowski et al. [18] postulate that thionylation increases S100A1's affinity for calcium ions by a rearrangement of aromatic residues of its hydrophobic core between the apo and holo states. Indeed, the mapping comparisons of the un-thionylated and thionylated wild-type species (although both in the holo state in the present study) un-veiled a dramatic difference in hydrophobic-associated Lennard-Jones atom-atom interactions with the thionylated species exhibiting a greater magnitude of non-covalent interaction energies by nearly four-fold (Table I). This stronger hydrophobic core thus appears to be associated with the higher Ca^{2+} binding affinities described by Nowakowski et al. [18]. Considering that the mutant strain exhibited the weakest energetic inter-chain interactions (Table 1) along with the fact that the mutant residue was observed in the persistent core (Table 2), it can be concluded that the mutation played a direct role in destabilizing the persistent core energetic landscape. Given the Lennard-Jones type interactions' importance in distinguishing between the three isoforms, Figure 7 shows plots of the energy values in kT units for those Lennard-Jones interactions that persisted across the ensemble of 10 structures for the three species. Figure 8 also presents via molecular representations five of the strongest Lennard-Jones interactions for the three isoforms. For completeness, it is to be noted that the mutation is not known to be associated with any known clinical pathology.

2LP3 Persistent Interaction Energies-Lennard-Jones



a

2LUX Persistent Interaction Energies-Lennard-Jones



b

2LP2 Persistent Interaction Energies-Lennard-Jones

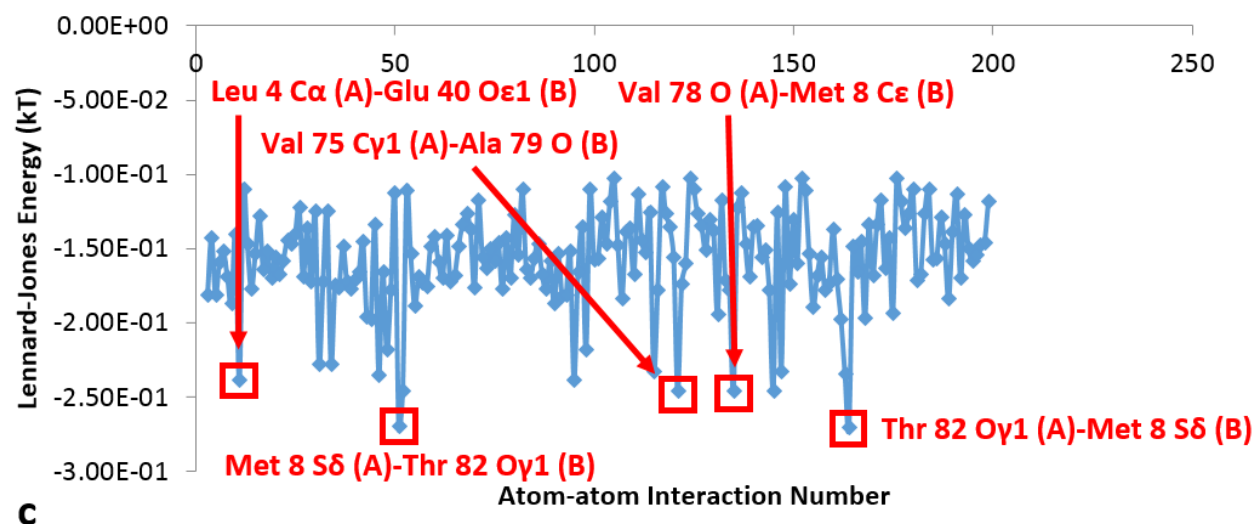
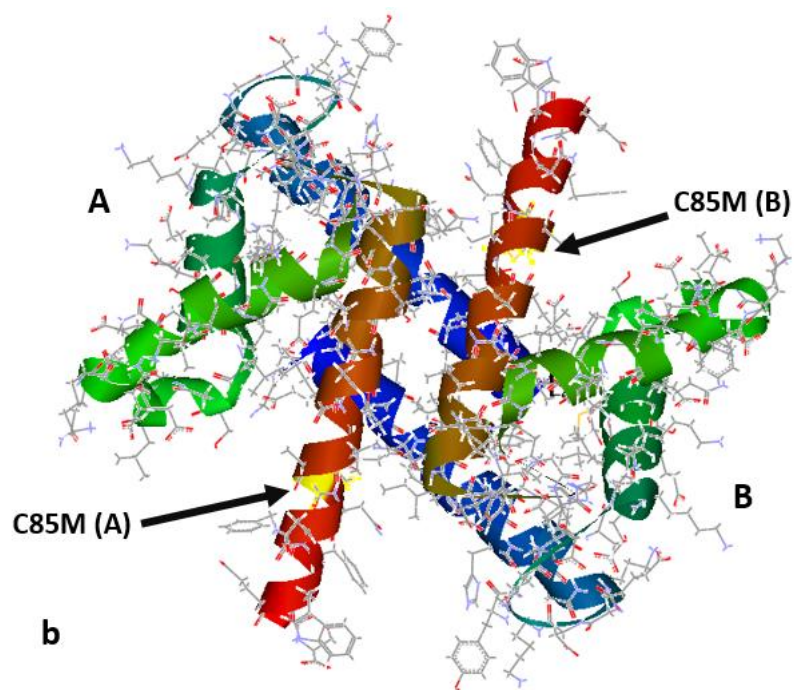
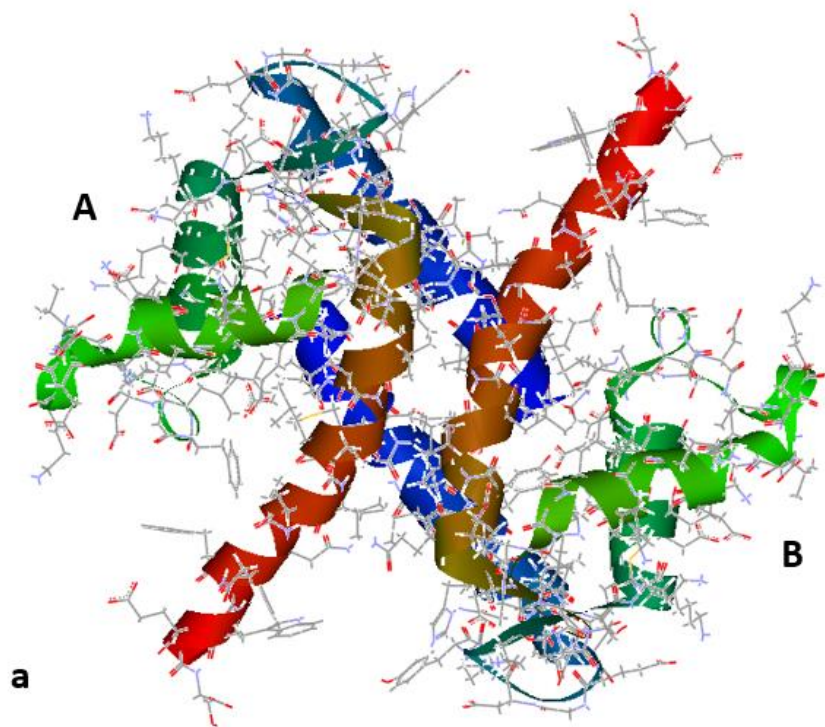
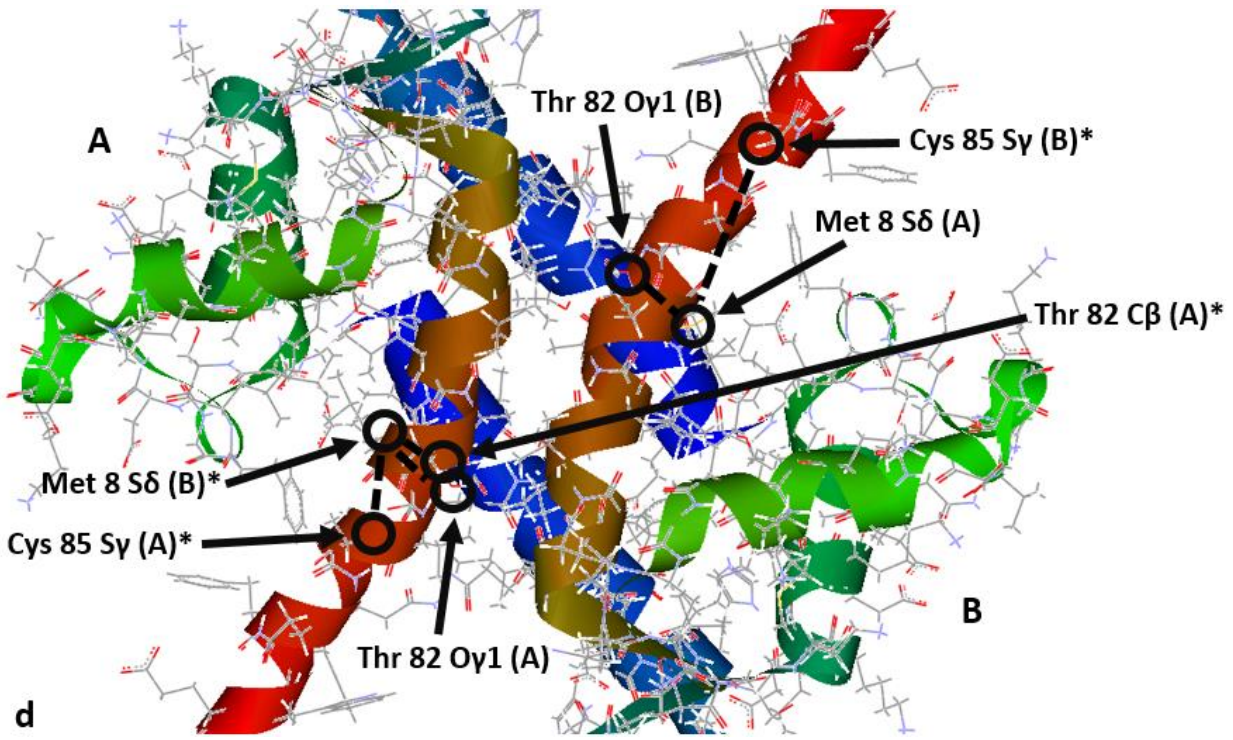
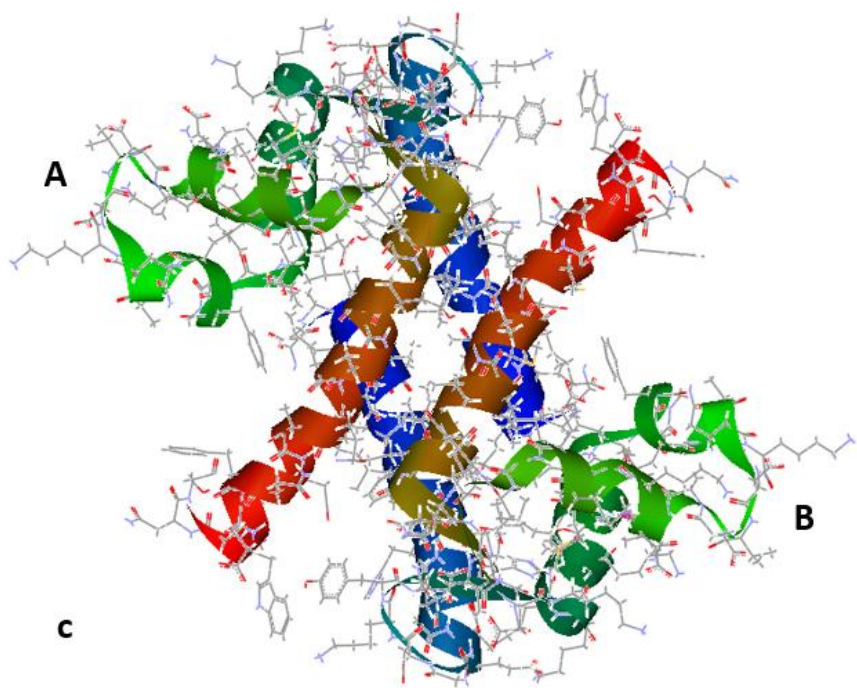
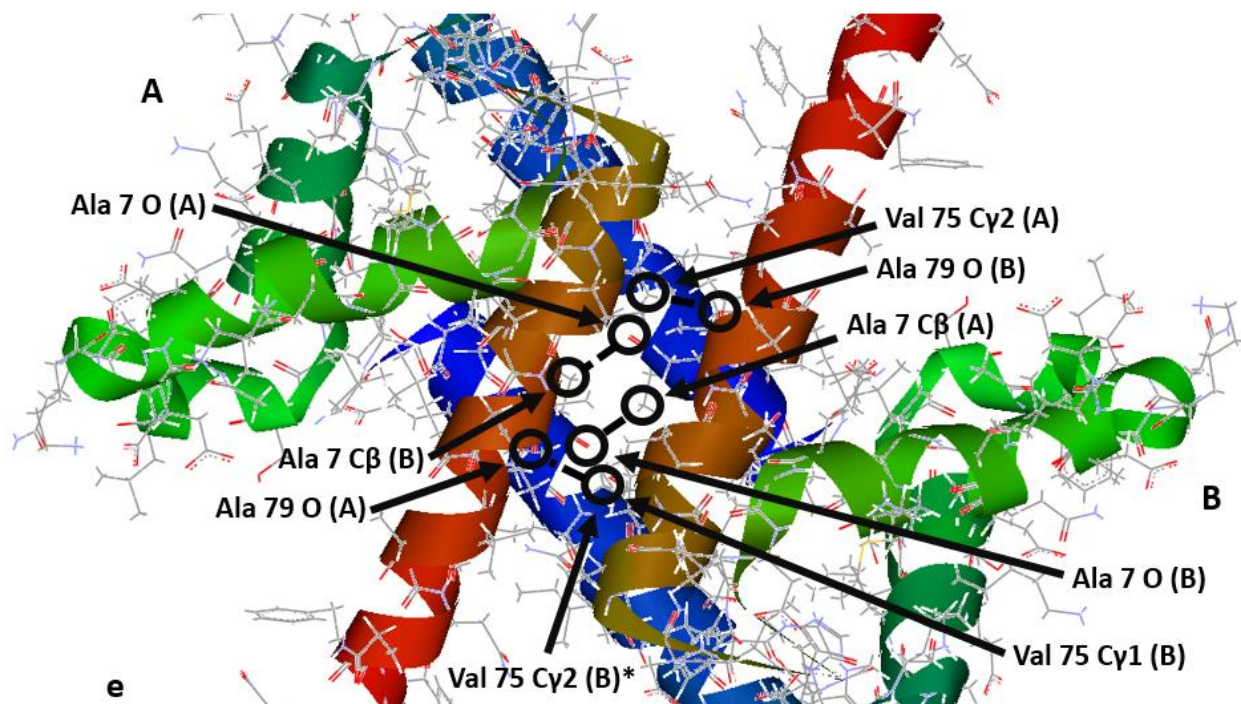


Figure 7. (a-c): Plots of the Lennard-Jones atom-atom interactions' energies that survived across the energy mapping of 10 ensemble structures for wild-type (a), mutant (b) and thionylated wild-type (c) S100A1. Five of the strongest atom-atom interactions are boxed for each respective set with the interacting atoms identified as follows: [residue name] [*].pdb residue number] [atomic element] (chain A)- [residue name] [*].pdb residue number] [atomic element] (chain B).







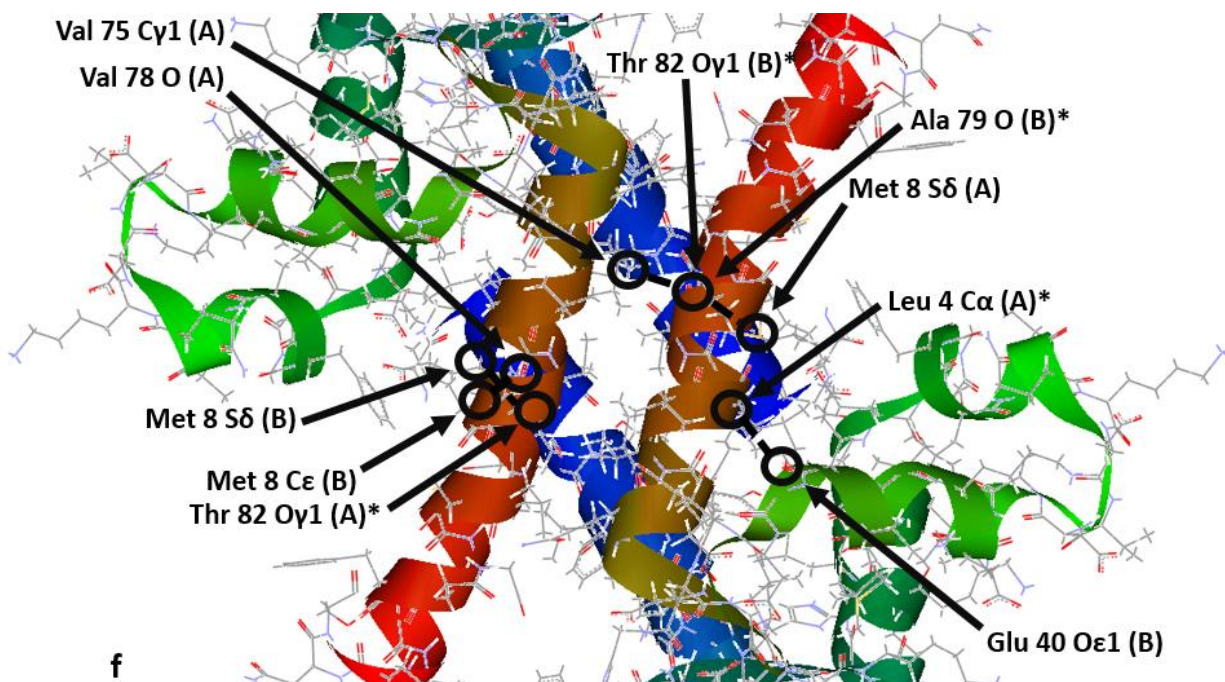
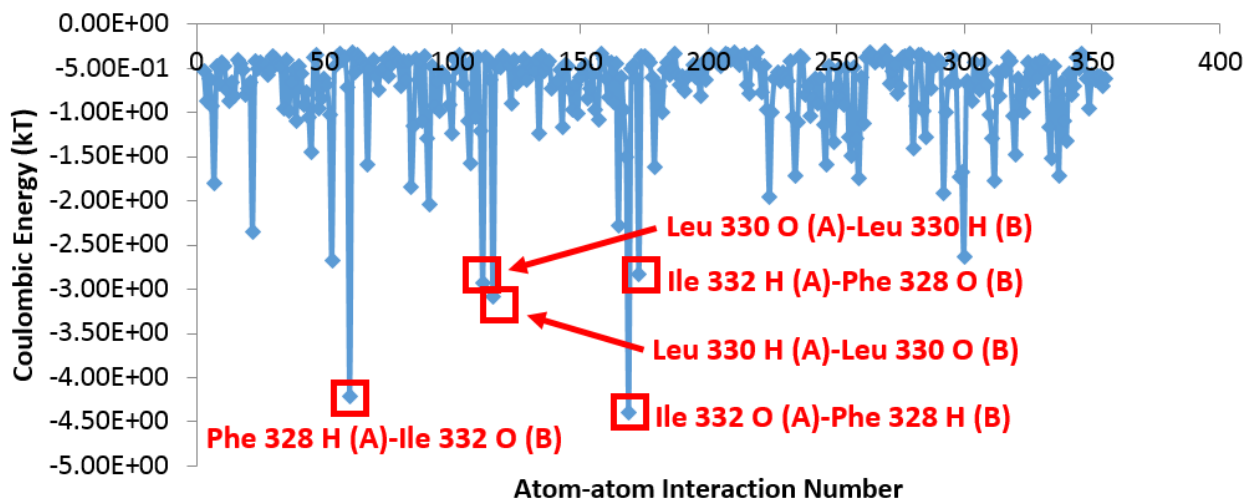


Figure 8 (a-f): Global view of the three S100A1 isoform structures: wild-type/pdb id: 2LP3 (a), mutant/pdb id: 2LUX (b) and thionylated wild-type/pdb id: 2LP2 (c). Mutant residue, C85M, is hi-lighted in yellow and labeled in the mutant structure. Close up of five strongest persistent core Lennard-Jones atom-atom interactions (from Figure 7) between S100A1 chains A and B for wild-type (d), mutant (e) and thionylated wild-type strains (f). Individual atom-atom interaction energy values across all 10 structure models were averaged to identify the five strongest for both strains. Asterisked atom corresponds to it being obscured behind another atom.

Wild-type vs. mutant p53: The final wild-type/mutant system investigated by our ensemble energy mapping method was the tetramerization domain of human p53. The mutant strain had three mutations (Y327S, T329G and Q331G). For both wild-type and mutant isoforms (*.pdb accession: 2J0Z and *.pdb accession: 2J11 respectively), all 4 chains were mapped against one another to ensure that all possible inter-chain interaction configurations were addressed (chain combinations mapped in the study were: A-B, A-C, A-D, B-C, B-D and C-D). Results from the

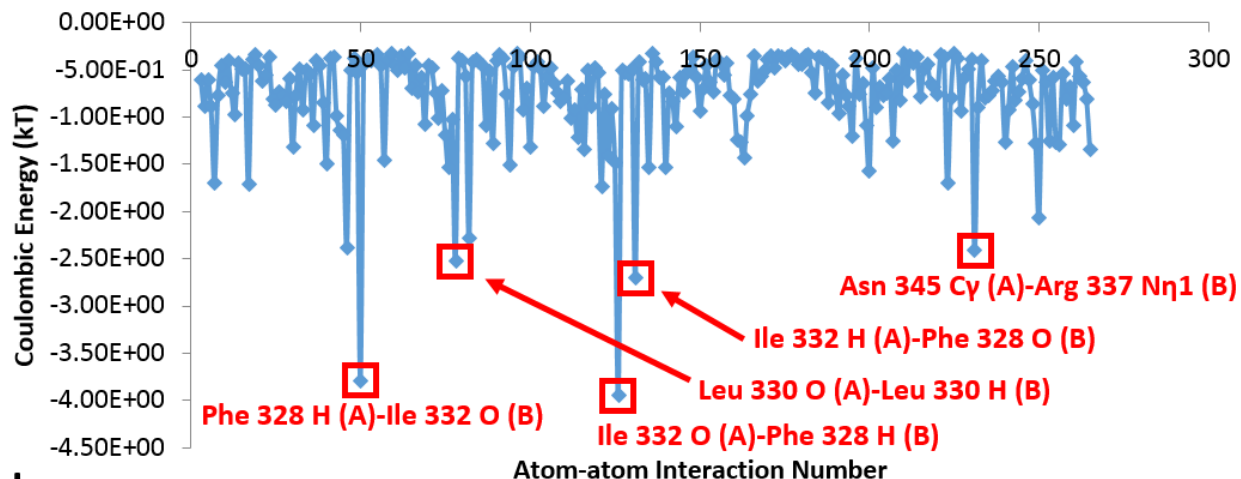
analysis of this system yielded notable interaction differences between the wild-type and mutant strains where the wild-type strain tended to exhibit a greater quantity of both Coulombic and Lennard-Jones inter-chain interactions as well as stronger energetics (Table 1). One inter-chain combination, however (B-D), showed the mutant variant to have a greater quantity of both Coulombic and Lennard-Jones atom-atom interactions as well as stronger attractive interaction energies (Table 1). Yet even these results for B-D corresponded to smaller measures of atom-atom interaction quantities and weaker attractive interaction energies compared to the more dominantly interacting chains (A-B and C-D) as seen in Table 1. Overall, these observations were consistent with the nature of the mutations (Y327S, T329G and Q331G) which were in turn *in vitro* mutations purposefully selected to destabilize the tetramerization domain and were experimentally corroborated to do so by Mora et al. [19]. Atoms from most of the mutant residues were also observed to be present in both the Coulombic and Lennard-Jones persistent cores, but for only two chain interaction combinations, A-B and C-D (Table 2) thus indicating that the mutations played a direct role in destabilizing the interaction energies in the mutant's core. Figure 9 shows plots of the energy values in kT units for those Coulombic interactions that persisted across the ensemble of 10 structures for both the wild-type and mutant strains of APP's A-B inter-chain interactions. Figure 10 also presents via molecular representations five of the strongest Coulombic interactions for the two strains' A-B chains.

2J0Z (A-B) Persistent Interaction Energies-Coulombic



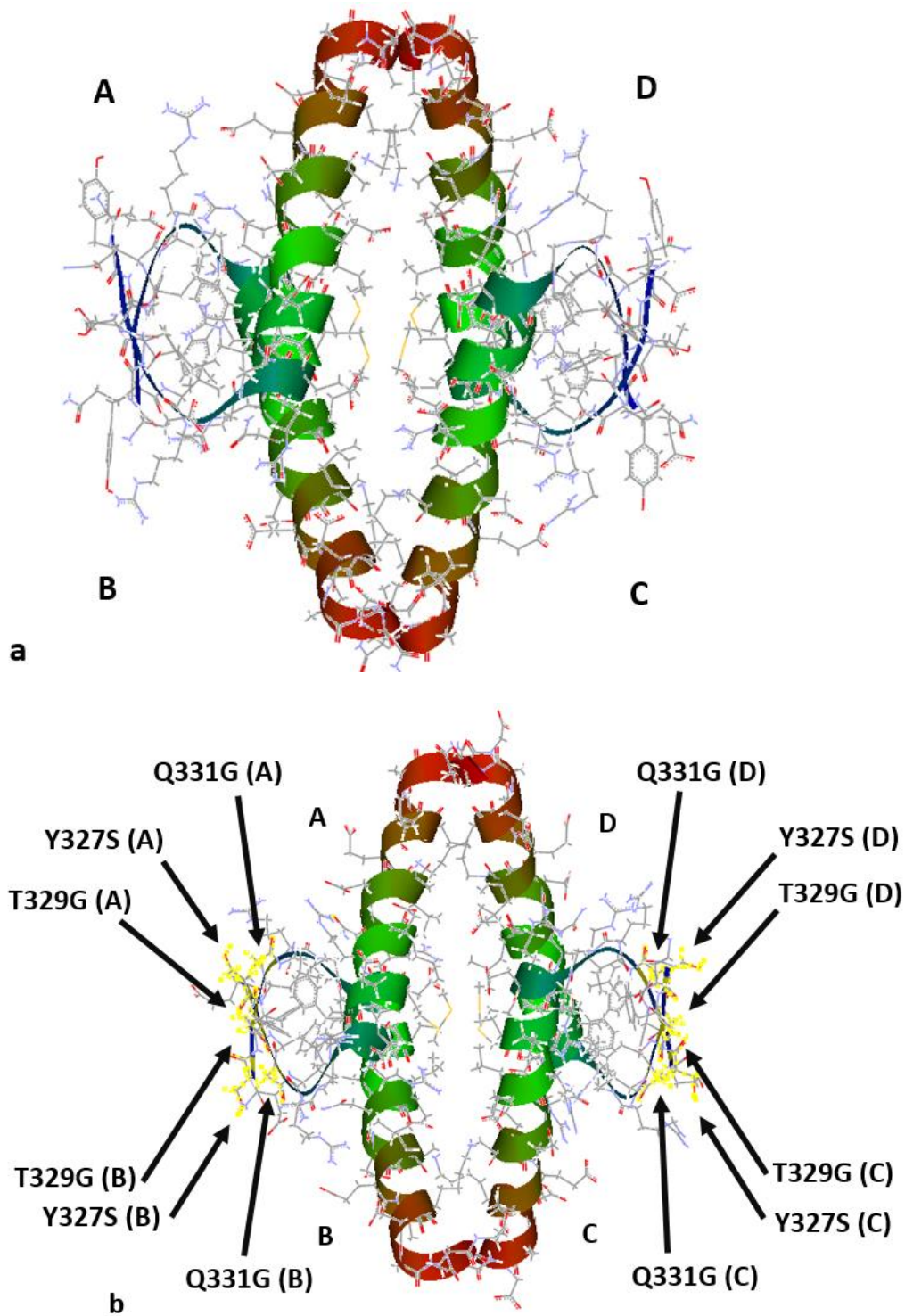
a

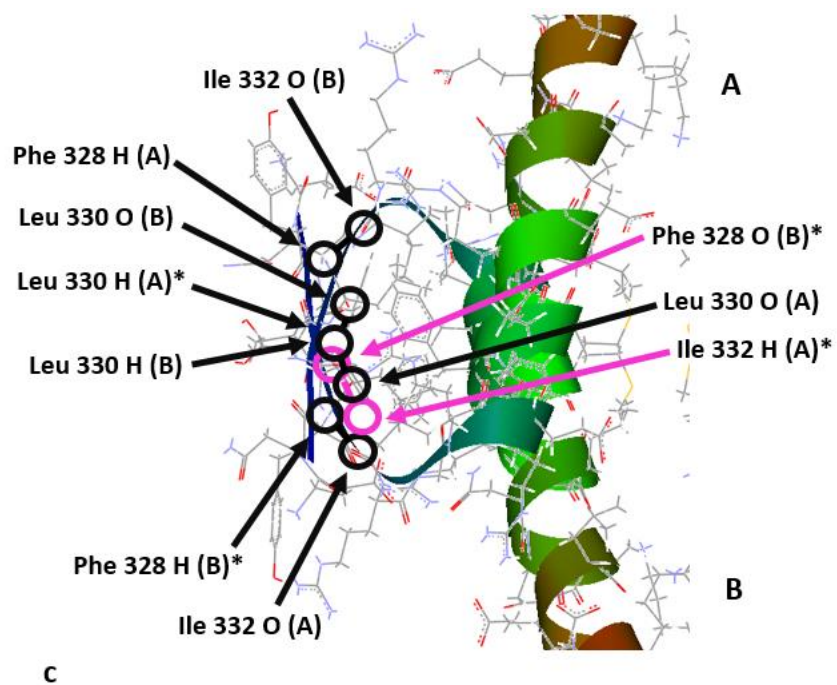
2J11 (A-B) Persistent Interaction Energies-Coulombic

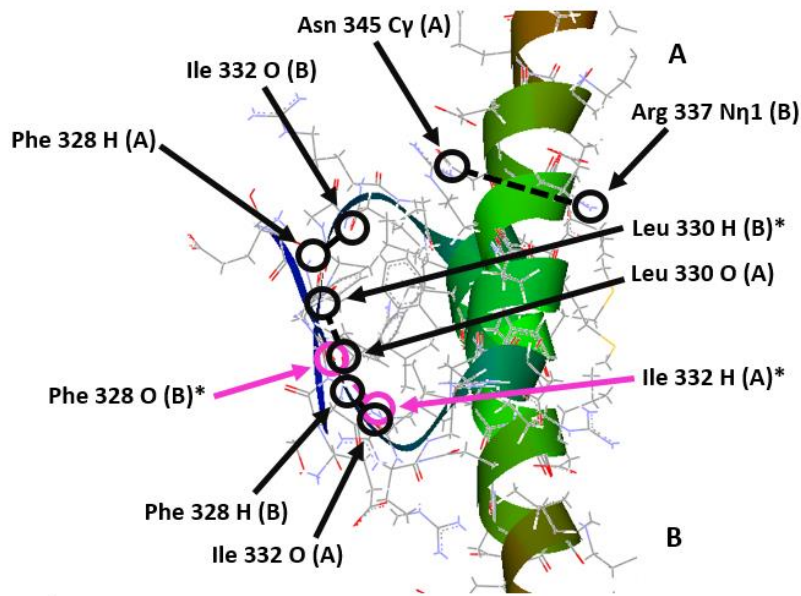


b

Figure 9. (a, b): Plots of the Lennard-Jones atom-atom interactions' energies that survived across the energy mapping of interacting chains A-B for 10 ensemble structures for wild-type (a) and mutant (b) p53. Five of the strongest atom-atom interactions are boxed for each respective set with the interacting atoms identified as follows: [residue name] [*pdb residue number] [atomic element] (chain A)- [residue name] [*pdb residue number] [atomic element] (chain B).







d
Figure 10. (a-d): Global view of wild-type and mutant p53 structures: wild-type/pdb id: 2J0Z (a) and mutant/pdb id: 2J11 (b). Mutant residues (Y327S, T329G and Q331G) are hi-lighted in yellow and labeled in the mutant structure. Close up of five strongest persistent core Coulombic atom-atom interactions (from Figure 9) between p53 chains A and B for wild-type (c) and mutant (d). Individual atom-atom interaction energy values across all 10 structure models were averaged to identify the four strongest for both strains. Asterisked and magenta atoms correspond to their being obscured behind another atom.

III. Conclusions:

In all, this study has established a protocol for carrying out energy mappings on ensemble structure data by using a minimum quantity of those structure ensemble members in the energy mapping approach. The approach yields statistically acceptable results as determined by a margin of error (MOE) analysis in order to identify non-covalent intra-protein/inter-chain atom-atom interactions that survive across the ensemble. The minimum quantity of ensemble members necessary was thus determined to be approximately ten structures across a broad range

of protein functions. Gratifyingly, many reported structure ensembles for proteins typically have a minimum of 10 structures already. It is further demonstrated that the methods here developed were able to identify regions of known functional significance that differ between wild-type and pathogenic mutants as well as post-translationally modified species (thionylated S100A1). For example, in the case of APP, the energy mapping results point to a potential destabilization of a protease binding site caused by a mutation located upstream therefrom in the mutant form. Similarly, for S100A1, the energy mappings showed that a thionylated form of the wild-type protein experienced the strongest interaction energies, particularly, hydrophobic-associated Lennard-Jones interactions, when compared to un-thionylated wild-type and mutant strains. These observations are consistent with experiments that demonstrate the thionylated isoform as experiencing stronger interactions, particularly, in retaining metal ions within the protein compared to un-thionylated and mutant varieties. Our analysis of the tetramerization domain of p53 likewise showed agreement with known experimental results regarding the destabilization effects on this domain incurred by the three mutant residues found in the mutant strain. Our study has thus resulted in the development of a novel technique to study protein inter-chain interactions by carrying out protein energy mappings on an ensemble of structures. This new method thus has the potential to benefit drug design efforts (specifically, peptide bio-mimetic design) in addition to facilitating the characterization of readily available ensemble structure data for protein functional insight.

III. References:

- 1) Davis, A. M., Teague, S. J., & Kleywegt, G. J. (2003). Application and limitations of X-ray crystallographic data in structure-based ligand and drug design. *Angewandte Chemie International Edition*, 42(24), 2718-2736.
- 2) Krall, A., Brunn, J., Kankanala, S., & Peters, M. H. (2014). A simple contact mapping algorithm for identifying potential peptide mimetics in protein–protein interaction partners. *Proteins: Structure, Function, and Bioinformatics*, 82(9), 2253-2262.
- 3) Bastidas, O. H., Green, B., Sprague, M., & Peters, M. H. (2016). Few ramachandran angle changes provide interaction strength increase in Abeta42 versus Abeta40 amyloid fibrils. *Scientific Reports*, 6
- 4) Babine, R. E., & Bender, S. L. (1997). Molecular recognition of protein– ligand complexes: Applications to drug design. *Chemical Reviews*, 97(5), 1359-1472.
- 5) Hardy, L. W., & Malikayil, A. (2003). The impact of structure-guided drug design on clinical agents. *Curr. Drug Discov*, 3, 15-20.
- 6) Jorgensen, W. L. (2004). The many roles of computation in drug discovery. *Science (New York, N.Y.)*, 303(5665), 1813-1818.
- 7) Billeter, M. (1992). Comparison of protein structures determined by NMR in solution and by X-ray diffraction in single crystals. *Quarterly Reviews of Biophysics*, 25(3), 325-377.
- 8) Carlson, H. A., Masukawa, K. M., & McCammon, J. A. (1999). Method for including the dynamic fluctuations of a protein in computer-aided drug design. *J. Phys. Chem. A*, 103(49), 10213-10219.
- 9) Greenwald, J., Le, V., Butler, S. L., Bushman, F. D., & Choe, S. (1999). The mobility of an HIV-1 integrase active site loop is correlated with catalytic activity†. *Biochemistry*, 38(28), 8892-8898.
- 10) Meagher, K. L., & Carlson, H. A. (2004). Incorporating protein flexibility in structure-based drug discovery: Using HIV-1 protease as a test case. *Journal of the American Chemical Society*, 126(41), 13276-13281.
- 11) Carlson, H. A. et al. (2000). Developing a dynamic pharmacophore model for HIV-1 integrase. *Journal of Medicinal Chemistry*, 43(11), 2100-2114.
- 12) Meagher, K. L., Lerner, M. G., & Carlson, H. A. (2006). Refining the multiple protein structure pharmacophore method: Consistency across three independent HIV-1 protease models. *Journal of Medicinal Chemistry*, 49(12), 3478-3484.

- 13) Damm, K. L., & Carlson, H. A. (2007). Exploring experimental sources of multiple protein conformations in structure-based drug design. *Journal of the American Chemical Society*, 129(26), 8225-8235.
- 14) Markley, J. L., Bax, A., Arata, Y., Hilbers, C., Kaptein, R., Sykes, B. D., . . . Wüthrich, K. (1998). Recommendations for the presentation of NMR structures of proteins and nucleic acids. *Journal of Molecular Biology*, 280(5), 933-952.
- 15) Stöbener, K., Klein, P., Reiser, S., Horsch, M., Küfer, K., & Hasse, H. (2014). Multicriteria optimization of molecular force fields by pareto approach. *Fluid Phase Equilibria*, 373, 100-108.
- 16) Peters M. Force descriptions. In: McCombs KP, ed. *Real-Time Biomolecular Simulations*. New York, New York: McGraw Hill; 2007:58-62.
- 17) Chen, W., Gamache, E., Rosenman, D. J., Xie, J., Lopez, M. M., Li, Y., & Wang, C. (2014). Familial Alzheimer's mutations within APPTM increase A β 42 production by enhancing accessibility of ϵ -cleavage site. *Nature Communications*, 5
- 18) Nowakowski, M. et al. (2013). Impact of calcium binding and thionylation of S100A1 protein on its nuclear magnetic resonance-derived structure and backbone dynamics. *Biochemistry*, 52(7), 1149-1159.
- 19) Mora, P., Carbajo, R. J., Pineda-Lucena, A., Sánchez del Pino, Manuel M, & Pérez-Payá, E. (2008). Solvent-exposed residues located in the β -sheet modulate the stability of the tetramerization domain of p53—A structural and combinatorial approach. *Proteins: Structure, Function, and Bioinformatics*, 71(4), 1670-1685.

III. Aim 2: Static Mapping of Amyloid Systems⁴

Abstract:

The pathology of Alzheimer's disease can ultimately be traced to the increased aggregation stability of A β 42 peptides which possess two extra residues (Ile 41 & Ala 42) that the non-pathological strain (A β 40) lacks. We have found A β 42 fibrils to exhibit stronger energies in inter-chain interactions and we have also identified the cause for this increase to be the result of different Ramachandran angle values in certain residues of the A β 42 strain compared to A β 40. These unique angle configurations result in the peptide planes in the fibril structures to be more vertical along the fibril axis for A β 42 which thus reduces the inter-atomic distance between interacting atoms on vicinal peptide chains thereby increasing the electrostatic interaction energies. We lastly postulate that these different Ramachandran angle values could possibly be traced to the unique conformational folding avenues sampled by the A β 42 peptide owing to the presence of its two extra residues.

IIIA. Introduction:

The neurodegeneration that marks the onset of Alzheimer's disease (AD) is believed to be caused by neurotoxic soluble aggregate oligomers of A β 42 peptides that result from the cleavage of the Alzheimer precursor protein¹. In this disorder, A β 42 peptides co-exist with the more benign A β 40 peptide but at a greater A β 42/A β 40 ratio, where the A β 42 is much more pathogenic²⁻⁴. This has recently been demonstrated to be clinically significant as measurements of A β 42/A β 40 ratios in cerebrospinal fluid can function as an important clinical diagnostic marker of AD⁵. A β 42's pathogenicity is consequently owed to its greater neuronal toxicity,

⁴ Published: Bastidas, O. H., et al. "Few Ramachandran Angle Changes Provide Interaction Strength Increase in Abeta42 Versus Abeta40 Amyloid Fibrils." Scientific reports 6 (2016): 1-10.

greater aggregation propensity, and its increased kinetics or rate of aggregate formation compared to A β 40⁶⁻¹⁰. Small, prefibrillar/oligomeric aggregate species of A β 42 are now recognized as the primary neurotoxic species responsible for neuronal death in Alzheimer's disease¹¹⁻¹⁵ although there is also a recognized appreciable toxicity of A β 42 mature fibrils as has been seen in cell culture experiments¹⁶⁻¹⁹. In this regard, mature fibril aggregates are also known to act as a source of these toxic pre-fibrillar oligomers and aggregates in aggregation pathway schemes²⁰⁻²². Neurotoxicity is thought to proceed by A β 42 targeting the synapse of neurons²³ with the likely mechanism of cell death being apoptosis²⁴.

Despite the obvious clinical importance of both oligomers and fibrils, their structural details at the atomic level have been unfortunately difficult to characterize^{12, 25-28}. It is known, however, that in these aggregate species, the constituent peptide chains, or monomers, of both A β 40 and A β 42 are held together by hydrogen bonds that stabilize the aggregate formation²⁹⁻³¹. In spite of the enigmatic nature of A β 40 and A β 42 oligomeric structure, there is a recognized considerable difference in morphology between A β 40 and A β 42 aggregates as evidenced by aggregation seeds of one strain failing to initiate fibril formation in the other³²⁻³⁴. These differences in morphology have been observed in experimentally determined structures of A β 40 and A β 42 mature fibrils, which demonstrate distinct differences in both their conformations and size, or number of constituent monomer A β chains. The addition of only two residues, as seen in the A β 42 strain, significantly alters the folded state conformations of the monomer chains in the mature fibril structure. Such distinctions have even been proposed as clinically significant in their exploitation as potential novel biomarkers for diagnosing late phase Alzheimer's disease specifically exploiting the more β -sheet rich A β 42 isoform³⁵. A comparison of the structural and

energetic properties of mature A β 40 and A β 42 fibrils may therefore provide insight into key differences between the two isoforms and thus help to establish the structural and energetic constraints on their fibril formation pathways. Such a comparative analysis may in turn help to characterize the long-term stability and associated neuronal toxicity of A β 42. Additionally, identifying the underlying key features of the differences of the two strains may provide insight into new therapeutic approaches to inhibit A β 42 aggregation formation. We therefore attempt to identify and characterize the underlying behavior of inter-peptide chain non-covalent interactions by carrying out detailed atomic level energy mappings for both A β 40 and A β 42 mature fibril structures. In doing so, we aim to answer the following two questions: 1) What are the key differences in the inter-chain interaction energetic profiles of A β 40 fibrils and A β 42 fibrils? and 2) What are the underlying conformational changes that are responsible for these differences?

IIIB. Results and Discussion:

For our study, we initially analyzed and compared the fibril structures of A β 40 (PDB ID: 2M4J by Lu et al.³⁶) and A β 42 (PDB ID: 2MXU by Xiao et al.³²) according to the Coulombic (charge and partial atomic charge) and Lennard-Jones (Born and van der Waals forces) atom-atom interaction forces as laid out in the open-source energy mapping algorithm developed by Krall, Brunn, Kankanala and Peters³⁷. This mapping algorithm efficiently parses the strongest non-covalent atom-atom interactions and their inter-atomic distances from structure file data according to empirically established criteria based on the AMBER 03 force field model to ensure that all dominant interactions are accounted for³⁷⁻³⁹. Those parsing criteria were taken as the upper limit of $-0.1 kT$ units for Lennard-Jones criteria and $-0.3 kT$ units for Coulombic interactions³⁷. The A β 40 PDB structure file was composed of three A β 40 peptide stacks, each

stack containing three A β 40 peptide chains, arranged in a triangular three-fold symmetry³⁶ whereas the A β 42 structure was comprised of only one stack possessing twelve A β 42 peptide chains³². These two published structures were selected for our analysis due to the fact that they are believed to represent the *in vivo* forms of mature fibrils^{32, 36}; very recently, two additional structures of mature A β 42 fibrils have also appeared (PDB ID: 2NAO by Walti et al.⁴⁰ and PDB ID: 5KK3 by Colvin et al.⁴¹), which are analyzed and compared following the present analysis of 2MXU. Given the ensemble nature of the structure data for both isoforms, the mapping results for each ensemble member were averaged to obtain the data reported here in the form of 95% confidence intervals for each isoform. The method of Aim 1 was employed to obtain this data. For the A β 40 structure, we found the results of our energy mappings for each stack to be virtually identical, deviating by only a few percent. Thus, we present the data of the A-D-G stack as representative for what we observed for the entire A β 40 isoform. Our energy mappings thus involved the investigation of any two inter-chain interaction configurations within one A β peptide chain stack: 1) mapping the atom-atom interactions between consecutive/vicinal chains (1:2 interactions) and 2) mapping the atom-atom interactions between non-vicinal chains (1:3 interactions, 1:4, etc...). We also note that, within each isoform, the mapping results between any 1:2, 1:3, etc... chain interactions in the fibril structures were virtually identical to the results of other 1:2, 1:3, etc... interaction systems in the respective fibril structure; so, we report the results for the mapping of the first two chains of each isoform as representative data for their respective strains (mapping chains A-D and A-G for 1:2 and 1:3 interactions respectively for A β 40 and mapping chains A-B and A-C for 1:2 and 1:3 interactions respectively for A β 42). The results of the energy mappings found that the A β 42 isoform has appreciably stronger inter-chain atom-atom interaction binding energies and smaller inter-atomic distances than A β 40 for both

1:2 and 1:3 interactions thus implying its superior aggregate stability. Interestingly, we observed that for the 1:2 interactions, despite A β 42 having stronger inter-chain atom-atom interactions, the quantity of those interactions for that isoform were fewer in number than the quantity of atom-atom interactions observed in the A β 40 isoform. These results are summarized in Table 1 for A β 40 compared against A β 42.

Table 1: Comparison of the quantity of the number of dominant atom-atom interaction pairs, average energy (per interaction pair) and average inter-atomic distance (per interaction pair) of 1:2 atom-atom interactions between two chains for A β 40 (A-D chain mapping results) and A β 42 (A-B chain mapping results) with 95% confidence intervals for analysis across all ensemble members. Energy units are in kT and distance units are in nanometers.

	A β 40 (A-D)	A β 42 (A-B)
Coulombic Interactions:	811	779
Coulombic Average E (kT):	-0.729 \pm 0.006	-0.819 \pm 0.008
Coulombic Average D (nm):	0.575 \pm 0.001	0.568 \pm 0.001
Lennard-Jones Interactions:	135	118
Lennard-Jones Average E (kT):	-0.177 \pm 0.001	-0.188 \pm 0.002
Lennard-Jones Average D (nm)	0.397 \pm 0.001	0.393 \pm 0.001

As can be seen, the magnitude of both Coulombic and Lennard-Jones interactions are statistically distinct between the two isoforms according to a 95% confidence interval analysis (i.e. the intervals do not overlap) thus showing that the two strains are energetically different from each other in their inter-chain interaction profiles. Coulombic type interactions were further found to dominate as the primary force for either fibril which stabilizes both strains' infrastructure (Coulombic force interactions being up to 3 to 4 times greater in magnitude than Lennard-Jones

interactions). As is widely recognized in the literature, hydrogen bonds were observed to be the greatest constituent contributor to the Coulombic interactions^{29, 30} holding the 1:2 chain configuration together for both A β 40 and A β 42 and they were observed to be primarily from backbone carbonyl oxygens and amino hydrogens from the same residues in both strains as discussed in more detail below.

Looking at the longer-range 1:3 interactions, we found that the A β 42 isoform likewise exhibited stronger overall interactions and smaller atom-atom separation distances than A β 40. Unlike the 1:2 interactions, however, all of these 1:3 interactions were exclusively composed of Coulombic atom-atom interactions. No Lennard-Jones interactions were observed for the 1:3 configuration in either fibril. This data is summarized in Table 2.

Table 2: Comparison of the quantity of the number of dominant atom-atom interaction pairs, average energy (per interaction pair) and average inter-atomic distance (per interaction pair) of 1:3 atom-atom interactions between two chains for A β 40 (A-G chain mapping results) and A β 42 (A-C chain mapping results) with 95% confidence intervals for analysis across all ensemble members. Energy units are in kT and distance units are in nanometers.

	A β 40 (A-D)	A β 42 (A-B)
Coulombic Interactions:	19	36
Coulombic Average E (kT):	-0.352 ± 0.004	-0.398 ± 0.003
Coulombic Average D (nm):	0.892 ± 0.006	0.877 ± 0.004
Lennard-Jones Interactions:	0	0
Lennard-Jones Average E (kT):	0	0
Lennard-Jones Average D (nm)	0	0

Like the 1:2 interactions, the observed average energies were statistically different for each isoform. Unlike the 1:2 interactions, however, the stronger bound A β 42 has a superior number of strong atom-atom interactions in addition to a superior average energy per interaction pair for those interactions. An additional noteworthy distinction is that the 1:3 non-vicinal interactions for both strains are not stabilized by hydrogen bonds, but rather carbonyl carbon atoms interacting with carbonyl oxygen atoms serve as the main long-range inter-chain-stabilizing interacting atoms. This is in contrast to the hydrogen bond-rich scenario that marks the 1:2 interactions. No dominant interactions beyond 1:3 interactions (1:4 and up) were observed for either strain. A complete listing of the 1:2 configuration atom-atom pair interaction data is provided as Supplementary Tables 1a and 1b (A β 40 Coulombic and Lennard-Jones interactions respectively) and Supplementary Tables 2a and 2b (A β 42 Coulombic and Lennard-Jones interactions respectively). 1:3 interaction data are in Supplementary Tables 3 and 4. All supplementary information is found in Appendix D.

Due to the fact that the dominant atom-atom interactions involved nearly identical residues in both A β 40 and A β 42 and that the overall average atom-atom distances were smaller in A β 42 (Tables 1 and 2), we postulated that the differences observed for the stronger A β 42 were due to a reduced distance between a smaller set of key interacting atoms in that isoform. Statistical data in the form of 95% confidence intervals for the average distance of the mapping results for both isoforms indeed revealed that the distances were statistically distinct between the two strains for both 1:2 and 1:3 interactions (see Tables 1 and 2). This motivated us to identify those atom-atom interactions, and their corresponding residues, that were primarily responsible for the changes in interacting energies that marked A β 42's superior aggregation interaction

stabilities. We note that the strongest 1:2 interaction inter-atomic hydrogen bonds of A β 40 had energy potential values within -4 to -5 kT whereas A β 42's hydrogen bond energy values exhibited a range between -6 to -10 kT for these vicinal chain energy mappings (mapping results for each isoform in Supplementary Tables 1a-1b and Supplementary Tables 2a-2b). From these results of the mapping analysis, we identified 12 atom-atom interaction pairs spanning residues between Lys 16 to Ala 42 that imparted the aforementioned exceptionally strong hydrogen bonds observed throughout the 1:2 chain configuration for A β 42. These residues were identified as those engaging in the exceptionally strong atom-atom interaction pairs that were found in the -6 to -10 kT range for A β 42 which marked that isoform's unique interaction energy profile. Seven of those 12 interactions involved the same atom-atom pairs in the A β 40 strain, but their magnitudes in A β 40 were noticeably weaker. These residues' interactions, their average Coulombic energies and average inter-atomic distances are shown below in Figures 1a and 1b.



Figures 1a & 1b: Atom-atom interactions imparting exceptionally strong hydrogen bonding energies in the 1:2 configuration of Aβ42 compared to Aβ40 (Figure 1a) and their respective atom-atom interaction distances (Figure 1b). 95% confidence interval error bars included for analysis across all ensemble members. The first three and last interactions were not observed in Aβ40. Interaction partners are presented as the residue, residue number in the sequence and the residue's atom of one chain (chain A for both strains) interacting with its partner atom in the 1:2 configuration (on the D-chain in Aβ40 or on the B-chain in Aβ42).

Those interaction energies which were observed in both isoforms were seen to be statistically distinct and considerably weaker in the Aβ40 strain (Figure 1a) owing to larger inter-atomic distances (Figure 1b). Interestingly, Aβ42 inter-atomic distances for these exceptionally strong

interactions were appreciably uniform unlike those of A β 40 which showed greater variability. Lastly, we note that for 1:3 interactions, although inter-atomic distances were statistically smaller in A β 42, atom-atom interaction energy values resided within the same range for both strains (A β 40 minimum and maximum of $-0.3 kT$ and $-0.4 kT$ respectively vs. A β 42 minimum and maximum of $-0.3 kT$ and $-0.5 kT$ respectively) indicating that A β 42's superior 1:3 interaction strength is owed to a greater number of uniform interactions instead of any single interactions of exceptional energy as was seen in the 1:2 configuration (1:3 interaction mapping results for A β 40 are in Supplementary Table 3 and 1:3 interaction mapping data for A β 42 are in Supplementary Table 4).

In light of these findings, we next sought to identify the detailed atomic configurational reasons for the reduced inter-atomic distances of the homologous residues and associated atom-atom interactions seen in the 1:2 configuration's exceptionally strong interactions; it was natural, therefore, to investigate the Ramachandran angle (φ and ψ) differences. The seven exceptionally strong atom-atom interaction pairs that were in both A β 40 and A β 42 were found to have φ and ψ angles that oriented the peptide planes more vertically in the A β 42 isoform which consequently placed the backbone carbonyl oxygen and amino hydrogen atoms closer to each other. Overall, two particular observations are of note for the observed Ramachandran angles: 1) the A β 42 strain shows more well-defined secondary structure primarily favoring β -sheet or left-handed α -helix regions on the Ramachandran plot and 2) the spread of φ and ψ angle values tends to be significantly reduced in A β 42. A summary of these more well-defined secondary structure motifs acquired in A β 42's seven exceptionally strong interactions are shown below in Table 3.

Table 3: Secondary structure motifs that are more well-defined in A β 42 compared to A β 40.

Atom-atom Interaction Pairs		Secondary Structure Acquired in A β 42 Interaction Pairs	
A Chain	Partner Chain: D (A β 40) or B (A β 42)	A Chain Residue (A β 42)	B Chain Residue (A β 42)
Ser 26 O	Asn 27 H	β -sheet increase	β -sheet increase
Asp 23 O	Val 24 H	Left-hand α -helix increase	β -sheet increase
Gly 29 O	Ala 30 H	Left-hand α -helix increase	No change
Lys 28 O	Gly 29 H	No change	Left-hand α -helix increase
Ile 31 O	Ile 32 H	β -sheet decrease	β -sheet increase
Val 39 O	Val 40 H	No change	β -sheet increase
Val 39 H	Gly 38 O	No change	β -sheet increase

Additionally, the φ and ψ values proved to be statistically unique between the two isoforms thus illustrating distinctiveness between the two structures (complete φ and ψ angle data is in Supplementary Table 5). Ramachandran angle changes for three representative interactions are depicted in the figures for the following discussion on these results. The remaining interaction illustrations and Ramachandran angle data are found in Supplementary Figs. 1a & 1b through Supplementary Figs. 8a-8d.

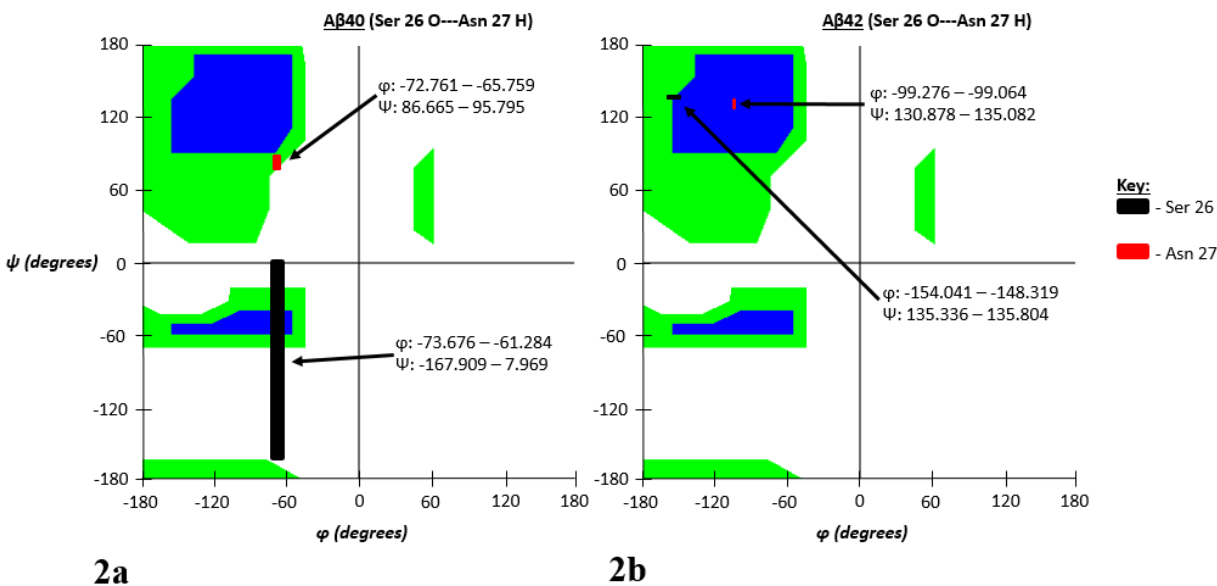
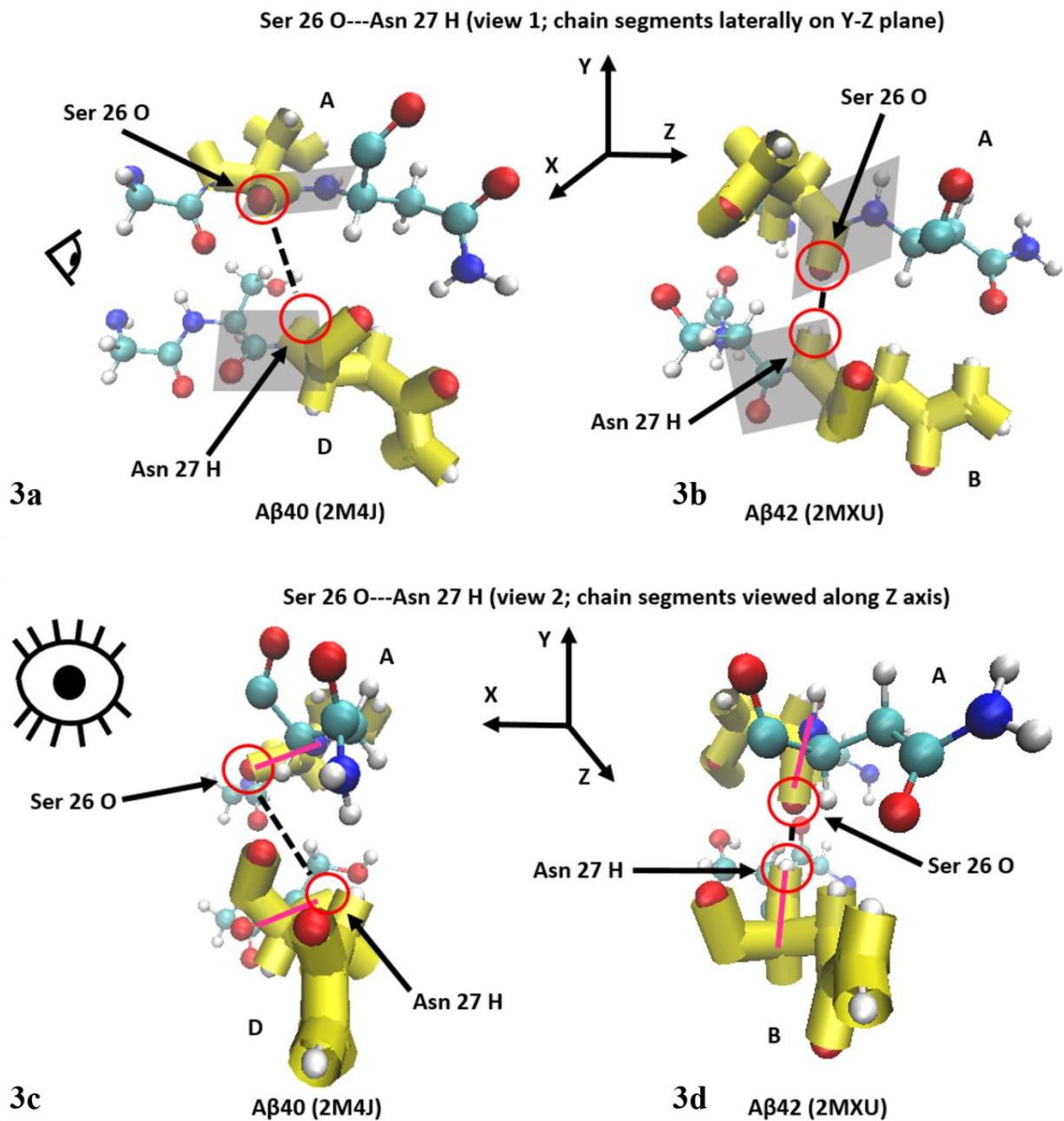


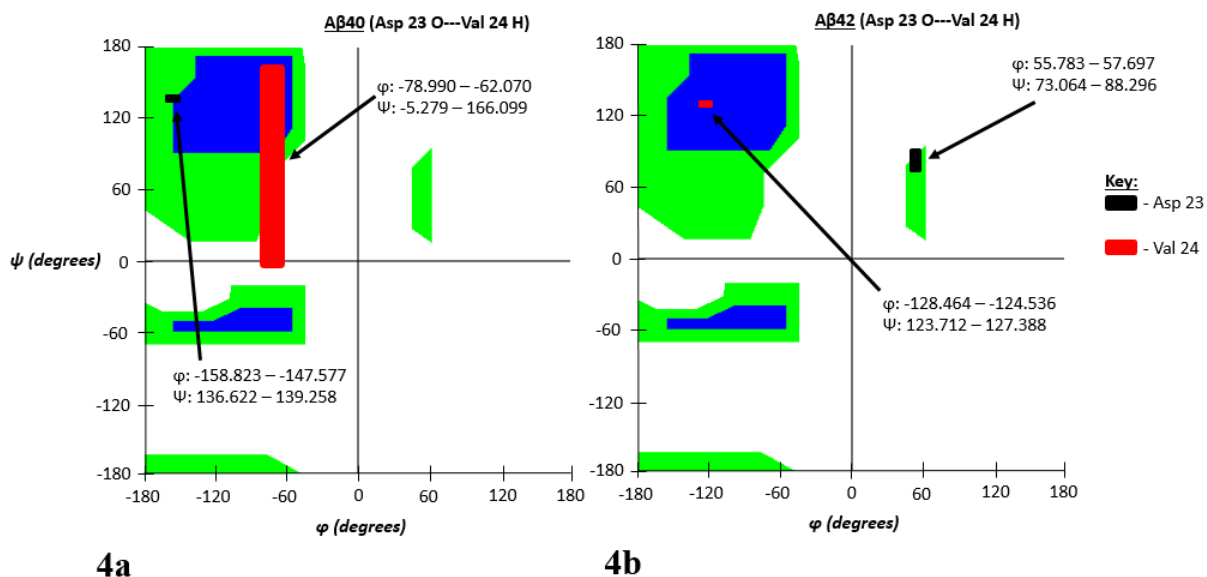
Figure 2a & 2b: Ramachandran angle profiles for an exceptionally strong atom-atom interaction (Ser 26 O interacting with Asn 27 H) for A β 40 (2a) and A β 42 (2b). Ranges for ϕ and ψ correspond to data spread according to 95% confidence interval analysis for all ensemble members as previously described. As stated before, the first atom is from the A chain of both isoforms and the second corresponds to the partner atom on the appropriate 1:2 interaction chain configuration. Note noticeable increase in β -sheet Ramachandran angle values for both residues of A β 42.

This particular interaction shows the Ramachandran angle values for the A β 42 isoform to clearly reside in β -sheet territory compared to A β 40 thus showing the increased secondary structure characteristics of A β 42 that favor the β -sheet motif for both interacting residues. The resulting changes in peptide plane orientations for the interaction in Figures 2a and 2b are further depicted in Figures 3a-3d for different viewing perspectives.



Figures 3a-3d: Molecule representations of peptide plane alignment for Aβ40 (3a & 3c) and Aβ42 (3b & 3d). Shaded parallelograms in Figures 3a and 3b are the peptide planes for the residues whose atoms are participating in the hydrogen bonding. Figures 3c and 3d correspond to a view down the peptide bonds showing the peptide plane profile orientation in magenta. Eye icons indicate view perspective.

As can be seen in Figure 3, the carbonyl oxygen and amino hydrogen that are involved in the hydrogen bond are considerably closer to each other in the A β 42 isoform thus illustrating that the cause of reduced inter-atomic distances is indeed a vertically-oriented peptide plane. Two additional interactions are shown below that further illustrate this behavior in Ramachandran angles and their effects on peptide plane orientations.



Figures 4a & 4b: Ramachandran angle profiles for an exceptionally strong atom-atom interaction (Asp 23 O interacting with Val 24 H) for A β 40 (4a) and A β 42 (4b). Ranges for ϕ and ψ correspond to data spread according to 95% confidence interval analysis for all ensemble members as previously described. As stated before, the first atom is from the A chain of both isoforms and the second corresponds to the partner atom on the appropriate 1:2 interaction chain configuration. Note noticeable increase in left-handed α -helix and β -sheet Ramachandran angle values for Asp 23 and Val 24 respectively in the A β 42 isoform.

Like the first atom-atom interaction case shown in Figures 2a and 2b, this interaction pair shows much more defined secondary structure in the A β 42 strain compared to A β 40. Unlike the preceding case, however, each residue takes on a different secondary structure motif, either left-handed α -helix (Asp 23) or β -sheet (Val 24) as summarized in Table 3. Such differing structure motifs are interesting given the proximal nature of these two residues relative to the primary sequence. Despite the differences in secondary structure characteristics assumed by the interacting residues of A β 42 for this interaction, the peptide planes of the participant atoms were likewise more vertical in the A β 42 isoform as was also seen in the preceding case. This orientation likewise contributed to decreased atom-atom interaction distances and therefore results in the stronger hydrogen bonding observed in that isoform. Images for these peptide plane configurations are shown below in Figures 5a-5d.

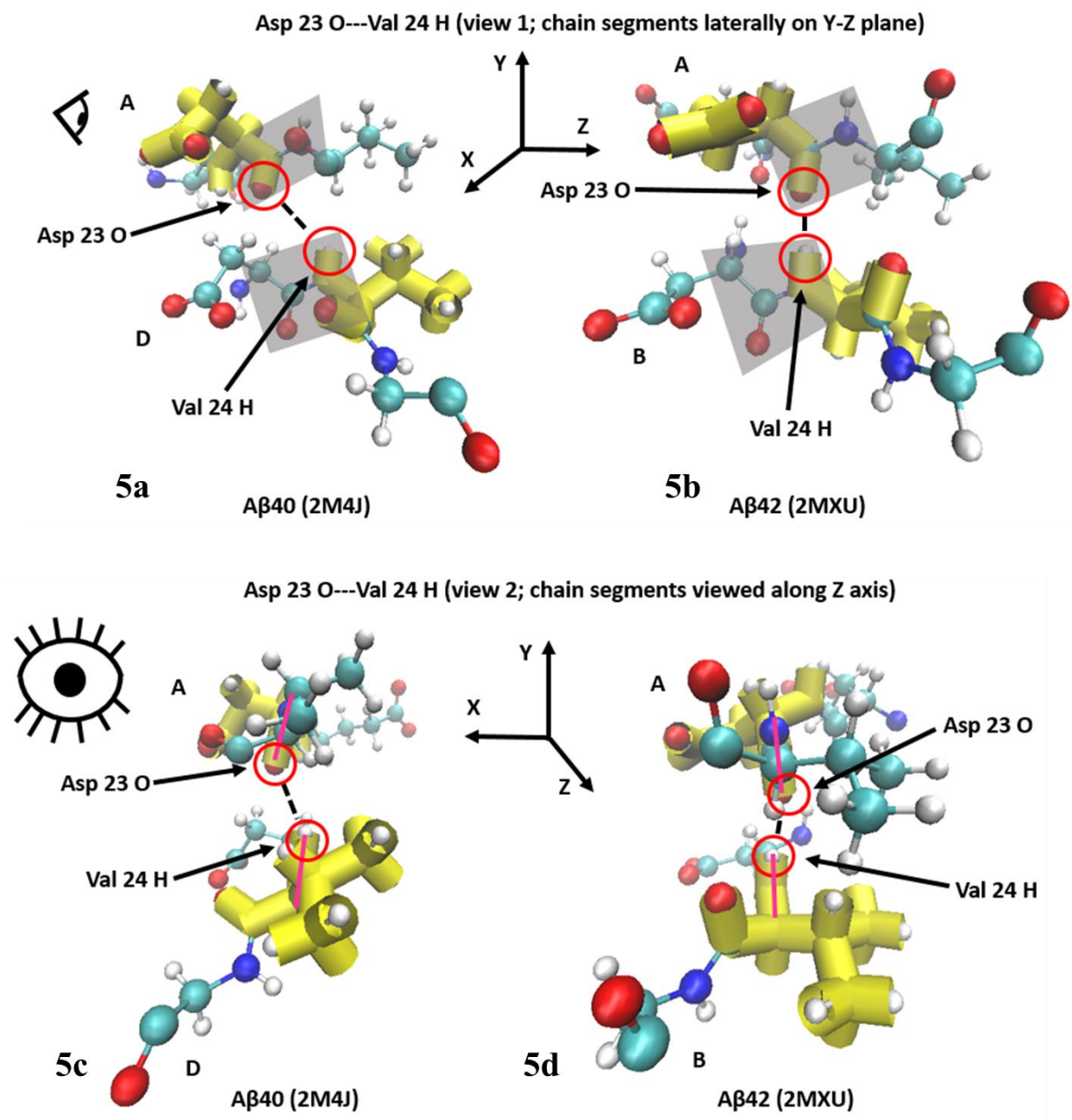
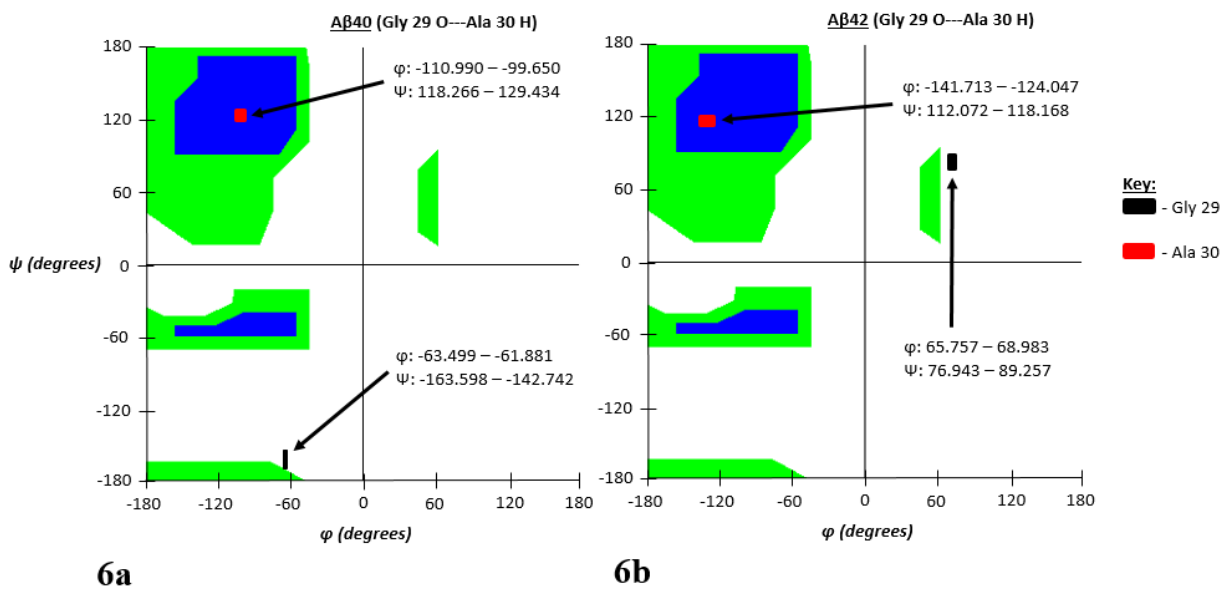


Figure 5a-5d: Molecule representations of peptide plane alignment for Aβ40 (5a & 5c) and Aβ42 (5b & 5d). Shaded parallelograms in Figures 5a and 5b are the peptide planes for the residues whose atoms are participating in the hydrogen bonding. Figures 5c and 5d correspond to a view down the peptide bonds showing the peptide plane profile orientation in magenta. Eye icons indicate view perspective.

Although the atoms involved in this example did not show as exaggerated vertical orientation of the peptide planes in the A β 42 strain, inter-atomic distance is nonetheless reduced in that isoform which corresponded to the observed superior interaction energy for this atom-atom pair interaction. For hydrogen bond Coulombic interactions, given the mathematical inverse relationship between the inter-atomic interacting energies and their inter-atomic distances, any appreciable increases in the interaction energy due to reduced distances, however small, are understandable and mathematically expected.

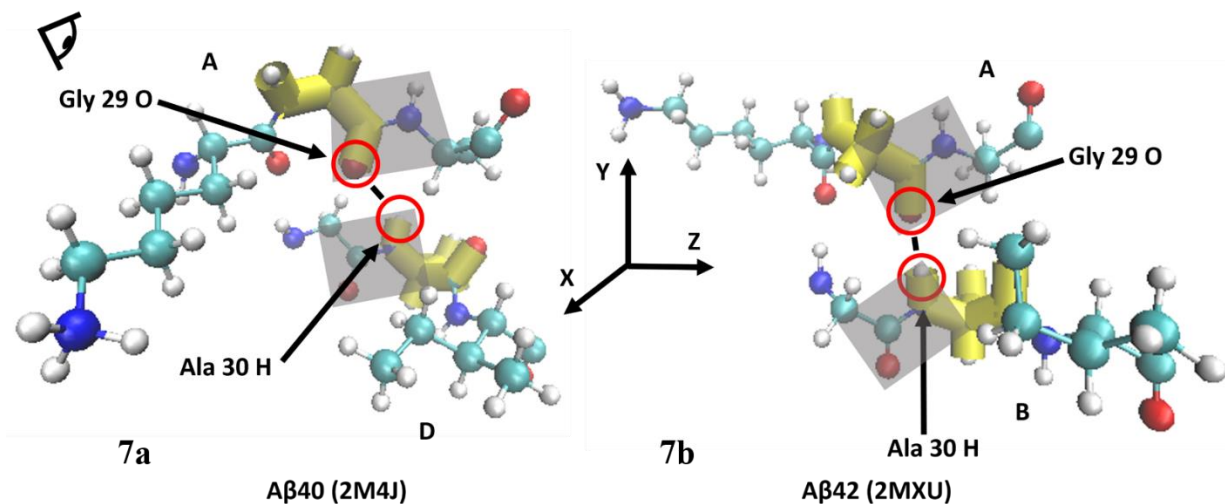
We lastly present a final case where secondary structure was more well-defined in the A β 42 isoform but for only one residue as opposed to both as has been seen in the previous two cases. Ramachandran plots for the respective angles of both A β 40 and A β 42 are shown below in Figures 6a and 6b.



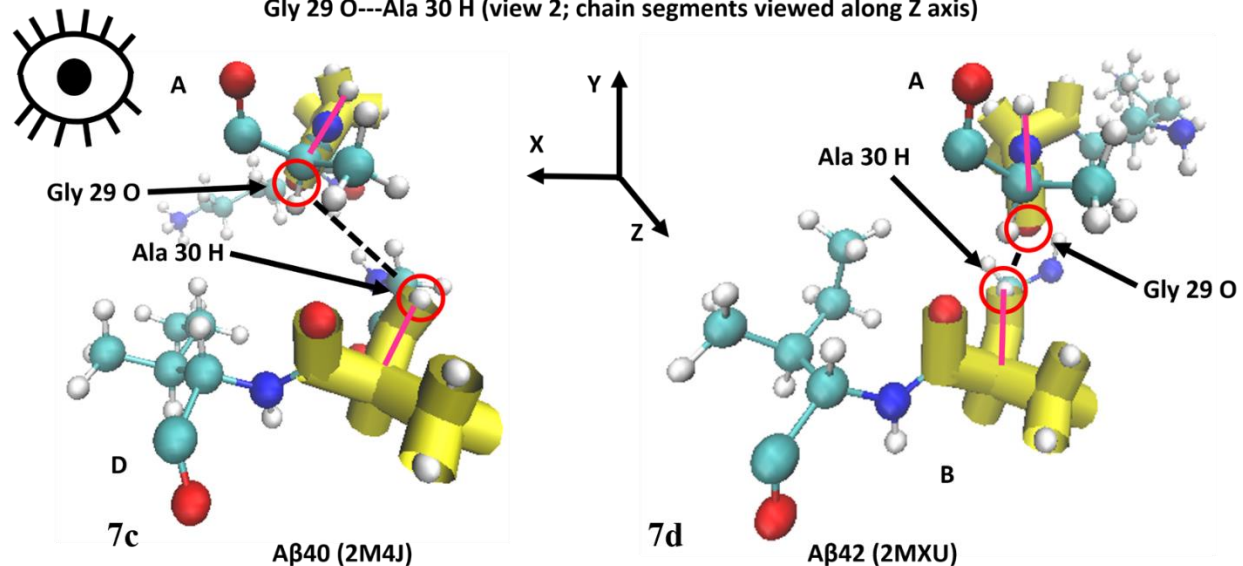
Figures 6a and 6b: Ramachandran angle profiles for an exceptionally strong atom-atom interaction (Gly 29 O interacting with Ala 30 H) for A β 40 (6a) and A β 42 (6b). Ranges for ϕ and ψ correspond to data spread according to 95% confidence interval analysis for all ensemble members as previously described. As stated before, the first atom is from the A chain of both isoforms and the second corresponds to the partner atom on the appropriate 1:2 interaction chain configuration. Note left-handed α -helix Ramachandran angle values for Gly 29 and the retention of β -sheet Ramachandran angle values for Ala 30 in A β 42 compared to A β 40.

In spite of the variation for the types of secondary characteristics acquired in the A β 42 isoform observed from case to case, the main motif of A β 42 possessing more vertical peptide planes (and hence reduced inter-atomic distances) remained true to this case as well as can be seen in Figures 7a-7d.

Gly 29 O---Ala 30 H (view 1; chain segments laterally on Y-Z plane)



Gly 29 O---Ala 30 H (view 2; chain segments viewed along Z axis)



Figures 7a-7d: Molecule representations of peptide plane alignment for Aβ40 (7a & 7c) and Aβ42 (7b & 7d). Shaded parallelograms in Figures 7a and 7b are the peptide planes for the residues whose atoms are participating in the hydrogen bonding. Figures 7c and 7d correspond to a view down the peptide bonds showing the peptide plane profile orientation in magenta. Eye icons indicate view perspective.

Although specific attributes regarding acquired secondary characteristics in the A β 42 strain are observed to vary from different interaction cases, the increased inter-chain interaction strength and stability of the A β 42 fibrils, compared to A β 40 fibrils, can confidently be attributed to Ramachandran angular changes that favor atom orientations that reduce key atom-atom interaction distances. These reduced distances thus favor strong attractive atom-atom interactions (particularly hydrogen bonding) between neighboring chains which appear to result in the superior aggregation stabilities and propensities observed in the A β 42 fibril isoform.

Recently, two additional structures of A β 42 aggregates have been published (PDB ID: 2NAO by Walti et al.⁴⁰ and 5KK3 by Colvin et al.⁴¹) that allow more comprehensive inter-chain interaction comparisons between A β 42 and A β 40 across independently published structure files. As described below, nearly identical conformational attributes noted above for the A β 42 structure by Xiao et al.³² (PDB ID: 2MXU) also occur for these two newly available structure files. Both 2NAO and 5KK3 were comprised of two stacks, but each structure's energy mappings were virtually identical for both stacks so representative data for one stack (the A-C and A-I stacks for 2NAO and 5KK3 respectively) is provided below.

In the case of 2NAO (for the A-B chain interactions) by Walti et al.⁴⁰, we found that the average energy per atom-atom interaction pair and the average distance, likewise per atom-atom interaction pair, were -0.828 ± 0.010 *kT* and 0.558 ± 0.002 *nm* respectively. This compares as appreciably similar to the results we obtained for 2MXU's average inter-atomic energy and distance of -0.819 ± 0.008 *kT* and 0.568 ± 0.001 *nm* respectively. This comparative analysis between these two A β 42 structures also led to our observing similar results for 2NAO

concerning that structure's β -sheet characteristics likewise reported by Walti et al.⁴⁰. Those residues we identified as contributing to the strongest inter-chain hydrogen bond energies for 2NAO (which also possessed more well-defined secondary structure characteristics through our Ramachandran plot analysis), were also identified as key β -sheet residues by Walti et al.'s⁴⁰ experimental chemical shift data. A complete comparison between 2MXU and 2NAO following our above analysis for the 2MXU structure can be found in the Supplemental Information.

In the case of 5KK3 (for the A-B chain interactions) by Colvin et al.⁴¹, concurrently, we found that the results were likewise similar to the 2MXU structure. Average energy and distance data per atom-atom interaction pair for 5KK3 were -0.889 ± 0.009 *kT* and 0.544 ± 0.002 *nm* respectively compared to 2MXU's -average energy and distance data of 0.819 ± 0.008 *kT* and 0.568 ± 0.001 *nm* respectively. As with the study by Walti et al.⁴⁰ for 2NAO, Colvin et al.⁴¹ also determined β -sheet structure regions using chemical shift data for their A β 42 fibril structure. Our energetic analysis likewise yielded the identification of the same key residues involved in β -sheet structure as Colvin et al.'s⁴¹ chemical shift data. The full analysis data for our comparison of 5KK3 and 2MXU is found in the Supplemental Information.

III.C. Conclusions:

A β 42 is known to engage in persistent aggregation structures more readily than A β 40, but until now, the details of why this is the case have not been clear. Our studies have clearly indicated, however, that the underlying reason behind increased aggregation attractive interactions and their corresponding superior attractive energies in mature A β 42 fibrils is due to a more vertical orientation of peptide planes within each constituent chain that places backbone

carbonyl oxygens and amino hydrogens in closer proximity to each other as evidenced by Ramachandran angle data. This consequently allows distance-dependent non-covalent attractive interaction energies in the form of hydrogen bonds to flourish in A β 42 which results in that isoform's stronger inter-chain interactions compared to the weaker A β 40 strain. Additionally, Ramachandran angles of A β 42 peptide chains in the fibril structure indicate that A β 42 has more well-defined secondary structure characteristics (specifically, β -sheet and left-handed α -helix) compared to A β 40. Indeed, the importance of Ramachandran angle changes have even been observed in the study of aggregation transition from pre-fibrillar aggregate structures to mature fibrils^{42, 43}.

A natural follow-up inquiry to these observations would then seek to probe the reason(s) why the A β 42 strain adopts more vertical peptide plane configurations. We postulate that, given A β 42's additional two C-terminal residues (Ile 41 and Ala 42), individual A β 42 peptide chains are perhaps able to sample fold-like configurations in the early aggregation process that allow Ramachandran angles which permit the more vertical peptide planes that favor stronger hydrogen bonding attractive interaction energies. Given A β 40's lack of these two C-terminal residues, it, by contrast, may perhaps not favorably sample those same conformations that favor reduced inter-atomic distances. Indeed, Urbanc et al.⁴⁴ discerned differences in the conformations assumed by monomer peptides of A β 40 and A β 42 during their computational simulation of the actual aggregation process for both isoforms. Such differences between isoforms observed during aggregation growth may yet be observed in the range of individual monomer motion preceding the actual aggregation process when considering the potential effects on individual monomer movement imparted by the last two C-terminal residues in A β 42.

Ultimately, therefore, the phenomenon behind A β 42's superior attractive interactions and superior stability, may be traced to concepts in the protein folding problem as they pertain to the three-dimensional configurations both isoforms' monomers distinctively sample prior to the early aggregation/oligomer stages leading up to mature fibril formation.

IIID. References:

- 1) Annaert, W., & De Strooper, B. (2002). A cell biological perspective on Alzheimer's disease. *Annual review of cell and developmental biology*, **18**(1), 25-51.
- 2) LaFerla, F. M., Green, K. N., & Oddo, S. (2007). Intracellular amyloid- β in Alzheimer's disease. *Nature Reviews Neuroscience*, **8**(7), 499-509.
- 3) Selkoe, D. J. (2001). Alzheimer's disease: genes, proteins, and therapy. *Physiological reviews*, **81**(2), 741-766.
- 4) Selkoe, D. J. (2004). Cell biology of protein misfolding: the examples of Alzheimer's and Parkinson's diseases. *Nature cell biology*, **6**(11), 1054-1061.
- 5) Klafki et al. (2016). Validation of a commercial chemiluminescence immunoassay for the simultaneous measurement of three different amyloid- β peptides in human cerebrospinal fluid and application to a clinical cohort. *Journal of Alzheimer's Disease*, (Preprint), 1-15.
- 6) Davis, J., & Van Nostrand, W. E. (1996). Enhanced pathologic properties of Dutch-type mutant amyloid beta-protein. *Proceedings of the National Academy of Sciences*, **93**(7), 2996-3000.
- 7) Davis-Salinas, J., Saporito-Irwin, S. M., Cotman, C. W., & Van Nostrand, W. E. (1995). Amyloid β -protein induces its own production in cultured degenerating cerebrovascular smooth muscle cells. *Journal of neurochemistry*, **65**(2), 931-934.
- 8) Luheshi, L. M., et al. (2007). Systematic in vivo analysis of the intrinsic determinants of amyloid β pathogenicity. *PLoS Biol*, **5**(11), e290.
- 9) Murakami, K., et al. (2003). Neurotoxicity and physicochemical properties of A β mutant peptides from cerebral amyloid angiopathy implication for the pathogenesis of cerebral amyloid angiopathy and alzheimer's disease. *Journal of Biological Chemistry*, **278**(46), 46179-46187.
- 10) Bitan, G., et al. (2003). Amyloid β -protein (A β) assembly: A β 40 and A β 42 oligomerize through distinct pathways. *Proceedings of the National Academy of Sciences*, **100**(1), 330-335.

- 11) Gong, Y., et al. (2003). Alzheimer's disease-affected brain: presence of oligomeric A β ligands (ADDLs) suggests a molecular basis for reversible memory loss. *Proceedings of the National Academy of Sciences*, **100**(18), 10417-10422.
- 12) Mastrangelo, I. A., et al. (2006). High-resolution atomic force microscopy of soluble A β 42 oligomers. *Journal of molecular biology*, **358**(1), 106-119.
- 13) Ahmed, M., et al. (2010). Structural conversion of neurotoxic amyloid-[beta] 1-42 oligomers to fibrils. *Nature structural & molecular biology*, **17**(5), 561-567.
- 14) Walsh, D. M., et al. (2002). Naturally secreted oligomers of amyloid β protein potently inhibit hippocampal long-term potentiation in vivo. *Nature*, **416**(6880), 535-539.
- 15) Dahlgren, K. N., et al. (2002). Oligomeric and fibrillar species of amyloid- β peptides differentially affect neuronal viability. *Journal of Biological Chemistry*, **277**(35), 32046-32053.
- 16) Chimon, S., et al. Evidence of fibril-like β -sheet structures in a neurotoxic amyloid intermediate of Alzheimer's β -amyloid. *Nature structural & molecular biology*, **14**(12), 1157-1164.
- 17) Petkova, A. T., et al. (2005). Self-propagating, molecular-level polymorphism in Alzheimer's β -amyloid fibrils. *Science*, **307**(5707), 262-265.
- 18) Qiang, W., Yau, W. M., Luo, Y., Mattson, M. P., & Tycko, R. (2012). Antiparallel β -sheet architecture in Iowa-mutant β -amyloid fibrils. *Proceedings of the National Academy of Sciences*, **109**(12), 4443-4448.
- 19) Walsh, D. M., et al. (1999). Amyloid β -protein fibrillogenesis structure and biological activity of protofibrillar intermediates. *Journal of Biological Chemistry*, **274**(36), 25945-25952.
- 20) Knowles, T. P., Vendruscolo, M., & Dobson, C. M. (2014). The amyloid state and its association with protein misfolding diseases. *Nature reviews Molecular cell biology*, **15**(6), 384-396.
- 21) Knowles, T. P., et al. (2009). An analytical solution to the kinetics of breakable filament assembly. *Science*, **326**(5959), 1533-1537.
- 22) Collins, S. R., Douglass, A., Vale, R. D., & Weissman, J. S. (2004). Mechanism of prion propagation: amyloid growth occurs by monomer addition. *PLoS Biol*, **2**(10), e321.
- 23) Mucke, L., et al. (2000). High-level neuronal expression of A β 1-42 in wild-type human amyloid protein precursor transgenic mice: synaptotoxicity without plaque formation. *The Journal of neuroscience*, **20**(11), 4050-4058.
- 24) Deshpande, A., Mina, E., Glabe, C., & Busciglio, J. (2006). Different conformations of amyloid β induce neurotoxicity by distinct mechanisms in human cortical neurons. *The Journal of neuroscience*, **26**(22), 6011-6018.

- 25) Lührs, T., et al. (2005). 3D structure of Alzheimer's amyloid- β (1–42) fibrils. *Proceedings of the National Academy of Sciences of the United States of America*, **102**(48), 17342-17347.
- 26) Olofsson, A., Sauer-Eriksson, A. E., & Öhman, A. (2006). The solvent protection of Alzheimer amyloid- β -(1–42) fibrils as determined by solution NMR spectroscopy. *Journal of Biological Chemistry*, **281**(1), 477-483.
- 27) Masuda, Y., et al. (2009). Identification of physiological and toxic conformations in A β 42 aggregates. *ChemBioChem*, **10**(2), 287-295.
- 28) Sakono, M., & Zako, T. (2010). Amyloid oligomers: formation and toxicity of A β oligomers. *FEBS journal*, **277**(6), 1348-1358.
- 29) Petkova, A. T., et al. (2002). A structural model for Alzheimer's β -amyloid fibrils based on experimental constraints from solid state NMR. *Proceedings of the National Academy of Sciences*, **99**(26), 16742-16747.
- 30) Sunde, M., et al. (1997). Common core structure of amyloid fibrils by synchrotron X-ray diffraction. *Journal of molecular biology*, **273**(3), 729-739.
- 31) Inouye, H., Fraser, P. E., & Kirschner, D. A. (1993). Structure of beta-crystallite assemblies formed by Alzheimer beta-amyloid protein analogues: analysis by x-ray diffraction. *Biophysical journal*, **64**(2), 502-519.
- 32) Xiao, Y., et al. (2015). A [beta](1-42) fibril structure illuminates self-recognition and replication of amyloid in Alzheimer's disease. *Nature structural & molecular biology*, **22**(6), 499-505.
- 33) Pauwels, K., et al. (2012). Structural basis for increased toxicity of pathological a β 42: a β 40 ratios in Alzheimer disease. *Journal of biological chemistry*, **287**(8), 5650-5660.
- 34) Stöhr, J., et al. (2014). Distinct synthetic A β prion strains producing different amyloid deposits in bigenic mice. *Proceedings of the National Academy of Sciences*, **111**(28), 10329-10334.
- 35) Nabers, A. et al. (2016). Amyloid- β -secondary structure distribution in cerebrospinal fluid and blood measured by an immuno-infrared-sensor: A biomarker candidate for Alzheimer's disease. *Analytical Chemistry*, **88**(5), 2755-2762.
- 36) Lu, J. X., et al. (2013). Molecular structure of β -amyloid fibrils in Alzheimer's disease brain tissue. *Cell*, **154**(6), 1257-1268.
- 37) Krall, A., Brunn, J., Kankanala, S., & Peters, M. H. (2014). A simple contact mapping algorithm for identifying potential peptide mimetics in protein–protein interaction partners. *Proteins: Structure, Function, and Bioinformatics*, **82**(9), 2253-2262.

- 38) Peters M. Force descriptions. In: McCombs KP, ed. *Real-Time Biomolecular Simulations*. New York, New York: McGraw Hill; 2007:58-62.
- 39) Stöbener, K., et al. (2014). Multicriteria optimization of molecular force fields by Pareto approach. *Fluid Phase Equilibria*, **373**, 100-108.
- 40) Walti, M. A. et al. (2016). Atomic-resolution structure of a disease-relevant abeta(1-42) amyloid fibril. *Proceedings of the National Academy of Sciences of the United States of America*, **113**(34), E4976-E4984.
- 41) Colvin, M. T. et al. (2016). Atomic resolution structure of monomorphic A β 42 amyloid fibrils. *Journal of the American Chemical Society*, **138**(30), 9663-9674.
- 42) Armen RS, DeMarco ML, Alonso DO & Daggett V. (2004). Pauling and Corey's alpha-pleated sheet structure may define the prefibrillar amyloidogenic intermediate in amyloid disease. *Proc Natl Acad Sci U S A*, **101**(32),11622-11627.
- 43) Milner-White, J. E., Watson, J. D., Qi, G., & Hayward, S. (2006). Amyloid formation may involve α -to β sheet interconversion via peptide plane flipping. *Structure*, **14**(9), 1369-1376.
- 44) Urbanc, B. et al. (2004). In silico study of amyloid beta-protein folding and oligomerization. *Proceedings of the National Academy of Sciences of the United States of America*, **101**(50), 17345-17350.

IV. Aim 3: Long-Time Dynamic Simulations of Protein Fluctuation States⁵

Abstract:

There are many important biological processes involving proteins and their fluctuations at nanosecond time-scales and up. Being able to study these fluctuations within reasonable user time frames is presently a challenge with existing computational techniques. Here, we present the application of an all-atom implicit solvent method for proteins applied to six distinct protein systems in a nanosecond time regime. We compared the results with known fluctuation data from the literature to see if known domains of exceptional motion can be recovered with our implicit solvent method. We also compare the implicit solvent results with results from all-atom explicit solvent molecular dynamics to compare the performance of the two methods to each other. We lastly look at whether the statistical variations in structure ensembles obtained from protein NMR correlate with known regions of exceptional flexibility from the literature. Results indicated that our implicit solvent algorithm was able to recover known regions of exceptional protein flexibility as described in the literature and we also conclude that NMR ensembles do not reliably convey regions of true protein motion.

IVA. Introduction:

The study of protein flexibility or dynamic protein conformational changes is critically important to the understanding of protein function including, for example, folding/misfolding, ligand-receptor signaling, enzymatic reactions, and protein-DNA interactions, to name a few. Short-lived energy fluctuations associated with conformational changes in proteins have also been shown to be important in a number of disease processes including pathogenic plaque

⁵ In preparation for submission.

formations [1]. Such a scenario of harmful aggregation-prone conformations in proteins, though short-lived and rare in occurrence, is nonetheless part of natural protein structural fluctuations whose ultimate biological consequences are energetically driven [2]. Missense genetic mutations can also lead to a plethora of altered folded states of proteins (“misfolded states”) that radically change their functional behavior and result in the cancerous states of cells [3]; these changes can be both static, such as by altering the structure of the binding domain sites, and/or dynamic, by altering the time dependent structure that may be critical to functionality. Missense genetic mutations also fundamentally alter the intra-atomic energy landscape of proteins and the interplay between shifts in protein energy landscapes and structure/dynamic changes may therefore be critical to understanding the role of missense mutations. The critical challenge of incorporating a more rigorous accounting of protein flexibility in drug design and development has also been recently highlighted [4]. Enzymatic reactions, in general, also involve time-dependent conformational states that ultimately depend on fluctuating intra-protein and inter-protein energetic interactions traceable to specific atom-atom interactions of amino acid residue groups [5].

In general, protein fluctuations take place over a wide variety of time scales and are often intimately connected to their functionality [6]. Major domain motions in proteins can take place over micro to milliseconds and allosteric transitions occupy a time regime spanning hundreds of nanoseconds to seconds [7]. Domain motions associated with enzymatic function are known to be associated with micro- to millisecond time regimes [8-12]. Due to the large range in time scales exhibited in protein dynamics in general, it is clear that robust methods are needed in order to capture the wide range of possible protein dynamic phenomena. *Natural fluctuation*

states of proteins about equilibrium configurations, involving thermal fluctuations, bond vibrations and bending motions, and side chain and dihedral angle rotations, are additionally known to reside within the picosecond to nanosecond time window [7]. Thus, as a first step to developing a comprehensive pathway for analyzing protein dynamics under one rigorous and broadly usable approach, we investigate the use of a generalized, all-atom implicit solvent protein computational dynamics previously developed [13-16] to predict and analyze those *natural protein fluctuation states* in systems where independent experimental dynamic data is available in order to test its potential efficacy.

Computational Approaches to Protein Fluctuations

In the consideration of computational approaches to protein dynamics, it is first noted that intra-atomic energy mappings in proteins demonstrate specific and conspicuous “hot-spots” or regions of dominant non-covalent interactions rather than a more uniform distribution across the protein [17] (Figure 1).

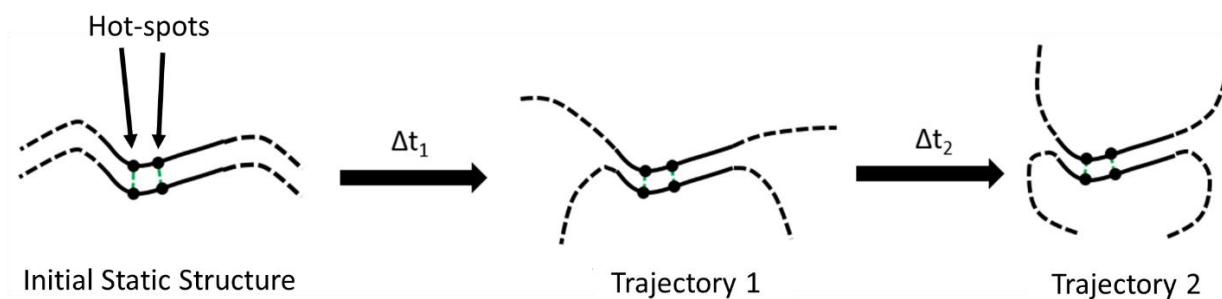


Figure 1: Schematic illustration of computationally-derived protein chain trajectories. The initial static structure may be obtained, for example, from crystallography. A real-time, dynamic protein trajectory over time steps Δt_1 and Δt_2 is illustrated. A collection/ensemble of these

structures superimposed one on another would constitute a simulation-derived dynamic ensemble. Green dashed lines are called “hot-spots,” or persistent dominant energy interactions.

These energy hot-spots are due to relatively large charge, partial atomic charge, and van der Waals type interactions that ultimately require force field models for their quantitative analysis. It is to be noted that charge interactions are typically associated with salt bridges, partial charge interactions are associated with hydrogen bonding, π interactions, etc., whereas van der Waals interactions dominate in hydrophobic regions of proteins. These interactions are traceable through the identification of the relatively strong atom pair interactions within the protein which act as “glue” points for protein stability, whereas weaker energetic interactions may be associated with more flexible regions of proteins.

Computational approaches to protein dynamics, therefore, should include all-atom methods where atomic level resolution is required to tease out critical details of observed dynamics. All-atom molecular dynamics (MD), or alternatively, all-atom implicit solvent (IS) methods can provide a time-dependent ensemble of structures at the atomic level which can truly be considered time-dependent snapshots of protein motion. Both all-atom molecular dynamics and all-atom implicit solvent models are based on simulating protein atomic motions from classical mechanics and statistical mechanics using interaction parameters to model the potential energy experienced by interacting atoms [18, 19]. Thus snapshots of trajectories of actual protein motions and fluctuations can be generated by these computational methods in order to provide insight on time-dependent protein motion across the entire protein, or any domains of interest (Figure 1). Differences between these two techniques are that in molecular dynamics

simulations the molecules of the protein's solvent, usually water, are treated explicitly, as opposed to implicit solvent simulations where the properties of the solvent are instead averaged [20]. The latter is formally accomplished by carrying out a short-time averaging of the host solvent dynamics [13-16]. This short time step, in turn, is formally coupled to a relatively longer-time, macromolecule (Generalized Langevin) dynamics step [13-16]. On a practical level, the diffusion and implicit fluid force terms can be approximated via separate analytical or computational studies for any given system as previously demonstrated [13-16]. Therefore, IS methods have demonstrated the potential to greatly reduce the computational work load for protein dynamic simulations by reducing both the total atom-atom force computations load and increasing the integration time steps required. Implicit solvent methods, in general, are able to probe longer time scales of protein motions as compared to molecular dynamics methods due to the averaging out of hundreds of thousands of protein associated solvent atoms necessary in explicit solvent methods. On the other hand, implicit solvent methods would not be able to tease out localized, discrete solvent effects, where possibly a relatively small number of localized solvent molecules could not simply be averaged in that region. However, in the consideration of determining fluctuation states and long-time domain motions in proteins considered here, these limitations do not appear as important. In some cases given below, we also give results for explicit solvent molecular dynamics (MD) computations for comparison purposes.

It is to be noted that explicit solvent MD methods often require thousands of core processing unit (CPU) hours and often specialized machines, such as hundreds of parallel core processors or graphical units [21]; whereas, implicit solvent methods can be performed on the order of a tenth to a hundredth of that time and on any type of computer. Thus, demonstrating

that efficacies of IS methods in general is critical in the pursuit of broad usability of atom-level protein dynamic simulations of a plethora of scientific activities and endeavors.

Experimental Approaches to Dynamic Protein Fluctuation States

Numerous experimental techniques can be employed to study protein fluctuation dynamics and no attempt is made here to exhaustively review the field. Techniques include, for example, fast relaxation imaging [22], fluorescence polarization anisotropy [23], hole burning spectroscopy [24, 25], dynamic NMR, which includes chemical shifts, relaxation rates, paramagnetic relaxation enhancement and residual dipolar couplings [1], and B-factors reported in x-ray crystallography protein structure data. As noted in these cited references, all methods have both advantages and disadvantages in any particular application depending on the specific protein properties. For completeness, we also note that several studies have identified the ill-defined regions of NMR structural ensembles as associated with flexible domains of proteins [26-28]. For example, Bertini et al. [26] state that in their structure determination of a matrix metalloproteinase 12 by NMR, loop regions with reduced Nuclear Overhauser Effect, or NOE, interactions (thus showing greater variability in the superimposed ensembles) are linked to local protein motion whereas superimposed regions with little variability are associated with more rigid protein regions. However, those authors also note that regions with such reduced NOE interactions may likewise be due to low data quality and/or severe overlap of NOESY cross peaks and are not necessarily due to local motion strictly speaking. Our focus here, therefore, is on direct experimental dynamic studies and their comparisons to IS methods.

IVB. Materials and Methods:

Implicit Solvent Method

In the implicit solvent method, the ligands (Brownian units) of a protein are smaller almost rigid segments flexibly connected at the α -carbon of each amino acid residue; namely peptide planes and R-groups as shown in Figure 2. A Generalized Langevin equation for each atomic-structured Brownian unit can be rigorously derived from multi-time scale perturbation theory as shown previously [15]. We note that the molecular theory derivations [13-16] are general and comprehensive and that they provide all possible rotational, translational, and coupled rotational-translational modes of motion and formally establish quantitative limits on the use of implicit solvent methods. They also include any external surfaces such as other biological macromolecules or other interacting proteins, and provide a formal, comprehensive prescription of all implicit solvent terms via time force autocorrelation expressions. The details of this derivation are given in the cited references, and no attempt is made here to present them for the sake of brevity.

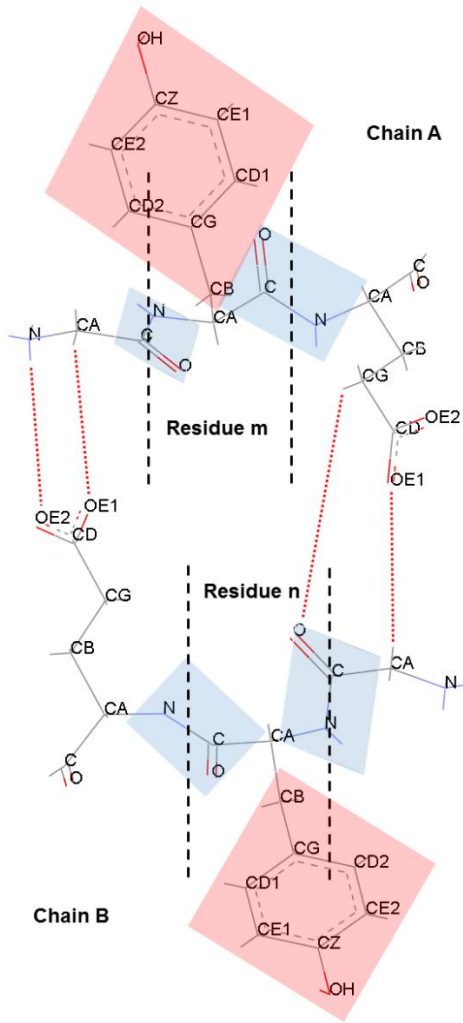


Figure 2: Implicit solvent rigid ligand structures: peptide planes (blue) and R-groups (red).

Briefly, the Brownian dynamics method is in the form of dimensionless translational and rotational displacement equations describing the change in the position of the ligand center of mass, \mathbf{R}_l , and the orientation about the center of mass, ϕ_l , for the l th ligand or B-particle as [13-16]

$$\mathbf{R}_{i1} = \mathbf{R}_{i1}^0 + \epsilon t \left[\sum_j (\mathbf{D}_{ij}^{0\text{TI}} \mathbf{F}_{j1}^0 + \mathbf{D}_{ij}^{0\text{TRI}} \mathbf{T}_{j1}^0) \right] + \mathbf{C}_{i1}(\mathbf{D}_{ij1}^0, t), \quad (1 \leq i \leq 3, 1 \leq j \leq 6) \quad (1)$$

$$\phi_{i1} = \phi_{i1}^0 + \epsilon t [\sum_j (D_{ij}^{0,RTI} F_{j1}^0 + D_{ij}^{0,RI} T_{j1}^0)] + C_{i1}(D_{ij1}^0, t), \quad (4 \leq i \leq 6, 1 \leq j \leq 6) \quad (2)$$

where i and j represent the Cartesian coordinates for coupled translation and rotation of the l th particle, ϵ is a particle Stokes' number, \mathbf{D} is a 6 by 6 grand diffusion tensor for the B-particle, \mathbf{F} and \mathbf{T} are the forces and torques acting on the B-particle as specified below, t is the time step, and the superscript (o) indicates values at the beginning of the time step. Thus Eq. 1 determines lateral displacement along the axes of a Cartesian lab reference frame and Eq. 2 determines angular rotational motion about the axes themselves. The stochastic function $C_{i1}(D_{ij1}^0, t)$ is a multivariate, Gaussian random number with zero mean and variance-covariance given by

$$\langle C_{i_l}(D_{ij_l}^0, \Delta t) C_{j_l}(D_{ij_l}^0, \Delta t) \rangle = 2D_{ij_l}^0 \Delta t \epsilon \quad (3)$$

For enhanced numerical stability, a variable time step method is used [15]. The force and torque terms appearing in the Brownian displacement equations above consist of two parts: (a) the local equilibrium average force and torque of the solvent acting on each ligand or B-particle (also, called the implicit solvent force) and (b) the external field force or torque due to the interactions of the ligand with the receptor molecule atoms, or in symbols, respectively [15]

$$\mathbf{F}'_l \equiv \langle \mathbf{F}_{fl} \rangle_{eq} + \sum_{kl} \sum_{ks} \mathbf{F}_{kl-ks} \quad (4)$$

$$\mathbf{T}'_l \equiv \langle \mathbf{T}_{fl} \rangle_{eq} + \sum_{kl} \sum_{ks} \mathbf{T}_{kl-ks} \quad (5)$$

where k_l represents the atom of the l th B-particle and k_s represents the atom of the target receptor (s). These atom-atom interaction forces and associated torques are taken from the AMBER 03 force field model for all results shown here [29]. Fixed bond distances and bond angles around each α -carbon are maintained by stiff potential functions, as described previously [15]. Dihedral angle potential functions are taken from AMBER03 [29]; see [15]. Atomic structural information (for ligand and receptor) is supplied by *.pdb or equivalent structure files.

Solvent Considerations

The local equilibrium average force of the solvent on the ligand consists of polar and apolar contributions as described below.

Polar Implicit Solvent Forces

Polar implicit solvent forces lead to the so-called dielectric behavior of the solvent. In the calculations given here, following the work of Ramstein and Lavery [30] as reviewed by Smith and Pettitt [31], we employ a distance dependent dielectric of sigmoidal shape with a decay constant of 0.5\AA^{-1} .

Apolar Implicit Solvent Forces

Following previous studies [15], the apolar implicit solvent potential was taken to be proportional to the solvent accessible surface area with the surface tension parameter set to $0.5\text{kcal/mol}\text{\AA}^2$. The solvent accessible surface area was calculated at the beginning of each Brownian dynamics step using the method of Hasel et al. [32].

Diffusion Tensor for the Ligand

For the purposes of calculating the diffusion tensor, each ligand is modeled as a sphere in a continuum with an effective diameter based on their respective van der Waals volume [15]. The hydrodynamic interaction of the ligand with the receptor is neglected in all calculations given here [14]. We note that any of these assumptions can be relaxed through the incorporation of short-time force autocorrelation or analytical studies.

Molecular Dynamics

In some results given below, implicit solvent simulations were compared to explicit solvent molecular dynamics (MD) simulations of the protein systems as performed by the NAMD2 program [33]. We used the CHARMM22 force field along with TIP3P [34, 35] water molecules to explicitly solvate the proteins. Simulations were performed maintaining the number of simulated particles, pressure and temperature (the NPT ensemble) constant with the Langevin piston method [33, 36, 37] specifically used to maintain a constant pressure of 1 atm. We employed boundary conditions for a water box simulation volume as well as the particle mesh Ewald (PME) method [38] with a 9 Å cutoff distance between the simulated protein and water box edge, and the integration time step was fixed at 2 femtoseconds. Given the computational cost of modelling solvent water molecules explicitly, this aspect of our study was therefore used for relatively short time simulations to compare with implicit solvent simulation results over the same time interval. Instructions for setting up a molecular dynamics simulation are found in Appendix E.

We make a final note of stating that we carried out all of our protein simulations under physiological conditions (i.e. 1 atm, 37 °C and pH of 7.4). Since the focus of this study is to strictly ascertain information regarding protein fluctuations as it relates to available experimental protein dynamic data, we did not introduce additional variables such as variable ionic strength, temperature and/or pH into our dynamic studies although they can readily be included.

Protein Experimental Selection Criteria

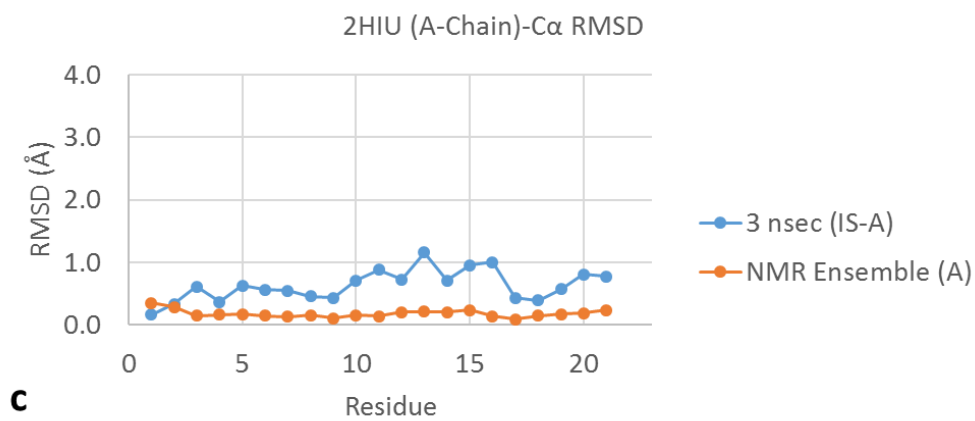
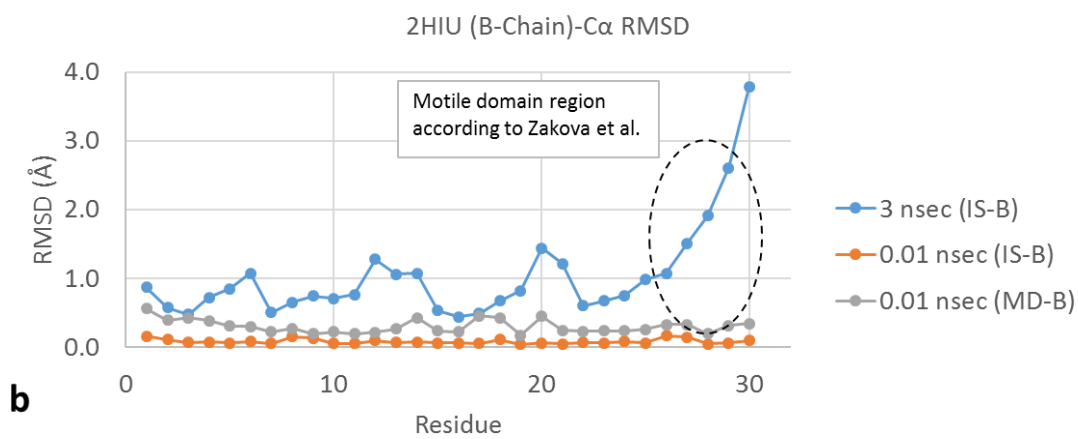
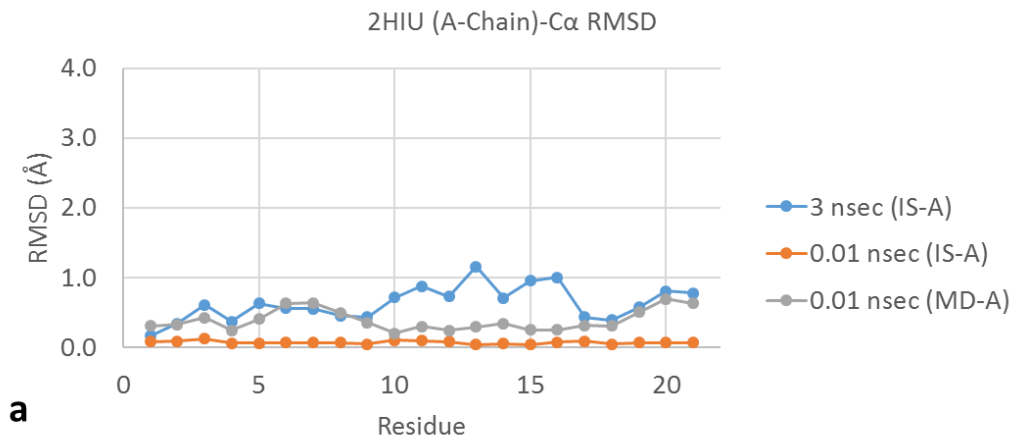
For the starting structures of the simulations, a total of 6 protein species were analyzed from a variety of different organisms. All proteins used in this study were selected from the Database of Molecular Movements [39]. Our selection criteria for picking species for study entailed selecting proteins that were composed of 1 to 2 chains with no attached ligand molecules/atoms and that had independent fluctuation data available to compare to our results. We employed structures elucidated from both X-ray diffraction studies as well as nuclear magnetic resonance experiments as our starting structures for simulation. In all, the forthcoming results are presented for: a long-time implicit solvent simulation (several tenths of a nanosecond to multiple nanoseconds), a short-time implicit solvent simulation (0.01 nanoseconds), a short-time molecular dynamics simulation (0.01 nanoseconds) and fluctuation data from the literature as obtained from the Database of Molecular Movements.

We finally note that all IS simulations were carried out on a single 2.3 GHz Opteron Processor Model 6276 CPU of a Linux cluster with no parallel processing or code optimization and all MD simulations were carried out on a Hewlett-Packard Stream 11 with a 2.16 GHz Intel Celeron N2840 processor with Turbo Boost Technology up to 2.58 GHz. We purposefully

employed readily available single processors in order to develop and analyze methods that could be of reach to the widest audience.

IVC. Results and Discussion:

Insulin: The first protein we analyzed to reconcile known literature fluctuation data with the results of our IS simulations was the two-chain insulin from *H. sapiens* (12.0 kDa, *.pdb ID: 2HIU). For this system and those that follow, we sought to identify those residues within the primary sequence that were particularly motile and see if these same residues have been heretofore identified by independent studies available in the literature. To this end, we specifically focused on determining RMSD data for the individual residues' α -carbons in the main chain backbone as potential representative regions of local motion. Consequently, regions of local RMSD value maxima are indicative of regions in the protein that experience significant fluctuations relative to the more static regions which are represented by local minima in the forthcoming figures. All simulation results therefore yielded an ensemble of a total of 10 structures whose statistical variations in atom positions correspond to actual local fluctuations. It is these structure ensembles that are henceforth analyzed. For this particular system, we carried out a long-time IS simulation of 3 nanoseconds in tandem with the short-time 0.01 nanosecond IS and MD runs. Literature data for comparison for the insulin protein was in the form of the results of a 50 nanosecond molecular dynamics simulation carried out by Zakova et al. which showed that a tens of nanoseconds time regime simulation was necessary to capture the full range of motion of the most motile domain [21]. We note that the two chains of this protein are different with the A chain being shorter (21 residues) than the B chain (30 residues). Results for this system are shown in Figure 3.



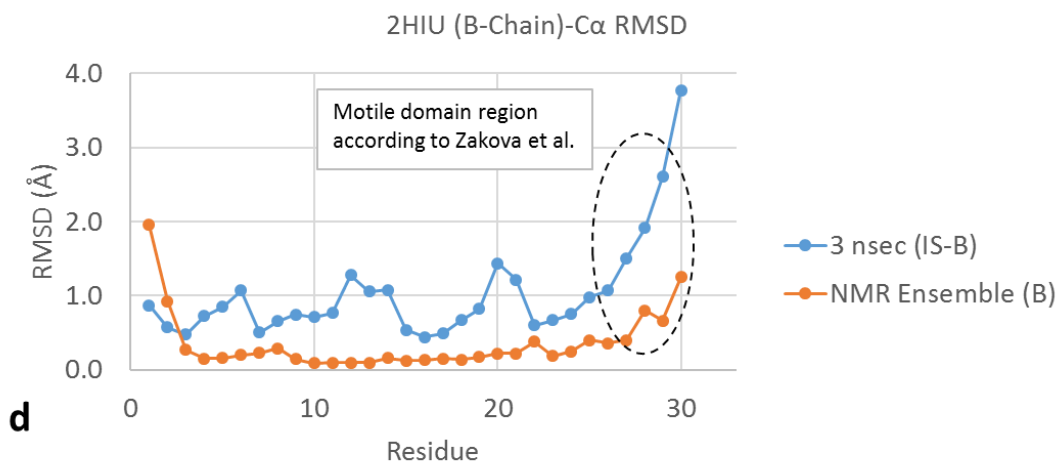
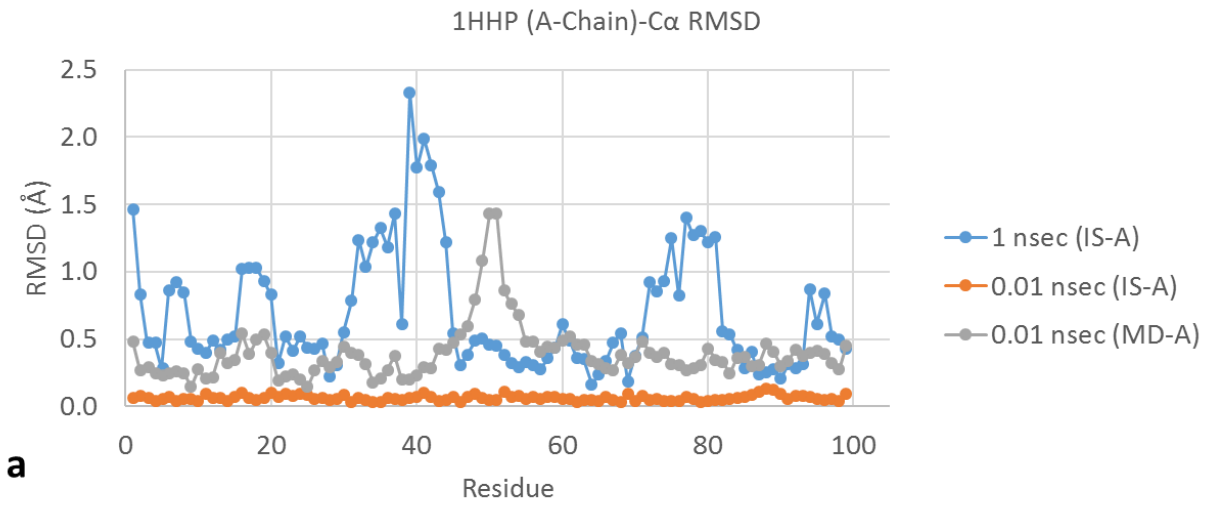


Figure 3: Simulation RMSD results data for IS, MD and region of motility as identified by a 50 nanosecond MD simulation carried out by Zakova et al [21]. Simulation RMSD data for both long-time 3 nanosecond IS and short-time 0.01 nanosecond IS and MD simulations for chains A and B (a & b), and long-time 3 nanosecond IS RMSD data compared to structure ensemble provided by NMR structure elucidation (c & d).

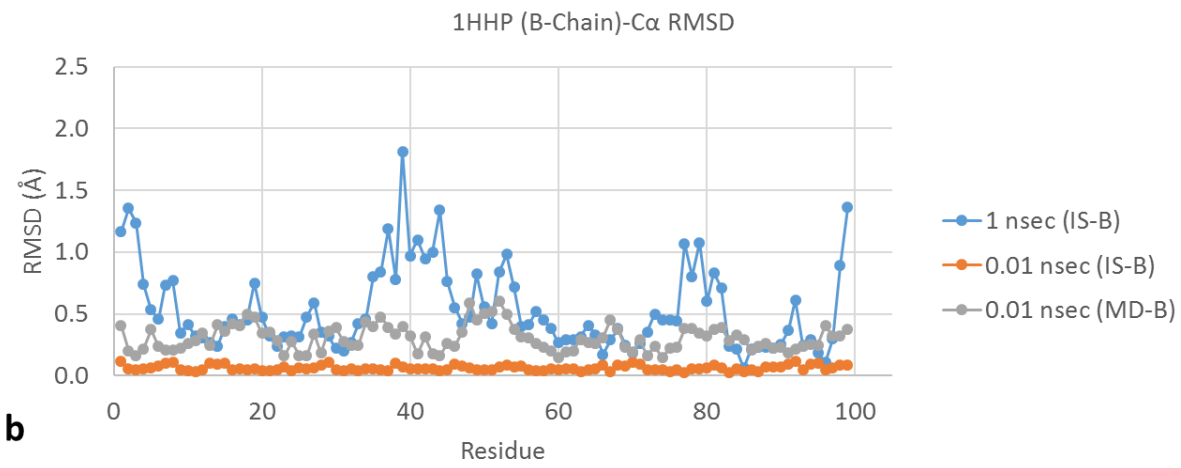
As expected, the short-time IS and MD simulations exhibited relatively small RMSD values residing stably around 0.2 Å (A chain) and 0.4 Å (B chain) respectively without any sharp and noticeable maxima for the short-time simulations (Figure 3a and 3b). The long-time 3 nanosecond IS simulation, however, yielded noticeably high RMSD values particularly for the B chain's residues closest to its C-terminus (the higher numbered residues for this structure) whereas results the A-chain provided no noticeable regions of high flexibility (Figure 3a and 3b). These long-time IS results for the B chain thus reflected a region of high motility that has been previously identified by the 50 nanosecond MD study carried out by Zakova et al. [21]. Since this protein's initial structure data was available as a NMR ensemble, we also sought to see if this ensemble reflected the C-terminal region's fluctuations. Indeed, the NMR ensemble did

reflect relatively larger RMSD values at the identified region of flexibility, but they were not as pronounced as the RMSD values from the 3 nanosecond IS simulation (Figure 3d). Furthermore, the NMR ensemble's RMSD analysis suggests that there is considerable motion at the N-terminus of the B chain ($\sim 2 \text{ \AA}$), even greater than the NMR ensemble's C-terminus region ($\sim 1.25 \text{ \AA}$), which is in contrast to our long-time IS simulation results and the findings by Zakova et al. [21] that suggest that this N-terminus region may actually be more stable. We note that in our methods described above, the computational time in carrying out an equivalent 3 nanosecond MD simulation were not reasonable. The CPU time for the MD simulations were approximately 10 to 20 times those for IS for all proteins studied here. We note that the average CPU times for long time IS simulations (on the order of nanoseconds) were 1-3 days.

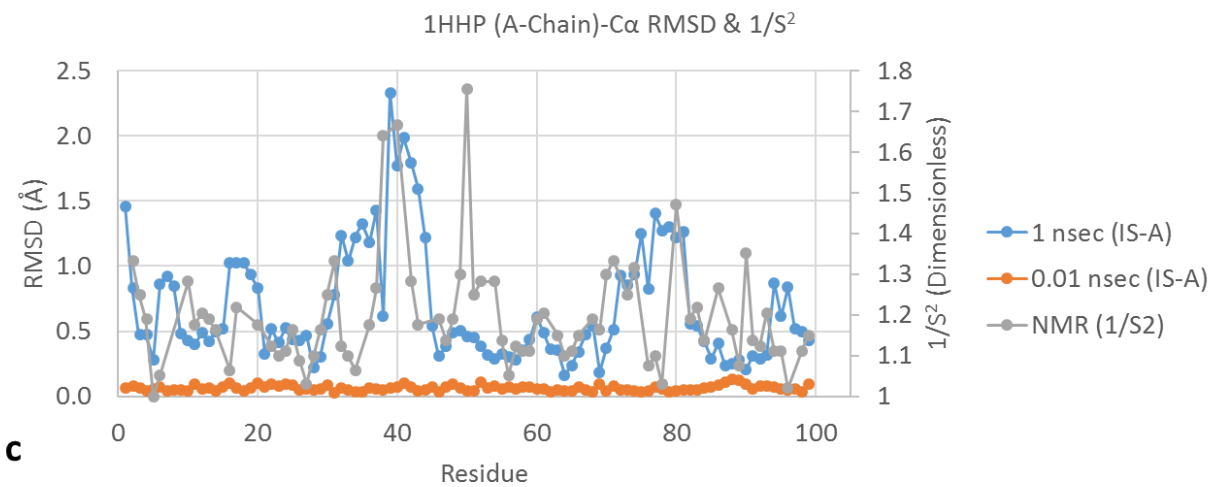
HIV-1 Protease: Results for the homodimer two-chain HIV-1 protease (21.6 kDa, *.pdb ID: 1HHP) were obtained for a 1.0 nanosecond long-time IS simulation along with short-time 0.01 nanosecond simulations from IS and MD. Both chains are identical for this system. Literature data for comparison is in the form of dimensionless order parameters (S^2) from nuclear magnetic resonance dynamics experiments which showed that motion for a pharmaceutically-relevant flap domain was on the tens of nanoseconds timescale [40, 41]. Since the relationship between order parameters and motility is of an inverse nature, we note that we present the inverse of the order parameters where larger valued data points correspond to greater degrees of fluctuations. RMSD data and inverse experimental order parameters are shown in Figure 4.



a



b



c

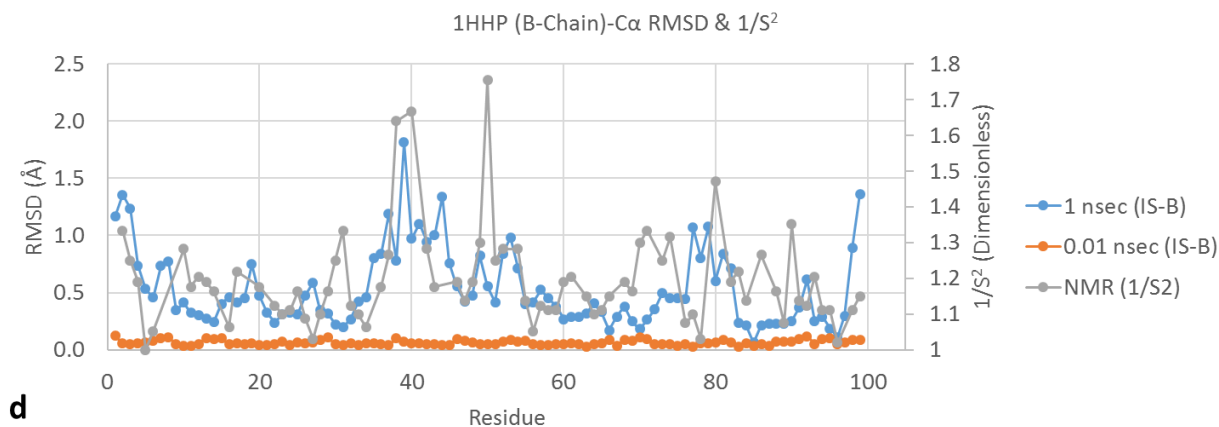


Figure 4: Simulation RMSD results data for IS, MD and inverse order parameters from NMR spectroscopy [40, 41]. RMSD data for long-time 1 nanosecond IS and short-time 0.01 nanosecond IS and MD for A and B chains (a & b), RMSD data for long-time 1 nanosecond and short-time 0.01 nanosecond IS with inverse order parameters from NMR (c & d).

As can be seen in Figures 4a and 4b, the long-time 1 nanosecond run yielded the highest RMSD values of all the simulations as expected. There were several prominent regions associated with exceptionally high RMSD values which ranged from 1 to in excess of 2 Å for both chains (i.e. Val 32-Pro 44 and Val 77-Pro 81). The more stable regions of the protein were observed to have RMSD values that resided between 0.3 and 0.5 Å. Profiles for both chains were very similar with large RMSD peaks appearing in the same regions. As discussed more fully below, differences seen between the short-time (0.01 nanosecond) MD and IS RMSD results are due to lack of an equilibration time for MD and the use of a constant time step as opposed to the variable time step used in IS. Comparing the simulation results to the experimental order parameter data in Figures 4c and 4d shows that the long-time IS simulation recovers many of the experimentally-identified residues of greatest fluctuation. The most prominent region thus identified for both A and B chains is Leu 38-Pro 44 which the long-time IS predicted specific a

maximum RMSD value of 2.33 Å for Pro 39 on the A chain and 1.28 Å for Trp 42 on the B chain. These residues correspond to known regions on the highly motile flap of HIV-1 protease and are a key binding region for pharmaceutically-relevant HIV protease inhibitors [40, 41]. Another highly fluctuating region identified by both methods was His 69-Thr 80 for which IS predicted a local maximum of 1.4 Å and 1.07 Å for Val 77 on both the A and B chains (Figures 4c and 4d). One region that was not in agreement, however, was the experimentally determined motion of Ile 50 that the long-time IS simulation did not pick up. This residue was prominently identified, however, by the short-time MD simulation which predicted a RMSD value of 1.43 Å for it and also the same RMSD value for Gly 51 (Figure 4a). We note that this was the only noticeable agreement between the MD simulation and the experimentally-derived order parameters.

It is worth mentioning that in addition to analyzing the experimentally-derived order parameter data that we've considered in our study thus far for HIV-1 protease, Hornak et al. [40] also generated order parameters for this protein from their 50 nanosecond MD simulation. Their comparison between the order parameters from these two sources resulted in the observation that MD predicts greater flexibility than may actually occur [40].

Endothiapepsin: The one chain endothiapepsin proteinase from *C. parasitica* (33.8 kDa, *.pdb id: 4APE) was analyzed for a 0.17 nanosecond long-time IS simulation and for 0.01 nanosecond short time IS and MD runs. Fluctuation information was available from X-ray diffraction studies with particular attention to the active site cleft, the most motile domain of this protein [42, 43].

No dynamic information for this protein was found in the literature. Our data results are shown in Figure 5.

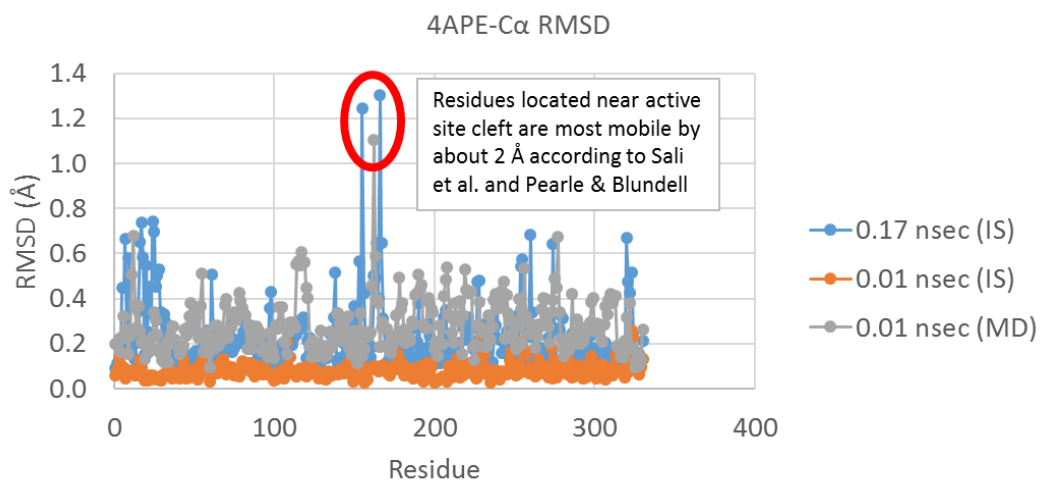


Figure 5: Simulation RMSD data for long-time 0.17 nanosecond IS and short-time 0.01 nanosecond IS and MD. Region of large flexibility was identified by X-ray diffraction studies [42, 43].

As can be seen in Figure 5, there is a particularly prominent region that corresponds to pronounced fluctuation dynamics. This region, which roughly spans residues Leu 155-Thr 172, constitutes the active site cleft of this protein. RMSD data from the long-time IS simulations indicates that local α -carbon RMSD values are 1.25 and 1.35 Å for Leu 155 and Asn 166 respectively which is remarkably close to the RMSDs predicted by the crystallography studies of 2 Å [42]. The location of both these residues in the active site cleft are shown in Figure 6. Short-time 0.01 nanosecond MD simulations similarly predicted a relatively large RMSD value of 1.11 Å for Asp 171 which also lies in this active site cleft region. As before, these short-time 0.01 nanosecond MD simulations predicted considerably larger RMSD values than their short-

time IS counterpart whose RMSD values instead tended to reside relatively stable between 0.03-0.2 Å.

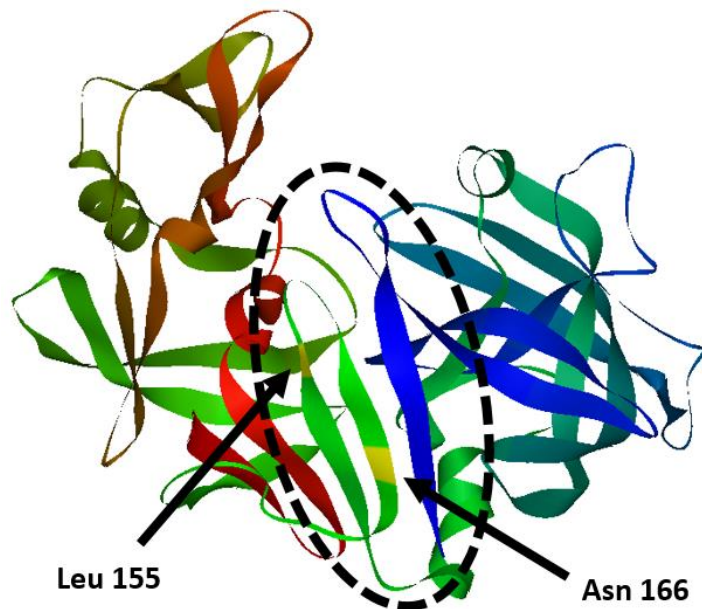
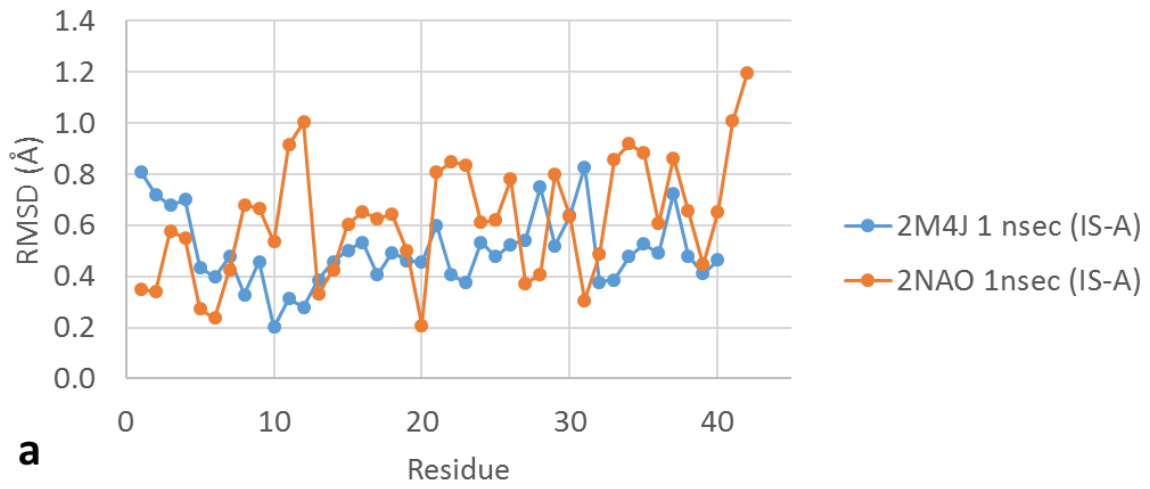


Figure 6: Active site cleft for endothiapepsin (4APE) with residues Leu 155 and Asn 166 identified by IS at 0.17 nanoseconds high-lighted in yellow.

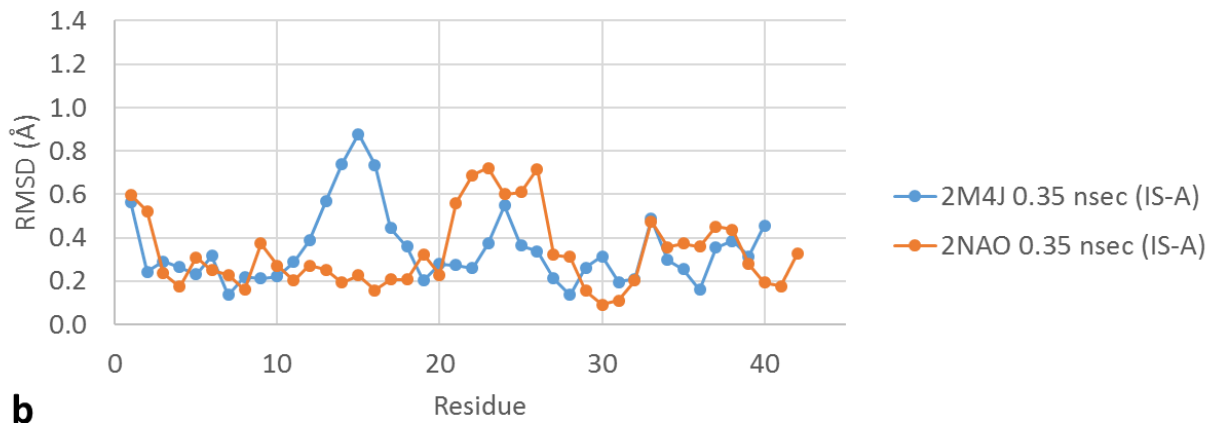
A β 40/42: The next system we analyzed were the A β 40 (*.pdb ID: 2M4J) and A β 42 (*.pdb ID: 2NAO) peptides, both, as dimer 2-chain units. Fluctuation data we present are for a long-time 1 nanosecond, a median 0.35 nanosecond and a short-time 0.01 nanosecond IS simulations along with a short-time 0.01 nanosecond MD simulation for both chains and both isoforms as shown in Figures 7 and 8. Experimental information cataloging fluctuation behavior for either isoform was found to be lacking in the literature although data for a truncated mature fibril (A β 9-40) was available [44].

2M4J & 2NAO (A-Chain)-C α RMSD



a

2M4J & 2NAO (A-Chain)-C α RMSD



b

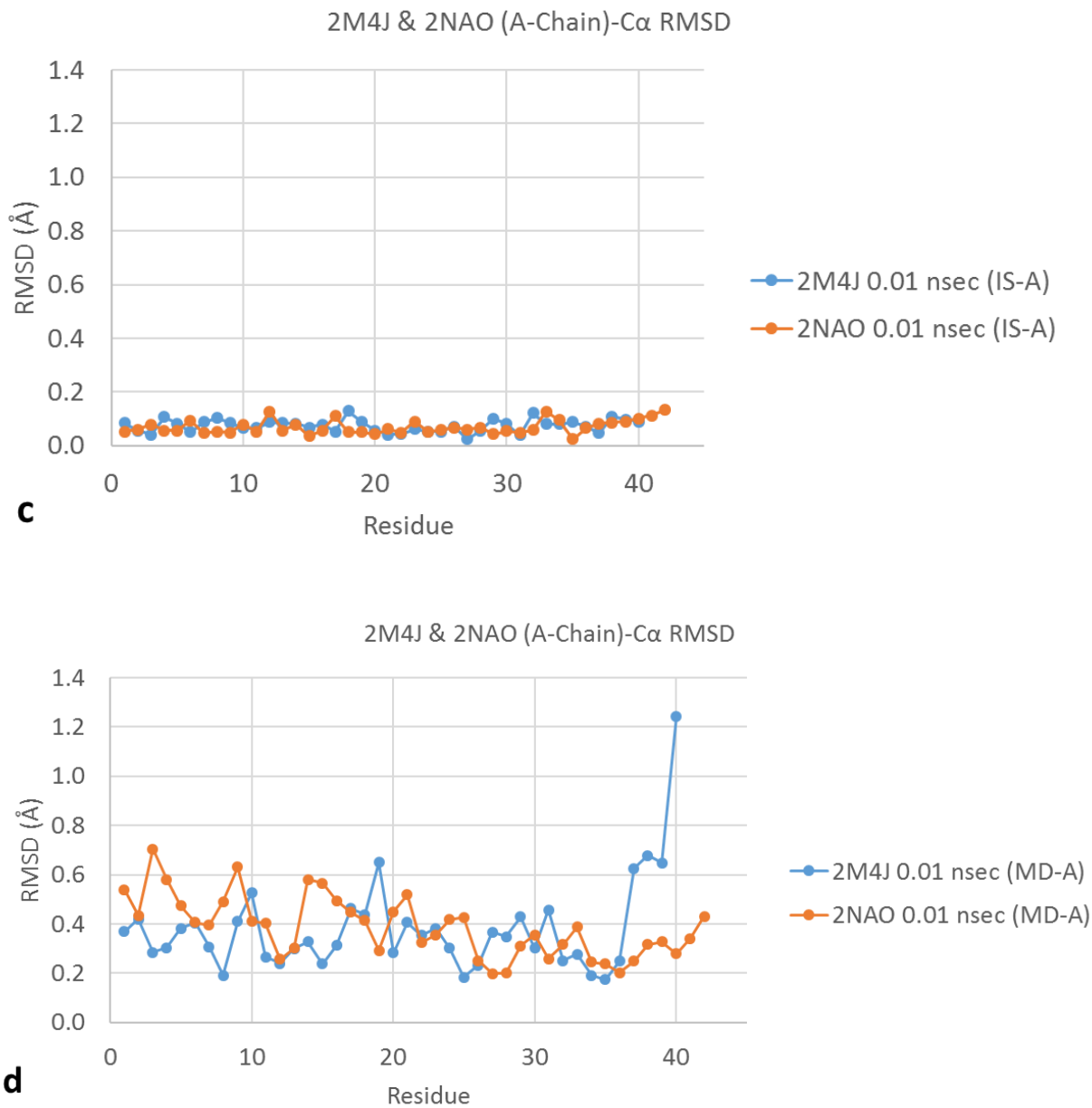
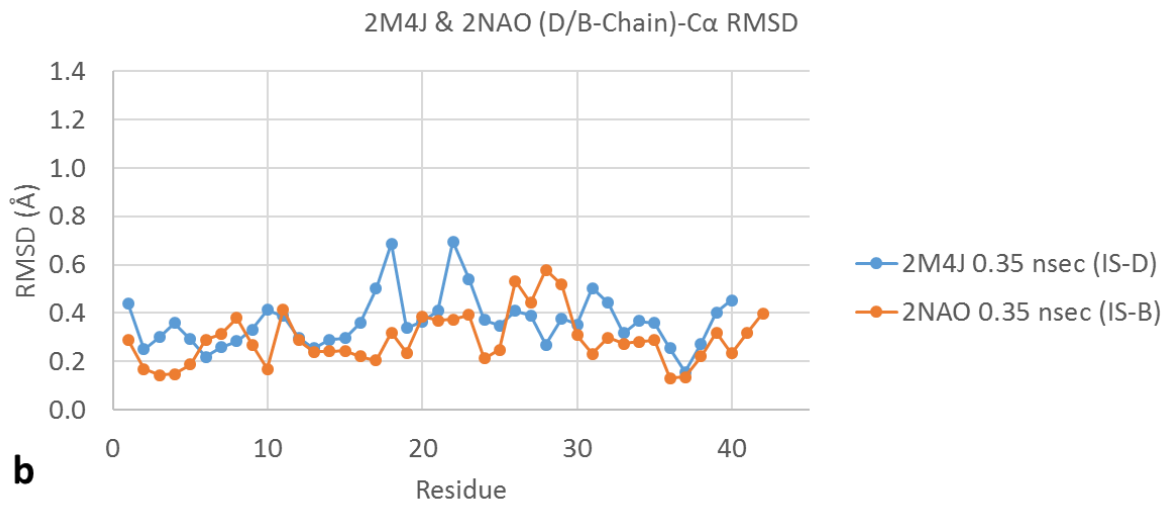
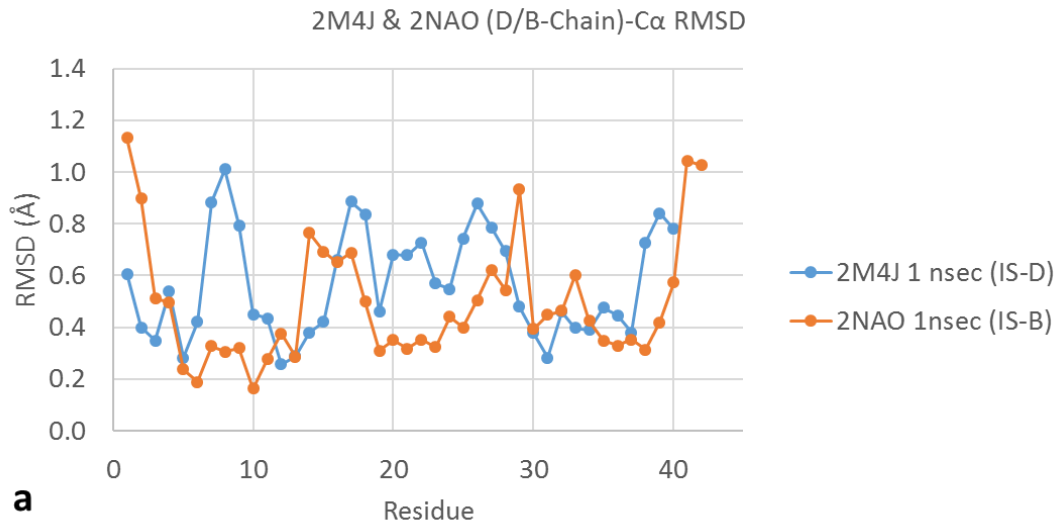


Figure 7: RMSD data for the A chains of A β 40 (*.pdb ID: 2M4J) and A β 42 (*.pdb ID: 2NAO). Long-time IS 1 nanosecond (a), median time IS 0.35 nanosecond (b) and short-time 0.01 nanosecond for IS and MD (c & d).



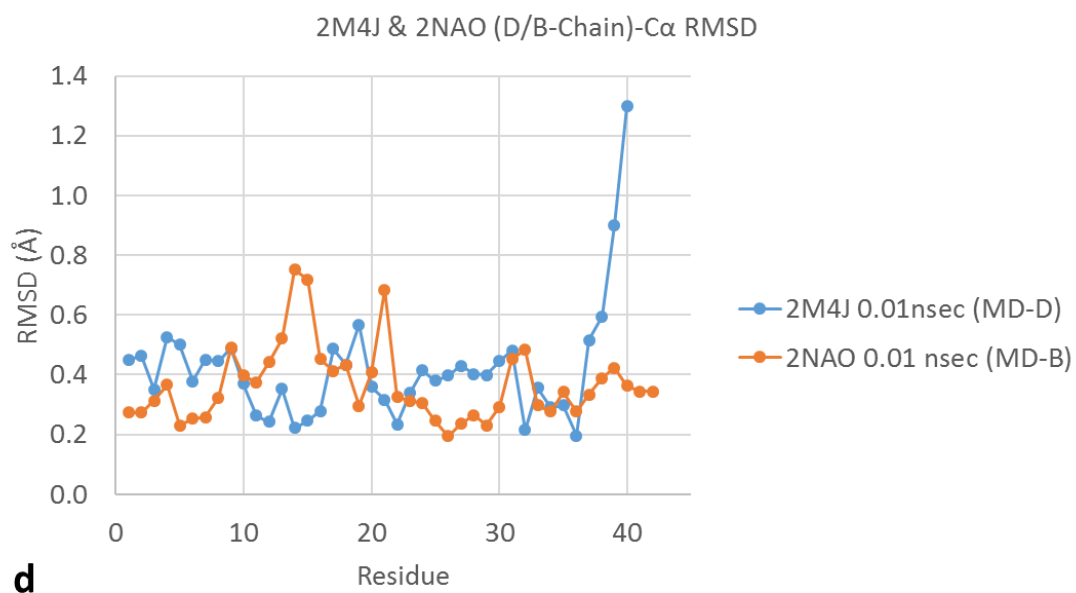
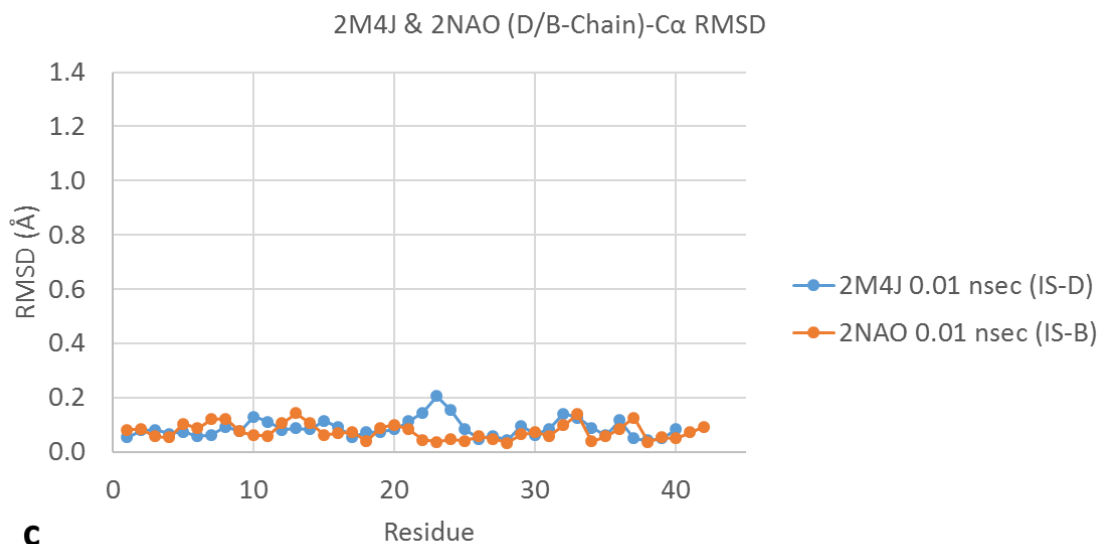


Figure 8: RMSD data for the partner chain (D or B) of A β 40 (*.pdb ID: 2M4J) and A β 42 (*.pdb ID: 2NAO). Long-time IS 1 nanosecond (a), median time IS 0.35 nanosecond (b) and short-time 0.01 nanosecond for IS and MD (c & d).

As can be seen in Figures 7a and 8a for long-time 4 nanosecond fluctuations, both isoforms experience a wide bandwidth of motions throughout the primary sequence ranging from 0.2-1.2

Å. No specific residues are observed to contribute any particularly outstanding RMSD values. Median-time IS simulations for 0.35 nanoseconds show similar behavior although some of the residues in the first half in the primary sequence of both isoforms (residues Arg 5-Phe 20) do appear relatively more stable compared to the latter residues. RMSD ranges thus observed for the 0.35 nanosecond simulations encompass a breadth of around 0.2-0.9 Å and 0.2-0.7 Å for the A chain and D/B partner chain respectively for both isoforms (Figures 7b and 8b). Short-time 0.01 nanosecond IS simulations show extremely stable RMSD values for both isoforms' chains with RMSD values being around 0.05 Å and 0.07 Å for the A and partner chains (D or B) respectively (Figures 7c and 8c). Short-time 0.01 nanosecond MD, on the other hand, predicts greater motion throughout the primary sequence for both isoforms' RMSD value ranges. The A chain is predicted to exhibit motion corresponding to overall RMSD values between 0.2-0.7 Å and the B chain between 0.2-0.8 Å (Figures 7d and 8d). Of note for the MD simulation is that the C-terminus of the Aβ40 isoform appears to be extremely motile with its last residue, Val 40, showing an outstandingly high RMSD value of 1.24 Å and 1.30 Å for the A and partner D chain respectively (Figure 7d and 8d). The short-time 0.01 nanosecond MD simulation for the Aβ42 isoform did not yield similar C-terminus behavior. Previously published MD simulation data for a truncated mature fibril (Aβ9-40) indicated an extremely motile N-terminus glycine (G9) [44]. However, neither of our simulations identified outstanding motion either at the 9th residue (G9) or the actual N-terminus of the complete structure (D1) which may not be too surprising given that we employed complete Aβ40/42 structures in our simulations. In all, our simulation data for both isoforms thus suggests both isoforms to be more or less equally stable relative to each other as far as motions/fluctuations are concerned thereby suggesting comparable degrees of motions for dimer units of Aβ40 and Aβ42.

Calbindin:

For all the protein systems with the pertinent data, it is also noted that MD results shown thus far for small times were done without equilibration, which is not a necessary consideration for IS simulations. The equilibration time for MD simulations is associated with explicit water stabilization since solvating schemes are geometric not thermal in nature. This is not an issue for IS, since thermal solvent equilibrium is part of the *a priori* averaging process. Thus, we carried out a root-mean-square deviation (RMSD) on the MD simulation of calbindin for the average of the entire backbone α -carbons of the protein (alternatively referred to here as global RMSD analyses) over a total simulation period of 0.6 nanoseconds in an effort to identify any potential causes for the inconsistencies observed between the short-time MD simulation results and the experimental data. As shown in Fig. 9, the resultant profile of time-dependent RMSD values for the entire protein begin to gradually stabilize with increasing simulation times plateauing out to around 2.5 Å for the obtained data.

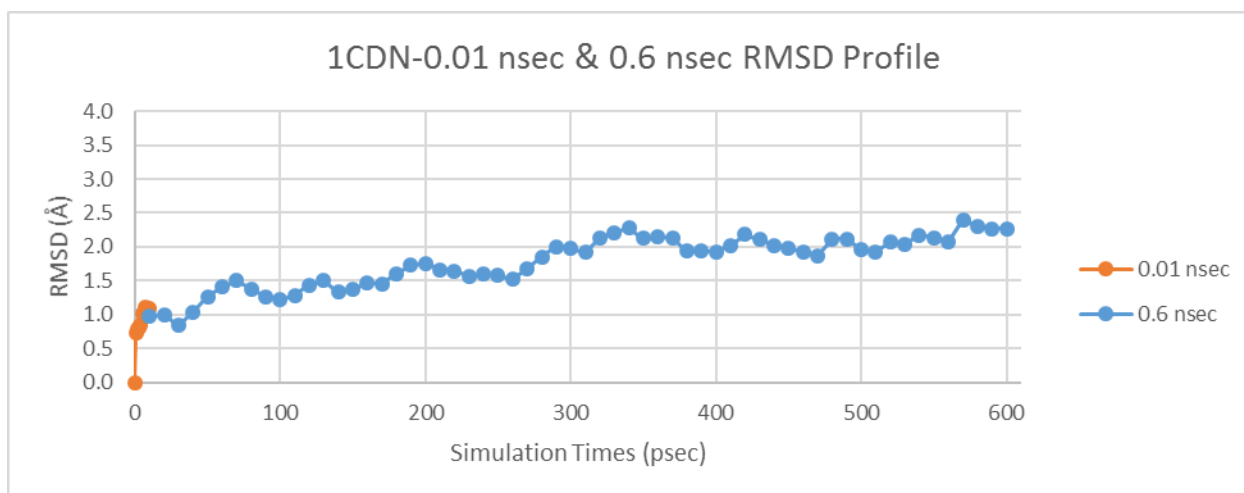
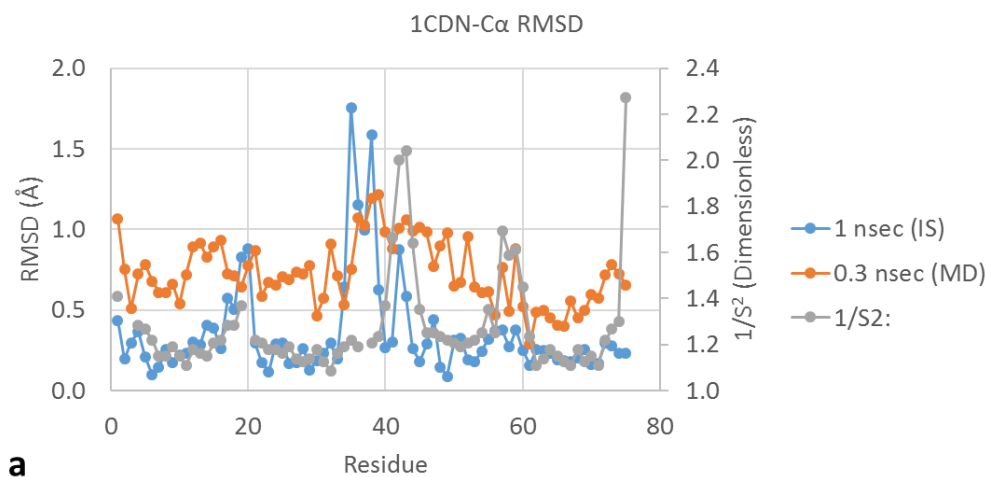


Figure 9: Global RMSD (Å) profile of calbindin (*.pdb ID: 1CDN) vs MD simulation time (picoseconds).

As can be seen in Figure 9, global RMSD values continue to clearly rise past the 600 picosecond (0.6 nanosecond) mark implying that a properly equilibrated system might well need to at least reach, if not surpass, 1000 picoseconds (1 nanosecond) in order to capture legitimate fluctuations and dynamics that mirror known fluctuation data. In an attempt to capture global RMSD behavior for earlier simulation times for the sake of comparison, we also show results in Figure 9 for a simulation of the very first 10 picoseconds of calbindin motion as seen in the orange portion of the curve. As can be seen from these two superimposed structures, such a short MD simulation time is inadequate to represent a stably fluctuation molecule and a significant equilibration time on top of an actual “analysis time” associated with the native or non-computational fluctuations is necessary for MD. This all comes with the significant increases in computational processor time as compared to the shorter processing times observed for IS.

The final system we analyzed was the single-chain calbindin from *B. taurus* (30.0 kDa, *.pdb ID: 1CDN). For calbindin, we carried out a long-time IS simulation of 1 nanosecond for which we identified three regions of considerable local fluctuations, namely, for residues Pro 20, Glu 35 and Gly 42. We also include the results for 0.3 nanoseconds MD simulation time specifically from the semi-stabilized plateau region observed in Figure 9 to see how individual α -carbon RMSD values for this relatively stable region predicted by MD compare to additional IS and experimental data. These results are shown together with dimensionless inverse order parameters ($1/S^2$) from nuclear magnetic resonance dynamics experiments [45]. Additional work from that study also specifically suggests two timescales of motion for the last C-terminal residue of this protein (Q75), one on the order of picoseconds to nanoseconds and another on the order of microseconds to milliseconds, specifically associated with outstanding conformational

changes for that residue [45]. We note, however, that our study did not probe such long timescales to observe these particular outstanding fluctuations for residue Q75, but as shall be seen shortly, nonetheless, we observed relatively good agreement between our data and the experimental order parameter data. We note that since short time MD and IS (0.01 nanosecond) simulations have thus far not revealed consistent insight into known domains of motion, that specific data is not included in this analysis. As noted previously for HIV-1 protease, since the relationship between order parameters and motility is of an inverse nature, we note that we present the inverse of the order parameters to reflect the paradigm encountered thus far where larger valued data points correspond to greater degrees of fluctuations. RMSD data and experimental order parameters are shown in Figure 10.



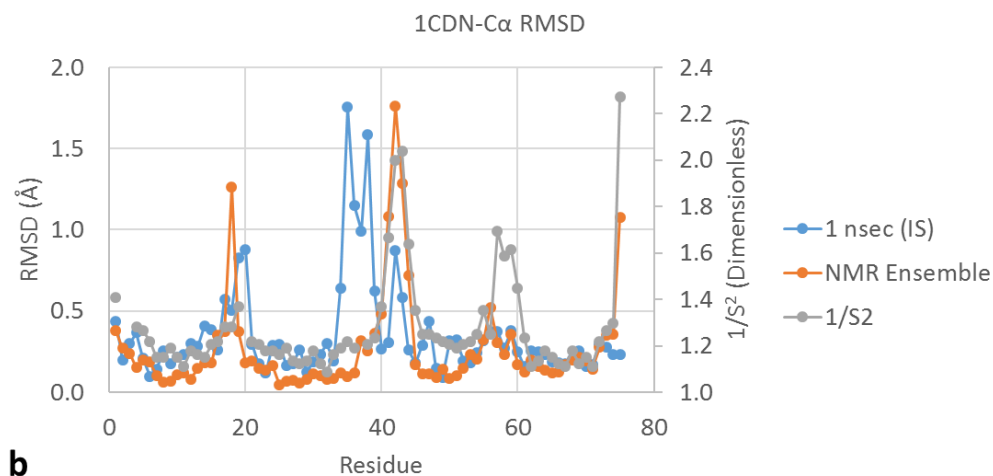


Figure 10: Simulation RMSD results data for IS, MD and inverse order parameters ($1/S^2$) as determined from nuclear magnetic resonance spectroscopy [45]. Simulation data for both 1 and 0.3 nanoseconds and inverse order parameters determined by nuclear magnetic resonance spectroscopy (NMR) (a) and simulation data for 1 nanosecond, NMR structure ensemble and inverse order parameters (b).

As can be seen in Figure 10a, there are the beginnings of what appear to be some agreement between the 1 nanosecond IS and 0.3 nanosecond MD simulations. Although rough in comparison to the 1 nanosecond profile, there are some notable maxima beginning to take shape around Lys 16, Leu 39 and the Gly 57-Gly 59 region that the MD data starts predicting which bears a budding resemblance to RMSD peaks identified by the 1 nanosecond IS data. MD RMSD maxima for these three residues are 1, 1.2 and 0.8 Å respectively. Turning to the comparison of the 0.3 nanosecond MD data to the experimental order parameter data likewise shows similar agreement. Although the Leu 19 and Gly 57 regions are captured by both MD and experiment, the experimental order parameter data identifies prominently outstanding fluctuations at Lys 41 while MD suggests a budding peak shifted at Leu 39 instead. Comparison

of the 1 nanosecond IS simulation results to the experimentally-determined order parameters (Figures 10a and 10 b) indicates that both data sets identify similar regions of pronounced motility as well. Two such regions that bear similarity are around residues Asp 19 and Lys 41. This fluctuation agreement can be seen by the overlapping maxima peaks of these regions as seen in Figure 10a. We do note that while our IS simulation predicted Glu 35 and Ser 38 as being particularly flexible, the order parameter data did not. In this regard, for this particular region, the IS and MD data were in stronger agreement since MD likewise appeared to hint at motions in this region. Similarly, the experimental data identified Gly 57-Gly 59 as being particularly motile but not the 1 nanosecond IS simulation results. We finally sought to see if there was any agreement between our structure ensemble set for the 1 nanosecond long-time simulation and the ensemble structure set determined by the NMR experiment. We should note that the aforementioned order parameter dynamic studies and the structure elucidation of generating structure ensembles that are about to be discussed are mutually exclusive processes and the implications of one do not necessarily indicate the results of the other despite the fact that both sets of data generally result from the same experiment. Since we employed 10 structures from our simulations, we likewise conducted a RMSD analysis on 10 structures from the NMR ensemble. As can be seen in Figure 10b, motility predicted by the NMR ensemble is intermediate between the 1 nanosecond IS simulation and the dynamics determined by the order parameter study. In this regard, the NMR ensemble suggests motility at Gly 18 which is in close proximity to the region of the Asp 19 fluctuations that the 1 nanosecond IS and order parameter detected. By contrast, the NMR ensemble did not identify the peak at Glu 35 identified by the 1 nanosecond simulation (nor identified by the order parameter data either, though hinted at by the MD simulation). Yet the NMR ensemble did show a relatively prominent peak at Lys 55 in

tandem with the order parameter data peak at Gly 57 which was not prominently identified by the 1 nanosecond IS simulation (although it was hinted at by the MD results).

In light of all the data thus encountered, we next sought to characterize the global RMSD profile for an IS simulated system. To examine this IS behavior, we prepared global RMSD profiles from a variety of simulation times (0.01, 0.35, 1, 2.5 and 4 nanoseconds) by averaging the RMSDs of all α -carbons for every simulation time data point. Such an example is shown in Figure 11 for both chains of A β 40 (*.pdb ID: 2M4J) with 95% confidence interval error bars.

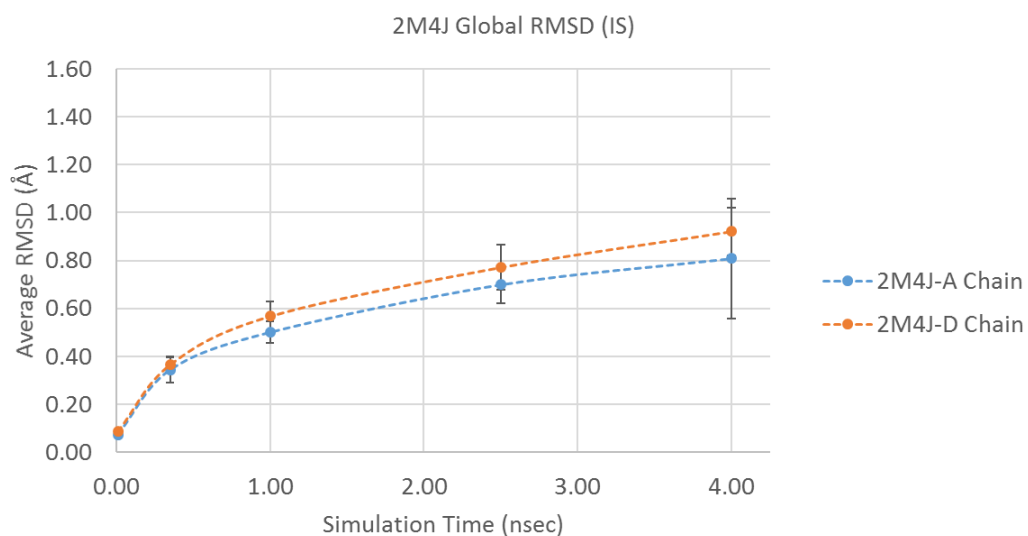


Figure 11: Global RMSD data for A β 40 (*.pdb ID: 2M4J) using data from 0.01, 0.35, 1, 2.5 and 4 nanoseconds. Error bars for 95% confidence intervals shown for the average RMSD values of each discrete time analyzed.

As Figure 11 shows, shorter simulation times produce little deviations from average RMSD values as evidenced by their smaller 95% confidence intervals. The general trend observed

previously for calbindin for MD global RMSD behavior leveling out over long time scales appears to be reproduced here as well. Although the data suggests RMSD values that continue to rise, a noticeable degree of RMSD value stabilization appears to occur at the 1 nanosecond mark. This exact behavior was also observed by Buchete, Tycko and Hummer [44] in their MD simulations of a mature A β 40 fibril composed of truncated monomer peptides (A β 9-40). These observations for these different systems may therefore suggest that the 1 nanosecond mark may indeed be an adequate time regime to begin observing relevant fluctuations as was suggested earlier for calbindin.

IVD. Conclusions:

In this study, we have presented an implicit solvent method by which protein fluctuations can be studied at a variety of different time scales. We have found that due to the implicit treatment of the host water solvent environment, we were able to obtain fluctuation data in the time regime of several nanoseconds over the course of less than one hundred (<100) CPU hours. Additionally, the IS method presented here was able to recover almost all fluctuations previously and independently identified by experimental and computational methods as found in the literature. Thus were some key regions of protein fluctuations identified through our methods that, in the case of HIV-1 protease, are even known to have a pharmaceutical significance in present drug targeting strategies thus showing potential applications for our methods in drug discovery and drug design. Such agreement between our IS results and the inverse experimental NMR order parameter data can be seen through the remarkably similar profiles between those two data sets. We additionally note particular agreement between our IS simulation results with the results of NMR experimental order parameter data for calbindin (*.pdb id: 1CDN) where our

IS RMSD profile and the profile of the inverse order parameter data were almost perfectly superimposable. Furthermore, literature acknowledgement regarding the most motile domain of endothiapepsin (Leu 155-Thr 172) was also in near perfect agreement with our own IS RMSD results data which prominently picked up on this region as an outstanding maxima of RMSD values. We also characterized the fluctuation behavior for A β 40 and A β 42 dimers which are shown to exhibit relatively small RMSD values associated with overall rigidity and stability created by multiple β strands, as seen previously [46]. Addressing the issue of whether statistical variations in the individual structure models of NMR structure ensembles communicate actual protein fluctuations, we found that they do not necessarily do so. As was seen with insulin (*.pdb id: 2HIU), the NMR ensemble over-estimated a global maximum of N-terminus motion where none has been experimentally acknowledged with the C-terminus in fact being experimentally recognized instead as the most motile domain. We also engaged the question regarding the identification of potentially suitable time regimes that would permit the simulated protein to reach an equilibrated point in its simulated fluctuations, so as to observe fluctuations that may more accurately reflect the natural physical phenomena of atomic motions. In this regard, global RMSD data analyses seems to suggest that simulating for at least 1 nanosecond may be necessary lest one obtain questionable results for want of greater protein equilibration times. The comparisons of IS and MD simulation results to dynamic NMR and other independent data may thus be an excellent tool for critically analyzing computational simulation methods and protocols for studying protein fluctuation states.

IVE. References:

(1) Kleckner IR, Foster MP. An introduction to NMR-based approaches for measuring protein dynamics. *Biochimica et Biophysica Acta* 2011;1814(8):942-968.

- (2) Zhuravlev PI, Reddy G, Straub JE, Thirumalai D. Propensity to form amyloid fibrils is encoded as excitations in the free energy landscape of monomeric proteins. *J Mol Biol* 2014;426(14):2653-2666.
- (3) Kato S, Han SY, Liu W, Otsuka K, Shibata H, Kanamaru R, et al. Understanding the function-structure and function-mutation relationships of p53 tumor suppressor protein by high-resolution missense mutation analysis. *Proc Natl Acad Sci U S A* 2003 Jul 8;100(14):8424-8429.
- (4) Antunes DA, Devaurs D, Kavarakı LE. Understanding the challenges of protein flexibility in drug design. *Expert Opin Drug Discov* 2015; Sept 28:1-13.
- (5) Henzler-Wildman KA, Lei M, Thai V, Kerns SJ, Karplus M, Kern D. A hierarchy of timescales in protein dynamics is linked to enzyme catalysis. *Nature* 2007;450(7171):913-916.
- (6) Ode H, Nakashima M, Kitamura S, Sugiura W, Sato H. Molecular dynamics simulation in virus research. *Frontiers in microbiology* 2012 July;3(258):1-9.
- (7) McCammon JA, Harvey CS. *Protein Dynamics. Dynamics of proteins and Nucleic Acids* Cambridge, UK: Cambridge University Press; 1987. p. 28-30.
- (8) Austin, Rv H., et al. "Dynamics of Ligand Binding to Myoglobin." *Biochemistry* 14.24 (1975): 5355-73.
- (9) Boehr, David D., H. Jane Dyson, and Peter E. Wright. "An NMR Perspective on Enzyme Dynamics." *Chemical reviews* 106.8 (2006): 3055-79.
- (10) Henzler-Wildman, Katherine A., et al. "A Hierarchy of Timescales in Protein Dynamics is Linked to Enzyme Catalysis." *Nature* 450.7171 (2007): 913-6.
- (11) Henzler-Wildman, Katherine A., et al. "Intrinsic Motions Along an Enzymatic Reaction Trajectory." *Nature* 450.7171 (2007): 838-44.
- (12) Wolf-Watz, Magnus, et al. "Linkage between Dynamics and Catalysis in a Thermophilic-Mesophilic Enzyme Pair." *Nature structural & molecular biology* 11.10 (2004): 945-9.
- (13) Peters MH. The Smoluchowski diffusion equation for structured macromolecules near structured surfaces. *J Chem Phys* 2000;112(12):5488-5498.
- (14) Zhang Y, Peters MH, Li Y. Nonequilibrium, multiple-timescale simulations of ligand-receptor interactions in structured protein systems. *Proteins: Structure, Function, and Bioinformatics* 2003;52(3):339-348.
- (15) Peters MH. Langevin dynamics for the transport of flexible biological macromolecules in confined geometries. *J Chem Phys* 2011;134(025105):1-11.

- (16) Peters MH. Fokker-Planck equation and the grand molecular friction tensor for coupled rotational and translational motions of structured Brownian particles near structured surfaces. *J Chem Phys* 1999;110(1):528-538.
- (17) Krall A, Brunn J, Kankanala S, Peters MH. A simple contact mapping algorithm for identifying potential peptide mimetics in protein–protein interaction partners. *Proteins: Structure, Function, and Bioinformatics* 2014;82(9):2253-2262.
- (18) Karplus M, Petsko GA. Molecular dynamics simulations in biology. *Nature* 1990 Oct 18;347(6294):631-639.
- (19) MacKerell AD, Feig M, Brooks CL. Extending the treatment of backbone energetics in protein force fields: Limitations of gas-phase quantum mechanics in reproducing protein conformational distributions in molecular dynamics simulations. *Journal of computational chemistry* 2004;25(11):1400-1415.
- (20) Anandakrishnan R, Drozdetski A, Walker RC, Onufriev AV. Speed of conformational change: comparing explicit and implicit solvent molecular dynamics simulations. *Biophys J* 2015;108(5):1153-1164.
- (21) Zakova, L., et al. "Structural Integrity of the B24 Site in Human Insulin is Important for Hormone Functionality." *The Journal of biological chemistry* 288.15 (2013): 10230-40.
- (22) Dhar A, Gruebele M. Fast relaxation imaging in living cells. *Current Protocols in Protein Science* 2011:28.1. 1-28.1. 19.
- (23) Schröder GF, Alexiev U, Grubmüller H. Simulation of fluorescence anisotropy experiments: probing protein dynamics. *Biophys J* 2005;89(6):3757-3770.
- (24) Shibata Y, Kurita A, Kushida T. Solvent effects on conformational dynamics of Zn-substituted myoglobin observed by time-resolved hole-burning spectroscopy. *Biochemistry (N Y)* 1999;38(6):1789-1801.
- (25) Shibata Y. Time-domain observation of conformational fluctuation of protein by time-resolved hole-burning spectroscopy. *Sci Prog* 1999;83(2):193-208.
- (26) Bertini I, Calderone V, Cosenza M, Fragai M, Lee YM, Luchinat C, et al. Conformational variability of matrix metalloproteinases: beyond a single 3D structure. *Proc Natl Acad Sci U S A* 2005 Apr 12;102(15):5334-5339.
- (27) Chalaoux F, O'Donoghue SI, Nilges M. Molecular dynamics and accuracy of NMR structures: effects of error bounds and data removal. *Proteins: Structure, Function, and Bioinformatics* 1999;34(4):453-463.
- (28) Andersen CA, Palmer AG, Brunak S, Rost B. Continuum secondary structure captures protein flexibility. *Structure* 2002;10(2):175-184.

- (29) Duan Y, Wu C, Chowdhury S, Lee M.C., Xiong G, Zhang W, et al. A point charge force field for molecular mechanics simulations of proteins based on condensed phase quantum mechanical calculations. *Journal of Computational Chemistry* 2003; 24(16):1999-2012.
- (30) Ramstein J, Lavery R. Energetic coupling between DNA bending and base pair opening. *Proc. Natl. Acad. Sci. U.S.A.* 1988; 85: 7231-7235.
- (31) Smith P.E., Pettitt B.M. Modeling solvent in biomolecular systems. *J. Phys. Chem.* 1994; 98: 9700-9711.
- (32) Hasel W, Hendrickson T.F., W. Clark Still. A rapid approximation to the solvent accessible surface areas of atoms. *Tetrahedron Computer Methodology.* 1988; 1: 103-116.
- (33) Kalé, L., Skeel, R., Bhandarkar, M., Brunner, R., Gursoy, A., Krawetz, N., . . . Schulten, K. (1999). NAMD2: Greater scalability for parallel molecular dynamics. *Journal of Computational Physics*, 151(1), 283-312.
- (34) Mahoney, M. W., & Jorgensen, W. L. (2000). A five-site model for liquid water and the reproduction of the density anomaly by rigid, nonpolarizable potential functions. *The Journal of Chemical Physics*, 112(20), 8910-8922.
- (35) Jorgensen, W. L., Chandrasekhar, J., Madura, J. D., Impey, R. W., & Klein, M. L. (1983). Comparison of simple potential functions for simulating liquid water. *The Journal of Chemical Physics*, 79(2), 926-935.
- (36) Martyna, G. J., Tobias, D. J., & Klein, M. L. (1994). Constant pressure molecular dynamics algorithms. *The Journal of Chemical Physics*, 101(5), 4177-4189.
- (37) Feller, S. E., Zhang, Y., Pastor, R. W., & Brooks, B. R. (1995). Constant pressure molecular dynamics simulation: The langevin piston method. *The Journal of Chemical Physics*, 103(11), 4613-4621.
- (38) Darden, T., York, D., & Pedersen, L. (1993). Particle mesh ewald: An $N \cdot \log(N)$ method for ewald sums in large systems. *The Journal of Chemical Physics*, 98(12), 10089-10092.
- (39) Echols, N., D. Milburn, and M. Gerstein. "MolMovDB: Analysis and Visualization of Conformational Change and Structural Flexibility." *Nucleic acids research* 31.1 (2003): 478-82.
- (40) Hornak, V., et al. "HIV-1 Protease Flaps Spontaneously Open and Reclose in Molecular Dynamics Simulations." *Proceedings of the National Academy of Sciences of the United States of America* 103.4 (2006): 915-20.
- (41) Freedberg, Darón I., et al. "Rapid Structural Fluctuations of the Free HIV Protease Flaps in Solution: Relationship to Crystal Structures and Comparison with Predictions of Dynamics Calculations." *Protein science* 11.2 (2002): 221-32.

(42) Sali, A., et al. "High-Resolution X-Ray Diffraction Study of the Complex between Endothiapepsin and an Oligopeptide Inhibitor: The Analysis of the Inhibitor Binding and Description of the Rigid Body Shift in the Enzyme." *The EMBO journal* 8.8 (1989): 2179-88.

(43) Pearl, Laurence, and Tom Blundell. "The Active Site of Aspartic Proteinases." *FEBS letters* 174.1 (1984): 96-101.

(44) Buchete, N., Tycko, R., & Hummer, G. (2005). Molecular dynamics simulations of alzheimer's β -amyloid protofilaments. *Journal of Molecular Biology*, 353(4), 804-821.

(45) Akke, Mikael, et al. "Effects of Ion Binding on the Backbone Dynamics of Calbindin D9k Determined by Nitrogen-15 NMR Relaxation." *Biochemistry* 32.37 (1993): 9832-44.

(46) Bastidas, O. H., et al. "Few Ramachandran Angle Changes Provide Interaction Strength Increase in Abeta42 Versus Abeta40 Amyloid Fibrils." *Scientific reports* 6 (2016): 1-10.

V. Aim 4: Inhibitor Design⁶

Abstract:

The etiology of Alzheimer's disease results from the aggregation of A β 42 peptides into oligomeric structures which are toxic to neuronal cells. Disrupting the oligomerization process early on therefore has the potential to decrease neurotoxic species and may therefore play a role in retarding the progress of Alzheimer's disease in *in vivo* systems. Here, we discuss the results of two novel inhibitors, Compound A and Compound B on their inhibition performance of A β 42. Both compounds were found to be successful in inhibiting the aggregation process by statistically significant margins and so intellectual property protection on these compounds has been sought in the form of a provisional patent application which was recently granted.

VA. Introduction:

Alzheimer's disease is a neurodegenerative disorder caused by toxic aggregate species of A β peptide that adversely affect neuronal cells and results in their death. The A β peptides are generated by enzyme proteolysis of γ -secretase of the neuronal transmembrane domain of amyloid precursor protein (APP)¹⁻³. This proteolysis results in A β peptides that can range from 38 to 42 amino acids in length with the 42 amino acid isoform being particularly known for its toxic aggregation properties⁴⁻⁶. The A β peptide monomers first aggregate as small oligomers before further aggregating into protofibril and finally full fibril structures^{4, 7, 8}. It is the mature A β 42 fibril structures that are rich in beta-sheets that further aggregate among themselves into neuritic plaques that form the hallmark of plaque structures seen in post-mortem tissue samples of central nervous system tissue affected by Alzheimer's disease⁹⁻¹². Although the macro plaque

⁶ Provisional Patent Application: O. Bastidas and M.H. Peters, Preliminary Patent Application No. PET-17-054, Virginia Commonwealth University, April 2017.

structures were initially believed to be the culprits in conveying cytotoxicity to neurons, recent work has suggested that the early oligomeric species comprised of only a few A β 42 monomers may be the real mediators of toxic properties to neuronal cells that result in declining brain function^{4, 13-16}. Nevertheless, mature fibrillar structures are known to still possess toxicity to neurons as they can serve as a reservoir source of toxic pre-fibrillar oligomers and aggregates in aggregation pathway schemes¹⁷⁻¹⁹. We therefore note that this study will focus exclusively on oligomers and oligomerization and so these terms “oligomers” and “oligomerization” will be used henceforth in describing our work.

An additional consideration to the clinical significance of the oligomer species is that evidence suggests that formation of these soluble oligomers is a critical event leading to the growth and formation of fibrils that form amyloid plaques^{4, 16, 20-24}. This relationship between one aggregate type and its subsequent follow-up species (i.e. oligomer to protofibril) has consequently been found to be fundamentally linked to a time dependence evolution spanning individual monomers aggregating to oligomers, then to protofibrils and finally to mature fibril structures⁴. Furthermore, it is generally acknowledged that the oligomer structures are spherical in nature²⁵⁻²⁷ although finer characterization of the structures at the atomic level have been unfortunately difficult to carry out^{4, 28-31} unlike the mature fibrils for which several atomic level structure characterizations are available³²⁻³⁴.

Previous characterization efforts for the clinically important oligomers has proceeded by analyzing the "macro" structure of the oligomers (at the nanometer level scale) via either electron microscopy (EM) or atomic force microscopy (AFM). A notable advantage of AFM over EM is

its ability to image samples at ambient conditions, i.e. atmospheric pressure and room temperature (thus eliminating the need to expose the sample to vacuum or electron beam), as well as affording very high spatial resolution in providing three-dimensional topographic images³⁵. Additionally, in contrast to other alternative established microscopy techniques, AFM allows for imaging without the need for stains or fixatives. In this regard, AFM has been particularly useful for analyzing oligomer heights and has already provided insight into structure morphology for both oligomers and fibrils^{4, 35, 36}. The technique has found particular utility in assaying the effectiveness of proposed inhibitor compounds as carried out by Mastrangelo et al.⁴ by examining oligomer heights of A β 42 in the absence and presence of peptide inhibitors. In this study we propose two potential inhibitors of A β 42 fibril formation based on all-atom inter-protein energy landscape mappings of A β 42 amyloid fibril structures.³⁷ These two compounds, referred to as Compounds A and B here (Bastidas and Peters, 2017), were experimentally tested with A β 42 in *in vitro* oligomer formation studies using AFM following the protocol of Mastrangelo et al.⁴. It is demonstrated that these compounds can inhibit oligomer formation in a dose-dependent manner and on an approximate equimolar ratio of inhibitor to A β 42 aggregate monomer.

We also remark that A β 42 oligomers have previously been targeted with inhibitors designed to engage a variety of locations on A β 42 monomers. Table 1 lists a variety of such inhibitors that have shown varying degrees of success in preventing the formation of oligomer structures. This list is by no means exhaustive of inhibitor compounds that have been and continue to presently be developed.

Table 1: Examples of inhibitors for Alzheimer disease fibril and oligomer formation.

Research Group Source	Based on A β 42 Residue Region
Mastrangelo et al. [4]	32-39 (A β 42)
Takahashi, Mihara [37]	16-20, 17-21; respectively (A β 42)
Hetenyi et al. [38]	38-42; for both (A β 42)
Fulop, Zarandi, Datki, Soos, Penke [39]	31-35 (A β 42)
Hughes, Burke, Doig [40]	25-35 (A β 42)

The development of such inhibitor compounds (though not known to be presently commercially available) is an illustration that A β 42 has potential target regions, or non-covalent interaction hot-spots, that are druggable and that have been previously investigated and exploited. We also note that these inhibitors have been developed by some random combinatorial method that did not reflect more rational computational analyses.

A final consideration we raise is the issue of any successful inhibitor compounds that show promise as potential pharmaceutical agents reaching the brain. Doing so requires a successful crossing of the blood brain barrier (BBB) by the molecular species, preferably, by the least invasive means possible. As consideration to this, we give a more detailed description of the BBB in Appendix F where we discuss its properties and general schematic of operation.

VB. Materials and Methods:

A β 42 Characterization: The first step was to obtain a detailed characterization of the A β 42 non-covalent interactions at the atomic level to identify potential regions in the peptide that might be amenable to drug targeting. We thus consulted the results of our energy mappings on A β 42 wherein we identified specific regions of exceptionally strong hydrogen bonding between

vicinal peptide monomers.³⁷ Specifically, these regions were found to be caused by Ramachandran angle values of ϕ and ψ that resulted in a more vertical orientation of certain peptide planes, especially, compared to the A β 40 isoform. Since the amide hydrogens and carbonyl oxygens of the peptide planes of A β 42 were more vertical in their respective peptide monomer stacks, the inter-atomic distance between these species were found to be shorter and so partial-charge interaction forces were stronger between these atoms. These regions of increased hydrogen bond interaction strength therefore served as potential drug targets for the study henceforth described.

Inhibitor Compounds: Compounds A and B inhibitors are peptide-based and they are a few residues or less in length in order to maximize the potential to cross the BBB. We direct the reader to Appendix G for a discussion of the unique considerations and challenges associated with using peptides as drugs.

A β 42 Preparation: A β 42 peptide was purchased from Genscript (China). PBS solution used was Dulbecco's phosphate buffered saline (DPBS) with calcium chloride and magnesium chloride purchased from Sigma-Aldrich (St. Louis, MO). Ionic solute concentrations were: 0.905 mM CaCl₂ • 2H₂O, 0.492 mM MgCl₂ • 6H₂O, 2.683 mM KCl, 1.470 mM KH₂PO₄, 136.885 mM NaCl and 8.101 mM Na₂HPO₄. Potential A β 42 aggregate inhibitors were also synthesized by outside sources. Glacial acetic acid for a negative control study was likewise purchased from Sigma-Aldrich, as oligomerization is known to be inhibited in acidic conditions^{42, 43}. All forthcoming solutions described were thus prepared with DPBS. Stock solutions of peptide, inhibitors and acetic acid were first prepared and a total of 8 reaction

solutions were established in 8 wells of a 96 well plate with each well containing a total reaction volume of 100 μ L. The 8 samples corresponded to positive and negative controls of A β 42 in DPBS and A β 42 in an acetic acid/DPBS solution respectively as well as varying inhibitor concentrations of 10 μ M, 50 μ M, and 100 μ M for both compound A and compound B inhibitors. All 8 well plates contained a standard 50 μ M concentration of A β 42 peptide and the acetic acid/DPBS reaction well was set to a pH of 3.3 as this was found to be an optimum pH for inhibiting A β 42 peptide aggregation⁴². The well plate reaction volumes were then allowed to incubate under ambient conditions (25 °C, 1 atm) for 45 minutes with gentle agitation. This experimental setup is summarized in Table 2 and schematically represented in Figure 1. An empirical curve for determining the pH dependency on DPBS/acetic acid ratios is found in Appendix G and was employed for this portion of the study.

Table 2: Experimental data collection setup.

Experimental Parameters	Modified Mastrangelo ⁴ Method
Time	45 minutes
Inhibitor Concentration	10 μ M, 50 μ M & 100 μ M
A β 42 Concentration	50 μ M
Solvent	DPBS
Temperature	25 °C
Positive Control	A β 42 in DPBS
Negative Control	Acetic acid, pH=3.3
Expected Oligomer Height	nm scale

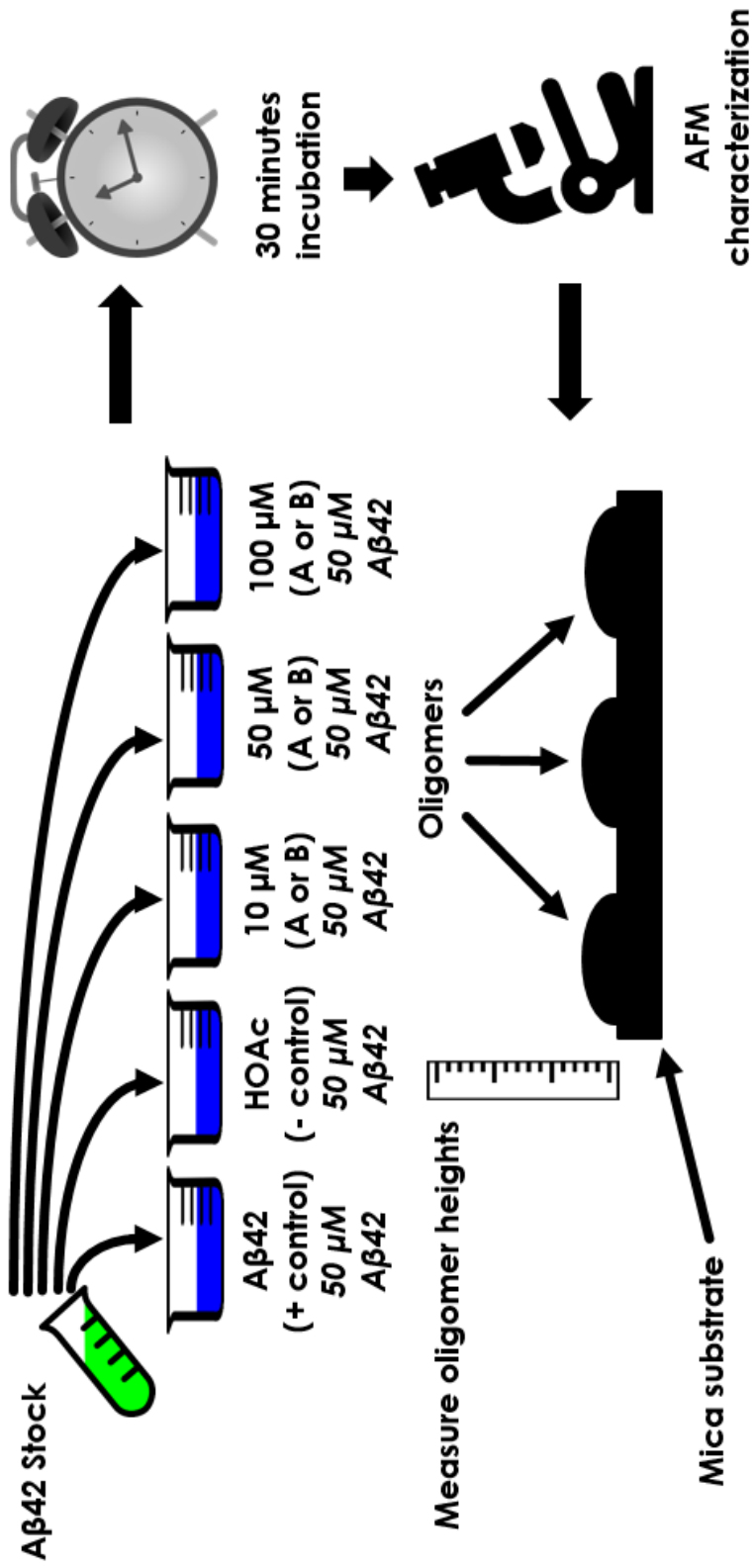


Figure 1: Process flow diagram of experimental set up and procedure.

First, inhibitor stock solutions for Compounds A (1 mg inhibitor and 19.21 mL DPBS) and B (2 mg inhibitor and 68.40 DPBS) are each prepared. From these stock solutions, volumes of 5, 25 and 50 μL are each pipetted into three wells of a 96 well plate (these volumes are applicable to both Compounds A and B). This is schematically represented by the blue volumes in Figure 1. Next, 45 and 25 μL of DPBS are pipetted into the 5 and 25 μL inhibitor volumes respectively. At this point, from a 2.4% by volume of glacial acetic acid in DPBS stock solution, 50 μL of that acetic acid/DPBS solution is pipetted into a new well to serve as the negative control. 50 μL of DPBS is pipetted into another clean well to serve as the positive control. At this point, An A β 42 stock solution is then prepared (2mg A β 42 and 4.43 mL DPBS) from which 50 μL are then pipetted into each of the wells just described. This is schematically represented as the green vial in Figure 1. The total reaction volumes are therefore 100 μL in each well and there are thus 8 total samples for subsequent testing, as identified by their unique reagent: 1) 5 μL of Compound A, 2) 5 μL of Compound B, 3) 25 μL of Compound A, 4) 25 μL of Compound B, 5) 50 μL of Compound A, 6) 50 μL of Compound B, 7) positive control and 8) negative control at a final pH of 3.3. It is important to note that the inhibitor reaction volumes/wells at this point thus contain 10, 50 and 100 μM concentrations of both Compounds A and B inhibitor as corresponding to the 5, 25 and 50 μL inhibitor volumes respectively. The well plate is then incubated at ambient conditions (25 $^{\circ}\text{C}$, 1 atm) for 30 minutes before being assayed by AFM for oligomer heights.

It is important to note that the A β 42 peptides employed in this study were click peptides which are peptide species with a strategically-placed O-acyl moiety replacing a naturally-occurring N-acyl bond in the native peptide. The resulting peptide, known as an O-acyl isopeptide, exhibits enhanced solubility and minimal peptide self-assembly due to a reduction in

inter-molecular hydrogen bond interactions between peptide chains. By adjusting the final reaction volume pH to ≥ 7.4 , a rapid O \rightarrow N inter-molecular acyl migration rapidly converts the insoluble click peptide to its soluble native form wherein the O-acyl bond converts to an N-acyl bond. No byproducts are released making the click peptide advantageous for both *in vivo* and *in vitro* experiments. This line of A β 42 was therefore specifically used for this study to prevent premature oligomerization of A β 42 until placement into the well plate reaction volumes where slightly alkaline pHs were to be found upon addition of all listed reagents.

AFM Specimen Preparation: AFM was used to assay oligomer height of specimens mounted on freshly cleaved mica chips purchased from Ted Pella (Redding, CA). Droplets of 5 μ L of the various sample solutions were deposited on the mica substrates, 1 mica chip for each sample, for a total of 8 mica chips. The droplets were then left to dry at room temperature for 5 minutes. In order to minimize the background of salts from the DPBS, the mica chips were rinsed with deionized-distilled water following the complete drying of the specimen droplets. The chips were then left to dry for an additional 5-10 minutes to eliminate water from the rinsing. Chips with no analyte and chips initially loaded with DPBS but then rinsed with water (henceforth referred to as DPBS-rinsed mica) were also prepared as mica controls to compare with actual specimen results so as to establish expected surface morphologies for actual specimens and rule out those morphologies that may be associated with bare mica or residual DPBS remaining after rinsing. Sample imaging was carried out on a Veeco Dimension Icon AFM instrument using tapping mode with cantilever tips by Veeco, model TESP, with a frequency range of 312-347 kHz.

VC. Results and Discussion:

Of the two inhibitors, compound A and compound B, compound B was found to be the most effective in diminishing oligomer size throughout the incubation period. Clean mica and DPBS-rinsed mica yielded statistically indistinguishable reduced (short) surface morphologies. This was followed by the acetic acid negative control (pH=3.3) which was found to be effective in maintaining short A β 42 oligomer heights that were statistically distinct from the clean mica and DPBS-rinsed substrates. Three scans were taken for each chip sample on three different locations of the chip to obtain a statistical portrait of oligomer size. Data for average oligomer sizes/surface morphologies are thus shown in Figure 1 along with 95% confidence intervals for each sample. Experimental results of oligomer heights under the different experimental conditions are displayed in Figures 2-4.

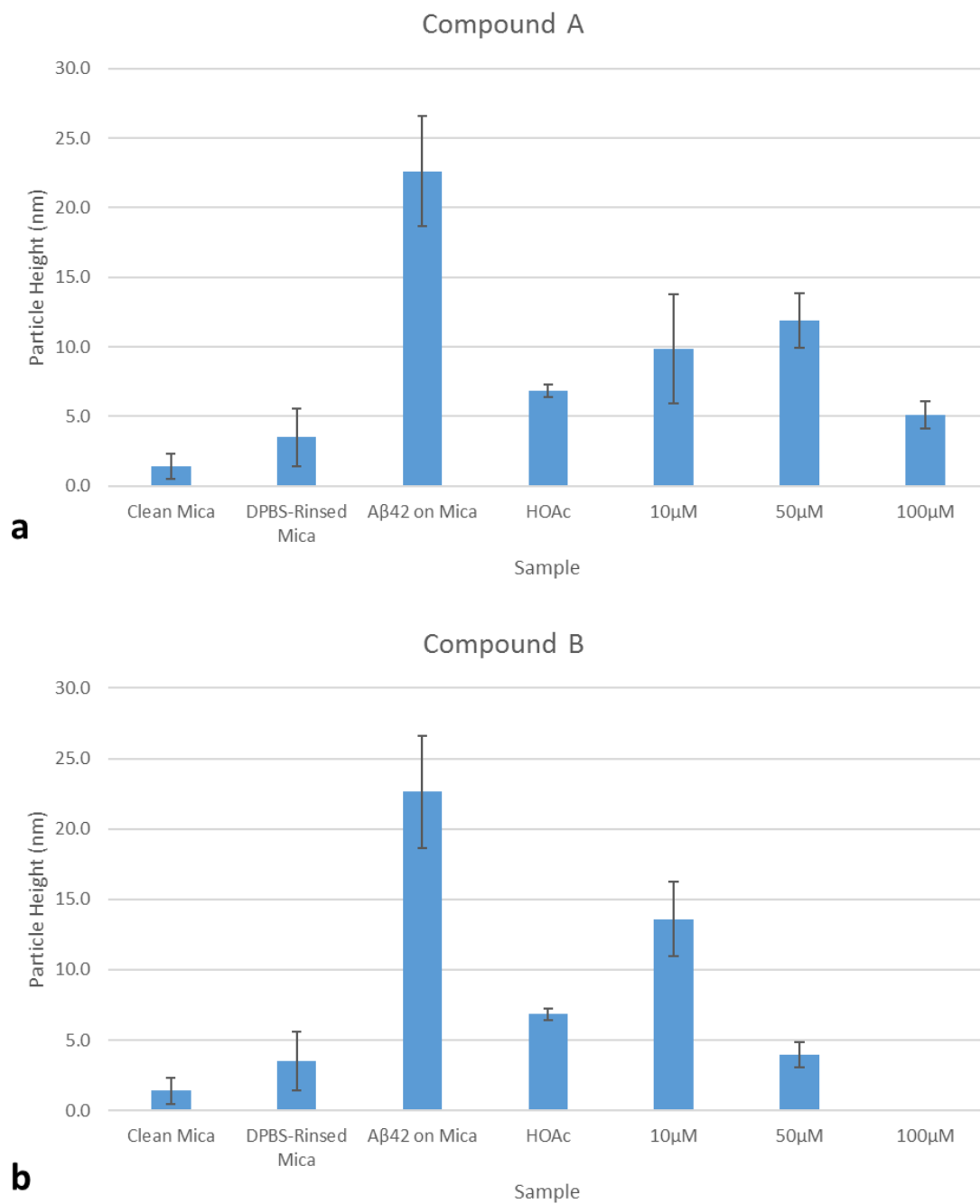


Figure 1: Surface morphology/particle heights for various concentrations of compound A (a) and compound B (b). 95% confidence intervals shown for three different scans of distinct regions of the mica chip substrate.

As expected, oligomer sizes were largest for A β 42/DPBS solutions with heights being 22.6 \pm 4.0 nm for this sample. A β 42/DPBS sample also had the greatest variability in oligomer heights (as given by the magnitude of its 95% confidence interval margin of error) and its lower limit did not overlap with any inhibitor samples' 95% confidence interval range thus demonstrating the efficacy of both inhibitors in exercising a statistically significant effect on reducing oligomer sizes. There was statistical overlap, however, involving oligomer heights for the various compound A-tested samples thus making the specific effect on reducing oligomer sizes by varying inhibitor concentrations somewhat difficult to conclude upon for compound A (Figure 1a). Compound B, on the other hand, exhibited clear statistical differentiation for the different inhibitor concentrations with no observed oligomers for the highest inhibitor concentration, 100 μ M (Figure 1b). Representative images for all 8 samples are shown in Figures 2-4.

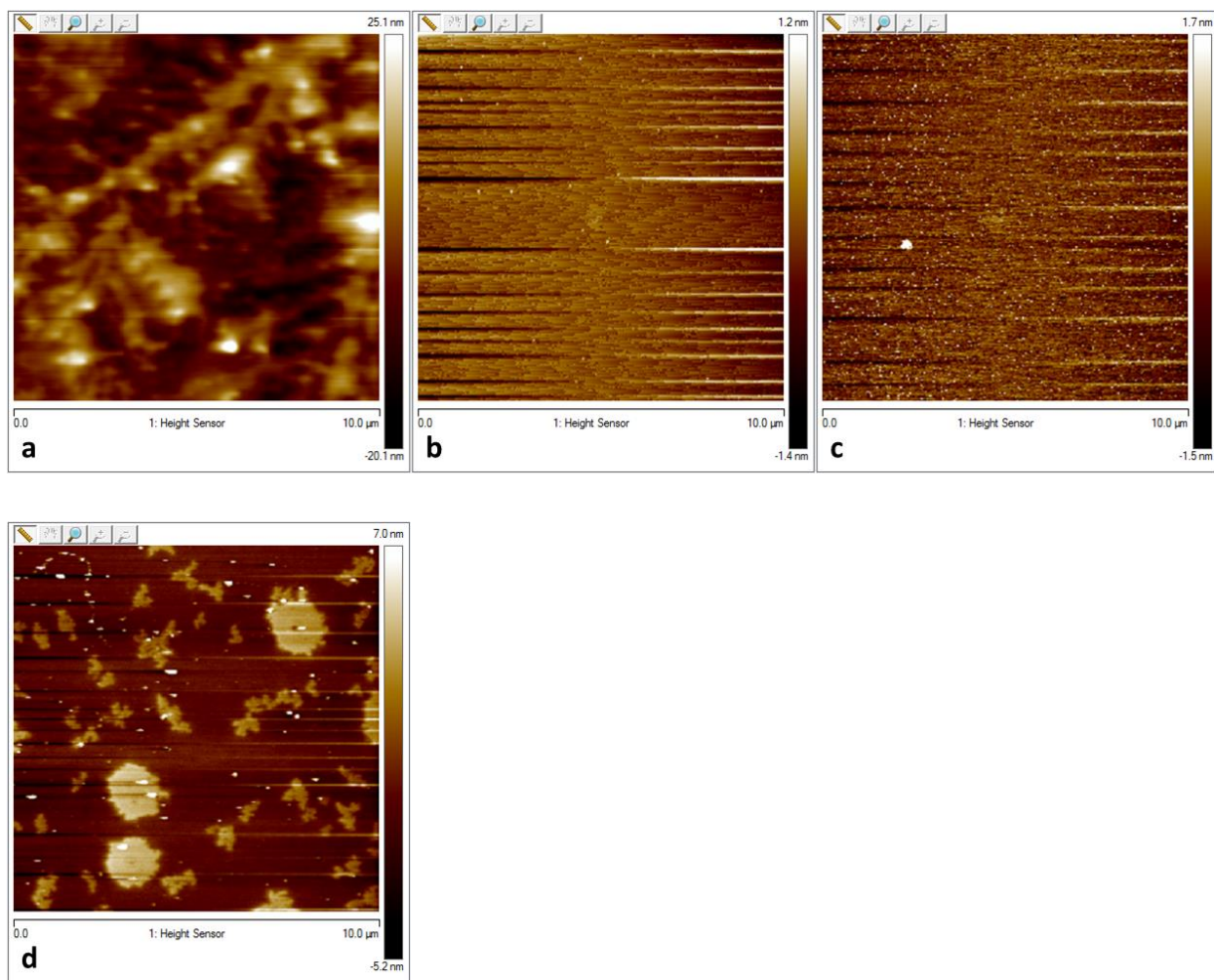


Figure 2: Control images for 50 μM Aβ42 with no inhibitor (a), clean mica chip (b), DPBS-rinsed mica chip (c) and 50 μM Aβ42 with acetic acid at pH=3.3 (d).

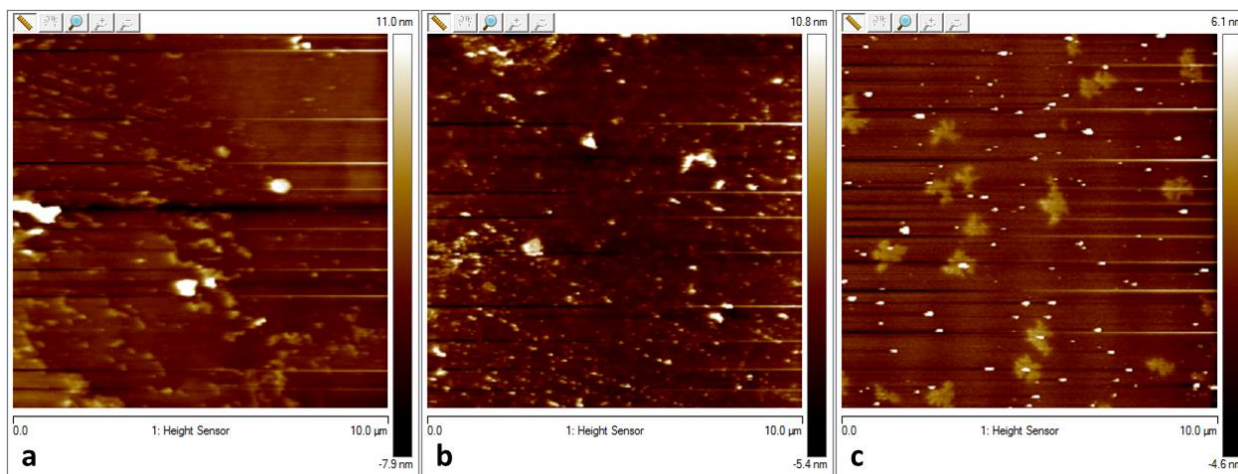


Figure 3: Oligomer size images for Compound A with inhibitor concentrations of 10 μM (a), 50 μM (b) and 100 μM (c).

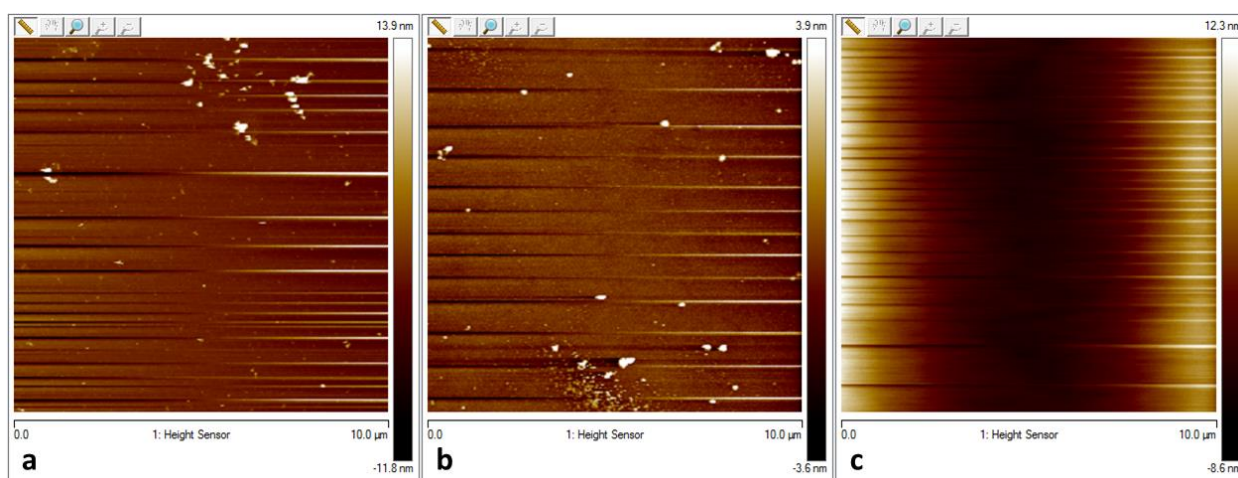


Figure 4: Oligomer size images for Compound B with inhibitor concentrations of 10 μM (a), 50 μM (b) and 100 μM (c).

In all, lateral size and height distributions of oligomers were regular for each sample assayed indicating a consistent inhibitory effect on A β 42 monomers throughout each respective reaction solution volume. We note that the surface morphology profile for compound B at 100 μ M appeared to be due to the mica substrate itself as opposed to actual oligomerization of monomer. It is interesting to note that particle sizes reported by Mastrangelo et al. were smaller overall with their maximum oligomer heights, in the absence of their inhibitor, being around 6 nanometers tall. Additionally, the concentration ratio of A β 42 to inhibitor used by Mastrangelo et al. was 1:20 which far exceeded our highest ratio of A β 42 to inhibitor which was 1:2. We also note that the results of the range of near equimolar concentrations of inhibitors that we used on oligomer size are indicative of possible 1:1 Langmuir binding of the inhibitor to A β 42 monomer. Lastly, we note that the horizontal lines seen in Figures 3 and 4 are artifacts due to imperfect tracking during the AFM cantilever tip scanning process.

VD. Conclusions:

Two inhibitor compounds, compound A and compound B, were proposed as potential oligomerization inhibitors for the pathogenic A β 42 peptide, the etiological agent responsible for Alzheimer's disease. Both inhibitors were found to be successful in hindering oligomerization of A β 42 as verified by AFM in a preliminary *in vitro* study. Compound B was found to be the most effective inhibitor as gauged by the smaller oligomer sizes it produced and its increasing concentration was correlated to statistically significant decreasing oligomer heights. This particular observation was in contrast to compound A whose increasing concentrations of inhibitor did not appear to have a statistically significant effect on reducing oligomer sizes although oligomer sizes were reduced by presence of this inhibitor nonetheless. As expected, a

positive control of A β 42 without inhibitor produced oligomer structures of greatest size and a negative control inhibitor of acetic acid at a pH of 3.3 was effective at suppressing oligomerization, although not as effective as the compound B inhibitor. Both these controls, however, served to provide a benchmark for gauging the success of both compound A and B inhibitors. It is to be noted that these *in vitro* experimental studies are very preliminary and further studies would be needed to explore any potential clinical or pre-clinical applications. These studies would include, for example, the use of “nonsense” inhibitors and other proposed inhibitors as controls/references along with collaborative experimental methods such as dynamic light scattering (DLS) and repeat AFM runs to help verify oligomer size data.

VE. References:

- (1) O'Brien RJ, Wong PC. Amyloid precursor protein processing and Alzheimer's disease. *Annu Rev Neurosci* 2011;34:185-204.
- (2) Selkoe, D. J. (2001). Presenilin, notch, and the genesis and treatment of alzheimer's disease. *Proceedings of the National Academy of Sciences of the United States of America*, 98(20), 11039-11041.
- (3) Hardy, J., & Selkoe, D. J. (2002). The amyloid hypothesis of alzheimer's disease: Progress and problems on the road to therapeutics. *Science (New York, N.Y.)*, 297(5580), 353-356.
- (4) Mastrangelo, I. A., Ahmed, M., Sato, T., Liu, W., Wang, C., Hough, P., & Smith, S. O. (2006). High-resolution atomic force microscopy of soluble A β 42 oligomers. *Journal of Molecular Biology*, 358(1), 106-119.
- (5) Selkoe, D. J. (2001). Alzheimer's disease: Genes, proteins, and therapy. *Physiological Reviews*, 81(2), 741-766.
- (6) Selkoe, D. J. (2004). Cell biology of protein misfolding: The examples of alzheimer's and parkinson's diseases. *Nature Cell Biology*, 6(11), 1054-1061.
- (7) Walsh, D. M., Hartley, D. M., Kusumoto, Y., Fezoui, Y., Condron, M. M., Lomakin, A., . . . Teplow, D. B. (1999). Amyloid beta-protein fibrillogenesis. structure and biological activity of protofibrillar intermediates. *The Journal of Biological Chemistry*, 274(36), 25945-25952.

- (8) Walsh, D. M., Lomakin, A., Benedek, G. B., Condron, M. M., & Teplow, D. B. (1997). Amyloid β -protein fibrillogenesis detection of a protofibrillar intermediate. *Journal of Biological Chemistry*, 272(35), 22364-22372.
- (9) Chiti F, Dobson CM. Protein misfolding, functional amyloid, and human disease. *Annu Rev Biochem* 2006;75:333-366.
- (10) Gravina, S. A., Ho, L., Eckman, C. B., Long, K. E., Otvos, L., Jr, Younkin, L. H., . . . Younkin, S. G. (1995). Amyloid beta protein (A beta) in alzheimer's disease brain. biochemical and immunocytochemical analysis with antibodies specific for forms ending at A beta 40 or A beta 42(43). *The Journal of Biological Chemistry*, 270(13), 7013-7016.
- (11) Roher, A. E., Lowenson, J. D., Clarke, S., Woods, A. S., Cotter, R. J., Gowing, E., & Ball, M. J. (1993). Beta-amyloid-(1-42) is a major component of cerebrovascular amyloid deposits: Implications for the pathology of alzheimer disease. *Proceedings of the National Academy of Sciences of the United States of America*, 90(22), 10836-10840.
- (12) Iwatsubo, T., Odaka, A., Suzuki, N., Mizusawa, H., Nukina, N., & Ihara, Y. (1994). Visualization of A β 42 (43) and A β 40 in senile plaques with end-specific A β monoclonals: Evidence that an initially deposited species is A β 42 (43). *Neuron*, 13(1), 45-53.
- (13) Gong, Y., Chang, L., Viola, K. L., Lacor, P. N., Lambert, M. P., Finch, C. E., . . . Klein, W. L. (2003). Alzheimer's disease-affected brain: Presence of oligomeric A beta ligands (ADDLs) suggests a molecular basis for reversible memory loss. *Proceedings of the National Academy of Sciences of the United States of America*, 100(18), 10417-10422.
- (14) Ahmed, M., Davis, J., Aucoin, D., Sato, T., Ahuja, S., Aimoto, S., . . . Smith, S. O. (2010). Structural conversion of neurotoxic amyloid-[beta] 1-42 oligomers to fibrils. *Nature Structural & Molecular Biology*, 17(5), 561-567.
- (15) Walsh, D. M., Klyubin, I., Fadeeva, J. V., Cullen, W. K., Anwyl, R., Wolfe, M. S., . . . Selkoe, D. J. (2002). Naturally secreted oligomers of amyloid β protein potently inhibit hippocampal long-term potentiation in vivo. *Nature*, 416(6880), 535-539.
- (16) Dahlgren, K. N., Manelli, A. M., Stine, W. B., Baker, L. K., Krafft, G. A., & LaDu, M. J. (2002). Oligomeric and fibrillar species of amyloid- β peptides differentially affect neuronal viability. *Journal of Biological Chemistry*, 277(35), 32046-32053.
- (17) Knowles, T. P., Vendruscolo, M., & Dobson, C. M. (2014). The amyloid state and its association with protein misfolding diseases. *Nature Reviews Molecular Cell Biology*, 15(6), 384-396.
- (18) Knowles, T. P., Waudby, C. A., Devlin, G. L., Cohen, S. I., Aguzzi, A., Vendruscolo, M., . . . Dobson, C. M. (2009). An analytical solution to the kinetics of breakable filament assembly. *Science (New York, N.Y.)*, 326(5959), 1533-1537.

- (19) Collins, S. R., Douglass, A., Vale, R. D., & Weissman, J. S. (2004). Mechanism of prion propagation: Amyloid growth occurs by monomer addition. *PLoS Biol*, 2(10), e321.
- (20) Hartley, D. M., Walsh, D. M., Ye, C. P., Diehl, T., Vasquez, S., Vassilev, P. M., . . . Selkoe, D. J. (1999). Protofibrillar intermediates of amyloid beta-protein induce acute electrophysiological changes and progressive neurotoxicity in cortical neurons. *The Journal of Neuroscience : The Official Journal of the Society for Neuroscience*, 19(20), 8876-8884.
- (21) Lambert, M. P., Barlow, A. K., Chromy, B. A., Edwards, C., Freed, R., Liosatos, M., . . . Klein, W. L. (1998). Diffusible, nonfibrillar ligands derived from Abeta1-42 are potent central nervous system neurotoxins. *Proceedings of the National Academy of Sciences of the United States of America*, 95(11), 6448-6453.
- (22) Kuo, Y. M., Emmerling, M. R., Vigo-Pelfrey, C., Kasunic, T. C., Kirkpatrick, J. B., Murdoch, G. H., . . . Roher, A. E. (1996). Water-soluble abeta (N-40, N-42) oligomers in normal and alzheimer disease brains. *The Journal of Biological Chemistry*, 271(8), 4077-4081.
- (23) McLean, C. A., Cherny, R. A., Fraser, F. W., Fuller, S. J., Smith, M. J., Bush, A. I., & Masters, C. L. (1999). Soluble pool of A β amyloid as a determinant of severity of neurodegeneration in alzheimer's disease. *Annals of Neurology*, 46(6), 860-866.
- (24) Lue, L., Kuo, Y., Roher, A. E., Brachova, L., Shen, Y., Sue, L., . . . Rogers, J. (1999). Soluble amyloid β peptide concentration as a predictor of synaptic change in alzheimer's disease. *The American Journal of Pathology*, 155(3), 853-862.
- (25) Huang, T. J., Yang, D., Plaskos, N. P., Go, S., Yip, C. M., Fraser, P. E., & Chakrabartty, A. (2000). Structural studies of soluble oligomers of the alzheimer β -amyloid peptide. *Journal of Molecular Biology*, 297(1), 73-87.
- (26) Kaye, R., Head, E., Thompson, J. L., McIntire, T. M., Milton, S. C., Cotman, C. W., & Glabe, C. G. (2003). Common structure of soluble amyloid oligomers implies common mechanism of pathogenesis. *Science (New York, N.Y.)*, 300(5618), 486-489.
- (27) Lashuel, H. A., Hartley, D. M., Petre, B. M., Wall, J. S., Simon, M. N., Walz, T., & Lansbury, P. T. (2003). Mixtures of wild-type and a pathogenic (E22G) form of A β 40 in vitro accumulate protofibrils, including amyloid pores. *Journal of Molecular Biology*, 332(4), 795-808.
- (28) Luhrs, T., Ritter, C., Adrian, M., Riek-Loher, D., Bohrmann, B., Dobeli, H., . . . Riek, R. (2005). 3D structure of alzheimer's amyloid-beta(1-42) fibrils. *Proceedings of the National Academy of Sciences of the United States of America*, 102(48), 17342-17347.
- (29) Olofsson, A., Sauer-Eriksson, A. E., & Ohman, A. (2006). The solvent protection of alzheimer amyloid-beta-(1-42) fibrils as determined by solution NMR spectroscopy. *The Journal of Biological Chemistry*, 281(1), 477-483.

- (30) Masuda, Y., Uemura, S., Ohashi, R., Nakanishi, A., Takegoshi, K., Shimizu, T., . . . Irie, K. (2009). Identification of physiological and toxic conformations in A β 42 aggregates. *Chembiochem*, 10(2), 287-295.
- (31) Sakono, M., & Zako, T. (2010). Amyloid oligomers: Formation and toxicity of A β oligomers. *The FEBS Journal*, 277(6), 1348-1358.
- (32) Xiao, Y., Ma, B., McElheny, D., Parthasarathy, S., Long, F., Hoshi, M., . . . Ishii, Y. (2015). A [beta](1-42) fibril structure illuminates self-recognition and replication of amyloid in alzheimer's disease. *Nature Structural & Molecular Biology*, 22(6), 499-505.
- (33) Walti, M. A., Ravotti, F., Arai, H., Glabe, C. G., Wall, J. S., Bockmann, A., . . . Riek, R. (2016). Atomic-resolution structure of a disease-relevant abeta(1-42) amyloid fibril. *Proceedings of the National Academy of Sciences of the United States of America*, 113(34), E4976-E4984.
- (34) Colvin, M. T., Silvers, R., Ni, Q. Z., Can, T. V., Sergeyev, I., Rosay, M., . . . Linse, S. (2016). Atomic resolution structure of monomorphic A β 42 amyloid fibrils. *Journal of the American Chemical Society*, 138(30), 9663-9674.
- (35) Stine, W., Snyder, S., Ladrör, U., Wade, W., Miller, M., Perun, T., . . . Krafft, G. (1996). The nanometer-scale structure of amyloid- β visualized by atomic force microscopy. *Journal of Protein Chemistry*, 15(2), 193-203.
- (36) Roher, A. E., Chaney, M. O., Kuo, Y., Webster, S. D., Stine, W. B., Haverkamp, L. J., . . . Krafft, G. A. (1996). Morphology and toxicity of A β -(1-42) dimer derived from neuritic and vascular amyloid deposits of alzheimer's disease. *Journal of Biological Chemistry*, 271(34), 20631-20635.
- (37) Bastidas, O. H., Green, B., Sprague, M., & Peters, M. H. (2016). Few ramachandran angle changes provide interaction strength increase in Abeta42 versus Abeta40 amyloid fibrils. *Scientific Reports*, 6 (2016).
- (38) Takahashi T, Mihara H. Peptide and protein mimetics inhibiting amyloid β -peptide aggregation. *Acc Chem Res* 2008;41(10):1309-1318.
- (39) Hetényi C, Szabó Z, Klement É, Datki Z, Körtvélyesi T, Zarándi M, et al. Pentapeptide amides interfere with the aggregation of β -amyloid peptide of Alzheimer's disease. *Biochem Biophys Res Commun* 2002;292(4):931-936.
- (40) Fülöp L, Zarándi M, Datki Z, Soós K, Penke B. β -Amyloid-derived pentapeptide RIIGL a inhibits A β 1–42 aggregation and toxicity. *Biochem Biophys Res Commun* 2004;324(1):64-69.
- (41) Hughes E, Burke RM, Doig AJ. Inhibition of toxicity in the beta-amyloid peptide fragment beta -(25-35) using N-methylated derivatives: a general strategy to prevent amyloid formation. *J Biol Chem* 2000 Aug 18;275(33):25109-25115.

(42) Wood, S. J., Maleeff, B., Hart, T., & Wetzel, R. (1996). Physical, morphological and functional differences between pH 5.8 and 7.4 aggregates of the alzheimer's amyloid peptide A β . *Journal of Molecular Biology*, 256(5), 870-877.

(43) Fraser, P. E., Nguyen, J. T., Surewicz, W. K., & Kirschner, D. A. (1991). pH-dependent structural transitions of alzheimer amyloid peptides. *Biophysical Journal*, 60(5), 1190-1201.

O. Bastidas and M.H. Peters, Preliminary Patent Application No. PET-17-054, Virginia Commonwealth University, April 2017.

VI. Future Work:

Future work on the studies featured in this thesis will attempt to refine the methods and data obtained and in general, take the studies to the next level in scientific inquiry. Notable areas for which we foresee opportunities to apply future work are in Aims 3 and 4.

For Aim 3, we note that the implicit solvent code can potentially be optimized to cut down on processing times while maintaining computational equivalence so that the algorithm provides results in a shorter period of time. Additionally, for Aim 3, we would like to investigate the causes for the minor discrepancies observed between the implicit solvent RMSD results and the literature data. Despite very impressive agreement currently observed between the two methods, being able to identify factors that lead to differing RMSD maxima values, shifts (or absences) and even profile shapes, would be extremely informative for the application of our implicit solvent method to the rigorous study of protein dynamics in general. For Aim 3, we also intend to calculate order parameters (S^2) from the implicit solvent simulations according to the paradigm previously established for the decay of fluorescence polarization anisotropy [1] to see how these values compare to both the experimental order parameters as well as the calculated α -carbon RMSDs. Using IS to study dynamic changes leading to dihedral angle shifts determined in Aim 2 may shed light on amyloid fibril formation.

For Aim 4, we note that carrying out further duplicate experiments will be necessary to obtain a more statistically significant data set of the results presently observed. Additionally, we would like to include more controls in our experimental testing specifically using nonsense peptides. We would also like to include further additional characterization methods, such as

dynamic light scattering and FTIR, in the analysis of A β 42 controls and with our inhibitors. Should such a battery of tests prove fruitful, then we would like to see our inhibitor candidates proceed to further *in vitro* then the appropriate animal studies.

VIA. References:

(1) Ying, Ruoxian, and Michael H. Peters. "Brownian Dynamics Simulation of Rotational Correlation Functions for a three-body Macromolecular Model." *The Journal of chemical physics* 95.2 (1991): 1234-41.

VII. Thesis Summary:

In all, this thesis has aspired to address questions pertinent to the phenomena of protein fluctuations and dynamics, specifically, in developing methods to better understand and study these phenomena. To that end, the contents of this thesis were subdivided into four distinct aims.

Aim 1 sought to develop a protocol by which an ensemble of protein structures, such as those commonly encountered from protein NMR spectroscopy, can be analyzed to obtain informative energy mapping data of the potential energy landscape within a protein. Additionally, Aim 1 also sought to determine the minimum data set of ensemble structure members necessary to obtain statistically meaningful results. The results of this deliverable have materialized in the form of an algorithm especially designed to handle energy mapping output data from individual protein structures so that a collection of mapping output results of individual structures can be analyzed and organized so that only those atom-atom interactions that survive across all ensemble members (energetic "hot-spots") are thus identified. A margin of error analysis provided us with the conclusion that 10 ensemble structures were sufficient to obtain this mapping information.

Aim 2 then sought to apply this method to a case study characterization of A β 40 and A β 42 to see if any insight could be gained regarding differences in aggregation propensities between the two A β strains. Indeed, we were able to identify unique energy hot-spot profiles between these two isoforms which were linked to statistically significant differences in binding energies, and inter-atomic distances, between the two species. Furthermore, we were able to trace the causes of the differences of the interaction energies to differences in Ramachandran angle values between the two isoforms wherein A β 42 peptide planes were observed to be more vertical in nature resulting in reduced distances between hydrogen bonding atoms of neighboring A β 42 monomers. These unique peptide plane orientations thus led to increased attractive energies between neighboring A β 42 monomer chains and hence the observed interaction energy differences.

Aim 3's objective centered on determining whether or not our previously developed implicit solvent algorithm could recover fluctuation data identified by previous computational and experimental studies. Additionally, Aim 3 sought to see if the statistical variation in atomic positions of NMR structure ensembles capture true protein fluctuations. Results showed that the implicit solvent model was indeed able to recover known domain motion identified in the literature. Most encouraging was the high degree of similitude between the dynamic NMR order parameter data sets (S^2) and our own RMSD data for systems that had this detailed experimental data available. It should be noted that there were some nuanced differences observed nonetheless between the results of the two methods. Results of analyzing the NMR structure ensembles showed that the ensembles do not correlate well with known regions of outstanding motion. For example, the NMR structure ensemble for insulin suggested that the N-terminus of

that protein was the most motile domain, whereas experimental dynamic NMR data indicated the C-terminus as exhibiting the greatest motions (our implicit solvent RMSD data was in agreement with the literature data).

Lastly, Aim 4 attempted to reconcile the information specifically gleaned from A β 42 obtained from Aims 2 and 3 to see if an inhibitor compound for that system could be designed and then tested *in vitro*. Two inhibitors were proposed and subsequently tested via atomic force microscopy (AFM) for reduced A β 42 aggregation sizes which showed very promising results. Aggregation sizes were seen to be reduced by statistically significant margins in the presence of our inhibitor compounds. This motivated us to seek intellectual property protection in the form of a provisional patent application for our compounds pending further studies.

structure motifs, the alpha helix (α helix) and the beta sheet (β sheet), both of which are stabilized through a series of hydrogen bonds (see Figure 2).

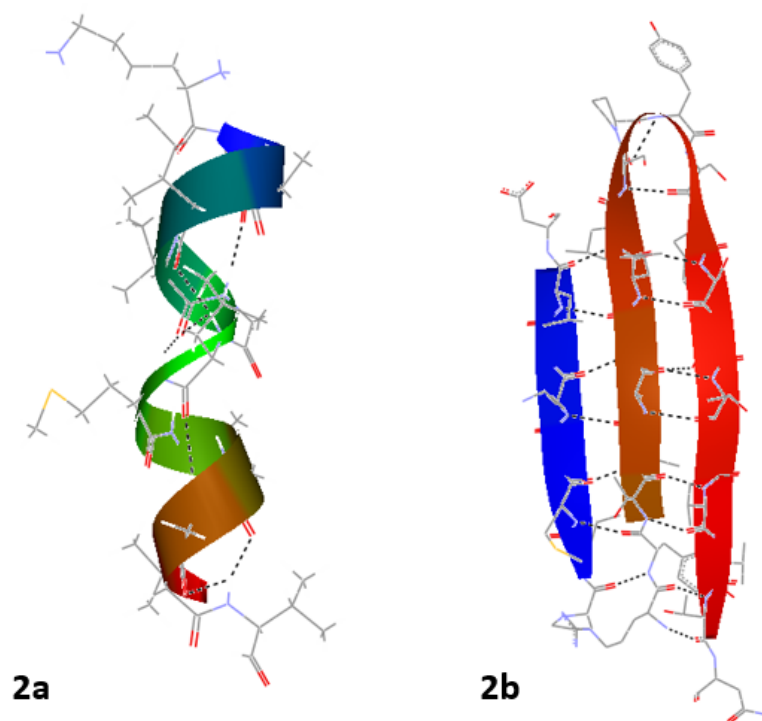


Figure 2: Secondary structure alpha helix motif (2a) and beta sheet motif (2b). Stabilizing hydrogen bonds between oxygens (red line designs) and hydrogens (light blue line designs) are shown by the black dashed lines.

The higher order tertiary structure in turn refers to how these secondary structure motifs are oriented together, each motif relative to the other, to confer the actual three-dimensional structure of a single amino acid chain protein (see Figure 3).

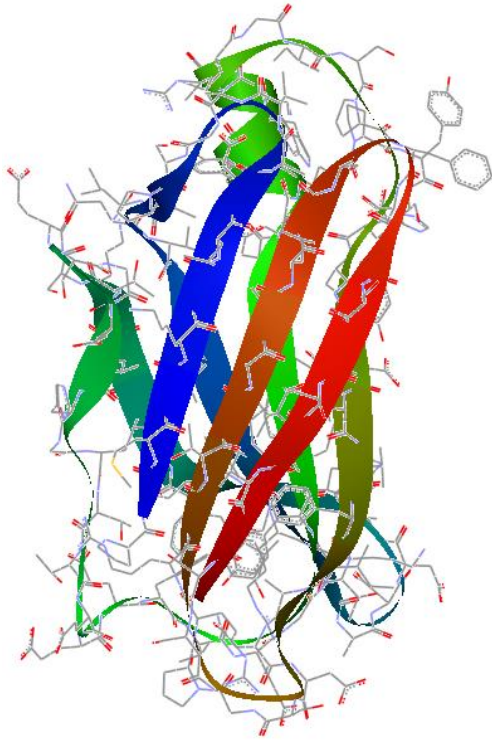


Figure 3: Tertiary structure of a single amino acid chain from the multi-chain transport protein transthyretin. Note how the spatial relationship is realized between the alpha helix and the beta sheets.

Quaternary structure then refers to the resulting structure that forms when *two or more* of such amino acid chains with tertiary structure come together in their appropriate arrangement via non-covalent interactions (incidentally it is these non-covalent interactions that our study shall explore for several systems) thus resulting in chain-chain interactions for the complete protein structure (see Figure 4).

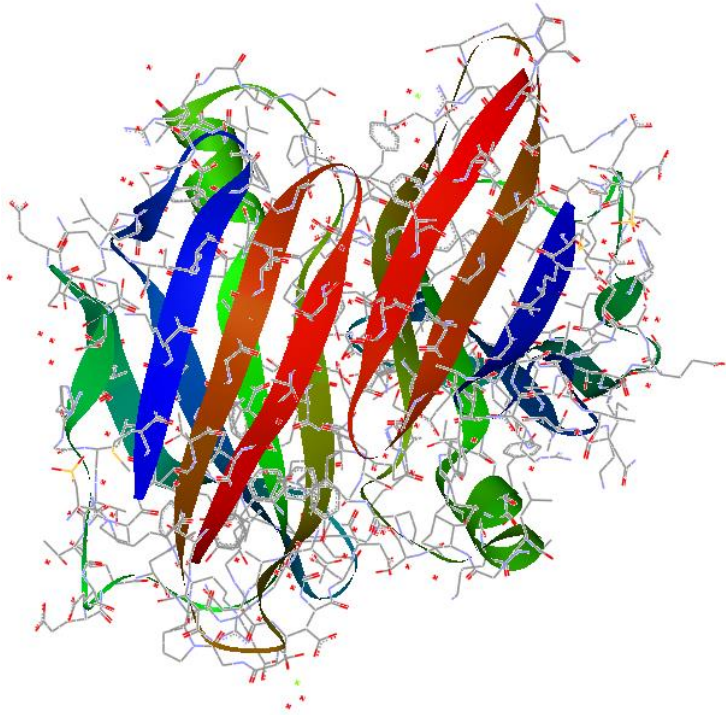


Figure 4: Quaternary structure of a dimer of the transporter protein transthyretin. Note how two identical subunit chains of the kind presented in Figure 3 come together.

In nature there may be single chain proteins that consequently only have tertiary structure, or there may be multi-chain proteins with quaternary structure, so which is the highest order of structure a protein can have depends on the actual protein species. The difference between peptides and proteins lies mostly in the definition of their architecture where proteins have a clearly defined tertiary structure, at the very minimum, whereas peptides do not [2]. It is therefore on account of these peptide bonds enjoining identical amino acid repeat units (save for the non-participating R group) that both peptide chains and proteins are considered biopolymers. The property of a unique structure plays a central role in the pertinent biology associated with proteins in particular [2, 4, 5, 6, 7].

References:

(1) Young TS, Schultz PG. Beyond the canonical 20 amino acids: expanding the genetic lexicon. *J Biol Chem* 2010 Apr 9;285(15):11039-11044.

(2) Creighton TE. Proteins: Structures and Molecular Properties. 2nd ed. New York: W.H. Freeman and Company; 1993.

(3) Mathews CK, Van Holde KE. Introduction to Proteins: The Primary Level of Protein Structure. Biochemistry. 2nd ed. Menlo Park, CA: Benjamin/Cummings Publishing Company, Inc.; 1996. p. 131-132.

(4) Koshland DE. The lock-key theory and the induced fit theory. Angewandte Chemie International Edition 1995;33:2375-2378.

(5) Fischer E. Einfluss der configuration auf die wirkung der enzyme. Ber Dtsch Chem Ges 1894;27:2985-2993.

(6) Koshland DE. Application of a Theory of Enzyme Specificity to Protein Synthesis. Proceedings of the National Academy of Sciences of the United States of America 1958;44:98-105.

(7) Norel R, Lin SL, Wolfson HJ, Nussinov R. Shape complementarity at protein-protein interfaces. Biopolymers 1994;34(7):933-940.

Appendix B:

Extended Literature Review: Covalent & Non-Covalent interactions in Proteins

The aims of the project and its subordinate parts are fundamental to acquire a greater understanding of the non-covalent interactions that maintain protein structure as well as accompany protein motion. Aim 1 of the project thus seeks to accomplish this by devising a strategy to identify the atoms from their respective residues responsible for inter-chain and intra-protein interaction stability from a set of ensemble structures. At this point, it becomes appropriate to provide an in-depth discussion of the concepts behind the AMBER03 force-field and computational force-fields in general (all mathematical explanations in this work serve the purpose to provide a background of the theory of the relevant equations and therefore no attempt is made here to derive these governing equations). The computational necessity for quantitatively determining the interatomic attractions and forces is founded on the discipline of molecular mechanics. Molecular mechanics is an application of classical mechanics (or Newtonian mechanics, the most common branch of physics) to model the movement of the individual atomic constituents in molecular systems [1]. This discipline is used to study a wide range of chemical species behavior ranging from small organic molecules containing only a few atoms, to large biological macromolecules such as proteins and DNA which may contain anywhere from several thousand to several million atoms. As alluded to earlier, the calculations that provided the quantitative data for this project were ultimately executed by the energy mapping algorithm, but the fundamentals of the underlying code are all based upon what follows and needless to say, the calculations are performed by the algorithm for as many atoms that are present in the system being analyzed.

In its most basic manifestation, molecular mechanics models systems via an “all-atom” approach: each individual atom in the molecule is treated as a single particle [1]. Each particle in turn, is then assigned a radius (most typically the van der Waals radius), along with a variety of different parameters (derived from quantum mechanical calculations) that account for polarization (partial atomic charge), fixed ion charges and bond angles (more on these parameters later) [1]. The bonded interactions are

modeled as stiff mechanical springs with an equilibrium distance equal to the experimental or calculated bond length [2]. As will be explored in greater detail shortly, the particular force field parameters assigned to each atom follow from large scale quantum mechanical calculations. Note that there are additional variations of this paradigm in use such as the “united-atom” model, which treats each terminal methyl group or intermediate methylene unit as a single particle, and the so-called “bead” model which assigns two to four particles to an individual amino acid in a protein system [1]. It is the “all-atom” model however that finds use in this project via the Open Contact© software and, thus, the data that follows in the coming sections is entirely *from an atomistic perspective*.

Now that the modeling technique has conceptually been defined, it is appropriate at this point to specifically detail the mathematical treatment of the “all-atom” model or potential function. From a mathematical and physical perspective, the molecular mechanics calculations are based simply on a summation of a variety of different potentials inherent in a molecular system. The two most fundamental categories of these potentials are the collective potentials governing covalent bonding between atoms and the collective potentials governing non-covalent bonding (i.e. electrostatic attractions). These two master families (covalent and non-covalent) are then added together to give the total potential energy of the molecule under study. Therefore mathematically the functional form of the potential function is [3],

$$(1) E_{TOT} = E_{COVALENT} + E_{NON-COVALENT}$$

where the covalent term is,

$$(2) E_{COVALENT} = E_{BOND} + E_{ANGLE} + E_{DIHEDRAL}$$

and the non-covalent term is,

$$(3) E_{NON-COVALENT} = E_{ELECTROSTATIC} + E_{VAN DER WAALS}$$

Eqs. (2) and (3) contain some of the potentials briefly mentioned in the foregoing paragraphs and we now see where and how exactly these potentials are prescribed in the grand scheme of molecular mechanics calculations.

Each term in Eqs. (2) and (3), in turn, are defined according to specific potential models. Starting with Eq. (2) (modeling covalent bonding), the bond and angle terms (E_{BOND} and E_{ANGLE}) are typically modeled as harmonic potentials centered about equilibrium bond length values. This approach makes use of the classical setup commonly seen when analyzing the equations of motion for periodically occurring phenomena such as a swinging pendulum or (as is most appropriate in the present case of a chemical bond) a spring rapidly expanding and contracting. Such a harmonic potential may therefore be of the form,

$$(4) x(t) = A \cos(\omega t + \phi)$$

where,

$$\omega = \sqrt{\frac{k}{m}} = \frac{2\pi}{T}$$

which would represent the angular frequency of bond vibration. The dihedral term in Eq. 2 ($E_{DIHEDRAL}$) is modeled with the appropriate potentials, but they tend not to be harmonic oscillators and their various functional forms tend to vary with the specific implementation of the potential function. Improper dihedral mathematical models may be included to enforce the planarity of aromatic rings and conjugated systems [4].

For the non-covalent interactions considered in Eq. (3), the electrostatic term ($E_{ELECTROSTATIC}$) takes into account any inherent charges possessed by the constituent atoms of the protein due to electron

deficiencies or excesses as well as dipole, quadrupole, or higher moments due to shifting electron positions. It is modeled with Coulomb's law for two point charges [5],

$$(5) \quad u(r) = \frac{q_1 q_2}{r}$$

where q_1 and q_2 are the charges of each point and are given in electrostatic units ($1 \text{ esu} \equiv 1 \text{ dyne}^{1/2} \cdot \text{cm}$). The van der Waals term ($E_{\text{VAN DER WAALS}}$) in Equation 3 further considers BOTH the short range (Born) repulsive forces and the longer-range (van der Waals) attractive forces present at the intermolecular level [5]. These forces, although similar in concept to the electrostatic forces previously mentioned, primarily differ in the sense that van der Waals forces are associated with oscillating, time-dependent electric fields created by the wave, or probabilistic behavior, of electrons in atoms (by themselves, van der Waals forces are mathematically modeled as r^{-7} where r is the separation distance between the two species) [5]. This is in distinction to the more fixed nature of positive or negative charge that is modeled by Coulomb's law. Although the term in Eq. 3 primarily bears the name van der Waals, it is important to note that the specific potential function actually used incorporates both Born and van der Waals repulsions and attractions respectively. On the atomic scale, the precise nature of Born repulsive forces manifest themselves when two atoms (or molecules) approach each other at distances slightly larger than σ where σ is the atomic or molecular diameter. At these very small separation distances, the electron shells of the two molecular (or atomic) species partially penetrate each other [5]. The nuclei of the constituent atoms (which are positively charged) are now no longer shielded by their respective electron shells and so they now repel one another. It is important to note that the scenario of Born repulsion, despite the physical similarities with covalent bonding, differs from covalent bonding in that no electrons are shared by the two species in question in the Born set up. Both Born and van der Waals interactions are thus modeled in Eq.(3)'s $E_{\text{VAN DER WAALS}}$ term using the Lennard-Jones Potential [6],

$$(6) u(r) = 4\epsilon \left[-\left(\frac{\sigma}{r}\right)^6 + \left(\frac{\sigma}{r}\right)^{12} \right]$$

where ϵ and σ are constants related to the energy minimum and distance at minimum, respectively.

As previously stated, the ultimate manifestation of the mathematical engine that drives the energy mapping algorithm's calculations is the atomic force field and associated parameters. It is crucial to make the distinction however of what is meant by the term "force field" in chemistry and computational biology as opposed to its more common usage in physics. In chemistry, a force field refers to a system of potential energy functions like the kind that have been discussed in the Equations 2 and 3. This stands in contrast to the definition of a force field in physics as being the gradient of a scalar potential [5]. Another important concept to be cognizant of is that despite the fact that the equations in conjunction with their parameters are called "force fields", the quantities that the equations actually provide are potentials, not forces. Strictly speaking, the force is defined mathematically as the negative of the first derivative of the potential function with respect to separation distance. In addition to providing information on each element present in the molecule, the parameters also include specific constants for the properties of these atoms as they appear in different functional groups such as carbonyl and hydroxyl oxygens [6].

The parameter sets used in proper force field analysis include data for van der Waals radii, partial charges, atomic masses, equilibrium values for bond lengths and angles, dihedral angles for bonded atoms and the effective "spring constants" for each bond potential (recall that in molecular mechanics, bonds are well approximated by the physics of an actual expanding and contracting spring) [6]. An important point of emphasis is that despite the fact that these values and constants are ultimately employed on a holistic perspective of the entire protein under study, the values themselves are derived primarily from quantum mechanical models on small and simple organic molecules [4]. As will be seen in the next section, there are many force field models currently available for intra and inter molecular interaction studies, and each

model has its own set of parameters. These parameters are defined by force field developers to be self-consistent within the parameters' respective force field model and should therefore never be used in conjunction with the potential equations from another force field model, no matter how similar parts of the models may be.

As previously discussed, the specific force-field model employed by the energy mapping algorithm used in this work is AMBER03. AMBER is an acronym which stands for **A**ssisted **M**odel **B**uilding with **E**nergy **R**efinement. AMBER 03 follows the skeletons of Eqs. (2) and (3) and it has its own set of parameters for van der Waals radii, bond lengths, etc.... AMBER03 is currently the third generation of the AMBER force field family which was first started by the work of Weiner et al. [7]. Subsequent work by Jorgensen and Tirado-Rives [8] developed non-bonded parameters that reproduce the enthalpy and density in their Optimized Potentials for Liquid Simulations (OPLS) model which they combined with the Weiner et al. bond angle and dihedral parameters to create the first generation OPLS/AMBER force field for peptides and proteins [8]. The second generation of AMBER, also known as AMBER02, arose from the derivation of new van der Waals parameters from liquid simulations and thus includes hydrogen parameters which take into account the effects of any geminal electronegative atoms [4]. Duan et al. [9] then obtained new charge sets and main chain torsion parameters by quantum mechanical models which resulted in the development of AMBER03. As mentioned earlier in the Introduction section, there are additionally other force-fields available, but their most recent generations/versions are in good agreement with each other [10].

Given that the parameter sets are the only attributes that differ between AMBER family members, it should come as no surprise then that the foundational molecular mechanics potential function for the AMBER family of force fields remains the same for each currently available AMBER family member. The actual functional form of the AMBER equation is [4],

(7)

$$\begin{aligned} V(r^N) = & \sum_{\text{bonds}} k_b(l - l_0)^2 + \sum_{\text{angles}} k_a(\theta - \theta_0)^2 \\ & + \sum_{\text{torsions}} \sum_n \frac{1}{2} V_n [1 + \cos(n\omega - \gamma)] \\ & + \sum_{j=1}^{N-1} \sum_{i=j+1}^N f_{ij} \left\{ \epsilon_{ij} \left[\left(\frac{\sigma_{0ij}}{r_{ij}} \right)^{12} - 2 \left(\frac{\sigma_{0ij}}{r_{ij}} \right)^6 \right] + \frac{q_i q_j}{4\pi\epsilon_0 r_{ij}} \right\} \end{aligned}$$

For the right hand side of this equation, the first term, which sums over bonds, models the potential energy between covalently bonded atoms [4]. The classical spring model is a good approximation for atoms participating in bonds, so long as the bound atom distance (l) remains relatively close to the equilibrium bond length (l_0). This model begins to give poorer results, however, as the distance of binding is increased [4]. The second term, which sums over the angles of electron orbitals (θ), models the potential energy of electron orbitals involved in covalent bonding [4]. The third term, which sums over torsion angles (ω), models bond rotation as influenced by bond order (i.e. double bonds vs. single bonds) and neighboring charge clouds (i.e. vicinal bonds on the same atom and electron lone pairs) [4]. It is possible for any given individual bond to have more than one of these terms and in such cases, the total torsional energy potential would be expressed as a Fourier series [4]. The fourth and last term (the double summation over i and j) models the interactions arising from non-covalent force sources where r_{ij} is the distance between the two interacting atoms in the system [5]. Recall that these forces were identified as being modeled by the Lennard-Jones potential for those non-covalent interactions arising from time-dependent electron oscillation phenomena and Coulomb's law for charged atomic species.

References:

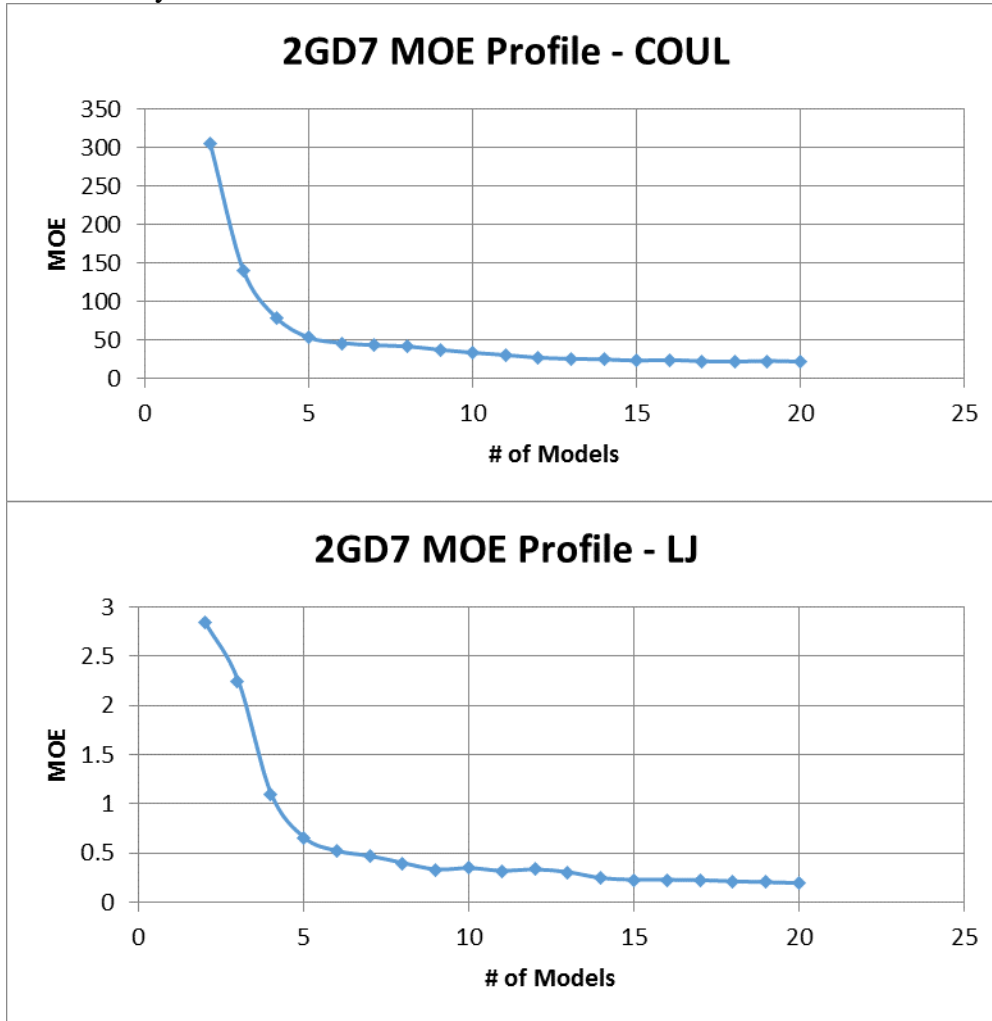
- (1) Kuhn B, Kollman PA. Binding of a diverse set of ligands to avidin and streptavidin: an accurate quantitative prediction of their relative affinities by a combination of molecular mechanics and continuum solvent models. *J Med Chem* 2000;43(20):3786-3791.
- (2) Truong PM, Viet MH, Nguyen PH, Hu C, Li MS. Effect of Taiwan Mutation (D7H) on Structures of Amyloid- β Peptides: Replica Exchange Molecular Dynamics Study. *The Journal of Physical Chemistry B* 2014;118(30):8972-8981.
- (3) Kollman PA, Massova I, Reyes C, Kuhn B, Huo S, Chong L, et al. Calculating structures and free energies of complex molecules: combining molecular mechanics and continuum models. *Acc Chem Res* 2000;33(12):889-897.
- (4) Cornell WD, Cieplak P, Bayly CI, Gould IR, Merz KM, Ferguson DM, et al. A second generation force field for the simulation of proteins, nucleic acids, and organic molecules. *J Am Chem Soc* 1995;117(19):5179-5197.
- (5) Peters M. Force descriptions. In: McCombs KP, ed. *Real-Time Biomolecular Simulations*. New York, New York: McGraw Hill; 2007:58-62.
- (6) Stöbener K, Klein P, Reiser S, Horsch M, Küfer K, Hasse H. Multicriteria optimization of molecular force fields by Pareto approach. *Fluid Phase Equilib* 2014;373:100-108.
- (7) Weiner SJ, Kollman PA, Case DA, Singh UC, Ghio C, Alagona G, et al. A new force field for molecular mechanical simulation of nucleic acids and proteins. *J Am Chem Soc* 1984;106(3):765-784.
- (8) Jorgensen WL, Tirado-Rives J. The OPLS [optimized potentials for liquid simulations] potential functions for proteins, energy minimizations for crystals of cyclic peptides and crambin. *J Am Chem Soc* 1988;110(6):1657-1666.
- (9) Duan Y, Wu C, Chowdhury S, Lee MC, Xiong G, Zhang W, et al. A point-charge force field for molecular mechanics simulations of proteins based on condensed-phase quantum mechanical calculations. *Journal of computational chemistry* 2003;24(16):1999-2012.
- (10) Martin-Garcia F, Papaleo E, Gomez-Puertas P, Boomsma W, Lindorff-Larsen K. Comparing molecular dynamics force fields in the essential subspace. *PLoS One* 2015 Mar 26;10(3):1-16.

Appendix C

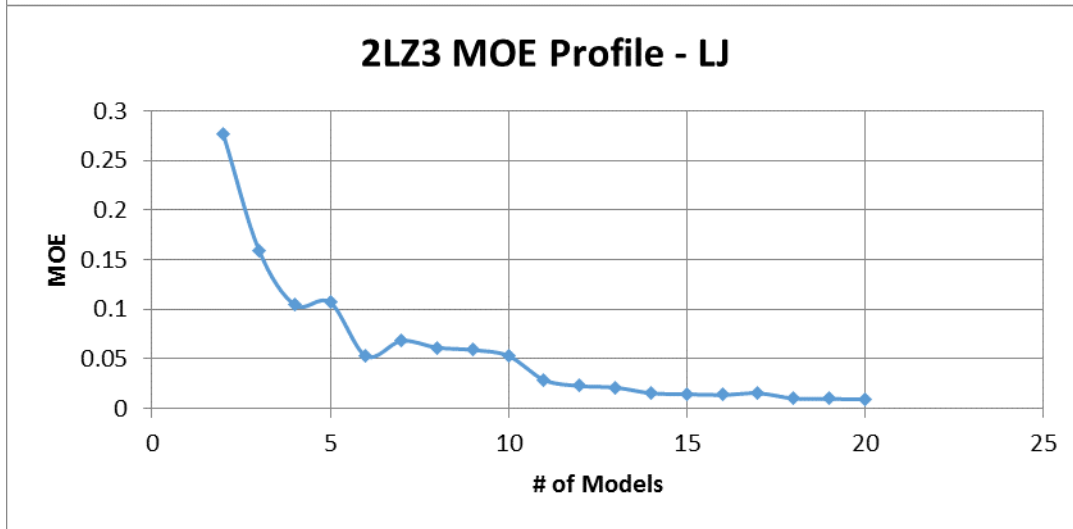
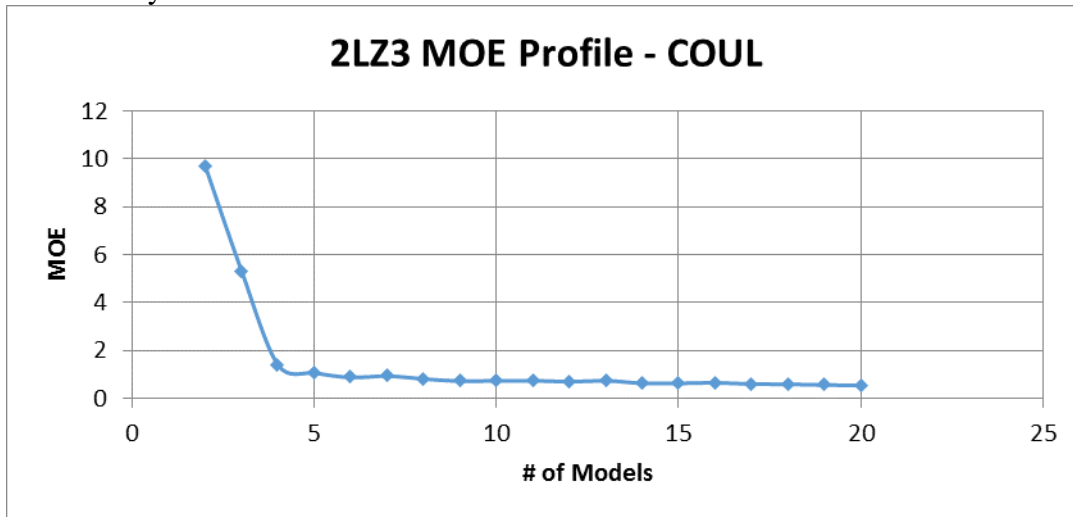
Supplementary Information:

20 Model Margin of Error (MOE) Analysis:

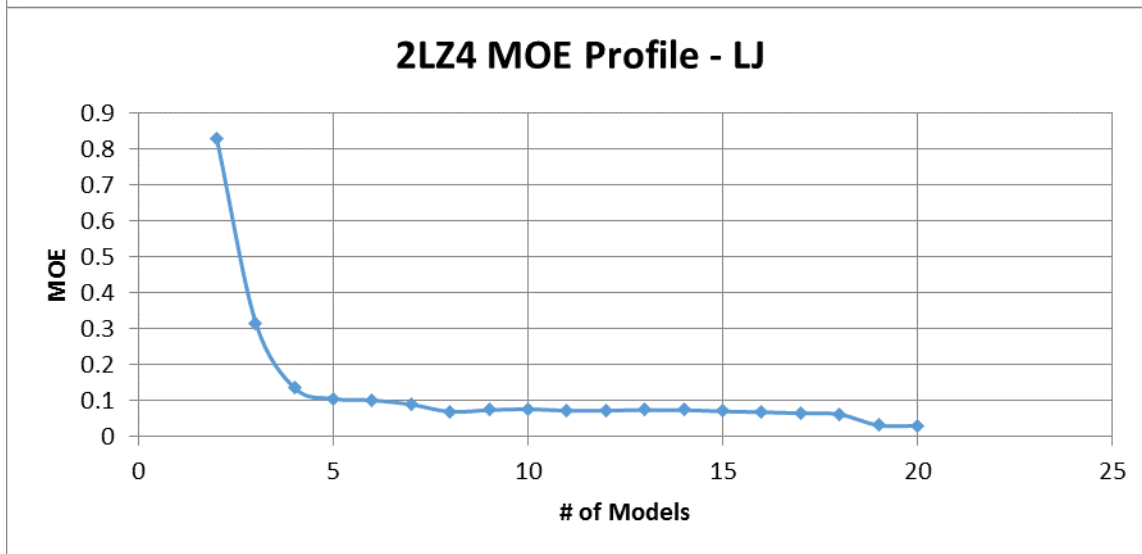
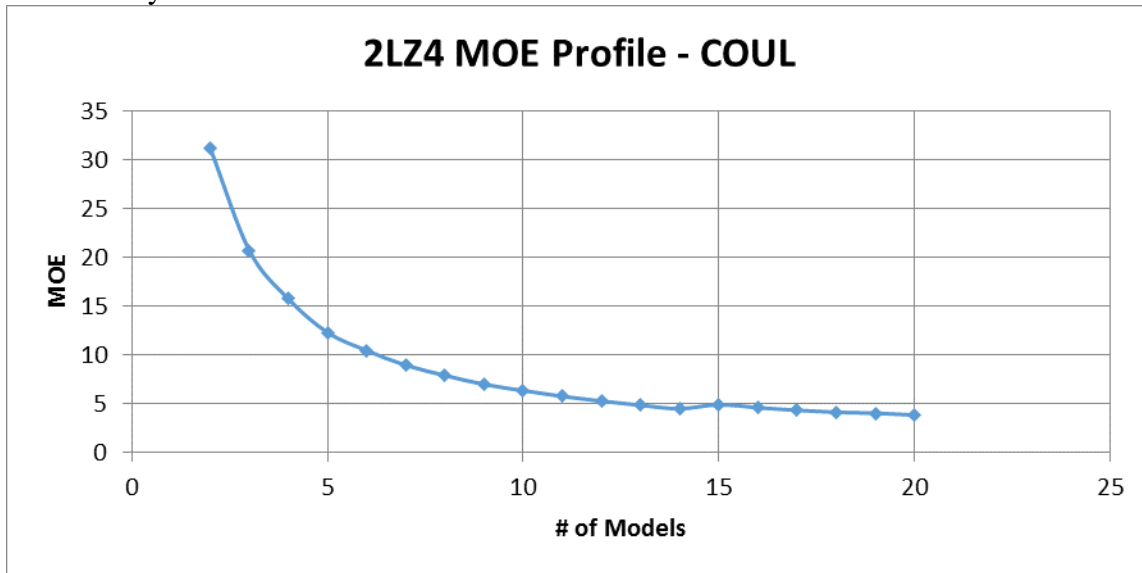
2GD7 Analysis 20:



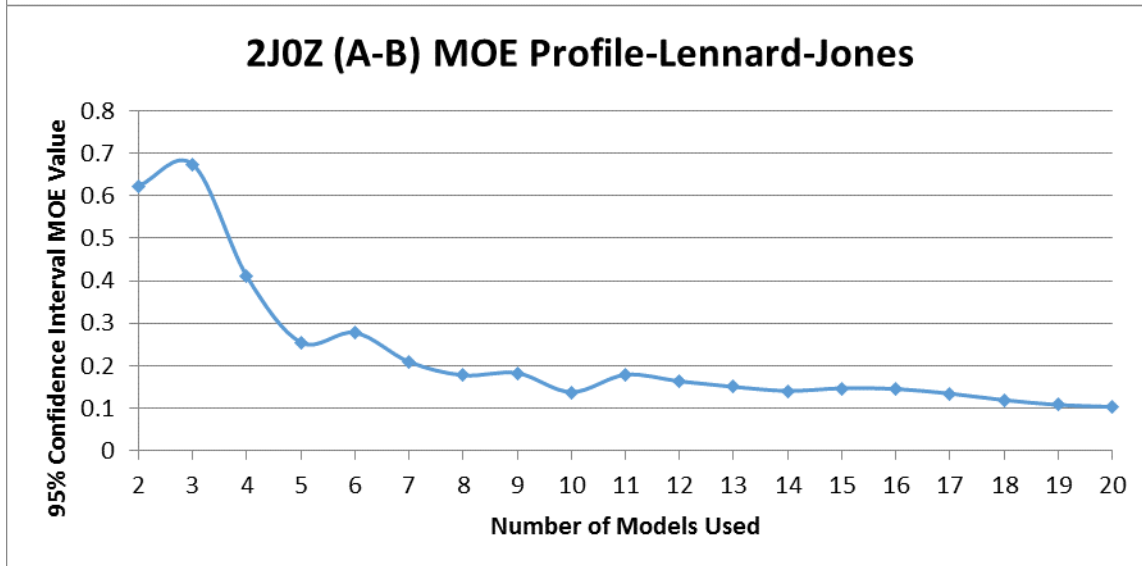
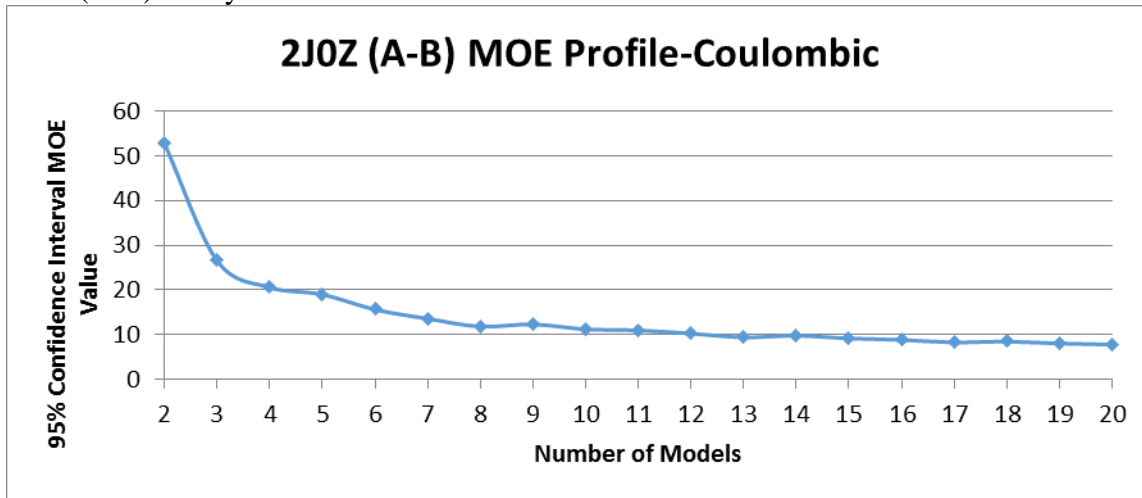
2LZ3 Analysis 20:



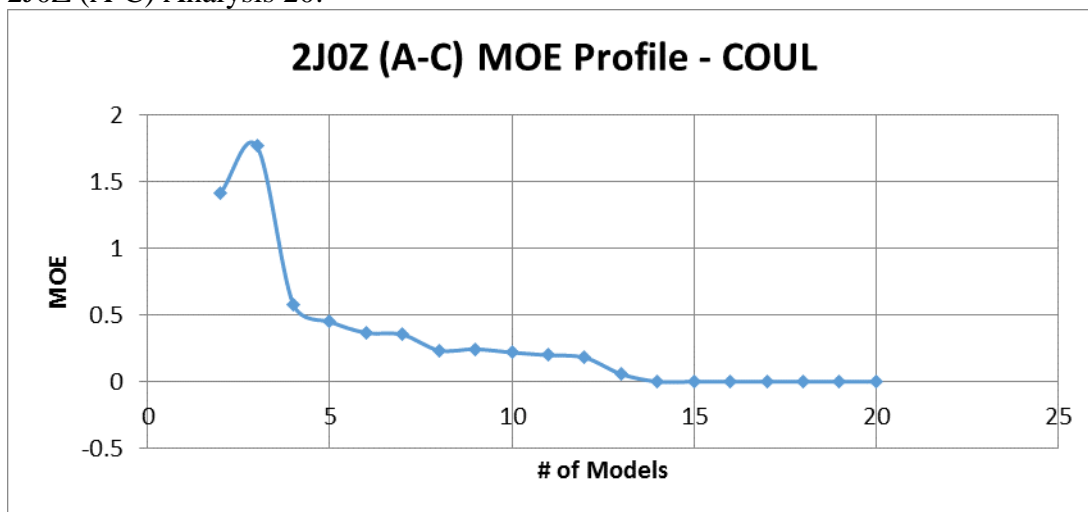
2LZ4 Analysis 20:



2J0Z (A-B) Analysis 20:

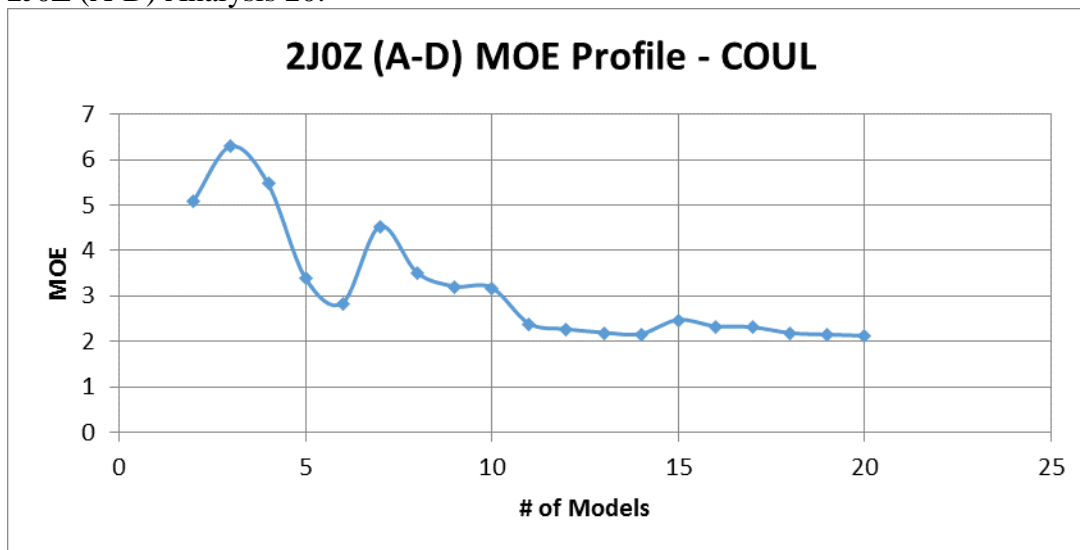


2J0Z (A-C) Analysis 20:



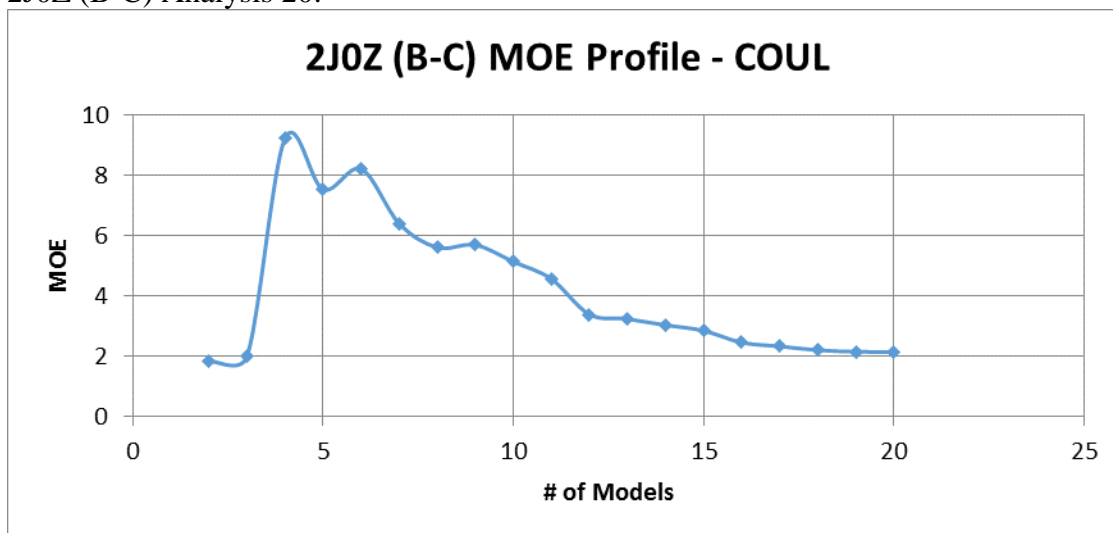
NO SURVIVING LENNARD-JONES A-C ATOM-ATOM INTERACTIONS ACROSS ENSEMBLE

2J0Z (A-D) Analysis 20:



NO SURVIVING LENNARD-JONES A-D ATOM-ATOM INTERACTIONS ACROSS ENSEMBLE

2J0Z (B-C) Analysis 20:



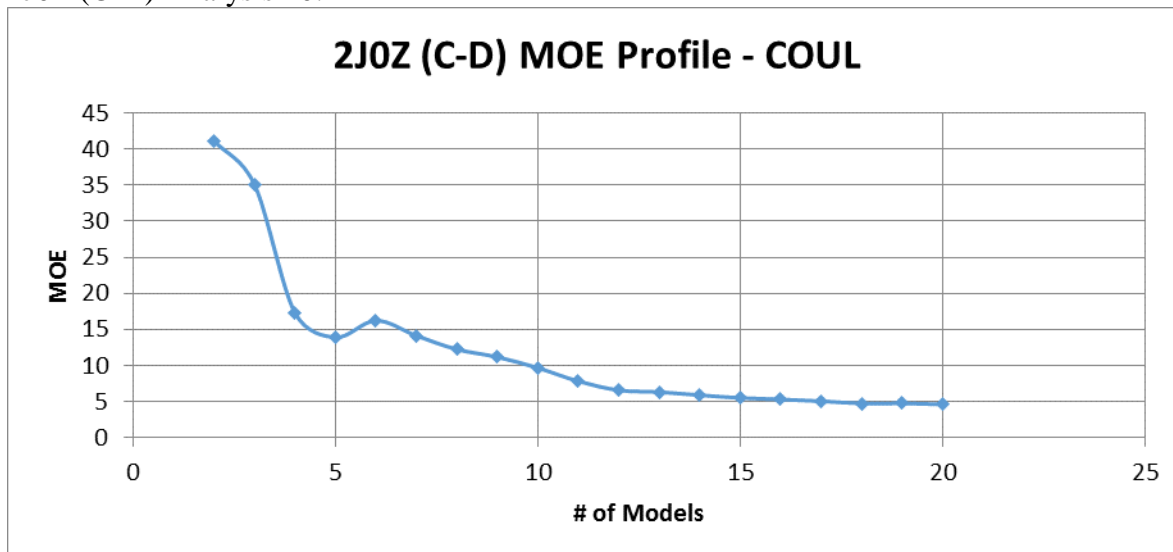
NO SURVIVING LENNARD-JONES B-C ATOM-ATOM INTERACTIONS ACROSS ENSEMBLE

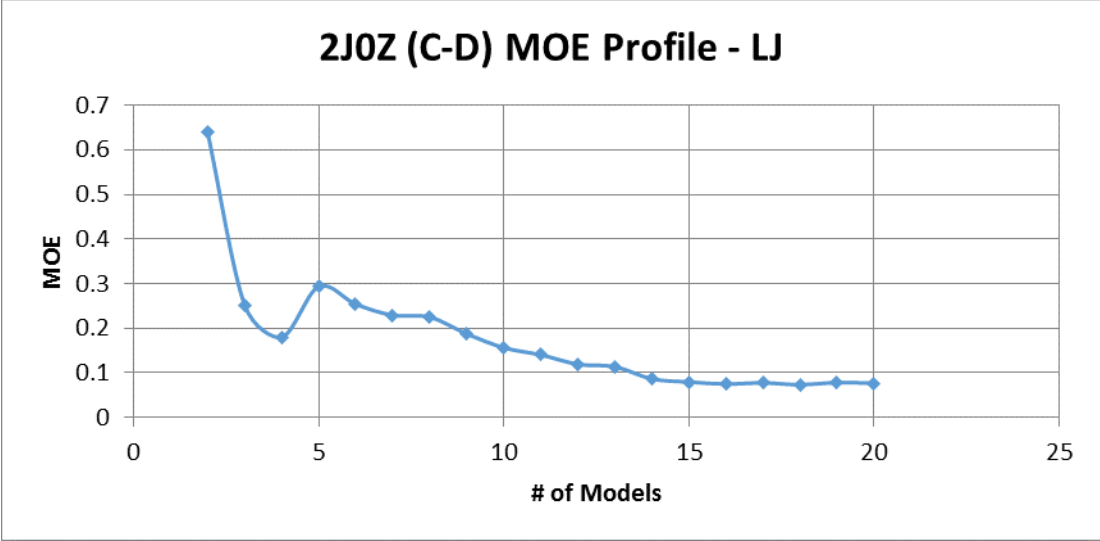
2J0Z (B-D) Analysis 20:

NO SURVIVING COULOMBIC B-D ATOM-ATOM INTERACTIONS ACROSS ENSEMBLE

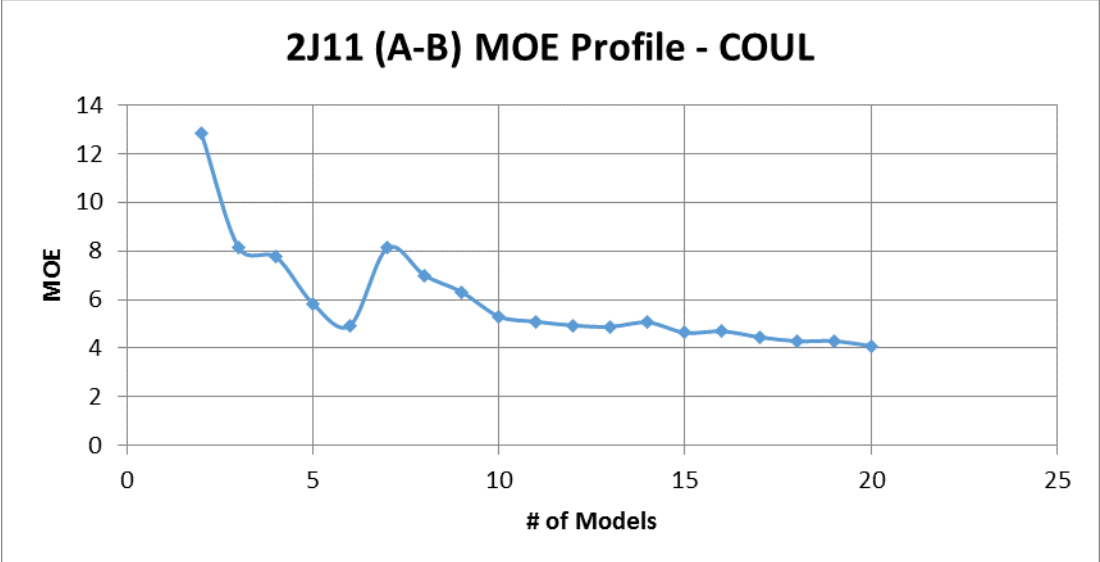
NO SURVIVING LENNARD-JONES B-D ATOM-ATOM INTERACTIONS ACROSS ENSEMBLE

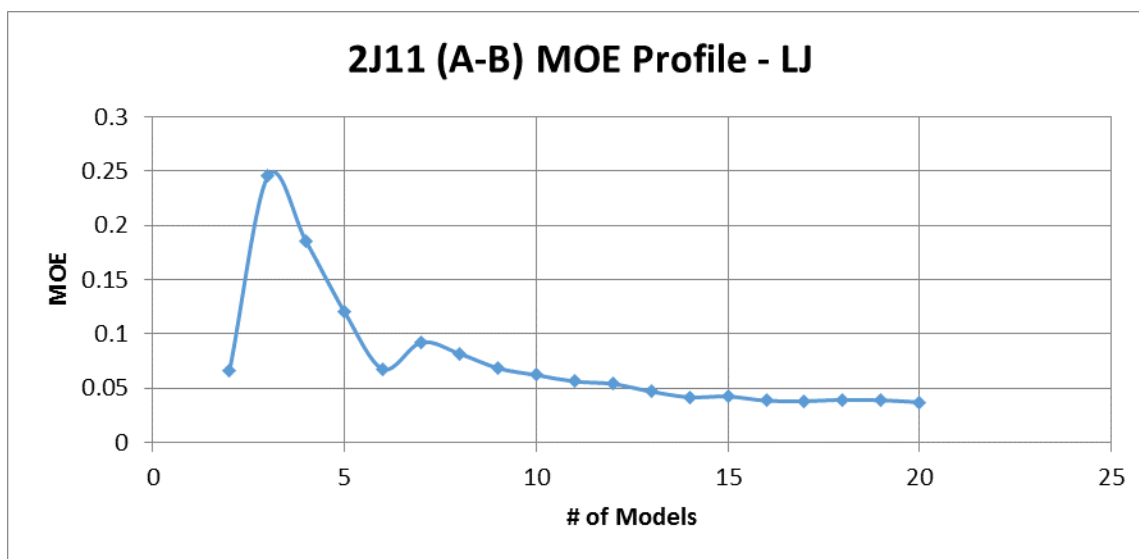
2J0Z (C-D) Analysis 20:





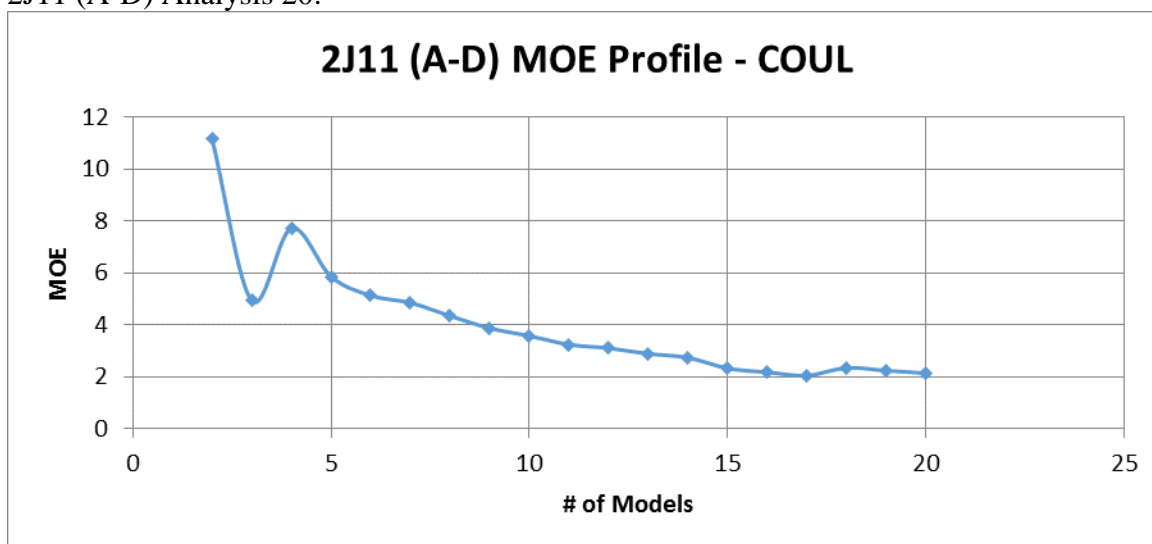
2J11 (A-B) Analysis 20:





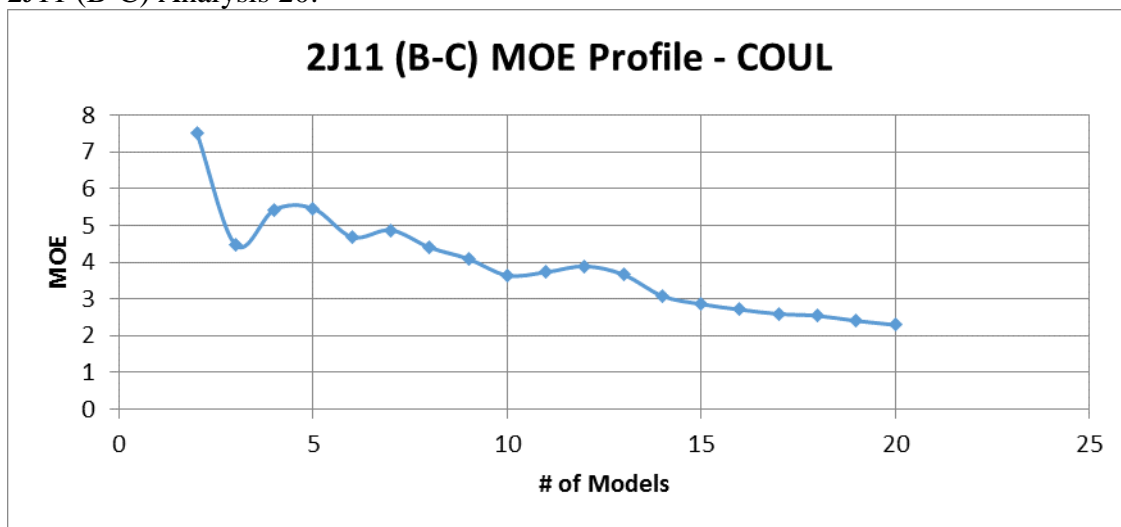
2J11 (A-C) Analysis 20:
 NO SURVIVING COULOMBIC A-C ATOM-ATOM INTERACTIONS ACROSS ENSEMBLE
 NO SURVIVING LENNARD-JONES A-C ATOM-ATOM INTERACTIONS ACROSS ENSEMBLE

2J11 (A-D) Analysis 20:



NO SURVIVING LENNARD-JONES A-D ATOM-ATOM INTERACTIONS ACROSS ENSEMBLE

2J11 (B-C) Analysis 20:



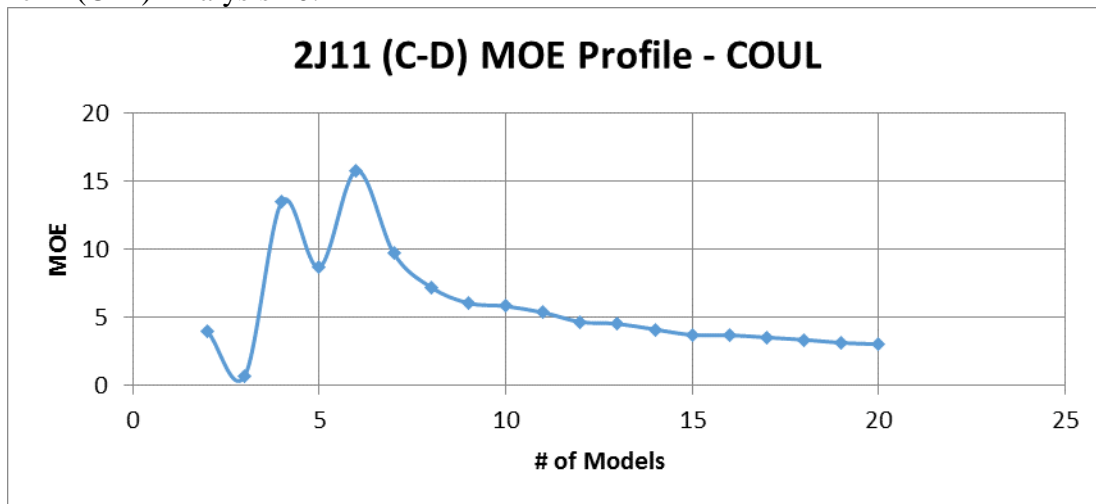
NO SURVIVING LENNARD-JONES B-C ATOM-ATOM INTERACTIONS ACROSS ENSEMBLE

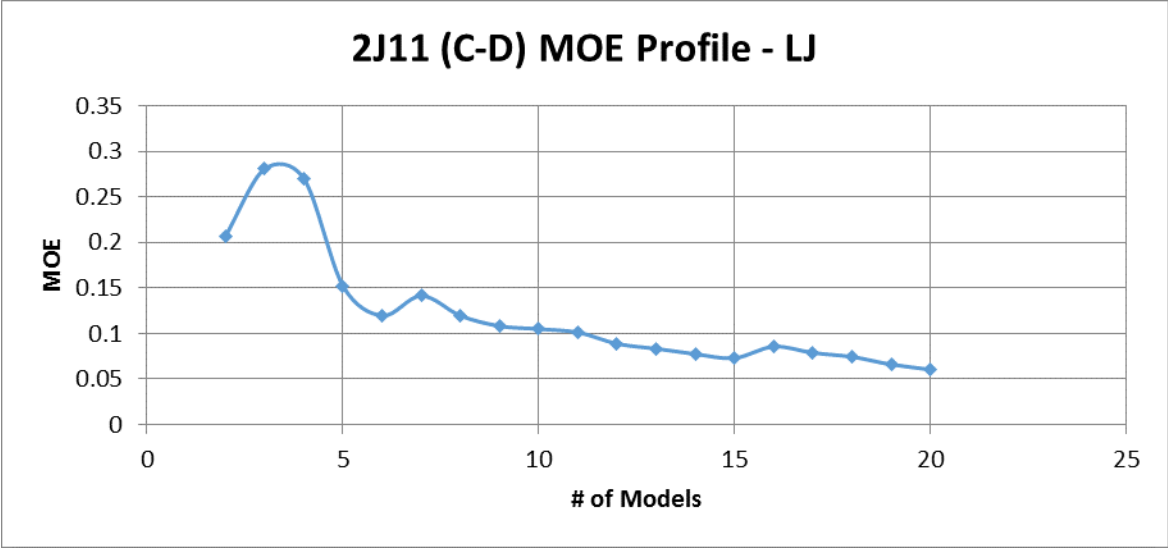
2J11 (B-D) Analysis 20:

NO SURVIVING COULOMBIC B-D ATOM-ATOM INTERACTIONS ACROSS ENSEMBLE

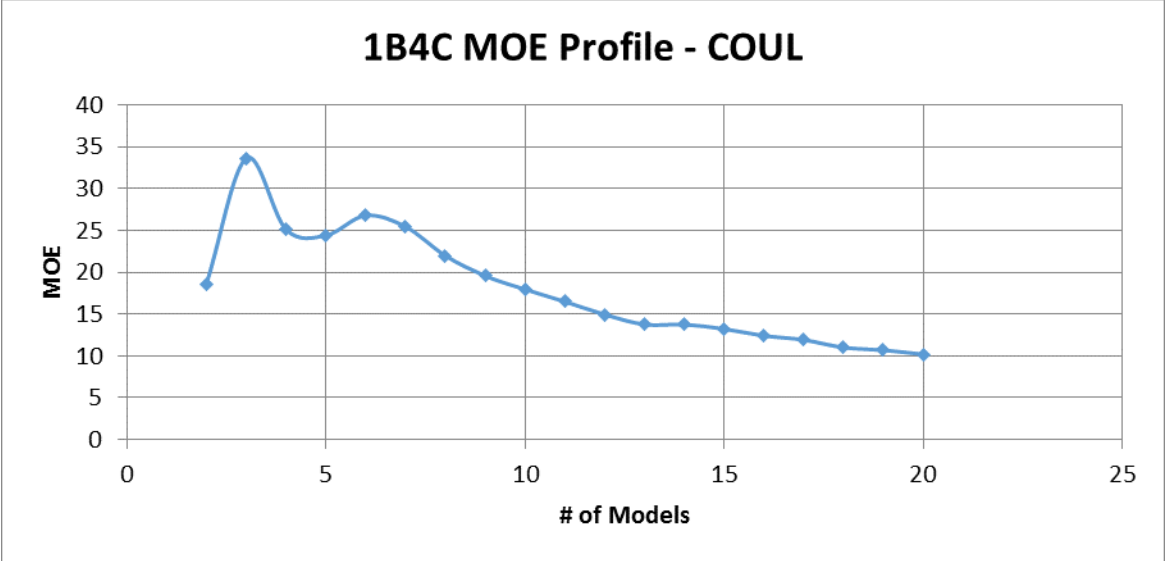
NO SURVIVING LENNARD-JONES B-D ATOM-ATOM INTERACTIONS ACROSS ENSEMBLE

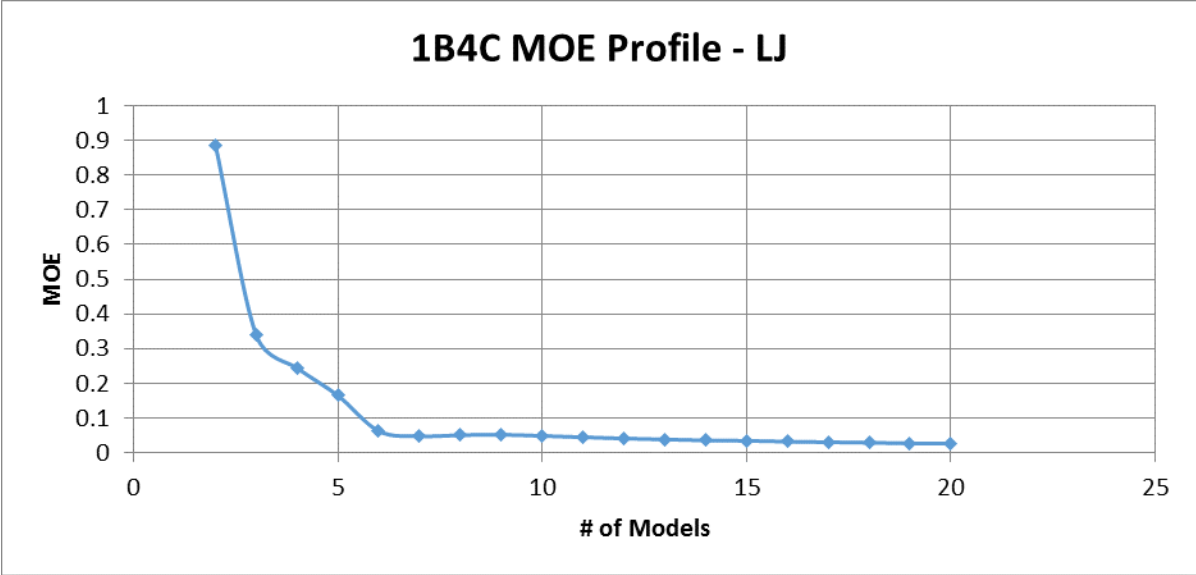
2J11 (C-D) Analysis 20:



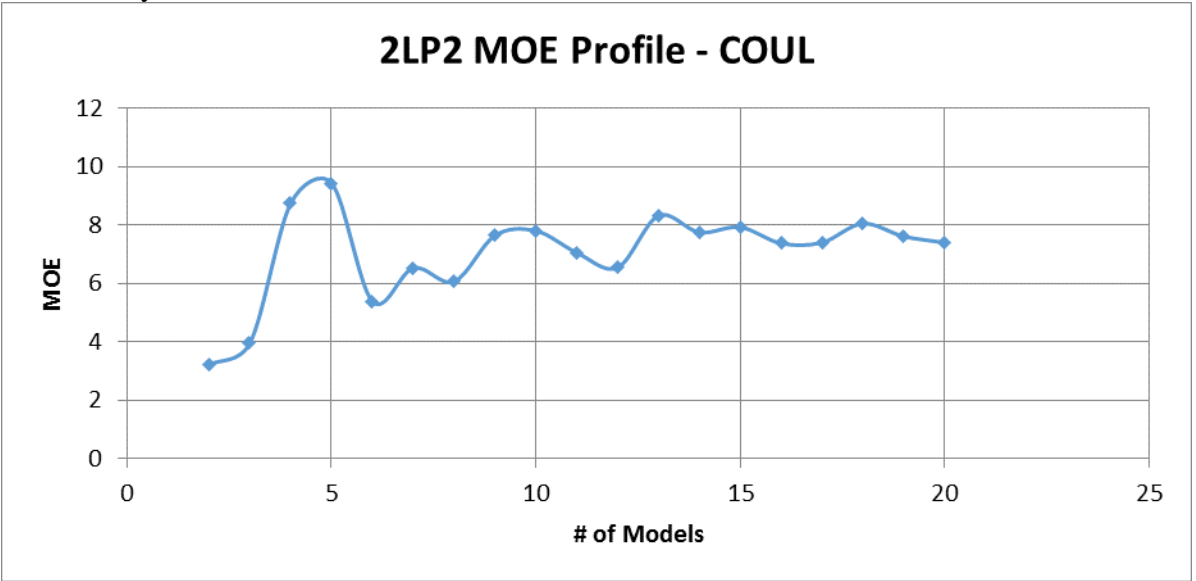


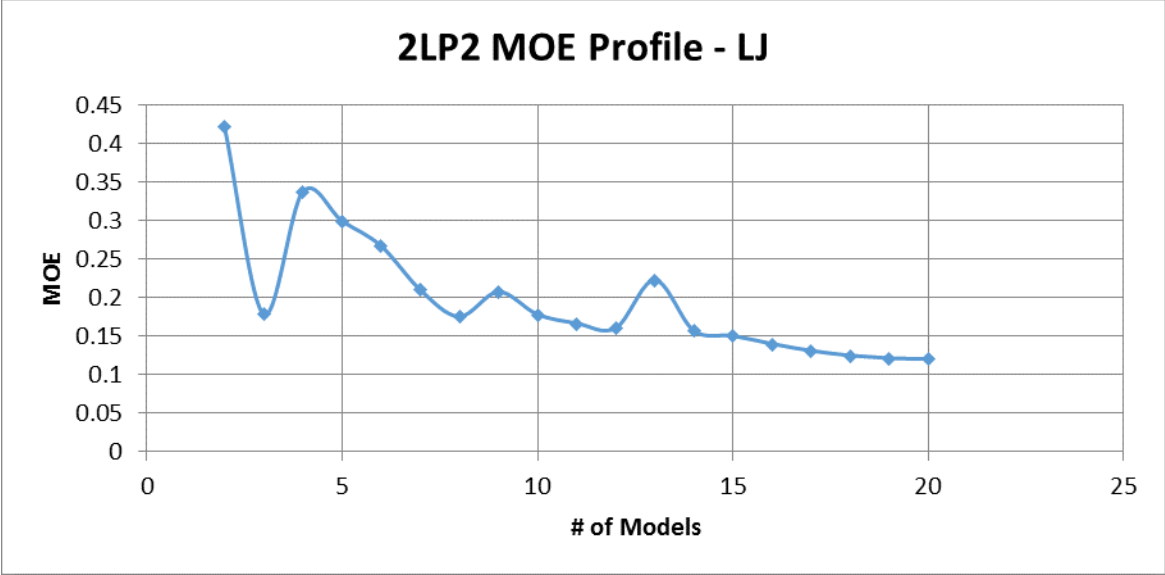
1B4C Analysis 20:



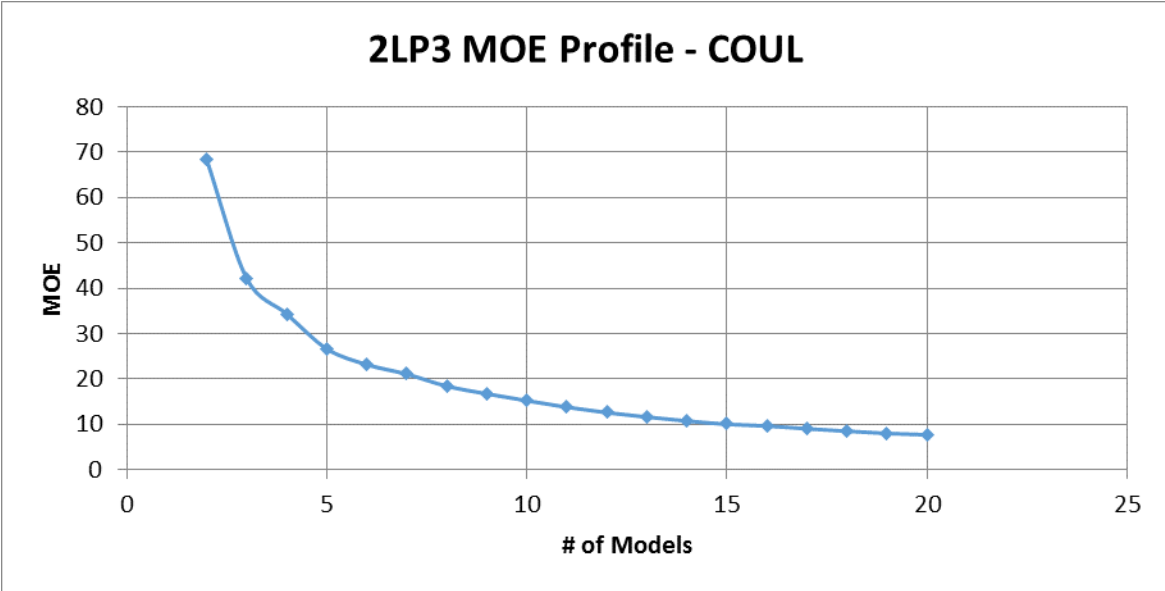


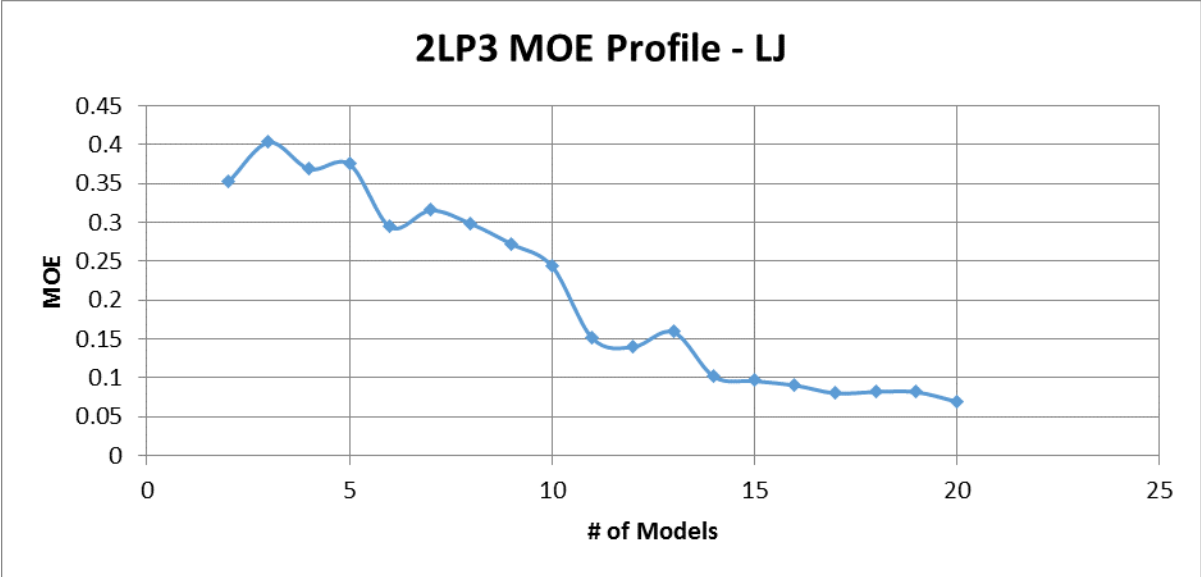
2LP2 Analysis 20:



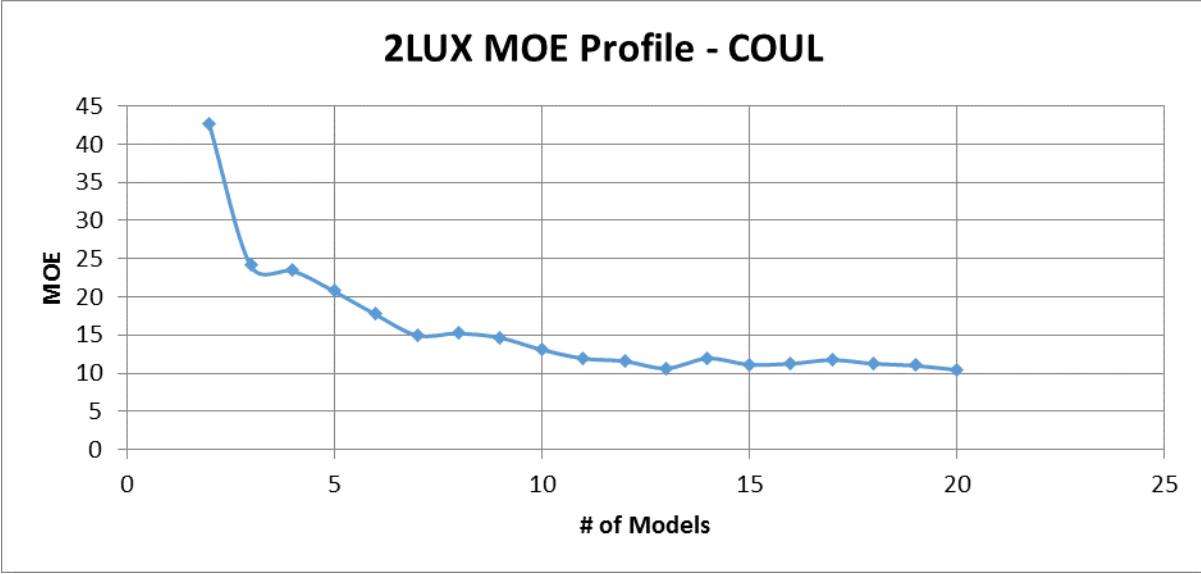


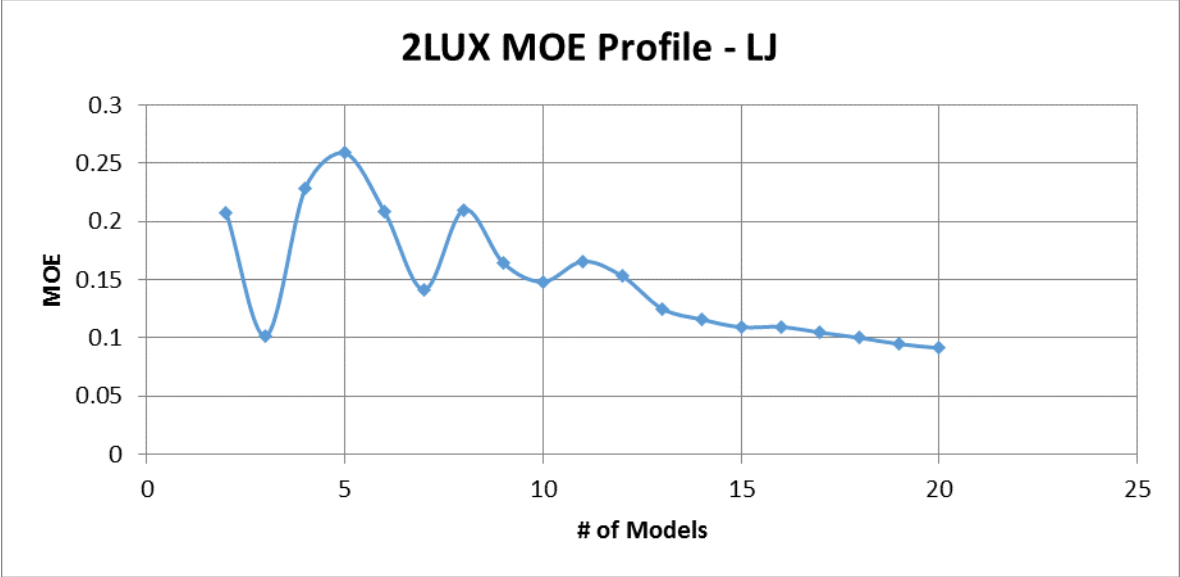
2LP3 Analysis 20:



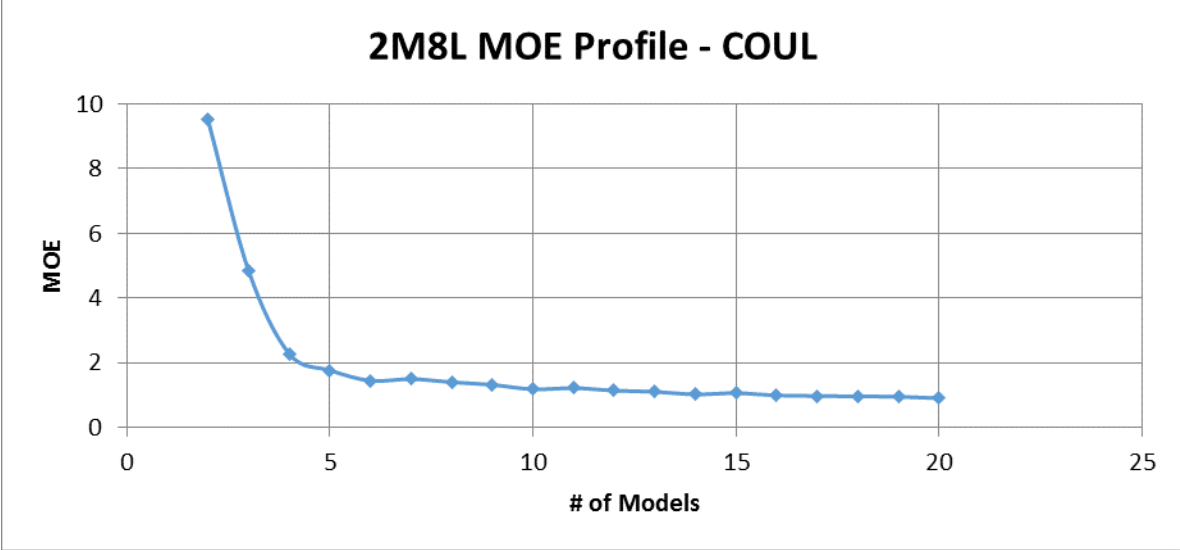


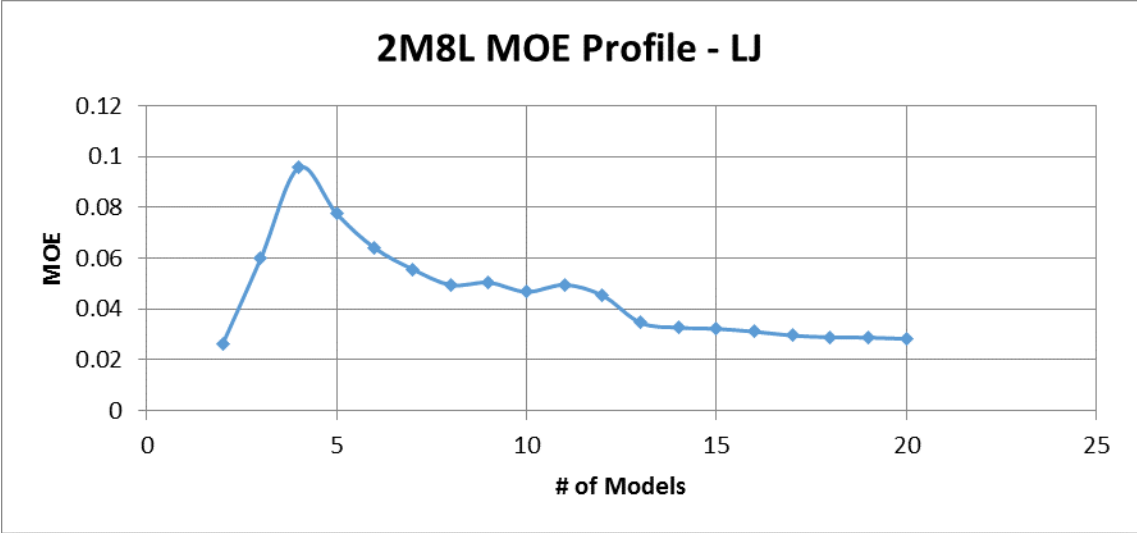
2LUX Analysis 20:



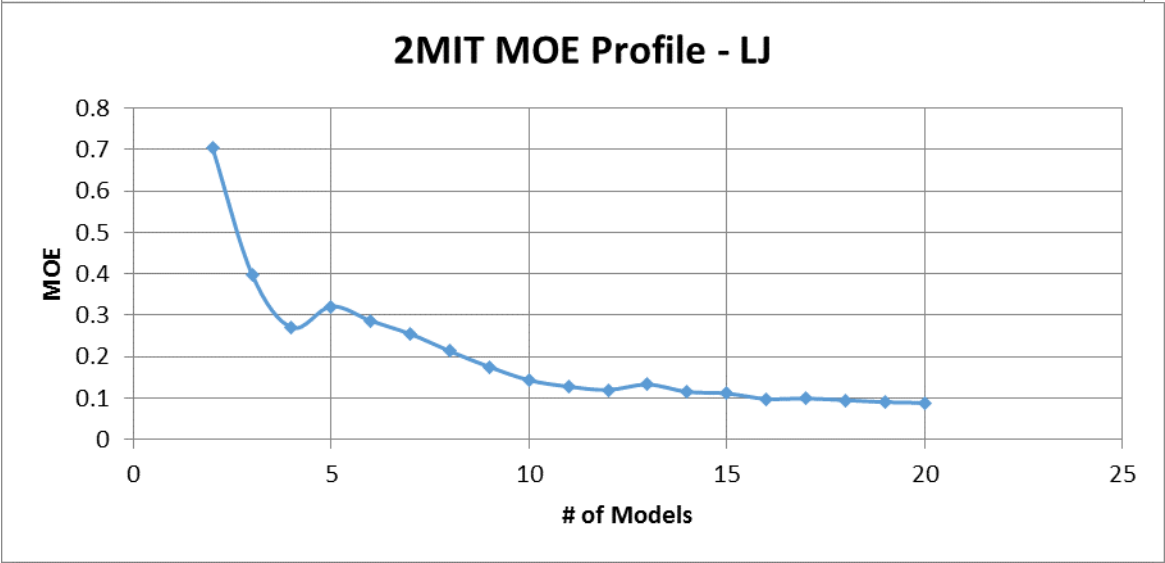
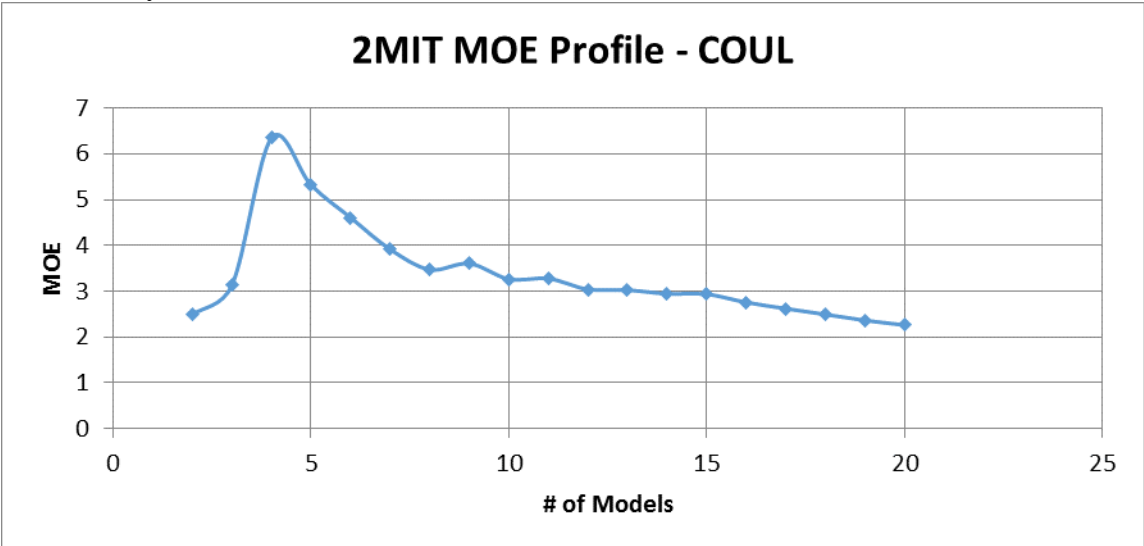


2M8L Analysis 20:

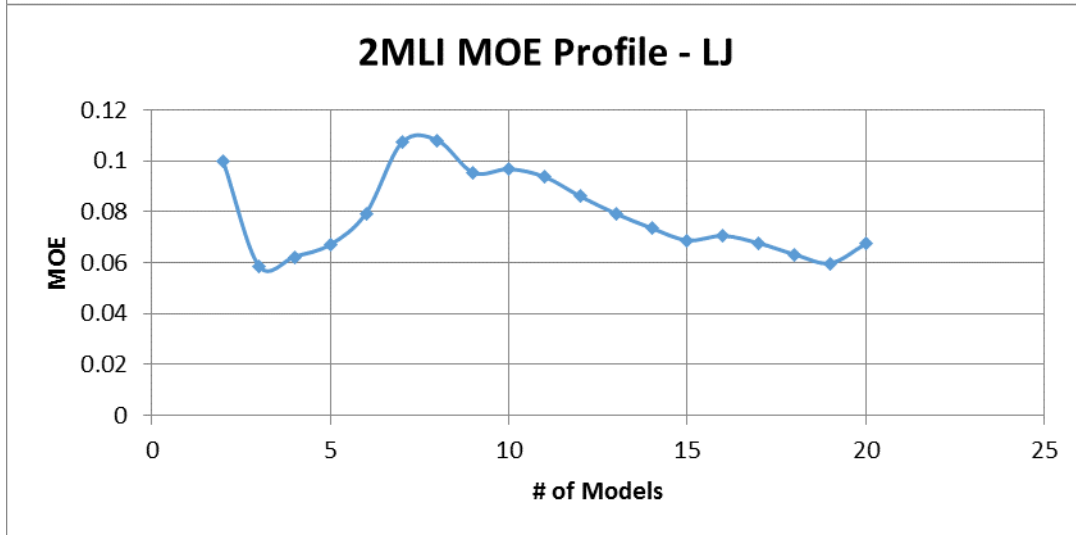
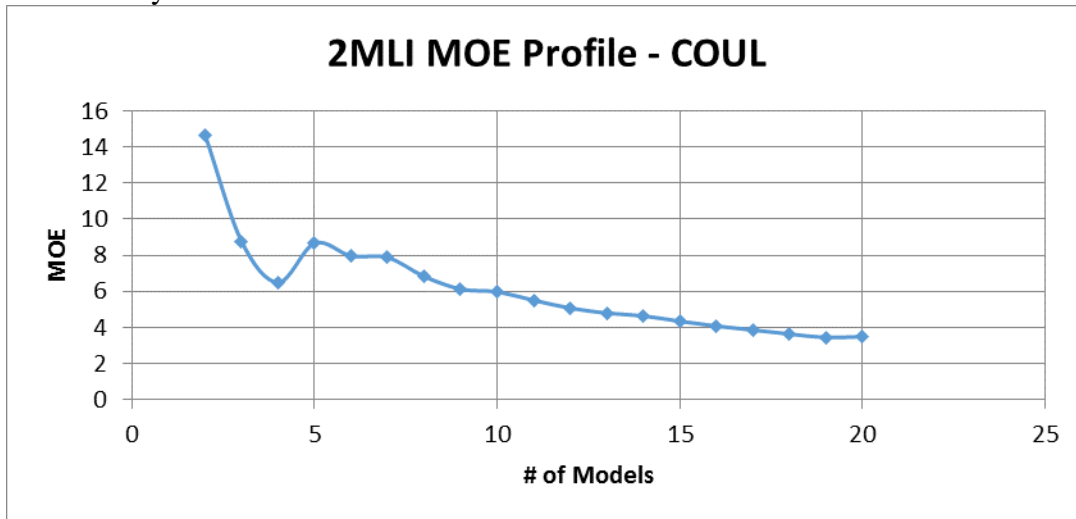




2MIT Analysis 20:

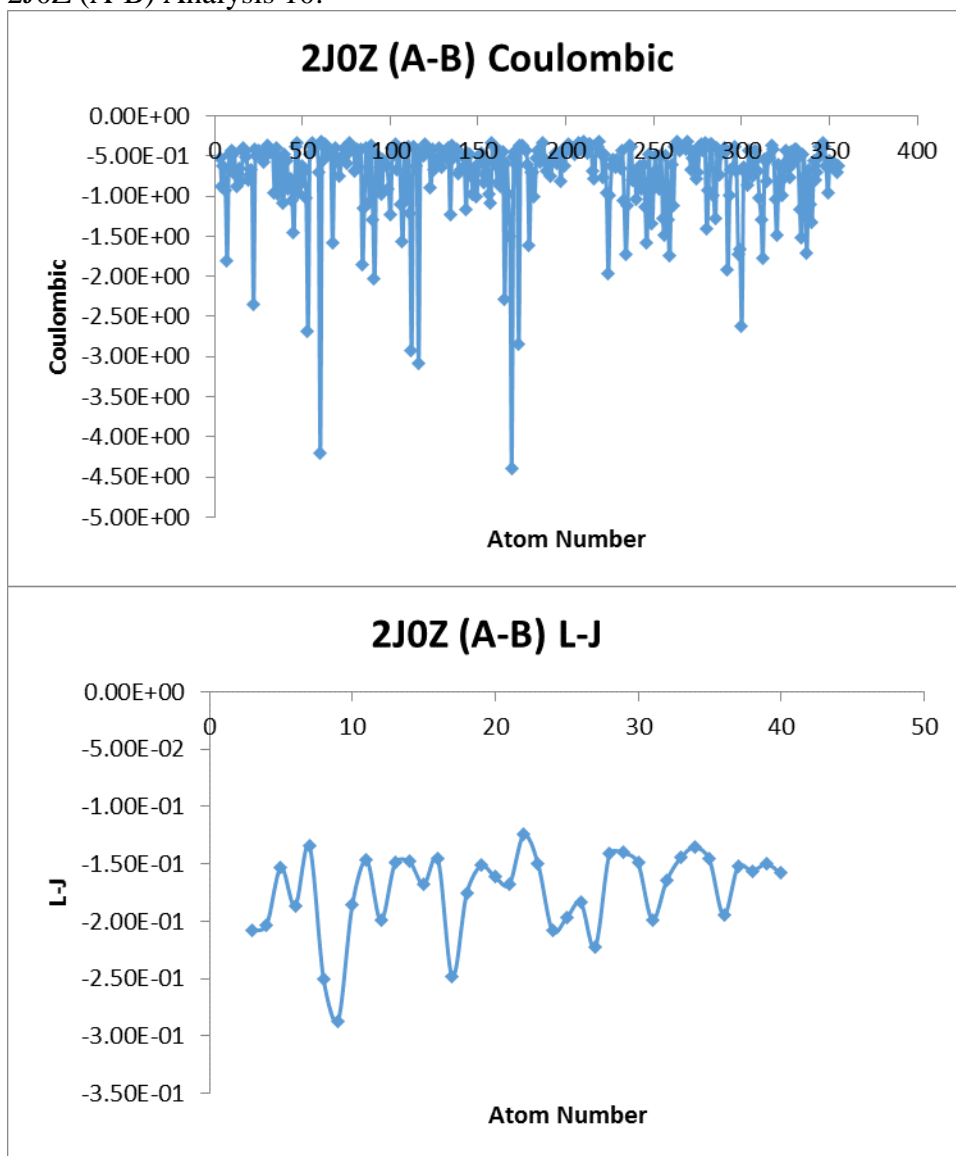


2MLI Analysis 20:

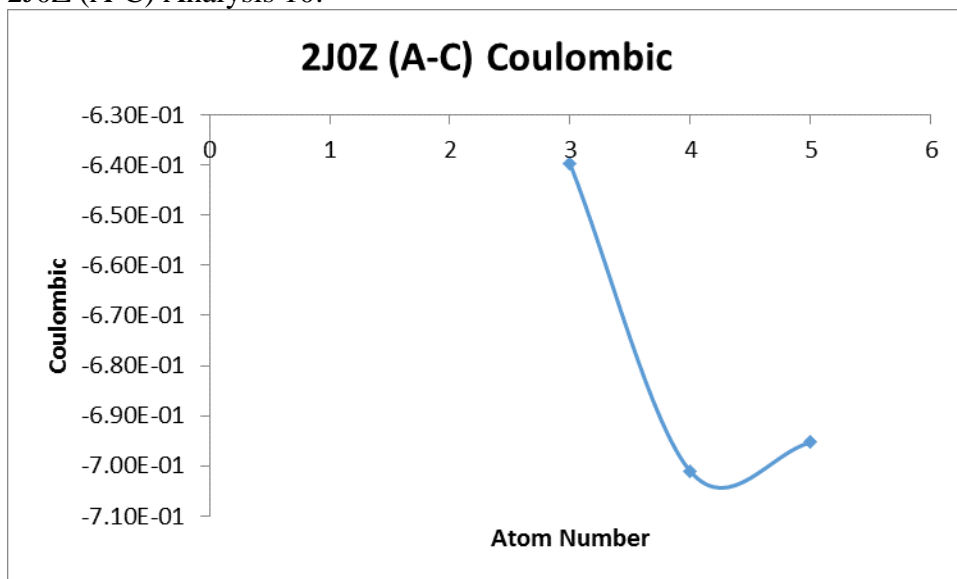


10 Model Surviving Interaction Analysis:

2J0Z (A-B) Analysis 10:

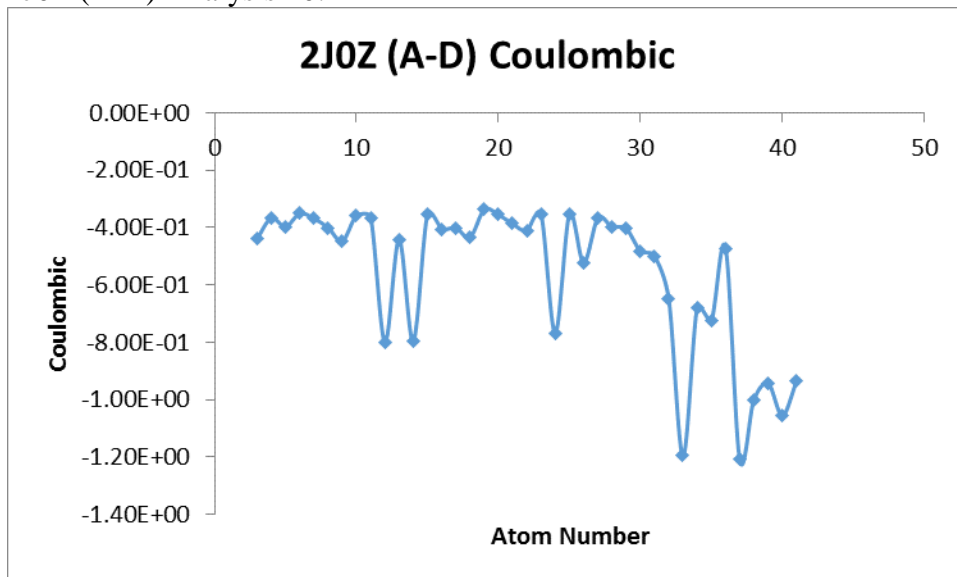


2J0Z (A-C) Analysis 10:



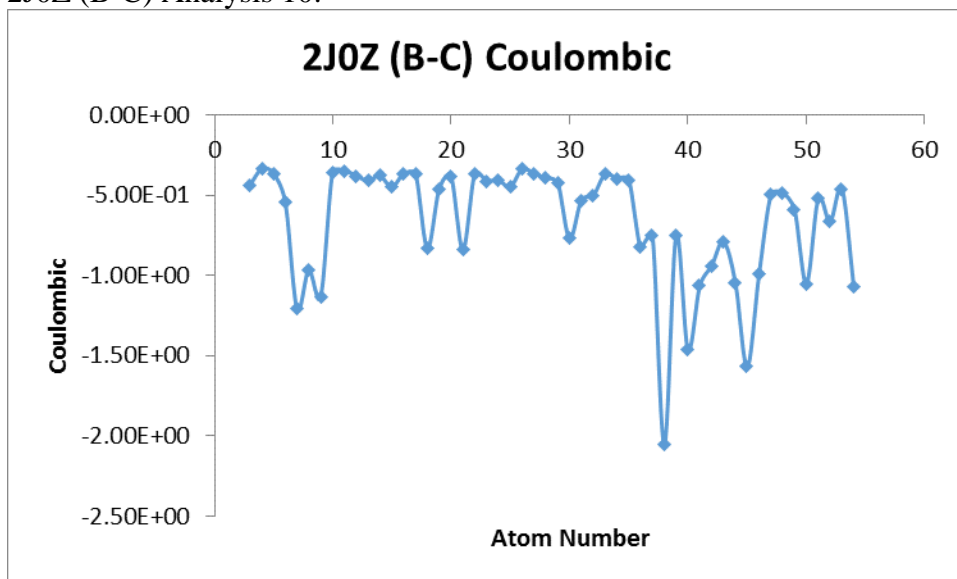
NO SURVIVING LENNARD-JONES A-C ATOM-ATOM INTERACTIONS ACROSS ENSEMBLE

2J0Z (A-D) Analysis 10:



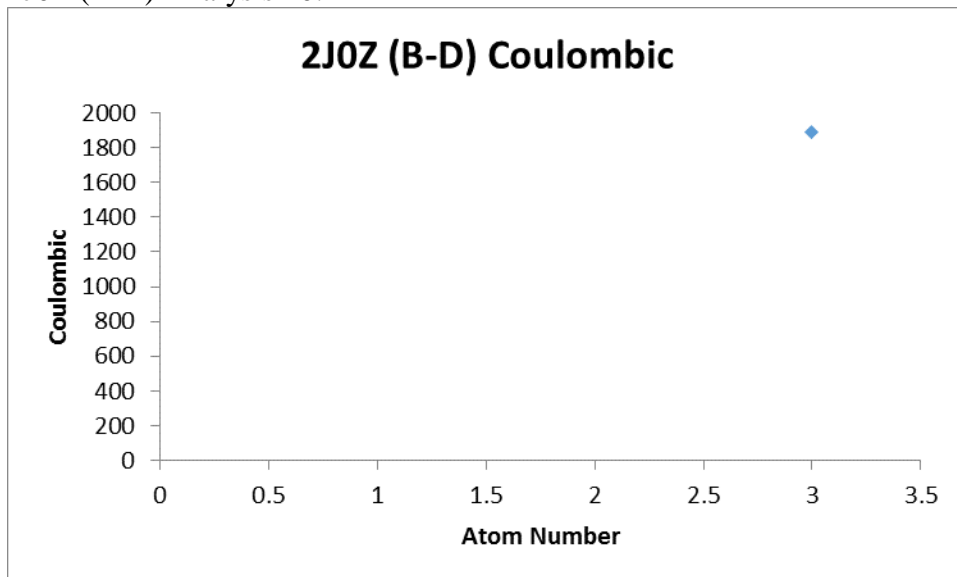
NO SURVIVING LENNARD-JONES A-D ATOM-ATOM INTERACTIONS ACROSS ENSEMBLE

2J0Z (B-C) Analysis 10:



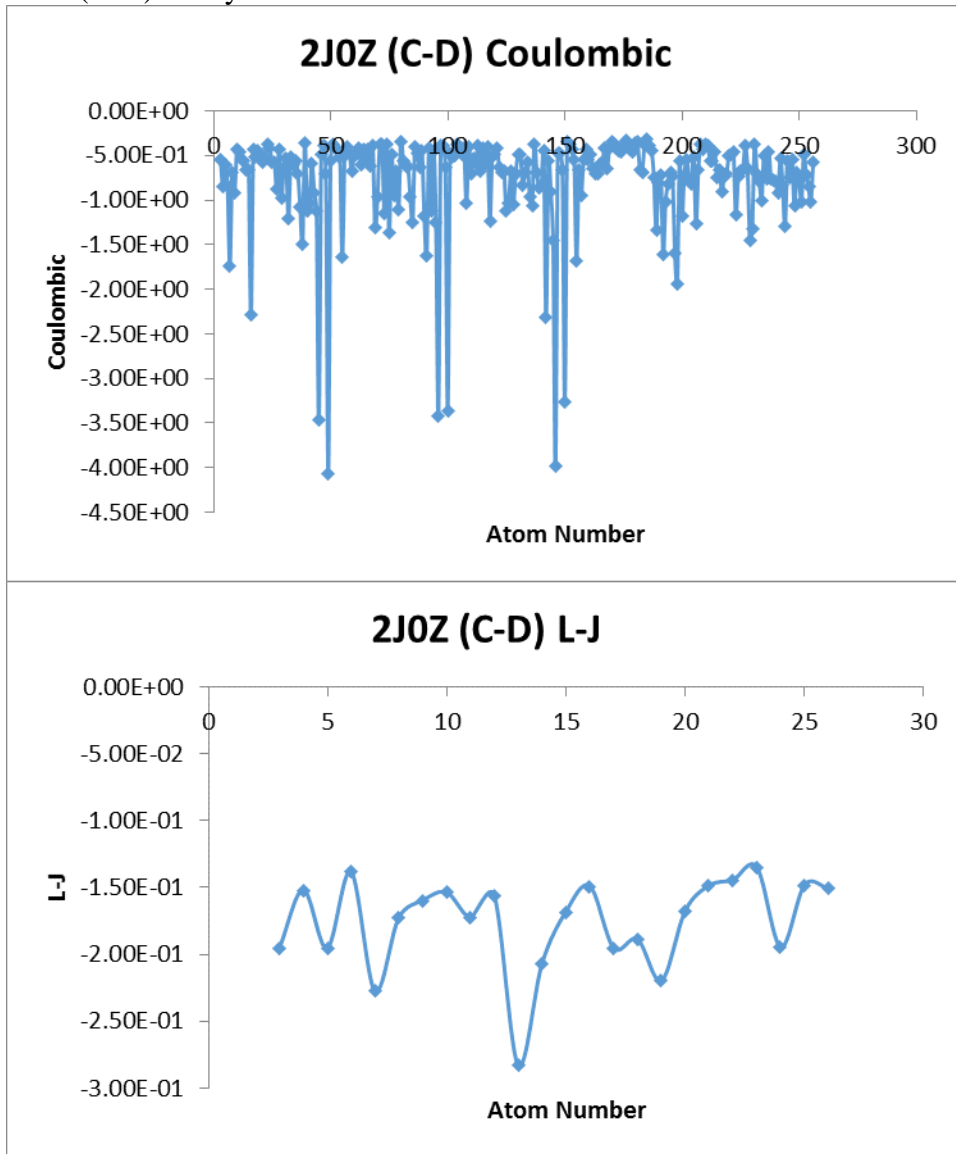
NO SURVIVING LENNARD-JONES B-C ATOM-ATOM INTERACTIONS ACROSS ENSEMBLE

2J0Z (B-D) Analysis 10:

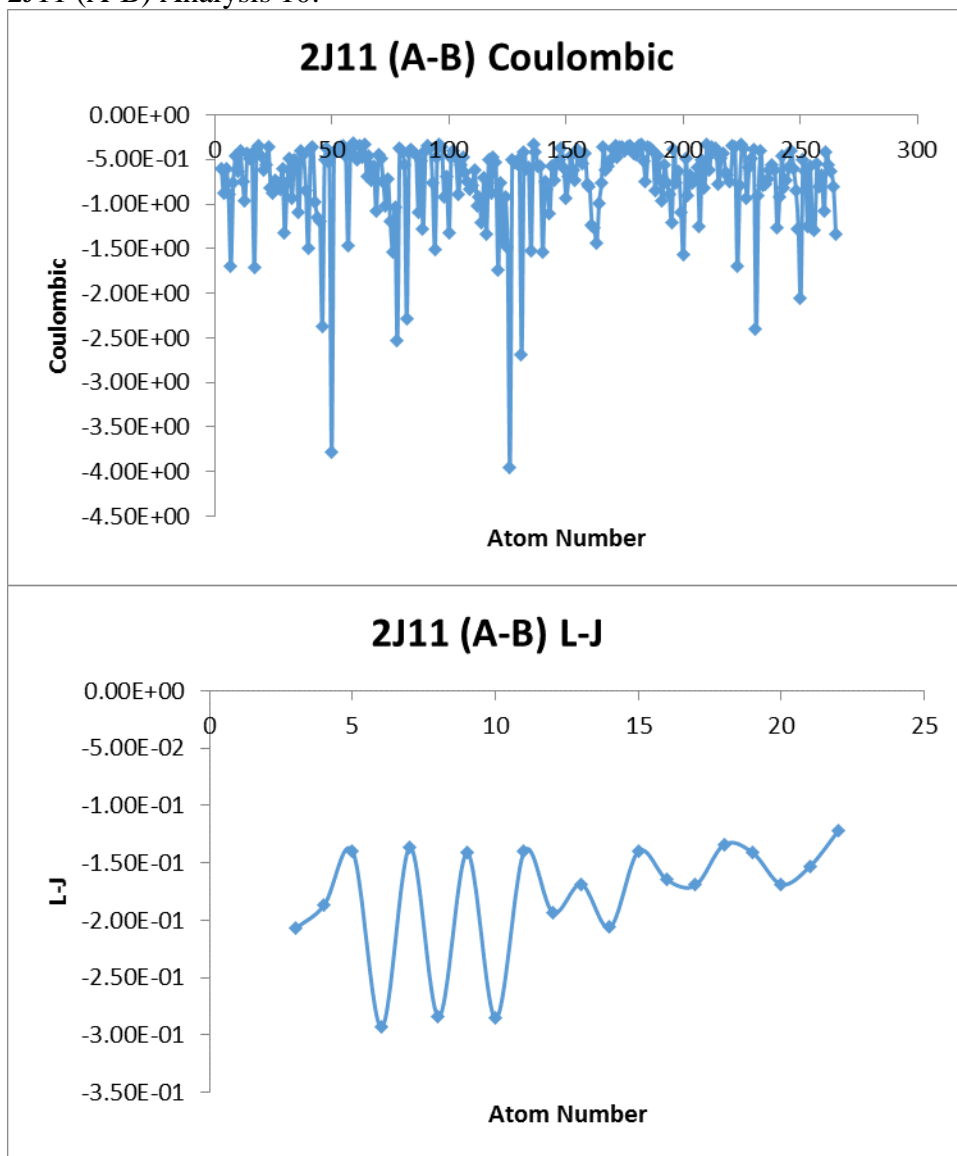


NO SURVIVING LENNARD-JONES B-D ATOM-ATOM INTERACTIONS ACROSS ENSEMBLE

2J0Z (C-D) Analysis 10:



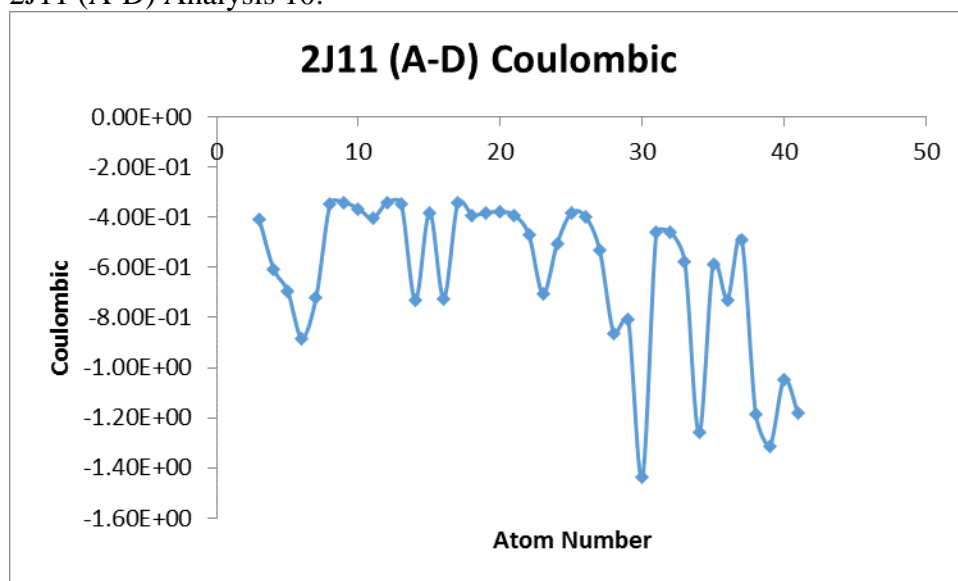
2J11 (A-B) Analysis 10:



2J11 (A-C) Analysis 10:

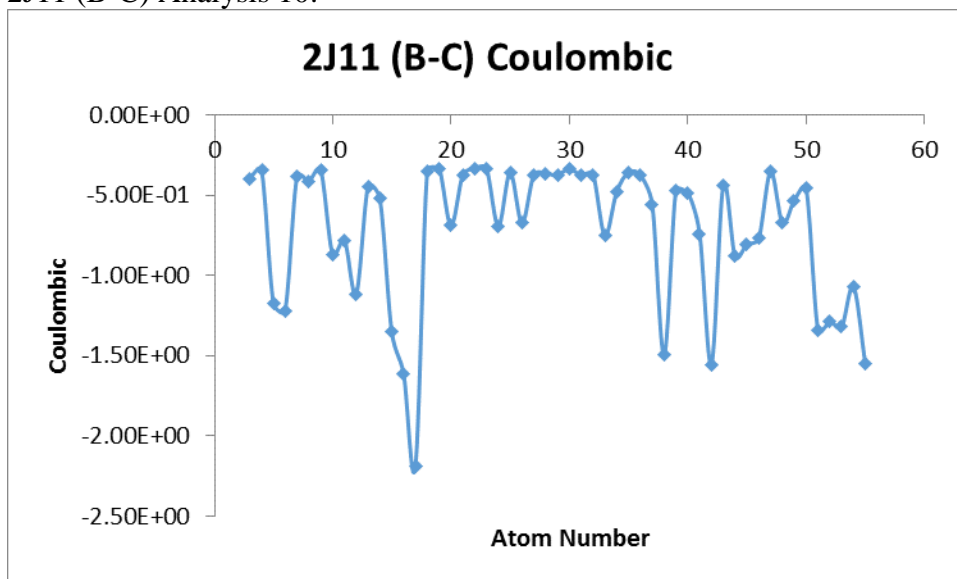
NO SURVIVING COULOMBIC A-C ATOM-ATOM INTERACTIONS ACROSS ENSEMBLE
NO SURVIVING LENNARD-JONES A-C ATOM-ATOM INTERACTIONS ACROSS ENSEMBLE

2J11 (A-D) Analysis 10:



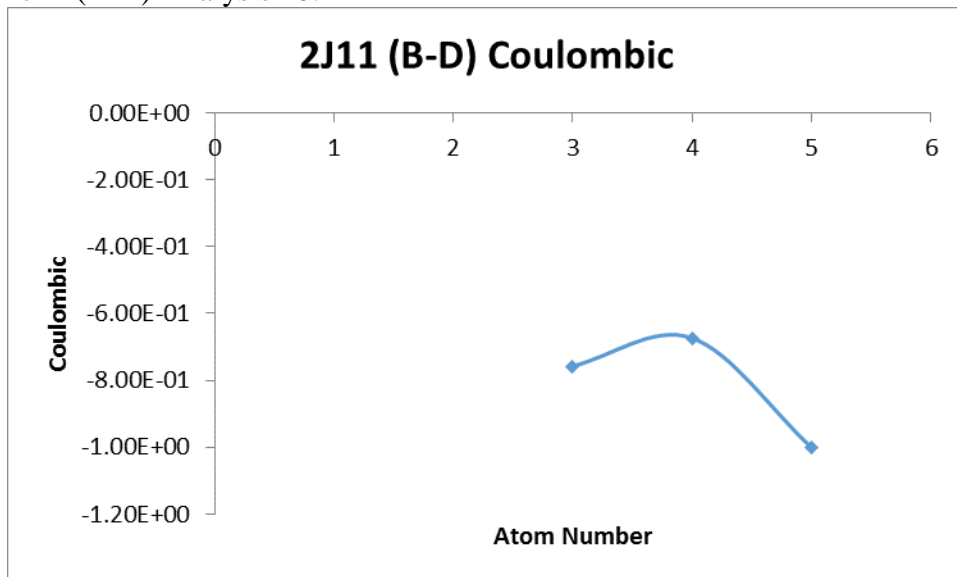
NO SURVIVING LENNARD-JONES A-D ATOM-ATOM INTERACTIONS ACROSS ENSEMBLE

2J11 (B-C) Analysis 10:



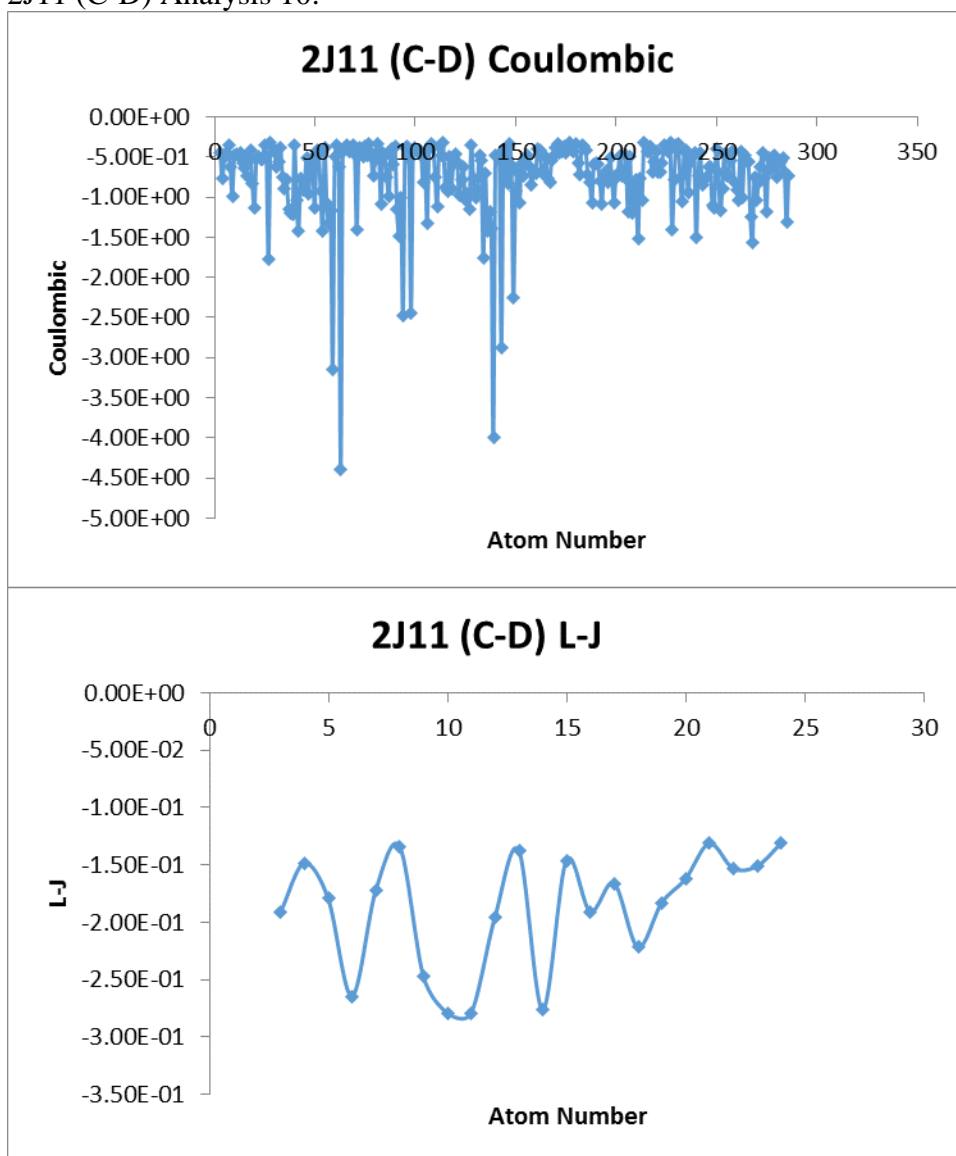
NO SURVIVING LENNARD-JONES B-C ATOM-ATOM INTERACTIONS ACROSS ENSEMBLE

2J11 (B-D) Analysis 10:

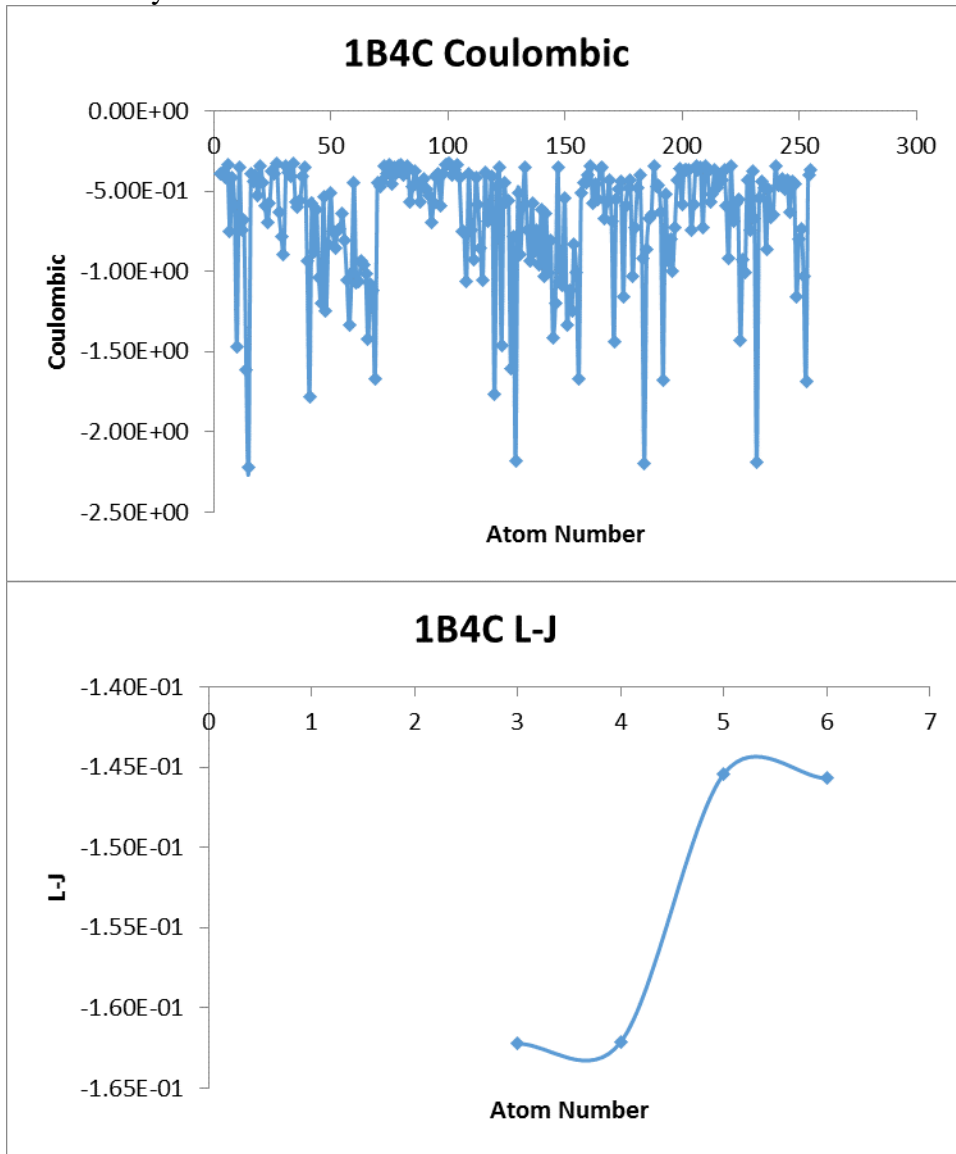


NO SURVIVING LENNARD-JONES B-D ATOM-ATOM INTERACTIONS ACROSS ENSEMBLE

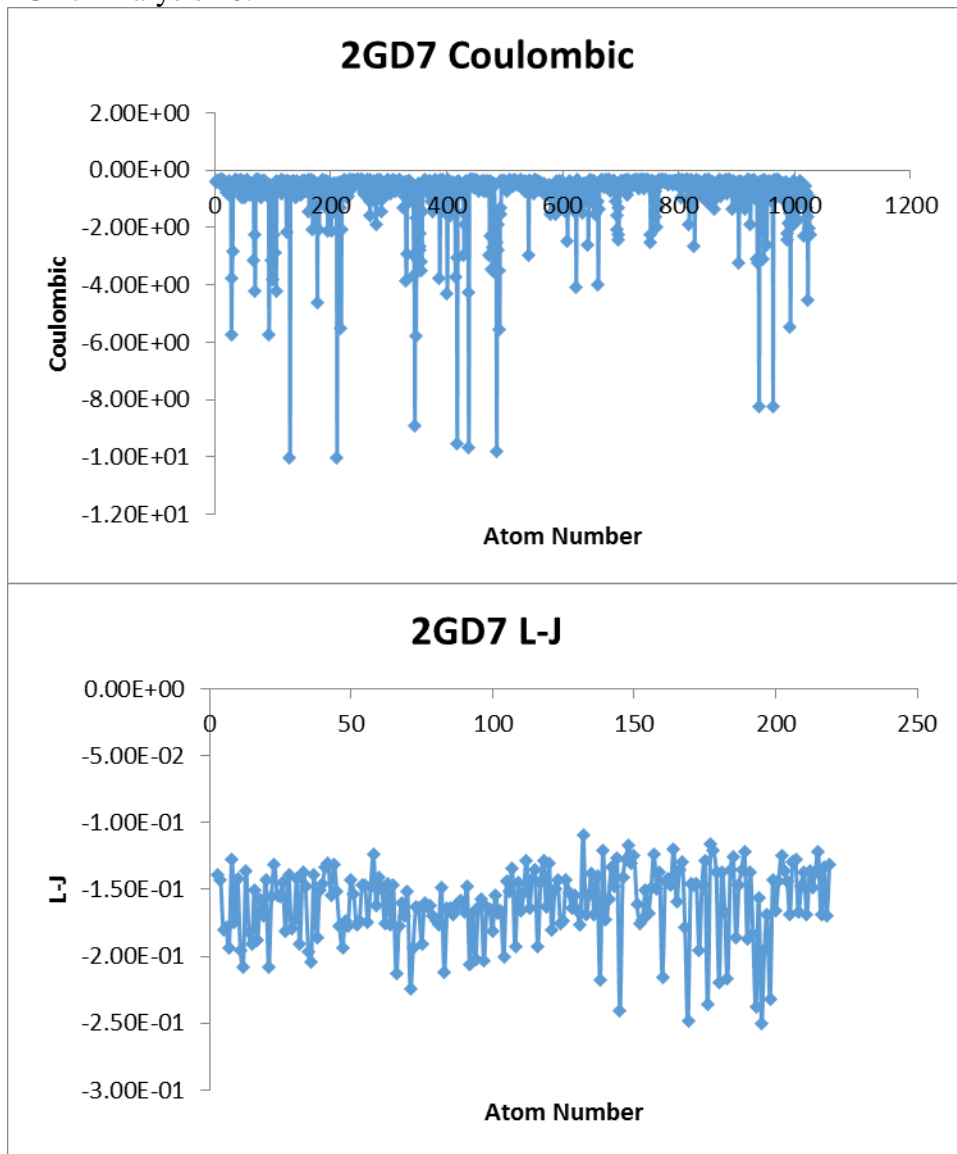
2J11 (C-D) Analysis 10:



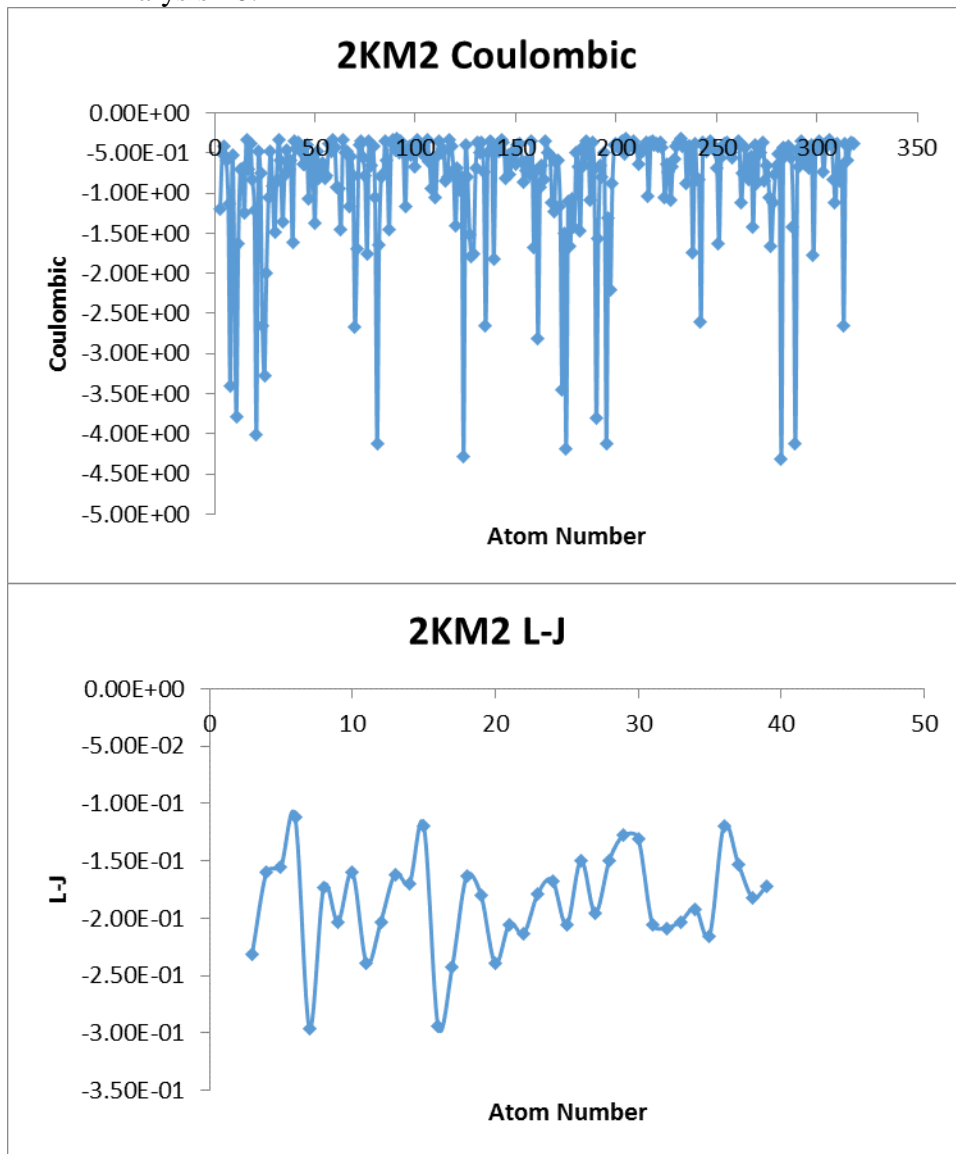
1B4C Analysis 10:



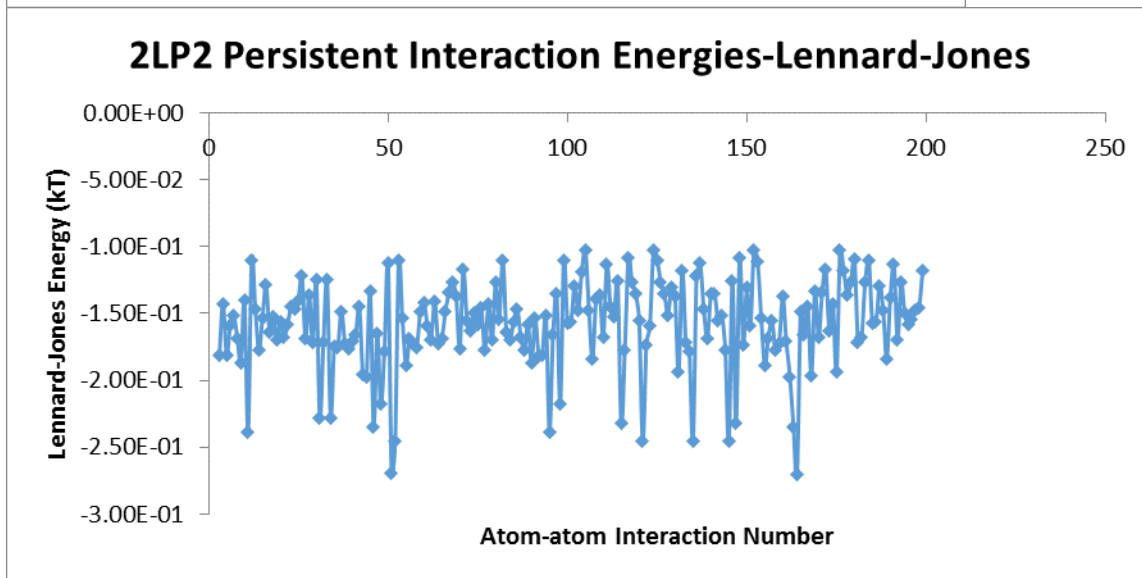
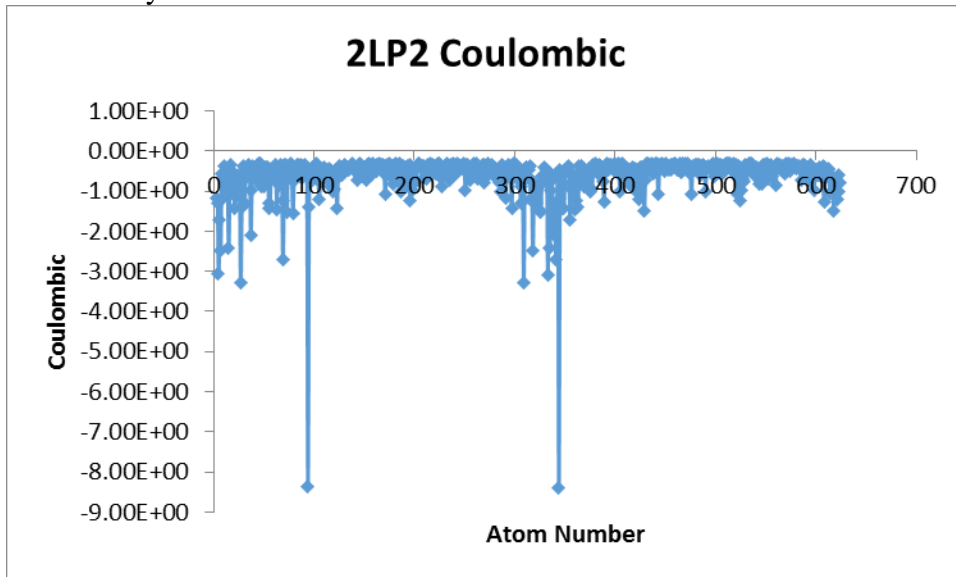
2GD7 Analysis 10:



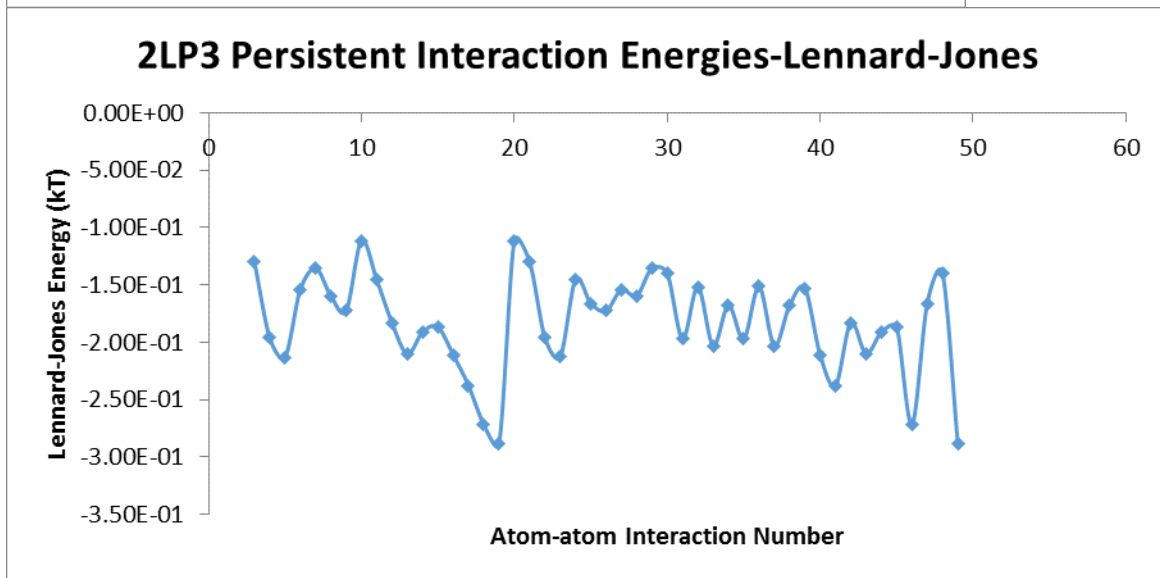
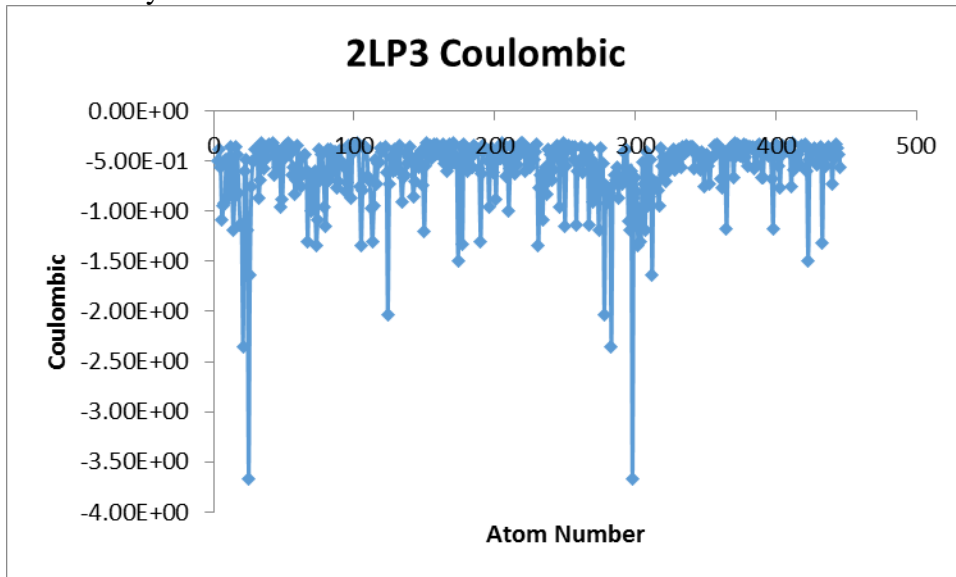
2KM2 Analysis 10:



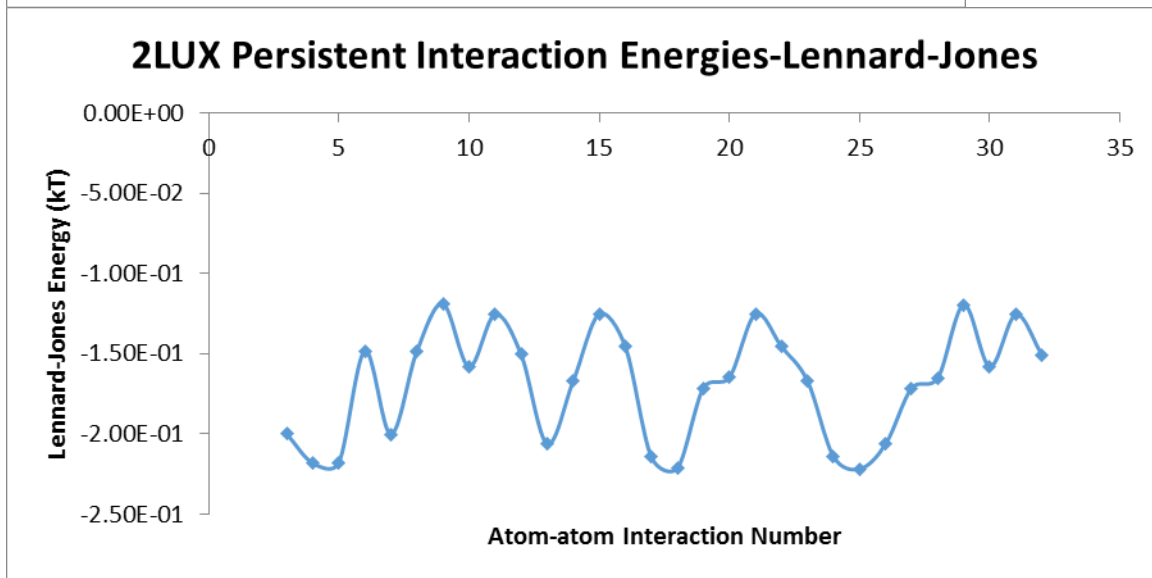
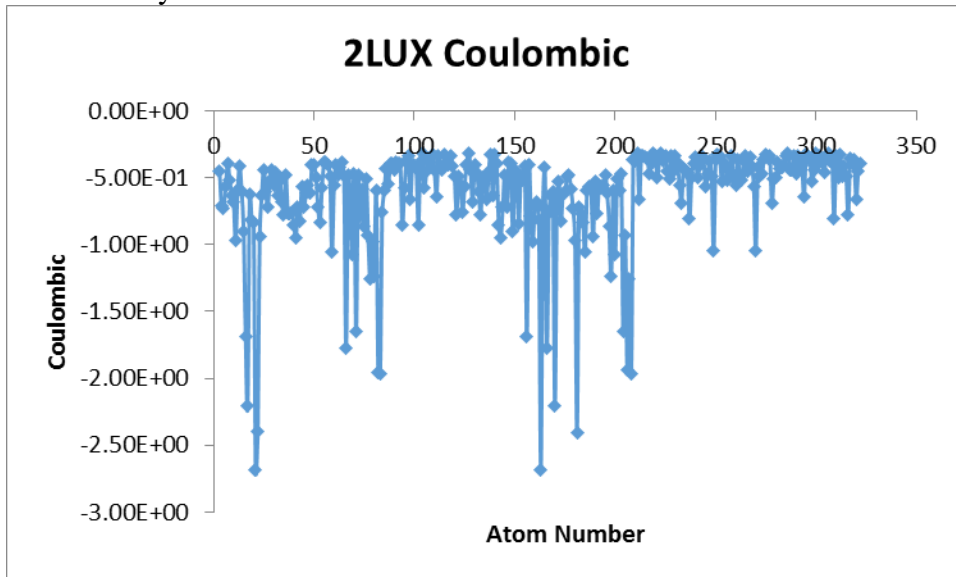
2LP2 Analysis 10:



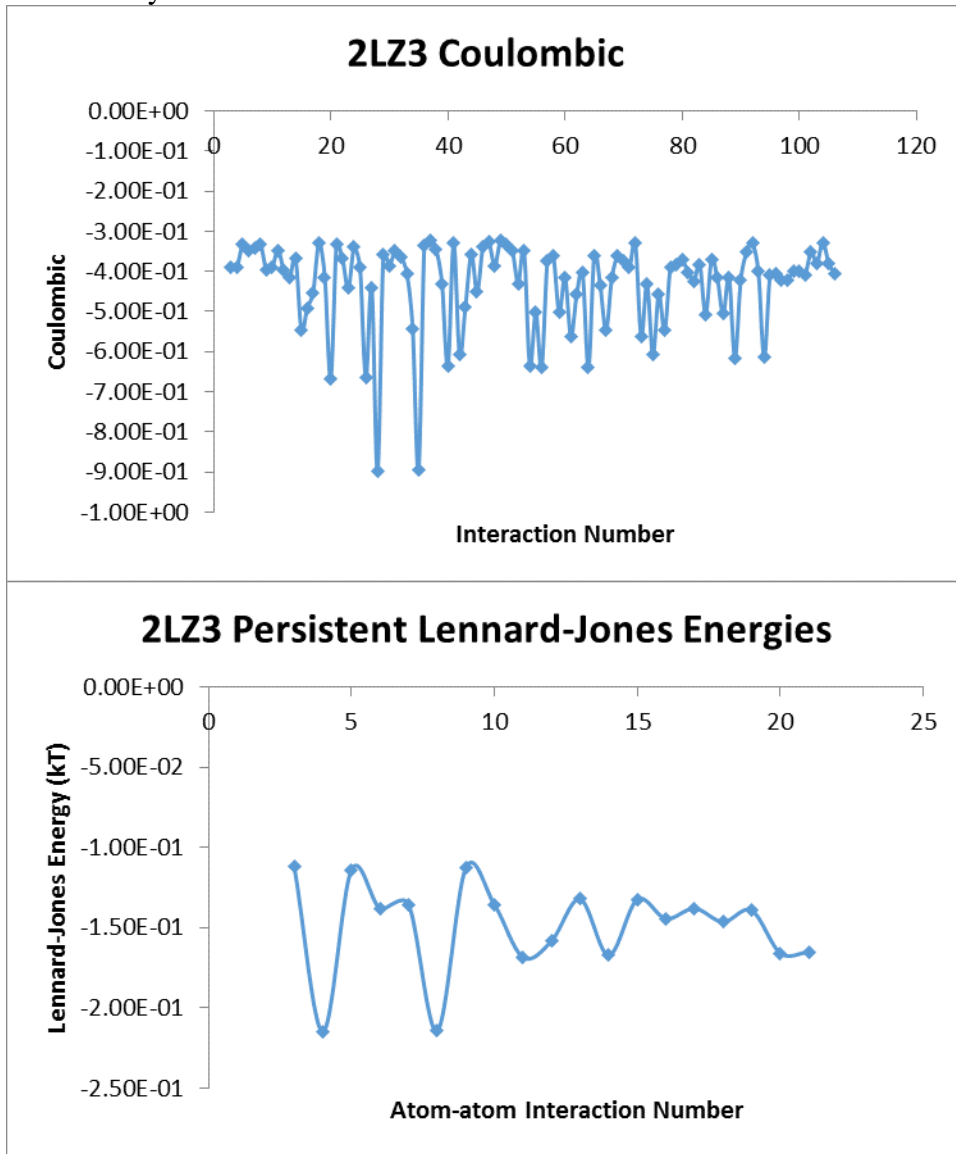
2LP3 Analysis 10:



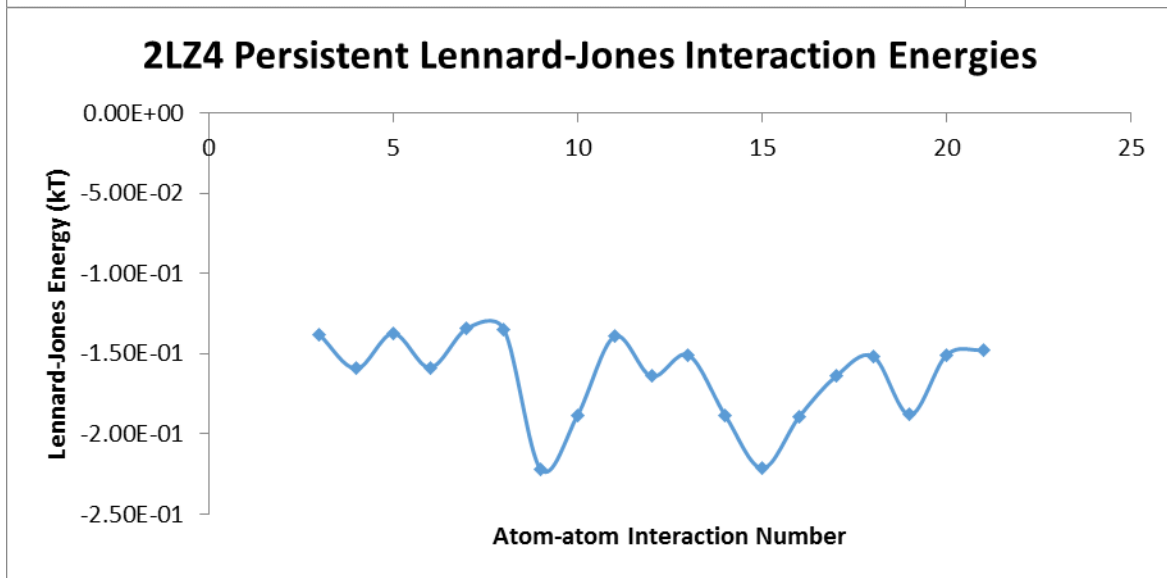
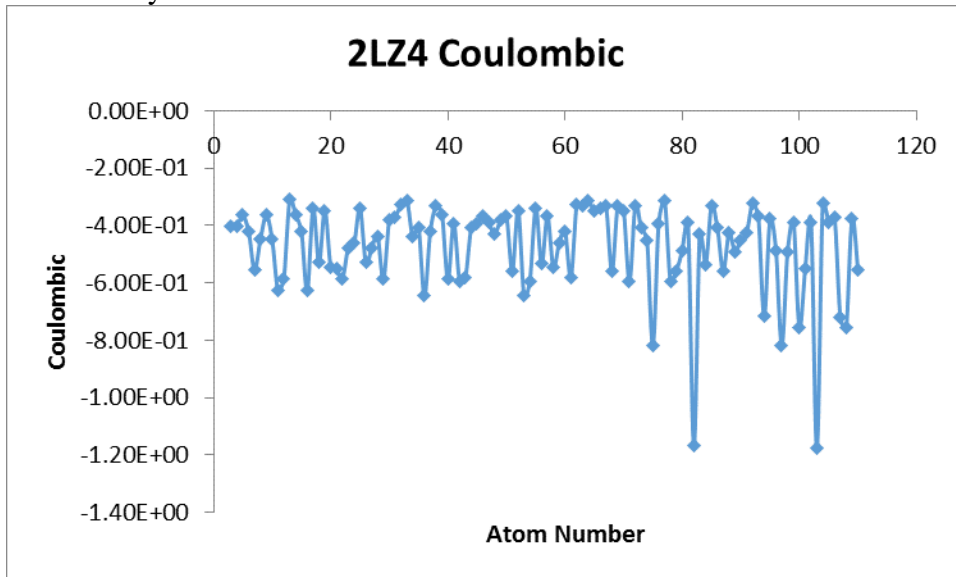
2LUX Analysis 10:



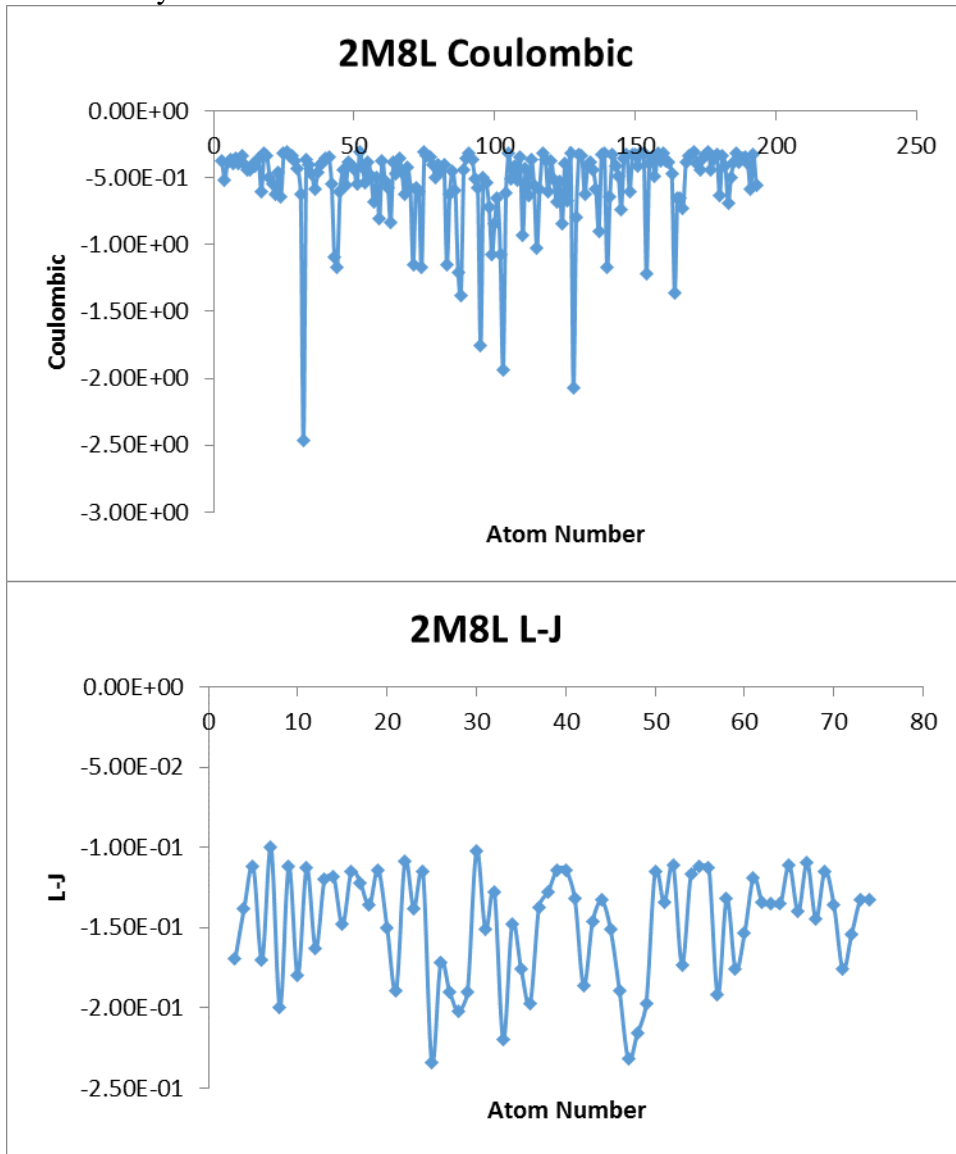
2LZ3 Analysis 10:



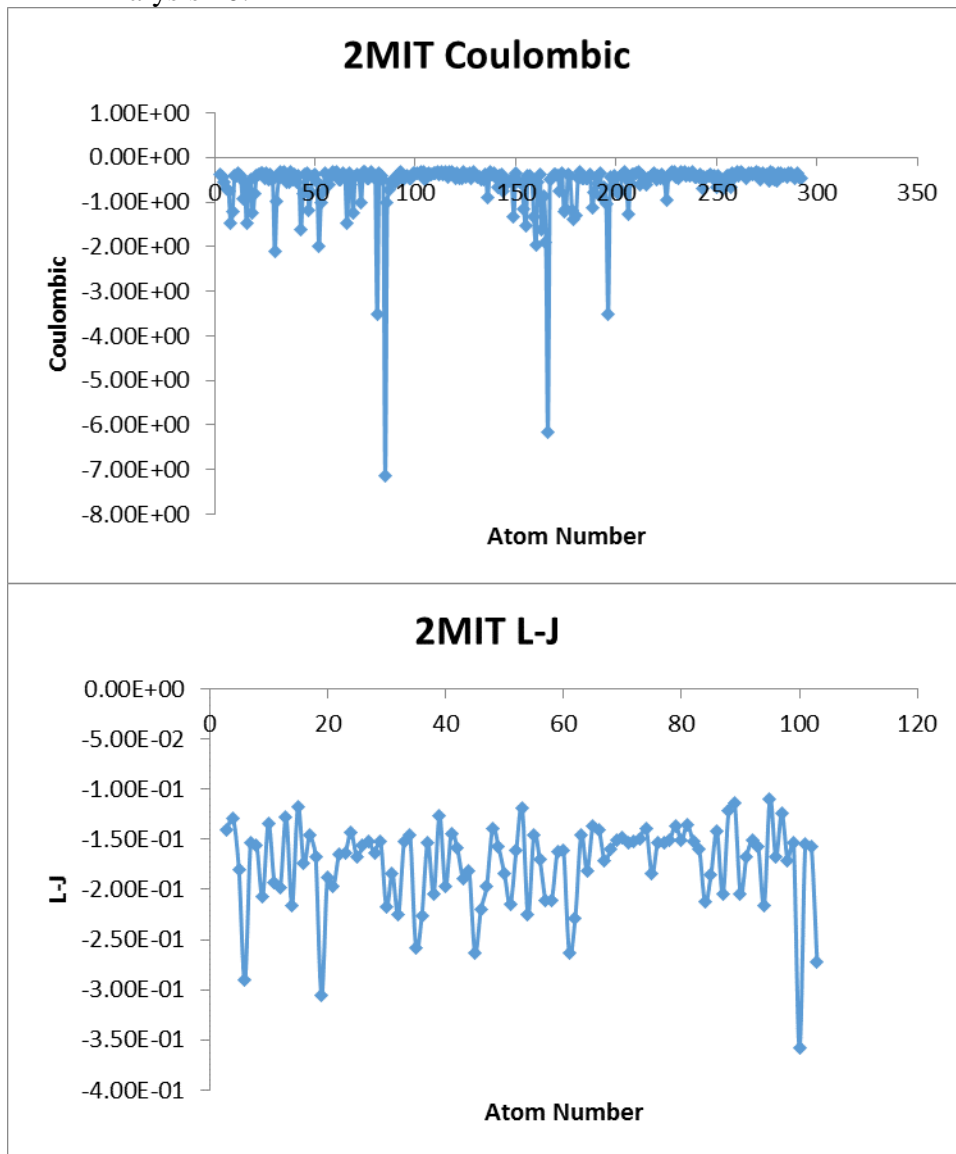
2LZ4 Analysis 10:



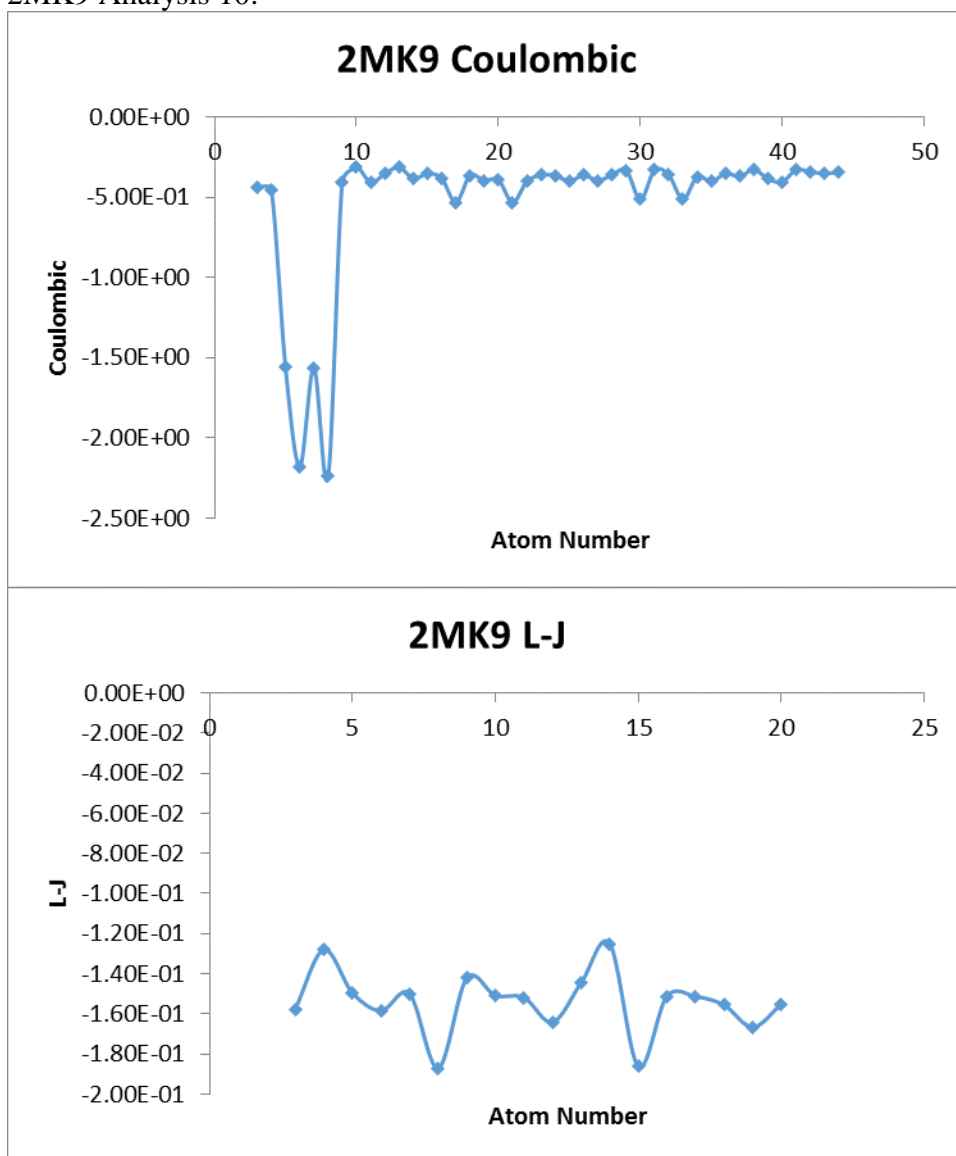
2M8L Analysis 10:



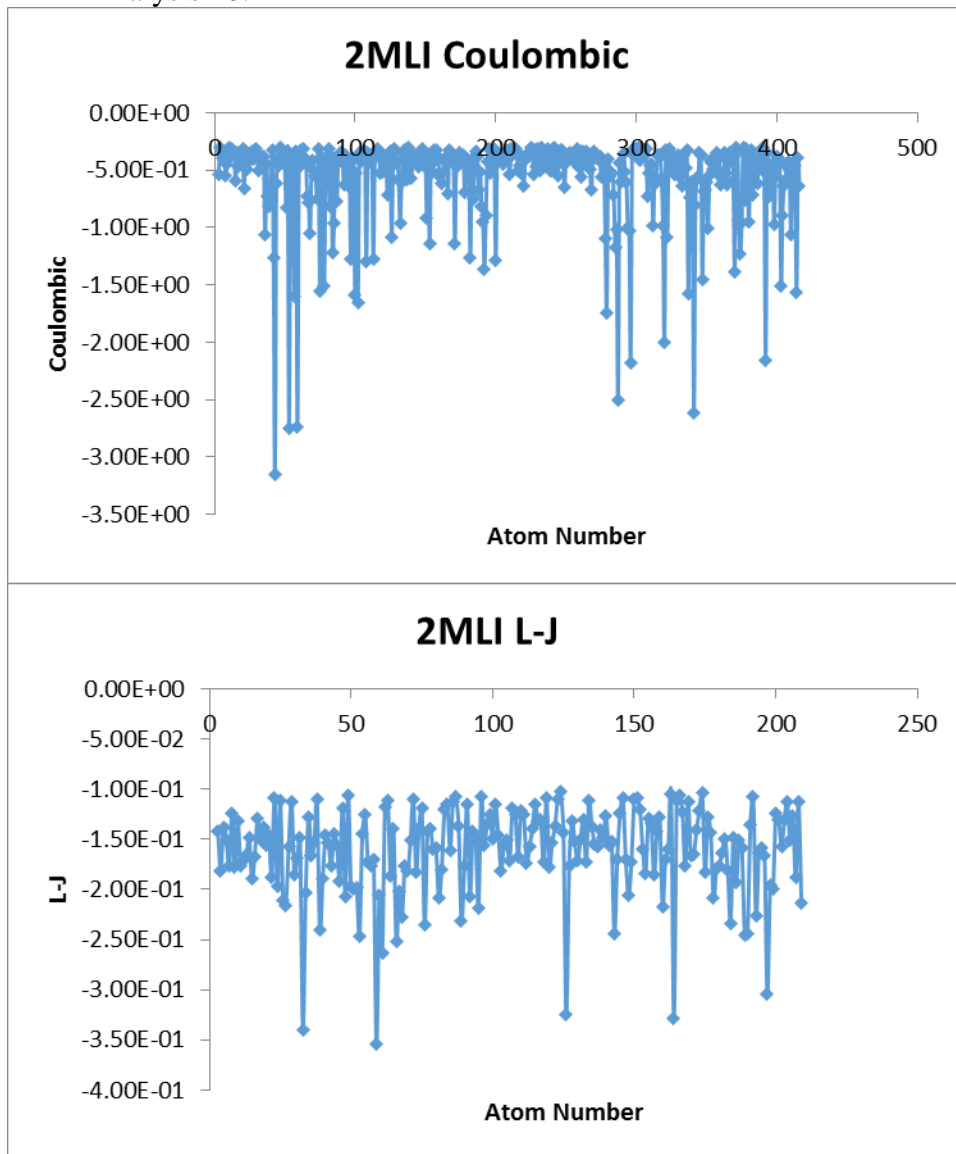
2MIT Analysis 10:



2MK9 Analysis 10:



2MLI Analysis 10:



Appendix D

A β 40 and A β 42 Case Study Mapping and Ramachandran Angle Data

Authors: Oscar H. Bastidas, Benjamin Green, Mary Sprague, Michael H. Peters

Supplementary Table 1a: Mapping results for A β 40's (PDB ID: 2M4J by Lu et al.) short range (1:2) dominant atom-atom Coulombic interactions across ensemble structures. Columns for each chain correspond to: residue abbreviation, residue number in peptide sequence, atom identity (IUPAC naming convention) and atom number in PDB file. Energy in kT , distance in nm . Mapping analysis began on the 11th residue for both isoforms because original structure data for A β 42 begins with the 11th residue.

Chain A				Chain D				Average Distance	Average Coulombic Values	Lower 95% Confidence Interval Bound	Upper 95% Confidence Interval Bound	Margin of Error
GLU	11	N	152	GLU	11	C	1951	5.75E-01	-4.21E-01	-4.26E-01	-4.16E-01	5.02E-03
GLU	11	N	152	GLU	11	CD	1955	6.25E-01	-5.73E-01	-5.80E-01	-5.66E-01	6.71E-03
GLU	11	N	152	VAL	12	H	1971	5.03E-01	-5.36E-01	-5.45E-01	-5.27E-01	8.92E-03
GLU	11	C	154	GLU	11	N	1949	5.60E-01	-4.46E-01	-4.50E-01	-4.42E-01	4.16E-03
GLU	11	C	154	GLU	11	O	1952	6.27E-01	-4.90E-01	-4.93E-01	-4.87E-01	2.76E-03
GLU	11	C	154	GLU	11	OE1	1956	7.22E-01	-5.28E-01	-5.88E-01	-4.68E-01	5.97E-02
GLU	11	C	154	GLU	11	OE2	1957	7.04E-01	-5.52E-01	-6.05E-01	-4.99E-01	5.30E-02
GLU	11	C	154	VAL	12	N	1964	4.47E-01	-8.07E-01	-8.14E-01	-8.00E-01	6.98E-03
GLU	11	C	154	VAL	12	O	1967	4.55E-01	-6.99E-01	-7.05E-01	-6.92E-01	6.19E-03
GLU	11	C	154	HIS	13	N	1980	6.66E-01	-3.87E-01	-3.88E-01	-3.85E-01	1.71E-03
GLU	11	C	154	HIS	13	ND1	1986	6.26E-01	-3.51E-01	-3.54E-01	-3.49E-01	2.79E-03
GLU	11	O	155	GLU	11	C	1951	3.99E-01	-1.43E+00	-1.44E+00	-1.42E+00	1.46E-02
GLU	11	O	155	GLU	11	CD	1955	6.26E-01	-8.01E-01	-8.04E-01	-7.97E-01	3.47E-03
GLU	11	O	155	GLU	11	H	1958	5.55E-01	-4.17E-01	-4.21E-01	-4.12E-01	4.11E-03
GLU	11	O	155	GLU	11	HA	1959	2.73E-01	-5.68E-01	-5.81E-01	-5.56E-01	1.25E-02
GLU	11	O	155	VAL	12	C	1966	4.69E-01	-9.00E-01	-9.08E-01	-8.92E-01	8.08E-03
GLU	11	O	155	VAL	12	CB	1968	4.57E-01	-8.48E-01	-8.62E-01	-8.33E-01	1.41E-02
GLU	11	O	155	VAL	12	H	1971	2.72E-01	-3.86E+00	-3.92E+00	-3.79E+00	6.26E-02
GLU	11	O	155	HIS	13	C	1982	8.06E-01	-4.27E-01	-4.29E-01	-4.25E-01	1.79E-03
GLU	11	CD	158	GLU	11	N	1949	7.24E-01	-4.28E-01	-4.30E-01	-4.25E-01	2.95E-03
GLU	11	CD	158	GLU	11	O	1952	8.84E-01	-4.22E-01	-4.24E-01	-4.21E-01	1.46E-03
GLU	11	CD	158	GLU	11	OE1	1956	5.55E-01	-1.61E+00	-2.00E+00	-1.22E+00	3.89E-01
GLU	11	CD	158	GLU	11	OE2	1957	5.15E-01	-1.88E+00	-2.26E+00	-1.50E+00	3.78E-01
GLU	11	CD	158	VAL	12	N	1964	7.59E-01	-4.17E-01	-4.19E-01	-4.15E-01	1.83E-03
GLU	11	CD	158	VAL	12	O	1967	8.02E-01	-3.40E-01	-3.42E-01	-3.39E-01	1.40E-03
GLU	11	CD	158	HIS	13	N	1980	9.55E-01	-3.33E-01	-3.34E-01	-3.32E-01	8.98E-04
GLU	11	CD	158	HIS	13	ND1	1986	7.15E-01	-4.38E-01	-4.42E-01	-4.34E-01	3.97E-03

GLU	11	OE1	159	GLU	11	C	1951	7.82E-01	-4.51E-01	-4.88E-01	-4.15E-01	3.66E-02
GLU	11	OE1	159	GLU	11	CD	1955	4.89E-01	-2.18E+00	-2.67E+00	-1.68E+00	4.93E-01
GLU	11	OE1	159	VAL	12	C	1966	8.81E-01	-3.46E-01	-3.58E-01	-3.34E-01	1.23E-02
GLU	11	OE1	159	VAL	12	H	1971	6.93E-01	-5.26E-01	-5.62E-01	-4.89E-01	3.66E-02
GLU	11	OE1	159	GLY	38	C	2358	8.60E-01	-4.71E-01	-4.98E-01	-4.43E-01	2.75E-02
GLU	11	OE1	159	VAL	39	CB	2367	7.09E-01	-4.58E-01	-5.06E-01	-4.10E-01	4.78E-02
GLU	11	OE1	159	VAL	39	H	2370	8.52E-01	-3.68E-01	-4.08E-01	-3.29E-01	3.96E-02
GLU	11	OE2	160	GLU	11	C	1951	8.19E-01	-4.16E-01	-4.48E-01	-3.83E-01	3.25E-02
GLU	11	OE2	160	GLU	11	CD	1955	5.33E-01	-1.80E+00	-2.28E+00	-1.32E+00	4.80E-01
GLU	11	OE2	160	VAL	12	H	1971	7.24E-01	-4.83E-01	-5.12E-01	-4.53E-01	2.93E-02
GLU	11	OE2	160	GLY	38	C	2358	8.64E-01	-4.69E-01	-5.04E-01	-4.34E-01	3.50E-02
GLU	11	OE2	160	VAL	39	CB	2367	7.02E-01	-4.80E-01	-5.57E-01	-4.04E-01	7.65E-02
GLU	11	H	161	GLU	11	N	1949	4.36E-01	-5.31E-01	-5.36E-01	-5.25E-01	5.66E-03
GLU	11	H	161	GLU	11	O	1952	6.29E-01	-3.19E-01	-3.21E-01	-3.16E-01	2.23E-03
GLU	11	H	161	GLU	11	OE1	1956	6.11E-01	-4.78E-01	-5.22E-01	-4.33E-01	4.42E-02
GLU	11	H	161	GLU	11	OE2	1957	5.93E-01	-5.06E-01	-5.42E-01	-4.71E-01	3.56E-02
GLU	11	H	161	VAL	12	N	1964	5.39E-01	-3.39E-01	-3.42E-01	-3.35E-01	3.28E-03
VAL	12	N	167	GLU	11	C	1951	5.93E-01	-4.19E-01	-4.21E-01	-4.16E-01	2.41E-03
VAL	12	N	167	GLU	11	CD	1955	7.55E-01	-4.21E-01	-4.24E-01	-4.18E-01	2.94E-03
VAL	12	N	167	VAL	12	C	1966	5.40E-01	-4.90E-01	-4.92E-01	-4.87E-01	2.59E-03
VAL	12	N	167	VAL	12	CB	1968	5.89E-01	-3.57E-01	-3.59E-01	-3.55E-01	2.22E-03
VAL	12	N	167	VAL	12	H	1971	4.21E-01	-8.83E-01	-8.92E-01	-8.75E-01	8.46E-03
VAL	12	N	167	HIS	13	C	1982	8.12E-01	-3.20E-01	-3.21E-01	-3.19E-01	9.45E-04
VAL	12	C	169	VAL	12	N	1964	5.81E-01	-4.16E-01	-4.18E-01	-4.13E-01	2.45E-03
VAL	12	C	169	VAL	12	O	1967	3.82E-01	-1.03E+00	-1.04E+00	-1.03E+00	8.37E-03
VAL	12	C	169	HIS	13	N	1980	5.91E-01	-4.70E-01	-4.72E-01	-4.69E-01	1.58E-03
VAL	12	C	169	HIS	13	ND1	1986	5.36E-01	-4.69E-01	-4.73E-01	-4.65E-01	3.97E-03
VAL	12	C	169	HIS	14	N	1997	6.74E-01	-3.58E-01	-3.59E-01	-3.56E-01	1.70E-03
VAL	12	O	170	VAL	12	C	1966	6.29E-01	-3.17E-01	-3.18E-01	-3.15E-01	1.28E-03
VAL	12	O	170	VAL	12	H	1971	6.14E-01	-3.28E-01	-3.30E-01	-3.26E-01	2.00E-03
VAL	12	O	170	HIS	13	C	1982	7.83E-01	-3.07E-01	-3.07E-01	-3.06E-01	7.76E-04
VAL	12	CB	171	VAL	12	N	1964	5.40E-01	-4.33E-01	-4.36E-01	-4.30E-01	3.09E-03
VAL	12	CB	171	VAL	12	O	1967	4.25E-01	-6.94E-01	-6.98E-01	-6.89E-01	4.21E-03
VAL	12	CB	171	HIS	13	N	1980	6.40E-01	-3.52E-01	-3.53E-01	-3.50E-01	1.06E-03
VAL	12	H	174	GLU	11	OE1	1956	8.49E-01	-3.71E-01	-4.12E-01	-3.30E-01	4.08E-02
VAL	12	H	174	GLU	11	OE2	1957	8.25E-01	-3.87E-01	-4.22E-01	-3.52E-01	3.50E-02
VAL	12	H	174	VAL	12	N	1964	5.97E-01	-3.86E-01	-3.88E-01	-3.84E-01	1.85E-03
VAL	12	H	174	VAL	12	O	1967	5.11E-01	-4.94E-01	-4.97E-01	-4.92E-01	2.57E-03

VAL	12	H	174	HIS	13	ND1	1986	6.33E-01	-3.21E-01	-3.24E-01	-3.19E-01	2.56E-03
HIS	13	N	183	GLU	11	C	1951	7.00E-01	-3.50E-01	-3.51E-01	-3.48E-01	1.67E-03
HIS	13	N	183	GLU	11	CD	1955	9.00E-01	-3.66E-01	-3.67E-01	-3.64E-01	1.31E-03
HIS	13	N	183	VAL	12	C	1966	4.46E-01	-9.07E-01	-9.13E-01	-9.00E-01	6.52E-03
HIS	13	N	183	VAL	12	CB	1968	5.97E-01	-4.08E-01	-4.09E-01	-4.06E-01	1.94E-03
HIS	13	N	183	VAL	12	H	1971	5.04E-01	-6.65E-01	-6.70E-01	-6.59E-01	5.40E-03
HIS	13	N	183	HIS	13	C	1982	5.59E-01	-7.86E-01	-7.90E-01	-7.83E-01	3.39E-03
HIS	13	N	183	HIS	13	CG	1985	4.95E-01	-4.37E-01	-4.42E-01	-4.32E-01	5.19E-03
HIS	13	N	183	HIS	14	C	1999	6.97E-01	-4.97E-01	-5.00E-01	-4.93E-01	3.43E-03
HIS	13	N	183	HIS	14	H	2007	4.78E-01	-4.84E-01	-4.89E-01	-4.80E-01	4.70E-03
HIS	13	C	185	GLU	11	O	1952	9.66E-01	-3.18E-01	-3.18E-01	-3.17E-01	7.87E-04
HIS	13	C	185	VAL	12	N	1964	7.53E-01	-3.66E-01	-3.68E-01	-3.65E-01	1.37E-03
HIS	13	C	185	VAL	12	O	1967	4.73E-01	-8.94E-01	-9.01E-01	-8.86E-01	7.25E-03
HIS	13	C	185	HIS	13	N	1980	5.67E-01	-7.63E-01	-7.66E-01	-7.59E-01	3.86E-03
HIS	13	C	185	HIS	13	O	1983	6.25E-01	-6.20E-01	-6.22E-01	-6.18E-01	1.70E-03
HIS	13	C	185	HIS	13	ND1	1986	5.23E-01	-7.33E-01	-7.41E-01	-7.25E-01	7.88E-03
HIS	13	C	185	HIS	14	N	1997	4.34E-01	-1.44E+00	-1.45E+00	-1.43E+00	9.89E-03
HIS	13	C	185	HIS	14	O	2000	4.57E-01	-1.27E+00	-1.28E+00	-1.26E+00	1.27E-02
HIS	13	C	185	GLN	15	N	2014	5.81E-01	-5.30E-01	-5.38E-01	-5.22E-01	7.73E-03
HIS	13	C	185	GLN	15	O	2017	8.20E-01	-3.95E-01	-3.98E-01	-3.92E-01	3.27E-03
HIS	13	C	185	GLN	15	OE1	2021	8.07E-01	-4.86E-01	-5.74E-01	-3.99E-01	8.73E-02
HIS	13	C	185	GLN	15	NE2	2022	7.53E-01	-7.48E-01	-8.47E-01	-6.49E-01	9.89E-02
HIS	13	O	186	VAL	12	C	1966	4.78E-01	-7.65E-01	-7.71E-01	-7.59E-01	6.09E-03
HIS	13	O	186	VAL	12	CB	1968	6.56E-01	-3.35E-01	-3.37E-01	-3.34E-01	1.59E-03
HIS	13	O	186	VAL	12	H	1971	6.51E-01	-3.79E-01	-3.81E-01	-3.77E-01	2.11E-03
HIS	13	O	186	HIS	13	C	1982	3.84E-01	-1.97E+00	-1.99E+00	-1.96E+00	1.51E-02
HIS	13	O	186	HIS	13	CG	1985	5.01E-01	-4.27E-01	-4.33E-01	-4.22E-01	5.67E-03
HIS	13	O	186	HIS	13	H	1990	5.52E-01	-3.46E-01	-3.48E-01	-3.44E-01	1.83E-03
HIS	13	O	186	HIS	13	HA	1991	2.66E-01	-7.07E-01	-7.19E-01	-6.94E-01	1.29E-02
HIS	13	O	186	HIS	14	C	1999	4.19E-01	-1.58E+00	-1.61E+00	-1.55E+00	2.69E-02
HIS	13	O	186	HIS	14	H	2007	2.34E-01	-3.43E+00	-3.53E+00	-3.33E+00	9.58E-02
HIS	13	O	186	GLN	15	CD	2020	7.19E-01	-4.95E-01	-5.72E-01	-4.19E-01	7.67E-02
HIS	13	O	186	GLN	15	H	2023	5.59E-01	-3.59E-01	-3.64E-01	-3.53E-01	5.74E-03
HIS	13	CG	188	VAL	12	O	1967	5.13E-01	-3.08E-01	-3.13E-01	-3.04E-01	4.43E-03
HIS	13	CG	188	HIS	13	ND1	1986	3.96E-01	-6.12E-01	-6.18E-01	-6.06E-01	6.37E-03
HIS	13	CD2	190	VAL	12	H	1971	5.32E-01	-3.31E-01	-3.36E-01	-3.27E-01	4.38E-03
HIS	13	CD2	190	HIS	13	HE1	1995	2.91E-01	-4.62E-01	-4.66E-01	-4.58E-01	4.07E-03
HIS	13	H	193	VAL	12	N	1964	4.95E-01	-3.78E-01	-3.81E-01	-3.75E-01	2.93E-03

HIS	13	H	193	VAL	12	O	1967	2.35E-01	-2.61E+00	-2.66E+00	-2.57E+00	4.43E-02
HIS	13	H	193	HIS	13	N	1980	4.09E-01	-7.14E-01	-7.19E-01	-7.10E-01	4.88E-03
HIS	13	H	193	HIS	13	O	1983	5.86E-01	-3.03E-01	-3.05E-01	-3.02E-01	1.25E-03
HIS	13	H	193	HIS	13	ND1	1986	3.99E-01	-6.10E-01	-6.20E-01	-6.00E-01	1.02E-02
HIS	13	H	193	HIS	14	N	1997	4.82E-01	-4.73E-01	-4.77E-01	-4.69E-01	4.05E-03
HIS	13	HD2	197	VAL	12	O	1967	3.74E-01	-3.93E-01	-4.03E-01	-3.83E-01	1.02E-02
HIS	13	HD2	197	HIS	13	ND1	1986	3.11E-01	-6.84E-01	-6.93E-01	-6.74E-01	9.49E-03
HIS	14	N	200	VAL	12	C	1966	6.93E-01	-3.39E-01	-3.41E-01	-3.38E-01	1.57E-03
HIS	14	N	200	HIS	13	C	1982	5.96E-01	-6.85E-01	-6.87E-01	-6.82E-01	2.47E-03
HIS	14	N	200	HIS	14	C	1999	5.09E-01	-9.79E-01	-9.89E-01	-9.69E-01	9.95E-03
HIS	14	N	200	HIS	14	H	2007	4.14E-01	-6.92E-01	-6.97E-01	-6.87E-01	4.83E-03
HIS	14	N	200	GLN	15	CD	2020	7.29E-01	-4.93E-01	-5.87E-01	-3.99E-01	9.42E-02
HIS	14	C	202	HIS	13	N	1980	8.84E-01	-3.25E-01	-3.26E-01	-3.24E-01	1.00E-03
HIS	14	C	202	HIS	13	O	1983	8.38E-01	-3.56E-01	-3.57E-01	-3.55E-01	9.89E-04
HIS	14	C	202	HIS	14	N	1997	6.13E-01	-6.45E-01	-6.48E-01	-6.42E-01	3.11E-03
HIS	14	C	202	HIS	14	O	2000	4.13E-01	-1.64E+00	-1.65E+00	-1.63E+00	1.12E-02
HIS	14	C	202	GLN	15	N	2014	5.48E-01	-6.03E-01	-6.10E-01	-5.96E-01	6.62E-03
HIS	14	C	202	GLN	15	O	2017	6.98E-01	-5.30E-01	-5.37E-01	-5.24E-01	6.75E-03
HIS	14	C	202	GLN	15	OE1	2021	7.53E-01	-5.78E-01	-7.20E-01	-4.36E-01	1.42E-01
HIS	14	C	202	GLN	15	NE2	2022	7.32E-01	-7.70E-01	-8.33E-01	-7.07E-01	6.29E-02
HIS	14	C	202	LYS	16	N	2031	6.29E-01	-5.05E-01	-5.14E-01	-4.95E-01	9.57E-03
HIS	14	C	202	LYS	16	O	2034	7.73E-01	-4.37E-01	-4.45E-01	-4.29E-01	8.28E-03
HIS	14	O	203	HIS	13	C	1982	8.32E-01	-3.60E-01	-3.61E-01	-3.59E-01	1.09E-03
HIS	14	O	203	HIS	14	C	1999	6.10E-01	-6.53E-01	-6.56E-01	-6.49E-01	3.71E-03
HIS	14	O	203	GLN	15	CD	2020	8.14E-01	-3.92E-01	-4.47E-01	-3.38E-01	5.42E-02
HIS	14	O	203	LYS	16	C	2033	8.68E-01	-3.68E-01	-3.74E-01	-3.62E-01	5.77E-03
HIS	14	CB	204	HIS	14	C	1999	4.44E-01	-3.93E-01	-4.03E-01	-3.82E-01	1.00E-02
HIS	14	CG	205	HIS	14	N	1997	5.19E-01	-3.92E-01	-3.95E-01	-3.88E-01	3.88E-03
HIS	14	CG	205	HIS	14	O	2000	2.88E-01	-1.85E+00	-1.89E+00	-1.80E+00	4.49E-02
HIS	14	ND1	206	HIS	13	C	1982	6.07E-01	-5.33E-01	-5.71E-01	-4.96E-01	3.76E-02
HIS	14	ND1	206	HIS	14	C	1999	3.75E-01	-1.69E+00	-1.74E+00	-1.65E+00	4.35E-02
HIS	14	ND1	206	HIS	14	CG	2002	4.16E-01	-5.69E-01	-6.51E-01	-4.88E-01	8.18E-02
HIS	14	ND1	206	HIS	14	H	2007	4.77E-01	-3.92E-01	-4.13E-01	-3.71E-01	2.07E-02
HIS	14	ND1	206	GLN	15	C	2016	5.48E-01	-4.33E-01	-4.99E-01	-3.67E-01	6.59E-02
HIS	14	CD2	207	HIS	14	C	1999	4.61E-01	-6.98E-01	-7.15E-01	-6.82E-01	1.67E-02
HIS	14	H	210	HIS	14	O	2000	5.28E-01	-3.83E-01	-3.86E-01	-3.81E-01	2.32E-03
HIS	14	HA	211	HIS	14	O	2000	2.45E-01	-9.01E-01	-9.09E-01	-8.94E-01	7.22E-03
HIS	14	HD2	214	HIS	14	O	2000	4.13E-01	-3.96E-01	-4.05E-01	-3.87E-01	9.06E-03

HIS	14	HE1	215	HIS	14	O	2000	3.70E-01	-4.21E-01	-4.34E-01	-4.09E-01	1.23E-02
GLN	15	N	217	HIS	13	C	1982	7.57E-01	-3.12E-01	-3.14E-01	-3.10E-01	2.07E-03
GLN	15	N	217	HIS	14	C	1999	5.00E-01	-7.46E-01	-7.53E-01	-7.40E-01	6.51E-03
GLN	15	N	217	GLN	15	C	2016	5.40E-01	-3.95E-01	-4.01E-01	-3.89E-01	5.77E-03
GLN	15	N	217	GLN	15	CD	2020	5.98E-01	-5.54E-01	-6.87E-01	-4.21E-01	1.33E-01
GLN	15	N	217	GLN	15	HA	2024	3.41E-01	-4.59E-01	-4.69E-01	-4.50E-01	9.68E-03
GLN	15	N	217	LYS	16	C	2033	7.01E-01	-3.95E-01	-4.02E-01	-3.87E-01	7.68E-03
GLN	15	C	219	HIS	14	O	2000	5.40E-01	-5.40E-01	-5.50E-01	-5.29E-01	1.05E-02
GLN	15	C	219	GLN	15	N	2014	5.83E-01	-3.33E-01	-3.36E-01	-3.29E-01	3.24E-03
GLN	15	C	219	GLN	15	O	2017	6.20E-01	-4.27E-01	-4.29E-01	-4.24E-01	2.58E-03
GLN	15	C	219	GLN	15	NE2	2022	6.84E-01	-5.49E-01	-5.77E-01	-5.21E-01	2.82E-02
GLN	15	C	219	LYS	16	N	2031	4.54E-01	-6.72E-01	-6.83E-01	-6.62E-01	1.06E-02
GLN	15	C	219	LYS	16	O	2034	4.82E-01	-7.53E-01	-7.80E-01	-7.25E-01	2.73E-02
GLN	15	O	220	HIS	13	C	1982	8.58E-01	-3.66E-01	-3.69E-01	-3.63E-01	2.64E-03
GLN	15	O	220	HIS	14	C	1999	5.15E-01	-1.01E+00	-1.03E+00	-9.97E-01	1.77E-02
GLN	15	O	220	GLN	15	C	2016	4.04E-01	-1.18E+00	-1.20E+00	-1.15E+00	2.47E-02
GLN	15	O	220	GLN	15	CD	2020	6.15E-01	-7.09E-01	-7.90E-01	-6.28E-01	8.09E-02
GLN	15	O	220	GLN	15	H	2023	5.77E-01	-3.58E-01	-3.65E-01	-3.51E-01	7.01E-03
GLN	15	O	220	GLN	15	HA	2024	2.80E-01	-1.17E+00	-1.23E+00	-1.11E+00	5.89E-02
GLN	15	O	220	LYS	16	C	2033	4.79E-01	-1.33E+00	-1.37E+00	-1.28E+00	4.65E-02
GLN	15	O	220	LYS	16	H	2040	3.01E-01	-1.59E+00	-1.73E+00	-1.45E+00	1.36E-01
GLN	15	O	220	LEU	17	C	2055	8.04E-01	-3.54E-01	-3.58E-01	-3.50E-01	3.98E-03
GLN	15	CD	223	HIS	14	N	1997	8.80E-01	-3.32E-01	-3.45E-01	-3.20E-01	1.25E-02
GLN	15	CD	223	HIS	14	O	2000	7.59E-01	-4.32E-01	-4.56E-01	-4.07E-01	2.45E-02
GLN	15	CD	223	GLN	15	O	2017	8.40E-01	-3.92E-01	-4.29E-01	-3.54E-01	3.77E-02
GLN	15	CD	223	GLN	15	OE1	2021	5.12E-01	-1.31E+00	-1.64E+00	-9.75E-01	3.34E-01
GLN	15	CD	223	GLN	15	NE2	2022	5.00E-01	-1.94E+00	-2.43E+00	-1.46E+00	4.82E-01
GLN	15	CD	223	LYS	16	N	2031	6.87E-01	-4.49E-01	-5.14E-01	-3.85E-01	6.44E-02
GLN	15	CD	223	LYS	16	O	2034	7.42E-01	-4.97E-01	-5.62E-01	-4.32E-01	6.49E-02
GLN	15	OE1	224	HIS	14	C	1999	8.36E-01	-4.37E-01	-4.84E-01	-3.90E-01	4.72E-02
GLN	15	OE1	224	GLN	15	CD	2020	5.25E-01	-1.21E+00	-1.48E+00	-9.34E-01	2.73E-01
GLN	15	OE1	224	GLN	15	HE22	2030	5.10E-01	-1.17E+00	-1.75E+00	-5.84E-01	5.82E-01
GLN	15	OE1	224	LYS	16	C	2033	7.77E-01	-5.79E-01	-6.89E-01	-4.69E-01	1.10E-01
GLN	15	NE2	225	HIS	14	C	1999	8.28E-01	-6.08E-01	-6.24E-01	-5.92E-01	1.59E-02
GLN	15	NE2	225	GLN	15	C	2016	7.86E-01	-4.26E-01	-4.58E-01	-3.93E-01	3.26E-02
GLN	15	NE2	225	GLN	15	CD	2020	5.39E-01	-1.60E+00	-1.97E+00	-1.23E+00	3.72E-01
GLN	15	NE2	225	GLN	15	HE21	2029	5.20E-01	-1.02E+00	-1.20E+00	-8.35E-01	1.84E-01
GLN	15	NE2	225	GLN	15	HE22	2030	5.00E-01	-1.05E+00	-1.07E+00	-1.03E+00	2.32E-02

GLN	15	NE2	225	LYS	16	C	2033	8.23E-01	-6.98E-01	-7.89E-01	-6.07E-01	9.11E-02
GLN	15	NE2	225	MET	35	C	2318	8.58E-01	-5.30E-01	-5.81E-01	-4.79E-01	5.13E-02
GLN	15	NE2	225	VAL	36	C	2335	7.19E-01	-5.56E-01	-6.44E-01	-4.68E-01	8.83E-02
GLN	15	NE2	225	VAL	36	CB	2337	6.49E-01	-6.51E-01	-8.25E-01	-4.77E-01	1.74E-01
GLN	15	NE2	225	VAL	36	H	2340	8.95E-01	-3.63E-01	-4.01E-01	-3.26E-01	3.76E-02
GLN	15	NE2	225	GLY	37	C	2351	8.17E-01	-5.54E-01	-6.02E-01	-5.05E-01	4.85E-02
GLN	15	NE2	225	GLY	37	H	2353	5.41E-01	-5.92E-01	-7.21E-01	-4.62E-01	1.30E-01
GLN	15	NE2	225	GLY	38	C	2358	9.48E-01	-4.30E-01	-4.51E-01	-4.09E-01	2.08E-02
GLN	15	H	226	HIS	14	N	1997	5.68E-01	-3.46E-01	-3.51E-01	-3.41E-01	5.13E-03
GLN	15	H	226	HIS	14	O	2000	3.82E-01	-9.14E-01	-9.44E-01	-8.84E-01	2.98E-02
GLN	15	H	226	GLN	15	N	2014	4.33E-01	-4.84E-01	-4.85E-01	-4.82E-01	1.70E-03
GLN	15	H	226	GLN	15	O	2017	5.85E-01	-3.47E-01	-3.51E-01	-3.44E-01	3.64E-03
GLN	15	H	226	GLN	15	NE2	2022	5.41E-01	-6.64E-01	-7.40E-01	-5.89E-01	7.57E-02
GLN	15	H	226	LYS	16	N	2031	4.95E-01	-3.92E-01	-4.00E-01	-3.84E-01	7.83E-03
GLN	15	HE21	232	GLN	15	NE2	2022	5.10E-01	-1.09E+00	-1.31E+00	-8.62E-01	2.25E-01
GLN	15	HE22	233	GLN	15	OE1	2021	5.75E-01	-7.49E-01	-1.05E+00	-4.48E-01	3.00E-01
GLN	15	HE22	233	GLN	15	NE2	2022	5.38E-01	-8.85E-01	-8.95E-01	-8.75E-01	1.01E-02
LYS	16	N	234	HIS	14	C	1999	7.30E-01	-3.76E-01	-3.79E-01	-3.72E-01	3.64E-03
LYS	16	N	234	GLN	15	C	2016	5.86E-01	-3.72E-01	-3.73E-01	-3.70E-01	1.41E-03
LYS	16	N	234	GLN	15	CD	2020	7.06E-01	-4.13E-01	-4.56E-01	-3.69E-01	4.34E-02
LYS	16	N	234	LYS	16	C	2033	5.30E-01	-8.05E-01	-8.22E-01	-7.87E-01	1.75E-02
LYS	16	N	234	LYS	16	H	2040	4.24E-01	-4.79E-01	-4.86E-01	-4.73E-01	6.57E-03
LYS	16	C	236	HIS	14	O	2000	8.72E-01	-3.65E-01	-3.68E-01	-3.61E-01	3.55E-03
LYS	16	C	236	GLN	15	O	2017	8.09E-01	-4.43E-01	-4.46E-01	-4.39E-01	3.03E-03
LYS	16	C	236	GLN	15	OE1	2021	8.36E-01	-4.86E-01	-5.55E-01	-4.17E-01	6.89E-02
LYS	16	C	236	GLN	15	NE2	2022	8.63E-01	-6.24E-01	-6.62E-01	-5.87E-01	3.73E-02
LYS	16	C	236	LYS	16	N	2031	5.91E-01	-6.31E-01	-6.38E-01	-6.23E-01	7.67E-03
LYS	16	C	236	LYS	16	O	2034	3.98E-01	-2.10E+00	-2.12E+00	-2.09E+00	1.18E-02
LYS	16	C	236	LEU	17	N	2053	5.77E-01	-5.40E-01	-5.43E-01	-5.37E-01	2.77E-03
LYS	16	C	236	LEU	17	O	2056	7.69E-01	-4.78E-01	-4.84E-01	-4.73E-01	5.53E-03
LYS	16	C	236	VAL	18	N	2072	6.74E-01	-4.96E-01	-5.02E-01	-4.89E-01	6.37E-03
LYS	16	O	237	LYS	16	C	2033	6.21E-01	-7.34E-01	-7.36E-01	-7.32E-01	2.08E-03
LYS	16	O	237	LEU	17	C	2055	7.64E-01	-3.86E-01	-3.89E-01	-3.84E-01	2.36E-03
LYS	16	O	237	VAL	18	H	2079	6.84E-01	-3.66E-01	-3.74E-01	-3.58E-01	8.32E-03
LYS	16	H	243	LYS	16	O	2034	5.25E-01	-3.68E-01	-3.78E-01	-3.58E-01	9.97E-03
LYS	16	HA	244	LYS	16	N	2031	3.81E-01	-3.25E-01	-3.33E-01	-3.17E-01	7.73E-03
LYS	16	HA	244	LYS	16	O	2034	2.47E-01	-1.42E+00	-1.47E+00	-1.38E+00	4.69E-02
LEU	17	N	256	LYS	16	C	2033	4.69E-01	-8.73E-01	-8.81E-01	-8.64E-01	8.48E-03

LEU	17	N	256	LEU	17	C	2055	5.71E-01	-4.37E-01	-4.40E-01	-4.34E-01	3.04E-03
LEU	17	N	256	LEU	17	HA	2062	3.62E-01	-3.23E-01	-3.27E-01	-3.19E-01	4.39E-03
LEU	17	N	256	VAL	18	H	2079	4.99E-01	-4.60E-01	-4.81E-01	-4.38E-01	2.13E-02
LEU	17	C	258	GLN	15	NE2	2022	9.61E-01	-4.20E-01	-4.54E-01	-3.85E-01	3.43E-02
LEU	17	C	258	LYS	16	N	2031	7.48E-01	-3.11E-01	-3.17E-01	-3.05E-01	5.76E-03
LEU	17	C	258	LYS	16	O	2034	4.83E-01	-1.02E+00	-1.07E+00	-9.77E-01	4.70E-02
LEU	17	C	258	LEU	17	N	2053	5.58E-01	-4.61E-01	-4.66E-01	-4.56E-01	5.19E-03
LEU	17	C	258	LEU	17	O	2056	6.25E-01	-5.67E-01	-5.71E-01	-5.63E-01	3.93E-03
LEU	17	C	258	VAL	18	N	2072	4.46E-01	-9.90E-01	-1.01E+00	-9.68E-01	2.27E-02
LEU	17	C	258	VAL	18	O	2075	5.16E-01	-6.29E-01	-6.53E-01	-6.06E-01	2.34E-02
LEU	17	O	259	GLN	15	CD	2020	8.83E-01	-3.49E-01	-3.60E-01	-3.37E-01	1.14E-02
LEU	17	O	259	LYS	16	C	2033	4.70E-01	-1.37E+00	-1.44E+00	-1.31E+00	6.51E-02
LEU	17	O	259	LEU	17	C	2055	3.86E-01	-1.79E+00	-1.84E+00	-1.74E+00	5.23E-02
LEU	17	O	259	LEU	17	CG	2058	3.83E-01	-6.83E-01	-8.36E-01	-5.29E-01	1.53E-01
LEU	17	O	259	LEU	17	H	2061	5.39E-01	-3.57E-01	-3.60E-01	-3.55E-01	2.67E-03
LEU	17	O	259	LEU	17	HA	2062	2.45E-01	-1.53E+00	-1.55E+00	-1.51E+00	1.89E-02
LEU	17	O	259	VAL	18	C	2074	5.00E-01	-7.32E-01	-7.73E-01	-6.91E-01	4.11E-02
LEU	17	O	259	VAL	18	CB	2076	4.59E-01	-7.91E-01	-8.16E-01	-7.66E-01	2.49E-02
LEU	17	O	259	VAL	18	H	2079	2.51E-01	-4.89E+00	-5.73E+00	-4.04E+00	8.46E-01
LEU	17	O	259	PHE	19	C	2090	8.23E-01	-3.21E-01	-3.28E-01	-3.15E-01	6.51E-03
LEU	17	H	264	LYS	16	N	2031	5.09E-01	-3.20E-01	-3.28E-01	-3.12E-01	8.32E-03
LEU	17	H	264	LYS	16	O	2034	3.10E-01	-1.50E+00	-1.52E+00	-1.48E+00	2.10E-02
LEU	17	H	264	LEU	17	N	2053	4.24E-01	-4.07E-01	-4.10E-01	-4.04E-01	2.91E-03
VAL	18	N	275	LYS	16	C	2033	6.88E-01	-4.75E-01	-4.85E-01	-4.66E-01	9.70E-03
VAL	18	N	275	LEU	17	C	2055	5.83E-01	-5.30E-01	-5.37E-01	-5.24E-01	6.48E-03
VAL	18	N	275	VAL	18	C	2074	5.88E-01	-4.06E-01	-4.10E-01	-4.02E-01	4.19E-03
VAL	18	N	275	VAL	18	CB	2076	5.53E-01	-4.11E-01	-4.24E-01	-3.99E-01	1.24E-02
VAL	18	N	275	VAL	18	H	2079	4.05E-01	-9.74E-01	-9.91E-01	-9.57E-01	1.73E-02
VAL	18	C	277	LEU	17	O	2056	7.43E-01	-3.15E-01	-3.17E-01	-3.12E-01	2.71E-03
VAL	18	C	277	VAL	18	N	2072	5.21E-01	-5.32E-01	-5.37E-01	-5.27E-01	4.86E-03
VAL	18	C	277	VAL	18	O	2075	3.84E-01	-1.03E+00	-1.04E+00	-1.01E+00	1.36E-02
VAL	18	C	277	PHE	19	N	2088	6.08E-01	-3.11E-01	-3.13E-01	-3.09E-01	2.14E-03
VAL	18	O	278	VAL	18	C	2074	6.14E-01	-3.33E-01	-3.34E-01	-3.32E-01	9.60E-04
VAL	18	O	278	VAL	18	H	2079	5.55E-01	-4.08E-01	-4.14E-01	-4.02E-01	6.18E-03
VAL	18	CB	279	VAL	18	N	2072	5.61E-01	-3.98E-01	-4.08E-01	-3.88E-01	9.74E-03
VAL	18	CB	279	VAL	18	O	2075	5.17E-01	-4.35E-01	-4.62E-01	-4.07E-01	2.73E-02
VAL	18	H	282	LYS	16	O	2034	6.77E-01	-3.74E-01	-3.80E-01	-3.67E-01	6.47E-03
VAL	18	H	282	VAL	18	N	2072	5.95E-01	-3.90E-01	-3.93E-01	-3.86E-01	3.37E-03

VAL	18	H	282	VAL	18	O	2075	5.82E-01	-3.68E-01	-3.75E-01	-3.60E-01	7.54E-03
PHE	19	N	291	LEU	17	C	2055	6.01E-01	-4.09E-01	-4.16E-01	-4.02E-01	6.81E-03
PHE	19	N	291	VAL	18	C	2074	4.01E-01	-8.35E-01	-8.39E-01	-8.31E-01	4.16E-03
PHE	19	N	291	VAL	18	CB	2076	4.73E-01	-4.92E-01	-5.21E-01	-4.62E-01	2.98E-02
PHE	19	N	291	VAL	18	H	2079	4.14E-01	-7.58E-01	-7.65E-01	-7.51E-01	7.04E-03
PHE	19	N	291	PHE	19	C	2090	5.66E-01	-4.60E-01	-5.22E-01	-3.99E-01	6.14E-02
PHE	19	C	293	VAL	18	N	2072	6.62E-01	-3.90E-01	-4.07E-01	-3.73E-01	1.70E-02
PHE	19	C	293	VAL	18	O	2075	3.94E-01	-1.20E+00	-1.33E+00	-1.08E+00	1.25E-01
PHE	19	C	293	PHE	19	N	2088	5.44E-01	-4.99E-01	-5.53E-01	-4.46E-01	5.35E-02
PHE	19	C	293	PHE	19	O	2091	5.98E-01	-5.48E-01	-5.93E-01	-5.02E-01	4.54E-02
PHE	19	C	293	PHE	20	N	2108	4.37E-01	-8.27E-01	-8.57E-01	-7.97E-01	3.00E-02
PHE	19	C	293	PHE	20	O	2111	6.78E-01	-4.33E-01	-4.95E-01	-3.71E-01	6.24E-02
PHE	19	C	293	ALA	21	N	2128	5.17E-01	-7.03E-01	-9.31E-01	-4.75E-01	2.28E-01
PHE	19	C	293	GLU	22	O	2141	8.65E-01	-3.14E-01	-3.15E-01	-3.12E-01	1.61E-03
PHE	19	C	293	ASP	23	OD1	2159	8.89E-01	-3.77E-01	-4.15E-01	-3.39E-01	3.78E-02
PHE	19	C	293	ASP	23	OD2	2160	8.45E-01	-4.19E-01	-4.74E-01	-3.64E-01	5.47E-02
PHE	19	O	294	LEU	17	C	2055	7.41E-01	-3.71E-01	-3.95E-01	-3.48E-01	2.34E-02
PHE	19	O	294	VAL	18	C	2074	4.38E-01	-9.83E-01	-1.16E+00	-8.09E-01	1.74E-01
PHE	19	O	294	VAL	18	CB	2076	5.40E-01	-4.95E-01	-5.36E-01	-4.55E-01	4.06E-02
PHE	19	O	294	VAL	18	H	2079	5.91E-01	-4.45E-01	-4.63E-01	-4.27E-01	1.79E-02
PHE	19	O	294	PHE	19	C	2090	4.13E-01	-1.38E+00	-1.62E+00	-1.15E+00	2.33E-01
PHE	19	O	294	PHE	20	C	2110	4.89E-01	-8.54E-01	-8.67E-01	-8.41E-01	1.33E-02
PHE	19	O	294	PHE	20	H	2119	3.06E-01	-2.09E+00	-2.82E+00	-1.36E+00	7.31E-01
PHE	19	O	294	ALA	21	C	2130	6.88E-01	-4.22E-01	-4.34E-01	-4.09E-01	1.27E-02
PHE	19	O	294	ALA	21	H	2133	3.79E-01	-8.88E-01	-9.70E-01	-8.07E-01	8.15E-02
PHE	19	H	302	VAL	18	N	2072	3.95E-01	-5.53E-01	-5.56E-01	-5.49E-01	3.20E-03
PHE	19	H	302	VAL	18	O	2075	1.91E-01	-4.03E+00	-4.16E+00	-3.90E+00	1.29E-01
PHE	19	H	302	PHE	19	N	2088	4.08E-01	-4.20E-01	-4.25E-01	-4.15E-01	4.77E-03
PHE	19	HB2	304	VAL	18	O	2075	2.52E-01	-4.53E-01	-4.56E-01	-4.51E-01	2.55E-03
PHE	20	N	311	PHE	19	C	2090	5.89E-01	-4.08E-01	-4.10E-01	-4.06E-01	2.30E-03
PHE	20	N	311	PHE	20	C	2110	5.91E-01	-4.53E-01	-5.71E-01	-3.35E-01	1.18E-01
PHE	20	C	313	PHE	19	O	2091	6.93E-01	-4.13E-01	-4.58E-01	-3.67E-01	4.54E-02
PHE	20	C	313	PHE	20	N	2108	5.05E-01	-6.53E-01	-7.90E-01	-5.17E-01	1.37E-01
PHE	20	C	313	PHE	20	O	2111	5.99E-01	-5.44E-01	-5.82E-01	-5.06E-01	3.80E-02
PHE	20	C	313	ALA	21	N	2128	4.18E-01	-1.01E+00	-1.05E+00	-9.74E-01	3.62E-02
PHE	20	C	313	ALA	21	O	2131	6.65E-01	-4.86E-01	-5.40E-01	-4.32E-01	5.41E-02
PHE	20	C	313	ALA	21	CB	2132	4.56E-01	-5.14E-01	-6.54E-01	-3.74E-01	1.40E-01
PHE	20	C	313	GLU	22	N	2138	5.43E-01	-5.58E-01	-5.69E-01	-5.47E-01	1.09E-02

PHE	20	C	313	GLU	22	O	2141	5.94E-01	-6.49E-01	-6.97E-01	-6.01E-01	4.79E-02
PHE	20	C	313	GLU	22	OE1	2145	9.40E-01	-3.82E-01	-3.97E-01	-3.67E-01	1.53E-02
PHE	20	C	313	GLU	22	OE2	2146	9.95E-01	-3.51E-01	-3.62E-01	-3.39E-01	1.16E-02
PHE	20	C	313	ASP	23	N	2153	7.29E-01	-4.12E-01	-4.57E-01	-3.66E-01	4.54E-02
PHE	20	C	313	ASP	23	OD1	2159	7.11E-01	-5.76E-01	-6.75E-01	-4.76E-01	9.92E-02
PHE	20	C	313	ASP	23	OD2	2160	6.84E-01	-6.76E-01	-8.35E-01	-5.17E-01	1.59E-01
PHE	20	O	314	PHE	19	C	2090	5.58E-01	-7.75E-01	-9.68E-01	-5.82E-01	1.93E-01
PHE	20	O	314	PHE	20	C	2110	4.04E-01	-1.47E+00	-1.71E+00	-1.22E+00	2.43E-01
PHE	20	O	314	ALA	21	C	2130	4.69E-01	-9.86E-01	-1.05E+00	-9.25E-01	6.09E-02
PHE	20	O	314	ALA	21	H	2133	2.71E-01	-3.53E+00	-4.74E+00	-2.32E+00	1.21E+00
PHE	20	O	314	GLU	22	C	2140	5.69E-01	-5.25E-01	-5.70E-01	-4.81E-01	4.46E-02
PHE	20	O	314	GLU	22	CD	2144	8.63E-01	-3.75E-01	-3.83E-01	-3.68E-01	7.61E-03
PHE	20	O	314	GLU	22	H	2147	3.90E-01	-8.46E-01	-8.57E-01	-8.34E-01	1.14E-02
PHE	20	O	314	ASP	23	CG	2158	6.19E-01	-7.68E-01	-9.21E-01	-6.14E-01	1.53E-01
ALA	21	N	331	PHE	20	C	2110	5.95E-01	-4.38E-01	-4.49E-01	-4.26E-01	1.18E-02
ALA	21	N	331	ALA	21	C	2130	6.06E-01	-4.39E-01	-4.63E-01	-4.14E-01	2.46E-02
ALA	21	N	331	ALA	21	H	2133	4.22E-01	-5.46E-01	-6.12E-01	-4.80E-01	6.60E-02
ALA	21	C	333	PHE	20	O	2111	6.87E-01	-4.23E-01	-4.27E-01	-4.18E-01	4.88E-03
ALA	21	C	333	ALA	21	N	2128	4.96E-01	-6.97E-01	-7.60E-01	-6.34E-01	6.32E-02
ALA	21	C	333	ALA	21	O	2131	5.98E-01	-6.19E-01	-6.56E-01	-5.81E-01	3.78E-02
ALA	21	C	333	ALA	21	CB	2132	4.10E-01	-6.30E-01	-6.75E-01	-5.86E-01	4.48E-02
ALA	21	C	333	GLU	22	N	2138	4.41E-01	-1.03E+00	-1.22E+00	-8.50E-01	1.84E-01
ALA	21	C	333	GLU	22	O	2141	4.31E-01	-1.50E+00	-1.74E+00	-1.26E+00	2.40E-01
ALA	21	C	333	GLU	22	OE1	2145	7.40E-01	-6.84E-01	-8.25E-01	-5.42E-01	1.42E-01
ALA	21	C	333	GLU	22	OE2	2146	7.85E-01	-5.71E-01	-6.62E-01	-4.81E-01	9.05E-02
ALA	21	C	333	ASP	23	N	2153	6.25E-01	-5.88E-01	-6.65E-01	-5.12E-01	7.62E-02
ALA	21	C	333	ASP	23	OD1	2159	6.99E-01	-6.24E-01	-7.27E-01	-5.21E-01	1.03E-01
ALA	21	C	333	ASP	23	OD2	2160	6.85E-01	-6.39E-01	-7.29E-01	-5.50E-01	8.92E-02
ALA	21	O	334	PHE	20	C	2110	5.55E-01	-7.35E-01	-8.41E-01	-6.29E-01	1.06E-01
ALA	21	O	334	ALA	21	C	2130	4.08E-01	-1.59E+00	-1.81E+00	-1.37E+00	2.19E-01
ALA	21	O	334	ALA	21	H	2133	4.08E-01	-9.72E-01	-1.23E+00	-7.15E-01	2.57E-01
ALA	21	O	334	ALA	21	HB2	2136	2.81E-01	-6.46E-01	-7.87E-01	-5.05E-01	1.41E-01
ALA	21	O	334	GLU	22	C	2140	4.21E-01	-1.44E+00	-1.82E+00	-1.06E+00	3.78E-01
ALA	21	O	334	GLU	22	CD	2144	6.77E-01	-7.64E-01	-9.37E-01	-5.90E-01	1.73E-01
ALA	21	O	334	GLU	22	H	2147	2.87E-01	-5.49E+00	-7.65E+00	-3.34E+00	2.16E+00
ALA	21	O	334	ASP	23	CG	2158	5.90E-01	-8.29E-01	-8.54E-01	-8.04E-01	2.50E-02
GLU	22	N	341	PHE	20	C	2110	6.98E-01	-3.31E-01	-3.47E-01	-3.14E-01	1.65E-02
GLU	22	N	341	ALA	21	C	2130	5.75E-01	-5.28E-01	-5.99E-01	-4.56E-01	7.12E-02

GLU	22	N	341	GLU	22	C	2140	5.31E-01	-5.08E-01	-5.43E-01	-4.74E-01	3.47E-02
GLU	22	N	341	GLU	22	CD	2144	6.96E-01	-4.90E-01	-5.60E-01	-4.19E-01	7.06E-02
GLU	22	N	341	GLU	22	H	2147	4.24E-01	-5.79E-01	-6.32E-01	-5.26E-01	5.30E-02
GLU	22	N	341	ASP	23	CG	2158	7.28E-01	-4.13E-01	-4.23E-01	-4.03E-01	1.02E-02
GLU	22	C	343	GLU	22	N	2138	5.77E-01	-4.19E-01	-4.43E-01	-3.95E-01	2.38E-02
GLU	22	C	343	GLU	22	O	2141	3.81E-01	-1.61E+00	-1.62E+00	-1.59E+00	1.31E-02
GLU	22	C	343	GLU	22	OE1	2145	6.79E-01	-6.74E-01	-8.28E-01	-5.20E-01	1.54E-01
GLU	22	C	343	GLU	22	OE2	2146	7.46E-01	-5.03E-01	-5.83E-01	-4.24E-01	7.95E-02
GLU	22	C	343	ASP	23	N	2153	5.95E-01	-5.16E-01	-5.19E-01	-5.12E-01	3.50E-03
GLU	22	C	343	ASP	23	OD1	2159	6.96E-01	-5.94E-01	-7.96E-01	-3.92E-01	2.02E-01
GLU	22	C	343	ASP	23	OD2	2160	7.18E-01	-4.68E-01	-5.07E-01	-4.29E-01	3.93E-02
GLU	22	O	344	ALA	21	C	2130	7.84E-01	-4.00E-01	-4.55E-01	-3.46E-01	5.43E-02
GLU	22	O	344	GLU	22	C	2140	6.24E-01	-4.95E-01	-4.97E-01	-4.93E-01	2.31E-03
GLU	22	O	344	GLU	22	CD	2144	7.82E-01	-5.41E-01	-6.05E-01	-4.77E-01	6.42E-02
GLU	22	O	344	ASP	23	CG	2158	7.74E-01	-5.27E-01	-5.79E-01	-4.75E-01	5.22E-02
GLU	22	CD	347	ALA	21	O	2131	8.97E-01	-4.09E-01	-4.78E-01	-3.40E-01	6.89E-02
GLU	22	CD	347	GLU	22	N	2138	6.96E-01	-5.14E-01	-6.44E-01	-3.85E-01	1.29E-01
GLU	22	CD	347	GLU	22	O	2141	5.72E-01	-1.06E+00	-1.29E+00	-8.18E-01	2.38E-01
GLU	22	CD	347	GLU	22	OE1	2145	4.60E-01	-2.69E+00	-3.42E+00	-1.97E+00	7.23E-01
GLU	22	CD	347	GLU	22	OE2	2146	5.23E-01	-1.83E+00	-2.32E+00	-1.35E+00	4.86E-01
GLU	22	CD	347	ASP	23	N	2153	7.52E-01	-5.81E-01	-7.17E-01	-4.45E-01	1.36E-01
GLU	22	OE1	348	ALA	21	C	2130	8.79E-01	-5.13E-01	-6.58E-01	-3.68E-01	1.45E-01
GLU	22	OE1	348	GLU	22	C	2140	7.13E-01	-6.29E-01	-8.36E-01	-4.22E-01	2.07E-01
GLU	22	OE1	348	GLU	22	CD	2144	5.47E-01	-1.71E+00	-2.21E+00	-1.22E+00	4.95E-01
GLU	22	OE2	349	ALA	21	C	2130	8.56E-01	-4.74E-01	-5.24E-01	-4.23E-01	5.01E-02
GLU	22	OE2	349	GLU	22	C	2140	6.93E-01	-5.83E-01	-6.75E-01	-4.91E-01	9.23E-02
GLU	22	OE2	349	GLU	22	CD	2144	4.94E-01	-2.05E+00	-2.41E+00	-1.68E+00	3.69E-01
GLU	22	H	350	GLU	22	O	2141	5.23E-01	-4.78E-01	-4.94E-01	-4.62E-01	1.63E-02
GLU	22	HA	351	GLU	22	O	2141	2.58E-01	-6.63E-01	-6.79E-01	-6.47E-01	1.59E-02
ASP	23	N	356	PHE	20	C	2110	7.89E-01	-3.46E-01	-3.56E-01	-3.36E-01	1.01E-02
ASP	23	N	356	ALA	21	C	2130	6.48E-01	-5.40E-01	-6.11E-01	-4.69E-01	7.10E-02
ASP	23	N	356	GLU	22	C	2140	4.33E-01	-1.09E+00	-1.09E+00	-1.08E+00	8.39E-03
ASP	23	N	356	GLU	22	CD	2144	6.73E-01	-6.66E-01	-7.31E-01	-6.02E-01	6.44E-02
ASP	23	N	356	GLU	22	H	2147	5.23E-01	-4.52E-01	-4.74E-01	-4.30E-01	2.19E-02
ASP	23	N	356	ASP	23	C	2155	6.02E-01	-4.75E-01	-4.95E-01	-4.54E-01	2.05E-02
ASP	23	N	356	ASP	23	CG	2158	5.66E-01	-9.37E-01	-1.06E+00	-8.15E-01	1.21E-01
ASP	23	N	356	ASP	23	H	2161	5.99E-01	-3.46E-01	-3.48E-01	-3.44E-01	1.85E-03
ASP	23	N	356	VAL	24	H	2172	5.56E-01	-5.75E-01	-6.47E-01	-5.04E-01	7.14E-02

ASP	23	C	358	GLU	22	O	2141	4.20E-01	-1.19E+00	-1.28E+00	-1.10E+00	8.78E-02
ASP	23	C	358	GLU	22	OE1	2145	7.92E-01	-4.27E-01	-4.81E-01	-3.73E-01	5.40E-02
ASP	23	C	358	GLU	22	OE2	2146	8.32E-01	-3.82E-01	-4.15E-01	-3.48E-01	3.37E-02
ASP	23	C	358	ASP	23	N	2153	5.17E-01	-6.69E-01	-7.00E-01	-6.38E-01	3.09E-02
ASP	23	C	358	ASP	23	O	2156	6.20E-01	-4.00E-01	-4.02E-01	-3.97E-01	2.21E-03
ASP	23	C	358	ASP	23	OD1	2159	5.66E-01	-7.53E-01	-8.97E-01	-6.09E-01	1.44E-01
ASP	23	C	358	ASP	23	OD2	2160	6.23E-01	-5.80E-01	-6.07E-01	-5.54E-01	2.66E-02
ASP	23	C	358	VAL	24	N	2165	4.75E-01	-6.65E-01	-7.24E-01	-6.06E-01	5.86E-02
ASP	23	O	359	ALA	21	C	2130	7.07E-01	-3.95E-01	-3.99E-01	-3.90E-01	4.40E-03
ASP	23	O	359	GLU	22	C	2140	4.27E-01	-1.02E+00	-1.08E+00	-9.62E-01	5.81E-02
ASP	23	O	359	GLU	22	CD	2144	7.26E-01	-5.04E-01	-5.16E-01	-4.93E-01	1.16E-02
ASP	23	O	359	ASP	23	C	2155	3.94E-01	-1.18E+00	-1.23E+00	-1.13E+00	4.79E-02
ASP	23	O	359	ASP	23	CG	2158	4.39E-01	-1.52E+00	-1.64E+00	-1.39E+00	1.26E-01
ASP	23	O	359	ASP	23	H	2161	5.04E-01	-4.60E-01	-4.76E-01	-4.43E-01	1.64E-02
ASP	23	O	359	ASP	23	HA	2162	2.44E-01	-8.30E-01	-8.33E-01	-8.28E-01	2.55E-03
ASP	23	O	359	VAL	24	C	2167	5.67E-01	-4.97E-01	-5.42E-01	-4.51E-01	4.54E-02
ASP	23	O	359	VAL	24	CB	2169	5.28E-01	-5.64E-01	-7.11E-01	-4.17E-01	1.47E-01
ASP	23	O	359	VAL	24	H	2172	3.07E-01	-2.78E+00	-3.83E+00	-1.74E+00	1.04E+00
ASP	23	CG	361	PHE	20	O	2111	8.47E-01	-3.81E-01	-4.04E-01	-3.58E-01	2.28E-02
ASP	23	CG	361	ALA	21	N	2128	7.28E-01	-4.05E-01	-4.44E-01	-3.65E-01	3.96E-02
ASP	23	CG	361	ALA	21	O	2131	7.75E-01	-5.05E-01	-5.83E-01	-4.27E-01	7.82E-02
ASP	23	CG	361	GLU	22	N	2138	6.76E-01	-4.76E-01	-4.87E-01	-4.65E-01	1.07E-02
ASP	23	CG	361	GLU	22	O	2141	4.79E-01	-1.43E+00	-1.46E+00	-1.39E+00	3.44E-02
ASP	23	CG	361	GLU	22	OE2	2146	9.95E-01	-4.78E-01	-5.04E-01	-4.52E-01	2.61E-02
ASP	23	CG	361	ASP	23	N	2153	6.00E-01	-8.12E-01	-8.69E-01	-7.55E-01	5.67E-02
ASP	23	CG	361	ASP	23	O	2156	7.48E-01	-4.70E-01	-5.05E-01	-4.35E-01	3.48E-02
ASP	23	CG	361	ASP	23	OD1	2159	5.17E-01	-1.70E+00	-2.23E+00	-1.17E+00	5.28E-01
ASP	23	CG	361	ASP	23	OD2	2160	5.58E-01	-1.24E+00	-1.31E+00	-1.17E+00	6.61E-02
ASP	23	CG	361	VAL	24	N	2165	6.77E-01	-5.06E-01	-5.24E-01	-4.87E-01	1.84E-02
ASP	23	OD1	362	PHE	20	C	2110	7.91E-01	-4.86E-01	-5.67E-01	-4.05E-01	8.11E-02
ASP	23	OD1	362	ALA	21	C	2130	7.57E-01	-5.10E-01	-5.43E-01	-4.77E-01	3.34E-02
ASP	23	OD1	362	GLU	22	C	2140	6.09E-01	-6.63E-01	-7.44E-01	-5.83E-01	8.05E-02
ASP	23	OD1	362	ASP	23	C	2155	6.59E-01	-5.55E-01	-6.48E-01	-4.61E-01	9.32E-02
ASP	23	OD1	362	ASP	23	CG	2158	5.07E-01	-1.66E+00	-1.95E+00	-1.36E+00	2.94E-01
ASP	23	OD1	362	VAL	24	H	2172	6.19E-01	-6.08E-01	-6.93E-01	-5.23E-01	8.54E-02
ASP	23	OD1	362	LYS	28	HZ3	2234	6.02E-01	-4.32E-01	-5.10E-01	-3.53E-01	7.88E-02
ASP	23	OD2	363	PHE	20	C	2110	7.12E-01	-5.82E-01	-6.70E-01	-4.93E-01	8.86E-02
ASP	23	OD2	363	ALA	21	C	2130	6.67E-01	-6.62E-01	-7.41E-01	-5.84E-01	7.83E-02

ASP	23	OD2	363	GLU	22	C	2140	5.52E-01	-8.05E-01	-8.60E-01	-7.50E-01	5.50E-02
ASP	23	OD2	363	GLU	22	CD	2144	9.16E-01	-4.97E-01	-5.30E-01	-4.64E-01	3.30E-02
ASP	23	OD2	363	ASP	23	C	2155	6.74E-01	-4.98E-01	-5.40E-01	-4.56E-01	4.20E-02
ASP	23	OD2	363	ASP	23	CG	2158	4.84E-01	-1.74E+00	-1.89E+00	-1.59E+00	1.50E-01
ASP	23	OD2	363	VAL	24	H	2172	6.64E-01	-5.09E-01	-5.51E-01	-4.66E-01	4.22E-02
ASP	23	H	364	GLU	22	N	2138	4.72E-01	-4.53E-01	-4.63E-01	-4.42E-01	1.04E-02
ASP	23	H	364	GLU	22	O	2141	2.20E-01	-5.26E+00	-5.49E+00	-5.04E+00	2.27E-01
ASP	23	H	364	GLU	22	OE1	2145	6.26E-01	-5.12E-01	-6.09E-01	-4.14E-01	9.74E-02
ASP	23	H	364	GLU	22	OE2	2146	6.75E-01	-4.08E-01	-4.57E-01	-3.59E-01	4.92E-02
ASP	23	H	364	ASP	23	N	2153	4.07E-01	-8.67E-01	-8.74E-01	-8.61E-01	6.56E-03
ASP	23	H	364	ASP	23	OD1	2159	5.23E-01	-8.35E-01	-1.22E+00	-4.47E-01	3.88E-01
ASP	23	H	364	ASP	23	OD2	2160	5.49E-01	-5.58E-01	-6.10E-01	-5.07E-01	5.13E-02
VAL	24	N	368	GLU	22	C	2140	6.21E-01	-3.83E-01	-4.05E-01	-3.60E-01	2.23E-02
VAL	24	N	368	GLU	22	CD	2144	8.47E-01	-3.45E-01	-3.60E-01	-3.30E-01	1.49E-02
VAL	24	N	368	ASP	23	C	2155	5.63E-01	-4.43E-01	-4.62E-01	-4.24E-01	1.87E-02
VAL	24	N	368	ASP	23	CG	2158	6.44E-01	-5.60E-01	-5.76E-01	-5.44E-01	1.59E-02
VAL	24	N	368	VAL	24	CB	2169	5.69E-01	-3.94E-01	-4.40E-01	-3.48E-01	4.57E-02
VAL	24	N	368	VAL	24	H	2172	4.12E-01	-9.31E-01	-9.46E-01	-9.15E-01	1.54E-02
VAL	24	C	370	GLU	22	O	2141	6.47E-01	-4.45E-01	-4.85E-01	-4.06E-01	3.96E-02
VAL	24	C	370	ASP	23	N	2153	6.47E-01	-4.22E-01	-4.64E-01	-3.80E-01	4.17E-02
VAL	24	C	370	ASP	23	O	2156	6.11E-01	-4.25E-01	-4.64E-01	-3.86E-01	3.90E-02
VAL	24	C	370	ASP	23	OD1	2159	6.19E-01	-6.11E-01	-6.88E-01	-5.34E-01	7.75E-02
VAL	24	C	370	ASP	23	OD2	2160	6.95E-01	-5.01E-01	-5.92E-01	-4.10E-01	9.12E-02
VAL	24	C	370	VAL	24	N	2165	4.23E-01	-8.93E-01	-9.63E-01	-8.23E-01	7.02E-02
VAL	24	C	370	VAL	24	O	2168	5.01E-01	-5.55E-01	-6.39E-01	-4.70E-01	8.46E-02
VAL	24	C	370	VAL	24	HB	2174	3.48E-01	-4.07E-01	-4.88E-01	-3.25E-01	8.17E-02
VAL	24	C	370	SER	26	N	2188	6.03E-01	-5.29E-01	-6.82E-01	-3.75E-01	1.54E-01
VAL	24	C	370	SER	26	OG	2193	7.09E-01	-4.35E-01	-5.39E-01	-3.31E-01	1.04E-01
VAL	24	O	371	ASP	23	C	2155	5.23E-01	-4.75E-01	-5.11E-01	-4.38E-01	3.62E-02
VAL	24	O	371	ASP	23	CG	2158	5.74E-01	-6.51E-01	-7.03E-01	-6.00E-01	5.13E-02
VAL	24	O	371	VAL	24	C	2167	5.34E-01	-5.13E-01	-6.59E-01	-3.67E-01	1.46E-01
VAL	24	O	371	VAL	24	CB	2169	5.10E-01	-5.44E-01	-7.45E-01	-3.43E-01	2.01E-01
VAL	24	O	371	VAL	24	H	2172	3.88E-01	-1.16E+00	-1.56E+00	-7.56E-01	4.00E-01
VAL	24	CB	372	VAL	24	N	2165	5.54E-01	-4.16E-01	-4.52E-01	-3.80E-01	3.59E-02
VAL	24	H	375	GLU	22	O	2141	6.01E-01	-5.07E-01	-5.37E-01	-4.76E-01	3.01E-02
VAL	24	H	375	ASP	23	N	2153	7.02E-01	-3.46E-01	-3.62E-01	-3.30E-01	1.60E-02
VAL	24	H	375	ASP	23	OD1	2159	7.42E-01	-4.17E-01	-4.66E-01	-3.67E-01	4.95E-02
VAL	24	H	375	ASP	23	OD2	2160	8.08E-01	-3.49E-01	-3.59E-01	-3.38E-01	1.04E-02

VAL	24	H	375	VAL	24	N	2165	5.98E-01	-3.86E-01	-3.88E-01	-3.84E-01	2.01E-03
GLY	25	N	384	VAL	24	C	2167	4.56E-01	-6.76E-01	-8.10E-01	-5.42E-01	1.34E-01
GLY	25	N	384	VAL	24	CB	2169	3.98E-01	-8.25E-01	-9.77E-01	-6.74E-01	1.51E-01
GLY	25	N	384	VAL	24	H	2172	3.62E-01	-1.39E+00	-1.79E+00	-1.00E+00	3.92E-01
GLY	25	N	384	GLY	25	C	2183	5.78E-01	-4.77E-01	-5.56E-01	-3.98E-01	7.93E-02
GLY	25	N	384	SER	26	H	2194	4.61E-01	-4.71E-01	-5.24E-01	-4.18E-01	5.28E-02
GLY	25	C	386	ASP	23	OD1	2159	7.38E-01	-5.91E-01	-7.02E-01	-4.79E-01	1.12E-01
GLY	25	C	386	VAL	24	N	2165	5.95E-01	-5.57E-01	-6.53E-01	-4.62E-01	9.54E-02
GLY	25	C	386	GLY	25	N	2181	5.45E-01	-5.31E-01	-5.84E-01	-4.77E-01	5.36E-02
GLY	25	C	386	GLY	25	O	2184	5.71E-01	-6.84E-01	-8.28E-01	-5.41E-01	1.44E-01
GLY	25	C	386	SER	26	N	2188	4.27E-01	-1.39E+00	-1.55E+00	-1.23E+00	1.60E-01
GLY	25	C	386	SER	26	O	2191	5.66E-01	-7.70E-01	-8.68E-01	-6.72E-01	9.77E-02
GLY	25	C	386	SER	26	OG	2193	5.19E-01	-1.03E+00	-1.15E+00	-9.03E-01	1.25E-01
GLY	25	C	386	ASN	27	N	2199	5.54E-01	-5.75E-01	-5.88E-01	-5.61E-01	1.36E-02
GLY	25	C	386	ASN	27	O	2202	6.60E-01	-4.93E-01	-5.40E-01	-4.46E-01	4.73E-02
GLY	25	C	386	ASN	27	ND2	2206	9.59E-01	-3.73E-01	-3.85E-01	-3.60E-01	1.26E-02
GLY	25	O	387	GLY	25	C	2183	4.57E-01	-1.16E+00	-1.36E+00	-9.51E-01	2.06E-01
GLY	25	O	387	SER	26	C	2190	4.40E-01	-1.18E+00	-1.47E+00	-8.85E-01	2.95E-01
GLY	25	O	387	SER	26	HA	2195	4.19E-01	-3.28E-01	-3.51E-01	-3.05E-01	2.31E-02
GLY	25	O	387	ASN	27	C	2201	5.80E-01	-7.58E-01	-9.25E-01	-5.91E-01	1.67E-01
GLY	25	O	387	ASN	27	CG	2204	7.87E-01	-3.39E-01	-3.53E-01	-3.24E-01	1.41E-02
GLY	25	O	387	ASN	27	H	2207	4.62E-01	-4.59E-01	-4.77E-01	-4.41E-01	1.80E-02
SER	26	N	391	ASP	23	CG	2158	8.02E-01	-4.45E-01	-4.64E-01	-4.25E-01	1.91E-02
SER	26	N	391	VAL	24	C	2167	6.20E-01	-4.53E-01	-5.08E-01	-3.97E-01	5.52E-02
SER	26	N	391	VAL	24	H	2172	5.95E-01	-4.72E-01	-5.05E-01	-4.39E-01	3.27E-02
SER	26	N	391	GLY	25	C	2183	6.01E-01	-6.16E-01	-6.79E-01	-5.53E-01	6.31E-02
SER	26	N	391	SER	26	C	2190	5.64E-01	-5.80E-01	-6.12E-01	-5.48E-01	3.19E-02
SER	26	N	391	SER	26	CB	2192	4.10E-01	-3.80E-01	-3.89E-01	-3.72E-01	8.69E-03
SER	26	N	391	SER	26	H	2194	4.70E-01	-6.63E-01	-7.59E-01	-5.68E-01	9.56E-02
SER	26	N	391	SER	26	HG	2198	5.49E-01	-5.75E-01	-6.30E-01	-5.20E-01	5.54E-02
SER	26	N	391	ASN	27	C	2201	6.72E-01	-5.15E-01	-5.46E-01	-4.84E-01	3.10E-02
SER	26	C	393	GLY	25	O	2184	7.05E-01	-3.54E-01	-4.04E-01	-3.05E-01	4.96E-02
SER	26	C	393	SER	26	N	2188	5.63E-01	-5.79E-01	-5.88E-01	-5.70E-01	8.62E-03
SER	26	C	393	SER	26	O	2191	5.79E-01	-5.86E-01	-6.07E-01	-5.66E-01	2.07E-02
SER	26	C	393	SER	26	OG	2193	5.02E-01	-9.15E-01	-1.01E+00	-8.17E-01	9.80E-02
SER	26	C	393	ASN	27	N	2199	4.90E-01	-6.38E-01	-6.74E-01	-6.02E-01	3.55E-02
SER	26	C	393	ASN	27	O	2202	4.71E-01	-8.78E-01	-9.81E-01	-7.75E-01	1.03E-01
SER	26	C	393	ASN	27	ND2	2206	8.07E-01	-4.13E-01	-4.39E-01	-3.88E-01	2.54E-02

SER	26	C	393	LYS	28	N	2213	5.71E-01	-4.84E-01	-5.61E-01	-4.07E-01	7.70E-02
SER	26	O	394	ASP	23	CG	2158	8.69E-01	-4.15E-01	-4.28E-01	-4.02E-01	1.30E-02
SER	26	O	394	GLY	25	C	2183	6.18E-01	-6.17E-01	-6.56E-01	-5.78E-01	3.90E-02
SER	26	O	394	SER	26	C	2190	4.60E-01	-1.04E+00	-1.19E+00	-8.83E-01	1.53E-01
SER	26	O	394	SER	26	CB	2192	3.98E-01	-4.71E-01	-5.72E-01	-3.69E-01	1.02E-01
SER	26	O	394	SER	26	H	2194	5.13E-01	-5.57E-01	-6.01E-01	-5.13E-01	4.39E-02
SER	26	O	394	SER	26	HG	2198	5.40E-01	-6.43E-01	-7.01E-01	-5.84E-01	5.85E-02
SER	26	O	394	ASN	27	C	2201	4.50E-01	-1.37E+00	-1.48E+00	-1.26E+00	1.11E-01
SER	26	O	394	ASN	27	CG	2204	6.85E-01	-5.01E-01	-5.20E-01	-4.82E-01	1.92E-02
SER	26	O	394	ASN	27	H	2207	4.49E-01	-6.71E-01	-9.08E-01	-4.34E-01	2.37E-01
SER	26	O	394	LYS	28	C	2215	6.10E-01	-8.62E-01	-1.02E+00	-7.05E-01	1.58E-01
SER	26	OG	396	GLY	25	C	2183	8.11E-01	-4.12E-01	-4.62E-01	-3.63E-01	4.95E-02
SER	26	OG	396	SER	26	C	2190	6.83E-01	-4.72E-01	-5.31E-01	-4.12E-01	6.00E-02
SER	26	OG	396	SER	26	H	2194	6.64E-01	-3.47E-01	-3.65E-01	-3.29E-01	1.79E-02
SER	26	OG	396	SER	26	HG	2198	5.36E-01	-7.37E-01	-8.52E-01	-6.23E-01	1.14E-01
SER	26	OG	396	ASN	27	C	2201	7.39E-01	-5.04E-01	-5.19E-01	-4.89E-01	1.50E-02
SER	26	OG	396	ASN	27	CG	2204	9.12E-01	-3.31E-01	-3.35E-01	-3.27E-01	4.15E-03
SER	26	OG	396	LYS	28	C	2215	9.49E-01	-3.86E-01	-3.91E-01	-3.81E-01	4.71E-03
SER	26	H	397	SER	26	N	2188	5.50E-01	-4.65E-01	-5.59E-01	-3.72E-01	9.34E-02
SER	26	H	397	SER	26	OG	2193	5.58E-01	-5.21E-01	-6.04E-01	-4.37E-01	8.37E-02
SER	26	HG	401	SER	26	OG	2193	4.95E-01	-8.95E-01	-1.03E+00	-7.57E-01	1.38E-01
ASN	27	N	402	SER	26	C	2190	5.62E-01	-4.63E-01	-4.65E-01	-4.60E-01	2.65E-03
ASN	27	N	402	ASN	27	C	2201	5.17E-01	-7.46E-01	-8.47E-01	-6.45E-01	1.01E-01
ASN	27	N	402	ASN	27	CG	2204	6.66E-01	-3.91E-01	-3.97E-01	-3.85E-01	5.89E-03
ASN	27	N	402	ASN	27	H	2207	4.67E-01	-3.86E-01	-4.32E-01	-3.40E-01	4.59E-02
ASN	27	C	404	SER	26	N	2188	7.95E-01	-3.74E-01	-3.90E-01	-3.58E-01	1.60E-02
ASN	27	C	404	SER	26	O	2191	7.09E-01	-4.97E-01	-5.28E-01	-4.65E-01	3.13E-02
ASN	27	C	404	SER	26	OG	2193	7.13E-01	-5.38E-01	-5.54E-01	-5.23E-01	1.58E-02
ASN	27	C	404	ASN	27	N	2199	6.07E-01	-5.25E-01	-6.15E-01	-4.36E-01	8.98E-02
ASN	27	C	404	ASN	27	O	2202	4.14E-01	-1.51E+00	-1.57E+00	-1.44E+00	6.99E-02
ASN	27	C	404	ASN	27	OD1	2205	6.45E-01	-5.46E-01	-5.82E-01	-5.10E-01	3.61E-02
ASN	27	C	404	ASN	27	ND2	2206	7.50E-01	-6.49E-01	-7.88E-01	-5.09E-01	1.39E-01
ASN	27	C	404	LYS	28	N	2213	5.77E-01	-5.71E-01	-6.05E-01	-5.37E-01	3.41E-02
ASN	27	C	404	LYS	28	O	2216	7.16E-01	-4.86E-01	-5.42E-01	-4.30E-01	5.60E-02
ASN	27	C	404	GLY	29	N	2235	5.67E-01	-5.48E-01	-6.47E-01	-4.49E-01	9.90E-02
ASN	27	O	405	ASN	27	C	2201	6.19E-01	-5.84E-01	-5.92E-01	-5.76E-01	8.05E-03
ASN	27	O	405	ASN	27	CG	2204	7.43E-01	-3.88E-01	-4.11E-01	-3.65E-01	2.32E-02
ASN	27	O	405	LYS	28	C	2215	6.95E-01	-5.61E-01	-6.25E-01	-4.97E-01	6.38E-02

ASN	27	CG	407	SER	26	O	2191	7.72E-01	-3.98E-01	-4.02E-01	-3.95E-01	3.50E-03
ASN	27	CG	407	SER	26	OG	2193	7.83E-01	-4.39E-01	-4.80E-01	-3.97E-01	4.17E-02
ASN	27	CG	407	ASN	27	N	2199	6.08E-01	-4.73E-01	-4.96E-01	-4.50E-01	2.32E-02
ASN	27	CG	407	ASN	27	O	2202	4.08E-01	-1.62E+00	-1.92E+00	-1.31E+00	3.02E-01
ASN	27	CG	407	ASN	27	OD1	2205	4.87E-01	-1.07E+00	-1.29E+00	-8.48E-01	2.19E-01
ASN	27	CG	407	ASN	27	ND2	2206	5.78E-01	-1.09E+00	-1.40E+00	-7.77E-01	3.12E-01
ASN	27	CG	407	LYS	28	N	2213	6.22E-01	-4.68E-01	-5.18E-01	-4.18E-01	5.01E-02
ASN	27	OD1	408	ASN	27	C	2201	5.52E-01	-7.87E-01	-9.12E-01	-6.61E-01	1.26E-01
ASN	27	OD1	408	ASN	27	CG	2204	5.44E-01	-9.38E-01	-1.31E+00	-5.65E-01	3.73E-01
ASN	27	OD1	408	LYS	28	C	2215	6.49E-01	-6.34E-01	-6.79E-01	-5.89E-01	4.52E-02
ASN	27	ND2	409	GLY	25	C	2183	9.92E-01	-3.54E-01	-3.64E-01	-3.45E-01	9.23E-03
ASN	27	ND2	409	SER	26	C	2190	7.24E-01	-5.11E-01	-5.60E-01	-4.62E-01	4.87E-02
ASN	27	ND2	409	ASN	27	C	2201	5.11E-01	-1.59E+00	-1.97E+00	-1.21E+00	3.78E-01
ASN	27	ND2	409	ASN	27	CG	2204	4.55E-01	-1.89E+00	-2.29E+00	-1.49E+00	4.02E-01
ASN	27	ND2	409	ASN	27	H	2207	5.88E-01	-4.10E-01	-4.45E-01	-3.74E-01	3.52E-02
ASN	27	ND2	409	ASN	27	HD21	2211	5.36E-01	-8.02E-01	-1.05E+00	-5.48E-01	2.53E-01
ASN	27	ND2	409	ASN	27	HD22	2212	5.43E-01	-6.69E-01	-6.77E-01	-6.61E-01	7.83E-03
ASN	27	ND2	409	LYS	28	C	2215	6.48E-01	-1.10E+00	-1.35E+00	-8.52E-01	2.47E-01
ASN	27	HD21	414	ASN	27	ND2	2206	4.91E-01	-9.08E-01	-1.06E+00	-7.54E-01	1.54E-01
ASN	27	HD22	415	ASN	27	O	2202	4.41E-01	-9.30E-01	-1.18E+00	-6.79E-01	2.51E-01
ASN	27	HD22	415	ASN	27	ND2	2206	4.97E-01	-8.30E-01	-8.92E-01	-7.68E-01	6.20E-02
LYS	28	N	416	ASN	27	C	2201	4.76E-01	-9.36E-01	-1.12E+00	-7.55E-01	1.81E-01
LYS	28	N	416	ASN	27	CG	2204	6.74E-01	-4.12E-01	-4.89E-01	-3.35E-01	7.70E-02
LYS	28	N	416	LYS	28	C	2215	5.28E-01	-8.41E-01	-9.48E-01	-7.34E-01	1.07E-01
LYS	28	N	416	GLY	29	H	2239	4.03E-01	-6.32E-01	-7.80E-01	-4.83E-01	1.48E-01
LYS	28	C	418	SER	26	O	2191	8.08E-01	-4.77E-01	-5.48E-01	-4.05E-01	7.11E-02
LYS	28	C	418	SER	26	OG	2193	9.08E-01	-4.37E-01	-5.09E-01	-3.65E-01	7.20E-02
LYS	28	C	418	ASN	27	N	2199	7.72E-01	-3.98E-01	-4.84E-01	-3.13E-01	8.54E-02
LYS	28	C	418	ASN	27	O	2202	4.95E-01	-1.59E+00	-2.36E+00	-8.27E-01	7.65E-01
LYS	28	C	418	ASN	27	OD1	2205	7.15E-01	-5.23E-01	-5.63E-01	-4.84E-01	3.94E-02
LYS	28	C	418	ASN	27	ND2	2206	8.36E-01	-6.86E-01	-8.99E-01	-4.73E-01	2.13E-01
LYS	28	C	418	LYS	28	N	2213	5.99E-01	-6.44E-01	-7.54E-01	-5.34E-01	1.10E-01
LYS	28	C	418	LYS	28	O	2216	6.26E-01	-7.20E-01	-7.30E-01	-7.11E-01	9.61E-03
LYS	28	C	418	GLY	29	N	2235	4.16E-01	-1.25E+00	-1.29E+00	-1.20E+00	4.58E-02
LYS	28	C	418	GLY	29	O	2238	6.53E-01	-6.04E-01	-6.45E-01	-5.62E-01	4.16E-02
LYS	28	C	418	ALA	30	N	2242	6.54E-01	-4.80E-01	-5.22E-01	-4.39E-01	4.14E-02
LYS	28	C	418	ALA	30	O	2245	7.64E-01	-4.90E-01	-5.40E-01	-4.41E-01	4.94E-02
LYS	28	O	419	ASN	27	C	2201	5.08E-01	-1.23E+00	-1.72E+00	-7.46E-01	4.89E-01

LYS	28	O	419	ASN	27	CG	2204	6.70E-01	-5.73E-01	-7.31E-01	-4.15E-01	1.58E-01
LYS	28	O	419	LYS	28	C	2215	4.01E-01	-2.07E+00	-2.19E+00	-1.94E+00	1.24E-01
LYS	28	O	419	LYS	28	HA	2223	3.41E-01	-6.36E-01	-8.13E-01	-4.58E-01	1.78E-01
LYS	28	O	419	GLY	29	C	2237	4.85E-01	-1.06E+00	-1.19E+00	-9.29E-01	1.30E-01
LYS	28	O	419	GLY	29	H	2239	2.20E-01	-3.97E+00	-4.21E+00	-3.72E+00	2.47E-01
LYS	28	O	419	ALA	30	C	2244	7.04E-01	-4.57E-01	-5.02E-01	-4.12E-01	4.47E-02
LYS	28	O	419	ALA	30	H	2247	5.33E-01	-4.35E-01	-5.03E-01	-3.66E-01	6.85E-02
LYS	28	NZ	424	ASP	23	CG	2158	5.94E-01	-3.69E-01	-3.87E-01	-3.50E-01	1.82E-02
LYS	28	H	425	ASN	27	O	2202	3.35E-01	-1.55E+00	-2.34E+00	-7.51E-01	7.95E-01
LYS	28	H	425	LYS	28	N	2213	4.33E-01	-4.54E-01	-4.65E-01	-4.42E-01	1.18E-02
LYS	28	HZ1	435	ASP	23	OD1	2159	6.26E-01	-3.84E-01	-4.11E-01	-3.57E-01	2.73E-02
LYS	28	HZ2	436	ASP	23	OD1	2159	5.84E-01	-4.67E-01	-5.51E-01	-3.83E-01	8.40E-02
LYS	28	HZ3	437	ASP	23	OD1	2159	5.55E-01	-5.21E-01	-6.04E-01	-4.38E-01	8.31E-02
GLY	29	N	438	LYS	28	C	2215	6.20E-01	-4.90E-01	-5.13E-01	-4.67E-01	2.29E-02
GLY	29	N	438	GLY	29	C	2237	6.56E-01	-3.50E-01	-3.65E-01	-3.36E-01	1.44E-02
GLY	29	N	438	GLY	29	H	2239	4.26E-01	-4.13E-01	-4.36E-01	-3.90E-01	2.32E-02
GLY	29	C	440	ASN	27	O	2202	7.05E-01	-4.72E-01	-5.90E-01	-3.54E-01	1.18E-01
GLY	29	C	440	LYS	28	O	2216	6.81E-01	-4.95E-01	-5.41E-01	-4.50E-01	4.53E-02
GLY	29	C	440	GLY	29	N	2235	4.61E-01	-8.19E-01	-9.81E-01	-6.58E-01	1.62E-01
GLY	29	C	440	GLY	29	O	2238	6.03E-01	-5.66E-01	-5.79E-01	-5.53E-01	1.30E-02
GLY	29	C	440	ALA	30	N	2242	5.10E-01	-6.56E-01	-6.87E-01	-6.25E-01	3.12E-02
GLY	29	C	440	ALA	30	O	2245	5.42E-01	-7.98E-01	-8.90E-01	-7.06E-01	9.22E-02
GLY	29	C	440	ILE	31	N	2252	6.79E-01	-3.95E-01	-4.15E-01	-3.74E-01	2.08E-02
GLY	29	O	441	ASN	27	C	2201	7.13E-01	-4.76E-01	-5.93E-01	-3.58E-01	1.18E-01
GLY	29	O	441	LYS	28	C	2215	5.01E-01	-1.19E+00	-1.49E+00	-8.82E-01	3.03E-01
GLY	29	O	441	GLY	29	C	2237	4.40E-01	-1.19E+00	-1.28E+00	-1.10E+00	9.30E-02
GLY	29	O	441	GLY	29	H	2239	3.13E-01	-2.03E+00	-3.19E+00	-8.60E-01	1.17E+00
GLY	29	O	441	ALA	30	C	2244	5.39E-01	-7.25E-01	-8.04E-01	-6.46E-01	7.88E-02
GLY	29	O	441	ALA	30	H	2247	4.26E-01	-6.82E-01	-8.05E-01	-5.60E-01	1.22E-01
ALA	30	N	445	LYS	28	C	2215	6.79E-01	-4.49E-01	-4.97E-01	-4.02E-01	4.77E-02
ALA	30	N	445	GLY	29	C	2237	5.45E-01	-5.63E-01	-5.91E-01	-5.35E-01	2.82E-02
ALA	30	N	445	ALA	30	C	2244	5.65E-01	-5.10E-01	-5.28E-01	-4.93E-01	1.75E-02
ALA	30	N	445	ALA	30	H	2247	4.44E-01	-4.68E-01	-4.98E-01	-4.38E-01	3.02E-02
ALA	30	C	447	GLY	29	O	2238	7.07E-01	-4.03E-01	-4.20E-01	-3.87E-01	1.64E-02
ALA	30	C	447	ALA	30	N	2242	5.64E-01	-5.16E-01	-5.56E-01	-4.76E-01	4.01E-02
ALA	30	C	447	ALA	30	O	2245	4.09E-01	-1.53E+00	-1.63E+00	-1.44E+00	9.53E-02
ALA	30	C	447	ILE	31	N	2252	5.74E-01	-5.49E-01	-5.70E-01	-5.28E-01	2.11E-02
ALA	30	C	447	ILE	31	O	2255	7.58E-01	-4.30E-01	-4.47E-01	-4.13E-01	1.70E-02

ALA	30	C	447	ILE	32	N	2271	6.39E-01	-4.36E-01	-4.57E-01	-4.16E-01	2.05E-02
ALA	30	C	447	ILE	32	O	2274	7.35E-01	-4.55E-01	-4.66E-01	-4.43E-01	1.17E-02
ALA	30	O	448	LYS	28	C	2215	9.13E-01	-3.60E-01	-3.86E-01	-3.34E-01	2.60E-02
ALA	30	O	448	GLY	29	C	2237	7.38E-01	-4.13E-01	-4.32E-01	-3.93E-01	1.95E-02
ALA	30	O	448	ALA	30	C	2244	6.15E-01	-5.81E-01	-5.97E-01	-5.65E-01	1.60E-02
ALA	30	O	448	ILE	31	C	2254	7.39E-01	-4.05E-01	-4.24E-01	-3.85E-01	1.97E-02
ALA	30	CB	449	ALA	30	C	2244	4.41E-01	-5.33E-01	-5.93E-01	-4.73E-01	5.98E-02
ALA	30	H	450	ALA	30	O	2245	5.56E-01	-3.73E-01	-3.86E-01	-3.60E-01	1.31E-02
ALA	30	HA	451	ALA	30	O	2245	2.96E-01	-8.17E-01	-9.73E-01	-6.62E-01	1.56E-01
ILE	31	N	455	LYS	28	C	2215	8.01E-01	-3.66E-01	-4.01E-01	-3.32E-01	3.47E-02
ILE	31	N	455	GLY	29	C	2237	6.28E-01	-4.63E-01	-4.92E-01	-4.34E-01	2.91E-02
ILE	31	N	455	ALA	30	C	2244	4.73E-01	-8.65E-01	-9.38E-01	-7.92E-01	7.32E-02
ILE	31	N	455	ILE	31	C	2254	5.66E-01	-5.64E-01	-5.81E-01	-5.46E-01	1.74E-02
ILE	31	N	455	ILE	31	HA	2261	3.61E-01	-5.25E-01	-5.51E-01	-4.99E-01	2.60E-02
ILE	31	N	455	ILE	32	C	2273	7.16E-01	-3.47E-01	-3.51E-01	-3.42E-01	4.79E-03
ILE	31	N	455	ILE	32	H	2279	4.79E-01	-4.81E-01	-4.99E-01	-4.63E-01	1.79E-02
ILE	31	C	457	ALA	30	O	2245	4.72E-01	-1.09E+00	-1.23E+00	-9.50E-01	1.40E-01
ILE	31	C	457	ILE	31	N	2252	5.56E-01	-5.86E-01	-6.04E-01	-5.67E-01	1.83E-02
ILE	31	C	457	ILE	31	O	2255	6.27E-01	-6.21E-01	-6.35E-01	-6.07E-01	1.36E-02
ILE	31	C	457	ILE	32	N	2271	4.44E-01	-1.00E+00	-1.06E+00	-9.50E-01	5.49E-02
ILE	31	C	457	ILE	32	O	2274	4.45E-01	-1.37E+00	-1.42E+00	-1.32E+00	4.95E-02
ILE	31	C	457	GLY	33	N	2290	6.55E-01	-3.43E-01	-3.50E-01	-3.36E-01	6.55E-03
ILE	31	C	457	GLY	33	O	2293	7.43E-01	-3.67E-01	-3.88E-01	-3.47E-01	2.04E-02
ILE	31	O	458	LYS	28	C	2215	9.51E-01	-3.74E-01	-3.89E-01	-3.59E-01	1.48E-02
ILE	31	O	458	GLY	29	C	2237	7.39E-01	-4.60E-01	-4.75E-01	-4.44E-01	1.51E-02
ILE	31	O	458	ALA	30	C	2244	4.68E-01	-1.23E+00	-1.34E+00	-1.11E+00	1.16E-01
ILE	31	O	458	ILE	31	C	2254	3.85E-01	-1.99E+00	-2.06E+00	-1.92E+00	6.84E-02
ILE	31	O	458	ILE	31	H	2260	5.42E-01	-4.94E-01	-5.05E-01	-4.83E-01	1.12E-02
ILE	31	O	458	ILE	31	HA	2261	2.51E-01	-2.04E+00	-2.19E+00	-1.89E+00	1.49E-01
ILE	31	O	458	ILE	32	C	2273	4.47E-01	-1.36E+00	-1.40E+00	-1.31E+00	4.73E-02
ILE	31	O	458	ILE	32	H	2279	2.36E-01	-4.63E+00	-5.08E+00	-4.17E+00	4.55E-01
ILE	31	O	458	GLY	33	C	2292	6.55E-01	-5.80E-01	-5.93E-01	-5.67E-01	1.28E-02
ILE	31	H	463	ALA	30	N	2242	5.02E-01	-3.95E-01	-4.44E-01	-3.46E-01	4.86E-02
ILE	31	H	463	ALA	30	O	2245	3.32E-01	-1.90E+00	-2.63E+00	-1.16E+00	7.31E-01
ILE	31	H	463	ILE	31	N	2252	4.29E-01	-6.32E-01	-6.61E-01	-6.02E-01	2.93E-02
ILE	31	H	463	ILE	31	O	2255	6.17E-01	-3.72E-01	-3.80E-01	-3.64E-01	7.66E-03
ILE	31	H	463	ILE	32	N	2271	5.19E-01	-3.97E-01	-4.13E-01	-3.81E-01	1.60E-02
ILE	31	H	463	ILE	32	O	2274	6.45E-01	-3.40E-01	-3.51E-01	-3.28E-01	1.15E-02

ILE	32	N	474	ALA	30	C	2244	6.70E-01	-3.97E-01	-4.15E-01	-3.79E-01	1.78E-02
ILE	32	N	474	ILE	31	C	2254	5.94E-01	-5.06E-01	-5.13E-01	-5.00E-01	6.53E-03
ILE	32	N	474	ILE	32	C	2273	5.40E-01	-6.27E-01	-6.40E-01	-6.13E-01	1.35E-02
ILE	32	N	474	ILE	32	H	2279	4.12E-01	-6.99E-01	-7.18E-01	-6.80E-01	1.93E-02
ILE	32	N	474	GLY	33	C	2292	6.79E-01	-3.93E-01	-4.06E-01	-3.80E-01	1.30E-02
ILE	32	C	476	ALA	30	O	2245	7.75E-01	-3.70E-01	-3.85E-01	-3.55E-01	1.51E-02
ILE	32	C	476	ILE	31	O	2255	8.18E-01	-3.75E-01	-3.82E-01	-3.67E-01	7.51E-03
ILE	32	C	476	ILE	32	N	2271	5.94E-01	-5.08E-01	-5.28E-01	-4.88E-01	1.98E-02
ILE	32	C	476	ILE	32	O	2274	4.08E-01	-1.71E+00	-1.80E+00	-1.62E+00	8.79E-02
ILE	32	C	476	GLY	33	N	2290	5.79E-01	-4.44E-01	-4.55E-01	-4.34E-01	1.05E-02
ILE	32	C	476	GLY	33	O	2293	5.39E-01	-7.12E-01	-7.43E-01	-6.81E-01	3.11E-02
ILE	32	O	477	ILE	31	C	2254	8.01E-01	-3.88E-01	-3.92E-01	-3.84E-01	3.77E-03
ILE	32	O	477	ILE	32	C	2273	6.27E-01	-6.21E-01	-6.31E-01	-6.11E-01	9.95E-03
ILE	32	O	477	ILE	32	H	2279	6.05E-01	-3.88E-01	-3.95E-01	-3.80E-01	7.91E-03
ILE	32	O	477	GLY	33	C	2292	6.49E-01	-5.93E-01	-6.17E-01	-5.70E-01	2.34E-02
ILE	32	H	482	ILE	32	O	2274	5.29E-01	-5.23E-01	-5.36E-01	-5.09E-01	1.34E-02
ILE	32	HA	483	ILE	32	N	2271	3.92E-01	-4.23E-01	-4.43E-01	-4.03E-01	2.01E-02
ILE	32	HA	483	ILE	32	O	2274	2.52E-01	-2.06E+00	-2.27E+00	-1.84E+00	2.18E-01
GLY	33	N	493	ILE	32	C	2273	4.79E-01	-6.97E-01	-7.70E-01	-6.24E-01	7.31E-02
GLY	33	N	493	GLY	33	C	2292	4.75E-01	-7.19E-01	-7.44E-01	-6.94E-01	2.52E-02
GLY	33	C	495	ILE	32	O	2274	5.39E-01	-9.09E-01	-1.04E+00	-7.79E-01	1.31E-01
GLY	33	C	495	GLY	33	N	2290	6.55E-01	-3.51E-01	-3.65E-01	-3.36E-01	1.46E-02
GLY	33	C	495	GLY	33	O	2293	4.37E-01	-1.22E+00	-1.37E+00	-1.08E+00	1.44E-01
GLY	33	C	495	LEU	34	N	2297	6.05E-01	-3.92E-01	-3.98E-01	-3.86E-01	5.99E-03
GLY	33	C	495	LEU	34	O	2300	8.14E-01	-3.47E-01	-3.51E-01	-3.43E-01	3.91E-03
GLY	33	C	495	MET	35	N	2316	7.02E-01	-3.22E-01	-3.28E-01	-3.16E-01	5.98E-03
GLY	33	C	495	MET	35	O	2319	7.62E-01	-3.97E-01	-4.09E-01	-3.85E-01	1.19E-02
GLY	33	O	496	ILE	32	C	2273	7.53E-01	-3.58E-01	-3.78E-01	-3.38E-01	2.00E-02
GLY	33	O	496	GLY	33	C	2292	6.10E-01	-5.51E-01	-5.60E-01	-5.42E-01	9.10E-03
GLY	33	O	496	LEU	34	C	2299	7.75E-01	-3.40E-01	-3.49E-01	-3.32E-01	8.63E-03
GLY	33	H	497	ILE	32	O	2274	3.22E-01	-1.64E+00	-2.19E+00	-1.09E+00	5.51E-01
GLY	33	H	497	GLY	33	N	2290	4.29E-01	-4.05E-01	-4.23E-01	-3.86E-01	1.84E-02
GLY	33	H	497	GLY	33	O	2293	4.07E-01	-6.34E-01	-6.89E-01	-5.79E-01	5.53E-02
LEU	34	N	500	ILE	32	C	2273	5.75E-01	-4.32E-01	-4.66E-01	-3.98E-01	3.43E-02
LEU	34	N	500	GLY	33	C	2292	4.54E-01	-7.72E-01	-8.50E-01	-6.94E-01	7.80E-02
LEU	34	N	500	LEU	34	C	2299	6.19E-01	-3.68E-01	-3.83E-01	-3.54E-01	1.45E-02
LEU	34	C	502	ILE	32	O	2274	5.99E-01	-6.90E-01	-7.09E-01	-6.71E-01	1.88E-02
LEU	34	C	502	GLY	33	O	2293	3.81E-01	-1.72E+00	-1.89E+00	-1.55E+00	1.69E-01

LEU	34	C	502	LEU	34	N	2297	5.12E-01	-5.60E-01	-5.74E-01	-5.45E-01	1.46E-02
LEU	34	C	502	LEU	34	O	2300	6.30E-01	-5.56E-01	-5.66E-01	-5.46E-01	1.00E-02
LEU	34	C	502	MET	35	N	2316	4.60E-01	-8.10E-01	-8.50E-01	-7.70E-01	4.03E-02
LEU	34	C	502	MET	35	O	2319	4.64E-01	-1.15E+00	-1.25E+00	-1.05E+00	9.73E-02
LEU	34	C	502	VAL	36	N	2333	6.82E-01	-3.84E-01	-4.02E-01	-3.66E-01	1.83E-02
LEU	34	O	503	ILE	32	C	2273	6.10E-01	-5.93E-01	-6.16E-01	-5.71E-01	2.22E-02
LEU	34	O	503	GLY	33	C	2292	3.72E-01	-2.01E+00	-2.14E+00	-1.88E+00	1.34E-01
LEU	34	O	503	LEU	34	C	2299	3.93E-01	-1.71E+00	-1.78E+00	-1.63E+00	7.30E-02
LEU	34	O	503	LEU	34	CG	2302	4.71E-01	-3.61E-01	-3.76E-01	-3.46E-01	1.52E-02
LEU	34	O	503	LEU	34	H	2305	4.96E-01	-4.36E-01	-4.51E-01	-4.20E-01	1.50E-02
LEU	34	O	503	LEU	34	HA	2306	2.48E-01	-1.48E+00	-1.53E+00	-1.42E+00	5.54E-02
LEU	34	O	503	MET	35	C	2318	4.83E-01	-1.08E+00	-1.18E+00	-9.75E-01	1.05E-01
LEU	34	O	503	MET	35	H	2324	2.73E-01	-2.42E+00	-2.86E+00	-1.97E+00	4.44E-01
LEU	34	O	503	VAL	36	H	2340	6.77E-01	-3.72E-01	-3.94E-01	-3.50E-01	2.16E-02
LEU	34	H	508	ILE	32	O	2274	3.81E-01	-9.66E-01	-1.11E+00	-8.22E-01	1.43E-01
LEU	34	H	508	GLY	33	O	2293	3.46E-01	-1.60E+00	-2.55E+00	-6.40E-01	9.55E-01
LEU	34	H	508	LEU	34	N	2297	4.56E-01	-3.44E-01	-3.75E-01	-3.12E-01	3.18E-02
MET	35	N	519	GLY	33	C	2292	5.91E-01	-4.59E-01	-4.72E-01	-4.46E-01	1.27E-02
MET	35	N	519	LEU	34	C	2299	5.88E-01	-4.56E-01	-4.63E-01	-4.49E-01	6.81E-03
MET	35	N	519	MET	35	C	2318	5.53E-01	-5.49E-01	-5.70E-01	-5.27E-01	2.16E-02
MET	35	N	519	MET	35	H	2324	4.21E-01	-4.95E-01	-5.07E-01	-4.83E-01	1.22E-02
MET	35	C	521	GLN	15	NE2	2022	8.06E-01	-5.92E-01	-6.54E-01	-5.29E-01	6.26E-02
MET	35	C	521	GLY	33	O	2293	6.71E-01	-4.69E-01	-4.85E-01	-4.54E-01	1.53E-02
MET	35	C	521	LEU	34	O	2300	8.07E-01	-3.64E-01	-3.71E-01	-3.56E-01	7.46E-03
MET	35	C	521	MET	35	N	2316	5.85E-01	-4.83E-01	-4.98E-01	-4.69E-01	1.49E-02
MET	35	C	521	MET	35	O	2319	4.01E-01	-1.71E+00	-1.74E+00	-1.69E+00	2.29E-02
MET	35	C	521	VAL	36	N	2333	5.90E-01	-5.41E-01	-5.56E-01	-5.26E-01	1.48E-02
MET	35	C	521	GLY	38	O	2359	7.83E-01	-3.52E-01	-3.73E-01	-3.31E-01	2.13E-02
MET	35	O	522	GLY	33	C	2292	8.47E-01	-3.29E-01	-3.34E-01	-3.23E-01	5.12E-03
MET	35	O	522	LEU	34	C	2299	7.97E-01	-3.60E-01	-3.67E-01	-3.54E-01	6.18E-03
MET	35	O	522	MET	35	C	2318	6.38E-01	-5.76E-01	-5.87E-01	-5.65E-01	1.07E-02
MET	35	CG	524	MET	35	C	2318	4.43E-01	-4.95E-01	-5.35E-01	-4.54E-01	4.03E-02
MET	35	CE	526	GLY	38	C	2358	4.45E-01	-6.72E-01	-7.82E-01	-5.61E-01	1.10E-01
MET	35	CE	526	VAL	40	H	2387	3.73E-01	-9.59E-01	-1.28E+00	-6.40E-01	3.20E-01
MET	35	H	527	MET	35	O	2319	5.23E-01	-4.17E-01	-4.30E-01	-4.04E-01	1.28E-02
MET	35	HA	528	MET	35	O	2319	2.48E-01	-1.35E+00	-1.43E+00	-1.27E+00	7.92E-02
MET	35	HE1	533	GLY	38	O	2359	3.65E-01	-4.45E-01	-5.24E-01	-3.65E-01	7.94E-02
MET	35	HE2	534	GLY	38	O	2359	3.13E-01	-6.59E-01	-7.38E-01	-5.79E-01	7.94E-02

MET	35	HE3	535	GLY	38	O	2359	3.66E-01	-4.37E-01	-5.06E-01	-3.67E-01	6.99E-02
VAL	36	N	536	GLN	15	CD	2020	7.47E-01	-3.93E-01	-4.53E-01	-3.32E-01	6.05E-02
VAL	36	N	536	LEU	34	C	2299	7.14E-01	-3.51E-01	-3.65E-01	-3.37E-01	1.40E-02
VAL	36	N	536	MET	35	C	2318	4.70E-01	-9.16E-01	-9.51E-01	-8.80E-01	3.58E-02
VAL	36	N	536	MET	35	H	2324	5.17E-01	-3.43E-01	-3.66E-01	-3.20E-01	2.32E-02
VAL	36	N	536	VAL	36	C	2335	5.78E-01	-4.23E-01	-4.43E-01	-4.04E-01	1.92E-02
VAL	36	N	536	VAL	36	CB	2337	4.89E-01	-5.54E-01	-6.00E-01	-5.08E-01	4.62E-02
VAL	36	N	536	VAL	36	H	2340	6.09E-01	-3.72E-01	-3.79E-01	-3.64E-01	7.56E-03
VAL	36	C	538	GLN	15	OE1	2021	5.79E-01	-8.10E-01	-1.15E+00	-4.69E-01	3.40E-01
VAL	36	C	538	GLN	15	NE2	2022	5.22E-01	-1.24E+00	-1.62E+00	-8.59E-01	3.78E-01
VAL	36	C	538	MET	35	O	2319	4.92E-01	-7.79E-01	-8.51E-01	-7.07E-01	7.21E-02
VAL	36	C	538	VAL	36	N	2333	5.55E-01	-4.62E-01	-4.78E-01	-4.47E-01	1.53E-02
VAL	36	C	538	VAL	36	O	2336	6.32E-01	-3.14E-01	-3.18E-01	-3.09E-01	4.47E-03
VAL	36	C	538	GLY	37	N	2349	4.63E-01	-5.91E-01	-6.25E-01	-5.58E-01	3.38E-02
VAL	36	C	538	GLY	38	O	2359	6.02E-01	-4.51E-01	-5.15E-01	-3.87E-01	6.39E-02
VAL	36	O	539	GLN	15	CD	2020	5.41E-01	-7.67E-01	-1.00E+00	-5.32E-01	2.36E-01
VAL	36	O	539	GLN	15	HE22	2030	3.85E-01	-1.52E+00	-2.33E+00	-7.11E-01	8.11E-01
VAL	36	O	539	MET	35	C	2318	4.74E-01	-8.12E-01	-8.72E-01	-7.51E-01	6.04E-02
VAL	36	O	539	VAL	36	C	2335	3.96E-01	-9.51E-01	-9.91E-01	-9.11E-01	3.99E-02
VAL	36	O	539	VAL	36	CB	2337	3.90E-01	-9.19E-01	-1.08E+00	-7.54E-01	1.65E-01
VAL	36	O	539	VAL	36	H	2340	5.25E-01	-4.64E-01	-4.74E-01	-4.53E-01	1.03E-02
VAL	36	O	539	GLY	37	C	2351	5.44E-01	-5.70E-01	-6.10E-01	-5.29E-01	4.07E-02
VAL	36	O	539	GLY	37	H	2353	2.75E-01	-1.60E+00	-1.95E+00	-1.25E+00	3.49E-01
VAL	36	O	539	GLY	38	C	2358	6.10E-01	-4.51E-01	-5.06E-01	-3.96E-01	5.50E-02
VAL	36	O	539	GLY	38	H	2360	4.41E-01	-4.18E-01	-4.66E-01	-3.70E-01	4.81E-02
VAL	36	CB	540	GLN	15	NE2	2022	6.17E-01	-6.89E-01	-8.23E-01	-5.54E-01	1.35E-01
VAL	36	CB	540	MET	35	O	2319	5.26E-01	-5.92E-01	-6.57E-01	-5.26E-01	6.56E-02
VAL	36	H	543	GLN	15	OE1	2021	6.77E-01	-4.41E-01	-5.16E-01	-3.67E-01	7.43E-02
VAL	36	H	543	GLN	15	NE2	2022	6.28E-01	-7.15E-01	-8.23E-01	-6.07E-01	1.08E-01
VAL	36	H	543	MET	35	N	2316	5.20E-01	-4.67E-01	-5.03E-01	-4.30E-01	3.65E-02
VAL	36	H	543	MET	35	O	2319	2.79E-01	-3.58E+00	-4.16E+00	-3.00E+00	5.80E-01
VAL	36	H	543	VAL	36	N	2333	4.19E-01	-8.91E-01	-9.02E-01	-8.80E-01	1.12E-02
VAL	36	H	543	VAL	36	O	2336	5.94E-01	-3.53E-01	-3.64E-01	-3.41E-01	1.14E-02
VAL	36	H	543	GLY	37	N	2349	5.07E-01	-4.71E-01	-5.14E-01	-4.28E-01	4.31E-02
VAL	36	H	543	GLY	38	O	2359	6.37E-01	-3.87E-01	-4.21E-01	-3.52E-01	3.46E-02
GLY	37	N	552	GLN	15	CD	2020	5.92E-01	-6.19E-01	-8.39E-01	-3.99E-01	2.20E-01
GLY	37	N	552	VAL	36	C	2335	5.86E-01	-3.40E-01	-3.45E-01	-3.34E-01	5.86E-03
GLY	37	N	552	GLY	37	C	2351	6.78E-01	-3.27E-01	-3.39E-01	-3.15E-01	1.21E-02

GLY	37	N	552	GLY	37	H	2353	4.18E-01	-4.31E-01	-4.40E-01	-4.21E-01	9.76E-03
GLY	37	C	554	HIS	13	ND1	1986	5.82E-01	-5.35E-01	-6.27E-01	-4.44E-01	9.12E-02
GLY	37	C	554	GLN	15	OE1	2021	6.14E-01	-7.96E-01	-1.01E+00	-5.79E-01	2.17E-01
GLY	37	C	554	GLN	15	NE2	2022	5.27E-01	-1.59E+00	-2.07E+00	-1.12E+00	4.79E-01
GLY	37	C	554	MET	35	O	2319	6.76E-01	-5.00E-01	-5.31E-01	-4.69E-01	3.11E-02
GLY	37	C	554	VAL	36	N	2333	6.59E-01	-4.18E-01	-4.37E-01	-3.98E-01	1.94E-02
GLY	37	C	554	VAL	36	O	2336	6.29E-01	-4.12E-01	-4.27E-01	-3.97E-01	1.50E-02
GLY	37	C	554	GLY	37	N	2349	4.32E-01	-9.21E-01	-1.00E+00	-8.41E-01	7.97E-02
GLY	37	C	554	GLY	37	O	2352	6.35E-01	-5.07E-01	-5.13E-01	-5.01E-01	5.86E-03
GLY	37	C	554	GLY	38	N	2356	4.44E-01	-8.51E-01	-9.04E-01	-7.98E-01	5.30E-02
GLY	37	C	554	GLY	38	O	2359	4.26E-01	-1.37E+00	-1.68E+00	-1.07E+00	3.06E-01
GLY	37	C	554	VAL	39	N	2363	6.33E-01	-4.65E-01	-5.23E-01	-4.06E-01	5.86E-02
GLY	37	O	555	HIS	13	C	1982	8.20E-01	-3.61E-01	-3.91E-01	-3.31E-01	2.96E-02
GLY	37	O	555	HIS	14	C	1999	8.40E-01	-3.44E-01	-3.62E-01	-3.26E-01	1.79E-02
GLY	37	O	555	GLN	15	CD	2020	5.48E-01	-8.86E-01	-1.09E+00	-6.84E-01	2.02E-01
GLY	37	O	555	GLN	15	HE22	2030	4.38E-01	-1.12E+00	-1.52E+00	-7.14E-01	4.06E-01
GLY	37	O	555	MET	35	C	2318	6.61E-01	-4.84E-01	-5.08E-01	-4.61E-01	2.36E-02
GLY	37	O	555	VAL	36	C	2335	4.36E-01	-9.44E-01	-1.04E+00	-8.44E-01	9.99E-02
GLY	37	O	555	VAL	36	CB	2337	5.68E-01	-4.51E-01	-5.08E-01	-3.94E-01	5.70E-02
GLY	37	O	555	VAL	36	H	2340	6.32E-01	-3.89E-01	-4.05E-01	-3.72E-01	1.66E-02
GLY	37	O	555	GLY	37	C	2351	3.91E-01	-1.60E+00	-1.63E+00	-1.56E+00	3.38E-02
GLY	37	O	555	GLY	37	H	2353	2.87E-01	-1.88E+00	-2.41E+00	-1.34E+00	5.35E-01
GLY	37	O	555	GLY	38	C	2358	4.25E-01	-1.41E+00	-1.78E+00	-1.04E+00	3.67E-01
GLY	37	O	555	GLY	38	H	2360	2.30E-01	-3.25E+00	-3.76E+00	-2.73E+00	5.17E-01
GLY	37	O	555	VAL	39	H	2370	6.15E-01	-4.24E-01	-4.84E-01	-3.65E-01	5.93E-02
GLY	38	N	559	GLY	37	C	2351	6.04E-01	-4.15E-01	-4.23E-01	-4.06E-01	8.87E-03
GLY	38	N	559	GLY	38	C	2358	5.27E-01	-5.69E-01	-6.26E-01	-5.12E-01	5.71E-02
GLY	38	N	559	GLY	38	H	2360	4.18E-01	-4.32E-01	-4.40E-01	-4.23E-01	8.82E-03
GLY	38	C	561	GLY	38	N	2356	6.11E-01	-4.06E-01	-4.26E-01	-3.86E-01	2.00E-02
GLY	38	C	561	GLY	38	O	2359	4.18E-01	-1.35E+00	-1.43E+00	-1.26E+00	8.49E-02
GLY	38	C	561	VAL	39	N	2363	5.69E-01	-5.68E-01	-5.96E-01	-5.40E-01	2.81E-02
GLY	38	C	561	VAL	40	N	2379	6.37E-01	-4.70E-01	-5.44E-01	-3.95E-01	7.48E-02
GLY	38	O	562	GLY	38	C	2358	6.24E-01	-5.25E-01	-5.34E-01	-5.16E-01	8.80E-03
VAL	39	N	566	GLY	38	C	2358	4.99E-01	-7.69E-01	-8.04E-01	-7.34E-01	3.54E-02
VAL	39	N	566	VAL	39	C	2365	5.56E-01	-4.77E-01	-5.45E-01	-4.10E-01	6.76E-02
VAL	39	N	566	VAL	39	CB	2367	4.62E-01	-6.39E-01	-7.10E-01	-5.69E-01	7.02E-02
VAL	39	N	566	VAL	39	H	2370	6.05E-01	-3.76E-01	-3.82E-01	-3.70E-01	5.68E-03
VAL	39	N	566	VAL	40	H	2387	4.65E-01	-8.19E-01	-1.07E+00	-5.64E-01	2.55E-01

VAL	39	C	568	GLY	38	O	2359	5.42E-01	-5.70E-01	-6.47E-01	-4.94E-01	7.63E-02
VAL	39	C	568	VAL	39	N	2363	5.88E-01	-4.12E-01	-4.47E-01	-3.77E-01	3.54E-02
VAL	39	C	568	VAL	40	N	2379	4.51E-01	-7.76E-01	-8.81E-01	-6.70E-01	1.06E-01
VAL	39	O	569	GLY	38	C	2358	5.21E-01	-6.57E-01	-7.66E-01	-5.49E-01	1.08E-01
VAL	39	O	569	VAL	39	C	2365	4.00E-01	-9.21E-01	-9.45E-01	-8.97E-01	2.38E-02
VAL	39	O	569	VAL	39	CB	2367	3.86E-01	-1.05E+00	-1.32E+00	-7.76E-01	2.73E-01
VAL	39	O	569	VAL	39	H	2370	5.63E-01	-4.05E-01	-4.50E-01	-3.60E-01	4.47E-02
VAL	39	O	569	VAL	40	C	2381	5.25E-01	-5.18E-01	-6.38E-01	-3.97E-01	1.21E-01
VAL	39	O	569	VAL	40	CB	2383	5.38E-01	-4.19E-01	-4.97E-01	-3.41E-01	7.80E-02
VAL	39	O	569	VAL	40	H	2387	2.49E-01	-4.13E+00	-5.49E+00	-2.76E+00	1.37E+00
VAL	39	H	573	GLY	38	O	2359	3.63E-01	-1.58E+00	-1.86E+00	-1.29E+00	2.87E-01
VAL	39	H	573	VAL	39	N	2363	4.38E-01	-8.01E-01	-8.45E-01	-7.56E-01	4.45E-02
VAL	39	H	573	VAL	40	N	2379	4.89E-01	-7.38E-01	-9.88E-01	-4.88E-01	2.50E-01
VAL	40	N	582	VAL	39	C	2365	6.06E-01	-3.81E-01	-3.91E-01	-3.70E-01	1.07E-02
VAL	40	N	582	VAL	40	H	2387	4.26E-01	-8.58E-01	-8.73E-01	-8.42E-01	1.54E-02
VAL	40	C	584	VAL	40	N	2379	4.51E-01	-7.82E-01	-8.84E-01	-6.79E-01	1.03E-01
VAL	40	C	584	VAL	40	OXT	2386	5.11E-01	-5.29E-01	-6.08E-01	-4.51E-01	7.86E-02
VAL	40	O	585	VAL	40	C	2381	4.52E-01	-7.50E-01	-9.02E-01	-5.99E-01	1.52E-01
VAL	40	O	585	VAL	40	H	2387	3.42E-01	-2.86E+00	-4.11E+00	-1.60E+00	1.25E+00
VAL	40	CB	586	VAL	40	N	2379	4.36E-01	-7.52E-01	-8.58E-01	-6.46E-01	1.06E-01
VAL	40	OXT	589	VAL	40	C	2381	5.38E-01	-5.05E-01	-6.49E-01	-3.61E-01	1.44E-01
VAL	40	OXT	589	VAL	40	H	2387	4.28E-01	-7.96E-01	-9.23E-01	-6.70E-01	1.27E-01
VAL	40	H	590	VAL	40	N	2379	6.13E-01	-3.66E-01	-3.77E-01	-3.55E-01	1.08E-02
VAL	40	HB	592	VAL	40	H	2387	2.71E-01	-9.34E-01	-1.24E+00	-6.32E-01	3.02E-01

Supplementary Table 1b: Mapping results for A β 40's (PDB ID: 2M4J) short range (1:2) dominant atom-atom Lennard-Jones interactions across ensemble structures. Columns for each chain correspond to: residue abbreviation, residue number in peptide sequence, atom identity (IUPAC naming convention) and atom number in PDB file. Energy in kT , distance in nm . Mapping analysis began on the 11th residue for both isoforms because original structure data for A β 42 begins with the 11th residue.

Chain A				Chain D				Average Distance	Average L-J Values	Lower 95% Confidence Interval Bound	Upper 95% Confidence Interval Bound	Margin of Error
GLU	11	C	154	VAL	12	N	1964	4.47E-01	-1.10E-01	-1.12E-01	-1.08E-01	1.72E-03
GLU	11	O	155	GLU	11	CA	1950	3.72E-01	-2.33E-01	-2.36E-01	-2.31E-01	2.82E-03
GLU	11	O	155	GLU	11	C	1951	3.99E-01	-1.67E-01	-1.70E-01	-1.65E-01	2.59E-03
GLU	11	O	155	VAL	12	N	1964	3.43E-01	-3.03E-01	-3.05E-01	-3.01E-01	1.75E-03
GLU	11	O	155	VAL	12	CA	1965	4.44E-01	-1.15E-01	-1.18E-01	-1.13E-01	2.65E-03
GLU	11	O	155	VAL	12	O	1967	4.04E-01	-1.79E-01	-1.83E-01	-1.76E-01	3.39E-03
GLU	11	O	155	VAL	12	CG1	1969	3.49E-01	-2.37E-01	-2.44E-01	-2.29E-01	7.04E-03
VAL	12	N	167	VAL	12	O	1967	4.34E-01	-1.43E-01	-1.45E-01	-1.41E-01	1.94E-03
VAL	12	CA	168	VAL	12	O	1967	3.41E-01	-2.22E-01	-2.25E-01	-2.19E-01	2.98E-03
VAL	12	CA	168	VAL	12	CG1	1969	3.95E-01	-1.71E-01	-1.72E-01	-1.70E-01	9.92E-04
VAL	12	C	169	VAL	12	O	1967	3.82E-01	-1.93E-01	-1.95E-01	-1.92E-01	1.48E-03
VAL	12	CB	171	VAL	12	O	1967	4.25E-01	-1.42E-01	-1.43E-01	-1.41E-01	1.47E-03
VAL	12	CB	171	VAL	12	CG1	1969	3.72E-01	-1.73E-01	-1.74E-01	-1.72E-01	8.52E-04
VAL	12	CG2	173	VAL	12	O	1967	4.32E-01	-1.32E-01	-1.34E-01	-1.31E-01	1.58E-03
VAL	12	CG2	173	VAL	12	CG1	1969	3.95E-01	-1.71E-01	-1.72E-01	-1.71E-01	7.36E-04
HIS	13	N	183	VAL	12	C	1966	4.46E-01	-1.11E-01	-1.13E-01	-1.10E-01	1.44E-03
HIS	13	N	183	VAL	12	O	1967	3.28E-01	-2.43E-01	-2.52E-01	-2.35E-01	8.49E-03
HIS	13	N	183	HIS	13	ND1	1986	4.49E-01	-1.36E-01	-1.39E-01	-1.33E-01	3.06E-03
HIS	13	CA	184	VAL	12	O	1967	4.44E-01	-1.15E-01	-1.17E-01	-1.13E-01	1.86E-03
HIS	13	C	185	HIS	14	N	1997	4.34E-01	-1.26E-01	-1.28E-01	-1.25E-01	1.41E-03
HIS	13	O	186	VAL	12	O	1967	4.08E-01	-1.71E-01	-1.74E-01	-1.68E-01	3.16E-03
HIS	13	O	186	HIS	13	CA	1981	3.65E-01	-2.42E-01	-2.44E-01	-2.41E-01	1.27E-03
HIS	13	O	186	HIS	13	C	1982	3.84E-01	-1.90E-01	-1.91E-01	-1.88E-01	1.61E-03
HIS	13	O	186	HIS	13	CB	1984	4.48E-01	-1.10E-01	-1.13E-01	-1.07E-01	2.76E-03
HIS	13	O	186	HIS	14	CA	1998	4.21E-01	-1.48E-01	-1.51E-01	-1.46E-01	2.57E-03
HIS	13	O	186	HIS	14	C	1999	4.19E-01	-1.35E-01	-1.39E-01	-1.31E-01	3.98E-03
HIS	13	O	186	HIS	14	O	2000	3.88E-01	-2.16E-01	-2.22E-01	-2.11E-01	5.69E-03
HIS	13	CB	187	HIS	13	ND1	1986	3.84E-01	-2.16E-01	-2.17E-01	-2.15E-01	1.34E-03
HIS	13	CG	188	HIS	13	ND1	1986	3.96E-01	-1.78E-01	-1.80E-01	-1.76E-01	1.84E-03
HIS	13	CG	188	HIS	13	CE1	1988	4.11E-01	-1.22E-01	-1.23E-01	-1.20E-01	1.55E-03
HIS	13	CD2	190	HIS	13	ND1	1986	3.67E-01	-1.94E-01	-1.95E-01	-1.92E-01	1.57E-03

HIS	13	CD2	190	HIS	13	NE2	1989	4.38E-01	-1.21E-01	-1.23E-01	-1.19E-01	2.19E-03
HIS	13	NE2	192	HIS	13	CE1	1988	4.20E-01	-1.46E-01	-1.48E-01	-1.43E-01	2.73E-03
HIS	14	N	200	HIS	14	O	2000	4.40E-01	-1.33E-01	-1.36E-01	-1.31E-01	2.26E-03
HIS	14	CA	201	HIS	14	C	1999	4.19E-01	-1.28E-01	-1.31E-01	-1.26E-01	2.37E-03
HIS	14	CA	201	HIS	14	O	2000	3.29E-01	-1.50E-01	-1.61E-01	-1.38E-01	1.14E-02
HIS	14	C	202	HIS	14	O	2000	4.13E-01	-1.44E-01	-1.46E-01	-1.43E-01	1.30E-03
HIS	14	CG	205	HIS	14	C	1999	4.06E-01	-1.26E-01	-1.30E-01	-1.22E-01	3.57E-03
HIS	14	ND1	206	HIS	14	C	1999	3.75E-01	-1.95E-01	-1.96E-01	-1.93E-01	1.64E-03
HIS	14	CD2	207	HIS	14	O	2000	3.42E-01	-1.94E-01	-2.03E-01	-1.84E-01	9.61E-03
HIS	14	CE1	208	HIS	14	C	1999	4.17E-01	-1.15E-01	-1.20E-01	-1.11E-01	4.22E-03
HIS	14	NE2	209	HIS	14	O	2000	3.61E-01	-2.93E-01	-3.00E-01	-2.86E-01	7.25E-03
GLN	15	N	217	HIS	14	O	2000	4.26E-01	-1.56E-01	-1.62E-01	-1.50E-01	5.59E-03
GLN	15	N	217	GLN	15	CA	2015	4.35E-01	-1.42E-01	-1.46E-01	-1.39E-01	3.44E-03
GLN	15	N	217	GLN	15	CB	2018	4.44E-01	-1.29E-01	-1.39E-01	-1.19E-01	1.00E-02
GLN	15	O	220	GLN	15	CA	2015	3.72E-01	-2.33E-01	-2.41E-01	-2.24E-01	8.39E-03
GLN	15	O	220	GLN	15	C	2016	4.04E-01	-1.59E-01	-1.64E-01	-1.54E-01	5.02E-03
GLN	15	O	220	GLN	15	CB	2018	4.15E-01	-1.60E-01	-1.78E-01	-1.42E-01	1.81E-02
GLN	15	O	220	LYS	16	N	2031	3.60E-01	-2.94E-01	-3.00E-01	-2.87E-01	6.59E-03
LYS	16	N	234	LYS	16	O	2034	4.49E-01	-1.20E-01	-1.28E-01	-1.12E-01	8.07E-03
LYS	16	CA	235	LYS	16	O	2034	3.42E-01	-2.20E-01	-2.30E-01	-2.09E-01	1.04E-02
LYS	16	C	236	LYS	16	O	2034	3.98E-01	-1.68E-01	-1.70E-01	-1.67E-01	1.44E-03
LYS	16	CB	238	LYS	16	O	2034	3.95E-01	-1.95E-01	-2.01E-01	-1.89E-01	5.97E-03
LYS	16	CG	239	LYS	16	O	2034	3.57E-01	-2.43E-01	-2.46E-01	-2.41E-01	2.26E-03
LEU	17	N	256	LYS	16	O	2034	3.74E-01	-2.70E-01	-2.74E-01	-2.67E-01	3.56E-03
LEU	17	N	256	LEU	17	CA	2054	4.54E-01	-1.16E-01	-1.20E-01	-1.11E-01	4.57E-03
LEU	17	N	256	LEU	17	CG	2058	4.03E-01	-1.75E-01	-2.08E-01	-1.42E-01	3.28E-02
LEU	17	O	259	LYS	16	O	2034	4.00E-01	-1.93E-01	-2.25E-01	-1.60E-01	3.27E-02
LEU	17	O	259	LEU	17	N	2053	4.52E-01	-1.16E-01	-1.18E-01	-1.14E-01	1.98E-03
LEU	17	O	259	LEU	17	C	2055	3.86E-01	-1.88E-01	-1.94E-01	-1.81E-01	6.48E-03
LEU	17	O	259	LEU	17	CB	2057	3.86E-01	-2.08E-01	-2.37E-01	-1.78E-01	2.94E-02
LEU	17	O	259	VAL	18	N	2072	3.36E-01	-2.51E-01	-2.73E-01	-2.29E-01	2.17E-02
VAL	18	CA	276	VAL	18	N	2072	4.58E-01	-1.11E-01	-1.13E-01	-1.09E-01	2.14E-03
VAL	18	CA	276	VAL	18	O	2075	4.08E-01	-1.71E-01	-1.82E-01	-1.60E-01	1.12E-02
VAL	18	C	277	VAL	18	O	2075	3.84E-01	-1.91E-01	-1.94E-01	-1.89E-01	2.72E-03
PHE	19	N	291	VAL	18	C	2074	4.01E-01	-1.72E-01	-1.73E-01	-1.71E-01	1.01E-03
PHE	19	CA	292	VAL	18	O	2075	3.52E-01	-2.40E-01	-2.42E-01	-2.38E-01	2.02E-03
PHE	19	C	293	VAL	18	O	2075	3.94E-01	-1.76E-01	-2.01E-01	-1.50E-01	2.53E-02
PHE	19	C	293	PHE	20	N	2108	4.37E-01	-1.24E-01	-1.32E-01	-1.16E-01	7.70E-03

PHE	19	O	294	VAL	18	O	2075	3.48E-01	-2.72E-01	-3.18E-01	-2.26E-01	4.61E-02
PHE	19	O	294	PHE	20	CA	2109	4.20E-01	-1.51E-01	-1.57E-01	-1.45E-01	6.17E-03
PHE	19	CB	295	VAL	18	O	2075	3.38E-01	-2.05E-01	-2.18E-01	-1.92E-01	1.32E-02
PHE	19	CB	295	PHE	19	CA	2089	4.34E-01	-1.26E-01	-1.45E-01	-1.07E-01	1.87E-02
PHE	20	C	313	ALA	21	N	2128	4.18E-01	-1.49E-01	-1.57E-01	-1.41E-01	7.59E-03
PHE	20	O	314	ALA	21	CA	2129	3.88E-01	-1.61E-01	-1.66E-01	-1.56E-01	4.74E-03
PHE	20	O	314	ALA	21	CB	2132	3.98E-01	-1.88E-01	-2.08E-01	-1.68E-01	2.00E-02
PHE	20	O	314	GLU	22	N	2138	4.56E-01	-1.11E-01	-1.14E-01	-1.07E-01	3.00E-03
PHE	20	CD2	318	PHE	20	CD1	2114	4.17E-01	-1.16E-01	-1.18E-01	-1.14E-01	2.13E-03
PHE	20	CE2	320	PHE	20	CE1	2116	4.18E-01	-1.15E-01	-1.17E-01	-1.12E-01	2.49E-03
ALA	21	CA	332	ALA	21	CB	2132	4.18E-01	-1.45E-01	-1.58E-01	-1.33E-01	1.24E-02
ALA	21	C	333	ALA	21	CB	2132	4.10E-01	-1.36E-01	-1.44E-01	-1.27E-01	8.45E-03
ALA	21	O	334	ALA	21	CA	2129	4.04E-01	-1.79E-01	-1.86E-01	-1.71E-01	7.21E-03
ALA	21	O	334	ALA	21	CB	2132	3.49E-01	-2.37E-01	-2.44E-01	-2.30E-01	7.21E-03
GLU	22	CA	342	GLU	22	O	2141	3.52E-01	-2.43E-01	-2.45E-01	-2.41E-01	2.03E-03
GLU	22	C	343	GLU	22	O	2141	3.81E-01	-1.95E-01	-1.97E-01	-1.93E-01	1.82E-03
ASP	23	N	356	GLU	22	C	2140	4.33E-01	-1.28E-01	-1.29E-01	-1.26E-01	1.69E-03
ASP	23	CA	357	GLU	22	O	2141	4.20E-01	-1.51E-01	-1.54E-01	-1.47E-01	3.39E-03
ASP	23	O	359	GLU	22	O	2141	3.57E-01	-2.95E-01	-3.25E-01	-2.64E-01	3.03E-02
ASP	23	O	359	ASP	23	N	2153	4.15E-01	-1.80E-01	-1.98E-01	-1.62E-01	1.81E-02
ASP	23	O	359	ASP	23	C	2155	3.94E-01	-1.75E-01	-1.84E-01	-1.66E-01	8.81E-03
ASP	23	O	359	VAL	24	N	2165	3.79E-01	-1.99E-01	-2.08E-01	-1.90E-01	8.96E-03
VAL	24	CA	369	VAL	24	CG2	2171	4.29E-01	-1.30E-01	-1.48E-01	-1.11E-01	1.88E-02
VAL	24	CG1	373	VAL	24	CG2	2171	4.14E-01	-1.50E-01	-1.64E-01	-1.35E-01	1.45E-02
GLY	25	CA	385	SER	26	N	2188	4.41E-01	-1.35E-01	-1.55E-01	-1.16E-01	1.92E-02
GLY	25	C	386	SER	26	CA	2189	4.35E-01	-1.11E-01	-1.14E-01	-1.08E-01	3.30E-03
SER	26	N	391	SER	26	CB	2192	4.10E-01	-1.81E-01	-1.86E-01	-1.76E-01	5.18E-03
SER	26	C	393	SER	26	CB	2192	4.12E-01	-1.35E-01	-1.45E-01	-1.26E-01	9.38E-03
SER	26	O	394	SER	26	CB	2192	3.98E-01	-1.52E-01	-1.69E-01	-1.36E-01	1.65E-02
SER	26	O	394	ASN	27	O	2202	4.19E-01	-1.51E-01	-1.66E-01	-1.35E-01	1.56E-02
ASN	27	CA	403	ASN	27	O	2202	3.63E-01	-1.59E-01	-1.79E-01	-1.40E-01	1.98E-02
ASN	27	C	404	ASN	27	O	2202	4.14E-01	-1.42E-01	-1.53E-01	-1.32E-01	1.06E-02
LYS	28	C	418	GLY	29	N	2235	4.16E-01	-1.51E-01	-1.59E-01	-1.43E-01	8.01E-03
LYS	28	O	419	LYS	28	CA	2214	4.15E-01	-1.59E-01	-1.95E-01	-1.23E-01	3.58E-02
LYS	28	O	419	LYS	28	C	2215	4.01E-01	-1.62E-01	-1.76E-01	-1.49E-01	1.33E-02
LYS	28	O	419	GLY	29	CA	2236	3.62E-01	-1.84E-01	-2.13E-01	-1.55E-01	2.87E-02
ALA	30	CA	446	ALA	30	O	2245	3.59E-01	-2.41E-01	-2.44E-01	-2.39E-01	2.60E-03
ALA	30	C	447	ALA	30	O	2245	4.09E-01	-1.52E-01	-1.67E-01	-1.37E-01	1.46E-02

ILE	31	N	455	ALA	30	O	2245	3.88E-01	-2.21E-01	-2.64E-01	-1.79E-01	4.21E-02
ILE	31	O	458	ALA	30	O	2245	3.96E-01	-2.06E-01	-2.61E-01	-1.52E-01	5.46E-02
ILE	31	O	458	ILE	31	CA	2253	3.44E-01	-2.18E-01	-2.28E-01	-2.08E-01	1.01E-02
ILE	31	O	458	ILE	31	C	2254	3.85E-01	-1.89E-01	-1.96E-01	-1.82E-01	6.91E-03
ILE	31	O	458	ILE	32	O	2274	3.72E-01	-2.59E-01	-2.79E-01	-2.38E-01	2.03E-02
ILE	32	N	474	ILE	32	O	2274	4.40E-01	-1.35E-01	-1.44E-01	-1.25E-01	9.40E-03
ILE	32	CA	475	ILE	32	O	2274	3.45E-01	-2.09E-01	-2.18E-01	-1.99E-01	9.34E-03
ILE	32	C	476	ILE	32	O	2274	4.08E-01	-1.52E-01	-1.64E-01	-1.40E-01	1.17E-02
LEU	34	C	502	GLY	33	O	2293	3.81E-01	-1.89E-01	-2.07E-01	-1.71E-01	1.77E-02
LEU	34	O	503	GLY	33	C	2292	3.72E-01	-2.02E-01	-2.12E-01	-1.93E-01	9.36E-03
LEU	34	O	503	LEU	34	N	2297	4.05E-01	-2.00E-01	-2.13E-01	-1.87E-01	1.33E-02
LEU	34	O	503	LEU	34	CA	2298	3.44E-01	-2.28E-01	-2.34E-01	-2.21E-01	6.74E-03
LEU	34	O	503	LEU	34	C	2299	3.93E-01	-1.76E-01	-1.85E-01	-1.67E-01	9.23E-03
LEU	34	O	503	MET	35	N	2316	3.51E-01	-2.66E-01	-2.91E-01	-2.42E-01	2.45E-02
MET	35	CA	520	MET	35	O	2319	3.43E-01	-2.09E-01	-2.26E-01	-1.92E-01	1.73E-02
MET	35	C	521	MET	35	O	2319	4.01E-01	-1.63E-01	-1.66E-01	-1.60E-01	3.12E-03
MET	35	CB	523	MET	35	O	2319	3.99E-01	-1.68E-01	-1.93E-01	-1.42E-01	2.53E-02
MET	35	CG	524	MET	35	O	2319	3.69E-01	-2.04E-01	-2.21E-01	-1.87E-01	1.69E-02
MET	35	SD	525	MET	35	SD	2322	5.08E-01	-1.71E-01	-1.78E-01	-1.63E-01	7.43E-03
VAL	36	N	536	MET	35	O	2319	3.61E-01	-2.80E-01	-2.89E-01	-2.70E-01	9.55E-03
VAL	36	O	539	VAL	36	C	2335	3.96E-01	-1.72E-01	-1.81E-01	-1.63E-01	9.23E-03
VAL	36	O	539	VAL	36	CB	2337	3.90E-01	-1.80E-01	-2.08E-01	-1.52E-01	2.81E-02
VAL	36	O	539	GLY	37	N	2349	3.55E-01	-2.53E-01	-2.81E-01	-2.25E-01	2.78E-02
GLY	37	O	555	GLY	37	CA	2350	3.62E-01	-2.20E-01	-2.39E-01	-2.01E-01	1.89E-02
GLY	37	O	555	GLY	37	C	2351	3.91E-01	-1.79E-01	-1.84E-01	-1.75E-01	4.62E-03
GLY	38	C	561	GLY	38	O	2359	4.18E-01	-1.37E-01	-1.51E-01	-1.23E-01	1.41E-02
VAL	39	O	569	VAL	39	C	2365	4.00E-01	-1.65E-01	-1.71E-01	-1.59E-01	6.07E-03
VAL	39	CG2	572	VAL	39	CB	2367	4.04E-01	-1.53E-01	-1.60E-01	-1.45E-01	7.82E-03

Supplementary Table 2a: Mapping results for A β 42's (PDB ID: 2MXU, by Xiao et al.) short range (1:2) dominant atom-atom Coulombic interactions across ensemble structures. Columns for each chain correspond to: residue abbreviation, residue number in peptide sequence, atom identity (IUPAC naming convention) and atom number in PDB file. Energy in kT , distance in nm . Mapping analysis began on the 11th residue for both isoforms because original structure data for A β 42 begins with the 11th residue.

Chain A				Chain B				Average Distance	Average Coulombic Values	Lower 95% Confidence Interval Bound	Upper 95% Confidence Interval Bound	Margin of Error
GLU	11	N	1	GLU	11	C	480	5.26E-01	-5.80E-01	-7.48E-01	-4.12E-01	1.68E-01
GLU	11	N	1	GLU	11	CD	484	6.60E-01	-5.24E-01	-5.80E-01	-4.69E-01	5.58E-02
GLU	11	C	3	GLU	11	O	481	5.12E-01	-1.01E+00	-1.40E+00	-6.21E-01	3.90E-01
GLU	11	C	3	GLU	11	OE1	485	7.36E-01	-5.11E-01	-5.73E-01	-4.49E-01	6.18E-02
GLU	11	C	3	GLU	11	OE2	486	8.05E-01	-4.28E-01	-4.58E-01	-3.98E-01	2.99E-02
GLU	11	C	3	VAL	12	N	493	4.82E-01	-7.58E-01	-9.29E-01	-5.87E-01	1.71E-01
GLU	11	C	3	HIS	13	N	509	6.56E-01	-3.99E-01	-4.08E-01	-3.89E-01	9.19E-03
GLU	11	O	4	GLU	11	C	480	4.67E-01	-1.25E+00	-1.65E+00	-8.59E-01	3.94E-01
GLU	11	O	4	GLU	11	CD	484	7.31E-01	-6.61E-01	-8.03E-01	-5.19E-01	1.42E-01
GLU	11	O	4	VAL	12	C	495	5.78E-01	-7.49E-01	-9.89E-01	-5.09E-01	2.40E-01
GLU	11	O	4	HIS	13	C	511	8.38E-01	-4.06E-01	-4.38E-01	-3.73E-01	3.25E-02
GLU	11	CD	7	GLU	11	N	478	5.52E-01	-8.94E-01	-1.17E+00	-6.14E-01	2.80E-01
GLU	11	CD	7	GLU	11	O	481	6.51E-01	-9.53E-01	-1.30E+00	-6.09E-01	3.44E-01
GLU	11	CD	7	GLU	11	OE1	485	4.96E-01	-1.93E+00	-2.15E+00	-1.71E+00	2.20E-01
GLU	11	CD	7	GLU	11	OE2	486	5.36E-01	-1.62E+00	-1.84E+00	-1.39E+00	2.21E-01
GLU	11	CD	7	VAL	12	N	493	6.73E-01	-5.42E-01	-6.11E-01	-4.72E-01	6.92E-02
GLU	11	CD	7	HIS	13	N	509	9.21E-01	-3.56E-01	-3.78E-01	-3.34E-01	2.19E-02
GLU	11	OE1	8	GLU	11	C	480	5.97E-01	-9.43E-01	-1.26E+00	-6.29E-01	3.14E-01
GLU	11	OE1	8	GLU	11	CD	484	5.00E-01	-1.91E+00	-2.17E+00	-1.64E+00	2.62E-01
GLU	11	OE1	8	VAL	12	C	495	8.26E-01	-3.93E-01	-4.33E-01	-3.53E-01	3.96E-02
GLU	11	OE1	8	VAL	12	H	500	6.38E-01	-6.70E-01	-8.42E-01	-4.98E-01	1.72E-01
GLU	11	OE2	9	GLU	11	C	480	6.70E-01	-6.25E-01	-7.22E-01	-5.28E-01	9.71E-02
GLU	11	OE2	9	GLU	11	CD	484	4.65E-01	-2.27E+00	-2.57E+00	-1.97E+00	2.99E-01
GLU	11	OE2	9	VAL	12	H	500	7.24E-01	-5.03E-01	-5.82E-01	-4.24E-01	7.91E-02
VAL	12	N	16	GLU	11	C	480	5.15E-01	-6.38E-01	-7.93E-01	-4.83E-01	1.55E-01
VAL	12	N	16	GLU	11	CD	484	7.87E-01	-3.92E-01	-4.07E-01	-3.76E-01	1.53E-02
VAL	12	N	16	VAL	12	C	495	5.42E-01	-4.89E-01	-5.10E-01	-4.67E-01	2.16E-02
VAL	12	N	16	VAL	12	CB	497	5.40E-01	-4.34E-01	-4.55E-01	-4.13E-01	2.09E-02
VAL	12	N	16	VAL	12	H	500	4.67E-01	-8.26E-01	-1.05E+00	-5.97E-01	2.29E-01
VAL	12	N	16	HIS	13	C	511	7.80E-01	-3.48E-01	-3.75E-01	-3.21E-01	2.72E-02
VAL	12	C	18	VAL	12	N	493	5.48E-01	-4.75E-01	-4.92E-01	-4.58E-01	1.68E-02
VAL	12	C	18	VAL	12	O	496	4.62E-01	-8.46E-01	-1.12E+00	-5.76E-01	2.70E-01
VAL	12	C	18	HIS	13	N	509	5.13E-01	-7.29E-01	-9.17E-01	-5.42E-01	1.87E-01
VAL	12	C	18	HIS	14	N	526	6.57E-01	-3.78E-01	-3.88E-01	-3.69E-01	9.50E-03
VAL	12	O	19	VAL	12	C	495	5.08E-01	-6.75E-01	-9.39E-01	-4.11E-01	2.64E-01
VAL	12	O	19	VAL	12	H	500	5.59E-01	-4.06E-01	-4.39E-01	-3.73E-01	3.26E-02

VAL	12	CB	20	VAL	12	N	493	5.50E-01	-4.17E-01	-4.40E-01	-3.95E-01	2.25E-02
VAL	12	CB	20	HIS	13	N	509	6.05E-01	-4.04E-01	-4.45E-01	-3.62E-01	4.12E-02
VAL	12	H	23	GLU	11	OE1	485	7.98E-01	-4.14E-01	-4.62E-01	-3.66E-01	4.77E-02
VAL	12	H	23	VAL	12	N	493	5.04E-01	-6.74E-01	-8.86E-01	-4.63E-01	2.11E-01
VAL	12	H	23	VAL	12	O	496	5.45E-01	-4.34E-01	-4.75E-01	-3.93E-01	4.13E-02
HIS	13	N	32	GLU	11	C	480	6.61E-01	-3.93E-01	-4.01E-01	-3.84E-01	8.07E-03
HIS	13	N	32	VAL	12	C	495	4.79E-01	-8.57E-01	-1.05E+00	-6.64E-01	1.92E-01
HIS	13	N	32	VAL	12	CB	497	5.73E-01	-4.58E-01	-5.10E-01	-4.06E-01	5.17E-02
HIS	13	N	32	HIS	13	C	511	5.47E-01	-8.29E-01	-8.62E-01	-7.95E-01	3.32E-02
HIS	13	N	32	HIS	13	H	519	5.05E-01	-5.16E-01	-6.85E-01	-3.47E-01	1.69E-01
HIS	13	N	32	HIS	14	C	528	7.61E-01	-4.29E-01	-4.67E-01	-3.91E-01	3.81E-02
HIS	13	C	34	GLU	11	O	481	8.60E-01	-3.90E-01	-4.25E-01	-3.54E-01	3.51E-02
HIS	13	C	34	VAL	12	N	493	7.59E-01	-3.66E-01	-3.95E-01	-3.37E-01	2.87E-02
HIS	13	C	34	VAL	12	O	496	5.70E-01	-8.04E-01	-1.07E+00	-5.37E-01	2.67E-01
HIS	13	C	34	HIS	13	N	509	5.40E-01	-8.53E-01	-8.85E-01	-8.20E-01	3.22E-02
HIS	13	C	34	HIS	13	O	512	5.07E-01	-1.34E+00	-1.87E+00	-7.99E-01	5.37E-01
HIS	13	C	34	HIS	13	ND1	515	6.05E-01	-6.24E-01	-8.24E-01	-4.23E-01	2.00E-01
HIS	13	C	34	HIS	14	N	526	4.76E-01	-1.30E+00	-1.60E+00	-9.97E-01	3.03E-01
HIS	13	C	34	HIS	14	O	529	5.84E-01	-9.82E-01	-1.30E+00	-6.63E-01	3.18E-01
HIS	13	C	34	GLN	15	N	543	6.59E-01	-4.08E-01	-4.24E-01	-3.93E-01	1.54E-02
HIS	13	C	34	GLN	15	O	546	8.20E-01	-4.13E-01	-4.75E-01	-3.51E-01	6.17E-02
HIS	13	O	35	HIS	13	C	511	4.61E-01	-1.60E+00	-2.09E+00	-1.11E+00	4.93E-01
HIS	13	O	35	HIS	13	H	519	5.46E-01	-3.58E-01	-3.85E-01	-3.30E-01	2.74E-02
HIS	13	O	35	HIS	14	C	528	5.74E-01	-1.05E+00	-1.40E+00	-6.96E-01	3.49E-01
HIS	13	ND1	38	HIS	13	C	511	7.36E-01	-3.64E-01	-3.94E-01	-3.34E-01	3.04E-02
HIS	13	H	42	HIS	13	N	509	4.66E-01	-6.15E-01	-7.81E-01	-4.49E-01	1.66E-01
HIS	14	N	49	VAL	12	C	495	6.56E-01	-3.79E-01	-3.91E-01	-3.68E-01	1.14E-02
HIS	14	N	49	HIS	13	C	511	5.09E-01	-1.11E+00	-1.40E+00	-8.14E-01	2.95E-01
HIS	14	N	49	HIS	14	C	528	5.39E-01	-8.60E-01	-9.12E-01	-8.08E-01	5.17E-02
HIS	14	N	49	HIS	14	H	536	4.62E-01	-6.39E-01	-8.16E-01	-4.61E-01	1.78E-01
HIS	14	C	51	HIS	13	N	509	7.80E-01	-4.11E-01	-4.50E-01	-3.72E-01	3.90E-02
HIS	14	C	51	HIS	13	O	512	6.36E-01	-8.93E-01	-1.29E+00	-4.98E-01	3.95E-01
HIS	14	C	51	HIS	14	N	526	5.45E-01	-8.40E-01	-8.88E-01	-7.92E-01	4.81E-02
HIS	14	C	51	HIS	14	O	529	4.58E-01	-1.66E+00	-2.19E+00	-1.13E+00	5.29E-01
HIS	14	C	51	HIS	14	ND1	532	6.54E-01	-5.06E-01	-6.48E-01	-3.64E-01	1.42E-01
HIS	14	C	51	GLN	15	N	543	5.09E-01	-8.09E-01	-1.02E+00	-5.98E-01	2.11E-01
HIS	14	C	51	GLN	15	O	546	5.85E-01	-1.00E+00	-1.32E+00	-6.90E-01	3.15E-01
HIS	14	C	51	GLN	15	OE1	550	7.40E-01	-5.73E-01	-6.81E-01	-4.64E-01	1.09E-01

HIS	14	C	51	GLN	15	NE2	551	7.70E-01	-6.95E-01	-7.39E-01	-6.50E-01	4.46E-02
HIS	14	C	51	LYS	16	N	560	6.58E-01	-4.62E-01	-4.80E-01	-4.44E-01	1.82E-02
HIS	14	O	52	HIS	13	C	511	6.40E-01	-8.55E-01	-1.22E+00	-4.90E-01	3.65E-01
HIS	14	O	52	HIS	14	C	528	5.07E-01	-1.29E+00	-1.79E+00	-8.01E-01	4.93E-01
HIS	14	O	52	GLN	15	CD	549	7.22E-01	-5.33E-01	-6.69E-01	-3.97E-01	1.36E-01
HIS	14	O	52	LYS	16	C	562	8.70E-01	-3.75E-01	-4.13E-01	-3.37E-01	3.82E-02
HIS	14	ND1	55	HIS	14	C	528	7.01E-01	-4.28E-01	-5.26E-01	-3.31E-01	9.74E-02
HIS	14	H	59	HIS	14	N	526	5.02E-01	-5.10E-01	-6.68E-01	-3.53E-01	1.57E-01
GLN	15	N	66	HIS	13	C	511	6.60E-01	-4.08E-01	-4.27E-01	-3.89E-01	1.93E-02
GLN	15	N	66	HIS	14	C	528	4.79E-01	-9.28E-01	-1.13E+00	-7.21E-01	2.07E-01
GLN	15	N	66	GLN	15	C	545	5.22E-01	-4.35E-01	-4.81E-01	-3.88E-01	4.62E-02
GLN	15	N	66	GLN	15	CD	549	6.55E-01	-4.21E-01	-4.56E-01	-3.86E-01	3.52E-02
GLN	15	C	68	GLN	15	O	546	4.60E-01	-1.11E+00	-1.46E+00	-7.59E-01	3.53E-01
GLN	15	C	68	GLN	15	OE1	550	6.94E-01	-3.89E-01	-4.32E-01	-3.45E-01	4.37E-02
GLN	15	C	68	GLN	15	NE2	551	7.52E-01	-4.69E-01	-5.24E-01	-4.14E-01	5.49E-02
GLN	15	C	68	LYS	16	N	560	5.10E-01	-5.81E-01	-7.39E-01	-4.22E-01	1.58E-01
GLN	15	O	69	HIS	14	C	528	6.38E-01	-8.38E-01	-1.15E+00	-5.25E-01	3.13E-01
GLN	15	O	69	GLN	15	C	545	5.09E-01	-8.65E-01	-1.20E+00	-5.35E-01	3.31E-01
GLN	15	O	69	GLN	15	CD	549	7.26E-01	-5.22E-01	-6.06E-01	-4.39E-01	8.37E-02
GLN	15	O	69	LYS	16	C	562	6.54E-01	-8.49E-01	-1.15E+00	-5.45E-01	3.04E-01
GLN	15	CD	72	HIS	14	N	526	7.68E-01	-4.25E-01	-4.60E-01	-3.90E-01	3.47E-02
GLN	15	CD	72	HIS	14	O	529	6.41E-01	-7.33E-01	-9.53E-01	-5.14E-01	2.20E-01
GLN	15	CD	72	GLN	15	N	543	6.46E-01	-4.33E-01	-4.67E-01	-3.99E-01	3.39E-02
GLN	15	CD	72	GLN	15	O	546	6.86E-01	-6.03E-01	-7.18E-01	-4.89E-01	1.14E-01
GLN	15	CD	72	GLN	15	OE1	550	4.84E-01	-1.65E+00	-2.18E+00	-1.12E+00	5.29E-01
GLN	15	CD	72	GLN	15	NE2	551	5.04E-01	-1.94E+00	-2.46E+00	-1.43E+00	5.18E-01
GLN	15	CD	72	LYS	16	N	560	7.52E-01	-3.62E-01	-3.87E-01	-3.38E-01	2.43E-02
GLN	15	OE1	73	HIS	13	C	511	8.34E-01	-4.34E-01	-4.73E-01	-3.95E-01	3.89E-02
GLN	15	OE1	73	HIS	14	C	528	6.93E-01	-7.29E-01	-1.00E+00	-4.52E-01	2.76E-01
GLN	15	OE1	73	GLN	15	CD	549	5.00E-01	-1.51E+00	-1.98E+00	-1.03E+00	4.75E-01
GLN	15	OE1	73	GLN	15	HE22	559	5.31E-01	-1.02E+00	-1.47E+00	-5.70E-01	4.51E-01
GLN	15	NE2	74	HIS	13	C	511	8.62E-01	-5.73E-01	-6.11E-01	-5.36E-01	3.77E-02
GLN	15	NE2	74	HIS	14	C	528	7.15E-01	-8.57E-01	-1.07E+00	-6.48E-01	2.09E-01
GLN	15	NE2	74	GLN	15	C	545	7.41E-01	-4.88E-01	-5.56E-01	-4.21E-01	6.73E-02
GLN	15	NE2	74	GLN	15	CD	549	4.99E-01	-1.99E+00	-2.52E+00	-1.47E+00	5.24E-01
GLN	15	NE2	74	GLN	15	HE21	558	5.11E-01	-1.14E+00	-1.43E+00	-8.48E-01	2.89E-01
GLN	15	NE2	74	GLN	15	HE22	559	5.06E-01	-1.03E+00	-1.10E+00	-9.63E-01	6.86E-02
GLN	15	H	75	GLN	15	O	546	5.04E-01	-5.98E-01	-8.40E-01	-3.55E-01	2.43E-01

GLN	15	HE21	81	GLN	15	NE2	551	4.96E-01	-1.24E+00	-1.57E+00	-9.11E-01	3.28E-01
GLN	15	HE22	82	GLN	15	OE1	550	5.19E-01	-1.08E+00	-1.53E+00	-6.22E-01	4.53E-01
GLN	15	HE22	82	GLN	15	NE2	551	5.15E-01	-9.92E-01	-1.08E+00	-9.08E-01	8.34E-02
LYS	16	N	83	HIS	14	C	528	6.44E-01	-4.91E-01	-5.50E-01	-4.33E-01	5.82E-02
LYS	16	N	83	GLN	15	C	545	4.77E-01	-6.75E-01	-8.31E-01	-5.20E-01	1.55E-01
LYS	16	N	83	GLN	15	CD	549	7.16E-01	-3.99E-01	-4.32E-01	-3.66E-01	3.32E-02
LYS	16	N	83	LYS	16	C	562	5.84E-01	-6.53E-01	-6.98E-01	-6.08E-01	4.51E-02
LYS	16	N	83	LEU	17	C	584	7.15E-01	-3.39E-01	-3.52E-01	-3.27E-01	1.26E-02
LYS	16	N	83	LEU	17	H	590	4.67E-01	-3.97E-01	-4.28E-01	-3.67E-01	3.08E-02
LYS	16	C	85	HIS	14	O	529	7.73E-01	-4.84E-01	-5.65E-01	-4.03E-01	8.10E-02
LYS	16	C	85	GLN	15	N	543	7.18E-01	-3.77E-01	-3.85E-01	-3.70E-01	7.14E-03
LYS	16	C	85	GLN	15	O	546	5.17E-01	-1.39E+00	-1.81E+00	-9.73E-01	4.18E-01
LYS	16	C	85	GLN	15	OE1	550	8.32E-01	-4.96E-01	-5.72E-01	-4.20E-01	7.59E-02
LYS	16	C	85	GLN	15	NE2	551	8.93E-01	-5.94E-01	-6.35E-01	-5.53E-01	4.09E-02
LYS	16	C	85	LYS	16	N	560	4.98E-01	-9.49E-01	-1.05E+00	-8.45E-01	1.04E-01
LYS	16	C	85	LYS	16	O	563	6.05E-01	-7.74E-01	-7.79E-01	-7.70E-01	4.41E-03
LYS	16	C	85	LEU	17	N	582	4.10E-01	-1.23E+00	-1.25E+00	-1.21E+00	2.05E-02
LYS	16	C	85	LEU	17	O	585	4.33E-01	-1.68E+00	-1.75E+00	-1.62E+00	6.40E-02
LYS	16	C	85	VAL	18	N	601	6.30E-01	-5.69E-01	-5.87E-01	-5.51E-01	1.81E-02
LYS	16	O	86	HIS	14	C	528	7.49E-01	-4.69E-01	-5.05E-01	-4.33E-01	3.65E-02
LYS	16	O	86	GLN	15	C	545	4.70E-01	-8.14E-01	-8.97E-01	-7.31E-01	8.27E-02
LYS	16	O	86	GLN	15	CD	549	7.83E-01	-4.49E-01	-5.09E-01	-3.89E-01	5.99E-02
LYS	16	O	86	LYS	16	C	562	3.68E-01	-2.59E+00	-2.65E+00	-2.52E+00	6.18E-02
LYS	16	O	86	LYS	16	H	569	4.54E-01	-6.74E-01	-9.44E-01	-4.05E-01	2.69E-01
LYS	16	O	86	LEU	17	C	584	4.08E-01	-1.57E+00	-1.66E+00	-1.48E+00	9.13E-02
LYS	16	O	86	LEU	17	H	590	1.96E-01	-5.86E+00	-6.39E+00	-5.33E+00	5.31E-01
LYS	16	O	86	VAL	18	CB	605	6.56E-01	-3.60E-01	-3.84E-01	-3.37E-01	2.34E-02
LYS	16	O	86	VAL	18	H	608	5.87E-01	-5.03E-01	-5.24E-01	-4.81E-01	2.13E-02
LEU	17	N	105	LYS	16	C	562	5.77E-01	-5.41E-01	-5.48E-01	-5.33E-01	7.37E-03
LEU	17	N	105	LEU	17	C	584	5.28E-01	-5.23E-01	-5.32E-01	-5.13E-01	9.59E-03
LEU	17	N	105	LEU	17	H	590	3.84E-01	-5.27E-01	-5.37E-01	-5.16E-01	1.07E-02
LEU	17	C	107	LYS	16	O	563	7.77E-01	-3.75E-01	-3.82E-01	-3.68E-01	6.62E-03
LEU	17	C	107	LEU	17	N	582	5.58E-01	-4.62E-01	-4.72E-01	-4.51E-01	1.03E-02
LEU	17	C	107	LEU	17	O	585	3.65E-01	-2.08E+00	-2.11E+00	-2.05E+00	2.94E-02
LEU	17	C	107	VAL	18	N	601	5.81E-01	-5.33E-01	-5.38E-01	-5.27E-01	5.57E-03
LEU	17	C	107	PHE	19	N	617	6.64E-01	-3.34E-01	-3.46E-01	-3.21E-01	1.22E-02
LEU	17	O	108	LYS	16	C	562	7.82E-01	-4.65E-01	-4.72E-01	-4.58E-01	7.00E-03
LEU	17	O	108	LEU	17	C	584	6.04E-01	-6.08E-01	-6.13E-01	-6.03E-01	4.63E-03

LEU	17	H	113	LEU	17	O	585	5.30E-01	-3.73E-01	-3.84E-01	-3.61E-01	1.13E-02
LEU	17	HA	114	LEU	17	O	585	2.59E-01	-1.33E+00	-1.48E+00	-1.19E+00	1.45E-01
VAL	18	N	124	LYS	16	C	562	6.59E-01	-5.19E-01	-5.35E-01	-5.02E-01	1.65E-02
VAL	18	N	124	LEU	17	C	584	4.11E-01	-1.22E+00	-1.26E+00	-1.19E+00	3.73E-02
VAL	18	N	124	LEU	17	H	590	4.79E-01	-3.81E-01	-3.94E-01	-3.68E-01	1.29E-02
VAL	18	N	124	VAL	18	C	603	5.63E-01	-4.47E-01	-4.62E-01	-4.32E-01	1.51E-02
VAL	18	N	124	VAL	18	CB	605	5.66E-01	-3.91E-01	-4.04E-01	-3.78E-01	1.33E-02
VAL	18	N	124	VAL	18	H	608	5.85E-01	-4.03E-01	-4.07E-01	-4.00E-01	3.72E-03
VAL	18	N	124	PHE	19	H	628	4.48E-01	-4.05E-01	-4.32E-01	-3.77E-01	2.77E-02
VAL	18	C	126	LEU	17	O	585	4.20E-01	-1.13E+00	-1.20E+00	-1.05E+00	7.27E-02
VAL	18	C	126	VAL	18	N	601	5.32E-01	-5.08E-01	-5.29E-01	-4.88E-01	2.04E-02
VAL	18	C	126	VAL	18	O	604	6.11E-01	-3.36E-01	-3.38E-01	-3.34E-01	1.79E-03
VAL	18	C	126	PHE	19	N	617	4.11E-01	-7.84E-01	-8.05E-01	-7.63E-01	2.09E-02
VAL	18	C	126	PHE	19	O	620	5.80E-01	-4.73E-01	-4.95E-01	-4.50E-01	2.27E-02
VAL	18	O	127	LYS	16	C	562	7.82E-01	-3.38E-01	-3.49E-01	-3.26E-01	1.11E-02
VAL	18	O	127	LEU	17	C	584	4.44E-01	-9.12E-01	-9.79E-01	-8.44E-01	6.74E-02
VAL	18	O	127	VAL	18	C	603	3.73E-01	-1.11E+00	-1.13E+00	-1.09E+00	2.05E-02
VAL	18	O	127	VAL	18	CB	605	4.70E-01	-5.44E-01	-5.77E-01	-5.12E-01	3.25E-02
VAL	18	O	127	VAL	18	H	608	5.33E-01	-4.51E-01	-4.75E-01	-4.26E-01	2.43E-02
VAL	18	O	127	PHE	19	C	619	4.76E-01	-7.31E-01	-7.69E-01	-6.94E-01	3.76E-02
VAL	18	O	127	PHE	19	H	628	1.92E-01	-3.95E+00	-4.13E+00	-3.77E+00	1.83E-01
VAL	18	CB	128	LEU	17	O	585	3.95E-01	-1.18E+00	-1.32E+00	-1.04E+00	1.41E-01
VAL	18	CB	128	VAL	18	N	601	5.21E-01	-4.73E-01	-4.97E-01	-4.49E-01	2.39E-02
VAL	18	CB	128	PHE	19	N	617	5.14E-01	-4.02E-01	-4.25E-01	-3.79E-01	2.30E-02
VAL	18	CB	128	PHE	19	O	620	6.46E-01	-3.33E-01	-3.47E-01	-3.18E-01	1.45E-02
VAL	18	H	131	LYS	16	O	563	6.60E-01	-3.93E-01	-4.09E-01	-3.78E-01	1.55E-02
VAL	18	H	131	LEU	17	N	582	4.56E-01	-5.72E-01	-6.02E-01	-5.42E-01	2.99E-02
VAL	18	H	131	LEU	17	O	585	1.93E-01	-1.01E+01	-1.08E+01	-9.43E+00	6.77E-01
VAL	18	H	131	VAL	18	N	601	3.90E-01	-1.07E+00	-1.09E+00	-1.06E+00	1.65E-02
VAL	18	H	131	VAL	18	O	604	5.99E-01	-3.47E-01	-3.59E-01	-3.35E-01	1.21E-02
VAL	18	H	131	PHE	19	N	617	4.75E-01	-5.43E-01	-5.78E-01	-5.07E-01	3.51E-02
PHE	19	N	140	LEU	17	C	584	6.42E-01	-3.57E-01	-3.70E-01	-3.44E-01	1.32E-02
PHE	19	N	140	VAL	18	C	603	5.89E-01	-3.34E-01	-3.38E-01	-3.29E-01	4.18E-03
PHE	19	N	140	PHE	19	C	619	6.17E-01	-3.71E-01	-3.81E-01	-3.60E-01	1.06E-02
PHE	19	N	140	PHE	19	H	628	3.94E-01	-4.61E-01	-4.67E-01	-4.54E-01	6.40E-03
PHE	19	C	142	LEU	17	O	585	7.09E-01	-4.22E-01	-4.35E-01	-4.08E-01	1.36E-02
PHE	19	C	142	PHE	19	N	617	4.76E-01	-6.71E-01	-7.08E-01	-6.34E-01	3.70E-02
PHE	19	C	142	PHE	19	O	620	5.07E-01	-7.83E-01	-8.09E-01	-7.57E-01	2.57E-02

PHE	19	C	142	PHE	20	N	637	5.47E-01	-4.81E-01	-4.93E-01	-4.70E-01	1.12E-02
PHE	19	C	142	PHE	20	O	640	5.39E-01	-6.85E-01	-7.22E-01	-6.48E-01	3.70E-02
PHE	19	O	143	VAL	18	C	603	5.91E-01	-4.54E-01	-4.77E-01	-4.32E-01	2.24E-02
PHE	19	O	143	PHE	19	C	619	4.96E-01	-8.28E-01	-8.54E-01	-8.02E-01	2.61E-02
PHE	19	O	143	PHE	19	H	628	4.15E-01	-5.55E-01	-6.00E-01	-5.09E-01	4.51E-02
PHE	19	O	143	PHE	20	C	639	6.14E-01	-5.12E-01	-5.37E-01	-4.88E-01	2.41E-02
PHE	20	N	160	PHE	19	C	619	4.67E-01	-7.02E-01	-7.41E-01	-6.64E-01	3.87E-02
PHE	20	N	160	PHE	20	C	639	5.67E-01	-4.45E-01	-4.56E-01	-4.34E-01	1.11E-02
PHE	20	C	162	PHE	19	N	617	6.39E-01	-3.48E-01	-3.76E-01	-3.20E-01	2.77E-02
PHE	20	C	162	PHE	19	O	620	5.16E-01	-7.74E-01	-8.86E-01	-6.61E-01	1.12E-01
PHE	20	C	162	PHE	20	N	637	5.47E-01	-4.83E-01	-4.99E-01	-4.68E-01	1.58E-02
PHE	20	C	162	PHE	20	O	640	3.73E-01	-1.71E+00	-1.73E+00	-1.68E+00	2.68E-02
PHE	20	C	162	ALA	21	N	657	5.90E-01	-4.44E-01	-4.49E-01	-4.40E-01	4.53E-03
PHE	20	C	162	ALA	21	O	660	5.92E-01	-6.05E-01	-6.15E-01	-5.95E-01	1.03E-02
PHE	20	C	162	GLU	22	N	667	6.56E-01	-3.72E-01	-3.77E-01	-3.66E-01	5.45E-03
PHE	20	C	162	ASN	27	ND2	735	9.07E-01	-3.87E-01	-4.11E-01	-3.62E-01	2.47E-02
PHE	20	O	163	PHE	19	C	619	6.41E-01	-4.69E-01	-4.95E-01	-4.43E-01	2.59E-02
PHE	20	O	163	PHE	20	C	639	6.16E-01	-5.08E-01	-5.12E-01	-5.03E-01	4.55E-03
PHE	20	O	163	ALA	21	C	659	7.00E-01	-4.07E-01	-4.11E-01	-4.04E-01	3.54E-03
PHE	20	HA	172	PHE	20	O	640	2.71E-01	-7.77E-01	-8.27E-01	-7.27E-01	4.97E-02
ALA	21	N	180	PHE	19	C	619	5.21E-01	-5.89E-01	-6.24E-01	-5.55E-01	3.42E-02
ALA	21	N	180	PHE	20	C	639	4.19E-01	-1.00E+00	-1.02E+00	-9.83E-01	1.74E-02
ALA	21	N	180	ALA	21	C	659	4.79E-01	-7.46E-01	-7.57E-01	-7.36E-01	1.05E-02
ALA	21	C	182	PHE	19	O	620	7.13E-01	-3.95E-01	-4.17E-01	-3.73E-01	2.21E-02
ALA	21	C	182	PHE	20	O	640	4.83E-01	-9.15E-01	-9.38E-01	-8.91E-01	2.37E-02
ALA	21	C	182	ALA	21	N	657	6.28E-01	-4.04E-01	-4.09E-01	-4.00E-01	4.10E-03
ALA	21	C	182	ALA	21	O	660	4.99E-01	-9.28E-01	-9.42E-01	-9.13E-01	1.45E-02
ALA	21	C	182	GLU	22	N	667	4.89E-01	-7.41E-01	-7.54E-01	-7.28E-01	1.30E-02
ALA	21	C	182	GLU	22	O	670	6.83E-01	-5.01E-01	-5.08E-01	-4.94E-01	6.61E-03
ALA	21	C	182	GLU	22	OE1	674	7.06E-01	-6.68E-01	-7.50E-01	-5.86E-01	8.19E-02
ALA	21	C	182	GLU	22	OE2	675	7.60E-01	-5.73E-01	-6.09E-01	-5.36E-01	3.64E-02
ALA	21	C	182	ASP	23	N	682	5.94E-01	-6.28E-01	-6.47E-01	-6.10E-01	1.85E-02
ALA	21	O	183	PHE	19	C	619	7.79E-01	-3.52E-01	-3.64E-01	-3.40E-01	1.19E-02
ALA	21	O	183	PHE	20	C	639	6.03E-01	-5.81E-01	-5.94E-01	-5.67E-01	1.37E-02
ALA	21	O	183	ALA	21	C	659	5.29E-01	-8.10E-01	-8.25E-01	-7.95E-01	1.51E-02
ALA	21	O	183	GLU	22	C	669	5.93E-01	-5.17E-01	-5.33E-01	-5.02E-01	1.53E-02
ALA	21	O	183	GLU	22	CD	673	7.73E-01	-5.03E-01	-5.40E-01	-4.65E-01	3.76E-02
ALA	21	O	183	GLU	22	H	676	5.94E-01	-3.37E-01	-3.46E-01	-3.27E-01	9.26E-03

ALA	21	O	183	ASP	23	CG	687	9.59E-01	-3.39E-01	-3.45E-01	-3.32E-01	6.64E-03
ALA	21	O	183	ASP	23	H	690	5.19E-01	-4.76E-01	-5.01E-01	-4.51E-01	2.51E-02
ALA	21	O	183	VAL	24	H	701	6.46E-01	-4.06E-01	-4.24E-01	-3.87E-01	1.85E-02
ALA	21	CB	184	PHE	20	C	639	4.54E-01	-4.63E-01	-4.76E-01	-4.50E-01	1.29E-02
ALA	21	CB	184	ALA	21	C	659	3.75E-01	-7.93E-01	-8.06E-01	-7.79E-01	1.33E-02
ALA	21	CB	184	GLU	22	H	676	3.67E-01	-4.52E-01	-4.71E-01	-4.33E-01	1.91E-02
ALA	21	H	185	PHE	19	O	620	4.10E-01	-7.28E-01	-8.33E-01	-6.22E-01	1.06E-01
ALA	21	H	185	PHE	20	N	637	4.46E-01	-4.20E-01	-4.34E-01	-4.06E-01	1.41E-02
ALA	21	H	185	PHE	20	O	640	1.96E-01	-5.87E+00	-6.09E+00	-5.65E+00	2.20E-01
ALA	21	H	185	ALA	21	N	657	3.97E-01	-6.16E-01	-6.26E-01	-6.07E-01	9.73E-03
ALA	21	H	185	ALA	21	O	660	4.09E-01	-7.86E-01	-8.05E-01	-7.68E-01	1.88E-02
ALA	21	H	185	GLU	22	N	667	4.75E-01	-4.11E-01	-4.21E-01	-4.01E-01	9.92E-03
GLU	22	N	190	PHE	20	C	639	6.92E-01	-3.34E-01	-3.38E-01	-3.30E-01	4.18E-03
GLU	22	N	190	ALA	21	C	659	5.46E-01	-5.73E-01	-5.79E-01	-5.68E-01	5.52E-03
GLU	22	N	190	GLU	22	C	669	5.71E-01	-4.28E-01	-4.35E-01	-4.20E-01	7.52E-03
GLU	22	N	190	GLU	22	CD	673	6.17E-01	-6.00E-01	-6.64E-01	-5.35E-01	6.46E-02
GLU	22	N	190	GLU	22	H	676	5.30E-01	-3.30E-01	-3.34E-01	-3.25E-01	4.33E-03
GLU	22	N	190	ASP	23	H	690	4.91E-01	-4.13E-01	-4.29E-01	-3.96E-01	1.65E-02
GLU	22	C	192	ALA	21	O	660	5.90E-01	-5.23E-01	-5.36E-01	-5.11E-01	1.26E-02
GLU	22	C	192	GLU	22	N	667	5.49E-01	-4.67E-01	-4.73E-01	-4.61E-01	6.12E-03
GLU	22	C	192	GLU	22	O	670	6.16E-01	-5.08E-01	-5.12E-01	-5.05E-01	3.29E-03
GLU	22	C	192	GLU	22	OE1	674	6.73E-01	-5.91E-01	-6.16E-01	-5.66E-01	2.51E-02
GLU	22	C	192	GLU	22	OE2	675	6.52E-01	-6.32E-01	-6.62E-01	-6.02E-01	2.98E-02
GLU	22	C	192	ASP	23	N	682	4.37E-01	-1.07E+00	-1.09E+00	-1.04E+00	2.90E-02
GLU	22	C	192	ASP	23	OD1	688	7.66E-01	-4.10E-01	-4.25E-01	-3.94E-01	1.50E-02
GLU	22	C	192	ASP	23	OD2	689	8.37E-01	-3.50E-01	-3.58E-01	-3.41E-01	8.31E-03
GLU	22	C	192	VAL	24	N	694	6.11E-01	-3.94E-01	-4.03E-01	-3.85E-01	9.44E-03
GLU	22	O	193	PHE	20	C	639	7.34E-01	-4.20E-01	-4.29E-01	-4.10E-01	9.61E-03
GLU	22	O	193	ALA	21	C	659	5.01E-01	-9.81E-01	-1.01E+00	-9.55E-01	2.55E-02
GLU	22	O	193	GLU	22	C	669	3.75E-01	-1.69E+00	-1.72E+00	-1.65E+00	3.42E-02
GLU	22	O	193	GLU	22	CD	673	5.61E-01	-1.02E+00	-1.05E+00	-9.79E-01	3.78E-02
GLU	22	O	193	GLU	22	H	676	5.06E-01	-5.15E-01	-5.23E-01	-5.06E-01	8.38E-03
GLU	22	O	193	GLU	22	HA	677	2.44E-01	-7.77E-01	-7.83E-01	-7.72E-01	5.49E-03
GLU	22	O	193	ASP	23	C	684	5.24E-01	-6.88E-01	-7.08E-01	-6.68E-01	2.01E-02
GLU	22	O	193	ASP	23	CG	687	6.63E-01	-6.94E-01	-7.16E-01	-6.72E-01	2.19E-02
GLU	22	O	193	ASP	23	H	690	2.29E-01	-4.72E+00	-5.22E+00	-4.22E+00	4.98E-01
GLU	22	O	193	VAL	24	C	696	7.12E-01	-3.62E-01	-3.68E-01	-3.56E-01	6.20E-03
GLU	22	O	193	VAL	24	CB	698	6.34E-01	-4.04E-01	-4.20E-01	-3.87E-01	1.63E-02

GLU	22	O	193	VAL	24	H	701	4.47E-01	-1.00E+00	-1.04E+00	-9.60E-01	4.11E-02
GLU	22	CD	196	PHE	20	O	640	9.51E-01	-3.23E-01	-3.40E-01	-3.07E-01	1.65E-02
GLU	22	CD	196	ALA	21	O	660	8.48E-01	-4.24E-01	-4.35E-01	-4.13E-01	1.07E-02
GLU	22	CD	196	GLU	22	N	667	6.92E-01	-4.68E-01	-4.81E-01	-4.55E-01	1.34E-02
GLU	22	CD	196	GLU	22	O	670	8.10E-01	-4.90E-01	-5.03E-01	-4.77E-01	1.29E-02
GLU	22	CD	196	GLU	22	OE1	674	4.95E-01	-1.91E+00	-2.09E+00	-1.73E+00	1.78E-01
GLU	22	CD	196	GLU	22	OE2	675	4.81E-01	-2.03E+00	-2.14E+00	-1.92E+00	1.08E-01
GLU	22	CD	196	ASP	23	N	682	6.84E-01	-6.33E-01	-6.64E-01	-6.03E-01	3.05E-02
GLU	22	OE1	197	ALA	21	C	659	8.47E-01	-4.79E-01	-5.30E-01	-4.28E-01	5.08E-02
GLU	22	OE1	197	GLU	22	C	669	7.52E-01	-4.79E-01	-4.96E-01	-4.62E-01	1.70E-02
GLU	22	OE1	197	GLU	22	CD	673	5.15E-01	-1.74E+00	-1.89E+00	-1.58E+00	1.59E-01
GLU	22	OE1	197	ASP	23	H	690	6.58E-01	-4.25E-01	-4.57E-01	-3.92E-01	3.22E-02
GLU	22	OE2	198	ALA	21	C	659	8.55E-01	-4.64E-01	-4.82E-01	-4.45E-01	1.83E-02
GLU	22	OE2	198	GLU	22	C	669	7.60E-01	-4.69E-01	-4.87E-01	-4.51E-01	1.77E-02
GLU	22	OE2	198	GLU	22	CD	673	5.15E-01	-1.72E+00	-1.80E+00	-1.64E+00	8.23E-02
GLU	22	OE2	198	ASP	23	H	690	6.71E-01	-4.11E-01	-4.47E-01	-3.74E-01	3.63E-02
GLU	22	H	199	ALA	21	O	660	5.87E-01	-3.46E-01	-3.54E-01	-3.37E-01	8.74E-03
GLU	22	H	199	GLU	22	N	667	4.95E-01	-3.88E-01	-3.93E-01	-3.83E-01	4.94E-03
GLU	22	H	199	GLU	22	OE1	674	5.72E-01	-5.55E-01	-6.17E-01	-4.93E-01	6.19E-02
GLU	22	H	199	GLU	22	OE2	675	6.28E-01	-4.51E-01	-4.95E-01	-4.07E-01	4.43E-02
GLU	22	H	199	ASP	23	N	682	6.08E-01	-3.22E-01	-3.30E-01	-3.14E-01	7.93E-03
ASP	23	N	205	ALA	21	C	659	7.24E-01	-4.20E-01	-4.26E-01	-4.15E-01	5.64E-03
ASP	23	N	205	GLU	22	C	669	5.75E-01	-5.56E-01	-5.62E-01	-5.51E-01	5.31E-03
ASP	23	N	205	GLU	22	CD	673	7.10E-01	-5.87E-01	-6.03E-01	-5.70E-01	1.61E-02
ASP	23	N	205	ASP	23	C	684	6.52E-01	-4.01E-01	-4.08E-01	-3.95E-01	6.52E-03
ASP	23	N	205	ASP	23	CG	687	7.45E-01	-5.21E-01	-5.31E-01	-5.12E-01	9.58E-03
ASP	23	N	205	ASP	23	H	690	3.91E-01	-9.64E-01	-9.77E-01	-9.51E-01	1.30E-02
ASP	23	N	205	VAL	24	H	701	5.30E-01	-6.24E-01	-6.44E-01	-6.04E-01	2.02E-02
ASP	23	C	207	ALA	21	O	660	6.65E-01	-3.84E-01	-3.92E-01	-3.77E-01	7.55E-03
ASP	23	C	207	GLU	22	O	670	6.34E-01	-4.52E-01	-4.60E-01	-4.43E-01	8.27E-03
ASP	23	C	207	GLU	22	OE1	674	8.81E-01	-3.45E-01	-3.66E-01	-3.23E-01	2.16E-02
ASP	23	C	207	GLU	22	OE2	675	8.21E-01	-3.87E-01	-4.08E-01	-3.67E-01	2.07E-02
ASP	23	C	207	ASP	23	N	682	4.24E-01	-1.08E+00	-1.12E+00	-1.05E+00	3.51E-02
ASP	23	C	207	ASP	23	O	685	6.09E-01	-4.16E-01	-4.19E-01	-4.13E-01	2.90E-03
ASP	23	C	207	ASP	23	OD1	688	5.87E-01	-6.59E-01	-6.90E-01	-6.27E-01	3.18E-02
ASP	23	C	207	ASP	23	OD2	689	7.24E-01	-4.28E-01	-4.43E-01	-4.14E-01	1.47E-02
ASP	23	C	207	VAL	24	N	694	4.21E-01	-8.86E-01	-9.09E-01	-8.63E-01	2.30E-02
ASP	23	C	207	VAL	24	O	697	4.55E-01	-6.59E-01	-6.83E-01	-6.35E-01	2.38E-02

ASP	23	O	208	ALA	21	C	659	6.58E-01	-4.57E-01	-4.73E-01	-4.41E-01	1.59E-02
ASP	23	O	208	GLU	22	C	669	4.44E-01	-9.21E-01	-9.68E-01	-8.74E-01	4.72E-02
ASP	23	O	208	GLU	22	CD	673	7.64E-01	-4.59E-01	-4.73E-01	-4.45E-01	1.41E-02
ASP	23	O	208	ASP	23	C	684	3.65E-01	-1.44E+00	-1.47E+00	-1.41E+00	3.14E-02
ASP	23	O	208	ASP	23	CG	687	5.22E-01	-9.87E-01	-1.01E+00	-9.59E-01	2.78E-02
ASP	23	O	208	ASP	23	H	690	2.78E-01	-2.27E+00	-2.53E+00	-2.01E+00	2.58E-01
ASP	23	O	208	ASP	23	HA	691	2.54E-01	-7.48E-01	-7.81E-01	-7.15E-01	3.30E-02
ASP	23	O	208	VAL	24	C	696	4.41E-01	-8.90E-01	-9.29E-01	-8.52E-01	3.81E-02
ASP	23	O	208	VAL	24	CB	698	4.56E-01	-7.30E-01	-7.89E-01	-6.72E-01	5.85E-02
ASP	23	O	208	VAL	24	H	701	2.06E-01	-7.59E+00	-8.34E+00	-6.85E+00	7.46E-01
ASP	23	O	208	GLY	25	C	712	6.95E-01	-4.17E-01	-4.26E-01	-4.08E-01	8.75E-03
ASP	23	CG	210	ALA	21	O	660	8.48E-01	-4.12E-01	-4.19E-01	-4.06E-01	6.84E-03
ASP	23	CG	210	GLU	22	N	667	8.08E-01	-3.42E-01	-3.50E-01	-3.34E-01	7.98E-03
ASP	23	CG	210	GLU	22	O	670	6.93E-01	-6.36E-01	-6.50E-01	-6.23E-01	1.35E-02
ASP	23	CG	210	GLU	22	OE1	674	8.48E-01	-6.32E-01	-7.22E-01	-5.43E-01	8.95E-02
ASP	23	CG	210	GLU	22	OE2	675	7.36E-01	-8.08E-01	-8.88E-01	-7.29E-01	7.99E-02
ASP	23	CG	210	ASP	23	N	682	4.75E-01	-1.37E+00	-1.42E+00	-1.32E+00	5.36E-02
ASP	23	CG	210	ASP	23	O	685	6.52E-01	-6.06E-01	-6.18E-01	-5.94E-01	1.19E-02
ASP	23	CG	210	ASP	23	OD1	688	4.75E-01	-1.82E+00	-1.97E+00	-1.67E+00	1.50E-01
ASP	23	CG	210	ASP	23	OD2	689	5.58E-01	-1.25E+00	-1.35E+00	-1.15E+00	1.01E-01
ASP	23	CG	210	VAL	24	N	694	5.38E-01	-8.29E-01	-8.63E-01	-7.94E-01	3.47E-02
ASP	23	CG	210	VAL	24	O	697	6.08E-01	-5.70E-01	-6.02E-01	-5.39E-01	3.17E-02
ASP	23	CG	210	GLY	25	N	710	7.49E-01	-3.46E-01	-3.59E-01	-3.34E-01	1.24E-02
ASP	23	CG	210	GLY	25	O	713	8.60E-01	-3.70E-01	-3.84E-01	-3.57E-01	1.35E-02
ASP	23	OD1	211	ALA	21	C	659	9.43E-01	-3.50E-01	-3.61E-01	-3.39E-01	1.09E-02
ASP	23	OD1	211	GLU	22	C	669	6.73E-01	-5.28E-01	-5.64E-01	-4.93E-01	3.56E-02
ASP	23	OD1	211	GLU	22	CD	673	8.74E-01	-5.34E-01	-5.63E-01	-5.05E-01	2.90E-02
ASP	23	OD1	211	ASP	23	C	684	5.63E-01	-7.31E-01	-8.09E-01	-6.54E-01	7.73E-02
ASP	23	OD1	211	ASP	23	CG	687	5.33E-01	-1.41E+00	-1.61E+00	-1.20E+00	2.04E-01
ASP	23	OD1	211	ASP	23	H	690	4.91E-01	-7.24E-01	-8.00E-01	-6.48E-01	7.58E-02
ASP	23	OD1	211	VAL	24	C	696	6.10E-01	-6.19E-01	-6.76E-01	-5.62E-01	5.72E-02
ASP	23	OD1	211	VAL	24	CB	698	7.30E-01	-3.79E-01	-4.02E-01	-3.55E-01	2.31E-02
ASP	23	OD1	211	VAL	24	H	701	4.55E-01	-1.21E+00	-1.37E+00	-1.06E+00	1.57E-01
ASP	23	OD1	211	GLY	25	C	712	7.93E-01	-4.79E-01	-5.07E-01	-4.50E-01	2.89E-02
ASP	23	OD2	212	ALA	21	C	659	9.26E-01	-3.61E-01	-3.72E-01	-3.50E-01	1.11E-02
ASP	23	OD2	212	GLU	22	C	669	6.28E-01	-6.08E-01	-6.49E-01	-5.66E-01	4.14E-02
ASP	23	OD2	212	GLU	22	CD	673	7.47E-01	-7.05E-01	-7.57E-01	-6.54E-01	5.15E-02
ASP	23	OD2	212	ASP	23	C	684	5.68E-01	-7.19E-01	-7.88E-01	-6.49E-01	6.97E-02

ASP	23	OD2	212	ASP	23	CG	687	4.45E-01	-2.17E+00	-2.43E+00	-1.91E+00	2.62E-01
ASP	23	OD2	212	ASP	23	H	690	4.66E-01	-8.21E-01	-8.99E-01	-7.43E-01	7.81E-02
ASP	23	OD2	212	VAL	24	C	696	7.16E-01	-4.45E-01	-4.73E-01	-4.18E-01	2.78E-02
ASP	23	OD2	212	VAL	24	H	701	5.27E-01	-8.47E-01	-9.29E-01	-7.65E-01	8.22E-02
ASP	23	OD2	212	GLY	25	C	712	9.33E-01	-3.64E-01	-3.78E-01	-3.49E-01	1.45E-02
ASP	23	H	213	ASP	23	N	682	5.90E-01	-3.58E-01	-3.61E-01	-3.55E-01	3.17E-03
VAL	24	N	217	GLU	22	C	669	6.42E-01	-3.55E-01	-3.69E-01	-3.42E-01	1.34E-02
VAL	24	N	217	ASP	23	C	684	5.72E-01	-4.28E-01	-4.33E-01	-4.22E-01	5.44E-03
VAL	24	N	217	ASP	23	CG	687	7.26E-01	-4.41E-01	-4.49E-01	-4.33E-01	8.23E-03
VAL	24	N	217	ASP	23	H	690	4.71E-01	-4.87E-01	-5.15E-01	-4.58E-01	2.83E-02
VAL	24	N	217	VAL	24	C	696	5.35E-01	-5.01E-01	-5.10E-01	-4.93E-01	8.65E-03
VAL	24	N	217	VAL	24	CB	698	5.61E-01	-3.98E-01	-4.14E-01	-3.82E-01	1.59E-02
VAL	24	N	217	VAL	24	H	701	3.84E-01	-1.12E+00	-1.14E+00	-1.11E+00	1.43E-02
VAL	24	N	217	GLY	25	C	712	7.10E-01	-3.59E-01	-3.65E-01	-3.53E-01	5.94E-03
VAL	24	C	219	ASP	23	N	682	7.18E-01	-3.36E-01	-3.45E-01	-3.27E-01	9.22E-03
VAL	24	C	219	ASP	23	OD1	688	7.47E-01	-4.08E-01	-4.19E-01	-3.96E-01	1.18E-02
VAL	24	C	219	VAL	24	N	694	5.51E-01	-4.68E-01	-4.76E-01	-4.60E-01	8.05E-03
VAL	24	C	219	VAL	24	O	697	3.62E-01	-1.20E+00	-1.21E+00	-1.19E+00	1.01E-02
VAL	24	C	219	GLY	25	N	710	5.76E-01	-3.52E-01	-3.56E-01	-3.48E-01	3.71E-03
VAL	24	C	219	GLY	25	O	713	4.82E-01	-7.24E-01	-7.51E-01	-6.97E-01	2.70E-02
VAL	24	C	219	SER	26	N	717	6.20E-01	-4.36E-01	-4.51E-01	-4.21E-01	1.50E-02
VAL	24	O	220	VAL	24	C	696	6.05E-01	-3.43E-01	-3.44E-01	-3.41E-01	1.50E-03
VAL	24	O	220	VAL	24	H	701	5.80E-01	-3.70E-01	-3.77E-01	-3.63E-01	7.02E-03
VAL	24	O	220	GLY	25	C	712	6.45E-01	-3.91E-01	-3.96E-01	-3.86E-01	5.33E-03
VAL	24	CB	221	ASP	23	N	682	6.53E-01	-3.59E-01	-3.77E-01	-3.40E-01	1.86E-02
VAL	24	CB	221	VAL	24	N	694	5.21E-01	-4.72E-01	-4.94E-01	-4.50E-01	2.21E-02
VAL	24	CB	221	VAL	24	O	697	4.13E-01	-7.54E-01	-8.21E-01	-6.88E-01	6.65E-02
VAL	24	CB	221	GLY	25	O	713	6.04E-01	-3.85E-01	-4.04E-01	-3.66E-01	1.89E-02
VAL	24	CB	221	SER	26	N	717	6.62E-01	-3.38E-01	-3.52E-01	-3.23E-01	1.46E-02
VAL	24	CB	221	ASN	27	ND2	735	7.42E-01	-3.95E-01	-4.24E-01	-3.66E-01	2.91E-02
VAL	24	H	224	ASP	23	N	682	6.16E-01	-4.49E-01	-4.68E-01	-4.31E-01	1.83E-02
VAL	24	H	224	ASP	23	OD1	688	7.62E-01	-3.87E-01	-3.99E-01	-3.75E-01	1.18E-02
VAL	24	H	224	VAL	24	N	694	5.82E-01	-4.08E-01	-4.11E-01	-4.04E-01	3.73E-03
VAL	24	H	224	VAL	24	O	697	5.28E-01	-4.57E-01	-4.67E-01	-4.47E-01	9.99E-03
GLY	25	N	233	VAL	24	C	696	4.13E-01	-7.80E-01	-7.88E-01	-7.72E-01	8.24E-03
GLY	25	N	233	VAL	24	CB	698	5.54E-01	-3.40E-01	-3.51E-01	-3.29E-01	1.06E-02
GLY	25	N	233	VAL	24	H	701	4.71E-01	-5.54E-01	-5.76E-01	-5.31E-01	2.25E-02
GLY	25	N	233	GLY	25	C	712	4.25E-01	-9.44E-01	-9.73E-01	-9.15E-01	2.90E-02

GLY	25	C	235	ASP	23	OD1	688	9.39E-01	-3.60E-01	-3.69E-01	-3.50E-01	9.28E-03
GLY	25	C	235	VAL	24	N	694	7.72E-01	-3.07E-01	-3.11E-01	-3.03E-01	4.03E-03
GLY	25	C	235	VAL	24	O	697	4.98E-01	-6.94E-01	-7.06E-01	-6.82E-01	1.24E-02
GLY	25	C	235	GLY	25	N	710	6.43E-01	-3.63E-01	-3.67E-01	-3.59E-01	3.65E-03
GLY	25	C	235	GLY	25	O	713	3.71E-01	-1.83E+00	-1.88E+00	-1.78E+00	5.33E-02
GLY	25	C	235	SER	26	N	717	5.60E-01	-7.07E-01	-7.18E-01	-6.95E-01	1.20E-02
GLY	25	C	235	SER	26	O	720	7.67E-01	-4.01E-01	-4.08E-01	-3.94E-01	7.02E-03
GLY	25	C	235	SER	26	OG	722	6.70E-01	-5.94E-01	-6.82E-01	-5.05E-01	8.87E-02
GLY	25	C	235	ASN	27	N	728	6.51E-01	-4.07E-01	-4.19E-01	-3.96E-01	1.15E-02
GLY	25	C	235	ASN	27	O	731	8.00E-01	-3.36E-01	-3.41E-01	-3.30E-01	5.45E-03
GLY	25	C	235	ASN	27	ND2	735	9.72E-01	-3.65E-01	-3.75E-01	-3.55E-01	1.03E-02
GLY	25	O	236	GLY	25	C	712	5.98E-01	-5.75E-01	-5.81E-01	-5.68E-01	6.06E-03
GLY	25	H	237	VAL	24	N	694	4.51E-01	-4.28E-01	-4.43E-01	-4.13E-01	1.52E-02
GLY	25	H	237	VAL	24	O	697	1.92E-01	-4.30E+00	-4.48E+00	-4.13E+00	1.74E-01
GLY	25	H	237	GLY	25	N	710	3.85E-01	-5.35E-01	-5.43E-01	-5.27E-01	7.72E-03
GLY	25	H	237	GLY	25	O	713	3.08E-01	-1.36E+00	-1.46E+00	-1.25E+00	1.06E-01
GLY	25	H	237	SER	26	N	717	4.40E-01	-5.52E-01	-5.85E-01	-5.18E-01	3.36E-02
SER	26	N	240	VAL	24	C	696	5.84E-01	-4.95E-01	-5.07E-01	-4.83E-01	1.16E-02
SER	26	N	240	VAL	24	H	701	7.17E-01	-3.21E-01	-3.29E-01	-3.13E-01	8.27E-03
SER	26	N	240	GLY	25	C	712	4.41E-01	-1.24E+00	-1.28E+00	-1.21E+00	3.35E-02
SER	26	N	240	SER	26	C	719	5.44E-01	-6.27E-01	-6.42E-01	-6.11E-01	1.54E-02
SER	26	N	240	SER	26	H	723	5.85E-01	-3.80E-01	-3.84E-01	-3.77E-01	3.27E-03
SER	26	N	240	SER	26	HA	724	3.40E-01	-6.08E-01	-6.33E-01	-5.82E-01	2.53E-02
SER	26	N	240	SER	26	HG	727	6.09E-01	-4.76E-01	-5.63E-01	-3.88E-01	8.78E-02
SER	26	N	240	ASN	27	C	730	7.14E-01	-4.54E-01	-4.62E-01	-4.45E-01	8.50E-03
SER	26	N	240	ASN	27	CG	733	8.14E-01	-3.39E-01	-3.50E-01	-3.27E-01	1.16E-02
SER	26	N	240	ASN	27	H	736	4.43E-01	-5.42E-01	-5.68E-01	-5.16E-01	2.61E-02
SER	26	C	242	VAL	24	O	697	6.09E-01	-3.66E-01	-3.79E-01	-3.53E-01	1.31E-02
SER	26	C	242	GLY	25	O	713	4.98E-01	-7.27E-01	-7.68E-01	-6.86E-01	4.10E-02
SER	26	C	242	SER	26	N	717	5.54E-01	-6.02E-01	-6.14E-01	-5.89E-01	1.22E-02
SER	26	C	242	SER	26	O	720	6.11E-01	-5.20E-01	-5.24E-01	-5.16E-01	3.96E-03
SER	26	C	242	SER	26	OG	722	5.76E-01	-7.11E-01	-8.81E-01	-5.41E-01	1.70E-01
SER	26	C	242	ASN	27	N	728	4.18E-01	-9.43E-01	-9.58E-01	-9.27E-01	1.52E-02
SER	26	C	242	ASN	27	O	731	4.64E-01	-8.85E-01	-9.24E-01	-8.47E-01	3.89E-02
SER	26	C	242	ASN	27	OD1	734	7.34E-01	-3.29E-01	-3.37E-01	-3.21E-01	8.12E-03
SER	26	C	242	ASN	27	ND2	735	6.52E-01	-6.21E-01	-6.64E-01	-5.78E-01	4.32E-02
SER	26	C	242	LYS	28	N	742	6.65E-01	-3.29E-01	-3.35E-01	-3.22E-01	6.52E-03
SER	26	O	243	VAL	24	C	696	6.23E-01	-4.65E-01	-4.80E-01	-4.49E-01	1.56E-02

SER	26	O	243	VAL	24	CB	698	6.44E-01	-3.84E-01	-4.02E-01	-3.66E-01	1.78E-02
SER	26	O	243	GLY	25	C	712	4.92E-01	-1.03E+00	-1.07E+00	-9.83E-01	4.51E-02
SER	26	O	243	SER	26	CA	718	3.43E-01	-5.28E-01	-5.55E-01	-5.01E-01	2.69E-02
SER	26	O	243	SER	26	C	719	3.68E-01	-1.79E+00	-1.82E+00	-1.75E+00	3.18E-02
SER	26	O	243	SER	26	CB	721	3.97E-01	-4.49E-01	-4.94E-01	-4.03E-01	4.53E-02
SER	26	O	243	SER	26	H	723	5.36E-01	-4.97E-01	-5.06E-01	-4.87E-01	9.23E-03
SER	26	O	243	SER	26	HA	724	2.53E-01	-1.52E+00	-1.61E+00	-1.42E+00	9.43E-02
SER	26	O	243	SER	26	HG	727	5.41E-01	-6.63E-01	-7.84E-01	-5.41E-01	1.21E-01
SER	26	O	243	ASN	27	C	730	4.35E-01	-1.47E+00	-1.52E+00	-1.42E+00	5.39E-02
SER	26	O	243	ASN	27	CG	733	5.47E-01	-8.09E-01	-8.59E-01	-7.59E-01	4.97E-02
SER	26	O	243	ASN	27	H	736	1.96E-01	-5.84E+00	-6.21E+00	-5.46E+00	3.78E-01
SER	26	O	243	ASN	27	HD21	740	5.37E-01	-5.22E-01	-5.73E-01	-4.71E-01	5.09E-02
SER	26	O	243	LYS	28	C	744	7.81E-01	-4.84E-01	-4.94E-01	-4.75E-01	9.28E-03
SER	26	OG	245	GLY	25	C	712	6.25E-01	-7.23E-01	-8.77E-01	-5.68E-01	1.55E-01
SER	26	OG	245	SER	26	C	719	6.14E-01	-6.10E-01	-7.28E-01	-4.93E-01	1.17E-01
SER	26	OG	245	SER	26	HG	727	5.87E-01	-7.04E-01	-9.31E-01	-4.78E-01	2.27E-01
SER	26	OG	245	ASN	27	C	730	6.80E-01	-6.03E-01	-6.64E-01	-5.43E-01	6.04E-02
SER	26	OG	245	ASN	27	H	736	5.04E-01	-4.94E-01	-5.82E-01	-4.06E-01	8.81E-02
SER	26	H	246	VAL	24	O	697	4.01E-01	-7.07E-01	-7.43E-01	-6.71E-01	3.61E-02
SER	26	H	246	GLY	25	N	710	5.26E-01	-3.34E-01	-3.44E-01	-3.24E-01	1.03E-02
SER	26	H	246	GLY	25	O	713	2.67E-01	-2.86E+00	-3.30E+00	-2.43E+00	4.32E-01
SER	26	H	246	SER	26	N	717	3.96E-01	-9.73E-01	-9.96E-01	-9.50E-01	2.33E-02
SER	26	H	246	SER	26	O	720	5.72E-01	-4.29E-01	-4.39E-01	-4.19E-01	1.02E-02
SER	26	H	246	SER	26	OG	722	5.17E-01	-6.35E-01	-7.66E-01	-5.03E-01	1.32E-01
SER	26	H	246	ASN	27	N	728	4.52E-01	-5.53E-01	-5.83E-01	-5.24E-01	2.92E-02
SER	26	HG	250	GLY	25	O	713	5.39E-01	-8.10E-01	-1.20E+00	-4.19E-01	3.91E-01
SER	26	HG	250	SER	26	OG	722	5.43E-01	-1.13E+00	-2.00E+00	-2.67E-01	8.67E-01
ASN	27	N	251	GLY	25	C	712	6.93E-01	-3.60E-01	-3.69E-01	-3.50E-01	9.31E-03
ASN	27	N	251	SER	26	C	719	5.83E-01	-4.27E-01	-4.33E-01	-4.20E-01	6.55E-03
ASN	27	N	251	ASN	27	C	730	5.60E-01	-5.97E-01	-6.14E-01	-5.80E-01	1.72E-02
ASN	27	N	251	ASN	27	CG	733	6.25E-01	-4.47E-01	-4.68E-01	-4.27E-01	2.07E-02
ASN	27	N	251	ASN	27	H	736	3.91E-01	-5.90E-01	-6.00E-01	-5.80E-01	1.02E-02
ASN	27	C	253	GLY	25	O	713	8.17E-01	-3.34E-01	-3.42E-01	-3.26E-01	8.37E-03
ASN	27	C	253	SER	26	N	717	8.15E-01	-3.56E-01	-3.61E-01	-3.52E-01	4.39E-03
ASN	27	C	253	SER	26	O	720	7.55E-01	-4.38E-01	-4.41E-01	-4.35E-01	3.17E-03
ASN	27	C	253	SER	26	OG	722	7.61E-01	-5.00E-01	-5.85E-01	-4.15E-01	8.49E-02
ASN	27	C	253	ASN	27	N	728	5.40E-01	-6.47E-01	-6.59E-01	-6.35E-01	1.16E-02
ASN	27	C	253	ASN	27	O	731	3.80E-01	-1.89E+00	-1.98E+00	-1.79E+00	9.49E-02

ASN	27	C	253	ASN	27	OD1	734	6.67E-01	-5.05E-01	-5.21E-01	-4.88E-01	1.67E-02
ASN	27	C	253	ASN	27	ND2	735	5.33E-01	-1.29E+00	-1.46E+00	-1.12E+00	1.67E-01
ASN	27	C	253	LYS	28	N	742	5.91E-01	-5.36E-01	-5.46E-01	-5.27E-01	9.47E-03
ASN	27	C	253	LYS	28	O	745	8.20E-01	-3.67E-01	-3.75E-01	-3.60E-01	7.57E-03
ASN	27	C	253	GLY	29	N	764	6.86E-01	-3.40E-01	-3.53E-01	-3.27E-01	1.30E-02
ASN	27	O	254	SER	26	C	719	7.54E-01	-3.10E-01	-3.14E-01	-3.06E-01	3.53E-03
ASN	27	O	254	ASN	27	C	730	5.99E-01	-6.27E-01	-6.34E-01	-6.20E-01	7.01E-03
ASN	27	O	254	ASN	27	CG	733	6.88E-01	-4.50E-01	-4.77E-01	-4.24E-01	2.66E-02
ASN	27	O	254	LYS	28	C	744	8.02E-01	-4.17E-01	-4.25E-01	-4.10E-01	7.58E-03
ASN	27	CG	256	SER	26	O	720	8.39E-01	-3.46E-01	-3.62E-01	-3.30E-01	1.58E-02
ASN	27	CG	256	ASN	27	N	728	6.20E-01	-4.57E-01	-4.95E-01	-4.19E-01	3.78E-02
ASN	27	CG	256	ASN	27	O	731	5.25E-01	-8.29E-01	-9.68E-01	-6.90E-01	1.39E-01
ASN	27	CG	256	ASN	27	OD1	734	6.09E-01	-5.78E-01	-6.08E-01	-5.47E-01	3.06E-02
ASN	27	CG	256	ASN	27	ND2	735	4.23E-01	-2.08E+00	-2.30E+00	-1.85E+00	2.22E-01
ASN	27	CG	256	LYS	28	N	742	6.82E-01	-3.83E-01	-4.15E-01	-3.50E-01	3.24E-02
ASN	27	CG	256	ALA	30	O	774	7.29E-01	-4.29E-01	-4.65E-01	-3.93E-01	3.60E-02
ASN	27	OD1	257	SER	26	C	719	6.97E-01	-3.63E-01	-3.80E-01	-3.47E-01	1.64E-02
ASN	27	OD1	257	ASN	27	C	730	5.08E-01	-9.20E-01	-9.75E-01	-8.66E-01	5.45E-02
ASN	27	OD1	257	ASN	27	CG	733	3.91E-01	-1.67E+00	-1.72E+00	-1.61E+00	5.82E-02
ASN	27	OD1	257	ASN	27	H	736	5.20E-01	-3.61E-01	-3.88E-01	-3.34E-01	2.70E-02
ASN	27	OD1	257	ASN	27	HD21	740	2.16E-01	-7.14E+00	-8.53E+00	-5.75E+00	1.39E+00
ASN	27	OD1	257	ASN	27	HD22	741	3.57E-01	-1.39E+00	-1.59E+00	-1.19E+00	1.97E-01
ASN	27	OD1	257	LYS	28	C	744	6.65E-01	-5.99E-01	-6.24E-01	-5.73E-01	2.56E-02
ASN	27	OD1	257	GLY	29	C	766	6.96E-01	-4.40E-01	-4.66E-01	-4.14E-01	2.61E-02
ASN	27	OD1	257	ALA	30	C	773	7.08E-01	-4.19E-01	-4.50E-01	-3.87E-01	3.15E-02
ASN	27	OD1	257	ALA	30	H	776	5.58E-01	-3.55E-01	-3.86E-01	-3.23E-01	3.16E-02
ASN	27	ND2	258	SER	26	C	719	8.73E-01	-3.62E-01	-3.88E-01	-3.36E-01	2.64E-02
ASN	27	ND2	258	ASN	27	C	730	6.95E-01	-7.26E-01	-8.74E-01	-5.78E-01	1.48E-01
ASN	27	ND2	258	ASN	27	CG	733	5.97E-01	-8.97E-01	-9.48E-01	-8.46E-01	5.10E-02
ASN	27	ND2	258	ASN	27	HD21	740	4.26E-01	-1.28E+00	-1.45E+00	-1.12E+00	1.67E-01
ASN	27	ND2	258	ASN	27	HD22	741	5.43E-01	-6.78E-01	-7.29E-01	-6.27E-01	5.08E-02
ASN	27	ND2	258	LYS	28	C	744	8.36E-01	-6.08E-01	-7.23E-01	-4.93E-01	1.15E-01
ASN	27	ND2	258	GLY	29	C	766	8.47E-01	-4.81E-01	-5.82E-01	-3.80E-01	1.01E-01
ASN	27	ND2	258	ALA	30	C	773	8.12E-01	-4.96E-01	-5.73E-01	-4.19E-01	7.71E-02
ASN	27	HD21	263	ASN	27	ND2	735	6.05E-01	-5.31E-01	-5.61E-01	-5.02E-01	2.91E-02
ASN	27	HD22	264	ASN	27	ND2	735	4.97E-01	-8.25E-01	-8.68E-01	-7.82E-01	4.29E-02
LYS	28	N	265	SER	26	C	719	6.34E-01	-3.63E-01	-3.70E-01	-3.56E-01	6.90E-03
LYS	28	N	265	ASN	27	C	730	4.05E-01	-1.32E+00	-1.35E+00	-1.29E+00	2.94E-02

LYS	28	N	265	ASN	27	CG	733	4.97E-01	-7.78E-01	-8.63E-01	-6.93E-01	8.52E-02
LYS	28	N	265	ASN	27	H	736	4.61E-01	-3.96E-01	-4.13E-01	-3.79E-01	1.69E-02
LYS	28	N	265	LYS	28	C	744	5.81E-01	-6.55E-01	-6.78E-01	-6.32E-01	2.30E-02
LYS	28	N	265	GLY	29	C	766	7.40E-01	-3.23E-01	-3.33E-01	-3.12E-01	1.07E-02
LYS	28	N	265	GLY	29	H	768	4.68E-01	-3.81E-01	-4.06E-01	-3.56E-01	2.50E-02
LYS	28	C	267	SER	26	O	720	8.52E-01	-4.17E-01	-4.26E-01	-4.08E-01	8.63E-03
LYS	28	C	267	SER	26	OG	722	9.19E-01	-4.15E-01	-4.57E-01	-3.72E-01	4.22E-02
LYS	28	C	267	ASN	27	N	728	6.74E-01	-4.75E-01	-4.91E-01	-4.59E-01	1.59E-02
LYS	28	C	267	ASN	27	O	731	4.07E-01	-1.86E+00	-1.98E+00	-1.75E+00	1.18E-01
LYS	28	C	267	ASN	27	OD1	734	5.89E-01	-7.79E-01	-8.41E-01	-7.17E-01	6.20E-02
LYS	28	C	267	ASN	27	ND2	735	4.70E-01	-2.21E+00	-2.63E+00	-1.79E+00	4.18E-01
LYS	28	C	267	LYS	28	N	742	5.10E-01	-8.82E-01	-9.12E-01	-8.52E-01	3.00E-02
LYS	28	C	267	LYS	28	O	745	6.07E-01	-7.68E-01	-7.72E-01	-7.65E-01	3.44E-03
LYS	28	C	267	GLY	29	N	764	4.12E-01	-1.28E+00	-1.30E+00	-1.25E+00	2.40E-02
LYS	28	C	267	GLY	29	O	767	6.99E-01	-5.22E-01	-5.35E-01	-5.10E-01	1.23E-02
LYS	28	C	267	ALA	30	N	771	5.72E-01	-6.32E-01	-6.56E-01	-6.07E-01	2.46E-02
LYS	28	C	267	ALA	30	O	774	6.93E-01	-5.79E-01	-5.93E-01	-5.66E-01	1.36E-02
LYS	28	C	267	ILE	31	N	781	8.57E-01	-3.20E-01	-3.24E-01	-3.16E-01	4.02E-03
LYS	28	O	268	SER	26	C	719	7.39E-01	-3.47E-01	-3.57E-01	-3.37E-01	9.94E-03
LYS	28	O	268	ASN	27	C	730	4.11E-01	-1.67E+00	-1.78E+00	-1.55E+00	1.13E-01
LYS	28	O	268	ASN	27	CG	733	4.53E-01	-1.28E+00	-1.47E+00	-1.10E+00	1.88E-01
LYS	28	O	268	LYS	28	C	744	3.66E-01	-2.63E+00	-2.67E+00	-2.60E+00	3.32E-02
LYS	28	O	268	LYS	28	H	751	4.97E-01	-4.20E-01	-4.40E-01	-3.99E-01	2.04E-02
LYS	28	O	268	LYS	28	HA	752	2.55E-01	-1.31E+00	-1.39E+00	-1.22E+00	8.32E-02
LYS	28	O	268	GLY	29	C	766	4.79E-01	-1.06E+00	-1.11E+00	-1.02E+00	4.67E-02
LYS	28	O	268	GLY	29	H	768	1.93E-01	-5.90E+00	-6.26E+00	-5.53E+00	3.67E-01
LYS	28	O	268	ALA	30	C	773	6.67E-01	-4.98E-01	-5.11E-01	-4.85E-01	1.25E-02
LYS	28	O	268	ALA	30	H	776	4.08E-01	-8.08E-01	-8.73E-01	-7.44E-01	6.44E-02
LYS	28	H	274	ASN	27	N	728	4.37E-01	-4.40E-01	-4.64E-01	-4.15E-01	2.43E-02
LYS	28	H	274	ASN	27	O	731	2.20E-01	-3.89E+00	-4.64E+00	-3.14E+00	7.49E-01
LYS	28	H	274	ASN	27	OD1	734	4.87E-01	-4.14E-01	-4.44E-01	-3.84E-01	3.02E-02
LYS	28	H	274	ASN	27	ND2	735	3.76E-01	-1.38E+00	-1.65E+00	-1.11E+00	2.70E-01
LYS	28	H	274	LYS	28	N	742	4.04E-01	-5.43E-01	-5.68E-01	-5.18E-01	2.49E-02
GLY	29	N	287	ASN	27	C	730	6.11E-01	-4.30E-01	-4.45E-01	-4.15E-01	1.46E-02
GLY	29	N	287	LYS	28	C	744	5.79E-01	-5.66E-01	-5.72E-01	-5.60E-01	6.20E-03
GLY	29	N	287	GLY	29	C	766	6.24E-01	-3.86E-01	-3.93E-01	-3.79E-01	7.08E-03
GLY	29	N	287	GLY	29	H	768	3.85E-01	-5.33E-01	-5.40E-01	-5.26E-01	6.95E-03
GLY	29	N	287	ALA	30	H	776	4.99E-01	-3.24E-01	-3.38E-01	-3.10E-01	1.40E-02

GLY	29	C	289	ASN	27	O	731	6.34E-01	-5.26E-01	-5.50E-01	-5.02E-01	2.39E-02
GLY	29	C	289	ASN	27	OD1	734	6.07E-01	-5.90E-01	-6.53E-01	-5.27E-01	6.33E-02
GLY	29	C	289	ASN	27	ND2	735	4.70E-01	-1.79E+00	-2.22E+00	-1.37E+00	4.22E-01
GLY	29	C	289	LYS	28	N	742	6.70E-01	-3.90E-01	-4.03E-01	-3.76E-01	1.36E-02
GLY	29	C	289	LYS	28	O	745	6.67E-01	-5.08E-01	-5.22E-01	-4.94E-01	1.38E-02
GLY	29	C	289	GLY	29	N	764	4.54E-01	-8.04E-01	-8.41E-01	-7.68E-01	3.66E-02
GLY	29	C	289	GLY	29	O	767	6.06E-01	-5.59E-01	-5.63E-01	-5.55E-01	4.06E-03
GLY	29	C	289	ALA	30	N	771	4.10E-01	-1.12E+00	-1.14E+00	-1.10E+00	2.06E-02
GLY	29	C	289	ALA	30	O	774	4.23E-01	-1.43E+00	-1.53E+00	-1.33E+00	9.98E-02
GLY	29	C	289	ILE	31	N	781	6.00E-01	-5.06E-01	-5.17E-01	-4.95E-01	1.10E-02
GLY	29	C	289	ILE	31	O	784	8.75E-01	-3.41E-01	-3.47E-01	-3.36E-01	5.12E-03
GLY	29	O	290	ASN	27	C	730	6.20E-01	-5.70E-01	-6.04E-01	-5.35E-01	3.49E-02
GLY	29	O	290	ASN	27	CG	733	5.05E-01	-8.95E-01	-1.06E+00	-7.32E-01	1.63E-01
GLY	29	O	290	LYS	28	C	744	4.87E-01	-1.15E+00	-1.21E+00	-1.09E+00	5.96E-02
GLY	29	O	290	GLY	29	C	766	3.65E-01	-1.91E+00	-1.97E+00	-1.86E+00	5.37E-02
GLY	29	O	290	GLY	29	H	768	3.20E-01	-1.22E+00	-1.33E+00	-1.11E+00	1.07E-01
GLY	29	O	290	GLY	29	HA2	769	2.82E-01	-6.22E-01	-7.00E-01	-5.45E-01	7.75E-02
GLY	29	O	290	ALA	30	C	773	4.00E-01	-1.48E+00	-1.54E+00	-1.42E+00	6.26E-02
GLY	29	O	290	ALA	30	H	776	1.90E-01	-6.39E+00	-6.65E+00	-6.14E+00	2.53E-01
GLY	29	O	290	ILE	31	C	783	7.28E-01	-3.79E-01	-3.87E-01	-3.71E-01	7.86E-03
GLY	29	O	290	ILE	31	H	789	5.71E-01	-3.60E-01	-3.71E-01	-3.49E-01	1.11E-02
ALA	30	N	294	LYS	28	C	744	6.88E-01	-4.29E-01	-4.42E-01	-4.16E-01	1.33E-02
ALA	30	N	294	GLY	29	C	766	5.81E-01	-4.87E-01	-4.95E-01	-4.79E-01	7.92E-03
ALA	30	N	294	ALA	30	C	773	5.09E-01	-6.44E-01	-6.55E-01	-6.34E-01	1.04E-02
ALA	30	N	294	ALA	30	H	776	3.89E-01	-6.52E-01	-6.66E-01	-6.38E-01	1.38E-02
ALA	30	C	296	ASN	27	ND2	735	6.53E-01	-7.56E-01	-8.45E-01	-6.66E-01	8.94E-02
ALA	30	C	296	GLY	29	O	767	8.11E-01	-3.13E-01	-3.18E-01	-3.07E-01	5.13E-03
ALA	30	C	296	ALA	30	N	771	5.89E-01	-4.64E-01	-4.76E-01	-4.53E-01	1.19E-02
ALA	30	C	296	ALA	30	O	774	3.80E-01	-1.85E+00	-1.94E+00	-1.77E+00	8.29E-02
ALA	30	C	296	ILE	31	N	781	5.72E-01	-5.52E-01	-5.66E-01	-5.37E-01	1.44E-02
ALA	30	C	296	ILE	31	O	784	7.76E-01	-4.12E-01	-4.22E-01	-4.02E-01	1.03E-02
ALA	30	C	296	ILE	32	N	800	6.68E-01	-3.98E-01	-4.10E-01	-3.86E-01	1.20E-02
ALA	30	C	296	ILE	32	O	803	7.86E-01	-4.03E-01	-4.13E-01	-3.92E-01	1.10E-02
ALA	30	O	297	LYS	28	C	744	9.70E-01	-3.24E-01	-3.30E-01	-3.18E-01	6.21E-03
ALA	30	O	297	GLY	29	C	766	8.16E-01	-3.43E-01	-3.48E-01	-3.39E-01	4.82E-03
ALA	30	O	297	ALA	30	C	773	6.17E-01	-5.76E-01	-5.80E-01	-5.71E-01	4.68E-03
ALA	30	O	297	ILE	31	C	783	7.75E-01	-3.68E-01	-3.76E-01	-3.60E-01	7.89E-03
ALA	30	CB	298	ALA	30	C	773	4.84E-01	-4.33E-01	-5.02E-01	-3.63E-01	6.97E-02

ALA	30	H	299	ALA	30	O	774	5.07E-01	-4.62E-01	-4.76E-01	-4.48E-01	1.39E-02
ALA	30	HA	300	ALA	30	O	774	2.43E-01	-1.39E+00	-1.41E+00	-1.38E+00	1.57E-02
ILE	31	N	304	GLY	29	C	766	7.08E-01	-3.63E-01	-3.77E-01	-3.48E-01	1.44E-02
ILE	31	N	304	ALA	30	C	773	4.50E-01	-9.77E-01	-1.04E+00	-9.16E-01	6.08E-02
ILE	31	N	304	ALA	30	H	776	5.23E-01	-3.50E-01	-3.70E-01	-3.30E-01	2.00E-02
ILE	31	N	304	ILE	31	C	783	5.56E-01	-5.86E-01	-6.01E-01	-5.71E-01	1.51E-02
ILE	31	N	304	ILE	31	HA	790	3.55E-01	-5.51E-01	-5.72E-01	-5.30E-01	2.10E-02
ILE	31	N	304	ILE	32	C	802	7.08E-01	-3.55E-01	-3.66E-01	-3.43E-01	1.16E-02
ILE	31	N	304	ILE	32	H	808	4.63E-01	-5.23E-01	-5.47E-01	-4.99E-01	2.37E-02
ILE	31	C	306	ALA	30	O	774	4.85E-01	-1.00E+00	-1.10E+00	-9.08E-01	9.71E-02
ILE	31	C	306	ILE	31	N	781	5.61E-01	-5.76E-01	-5.91E-01	-5.60E-01	1.55E-02
ILE	31	C	306	ILE	31	O	784	6.19E-01	-6.37E-01	-6.40E-01	-6.34E-01	2.73E-03
ILE	31	C	306	ILE	32	N	800	4.28E-01	-1.10E+00	-1.12E+00	-1.07E+00	2.13E-02
ILE	31	C	306	ILE	32	O	803	4.43E-01	-1.39E+00	-1.46E+00	-1.31E+00	7.71E-02
ILE	31	C	306	GLY	33	N	819	6.45E-01	-3.54E-01	-3.67E-01	-3.41E-01	1.31E-02
ILE	31	O	307	GLY	29	C	766	8.19E-01	-3.82E-01	-3.96E-01	-3.67E-01	1.46E-02
ILE	31	O	307	ALA	30	C	773	4.87E-01	-1.10E+00	-1.17E+00	-1.03E+00	6.95E-02
ILE	31	O	307	ILE	31	C	783	3.77E-01	-2.10E+00	-2.14E+00	-2.07E+00	3.31E-02
ILE	31	O	307	ILE	31	H	789	5.48E-01	-4.81E-01	-4.90E-01	-4.72E-01	8.82E-03
ILE	31	O	307	ILE	31	HA	790	2.58E-01	-1.89E+00	-1.99E+00	-1.78E+00	1.05E-01
ILE	31	O	307	ILE	32	C	802	4.35E-01	-1.45E+00	-1.56E+00	-1.35E+00	1.09E-01
ILE	31	O	307	ILE	32	H	808	2.12E-01	-6.42E+00	-6.95E+00	-5.90E+00	5.27E-01
ILE	31	O	307	GLY	33	C	821	7.70E-01	-4.27E-01	-4.46E-01	-4.08E-01	1.88E-02
ILE	31	H	312	ALA	30	N	771	5.09E-01	-3.75E-01	-4.02E-01	-3.48E-01	2.69E-02
ILE	31	H	312	ALA	30	O	774	2.51E-01	-3.86E+00	-4.88E+00	-2.85E+00	1.01E+00
ILE	31	H	312	ILE	31	N	781	3.98E-01	-7.66E-01	-7.76E-01	-7.57E-01	9.23E-03
ILE	31	H	312	ILE	31	O	784	5.80E-01	-4.24E-01	-4.36E-01	-4.12E-01	1.19E-02
ILE	31	H	312	ILE	32	N	800	4.76E-01	-4.88E-01	-5.12E-01	-4.63E-01	2.43E-02
ILE	31	H	312	ILE	32	O	803	6.18E-01	-3.72E-01	-3.91E-01	-3.52E-01	1.93E-02
ILE	32	N	323	ALA	30	C	773	6.97E-01	-3.66E-01	-3.80E-01	-3.52E-01	1.38E-02
ILE	32	N	323	ILE	31	C	783	5.87E-01	-5.20E-01	-5.24E-01	-5.15E-01	4.64E-03
ILE	32	N	323	ILE	32	C	802	5.37E-01	-6.34E-01	-6.49E-01	-6.20E-01	1.48E-02
ILE	32	N	323	ILE	32	H	808	3.96E-01	-7.73E-01	-7.85E-01	-7.62E-01	1.14E-02
ILE	32	C	325	ALA	30	O	774	8.19E-01	-3.36E-01	-3.49E-01	-3.22E-01	1.38E-02
ILE	32	C	325	ILE	31	O	784	7.92E-01	-3.96E-01	-4.02E-01	-3.89E-01	6.67E-03
ILE	32	C	325	ILE	32	N	800	5.71E-01	-5.53E-01	-5.69E-01	-5.36E-01	1.67E-02
ILE	32	C	325	ILE	32	O	803	3.76E-01	-2.11E+00	-2.16E+00	-2.05E+00	5.22E-02
ILE	32	C	325	GLY	33	N	819	5.88E-01	-4.29E-01	-4.32E-01	-4.26E-01	2.98E-03

ILE	32	C	325	GLY	33	O	822	7.90E-01	-3.51E-01	-4.37E-01	-2.64E-01	8.66E-02
ILE	32	O	326	ILE	31	C	783	7.92E-01	-3.96E-01	-4.03E-01	-3.89E-01	7.12E-03
ILE	32	O	326	ILE	32	C	802	6.18E-01	-6.41E-01	-6.50E-01	-6.31E-01	9.58E-03
ILE	32	O	326	ILE	32	H	808	5.96E-01	-4.00E-01	-4.12E-01	-3.88E-01	1.23E-02
ILE	32	O	326	GLY	33	C	821	8.16E-01	-3.89E-01	-4.20E-01	-3.57E-01	3.17E-02
ILE	32	H	331	ILE	32	O	803	5.26E-01	-5.28E-01	-5.40E-01	-5.17E-01	1.15E-02
ILE	32	HA	332	ILE	32	N	800	3.75E-01	-4.76E-01	-4.95E-01	-4.56E-01	1.92E-02
ILE	32	HA	332	ILE	32	O	803	2.52E-01	-2.00E+00	-2.15E+00	-1.85E+00	1.48E-01
GLY	33	N	342	ILE	31	C	783	6.76E-01	-3.22E-01	-3.31E-01	-3.13E-01	8.92E-03
GLY	33	N	342	ILE	32	C	802	4.32E-01	-8.89E-01	-9.31E-01	-8.48E-01	4.16E-02
GLY	33	N	342	ILE	32	H	808	4.93E-01	-3.72E-01	-3.90E-01	-3.54E-01	1.78E-02
GLY	33	N	342	GLY	33	C	821	5.95E-01	-4.37E-01	-4.96E-01	-3.79E-01	5.83E-02
GLY	33	C	344	ILE	31	O	784	8.82E-01	-3.37E-01	-3.46E-01	-3.28E-01	9.32E-03
GLY	33	C	344	ILE	32	N	800	7.01E-01	-3.70E-01	-3.80E-01	-3.59E-01	1.06E-02
GLY	33	C	344	ILE	32	O	803	4.25E-01	-1.57E+00	-1.67E+00	-1.47E+00	9.99E-02
GLY	33	C	344	GLY	33	N	819	5.20E-01	-5.84E-01	-6.26E-01	-5.42E-01	4.17E-02
GLY	33	C	344	GLY	33	O	822	5.92E-01	-6.67E-01	-9.16E-01	-4.18E-01	2.49E-01
GLY	33	C	344	LEU	34	N	826	4.93E-01	-6.32E-01	-6.84E-01	-5.79E-01	5.25E-02
GLY	33	C	344	LEU	34	O	829	7.90E-01	-3.74E-01	-4.19E-01	-3.29E-01	4.49E-02
GLY	33	O	345	ILE	32	C	802	4.43E-01	-1.24E+00	-1.43E+00	-1.05E+00	1.89E-01
GLY	33	O	345	GLY	33	C	821	4.11E-01	-1.51E+00	-1.72E+00	-1.30E+00	2.12E-01
GLY	33	O	345	LEU	34	C	828	6.15E-01	-5.45E-01	-5.92E-01	-4.99E-01	4.65E-02
GLY	33	H	346	ILE	32	N	800	4.78E-01	-3.75E-01	-3.99E-01	-3.51E-01	2.38E-02
GLY	33	H	346	ILE	32	O	803	2.18E-01	-4.65E+00	-5.36E+00	-3.94E+00	7.10E-01
GLY	33	H	346	GLY	33	N	819	4.01E-01	-4.79E-01	-4.89E-01	-4.70E-01	9.63E-03
LEU	34	N	349	ILE	32	C	802	6.15E-01	-3.74E-01	-4.02E-01	-3.45E-01	2.85E-02
LEU	34	N	349	GLY	33	C	821	5.36E-01	-5.31E-01	-6.28E-01	-4.34E-01	9.71E-02
LEU	34	C	351	ILE	32	O	803	6.24E-01	-6.39E-01	-6.88E-01	-5.90E-01	4.91E-02
LEU	34	C	351	GLY	33	O	822	5.58E-01	-6.98E-01	-8.53E-01	-5.43E-01	1.55E-01
LEU	34	C	351	LEU	34	N	826	4.04E-01	-1.07E+00	-1.22E+00	-9.18E-01	1.50E-01
LEU	34	C	351	LEU	34	O	829	5.93E-01	-6.77E-01	-8.46E-01	-5.09E-01	1.68E-01
LEU	34	C	351	MET	35	N	845	4.42E-01	-9.40E-01	-1.06E+00	-8.22E-01	1.18E-01
LEU	34	C	351	MET	35	O	848	6.47E-01	-6.75E-01	-9.30E-01	-4.19E-01	2.55E-01
LEU	34	C	351	VAL	36	N	862	6.06E-01	-4.95E-01	-5.35E-01	-4.54E-01	4.06E-02
LEU	34	O	352	ILE	32	C	802	6.80E-01	-4.88E-01	-5.39E-01	-4.36E-01	5.13E-02
LEU	34	O	352	GLY	33	C	821	4.28E-01	-1.51E+00	-1.74E+00	-1.28E+00	2.27E-01
LEU	34	O	352	LEU	34	C	828	3.95E-01	-1.82E+00	-2.08E+00	-1.56E+00	2.63E-01
LEU	34	O	352	MET	35	C	847	5.04E-01	-1.07E+00	-1.27E+00	-8.67E-01	2.00E-01

LEU	34	O	352	VAL	36	H	869	4.87E-01	-9.11E-01	-1.16E+00	-6.65E-01	2.46E-01
MET	35	N	368	GLY	33	C	821	5.46E-01	-5.61E-01	-6.36E-01	-4.85E-01	7.55E-02
MET	35	N	368	LEU	34	C	828	5.60E-01	-5.42E-01	-6.72E-01	-4.11E-01	1.30E-01
MET	35	N	368	MET	35	C	847	6.00E-01	-4.70E-01	-5.29E-01	-4.11E-01	5.87E-02
MET	35	C	370	ILE	32	O	803	8.06E-01	-4.10E-01	-4.41E-01	-3.79E-01	3.11E-02
MET	35	C	370	GLY	33	O	822	7.18E-01	-4.27E-01	-4.96E-01	-3.58E-01	6.89E-02
MET	35	C	370	LEU	34	N	826	6.01E-01	-4.16E-01	-4.54E-01	-3.79E-01	3.74E-02
MET	35	C	370	LEU	34	O	829	6.54E-01	-7.68E-01	-1.30E+00	-2.36E-01	5.32E-01
MET	35	C	370	MET	35	N	845	4.81E-01	-8.01E-01	-9.29E-01	-6.73E-01	1.28E-01
MET	35	C	370	MET	35	O	848	5.33E-01	-1.11E+00	-1.57E+00	-6.47E-01	4.61E-01
MET	35	C	370	VAL	36	N	862	4.63E-01	-1.06E+00	-1.27E+00	-8.44E-01	2.13E-01
MET	35	C	370	GLY	37	N	878	6.44E-01	-3.74E-01	-3.89E-01	-3.60E-01	1.44E-02
MET	35	O	371	GLY	33	C	821	6.65E-01	-5.27E-01	-5.80E-01	-4.73E-01	5.38E-02
MET	35	O	371	LEU	34	C	828	5.61E-01	-9.25E-01	-1.18E+00	-6.67E-01	2.58E-01
MET	35	O	371	MET	35	C	847	4.39E-01	-1.71E+00	-2.18E+00	-1.25E+00	4.65E-01
MET	35	O	371	MET	35	H	853	4.20E-01	-1.10E+00	-1.53E+00	-6.73E-01	4.30E-01
VAL	36	N	385	LEU	34	C	828	6.46E-01	-4.37E-01	-4.90E-01	-3.83E-01	5.36E-02
VAL	36	N	385	MET	35	C	847	5.28E-01	-7.77E-01	-9.88E-01	-5.67E-01	2.11E-01
VAL	36	N	385	VAL	36	C	864	5.38E-01	-4.96E-01	-5.19E-01	-4.72E-01	2.36E-02
VAL	36	N	385	VAL	36	CB	866	5.46E-01	-4.24E-01	-4.45E-01	-4.03E-01	2.10E-02
VAL	36	N	385	VAL	36	H	869	4.46E-01	-8.94E-01	-1.11E+00	-6.82E-01	2.12E-01
VAL	36	C	387	VAL	36	N	862	5.50E-01	-4.73E-01	-4.99E-01	-4.47E-01	2.59E-02
VAL	36	C	387	VAL	36	O	865	4.37E-01	-9.25E-01	-1.17E+00	-6.75E-01	2.50E-01
VAL	36	C	387	GLY	37	N	878	5.29E-01	-4.77E-01	-6.04E-01	-3.49E-01	1.28E-01
VAL	36	O	388	VAL	36	C	864	5.32E-01	-5.91E-01	-8.36E-01	-3.46E-01	2.45E-01
VAL	36	O	388	VAL	36	H	869	5.66E-01	-3.97E-01	-4.36E-01	-3.59E-01	3.86E-02
VAL	36	CB	389	VAL	36	N	862	5.46E-01	-4.25E-01	-4.49E-01	-4.01E-01	2.40E-02
VAL	36	H	392	VAL	36	N	862	5.23E-01	-6.11E-01	-8.10E-01	-4.11E-01	1.99E-01
VAL	36	H	392	VAL	36	O	865	5.46E-01	-4.31E-01	-4.69E-01	-3.92E-01	3.86E-02
GLY	37	N	401	MET	35	C	847	6.63E-01	-3.54E-01	-3.67E-01	-3.40E-01	1.37E-02
GLY	37	N	401	VAL	36	C	864	4.64E-01	-6.41E-01	-7.64E-01	-5.18E-01	1.23E-01
GLY	37	N	401	GLY	37	C	880	5.62E-01	-4.91E-01	-5.32E-01	-4.49E-01	4.15E-02
GLY	37	C	403	MET	35	O	848	8.29E-01	-3.46E-01	-3.78E-01	-3.14E-01	3.19E-02
GLY	37	C	403	GLY	37	N	878	5.32E-01	-5.64E-01	-6.42E-01	-4.85E-01	7.83E-02
GLY	37	C	403	GLY	37	O	881	5.54E-01	-8.15E-01	-1.13E+00	-5.03E-01	3.13E-01
GLY	37	C	403	GLY	38	N	885	4.55E-01	-8.44E-01	-9.75E-01	-7.13E-01	1.31E-01
GLY	37	C	403	GLY	38	O	888	4.30E-01	-1.27E+00	-1.38E+00	-1.16E+00	1.10E-01
GLY	37	C	403	VAL	39	N	892	6.13E-01	-4.87E-01	-5.22E-01	-4.52E-01	3.49E-02

GLY	37	O	404	GLY	37	C	880	4.33E-01	-1.43E+00	-1.74E+00	-1.12E+00	3.10E-01
GLY	37	O	404	GLY	38	C	887	4.57E-01	-1.19E+00	-1.43E+00	-9.49E-01	2.41E-01
GLY	38	N	408	GLY	37	C	880	5.40E-01	-5.47E-01	-6.25E-01	-4.69E-01	7.77E-02
GLY	38	N	408	GLY	38	C	887	4.96E-01	-6.89E-01	-8.39E-01	-5.40E-01	1.49E-01
GLY	38	C	410	GLY	37	O	881	7.27E-01	-4.10E-01	-4.81E-01	-3.38E-01	7.18E-02
GLY	38	C	410	GLY	38	N	885	5.93E-01	-4.40E-01	-4.82E-01	-3.99E-01	4.14E-02
GLY	38	C	410	GLY	38	O	888	3.71E-01	-1.84E+00	-1.92E+00	-1.76E+00	7.92E-02
GLY	38	C	410	VAL	39	N	892	5.72E-01	-5.61E-01	-5.74E-01	-5.47E-01	1.36E-02
GLY	38	C	410	VAL	40	N	908	6.56E-01	-4.20E-01	-4.33E-01	-4.07E-01	1.31E-02
GLY	38	O	411	GLY	37	C	880	7.82E-01	-3.40E-01	-3.51E-01	-3.29E-01	1.06E-02
GLY	38	O	411	GLY	38	C	887	6.09E-01	-5.54E-01	-5.60E-01	-5.47E-01	6.35E-03
GLY	38	O	411	VAL	40	H	915	6.59E-01	-3.58E-01	-3.74E-01	-3.41E-01	1.66E-02
GLY	38	H	412	GLY	38	O	888	4.61E-01	-9.63E-01	-1.81E+00	-1.13E-01	8.51E-01
GLY	38	HA2	413	GLY	38	O	888	2.60E-01	-7.87E-01	-8.81E-01	-6.93E-01	9.42E-02
VAL	39	N	415	GLY	37	C	880	6.65E-01	-4.13E-01	-4.43E-01	-3.83E-01	2.97E-02
VAL	39	N	415	GLY	38	C	887	4.32E-01	-1.11E+00	-1.19E+00	-1.02E+00	8.68E-02
VAL	39	N	415	VAL	39	C	894	5.54E-01	-4.64E-01	-4.75E-01	-4.53E-01	1.10E-02
VAL	39	N	415	VAL	39	CB	896	5.18E-01	-4.95E-01	-5.70E-01	-4.20E-01	7.48E-02
VAL	39	N	415	VAL	39	H	899	5.88E-01	-4.00E-01	-4.07E-01	-3.92E-01	7.36E-03
VAL	39	N	415	VAL	40	H	915	4.52E-01	-7.38E-01	-7.66E-01	-7.10E-01	2.76E-02
VAL	39	C	417	GLY	38	O	888	4.53E-01	-8.68E-01	-9.74E-01	-7.62E-01	1.06E-01
VAL	39	C	417	VAL	39	N	892	5.43E-01	-4.86E-01	-5.04E-01	-4.67E-01	1.86E-02
VAL	39	C	417	VAL	39	O	895	6.09E-01	-3.39E-01	-3.41E-01	-3.36E-01	2.63E-03
VAL	39	C	417	VAL	40	N	908	4.15E-01	-9.31E-01	-9.60E-01	-9.03E-01	2.86E-02
VAL	39	C	417	VAL	40	O	911	4.45E-01	-7.05E-01	-7.43E-01	-6.67E-01	3.83E-02
VAL	39	O	418	GLY	38	C	887	4.61E-01	-8.46E-01	-9.17E-01	-7.75E-01	7.10E-02
VAL	39	O	418	VAL	39	C	894	3.68E-01	-1.15E+00	-1.16E+00	-1.14E+00	1.31E-02
VAL	39	O	418	VAL	39	CB	896	4.21E-01	-7.57E-01	-9.08E-01	-6.06E-01	1.51E-01
VAL	39	O	418	VAL	39	H	899	5.34E-01	-4.46E-01	-4.59E-01	-4.33E-01	1.32E-02
VAL	39	O	418	VAL	40	C	910	4.29E-01	-7.72E-01	-8.17E-01	-7.27E-01	4.48E-02
VAL	39	O	418	VAL	40	CB	912	4.19E-01	-7.42E-01	-8.33E-01	-6.50E-01	9.16E-02
VAL	39	O	418	VAL	40	H	915	1.97E-01	-6.94E+00	-7.46E+00	-6.42E+00	5.18E-01
VAL	39	CB	419	GLY	38	O	888	4.73E-01	-7.35E-01	-8.84E-01	-5.85E-01	1.50E-01
VAL	39	CB	419	VAL	40	N	908	5.54E-01	-4.18E-01	-4.62E-01	-3.74E-01	4.43E-02
VAL	39	H	422	GLY	38	N	885	4.98E-01	-4.97E-01	-5.54E-01	-4.40E-01	5.70E-02
VAL	39	H	422	GLY	38	O	888	2.27E-01	-6.52E+00	-8.20E+00	-4.83E+00	1.69E+00
VAL	39	H	422	VAL	39	N	892	3.92E-01	-1.06E+00	-1.10E+00	-1.03E+00	3.54E-02
VAL	39	H	422	VAL	39	O	895	5.85E-01	-3.65E-01	-3.77E-01	-3.53E-01	1.21E-02

VAL	39	H	422	VAL	40	N	908	4.75E-01	-6.53E-01	-6.80E-01	-6.27E-01	2.64E-02
VAL	40	N	431	GLY	38	C	887	6.68E-01	-4.07E-01	-4.28E-01	-3.86E-01	2.13E-02
VAL	40	N	431	VAL	39	C	894	5.81E-01	-4.17E-01	-4.22E-01	-4.13E-01	4.35E-03
VAL	40	N	431	VAL	40	C	910	5.32E-01	-5.07E-01	-5.21E-01	-4.93E-01	1.40E-02
VAL	40	N	431	VAL	40	CB	912	5.40E-01	-4.36E-01	-4.62E-01	-4.11E-01	2.57E-02
VAL	40	N	431	VAL	40	H	915	3.88E-01	-1.09E+00	-1.10E+00	-1.08E+00	1.12E-02
VAL	40	C	433	VAL	40	N	908	5.58E-01	-4.57E-01	-4.69E-01	-4.44E-01	1.27E-02
VAL	40	C	433	VAL	40	O	911	3.65E-01	-1.18E+00	-1.20E+00	-1.16E+00	1.77E-02
VAL	40	C	433	ILE	41	N	924	5.81E-01	-4.18E-01	-4.22E-01	-4.14E-01	3.63E-03
VAL	40	C	433	ILE	41	O	927	7.90E-01	-3.12E-01	-3.16E-01	-3.08E-01	3.79E-03
VAL	40	O	434	VAL	40	C	910	6.05E-01	-3.44E-01	-3.47E-01	-3.40E-01	3.51E-03
VAL	40	O	434	VAL	40	H	915	5.85E-01	-3.64E-01	-3.74E-01	-3.53E-01	1.02E-02
VAL	40	CB	435	VAL	40	N	908	5.53E-01	-4.11E-01	-4.26E-01	-3.96E-01	1.50E-02
VAL	40	CB	435	VAL	40	O	911	4.42E-01	-6.34E-01	-6.70E-01	-5.97E-01	3.69E-02
VAL	40	H	438	GLY	38	O	888	6.39E-01	-3.84E-01	-4.12E-01	-3.55E-01	2.86E-02
VAL	40	H	438	VAL	40	N	908	5.84E-01	-4.05E-01	-4.09E-01	-4.01E-01	3.61E-03
VAL	40	H	438	VAL	40	O	911	5.26E-01	-4.63E-01	-4.77E-01	-4.49E-01	1.41E-02
ILE	41	N	447	VAL	39	C	894	6.59E-01	-3.20E-01	-3.30E-01	-3.10E-01	9.87E-03
ILE	41	N	447	VAL	40	C	910	4.12E-01	-9.50E-01	-9.74E-01	-9.25E-01	2.45E-02
ILE	41	N	447	VAL	40	CB	912	5.36E-01	-4.47E-01	-4.79E-01	-4.15E-01	3.20E-02
ILE	41	N	447	VAL	40	H	915	4.79E-01	-6.43E-01	-6.74E-01	-6.12E-01	3.12E-02
ILE	41	N	447	ILE	41	C	926	5.60E-01	-5.77E-01	-5.87E-01	-5.66E-01	1.03E-02
ILE	41	N	447	ILE	41	HA	933	3.75E-01	-4.75E-01	-4.94E-01	-4.56E-01	1.90E-02
ILE	41	N	447	ALA	42	C	945	7.10E-01	-3.54E-01	-3.67E-01	-3.41E-01	1.30E-02
ILE	41	N	447	ALA	42	H	949	4.50E-01	-5.02E-01	-5.25E-01	-4.79E-01	2.30E-02
ILE	41	C	449	VAL	40	N	908	7.09E-01	-3.53E-01	-3.63E-01	-3.42E-01	1.02E-02
ILE	41	C	449	VAL	40	O	911	4.20E-01	-1.04E+00	-1.10E+00	-9.79E-01	6.01E-02
ILE	41	C	449	ILE	41	N	924	5.29E-01	-6.56E-01	-6.73E-01	-6.38E-01	1.78E-02
ILE	41	C	449	ILE	41	O	927	6.07E-01	-6.65E-01	-6.71E-01	-6.58E-01	6.25E-03
ILE	41	C	449	ALA	42	N	943	4.10E-01	-1.10E+00	-1.12E+00	-1.08E+00	2.09E-02
ILE	41	C	449	ALA	42	O	946	5.91E-01	-6.77E-01	-8.24E-01	-5.30E-01	1.47E-01
ILE	41	C	449	ALA	42	CB	947	4.95E-01	-3.97E-01	-4.33E-01	-3.61E-01	3.59E-02
ILE	41	C	449	ALA	42	OXT	948	5.00E-01	-9.53E-01	-1.09E+00	-8.17E-01	1.36E-01
ILE	41	O	450	VAL	39	C	894	7.76E-01	-3.23E-01	-3.32E-01	-3.13E-01	9.11E-03
ILE	41	O	450	VAL	40	C	910	4.36E-01	-1.14E+00	-1.21E+00	-1.06E+00	7.20E-02
ILE	41	O	450	VAL	40	CB	912	5.88E-01	-5.02E-01	-5.48E-01	-4.56E-01	4.57E-02
ILE	41	O	450	VAL	40	H	915	6.38E-01	-4.65E-01	-4.82E-01	-4.47E-01	1.76E-02
ILE	41	O	450	ILE	41	C	926	3.70E-01	-2.21E+00	-2.25E+00	-2.16E+00	4.29E-02

ILE	41	O	450	ILE	41	H	932	5.26E-01	-5.28E-01	-5.47E-01	-5.10E-01	1.86E-02
ILE	41	O	450	ILE	41	HA	933	2.63E-01	-1.79E+00	-1.96E+00	-1.62E+00	1.70E-01
ILE	41	O	450	ALA	42	C	945	4.27E-01	-1.54E+00	-1.67E+00	-1.41E+00	1.29E-01
ILE	41	O	450	ALA	42	H	949	1.96E-01	-7.14E+00	-7.58E+00	-6.69E+00	4.44E-01
ILE	41	H	455	VAL	40	N	908	4.56E-01	-5.42E-01	-5.68E-01	-5.16E-01	2.59E-02
ILE	41	H	455	VAL	40	O	911	1.94E-01	-5.38E+00	-5.73E+00	-5.03E+00	3.49E-01
ILE	41	H	455	ILE	41	N	924	3.90E-01	-8.09E-01	-8.23E-01	-7.95E-01	1.40E-02
ILE	41	H	455	ILE	41	O	927	5.91E-01	-4.08E-01	-4.15E-01	-4.00E-01	7.48E-03
ILE	41	H	455	ALA	42	N	943	4.71E-01	-4.50E-01	-4.68E-01	-4.31E-01	1.84E-02
ALA	42	N	466	ILE	41	C	926	5.81E-01	-4.77E-01	-4.84E-01	-4.70E-01	7.23E-03
ALA	42	N	466	ALA	42	C	945	5.31E-01	-5.96E-01	-6.53E-01	-5.39E-01	5.71E-02
ALA	42	N	466	ALA	42	H	949	3.88E-01	-6.54E-01	-6.70E-01	-6.38E-01	1.57E-02
ALA	42	C	468	ILE	41	O	927	7.86E-01	-4.06E-01	-4.33E-01	-3.79E-01	2.68E-02
ALA	42	C	468	ALA	42	N	943	5.64E-01	-5.24E-01	-5.87E-01	-4.60E-01	6.32E-02
ALA	42	C	468	ALA	42	O	946	5.31E-01	-8.15E-01	-8.99E-01	-7.31E-01	8.43E-02
ALA	42	C	468	ALA	42	OXT	948	4.52E-01	-1.20E+00	-1.33E+00	-1.07E+00	1.30E-01
ALA	42	O	469	ILE	41	C	926	7.01E-01	-4.49E-01	-4.86E-01	-4.13E-01	3.65E-02
ALA	42	O	469	ALA	42	C	945	4.64E-01	-1.11E+00	-1.19E+00	-1.03E+00	7.62E-02
ALA	42	O	469	ALA	42	H	949	5.17E-01	-4.51E-01	-5.06E-01	-3.96E-01	5.50E-02
ALA	42	OXT	471	ILE	41	C	926	7.63E-01	-3.89E-01	-4.35E-01	-3.44E-01	4.57E-02
ALA	42	OXT	471	ALA	42	C	945	5.89E-01	-6.42E-01	-6.91E-01	-5.94E-01	4.84E-02

Supplementary Table 2b: Mapping results for A β 42's (PDB ID: 2MXU) short range (1:2) dominant atom-atom Lennard-Jones interactions across ensemble structures. Columns for each chain correspond to: residue abbreviation, residue number in peptide sequence, atom identity (IUPAC naming convention) and atom number in PDB file. Energy in kT , distance in nm . Mapping analysis began on the 11th residue for both isoforms because original structure data for A β 42 begins with the 11th residue.

Chain A				Chain B				Average Distance	Average L-J Values	Lower 95% Confidence Interval Bound	Upper 95% Confidence Interval Bound	Margin of Error
LYS	16	C	85	LEU	17	N	582	4.10E-01	-1.59E-01	-1.63E-01	-1.56E-01	3.45E-03
LYS	16	O	86	LYS	16	CA	561	3.51E-01	-2.33E-01	-2.42E-01	-2.24E-01	9.07E-03
LYS	16	O	86	LYS	16	C	562	3.68E-01	-2.11E-01	-2.14E-01	-2.08E-01	3.12E-03
LYS	16	O	86	LEU	17	CA	583	3.90E-01	-2.04E-01	-2.18E-01	-1.90E-01	1.38E-02
LYS	16	O	86	LEU	17	C	584	4.08E-01	-1.53E-01	-1.67E-01	-1.39E-01	1.38E-02
LYS	16	O	86	LEU	17	O	585	3.53E-01	-3.05E-01	-3.26E-01	-2.84E-01	2.11E-02
LEU	17	N	105	LEU	17	O	585	4.35E-01	-1.41E-01	-1.49E-01	-1.33E-01	7.98E-03

LEU	17	CA	106	LEU	17	O	585	3.50E-01	-2.28E-01	-2.38E-01	-2.17E-01	1.04E-02
LEU	17	C	107	LEU	17	O	585	3.65E-01	-2.14E-01	-2.16E-01	-2.13E-01	1.39E-03
VAL	18	N	124	LEU	17	C	584	4.11E-01	-1.59E-01	-1.65E-01	-1.52E-01	6.53E-03
VAL	18	CA	125	LEU	17	O	585	3.82E-01	-2.15E-01	-2.30E-01	-1.99E-01	1.56E-02
VAL	18	C	126	LEU	17	O	585	4.20E-01	-1.35E-01	-1.49E-01	-1.20E-01	1.45E-02
VAL	18	C	126	PHE	19	N	617	4.11E-01	-1.58E-01	-1.63E-01	-1.52E-01	5.56E-03
VAL	18	O	127	LEU	17	O	585	3.72E-01	-2.59E-01	-2.85E-01	-2.32E-01	2.65E-02
VAL	18	O	127	VAL	18	CA	602	3.63E-01	-2.34E-01	-2.43E-01	-2.25E-01	9.02E-03
VAL	18	O	127	VAL	18	C	603	3.73E-01	-2.06E-01	-2.09E-01	-2.03E-01	2.93E-03
VAL	18	O	127	PHE	19	CA	618	3.81E-01	-2.15E-01	-2.29E-01	-2.00E-01	1.43E-02
VAL	18	CB	128	LEU	17	O	585	3.95E-01	-1.91E-01	-2.17E-01	-1.65E-01	2.59E-02
PHE	19	CA	141	PHE	19	CB	621	3.94E-01	-1.69E-01	-1.73E-01	-1.64E-01	4.51E-03
PHE	20	CA	161	PHE	20	O	640	3.51E-01	-2.36E-01	-2.43E-01	-2.29E-01	7.12E-03
PHE	20	C	162	PHE	20	O	640	3.73E-01	-2.07E-01	-2.09E-01	-2.04E-01	2.45E-03
PHE	20	CB	164	PHE	20	O	640	3.80E-01	-2.10E-01	-2.39E-01	-1.82E-01	2.83E-02
ALA	21	N	180	PHE	20	C	639	4.19E-01	-1.47E-01	-1.51E-01	-1.43E-01	3.67E-03
ALA	21	CA	181	PHE	20	O	640	3.91E-01	-2.03E-01	-2.10E-01	-1.96E-01	6.54E-03
ALA	21	CB	184	PHE	20	O	640	3.65E-01	-2.40E-01	-2.45E-01	-2.34E-01	5.36E-03
ALA	21	CB	184	ALA	21	CA	658	3.85E-01	-1.76E-01	-1.77E-01	-1.75E-01	9.19E-04
ALA	21	CB	184	ALA	21	C	659	3.75E-01	-1.55E-01	-1.56E-01	-1.53E-01	1.31E-03
ALA	21	CB	184	ALA	21	O	660	4.30E-01	-1.35E-01	-1.41E-01	-1.29E-01	6.19E-03
ALA	21	CB	184	GLU	22	N	667	3.66E-01	-2.16E-01	-2.19E-01	-2.12E-01	3.41E-03
ALA	21	CB	184	GLU	22	CA	668	4.16E-01	-1.49E-01	-1.56E-01	-1.41E-01	7.19E-03
GLU	22	N	190	GLU	22	CA	668	4.53E-01	-1.17E-01	-1.21E-01	-1.12E-01	4.60E-03
GLU	22	C	192	GLU	22	CA	668	4.38E-01	-1.07E-01	-1.09E-01	-1.06E-01	1.58E-03
GLU	22	C	192	ASP	23	N	682	4.37E-01	-1.23E-01	-1.29E-01	-1.18E-01	5.56E-03
GLU	22	O	193	GLU	22	N	667	4.43E-01	-1.28E-01	-1.32E-01	-1.23E-01	4.54E-03
GLU	22	O	193	GLU	22	C	669	3.75E-01	-2.04E-01	-2.07E-01	-2.01E-01	3.23E-03
GLU	22	O	193	GLU	22	CB	671	3.50E-01	-2.29E-01	-2.38E-01	-2.20E-01	8.86E-03
ASP	23	CA	206	ASP	23	N	682	4.59E-01	-1.10E-01	-1.14E-01	-1.05E-01	4.57E-03
ASP	23	C	207	ASP	23	N	682	4.24E-01	-1.41E-01	-1.47E-01	-1.34E-01	6.92E-03
ASP	23	C	207	ASP	23	CA	683	4.35E-01	-1.11E-01	-1.14E-01	-1.08E-01	2.74E-03
ASP	23	C	207	VAL	24	N	694	4.21E-01	-1.44E-01	-1.50E-01	-1.38E-01	5.64E-03
ASP	23	O	208	ASP	23	C	684	3.65E-01	-2.14E-01	-2.17E-01	-2.11E-01	2.84E-03
ASP	23	O	208	VAL	24	CA	695	4.13E-01	-1.64E-01	-1.79E-01	-1.49E-01	1.47E-02
ASP	23	O	208	VAL	24	O	697	3.90E-01	-2.14E-01	-2.32E-01	-1.96E-01	1.83E-02
ASP	23	CB	209	ASP	23	N	682	4.15E-01	-1.73E-01	-1.83E-01	-1.63E-01	9.61E-03
ASP	23	CB	209	ASP	23	CA	683	4.28E-01	-1.34E-01	-1.40E-01	-1.28E-01	5.68E-03

VAL	24	N	217	VAL	24	O	697	4.40E-01	-1.33E-01	-1.40E-01	-1.27E-01	6.61E-03
VAL	24	CA	218	VAL	24	N	694	4.55E-01	-1.15E-01	-1.20E-01	-1.09E-01	5.65E-03
VAL	24	CA	218	VAL	24	O	697	3.39E-01	-2.08E-01	-2.23E-01	-1.92E-01	1.58E-02
VAL	24	C	219	VAL	24	O	697	3.62E-01	-2.17E-01	-2.17E-01	-2.16E-01	5.58E-04
VAL	24	CB	221	VAL	24	O	697	4.13E-01	-1.62E-01	-1.80E-01	-1.43E-01	1.88E-02
GLY	25	N	233	VAL	24	C	696	4.13E-01	-1.55E-01	-1.57E-01	-1.53E-01	2.23E-03
GLY	25	N	233	GLY	25	C	712	4.25E-01	-1.39E-01	-1.45E-01	-1.32E-01	6.85E-03
GLY	25	N	233	GLY	25	O	713	3.56E-01	-2.96E-01	-3.01E-01	-2.90E-01	5.57E-03
GLY	25	CA	234	VAL	24	O	697	3.95E-01	-1.94E-01	-2.02E-01	-1.87E-01	7.62E-03
GLY	25	C	235	GLY	25	O	713	3.71E-01	-2.07E-01	-2.11E-01	-2.03E-01	3.97E-03
SER	26	N	240	GLY	25	C	712	4.41E-01	-1.17E-01	-1.23E-01	-1.12E-01	5.50E-03
SER	26	N	240	SER	26	CA	718	4.41E-01	-1.33E-01	-1.39E-01	-1.27E-01	5.98E-03
SER	26	C	242	ASN	27	N	728	4.18E-01	-1.49E-01	-1.52E-01	-1.45E-01	3.53E-03
SER	26	O	243	SER	26	CA	718	3.43E-01	-2.14E-01	-2.39E-01	-1.88E-01	2.51E-02
SER	26	O	243	SER	26	C	719	3.68E-01	-2.12E-01	-2.15E-01	-2.10E-01	2.53E-03
SER	26	O	243	SER	26	CB	721	3.97E-01	-1.88E-01	-2.08E-01	-1.68E-01	2.00E-02
SER	26	O	243	ASN	27	CA	729	3.93E-01	-1.97E-01	-2.08E-01	-1.87E-01	1.02E-02
SER	26	O	243	ASN	27	O	731	3.84E-01	-2.28E-01	-2.49E-01	-2.07E-01	2.10E-02
ASN	27	CA	252	ASN	27	O	731	4.03E-01	-1.78E-01	-2.00E-01	-1.56E-01	2.23E-02
ASN	27	C	253	ASN	27	O	731	3.80E-01	-1.95E-01	-2.05E-01	-1.85E-01	1.03E-02
ASN	27	OD1	257	ASN	27	CB	732	3.97E-01	-1.90E-01	-2.03E-01	-1.76E-01	1.33E-02
ASN	27	OD1	257	ASN	27	CG	733	3.91E-01	-1.80E-01	-1.88E-01	-1.71E-01	8.52E-03
LYS	28	N	265	ASN	27	C	730	4.05E-01	-1.67E-01	-1.71E-01	-1.62E-01	4.84E-03
LYS	28	CA	266	ASN	27	O	731	3.70E-01	-2.32E-01	-2.41E-01	-2.23E-01	9.02E-03
LYS	28	C	267	ASN	27	O	731	4.07E-01	-1.55E-01	-1.70E-01	-1.40E-01	1.49E-02
LYS	28	C	267	GLY	29	N	764	4.12E-01	-1.57E-01	-1.61E-01	-1.53E-01	4.04E-03
LYS	28	O	268	ASN	27	O	731	3.58E-01	-2.93E-01	-3.16E-01	-2.69E-01	2.35E-02
LYS	28	O	268	LYS	28	N	742	4.13E-01	-1.84E-01	-2.02E-01	-1.67E-01	1.74E-02
LYS	28	O	268	LYS	28	CA	743	3.46E-01	-2.29E-01	-2.38E-01	-2.19E-01	9.96E-03
LYS	28	O	268	LYS	28	C	744	3.66E-01	-2.14E-01	-2.15E-01	-2.13E-01	1.31E-03
LYS	28	O	268	GLY	29	CA	765	3.90E-01	-2.03E-01	-2.15E-01	-1.92E-01	1.18E-02
LYS	28	CB	269	ASN	27	O	731	3.65E-01	-2.22E-01	-2.41E-01	-2.04E-01	1.84E-02
GLY	29	C	289	ALA	30	N	771	4.10E-01	-1.59E-01	-1.63E-01	-1.55E-01	3.80E-03
GLY	29	O	290	GLY	29	N	764	3.68E-01	-2.78E-01	-2.99E-01	-2.57E-01	2.08E-02
GLY	29	O	290	GLY	29	CA	765	3.48E-01	-2.15E-01	-2.31E-01	-1.98E-01	1.66E-02
GLY	29	O	290	GLY	29	C	766	3.65E-01	-2.13E-01	-2.17E-01	-2.09E-01	4.19E-03
GLY	29	O	290	ALA	30	CA	772	3.86E-01	-2.09E-01	-2.23E-01	-1.95E-01	1.38E-02
GLY	29	O	290	ALA	30	C	773	4.00E-01	-1.65E-01	-1.74E-01	-1.55E-01	9.68E-03

GLY	29	O	290	ALA	30	O	774	3.54E-01	-2.97E-01	-3.19E-01	-2.75E-01	2.16E-02
ALA	30	N	294	ALA	30	O	774	4.16E-01	-1.76E-01	-1.87E-01	-1.65E-01	1.09E-02
ALA	30	C	296	ALA	30	O	774	3.80E-01	-1.96E-01	-2.05E-01	-1.88E-01	8.56E-03
ILE	31	C	306	ILE	32	N	800	4.28E-01	-1.35E-01	-1.39E-01	-1.31E-01	3.96E-03
ILE	31	O	307	ILE	31	CA	782	3.48E-01	-2.31E-01	-2.42E-01	-2.20E-01	1.11E-02
ILE	31	O	307	ILE	31	C	783	3.77E-01	-2.02E-01	-2.04E-01	-1.99E-01	2.96E-03
ILE	31	O	307	ILE	31	CB	785	3.94E-01	-1.87E-01	-2.15E-01	-1.59E-01	2.81E-02
ILE	31	O	307	ILE	32	CA	801	4.12E-01	-1.65E-01	-1.77E-01	-1.53E-01	1.19E-02
ILE	31	O	307	ILE	32	O	803	3.78E-01	-2.44E-01	-2.78E-01	-2.11E-01	3.35E-02
ILE	32	N	323	ILE	32	O	803	4.39E-01	-1.36E-01	-1.46E-01	-1.26E-01	9.79E-03
ILE	32	CA	324	ILE	32	O	803	3.49E-01	-2.33E-01	-2.40E-01	-2.25E-01	7.86E-03
ILE	32	C	325	ILE	32	O	803	3.76E-01	-2.01E-01	-2.05E-01	-1.97E-01	3.91E-03
GLY	33	N	342	ILE	32	C	802	4.32E-01	-1.29E-01	-1.39E-01	-1.20E-01	9.22E-03
GLY	33	CA	343	ILE	32	O	803	4.18E-01	-1.55E-01	-1.74E-01	-1.36E-01	1.89E-02
GLY	38	C	410	GLY	38	O	888	3.71E-01	-2.07E-01	-2.14E-01	-1.99E-01	7.82E-03
VAL	39	C	417	VAL	40	N	908	4.15E-01	-1.53E-01	-1.60E-01	-1.46E-01	6.61E-03
VAL	39	O	418	VAL	39	N	892	4.45E-01	-1.27E-01	-1.38E-01	-1.15E-01	1.13E-02
VAL	39	O	418	VAL	39	CA	893	3.47E-01	-2.20E-01	-2.36E-01	-2.05E-01	1.58E-02
VAL	39	O	418	VAL	39	C	894	3.68E-01	-2.12E-01	-2.14E-01	-2.10E-01	1.66E-03
VAL	39	O	418	VAL	40	CA	909	3.94E-01	-1.97E-01	-2.14E-01	-1.79E-01	1.75E-02
VAL	39	O	418	VAL	40	O	911	3.78E-01	-2.45E-01	-2.70E-01	-2.20E-01	2.53E-02
VAL	39	O	418	VAL	40	CB	912	4.19E-01	-1.57E-01	-1.86E-01	-1.27E-01	2.92E-02
VAL	40	CA	432	VAL	40	O	911	3.49E-01	-2.34E-01	-2.40E-01	-2.28E-01	6.02E-03
VAL	40	C	433	VAL	40	O	911	3.65E-01	-2.15E-01	-2.16E-01	-2.13E-01	1.74E-03
ILE	41	N	447	VAL	40	C	910	4.12E-01	-1.57E-01	-1.63E-01	-1.51E-01	5.66E-03
ILE	41	CA	448	VAL	40	O	911	3.86E-01	-2.11E-01	-2.24E-01	-1.98E-01	1.31E-02
ILE	41	C	449	VAL	40	O	911	4.20E-01	-1.34E-01	-1.47E-01	-1.22E-01	1.28E-02
ILE	41	C	449	ALA	42	N	943	4.10E-01	-1.60E-01	-1.63E-01	-1.56E-01	3.93E-03
ILE	41	O	450	VAL	40	O	911	3.66E-01	-2.73E-01	-2.96E-01	-2.49E-01	2.32E-02
ILE	41	O	450	ILE	41	N	924	4.35E-01	-1.42E-01	-1.54E-01	-1.30E-01	1.22E-02
ILE	41	O	450	ILE	41	CA	925	3.56E-01	-2.39E-01	-2.44E-01	-2.34E-01	4.80E-03
ILE	41	O	450	ILE	41	C	926	3.70E-01	-2.10E-01	-2.13E-01	-2.07E-01	2.80E-03
ILE	41	O	450	ALA	42	CA	944	3.83E-01	-2.16E-01	-2.25E-01	-2.06E-01	9.43E-03
ILE	41	O	450	ALA	42	CB	947	3.91E-01	-2.00E-01	-2.26E-01	-1.74E-01	2.61E-02
ILE	41	CB	451	VAL	40	O	911	4.07E-01	-1.75E-01	-1.97E-01	-1.54E-01	2.16E-02

Supplementary Table 3: Mapping results for A β 40's (PDB ID: 2M4J) long range (1:3) dominant atom-atom Coulombic interactions across ensemble structures. Columns for each chain correspond to: residue abbreviation, residue number in peptide sequence, atom identity (IUPAC naming convention) and atom number in PDB file. Energy in *kT*, distance in *nm*. Mapping analysis began on the 11th residue for both isoforms because original structure data for A β 42 begins with the 11th residue.

Chain A				Chain G				Average Distance	Average Coulombic Values	Lower 95% Confidence Interval Bound	Upper 95% Confidence Interval Bound	Margin of Error
GLU	11	O	155	GLU	11	CD	3752	9.93E-01	-3.53E-01	-3.55E-01	-3.50E-01	2.17E-03
GLU	11	O	155	VAL	12	H	3768	7.60E-01	-3.15E-01	-3.17E-01	-3.13E-01	2.34E-03
HIS	13	C	185	HIS	14	O	3797	8.65E-01	-3.38E-01	-3.39E-01	-3.36E-01	1.55E-03
HIS	13	O	186	HIS	13	C	3779	8.95E-01	-3.20E-01	-3.20E-01	-3.19E-01	9.70E-04
HIS	13	O	186	HIS	14	C	3796	8.32E-01	-3.61E-01	-3.63E-01	-3.58E-01	2.48E-03
HIS	14	C	202	HIS	14	O	3797	9.21E-01	-3.05E-01	-3.06E-01	-3.04E-01	7.57E-04
GLN	15	O	220	LYS	16	C	3830	8.92E-01	-3.76E-01	-3.81E-01	-3.71E-01	4.85E-03
LYS	16	C	236	LYS	16	O	3831	9.06E-01	-3.65E-01	-3.66E-01	-3.64E-01	1.04E-03
LEU	17	O	259	LYS	16	C	3830	8.99E-01	-3.66E-01	-3.69E-01	-3.63E-01	3.09E-03
GLU	22	CD	347	GLU	22	O	3938	9.63E-01	-3.83E-01	-4.30E-01	-3.35E-01	4.78E-02
ASP	23	O	359	ASP	23	CG	3955	8.79E-01	-3.51E-01	-3.55E-01	-3.47E-01	3.95E-03
ASP	23	CG	361	GLU	22	O	3938	8.98E-01	-4.01E-01	-4.12E-01	-3.91E-01	1.07E-02
ASP	23	OD2	363	ASP	23	CG	3955	9.80E-01	-4.31E-01	-4.42E-01	-4.19E-01	1.15E-02
SER	26	O	394	ASN	27	C	3998	9.12E-01	-3.17E-01	-3.23E-01	-3.11E-01	5.75E-03
LYS	28	O	419	LYS	28	C	4012	9.09E-01	-3.64E-01	-3.73E-01	-3.55E-01	8.57E-03
ILE	31	C	457	ILE	32	O	4071	8.73E-01	-3.36E-01	-3.42E-01	-3.29E-01	6.85E-03
ILE	31	O	458	ILE	31	C	4051	8.89E-01	-3.26E-01	-3.31E-01	-3.20E-01	5.17E-03
ILE	31	O	458	ILE	32	C	4070	8.66E-01	-3.40E-01	-3.47E-01	-3.33E-01	6.91E-03
LEU	34	O	503	GLY	33	C	4089	8.12E-01	-3.49E-01	-3.58E-01	-3.39E-01	9.19E-03

Supplementary Table 4: Mapping results for A β 42's (PDB ID: 2MXU) long range (1:3) dominant atom-atom Coulombic interactions across ensemble structures. Columns for each chain correspond to: residue abbreviation, residue number in peptide sequence, atom identity (IUPAC naming convention) and atom number in PDB file. Energy in kT , distance in nm . Mapping analysis began on the 11th residue for both isoforms because original structure data for A β 42 begins with the 11th residue.

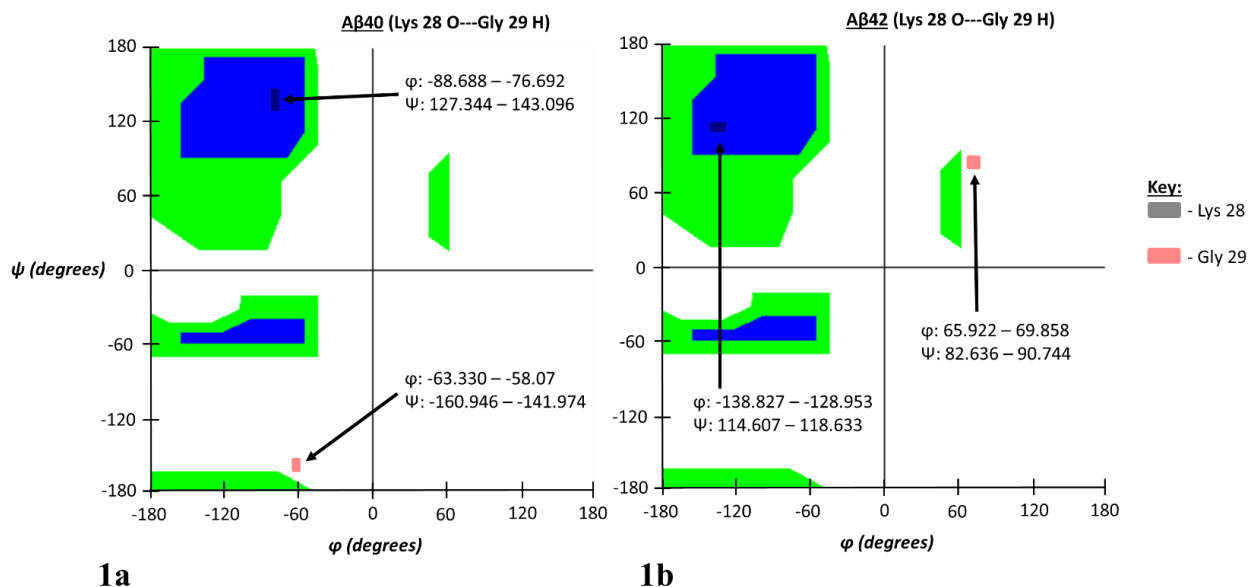
Chain A				Chain C				Average Distance	Average Coulombic Values	Lower 95% Confidence Interval Bound	Upper 95% Confidence Interval Bound	Margin of Error
GLU	11	CD	7	GLU	11	OE1	962	9.76E-01	-5.04E-01	-5.21E-01	-4.87E-01	1.74E-02
GLU	11	CD	7	GLU	11	OE2	963	9.82E-01	-5.03E-01	-5.32E-01	-4.74E-01	2.87E-02
GLU	11	OE1	8	GLU	11	CD	961	9.51E-01	-5.26E-01	-5.51E-01	-5.00E-01	2.59E-02
GLU	11	OE2	9	GLU	11	CD	961	9.24E-01	-5.50E-01	-5.76E-01	-5.24E-01	2.57E-02
LYS	16	C	85	LEU	17	O	1062	8.18E-01	-4.29E-01	-4.36E-01	-4.23E-01	6.53E-03
LYS	16	O	86	LYS	16	C	1039	8.54E-01	-4.02E-01	-4.05E-01	-3.99E-01	2.71E-03
LYS	16	O	86	LEU	17	C	1061	8.07E-01	-3.50E-01	-3.56E-01	-3.45E-01	5.44E-03
LEU	17	C	107	LEU	17	O	1062	8.49E-01	-3.18E-01	-3.20E-01	-3.16E-01	2.01E-03
VAL	18	H	131	LEU	17	O	1062	6.70E-01	-3.77E-01	-3.82E-01	-3.71E-01	5.57E-03
GLU	22	O	193	GLU	22	CD	1150	9.23E-01	-3.95E-01	-4.08E-01	-3.83E-01	1.26E-02
GLU	22	CD	196	GLU	22	OE1	1151	9.60E-01	-5.17E-01	-5.29E-01	-5.04E-01	1.23E-02
GLU	22	CD	196	GLU	22	OE2	1152	9.72E-01	-5.07E-01	-5.19E-01	-4.94E-01	1.23E-02
GLU	22	OE1	197	GLU	22	CD	1150	9.95E-01	-4.89E-01	-5.06E-01	-4.73E-01	1.65E-02
GLU	22	OE2	198	GLU	22	CD	1150	9.94E-01	-4.90E-01	-5.03E-01	-4.76E-01	1.34E-02
ASP	23	O	208	ASP	23	CG	1164	9.49E-01	-3.11E-01	-3.15E-01	-3.07E-01	3.83E-03
ASP	23	O	208	VAL	24	H	1178	6.79E-01	-3.30E-01	-3.35E-01	-3.25E-01	5.24E-03
ASP	23	CG	210	ASP	23	N	1159	8.85E-01	-3.87E-01	-3.93E-01	-3.80E-01	6.60E-03
ASP	23	CG	210	ASP	23	OD1	1165	9.65E-01	-4.42E-01	-4.52E-01	-4.32E-01	1.05E-02
ASP	23	OD2	212	ASP	23	CG	1164	9.25E-01	-4.72E-01	-4.88E-01	-4.57E-01	1.56E-02
SER	26	O	243	GLY	25	C	1189	8.78E-01	-3.18E-01	-3.23E-01	-3.12E-01	5.56E-03
SER	26	O	243	ASN	27	C	1207	8.48E-01	-3.58E-01	-3.63E-01	-3.53E-01	4.90E-03
LYS	28	C	267	ASN	27	O	1208	7.95E-01	-4.23E-01	-4.33E-01	-4.14E-01	9.20E-03
LYS	28	C	267	ALA	30	O	1251	9.87E-01	-3.16E-01	-3.23E-01	-3.09E-01	6.66E-03
LYS	28	O	268	ASN	27	C	1207	7.94E-01	-3.89E-01	-3.99E-01	-3.79E-01	9.77E-03
LYS	28	O	268	LYS	28	C	1221	8.53E-01	-4.03E-01	-4.05E-01	-4.01E-01	1.77E-03
GLY	29	C	289	ALA	30	O	1251	8.11E-01	-3.47E-01	-3.55E-01	-3.40E-01	7.40E-03
GLY	29	O	290	LYS	28	C	1221	9.04E-01	-3.32E-01	-3.39E-01	-3.25E-01	6.80E-03
GLY	29	O	290	ALA	30	C	1250	7.97E-01	-3.22E-01	-3.27E-01	-3.18E-01	4.48E-03
ILE	31	C	306	ILE	32	O	1280	8.46E-01	-3.53E-01	-3.58E-01	-3.48E-01	5.16E-03
ILE	31	O	307	ALA	30	C	1250	8.87E-01	-3.28E-01	-3.36E-01	-3.19E-01	8.49E-03

ILE	31	O	307	ILE	31	C	1260	8.71E-01	-3.36E-01	-3.37E-01	-3.35E-01	1.11E-03
ILE	31	O	307	ILE	32	C	1279	8.43E-01	-3.56E-01	-3.62E-01	-3.50E-01	6.09E-03
ILE	32	C	325	ILE	32	O	1280	8.72E-01	-3.35E-01	-3.39E-01	-3.32E-01	3.19E-03
GLY	33	C	344	ILE	32	O	1280	8.22E-01	-3.80E-01	-3.92E-01	-3.68E-01	1.20E-02
ILE	41	O	450	ILE	41	C	1403	8.54E-01	-3.48E-01	-3.51E-01	-3.44E-01	3.31E-03
ILE	41	O	450	ALA	42	C	1422	8.24E-01	-3.73E-01	-3.92E-01	-3.53E-01	1.95E-02

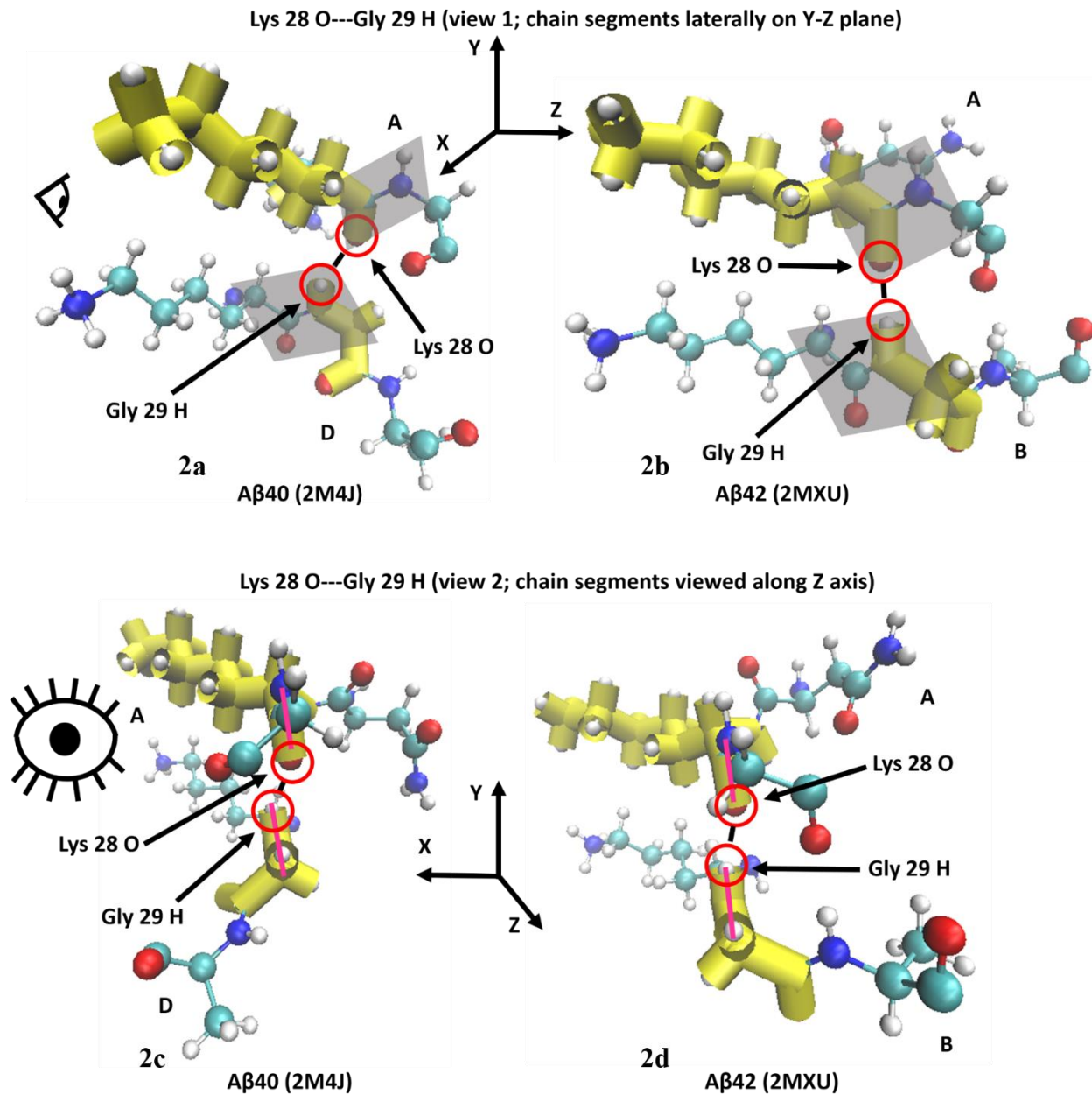
Supplementary Table 5: Ramachandran angle data for A β 40 and A β 42 for chains A-D (A β 40, PDB ID: 2M4J) and chains A-B (A β 42, PDB ID: 2MXU) for the 1:2 interaction configuration across ensemble structures.

	A β 40				A β 42			
	Chain A		Chain D		Chain A		Chain B	
	ϕ	ψ	ϕ	ψ	ϕ	ψ	ϕ	ψ
GLU 11	-	152.910 \pm 0.711	-	151.350 \pm 0.487	-	85.980 \pm 48.329	-	81.200 \pm 48.360
VAL 12	-153.140 \pm 0.201	128.500 \pm 0.357	-149.530 \pm 0.042	130.000 \pm 0.072	-130.860 \pm 4.541	132.920 \pm 2.150	-126.470 \pm 2.793	130.310 \pm 3.024
HIS 13	-135.180 \pm 0.296	146.43 \pm 0.743	-129.880 \pm 0.120	149.470 \pm 0.774	-130.400 \pm 4.486	138.120 \pm 3.514	-126.780 \pm 2.397	125.750 \pm 2.675
HIS 14	-165.320 \pm 0.569	97.570 \pm 0.373	-165.060 \pm 0.128	104.570 \pm 0.113	-139.520 \pm 1.844	135.130 \pm 3.390	-128.600 \pm 3.178	129.880 \pm 3.248
GLN 15	-107.590 \pm 2.008	-173.870 \pm 0.751	-111.070 \pm 2.030	-176.020 \pm 0.175	-99.300 \pm 49.056	121.450 \pm 16.646	-96.660 \pm 50.682	120.580 \pm 8.974
LYS 16	-166.350 \pm 1.700	97.950 \pm 0.938	-162.970 \pm 1.638	105.720 \pm 0.414	-66.370 \pm 51.461	74.450 \pm 41.173	-62.910 \pm 52.091	85.320 \pm 40.351
LEU 17	-117.790 \pm 5.123	158.580 \pm 2.486	-124.310 \pm 5.075	156.280 \pm 2.852	-106.350 \pm 8.094	128.920 \pm 5.349	-119.950 \pm 7.398	121.110 \pm 6.335
VAL 18	-120.610 \pm 9.229	124.710 \pm 2.477	-112.980 \pm 11.974	129.400 \pm 2.469	-131.080 \pm 1.889	121.890 \pm 3.649	-127.230 \pm 3.123	117.580 \pm 2.471
PHE 19	-109.630 \pm 16.980	133.770 \pm 10.920	-110.030 \pm 20.201	133.850 \pm 7.521	-81.020 \pm 3.879	158.850 \pm 30.529	-76.250 \pm 3.486	174.450 \pm 0.906
PHE 20	-13.800 \pm 67.407	34.610 \pm 39.682	-12.140 \pm 67.546	30.070 \pm 41.404	-29.740 \pm 43.085	146.220 \pm 6.041	-45.570 \pm 5.273	139.410 \pm 5.855
ALA 21	-67.680 \pm 12.282	-27.670 \pm 50.357	-68.800 \pm 13.231	-22.500 \pm 50.612	-82.390 \pm 2.151	-71.630 \pm 106.672	-79.190 \pm 1.994	-107.310 \pm 93.302
GLU 22	-99.030 \pm 13.950	117.940 \pm 17.139	-102.000 \pm 14.163	120.760 \pm 16.175	-64.210 \pm 1.979	164.500 \pm 2.354	-67.340 \pm 2.329	162.850 \pm 2.212
ASP 23	-153.20 \pm 5.623	137.940 \pm 1.318	-148.460 \pm 3.594	139.130 \pm 1.409	56.740 \pm 0.957	80.680 \pm 7.616	59.740 \pm 0.785	82.380 \pm 1.732
VAL 24	-67.650 \pm 8.347	79.540 \pm 83.862	-70.530 \pm 8.460	80.410 \pm 85.689	-120.910 \pm 5.218	129.850 \pm 4.328	-126.500 \pm 1.964	125.550 \pm 1.838
GLY 25	-114.140 \pm 3.094	50.210 \pm 2.290	-114.730 \pm 2.429	54.310 \pm 3.261	-69.410 \pm 1.837	-48.370 \pm 3.181	-64.700 \pm 0.905	-53.870 \pm 3.950
SER 26	-67.480 \pm 6.196	-79.970 \pm 87.939	-61.550 \pm 4.009	-83.240 \pm 87.483	-151.180 \pm 2.861	135.570 \pm 0.234	-148.780 \pm 2.944	135.650 \pm 0.221
ASN 27	-69.580 \pm 1.699	86.480 \pm 5.961	-69.260 \pm 3.501	91.230 \pm 4.565	-99.240 \pm 0.078	135.810 \pm 2.815	-99.170 \pm 0.106	132.980 \pm 2.102
LYS 28	-82.690 \pm 5.998	135.220 \pm 7.876	-87.910 \pm 5.247	137.660 \pm 8.087	-133.890 \pm 4.937	116.620 \pm 2.013	-128.180 \pm 4.710	115.470 \pm 1.180
GLY 29	-62.690 \pm 0.809	-153.170 \pm 10.428	-60.700 \pm 2.630	-151.460 \pm 9.486	67.370 \pm 1.613	83.100 \pm 6.157	67.890 \pm 1.968	86.690 \pm 4.054
ALA 30	-104.030 \pm 6.560	122.180 \pm 4.709	-105.320 \pm 5.670	123.850 \pm 5.584	-131.240 \pm 7.569	119.080 \pm 4.617	-132.880 \pm 8.833	115.120 \pm 3.048
ILE 31	-100.480 \pm 8.486	130.830 \pm 4.794	-103.190 \pm 8.379	137.610 \pm 3.972	-143.340 \pm 1.497	152.560 \pm 5.527	-139.650 \pm 2.449	149.700 \pm 5.180
ILE 32	-147.380 \pm 4.687	-78.070 \pm 95.222	-152.980 \pm 5.812	-77.810 \pm 96.409	-119.270 \pm 4.820	130.550 \pm 6.560	-118.550 \pm 2.265	126.340 \pm 6.973
GLY 33	63.670 \pm 0.773	21.120 \pm 16.942	63.990 \pm 0.473	20.500 \pm 16.506	125.780 \pm 69.398	54.270 \pm 93.645	60.750 \pm 102.966	52.780 \pm 89.964
LEU 34	-83.930 \pm 8.423	126.710 \pm 3.472	-84.830 \pm 7.589	134.400 \pm 2.025	-72.280 \pm 4.931	-36.940 \pm 5.140	-72.560 \pm 6.023	-39.810 \pm 2.733

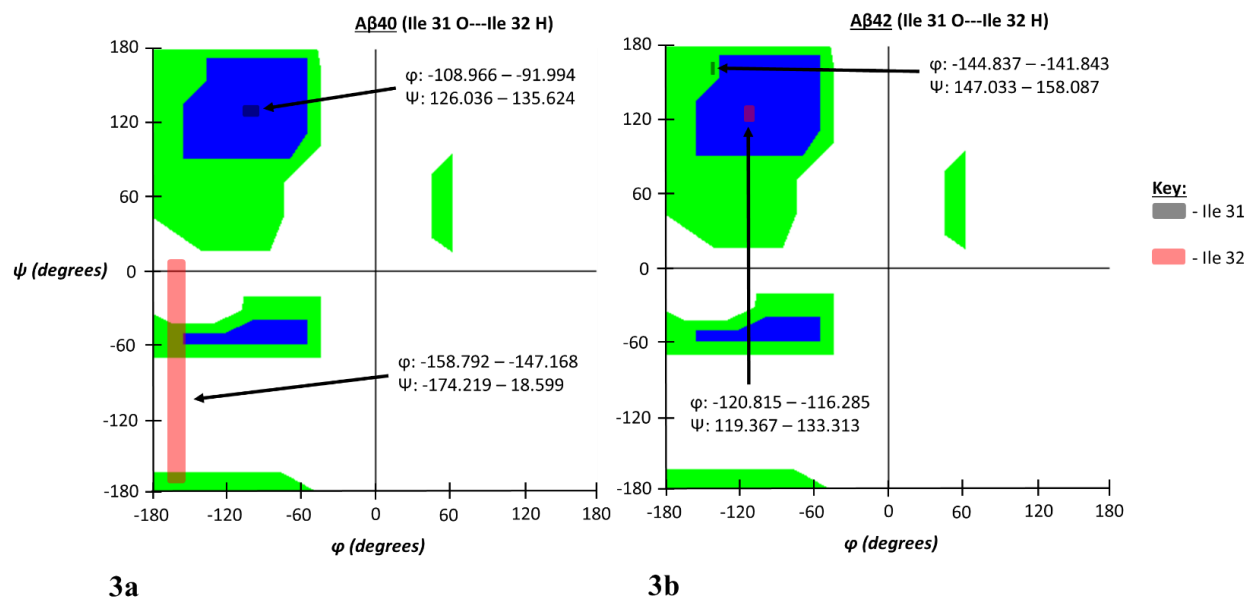
MET 35	-159.790 ± 2.975	150.550 ± 3.927	-157.400 ± 0.722	160.480 ± 2.626	-1.880 ± 56.148	76.720 ± 34.012	1.610 ± 55.991	80.430 ± 32.922
VAL 36	-154.990 ± 2.092	160.240 ± 4.458	-163.110 ± 1.703	161.350 ± 2.732	-122.660 ± 8.607	131.660 ± 5.849	-127.770 ± 3.156	121.400 ± 4.922
GLY 37	55.960 ± 0.472	69.450 ± 2.115	60.710 ± 0.370	64.440 ± 0.783	33.380 ± 78.191	-86.060 ± 80.912	44.710 ± 76.271	-71.030 ± 70.644
GLY 38	152.790 ± 7.822	7.410 ± 109.716	150.820 ± 7.315	8.980 ± 110.119	-73.180 ± 50.299	112.540 ± 28.090	-57.330 ± 76.223	114.640 ± 24.428
VAL 39	-122.680 ± 5.114	153.420 ± 4.657	-123.45 ± 4.172	151.310 ± 3.842	-130.890 ± 8.936	138.080 ± 7.006	-125.860 ± 5.951	134.690 ± 7.081
VAL 40	65.280 ± 0.705	-	73.420 ± 1.158	-	-121.460 ± 2.146	130.960 ± 2.269	-121.830 ± 2.170	125.290 ± 2.384
ILE 41	-	-	-	-	-126.650 ± 3.064	128.990 ± 6.494	-121.150 ± 3.527	121.410 ± 3.893
ALA 42	-	-	-	-	-114.710 ± 41.491	-	-121.570 ± 12.900	-



Supplementary Figure 1a & 1b: Ramachandran angle profiles for an exceptionally strong atom-atom interaction (Lys 28 O interacting with Gly 29 H) for A β 40 (PDB ID: 2M4J, 1a) and A β 42 (PDB ID: 2MXU, 1b). Ranges for ϕ and ψ correspond to data spread according to 95% confidence interval analysis for all ensemble members as previously described. As stated before, the first atom is from the A chain of both isoforms and the second corresponds to the partner atom on the appropriate 1:2 interaction chain configuration. Note the increase in left-handed α -helix secondary structure in A β 42 compared to A β 40.

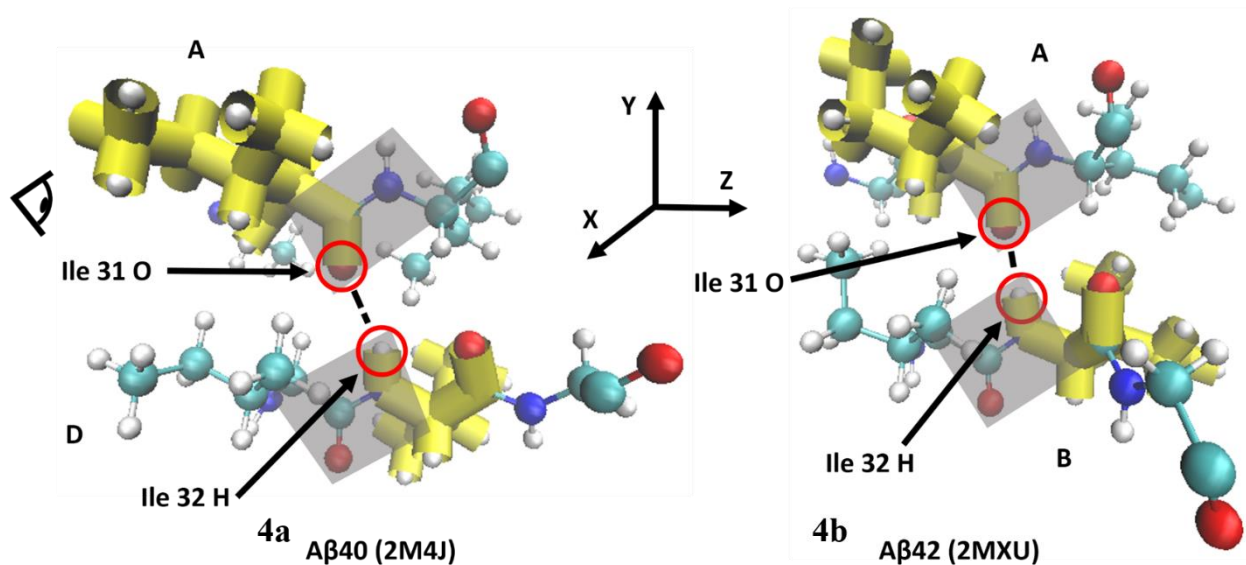


Supplementary Figure 2a-2d: Molecule representations of peptide plane alignment for Aβ40 (2a & 2c) and Aβ42 (2b & 2d). Shaded parallelograms in Figures 2a and 2b are the peptide planes for the residues whose atoms are participating in the hydrogen bonding. Figures 2c and 2d correspond to a view down the peptide bonds showing the peptide plane profile orientation in magenta. Eye icons indicate view perspective.

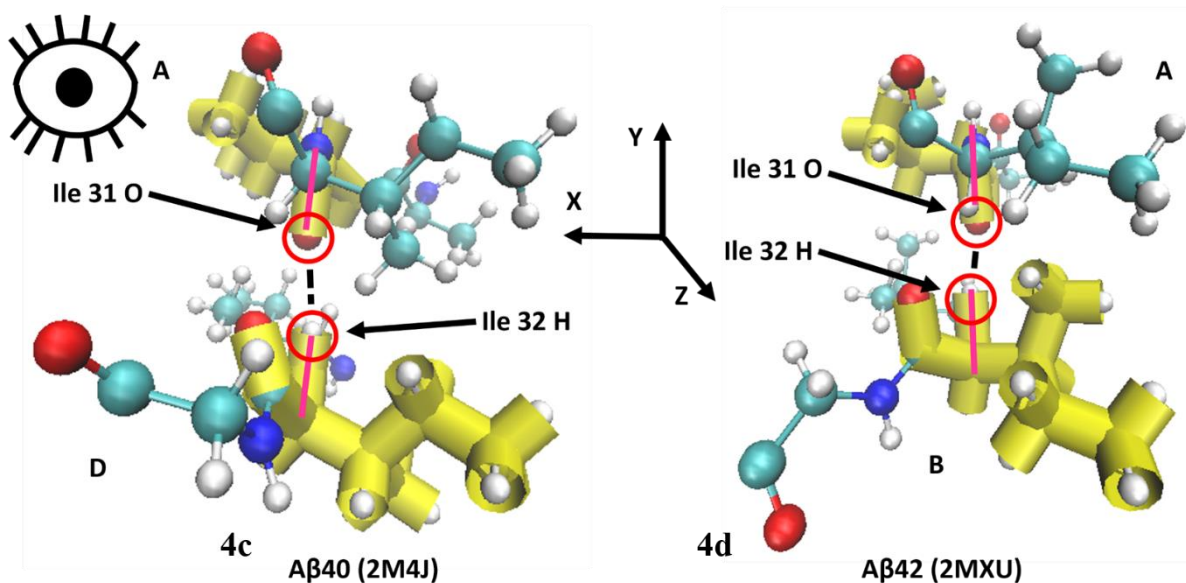


Supplementary Figure 3a & 3b: Ramachandran angle profiles for an exceptionally strong atom-atom interaction (Ile 31 O interacting with Ile 32 H) for Aβ40 (PDB ID: 2M4J, 3a) and Aβ42 (PDB ID: 2MXU, 3b). Ranges for φ and ψ correspond to data spread according to 95% confidence interval analysis for all ensemble members as previously described. As stated before, the first atom is from the A chain of both isoforms and the second corresponds to the partner atom on the appropriate 1:2 interaction chain configuration. Note the decrease in β -sheet and increase in β -sheet Ramachandran angle values for Ile 31 and Ile 32 respectively in Aβ42 compared to Aβ40.

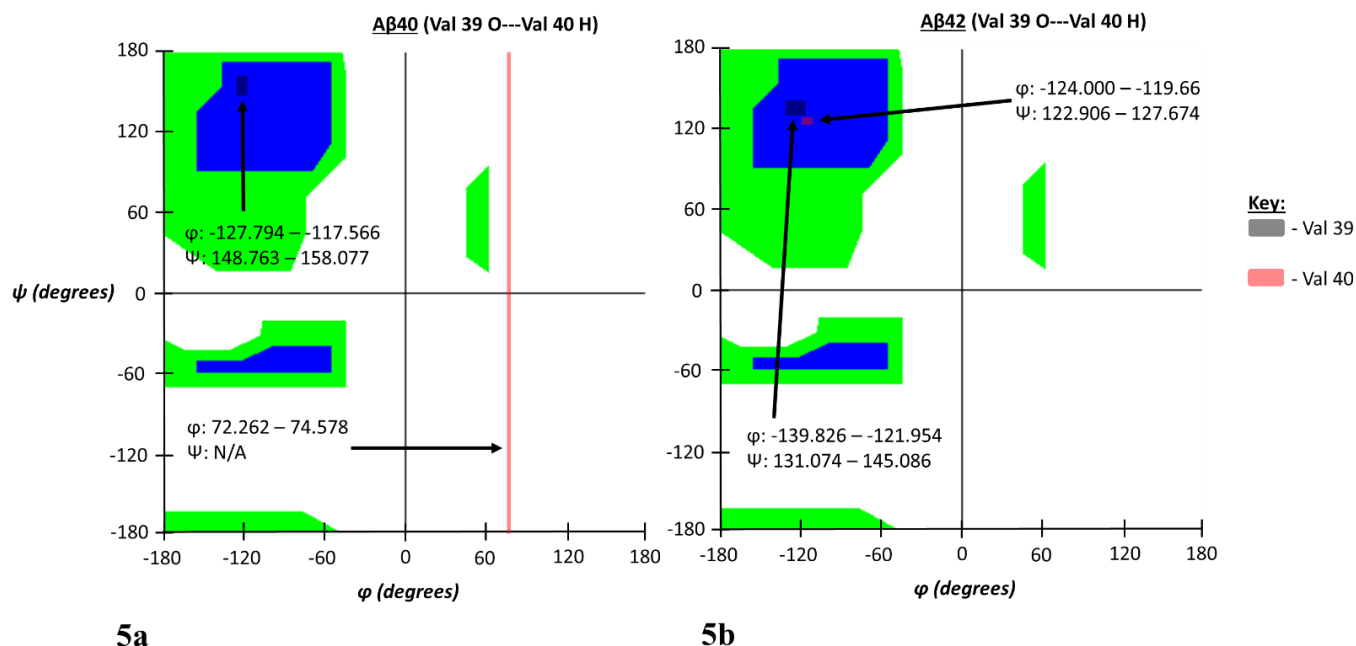
Ile 31 O---Ile 32 H (view 1; chain segments laterally on Y-Z plane)



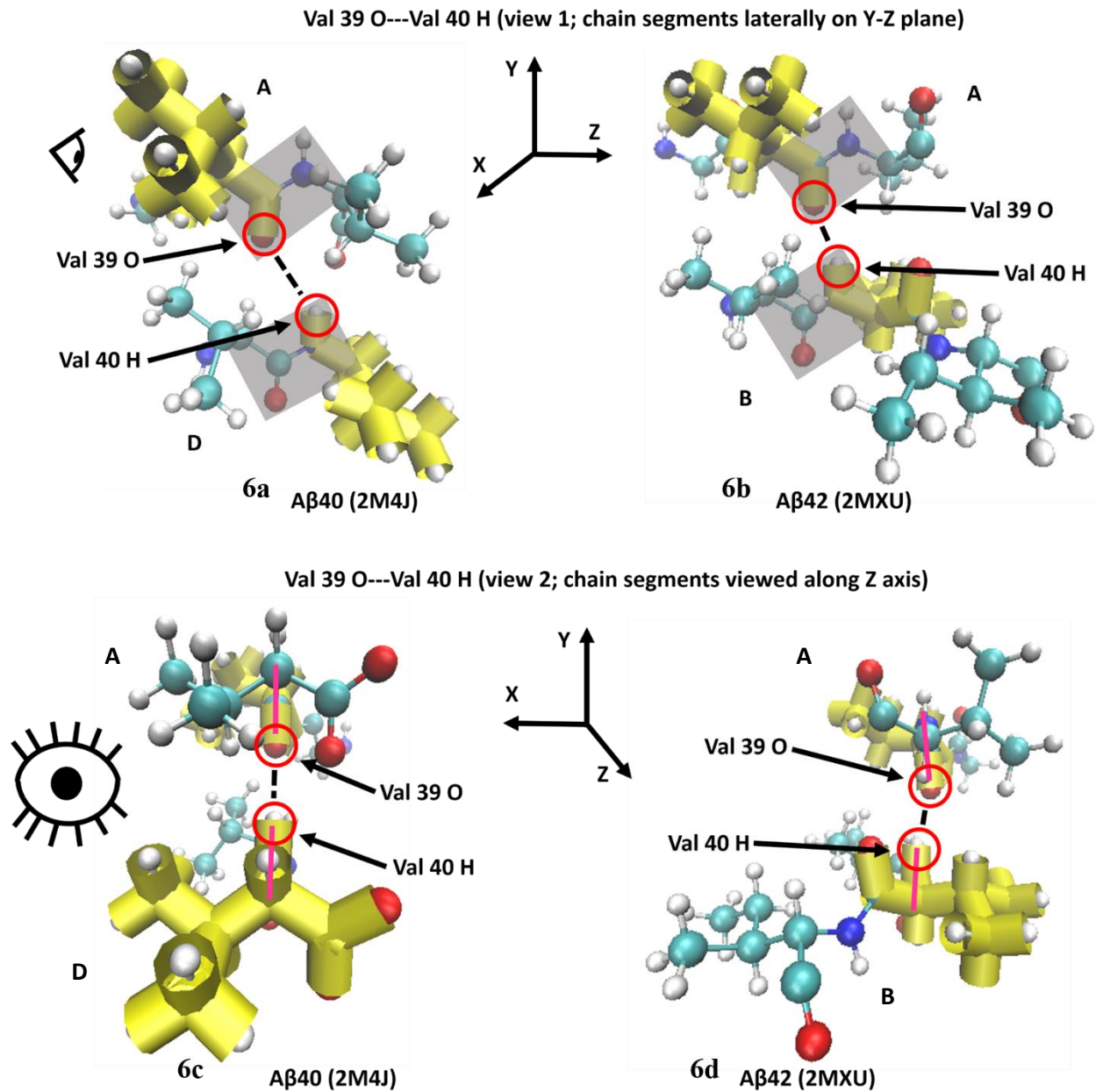
Ile 31 O---Ile 32 H (view 2; chain segments viewed along Z axis)



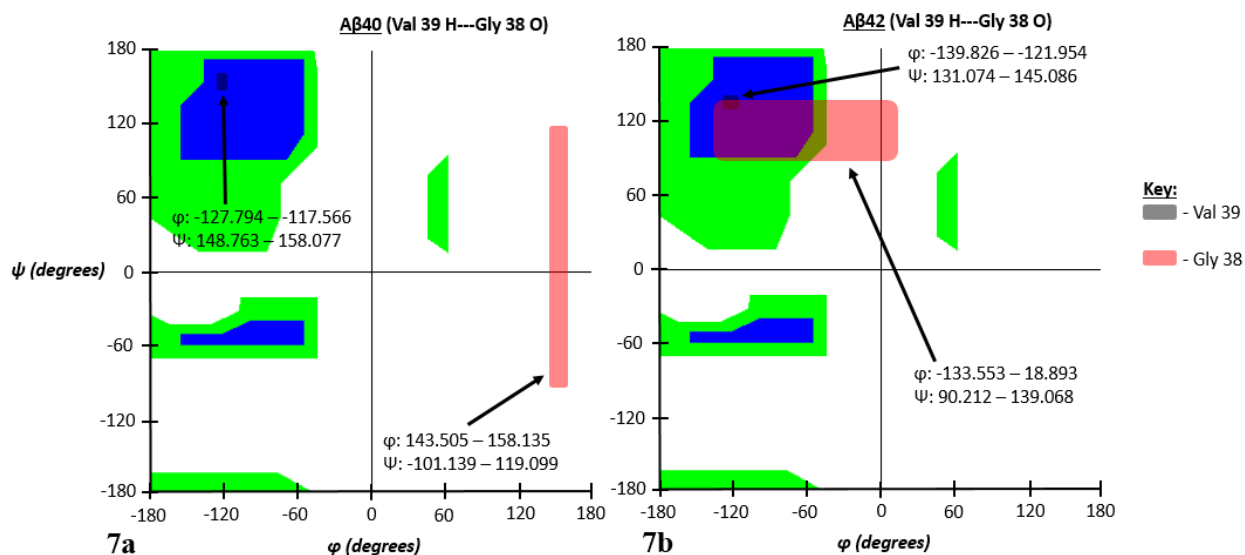
Supplementary Figure 4a-4d: Molecule representations of peptide plane alignment for Aβ40 (4a & 4c) and Aβ42 (4b & 4d). Shaded parallelograms in Figures 4a and 4b are the peptide planes for the residues whose atoms are participating in the hydrogen bonding. Figures 4c and 4d correspond to a view down the peptide bonds showing the peptide plane profile orientation in magenta. Eye icons indicate view perspective.



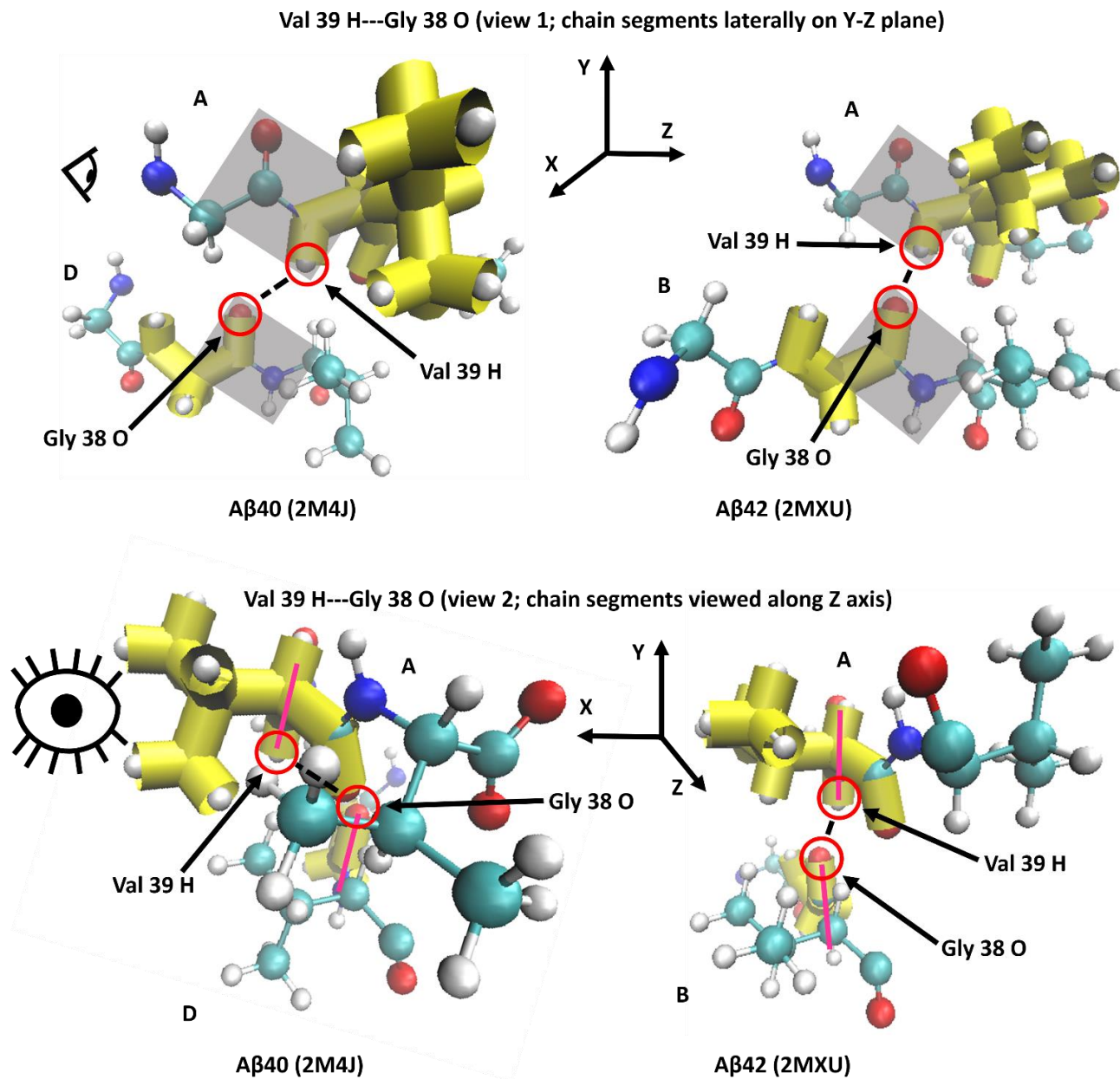
Supplementary Figure 5a & 5b: Ramachandran angle profiles for an exceptionally strong atom-atom interaction (Val 39 O interacting with Val 40 H) for Aβ40 (PDB ID: 2M4J, 5a) and Aβ42 (PDB ID: 2MXU, 5b). Ranges for ϕ and ψ correspond to data spread according to 95% confidence interval analysis for all ensemble members as previously described. As stated before, the first atom is from the A chain of both isoforms and the second corresponds to the partner atom on the appropriate 1:2 interaction chain configuration. Note the retention of β -sheet secondary structure for Val 39 and the acquisition of β -sheet Ramachandran angle values for Val 40 in Aβ42 compared to Aβ40. We also note the lack of Ramachandran ψ angles in Aβ40 due to it being the C-terminus residue which lacks a peptide plane.



Supplementary Figure 6a-6d: Molecule representations of peptide plane alignment for A β 40 (6a & 6c) and A β 42 (6b & 6d). Shaded parallelograms in Figures 6a and 6b are the peptide planes for the residues whose atoms are participating in the hydrogen bonding. Figures 6c and 6d correspond to a view down the peptide bonds showing the peptide plane profile orientation in magenta. Eye icons indicate view perspective.



Supplementary Figure 7a & 7b: Ramachandran angle profiles for an exceptionally strong atom-atom interaction (Val 39 H interacting with Gly 38 O) for A β 40 (PDB ID: 2M4J, 7a) and A β 42 (PDB ID: 2MXU, 7b). Ranges for ϕ and ψ correspond to data spread according to 95% confidence interval analysis for all ensemble members as previously described. As stated before, the first atom is from the A chain of both isoforms and the second corresponds to the partner atom on the appropriate 1:2 interaction chain configuration. Note the retention of β -sheet secondary structure for Val 39 and the acquisition of β -sheet Ramachandran angle values for Gly 38 in A β 42 compared to A β 40.



Supplementary Figure 8a-8d: Molecule representations of peptide plane alignment for Aβ40 (8a & 8c) and Aβ42 (8b & 8d). Shaded parallelograms in Figures 8a and 8b are the peptide planes for the residues whose atoms are participating in the hydrogen bonding. Figures 8c and 8d correspond to a view down the peptide bonds showing the peptide plane profile orientation in magenta. Eye icons indicate view perspective.

Supplementary Table 6a: Mapping results for A β 42's (PDB ID: 2NAO by Walti et al.) short range (1:2) dominant atom-atom Coulombic interactions across ensemble structures. Columns for each chain correspond to: residue abbreviation, residue number in peptide sequence, atom identity (IUPAC naming convention) and atom number in PDB file. Energy in kT , distance in nm . Mapping analysis began on the 11th residue for both isoforms because original structure data for A β 42 begins with the 11th residue.

Chain 1				Chain 2				Average Distance	Average Coulombic Values	Lower 95% Confidence Interval Bound	Upper 95% Confidence Interval Bound	Margin of Error
HIS	13	C	183	HIS	13	N	806	7.48E-01	-4.57E-01	-5.22E-01	-3.91E-01	6.51E-02
HIS	13	C	183	HIS	13	O	809	6.04E-01	-7.31E-01	-8.79E-01	-5.83E-01	1.48E-01
HIS	13	C	183	HIS	14	N	823	6.57E-01	-5.92E-01	-6.84E-01	-5.00E-01	9.22E-02
HIS	13	C	183	HIS	14	O	826	5.87E-01	-7.45E-01	-8.72E-01	-6.17E-01	1.28E-01
HIS	13	O	184	HIS	13	C	808	6.81E-01	-5.30E-01	-5.78E-01	-4.81E-01	4.85E-02
HIS	13	O	184	HIS	14	C	825	6.88E-01	-5.15E-01	-5.45E-01	-4.85E-01	3.00E-02
HIS	14	N	198	HIS	13	C	808	5.81E-01	-8.20E-01	-1.03E+00	-6.10E-01	2.11E-01
HIS	14	N	198	HIS	14	C	825	5.66E-01	-8.37E-01	-1.01E+00	-6.59E-01	1.78E-01
HIS	14	C	200	HIS	13	N	806	7.82E-01	-4.16E-01	-4.74E-01	-3.58E-01	5.78E-02
HIS	14	C	200	HIS	13	O	809	5.99E-01	-7.03E-01	-7.92E-01	-6.15E-01	8.87E-02
HIS	14	C	200	HIS	14	N	823	5.94E-01	-7.10E-01	-8.10E-01	-6.10E-01	9.98E-02
HIS	14	C	200	HIS	14	O	826	3.86E-01	-1.96E+00	-2.04E+00	-1.88E+00	8.00E-02
HIS	14	C	200	GLN	15	N	840	6.06E-01	-4.85E-01	-4.97E-01	-4.72E-01	1.28E-02
HIS	14	C	200	GLN	15	O	843	8.28E-01	-3.89E-01	-3.98E-01	-3.80E-01	8.79E-03
HIS	14	C	200	GLN	15	OE1	847	8.13E-01	-4.62E-01	-5.22E-01	-4.03E-01	5.94E-02
HIS	14	C	200	GLN	15	NE2	848	8.91E-01	-5.57E-01	-6.30E-01	-4.83E-01	7.38E-02
HIS	14	C	200	LYS	16	N	857	6.76E-01	-4.36E-01	-4.45E-01	-4.26E-01	9.60E-03
HIS	14	C	200	LYS	16	O	860	8.05E-01	-4.07E-01	-4.20E-01	-3.93E-01	1.32E-02
HIS	14	O	201	HIS	13	C	808	7.41E-01	-4.46E-01	-4.70E-01	-4.22E-01	2.42E-02
HIS	14	O	201	HIS	14	C	825	6.04E-01	-6.66E-01	-6.78E-01	-6.54E-01	1.24E-02
HIS	14	O	201	LYS	16	C	859	8.93E-01	-3.51E-01	-3.58E-01	-3.45E-01	6.77E-03
HIS	14	ND1	204	HIS	13	C	808	5.69E-01	-7.11E-01	-9.14E-01	-5.09E-01	2.03E-01
HIS	14	ND1	204	HIS	14	C	825	6.10E-01	-5.69E-01	-6.84E-01	-4.53E-01	1.16E-01
GLN	15	N	215	HIS	13	C	808	5.76E-01	-5.49E-01	-5.96E-01	-5.02E-01	4.69E-02
GLN	15	N	215	HIS	14	C	825	3.89E-01	-1.41E+00	-1.43E+00	-1.38E+00	2.63E-02
GLN	15	N	215	GLN	15	C	842	5.89E-01	-3.27E-01	-3.38E-01	-3.16E-01	1.08E-02
GLN	15	N	215	LYS	16	C	859	7.31E-01	-3.65E-01	-3.73E-01	-3.57E-01	7.79E-03
GLN	15	N	215	LYS	16	H	866	4.71E-01	-3.28E-01	-3.41E-01	-3.15E-01	1.31E-02
GLN	15	C	217	HIS	14	N	823	6.26E-01	-3.92E-01	-4.07E-01	-3.76E-01	1.52E-02
GLN	15	C	217	HIS	14	O	826	3.44E-01	-1.75E+00	-1.96E+00	-1.53E+00	2.15E-01
GLN	15	C	217	GLN	15	N	840	5.08E-01	-4.55E-01	-4.70E-01	-4.41E-01	1.47E-02
GLN	15	C	217	GLN	15	O	843	6.13E-01	-4.37E-01	-4.44E-01	-4.30E-01	6.83E-03
GLN	15	C	217	GLN	15	NE2	848	7.35E-01	-5.72E-01	-7.99E-01	-3.45E-01	2.27E-01

GLN	15	C	217	LYS	16	N	857	4.12E-01	-8.60E-01	-8.81E-01	-8.39E-01	2.09E-02
GLN	15	C	217	LYS	16	O	860	4.73E-01	-7.94E-01	-8.53E-01	-7.36E-01	5.87E-02
GLN	15	O	218	HIS	13	C	808	6.27E-01	-6.76E-01	-7.52E-01	-6.00E-01	7.58E-02
GLN	15	O	218	HIS	14	C	825	3.84E-01	-2.15E+00	-2.34E+00	-1.96E+00	1.90E-01
GLN	15	O	218	GLN	15	C	842	3.77E-01	-1.41E+00	-1.45E+00	-1.37E+00	4.26E-02
GLN	15	O	218	GLN	15	CD	846	5.89E-01	-8.59E-01	-1.08E+00	-6.41E-01	2.18E-01
GLN	15	O	218	GLN	15	H	849	5.10E-01	-4.74E-01	-4.90E-01	-4.57E-01	1.68E-02
GLN	15	O	218	GLN	15	HA	850	2.89E-01	-1.09E+00	-1.21E+00	-9.65E-01	1.25E-01
GLN	15	O	218	LYS	16	C	859	4.30E-01	-1.74E+00	-1.83E+00	-1.65E+00	8.91E-02
GLN	15	O	218	LYS	16	H	866	2.00E-01	-5.20E+00	-5.25E+00	-5.16E+00	4.67E-02
GLN	15	O	218	LEU	17	C	881	7.61E-01	-3.90E-01	-4.00E-01	-3.80E-01	9.98E-03
GLN	15	O	218	VAL	18	H	905	7.22E-01	-3.31E-01	-3.42E-01	-3.20E-01	1.13E-02
GLN	15	CD	221	HIS	14	N	823	6.85E-01	-6.92E-01	-1.01E+00	-3.78E-01	3.14E-01
GLN	15	CD	221	HIS	14	O	826	4.30E-01	-1.75E+00	-2.28E+00	-1.22E+00	5.28E-01
GLN	15	CD	221	GLN	15	N	840	5.36E-01	-7.21E-01	-8.99E-01	-5.42E-01	1.78E-01
GLN	15	CD	221	GLN	15	O	843	6.95E-01	-5.56E-01	-6.32E-01	-4.80E-01	7.63E-02
GLN	15	CD	221	GLN	15	OE1	847	4.80E-01	-1.57E+00	-2.02E+00	-1.12E+00	4.54E-01
GLN	15	CD	221	GLN	15	NE2	848	5.40E-01	-1.61E+00	-2.13E+00	-1.10E+00	5.14E-01
GLN	15	CD	221	LYS	16	N	857	5.71E-01	-6.84E-01	-8.62E-01	-5.07E-01	1.78E-01
GLN	15	CD	221	LYS	16	O	860	6.67E-01	-7.30E-01	-9.54E-01	-5.06E-01	2.24E-01
GLN	15	OE1	222	HIS	13	C	808	7.31E-01	-1.01E+00	-1.75E+00	-2.69E-01	7.42E-01
GLN	15	OE1	222	HIS	14	C	825	5.04E-01	-2.14E+00	-3.29E+00	-9.92E-01	1.15E+00
GLN	15	OE1	222	GLN	15	C	842	6.01E-01	-6.31E-01	-9.20E-01	-3.42E-01	2.89E-01
GLN	15	OE1	222	GLN	15	CD	846	5.03E-01	-1.33E+00	-1.63E+00	-1.04E+00	2.94E-01
GLN	15	OE1	222	GLN	15	HE22	856	6.02E-01	-8.64E-01	-1.64E+00	-8.86E-02	7.75E-01
GLN	15	OE1	222	LYS	16	C	859	7.09E-01	-8.47E-01	-1.29E+00	-4.09E-01	4.39E-01
GLN	15	NE2	223	HIS	13	C	808	7.80E-01	-8.24E-01	-1.13E+00	-5.16E-01	3.07E-01
GLN	15	NE2	223	HIS	14	C	825	5.39E-01	-1.72E+00	-2.37E+00	-1.07E+00	6.46E-01
GLN	15	NE2	223	GLN	15	C	842	5.95E-01	-7.92E-01	-9.43E-01	-6.41E-01	1.51E-01
GLN	15	NE2	223	GLN	15	CD	846	4.40E-01	-2.66E+00	-3.23E+00	-2.09E+00	5.71E-01
GLN	15	NE2	223	GLN	15	HE21	855	4.90E-01	-1.18E+00	-1.40E+00	-9.62E-01	2.21E-01
GLN	15	NE2	223	GLN	15	HE22	856	5.16E-01	-9.94E-01	-1.10E+00	-8.92E-01	1.02E-01
GLN	15	NE2	223	LYS	16	C	859	7.06E-01	-1.18E+00	-1.61E+00	-7.43E-01	4.32E-01
GLN	15	H	224	HIS	13	O	809	4.84E-01	-5.32E-01	-6.26E-01	-4.38E-01	9.39E-02
GLN	15	H	224	HIS	14	N	823	4.34E-01	-6.90E-01	-8.27E-01	-5.54E-01	1.37E-01
GLN	15	H	224	HIS	14	O	826	1.98E-01	-6.09E+00	-6.38E+00	-5.81E+00	2.85E-01
GLN	15	H	224	GLN	15	N	840	4.10E-01	-5.58E-01	-5.79E-01	-5.37E-01	2.12E-02
GLN	15	H	224	LYS	16	N	857	5.15E-01	-3.59E-01	-3.79E-01	-3.38E-01	2.03E-02
GLN	15	HA	225	HIS	14	O	826	4.26E-01	-3.49E-01	-3.61E-01	-3.36E-01	1.24E-02
GLN	15	HE21	230	HIS	14	O	826	4.95E-01	-9.66E-01	-1.69E+00	-2.39E-01	7.27E-01
GLN	15	HE21	230	GLN	15	NE2	848	4.78E-01	-1.27E+00	-1.55E+00	-9.98E-01	2.76E-01

GLN	15	HE22	231	HIS	14	O	826	5.24E-01	-7.24E-01	-1.10E+00	-3.48E-01	3.76E-01
GLN	15	HE22	231	GLN	15	OE1	847	4.28E-01	-1.74E+00	-2.56E+00	-9.22E-01	8.18E-01
GLN	15	HE22	231	GLN	15	NE2	848	4.57E-01	-1.40E+00	-1.67E+00	-1.13E+00	2.71E-01
LYS	16	N	232	HIS	14	C	825	5.80E-01	-6.02E-01	-6.31E-01	-5.74E-01	2.84E-02
LYS	16	N	232	GLN	15	C	842	5.95E-01	-3.59E-01	-3.67E-01	-3.52E-01	7.44E-03
LYS	16	N	232	LYS	16	C	859	5.58E-01	-7.15E-01	-7.32E-01	-6.99E-01	1.66E-02
LYS	16	N	232	LYS	16	H	866	4.03E-01	-5.47E-01	-5.62E-01	-5.31E-01	1.56E-02
LYS	16	C	234	HIS	14	O	826	6.68E-01	-5.97E-01	-6.30E-01	-5.65E-01	3.26E-02
LYS	16	C	234	GLN	15	O	843	7.72E-01	-4.81E-01	-4.94E-01	-4.69E-01	1.27E-02
LYS	16	C	234	LYS	16	N	857	5.49E-01	-7.44E-01	-7.79E-01	-7.08E-01	3.55E-02
LYS	16	C	234	LYS	16	O	860	3.86E-01	-2.27E+00	-2.30E+00	-2.25E+00	2.58E-02
LYS	16	C	234	LEU	17	N	879	6.07E-01	-4.85E-01	-4.90E-01	-4.80E-01	4.64E-03
LYS	16	C	234	LEU	17	O	882	8.29E-01	-4.20E-01	-4.27E-01	-4.12E-01	7.53E-03
LYS	16	C	234	VAL	18	N	898	6.68E-01	-5.05E-01	-5.22E-01	-4.88E-01	1.72E-02
LYS	16	C	234	VAL	18	O	901	7.05E-01	-4.09E-01	-4.25E-01	-3.94E-01	1.54E-02
LYS	16	O	235	HIS	14	C	825	8.61E-01	-3.63E-01	-3.73E-01	-3.53E-01	1.00E-02
LYS	16	O	235	LYS	16	C	859	6.14E-01	-7.52E-01	-7.68E-01	-7.37E-01	1.53E-02
LYS	16	O	235	LEU	17	C	881	8.01E-01	-3.55E-01	-3.59E-01	-3.50E-01	4.52E-03
LYS	16	O	235	VAL	18	H	905	6.54E-01	-4.00E-01	-4.10E-01	-3.89E-01	1.04E-02
LYS	16	HA	242	LYS	16	O	860	3.26E-01	-6.67E-01	-7.67E-01	-5.67E-01	1.00E-01
LEU	17	N	254	LYS	16	C	859	4.02E-01	-1.30E+00	-1.38E+00	-1.23E+00	7.32E-02
LEU	17	N	254	LEU	17	C	881	5.86E-01	-4.15E-01	-4.28E-01	-4.02E-01	1.32E-02
LEU	17	N	254	VAL	18	H	905	4.58E-01	-5.69E-01	-6.13E-01	-5.26E-01	4.32E-02
LEU	17	C	256	LYS	16	N	857	6.61E-01	-4.00E-01	-4.30E-01	-3.69E-01	3.06E-02
LEU	17	C	256	LYS	16	O	860	3.70E-01	-2.16E+00	-2.57E+00	-1.74E+00	4.17E-01
LEU	17	C	256	LEU	17	N	879	5.25E-01	-5.33E-01	-5.70E-01	-4.96E-01	3.70E-02
LEU	17	C	256	LEU	17	O	882	6.23E-01	-5.71E-01	-5.77E-01	-5.65E-01	5.70E-03
LEU	17	C	256	VAL	18	N	898	4.21E-01	-1.15E+00	-1.16E+00	-1.14E+00	1.01E-02
LEU	17	C	256	VAL	18	O	901	3.84E-01	-1.34E+00	-1.46E+00	-1.21E+00	1.24E-01
LEU	17	C	256	PHE	19	N	914	5.85E-01	-4.36E-01	-4.57E-01	-4.16E-01	2.06E-02
LEU	17	C	256	ILE	31	O	1081	8.54E-01	-3.51E-01	-3.62E-01	-3.39E-01	1.18E-02
LEU	17	C	256	ILE	32	O	1100	7.56E-01	-4.38E-01	-4.71E-01	-4.06E-01	3.24E-02
LEU	17	O	257	LYS	16	C	859	4.15E-01	-1.96E+00	-2.26E+00	-1.65E+00	3.05E-01
LEU	17	O	257	LEU	17	C	881	3.84E-01	-1.81E+00	-1.88E+00	-1.75E+00	6.44E-02
LEU	17	O	257	LEU	17	H	887	5.30E-01	-3.75E-01	-4.02E-01	-3.48E-01	2.67E-02
LEU	17	O	257	LEU	17	HA	888	2.86E-01	-1.01E+00	-1.16E+00	-8.61E-01	1.51E-01
LEU	17	O	257	VAL	18	C	900	3.73E-01	-1.55E+00	-1.70E+00	-1.40E+00	1.53E-01
LEU	17	O	257	VAL	18	CB	902	4.54E-01	-8.21E-01	-8.83E-01	-7.59E-01	6.21E-02
LEU	17	O	257	VAL	18	H	905	2.02E-01	-8.74E+00	-8.83E+00	-8.64E+00	9.96E-02
LEU	17	O	257	PHE	19	C	916	6.50E-01	-5.03E-01	-5.32E-01	-4.74E-01	2.90E-02
LEU	17	O	257	ILE	32	C	1099	7.32E-01	-4.14E-01	-4.34E-01	-3.95E-01	1.96E-02

LEU	17	CB	258	LYS	16	C	859	4.47E-01	-4.07E-01	-4.46E-01	-3.67E-01	3.94E-02
LEU	17	H	262	LYS	16	N	857	4.10E-01	-5.65E-01	-6.44E-01	-4.87E-01	7.83E-02
LEU	17	H	262	LYS	16	O	860	1.98E-01	-5.58E+00	-5.80E+00	-5.36E+00	2.18E-01
LEU	17	H	262	LEU	17	N	879	4.11E-01	-4.42E-01	-4.49E-01	-4.35E-01	6.74E-03
VAL	18	N	273	LYS	16	C	859	5.99E-01	-6.41E-01	-6.94E-01	-5.89E-01	5.25E-02
VAL	18	N	273	LEU	17	C	881	6.06E-01	-4.89E-01	-5.00E-01	-4.77E-01	1.12E-02
VAL	18	N	273	VAL	18	C	900	5.01E-01	-5.84E-01	-6.02E-01	-5.65E-01	1.88E-02
VAL	18	N	273	VAL	18	H	905	4.13E-01	-9.28E-01	-9.55E-01	-9.01E-01	2.70E-02
VAL	18	N	273	PHE	19	C	916	6.77E-01	-3.74E-01	-3.94E-01	-3.54E-01	1.98E-02
VAL	18	C	275	VAL	18	N	898	6.26E-01	-3.56E-01	-3.66E-01	-3.46E-01	1.01E-02
VAL	18	C	275	VAL	18	O	901	4.18E-01	-8.28E-01	-8.77E-01	-7.80E-01	4.86E-02
VAL	18	C	275	PHE	19	N	914	5.59E-01	-3.74E-01	-3.88E-01	-3.60E-01	1.40E-02
VAL	18	C	275	PHE	19	O	917	5.66E-01	-5.47E-01	-6.58E-01	-4.35E-01	1.11E-01
VAL	18	O	276	VAL	18	C	900	6.19E-01	-3.28E-01	-3.39E-01	-3.17E-01	1.08E-02
VAL	18	CB	277	LYS	16	O	860	5.92E-01	-4.60E-01	-5.27E-01	-3.92E-01	6.70E-02
VAL	18	CB	277	VAL	18	N	898	5.28E-01	-4.63E-01	-5.08E-01	-4.19E-01	4.42E-02
VAL	18	CB	277	VAL	18	O	901	3.87E-01	-1.08E+00	-1.48E+00	-6.85E-01	3.97E-01
VAL	18	CB	277	PHE	19	N	914	5.19E-01	-3.96E-01	-4.24E-01	-3.67E-01	2.83E-02
VAL	18	H	280	LYS	16	O	860	5.44E-01	-6.05E-01	-6.66E-01	-5.44E-01	6.11E-02
VAL	18	H	280	VAL	18	N	898	6.01E-01	-3.81E-01	-3.85E-01	-3.78E-01	3.23E-03
VAL	18	H	280	VAL	18	O	901	4.96E-01	-5.31E-01	-5.59E-01	-5.04E-01	2.76E-02
PHE	19	N	289	VAL	18	C	900	5.08E-01	-4.67E-01	-4.86E-01	-4.49E-01	1.86E-02
PHE	19	N	289	PHE	19	C	916	4.68E-01	-7.01E-01	-7.49E-01	-6.52E-01	4.89E-02
PHE	19	C	291	VAL	18	O	901	6.33E-01	-3.90E-01	-4.25E-01	-3.54E-01	3.54E-02
PHE	19	C	291	PHE	19	O	917	5.06E-01	-9.47E-01	-1.20E+00	-6.91E-01	2.56E-01
PHE	19	C	291	PHE	20	N	934	5.55E-01	-5.51E-01	-7.18E-01	-3.84E-01	1.67E-01
PHE	19	O	292	PHE	19	C	916	5.65E-01	-7.03E-01	-8.97E-01	-5.09E-01	1.94E-01
PHE	19	H	300	VAL	18	O	901	3.79E-01	-6.03E-01	-7.33E-01	-4.72E-01	1.30E-01
PHE	19	H	300	PHE	19	N	914	4.41E-01	-3.44E-01	-3.61E-01	-3.27E-01	1.70E-02
PHE	19	H	300	PHE	19	O	917	3.90E-01	-8.84E-01	-1.21E+00	-5.56E-01	3.28E-01
PHE	20	N	309	PHE	19	C	916	5.23E-01	-6.32E-01	-7.97E-01	-4.68E-01	1.64E-01
PHE	20	N	309	PHE	20	C	936	6.14E-01	-3.77E-01	-4.00E-01	-3.54E-01	2.32E-02
PHE	20	C	311	PHE	19	O	917	5.59E-01	-9.80E-01	-1.35E+00	-6.05E-01	3.75E-01
PHE	20	C	311	PHE	20	N	934	5.75E-01	-4.38E-01	-4.78E-01	-3.98E-01	4.02E-02
PHE	20	C	311	PHE	20	O	937	6.23E-01	-5.02E-01	-5.42E-01	-4.61E-01	4.04E-02
PHE	20	C	311	ALA	21	N	954	5.23E-01	-6.00E-01	-6.79E-01	-5.21E-01	7.93E-02
PHE	20	C	311	ALA	21	O	957	7.02E-01	-4.61E-01	-5.50E-01	-3.71E-01	8.94E-02
PHE	20	C	311	GLU	22	N	964	6.11E-01	-4.45E-01	-5.01E-01	-3.89E-01	5.57E-02
PHE	20	O	312	PHE	19	C	916	5.37E-01	-8.79E-01	-1.19E+00	-5.63E-01	3.16E-01
PHE	20	O	312	PHE	20	C	936	4.91E-01	-8.78E-01	-9.97E-01	-7.58E-01	1.20E-01

PHE	20	O	312	ALA	21	C	956	5.93E-01	-6.41E-01	-7.90E-01	-4.93E-01	1.49E-01
ALA	21	N	329	PHE	20	C	936	6.08E-01	-4.22E-01	-4.56E-01	-3.88E-01	3.37E-02
ALA	21	N	329	ALA	21	C	956	6.13E-01	-4.34E-01	-4.73E-01	-3.94E-01	3.97E-02
ALA	21	C	331	ALA	21	N	954	6.11E-01	-4.37E-01	-4.77E-01	-3.96E-01	4.09E-02
ALA	21	C	331	ALA	21	O	957	6.00E-01	-6.37E-01	-7.31E-01	-5.43E-01	9.43E-02
ALA	21	C	331	GLU	22	N	964	5.33E-01	-6.21E-01	-6.91E-01	-5.51E-01	6.98E-02
ALA	21	C	331	GLU	22	O	967	6.50E-01	-6.59E-01	-8.82E-01	-4.36E-01	2.23E-01
ALA	21	C	331	GLU	22	OE1	971	5.32E-01	-1.56E+00	-2.11E+00	-1.00E+00	5.55E-01
ALA	21	C	331	GLU	22	OE2	972	5.99E-01	-1.15E+00	-1.55E+00	-7.42E-01	4.03E-01
ALA	21	C	331	ASP	23	N	979	6.32E-01	-5.59E-01	-6.10E-01	-5.09E-01	5.06E-02
ALA	21	C	331	ASP	23	O	982	6.56E-01	-4.76E-01	-5.44E-01	-4.08E-01	6.82E-02
ALA	21	C	331	ASP	23	OD1	985	9.51E-01	-3.48E-01	-3.72E-01	-3.25E-01	2.34E-02
ALA	21	O	332	ALA	21	C	956	5.60E-01	-7.53E-01	-8.80E-01	-6.25E-01	1.28E-01
ALA	21	O	332	GLU	22	C	966	6.11E-01	-5.32E-01	-6.51E-01	-4.14E-01	1.19E-01
ALA	21	O	332	GLU	22	CD	970	4.65E-01	-1.72E+00	-2.16E+00	-1.29E+00	4.35E-01
ALA	21	O	332	ASP	23	CG	984	9.04E-01	-3.83E-01	-4.29E-01	-3.36E-01	4.65E-02
GLU	22	N	339	ALA	21	C	956	6.27E-01	-4.31E-01	-4.71E-01	-3.90E-01	4.06E-02
GLU	22	N	339	GLU	22	C	966	5.89E-01	-4.11E-01	-4.59E-01	-3.64E-01	4.75E-02
GLU	22	N	339	GLU	22	CD	970	5.66E-01	-8.71E-01	-1.18E+00	-5.61E-01	3.10E-01
GLU	22	C	341	GLU	22	O	967	5.98E-01	-5.99E-01	-7.46E-01	-4.51E-01	1.48E-01
GLU	22	C	341	GLU	22	OE1	971	6.18E-01	-8.42E-01	-1.14E+00	-5.47E-01	2.96E-01
GLU	22	C	341	GLU	22	OE2	972	6.87E-01	-6.55E-01	-8.73E-01	-4.38E-01	2.18E-01
GLU	22	C	341	ASP	23	N	979	5.58E-01	-6.30E-01	-7.28E-01	-5.32E-01	9.80E-02
GLU	22	C	341	ASP	23	O	982	4.58E-01	-9.44E-01	-1.22E+00	-6.67E-01	2.76E-01
GLU	22	C	341	ASP	23	OD1	985	7.73E-01	-4.12E-01	-4.53E-01	-3.71E-01	4.06E-02
GLU	22	O	342	GLU	22	C	966	5.57E-01	-6.96E-01	-8.40E-01	-5.53E-01	1.43E-01
GLU	22	O	342	GLU	22	CD	970	6.30E-01	-1.04E+00	-1.47E+00	-6.02E-01	4.36E-01
GLU	22	O	342	ASP	23	C	981	5.32E-01	-7.87E-01	-9.90E-01	-5.83E-01	2.04E-01
GLU	22	O	342	ASP	23	CG	984	6.83E-01	-7.55E-01	-9.64E-01	-5.47E-01	2.09E-01
GLU	22	CD	345	ALA	21	O	957	8.71E-01	-4.14E-01	-4.56E-01	-3.72E-01	4.23E-02
GLU	22	CD	345	GLU	22	O	967	8.61E-01	-5.36E-01	-7.75E-01	-2.97E-01	2.39E-01
GLU	22	CD	345	GLU	22	OE1	971	5.80E-01	-1.40E+00	-1.66E+00	-1.14E+00	2.60E-01
GLU	22	CD	345	GLU	22	OE2	972	6.20E-01	-1.24E+00	-1.52E+00	-9.66E-01	2.76E-01
GLU	22	CD	345	ASP	23	N	979	8.31E-01	-4.79E-01	-5.97E-01	-3.62E-01	1.17E-01
GLU	22	CD	345	ASP	23	O	982	8.42E-01	-4.13E-01	-5.01E-01	-3.25E-01	8.80E-02
GLU	22	OE1	346	ALA	21	C	956	9.08E-01	-4.28E-01	-4.68E-01	-3.87E-01	4.03E-02
GLU	22	OE1	346	GLU	22	CD	970	6.16E-01	-1.21E+00	-1.41E+00	-1.02E+00	1.95E-01
GLU	22	OE2	347	GLU	22	CD	970	5.76E-01	-1.45E+00	-1.73E+00	-1.16E+00	2.86E-01
ASP	23	N	354	ALA	21	C	956	7.96E-01	-3.59E-01	-3.89E-01	-3.29E-01	3.00E-02
ASP	23	N	354	GLU	22	C	966	6.05E-01	-5.29E-01	-6.28E-01	-4.31E-01	9.86E-02
ASP	23	N	354	GLU	22	CD	970	6.81E-01	-6.72E-01	-7.83E-01	-5.61E-01	1.11E-01

ASP	23	N	354	ASP	23	C	981	5.29E-01	-6.49E-01	-7.35E-01	-5.64E-01	8.56E-02
ASP	23	N	354	ASP	23	CG	984	6.76E-01	-6.56E-01	-7.62E-01	-5.50E-01	1.06E-01
ASP	23	C	356	ASP	23	N	979	6.90E-01	-3.61E-01	-3.84E-01	-3.38E-01	2.30E-02
ASP	23	C	356	ASP	23	O	982	4.48E-01	-8.53E-01	-9.04E-01	-8.01E-01	5.17E-02
ASP	23	C	356	ASP	23	OD1	985	8.07E-01	-3.52E-01	-3.67E-01	-3.37E-01	1.53E-02
ASP	23	C	356	VAL	24	N	991	6.27E-01	-3.52E-01	-3.70E-01	-3.34E-01	1.78E-02
ASP	23	O	357	ASP	23	C	981	6.77E-01	-3.34E-01	-3.40E-01	-3.27E-01	6.44E-03
ASP	23	O	357	ASP	23	CG	984	8.52E-01	-3.74E-01	-4.03E-01	-3.44E-01	2.94E-02
ASP	23	CG	359	GLU	22	O	967	7.34E-01	-7.34E-01	-1.10E+00	-3.66E-01	3.68E-01
ASP	23	CG	359	GLU	22	OE1	971	8.45E-01	-6.36E-01	-7.11E-01	-5.61E-01	7.53E-02
ASP	23	CG	359	GLU	22	OE2	972	9.11E-01	-5.54E-01	-6.02E-01	-5.07E-01	4.77E-02
ASP	23	CG	359	ASP	23	N	979	6.55E-01	-6.94E-01	-7.91E-01	-5.98E-01	9.63E-02
ASP	23	CG	359	ASP	23	O	982	4.76E-01	-1.56E+00	-2.20E+00	-9.20E-01	6.39E-01
ASP	23	CG	359	ASP	23	OD1	985	6.44E-01	-9.29E-01	-1.04E+00	-8.20E-01	1.09E-01
ASP	23	CG	359	ASP	23	OD2	986	5.72E-01	-1.23E+00	-1.45E+00	-1.02E+00	2.14E-01
ASP	23	CG	359	VAL	24	N	991	6.64E-01	-6.13E-01	-8.13E-01	-4.14E-01	2.00E-01
ASP	23	OD1	360	GLU	22	C	966	6.96E-01	-5.01E-01	-5.56E-01	-4.46E-01	5.51E-02
ASP	23	OD1	360	GLU	22	CD	970	8.46E-01	-5.85E-01	-6.73E-01	-4.98E-01	8.75E-02
ASP	23	OD1	360	ASP	23	C	981	5.26E-01	-9.75E-01	-1.27E+00	-6.81E-01	2.93E-01
ASP	23	OD1	360	ASP	23	CG	984	5.22E-01	-1.48E+00	-1.67E+00	-1.29E+00	1.88E-01
ASP	23	OD1	360	VAL	24	H	998	6.86E-01	-5.36E-01	-6.78E-01	-3.94E-01	1.42E-01
ASP	23	OD2	361	GLU	22	CD	970	8.84E-01	-5.39E-01	-6.09E-01	-4.69E-01	6.99E-02
ASP	23	OD2	361	ASP	23	C	981	6.35E-01	-6.88E-01	-1.00E+00	-3.73E-01	3.15E-01
ASP	23	OD2	361	ASP	23	CG	984	6.01E-01	-1.11E+00	-1.32E+00	-9.00E-01	2.12E-01
ASP	23	H	362	ASP	23	O	982	4.67E-01	-7.38E-01	-1.08E+00	-3.98E-01	3.40E-01
VAL	24	N	366	ASP	23	C	981	5.12E-01	-5.54E-01	-5.97E-01	-5.11E-01	4.27E-02
VAL	24	N	366	ASP	23	CG	984	7.38E-01	-4.37E-01	-4.85E-01	-3.89E-01	4.77E-02
VAL	24	N	366	VAL	24	C	993	5.60E-01	-4.61E-01	-5.11E-01	-4.10E-01	5.07E-02
VAL	24	N	366	VAL	24	CB	995	5.70E-01	-4.02E-01	-4.68E-01	-3.36E-01	6.56E-02
VAL	24	N	366	VAL	24	H	998	6.48E-01	-3.26E-01	-3.32E-01	-3.20E-01	6.32E-03
VAL	24	C	368	ASP	23	O	982	5.47E-01	-5.64E-01	-6.69E-01	-4.60E-01	1.05E-01
VAL	24	CB	370	ASP	23	O	982	5.48E-01	-4.92E-01	-5.71E-01	-4.13E-01	7.89E-02
VAL	24	H	373	ASP	23	N	979	5.92E-01	-5.06E-01	-5.74E-01	-4.37E-01	6.82E-02
VAL	24	H	373	ASP	23	O	982	3.31E-01	-2.10E+00	-2.64E+00	-1.55E+00	5.49E-01
VAL	24	H	373	ASP	23	OD1	985	7.10E-01	-4.47E-01	-4.80E-01	-4.14E-01	3.31E-02
VAL	24	H	373	ASP	23	OD2	986	7.11E-01	-4.76E-01	-5.89E-01	-3.63E-01	1.13E-01
VAL	24	H	373	VAL	24	N	991	4.64E-01	-6.96E-01	-7.31E-01	-6.60E-01	3.51E-02
VAL	24	H	373	GLY	25	N	1007	4.83E-01	-5.42E-01	-6.26E-01	-4.58E-01	8.41E-02
GLY	25	C	384	VAL	24	O	994	6.49E-01	-5.00E-01	-7.97E-01	-2.03E-01	2.97E-01
GLY	25	C	384	GLY	25	N	1007	4.72E-01	-7.41E-01	-8.12E-01	-6.70E-01	7.13E-02
GLY	25	C	384	GLY	25	O	1010	6.47E-01	-4.87E-01	-4.94E-01	-4.80E-01	7.01E-03

GLY	25	C	384	SER	26	N	1014	4.94E-01	-9.46E-01	-9.82E-01	-9.10E-01	3.63E-02
GLY	25	C	384	SER	26	O	1017	5.72E-01	-7.28E-01	-7.68E-01	-6.88E-01	4.00E-02
GLY	25	C	384	SER	26	OG	1019	6.16E-01	-7.10E-01	-8.15E-01	-6.04E-01	1.06E-01
GLY	25	O	385	VAL	24	C	993	4.80E-01	-7.76E-01	-9.30E-01	-6.22E-01	1.54E-01
GLY	25	O	385	GLY	25	C	1009	4.15E-01	-1.37E+00	-1.41E+00	-1.32E+00	4.61E-02
GLY	25	O	385	GLY	25	H	1011	3.34E-01	-1.33E+00	-1.77E+00	-8.85E-01	4.40E-01
GLY	25	O	385	SER	26	C	1016	5.64E-01	-5.50E-01	-5.88E-01	-5.12E-01	3.79E-02
GLY	25	O	385	SER	26	H	1020	3.19E-01	-1.72E+00	-1.98E+00	-1.46E+00	2.59E-01
GLY	25	O	385	SER	26	HG	1024	5.91E-01	-4.65E-01	-5.24E-01	-4.07E-01	5.82E-02
SER	26	N	389	VAL	24	C	993	6.73E-01	-3.79E-01	-4.30E-01	-3.28E-01	5.07E-02
SER	26	N	389	GLY	25	C	1009	5.86E-01	-6.39E-01	-6.58E-01	-6.20E-01	1.92E-02
SER	26	N	389	SER	26	C	1016	6.26E-01	-4.62E-01	-4.73E-01	-4.51E-01	1.13E-02
SER	26	N	389	SER	26	H	1020	4.29E-01	-7.93E-01	-8.12E-01	-7.74E-01	1.90E-02
SER	26	N	389	ASN	27	C	1027	8.78E-01	-3.14E-01	-3.20E-01	-3.09E-01	5.36E-03
SER	26	N	389	LYS	28	C	1041	9.60E-01	-3.21E-01	-3.26E-01	-3.16E-01	5.05E-03
SER	26	C	391	GLY	25	O	1010	7.21E-01	-3.29E-01	-3.44E-01	-3.14E-01	1.53E-02
SER	26	C	391	SER	26	N	1014	5.11E-01	-7.26E-01	-7.59E-01	-6.92E-01	3.36E-02
SER	26	C	391	SER	26	O	1017	3.99E-01	-1.44E+00	-1.46E+00	-1.42E+00	2.03E-02
SER	26	C	391	SER	26	OG	1019	5.73E-01	-7.42E-01	-9.31E-01	-5.52E-01	1.89E-01
SER	26	C	391	ASN	27	N	1025	6.23E-01	-3.70E-01	-3.73E-01	-3.67E-01	2.81E-03
SER	26	C	391	ASN	27	ND2	1032	8.72E-01	-3.73E-01	-4.21E-01	-3.24E-01	4.83E-02
SER	26	C	391	LYS	28	N	1039	6.14E-01	-3.87E-01	-3.98E-01	-3.77E-01	1.02E-02
SER	26	C	391	LYS	28	O	1042	7.02E-01	-3.83E-01	-4.00E-01	-3.67E-01	1.65E-02
SER	26	O	392	GLY	25	C	1009	7.28E-01	-4.44E-01	-4.64E-01	-4.24E-01	2.02E-02
SER	26	O	392	SER	26	C	1016	6.24E-01	-4.98E-01	-5.01E-01	-4.95E-01	2.94E-03
SER	26	O	392	SER	26	H	1020	5.46E-01	-4.77E-01	-4.96E-01	-4.59E-01	1.82E-02
SER	26	O	392	ASN	27	C	1027	7.77E-01	-4.16E-01	-4.21E-01	-4.11E-01	4.95E-03
SER	26	O	392	LYS	28	C	1041	7.73E-01	-4.95E-01	-5.07E-01	-4.82E-01	1.27E-02
SER	26	OG	394	GLY	25	C	1009	6.63E-01	-6.02E-01	-6.74E-01	-5.29E-01	7.27E-02
SER	26	OG	394	SER	26	C	1016	6.47E-01	-5.26E-01	-5.96E-01	-4.56E-01	6.95E-02
SER	26	OG	394	SER	26	H	1020	4.94E-01	-6.98E-01	-8.08E-01	-5.87E-01	1.10E-01
SER	26	OG	394	SER	26	HG	1024	5.25E-01	-7.61E-01	-8.42E-01	-6.80E-01	8.14E-02
SER	26	OG	394	ASN	27	C	1027	8.66E-01	-3.84E-01	-4.09E-01	-3.58E-01	2.54E-02
SER	26	OG	394	LYS	28	C	1041	9.09E-01	-4.16E-01	-4.38E-01	-3.94E-01	2.20E-02
SER	26	H	395	SER	26	N	1014	6.16E-01	-3.40E-01	-3.44E-01	-3.36E-01	3.91E-03
SER	26	H	395	SER	26	O	1017	6.20E-01	-3.61E-01	-3.71E-01	-3.52E-01	9.13E-03
SER	26	HA	396	SER	26	N	1014	3.44E-01	-5.89E-01	-6.26E-01	-5.52E-01	3.72E-02
SER	26	HA	396	SER	26	O	1017	3.55E-01	-5.82E-01	-6.20E-01	-5.43E-01	3.88E-02
SER	26	HG	399	SER	26	N	1014	6.00E-01	-5.01E-01	-6.04E-01	-3.98E-01	1.03E-01
SER	26	HG	399	SER	26	O	1017	6.03E-01	-5.04E-01	-5.54E-01	-4.55E-01	4.94E-02
SER	26	HG	399	SER	26	OG	1019	5.12E-01	-8.20E-01	-9.58E-01	-6.83E-01	1.37E-01

ASN	27	N	400	GLY	25	C	1009	5.66E-01	-5.53E-01	-5.93E-01	-5.14E-01	3.95E-02
ASN	27	N	400	SER	26	C	1016	4.05E-01	-1.02E+00	-1.04E+00	-1.00E+00	1.62E-02
ASN	27	N	400	SER	26	H	1020	3.87E-01	-8.31E-01	-9.00E-01	-7.63E-01	6.85E-02
ASN	27	N	400	ASN	27	C	1027	5.65E-01	-5.85E-01	-5.99E-01	-5.72E-01	1.35E-02
ASN	27	N	400	ASN	27	CG	1030	6.87E-01	-3.67E-01	-3.71E-01	-3.63E-01	4.13E-03
ASN	27	N	400	LYS	28	C	1041	6.22E-01	-5.60E-01	-5.78E-01	-5.41E-01	1.83E-02
ASN	27	N	400	LYS	28	H	1048	3.96E-01	-5.65E-01	-5.95E-01	-5.35E-01	3.01E-02
ASN	27	C	402	GLY	25	O	1010	8.38E-01	-3.20E-01	-3.31E-01	-3.09E-01	1.10E-02
ASN	27	C	402	SER	26	N	1014	6.39E-01	-5.67E-01	-5.90E-01	-5.44E-01	2.31E-02
ASN	27	C	402	SER	26	O	1017	3.85E-01	-2.03E+00	-2.15E+00	-1.90E+00	1.24E-01
ASN	27	C	402	SER	26	OG	1019	6.59E-01	-6.90E-01	-8.48E-01	-5.33E-01	1.57E-01
ASN	27	C	402	ASN	27	N	1025	5.53E-01	-6.14E-01	-6.28E-01	-6.00E-01	1.40E-02
ASN	27	C	402	ASN	27	O	1028	6.07E-01	-6.09E-01	-6.13E-01	-6.04E-01	4.34E-03
ASN	27	C	402	ASN	27	OD1	1031	7.38E-01	-4.28E-01	-4.74E-01	-3.82E-01	4.61E-02
ASN	27	C	402	ASN	27	ND2	1032	8.05E-01	-5.40E-01	-5.99E-01	-4.80E-01	5.90E-02
ASN	27	C	402	LYS	28	N	1039	3.89E-01	-1.47E+00	-1.50E+00	-1.44E+00	2.78E-02
ASN	27	C	402	LYS	28	O	1042	3.86E-01	-1.98E+00	-2.22E+00	-1.74E+00	2.38E-01
ASN	27	C	402	GLY	29	N	1061	5.14E-01	-6.35E-01	-6.80E-01	-5.91E-01	4.47E-02
ASN	27	C	402	GLY	29	O	1064	6.04E-01	-6.06E-01	-6.55E-01	-5.57E-01	4.94E-02
ASN	27	C	402	ALA	30	N	1068	6.19E-01	-4.54E-01	-4.75E-01	-4.33E-01	2.11E-02
ASN	27	C	402	ILE	41	O	1224	9.21E-01	-3.34E-01	-3.41E-01	-3.27E-01	7.48E-03
ASN	27	O	403	GLY	25	C	1009	7.56E-01	-3.72E-01	-3.85E-01	-3.59E-01	1.29E-02
ASN	27	O	403	SER	26	C	1016	4.55E-01	-9.32E-01	-9.74E-01	-8.89E-01	4.25E-02
ASN	27	O	403	ASN	27	C	1027	3.90E-01	-1.76E+00	-1.78E+00	-1.74E+00	2.26E-02
ASN	27	O	403	ASN	27	CG	1030	6.61E-01	-4.84E-01	-4.95E-01	-4.73E-01	1.10E-02
ASN	27	O	403	LYS	28	C	1041	3.11E-01	-3.87E+00	-4.17E+00	-3.57E+00	3.03E-01
ASN	27	O	403	LYS	28	H	1048	2.00E-01	-4.83E+00	-4.89E+00	-4.76E+00	6.25E-02
ASN	27	O	403	GLY	29	C	1063	5.02E-01	-8.87E-01	-9.55E-01	-8.18E-01	6.86E-02
ASN	27	O	403	GLY	29	H	1065	4.49E-01	-5.13E-01	-5.67E-01	-4.59E-01	5.41E-02
ASN	27	O	403	ALA	30	C	1070	7.55E-01	-3.66E-01	-3.78E-01	-3.54E-01	1.20E-02
ASN	27	O	403	ALA	30	H	1073	5.31E-01	-3.94E-01	-4.22E-01	-3.66E-01	2.82E-02
ASN	27	CG	405	GLY	25	N	1007	5.19E-01	-5.89E-01	-6.38E-01	-5.41E-01	4.83E-02
ASN	27	CG	405	GLY	25	O	1010	6.13E-01	-5.60E-01	-6.20E-01	-5.01E-01	5.94E-02
ASN	27	CG	405	SER	26	N	1014	4.64E-01	-1.11E+00	-1.17E+00	-1.04E+00	6.39E-02
ASN	27	CG	405	SER	26	O	1017	2.94E-01	-4.05E+00	-4.30E+00	-3.80E+00	2.55E-01
ASN	27	CG	405	SER	26	OG	1019	6.44E-01	-6.51E-01	-7.52E-01	-5.51E-01	1.00E-01
ASN	27	CG	405	ASN	27	N	1025	4.43E-01	-9.83E-01	-1.02E+00	-9.43E-01	4.07E-02
ASN	27	CG	405	ASN	27	O	1028	6.40E-01	-5.17E-01	-5.31E-01	-5.03E-01	1.42E-02
ASN	27	CG	405	ASN	27	OD1	1031	4.88E-01	-1.08E+00	-1.31E+00	-8.48E-01	2.33E-01
ASN	27	CG	405	ASN	27	ND2	1032	5.72E-01	-1.15E+00	-1.53E+00	-7.77E-01	3.78E-01
ASN	27	CG	405	LYS	28	N	1039	5.05E-01	-7.29E-01	-7.67E-01	-6.92E-01	3.75E-02

ASN	27	CG	405	LYS	28	O	1042	6.79E-01	-4.96E-01	-5.30E-01	-4.62E-01	3.40E-02
ASN	27	CG	405	GLY	29	O	1064	7.48E-01	-3.73E-01	-3.96E-01	-3.50E-01	2.31E-02
ASN	27	CG	405	ALA	30	N	1068	6.88E-01	-3.47E-01	-3.64E-01	-3.31E-01	1.64E-02
ASN	27	OD1	406	VAL	24	C	993	5.44E-01	-5.96E-01	-6.90E-01	-5.03E-01	9.39E-02
ASN	27	OD1	406	VAL	24	CB	995	4.69E-01	-8.15E-01	-1.02E+00	-6.10E-01	2.05E-01
ASN	27	OD1	406	GLY	25	C	1009	5.25E-01	-8.42E-01	-9.83E-01	-7.00E-01	1.41E-01
ASN	27	OD1	406	SER	26	C	1016	4.23E-01	-1.38E+00	-1.90E+00	-8.63E-01	5.16E-01
ASN	27	OD1	406	SER	26	H	1020	4.24E-01	-8.26E-01	-9.42E-01	-7.10E-01	1.16E-01
ASN	27	OD1	406	ASN	27	C	1027	5.90E-01	-7.31E-01	-9.27E-01	-5.36E-01	1.96E-01
ASN	27	OD1	406	ASN	27	CG	1030	5.46E-01	-8.85E-01	-1.20E+00	-5.72E-01	3.13E-01
ASN	27	OD1	406	LYS	28	C	1041	7.36E-01	-5.00E-01	-5.51E-01	-4.49E-01	5.12E-02
ASN	27	OD1	406	GLY	29	C	1063	7.99E-01	-3.43E-01	-3.70E-01	-3.15E-01	2.74E-02
ASN	27	ND2	407	PHE	19	C	916	7.97E-01	-4.83E-01	-5.20E-01	-4.45E-01	3.74E-02
ASN	27	ND2	407	PHE	20	C	936	8.83E-01	-4.02E-01	-4.19E-01	-3.84E-01	1.77E-02
ASN	27	ND2	407	ASP	23	C	981	7.42E-01	-4.41E-01	-4.69E-01	-4.13E-01	2.82E-02
ASN	27	ND2	407	VAL	24	C	993	5.24E-01	-9.34E-01	-1.05E+00	-8.22E-01	1.12E-01
ASN	27	ND2	407	VAL	24	CB	995	4.31E-01	-1.41E+00	-1.73E+00	-1.09E+00	3.19E-01
ASN	27	ND2	407	VAL	24	H	998	6.82E-01	-5.28E-01	-5.95E-01	-4.61E-01	6.69E-02
ASN	27	ND2	407	GLY	25	C	1009	5.01E-01	-1.36E+00	-1.52E+00	-1.19E+00	1.66E-01
ASN	27	ND2	407	GLY	25	H	1011	4.31E-01	-8.61E-01	-9.67E-01	-7.55E-01	1.06E-01
ASN	27	ND2	407	SER	26	C	1016	3.77E-01	-2.56E+00	-3.15E+00	-1.97E+00	5.91E-01
ASN	27	ND2	407	SER	26	H	1020	4.18E-01	-1.31E+00	-1.57E+00	-1.05E+00	2.60E-01
ASN	27	ND2	407	SER	26	HG	1024	6.92E-01	-5.57E-01	-6.91E-01	-4.22E-01	1.34E-01
ASN	27	ND2	407	ASN	27	C	1027	5.32E-01	-1.30E+00	-1.50E+00	-1.09E+00	2.04E-01
ASN	27	ND2	407	ASN	27	CG	1030	4.60E-01	-1.96E+00	-2.45E+00	-1.48E+00	4.84E-01
ASN	27	ND2	407	ASN	27	H	1033	5.03E-01	-6.34E-01	-7.60E-01	-5.09E-01	1.26E-01
ASN	27	ND2	407	ASN	27	HD21	1037	5.37E-01	-7.62E-01	-9.59E-01	-5.64E-01	1.98E-01
ASN	27	ND2	407	ASN	27	HD22	1038	5.42E-01	-6.71E-01	-6.82E-01	-6.60E-01	1.07E-02
ASN	27	ND2	407	LYS	28	C	1041	7.05E-01	-7.93E-01	-8.37E-01	-7.50E-01	4.36E-02
ASN	27	ND2	407	LYS	28	H	1048	4.63E-01	-7.10E-01	-7.92E-01	-6.27E-01	8.23E-02
ASN	27	ND2	407	GLY	29	C	1063	7.60E-01	-5.56E-01	-5.96E-01	-5.15E-01	4.05E-02
ASN	27	ND2	407	ALA	30	C	1070	8.42E-01	-4.56E-01	-4.91E-01	-4.22E-01	3.43E-02
ASN	27	H	408	SER	26	N	1014	3.66E-01	-9.01E-01	-9.81E-01	-8.21E-01	7.98E-02
ASN	27	H	408	SER	26	O	1017	2.00E-01	-5.42E+00	-5.57E+00	-5.27E+00	1.50E-01
ASN	27	H	408	SER	26	OG	1019	4.48E-01	-7.75E-01	-1.06E+00	-4.89E-01	2.85E-01
ASN	27	H	408	ASN	27	N	1025	4.24E-01	-4.81E-01	-4.86E-01	-4.75E-01	5.91E-03
ASN	27	H	408	LYS	28	N	1039	4.51E-01	-4.17E-01	-4.38E-01	-3.97E-01	2.06E-02
ASN	27	HB2	410	SER	26	O	1017	2.60E-01	-4.27E-01	-4.60E-01	-3.94E-01	3.30E-02
ASN	27	HD21	412	SER	26	N	1014	4.78E-01	-6.88E-01	-8.44E-01	-5.32E-01	1.56E-01
ASN	27	HD21	412	SER	26	O	1017	3.14E-01	-2.85E+00	-3.94E+00	-1.77E+00	1.09E+00
ASN	27	HD21	412	ASN	27	ND2	1032	4.94E-01	-9.05E-01	-1.07E+00	-7.43E-01	1.62E-01

ASN	27	HD22	413	GLY	25	N	1007	3.99E-01	-6.84E-01	-7.22E-01	-6.46E-01	3.78E-02
ASN	27	HD22	413	GLY	25	O	1010	5.25E-01	-5.03E-01	-6.05E-01	-4.00E-01	1.02E-01
ASN	27	HD22	413	SER	26	N	1014	4.28E-01	-8.57E-01	-9.91E-01	-7.22E-01	1.34E-01
ASN	27	HD22	413	SER	26	O	1017	3.60E-01	-1.47E+00	-1.71E+00	-1.23E+00	2.41E-01
ASN	27	HD22	413	ASN	27	N	1025	4.58E-01	-6.05E-01	-7.24E-01	-4.86E-01	1.19E-01
ASN	27	HD22	413	ASN	27	ND2	1032	5.08E-01	-7.80E-01	-7.90E-01	-7.69E-01	1.07E-02
LYS	28	N	414	SER	26	C	1016	6.14E-01	-3.88E-01	-4.00E-01	-3.76E-01	1.17E-02
LYS	28	N	414	ASN	27	C	1027	6.12E-01	-4.98E-01	-5.03E-01	-4.94E-01	4.24E-03
LYS	28	N	414	LYS	28	C	1041	4.83E-01	-1.00E+00	-1.04E+00	-9.63E-01	3.78E-02
LYS	28	N	414	LYS	28	H	1048	4.15E-01	-5.05E-01	-5.11E-01	-5.00E-01	5.59E-03
LYS	28	N	414	GLY	29	C	1063	6.44E-01	-4.25E-01	-4.49E-01	-4.01E-01	2.43E-02
LYS	28	C	416	SER	26	N	1014	9.68E-01	-3.17E-01	-3.23E-01	-3.10E-01	6.63E-03
LYS	28	C	416	SER	26	O	1017	7.15E-01	-5.71E-01	-5.87E-01	-5.55E-01	1.60E-02
LYS	28	C	416	ASN	27	O	1028	8.09E-01	-4.11E-01	-4.18E-01	-4.04E-01	6.81E-03
LYS	28	C	416	LYS	28	N	1039	6.03E-01	-6.03E-01	-6.16E-01	-5.91E-01	1.26E-02
LYS	28	C	416	LYS	28	O	1042	3.75E-01	-2.47E+00	-2.55E+00	-2.38E+00	8.45E-02
LYS	28	C	416	GLY	29	N	1061	5.64E-01	-6.00E-01	-6.18E-01	-5.82E-01	1.82E-02
LYS	28	C	416	GLY	29	O	1064	5.71E-01	-8.04E-01	-8.66E-01	-7.41E-01	6.23E-02
LYS	28	C	416	ALA	30	N	1068	6.89E-01	-4.27E-01	-4.40E-01	-4.15E-01	1.27E-02
LYS	28	C	416	ALA	30	O	1071	9.78E-01	-3.20E-01	-3.26E-01	-3.14E-01	5.81E-03
LYS	28	C	416	ILE	41	O	1224	7.39E-01	-5.75E-01	-6.07E-01	-5.44E-01	3.14E-02
LYS	28	C	416	ALA	42	O	1243	8.52E-01	-4.03E-01	-4.33E-01	-3.74E-01	2.94E-02
LYS	28	O	417	ASN	27	C	1027	8.47E-01	-3.47E-01	-3.51E-01	-3.43E-01	4.18E-03
LYS	28	O	417	LYS	28	C	1041	5.95E-01	-8.02E-01	-8.19E-01	-7.85E-01	1.72E-02
LYS	28	O	417	GLY	29	C	1063	6.93E-01	-4.72E-01	-4.87E-01	-4.56E-01	1.56E-02
LYS	28	H	423	SER	26	O	1017	5.45E-01	-3.49E-01	-3.62E-01	-3.36E-01	1.30E-02
LYS	28	H	423	LYS	28	O	1042	5.09E-01	-3.99E-01	-4.28E-01	-3.70E-01	2.91E-02
LYS	28	HA	424	LYS	28	O	1042	2.59E-01	-1.26E+00	-1.38E+00	-1.13E+00	1.27E-01
GLY	29	N	436	ASN	27	C	1027	6.85E-01	-3.40E-01	-3.53E-01	-3.28E-01	1.26E-02
GLY	29	N	436	LYS	28	C	1041	4.27E-01	-1.17E+00	-1.22E+00	-1.12E+00	5.00E-02
GLY	29	N	436	GLY	29	C	1063	4.75E-01	-7.19E-01	-7.57E-01	-6.82E-01	3.76E-02
GLY	29	C	438	SER	26	O	1017	8.60E-01	-3.30E-01	-3.40E-01	-3.19E-01	1.07E-02
GLY	29	C	438	LYS	28	O	1042	5.15E-01	-9.05E-01	-9.86E-01	-8.24E-01	8.08E-02
GLY	29	C	438	GLY	29	N	1061	5.97E-01	-4.24E-01	-4.36E-01	-4.12E-01	1.20E-02
GLY	29	C	438	GLY	29	O	1064	3.91E-01	-1.61E+00	-1.69E+00	-1.52E+00	8.60E-02
GLY	29	C	438	ALA	30	N	1068	5.80E-01	-4.90E-01	-4.98E-01	-4.82E-01	8.47E-03
GLY	29	C	438	ALA	30	O	1071	8.06E-01	-3.51E-01	-3.56E-01	-3.46E-01	5.07E-03
GLY	29	C	438	ILE	31	N	1078	6.61E-01	-4.14E-01	-4.22E-01	-4.05E-01	8.55E-03
GLY	29	C	438	ILE	31	O	1081	7.41E-01	-4.56E-01	-4.67E-01	-4.46E-01	1.06E-02
GLY	29	C	438	ILE	41	O	1224	8.52E-01	-3.58E-01	-3.69E-01	-3.46E-01	1.17E-02
GLY	29	O	439	LYS	28	C	1041	7.12E-01	-5.06E-01	-5.23E-01	-4.88E-01	1.74E-02

GLY	29	O	439	GLY	29	C	1063	5.79E-01	-6.18E-01	-6.31E-01	-6.05E-01	1.31E-02
GLY	29	O	439	ALA	30	C	1070	7.62E-01	-3.49E-01	-3.58E-01	-3.40E-01	9.01E-03
GLY	29	H	440	LYS	28	O	1042	2.63E-01	-2.68E+00	-3.49E+00	-1.88E+00	8.06E-01
GLY	29	H	440	GLY	29	N	1061	3.98E-01	-4.90E-01	-5.03E-01	-4.76E-01	1.36E-02
GLY	29	H	440	GLY	29	O	1064	3.89E-01	-7.35E-01	-8.45E-01	-6.24E-01	1.10E-01
ALA	30	N	443	LYS	28	C	1041	5.40E-01	-7.21E-01	-7.64E-01	-6.79E-01	4.23E-02
ALA	30	N	443	GLY	29	C	1063	4.00E-01	-1.20E+00	-1.24E+00	-1.15E+00	4.86E-02
ALA	30	N	443	ALA	30	C	1070	5.93E-01	-4.57E-01	-4.62E-01	-4.51E-01	5.71E-03
ALA	30	N	443	ILE	31	H	1086	4.91E-01	-4.07E-01	-4.12E-01	-4.02E-01	4.90E-03
ALA	30	C	445	PHE	19	CE2	923	4.30E-01	-3.81E-01	-4.03E-01	-3.59E-01	2.16E-02
ALA	30	C	445	PHE	19	CZ	924	3.58E-01	-3.90E-01	-4.07E-01	-3.73E-01	1.68E-02
ALA	30	C	445	LYS	28	O	1042	6.70E-01	-5.00E-01	-5.41E-01	-4.60E-01	4.05E-02
ALA	30	C	445	GLY	29	N	1061	6.48E-01	-3.51E-01	-3.60E-01	-3.41E-01	9.87E-03
ALA	30	C	445	GLY	29	O	1064	3.29E-01	-2.50E+00	-2.62E+00	-2.38E+00	1.23E-01
ALA	30	C	445	ALA	30	N	1068	4.84E-01	-7.27E-01	-7.42E-01	-7.12E-01	1.47E-02
ALA	30	C	445	ALA	30	O	1071	6.06E-01	-5.99E-01	-6.02E-01	-5.95E-01	3.44E-03
ALA	30	C	445	ALA	30	CB	1072	5.41E-01	-3.18E-01	-3.20E-01	-3.15E-01	2.81E-03
ALA	30	C	445	ILE	31	N	1078	4.17E-01	-1.17E+00	-1.18E+00	-1.16E+00	1.02E-02
ALA	30	C	445	ILE	31	O	1081	4.41E-01	-1.40E+00	-1.43E+00	-1.38E+00	2.34E-02
ALA	30	C	445	ILE	32	N	1097	6.47E-01	-4.23E-01	-4.26E-01	-4.20E-01	3.19E-03
ALA	30	O	446	PHE	19	HE2	932	3.66E-01	-4.53E-01	-5.01E-01	-4.04E-01	4.87E-02
ALA	30	O	446	PHE	19	HZ	933	2.50E-01	-1.21E+00	-1.21E+00	-1.21E+00	1.45E-16
ALA	30	O	446	ASN	27	C	1027	7.83E-01	-3.94E-01	-4.10E-01	-3.78E-01	1.62E-02
ALA	30	O	446	LYS	28	C	1041	6.49E-01	-6.61E-01	-6.90E-01	-6.32E-01	2.90E-02
ALA	30	O	446	GLY	29	C	1063	3.53E-01	-2.30E+00	-2.37E+00	-2.22E+00	7.43E-02
ALA	30	O	446	ALA	30	C	1070	3.61E-01	-2.11E+00	-2.13E+00	-2.08E+00	2.32E-02
ALA	30	O	446	ALA	30	H	1073	4.82E-01	-5.21E-01	-5.32E-01	-5.09E-01	1.14E-02
ALA	30	O	446	ALA	30	HA	1074	2.42E-01	-1.40E+00	-1.40E+00	-1.40E+00	1.45E-16
ALA	30	O	446	ILE	31	C	1080	4.33E-01	-1.31E+00	-1.33E+00	-1.29E+00	1.71E-02
ALA	30	O	446	ILE	31	H	1086	2.04E-01	-6.35E+00	-6.45E+00	-6.25E+00	9.96E-02
ALA	30	O	446	ILE	32	C	1099	7.82E-01	-3.63E-01	-3.66E-01	-3.60E-01	2.92E-03
ALA	30	O	446	ILE	32	H	1105	6.18E-01	-3.31E-01	-3.33E-01	-3.28E-01	2.63E-03
ALA	30	CB	447	PHE	19	HE2	932	2.78E-01	-3.99E-01	-4.26E-01	-3.72E-01	2.70E-02
ALA	30	CB	447	GLY	29	C	1063	4.69E-01	-4.54E-01	-4.68E-01	-4.40E-01	1.39E-02
ALA	30	CB	447	ALA	30	C	1070	5.49E-01	-3.07E-01	-3.09E-01	-3.05E-01	1.83E-03
ALA	30	H	448	LYS	28	O	1042	4.00E-01	-8.96E-01	-1.07E+00	-7.21E-01	1.75E-01
ALA	30	H	448	GLY	29	N	1061	4.46E-01	-4.24E-01	-4.38E-01	-4.09E-01	1.47E-02
ALA	30	H	448	GLY	29	O	1064	2.76E-01	-2.52E+00	-3.40E+00	-1.64E+00	8.79E-01
ALA	30	H	448	ALA	30	N	1068	4.14E-01	-5.55E-01	-5.76E-01	-5.33E-01	2.12E-02
ILE	31	N	453	PHE	19	HZ	933	3.15E-01	-5.12E-01	-5.54E-01	-4.70E-01	4.15E-02
ILE	31	N	453	LYS	28	C	1041	8.15E-01	-3.50E-01	-3.62E-01	-3.38E-01	1.19E-02

ILE	31	N	453	GLY	29	C	1063	5.50E-01	-6.14E-01	-6.31E-01	-5.97E-01	1.70E-02
ILE	31	N	453	ALA	30	C	1070	5.73E-01	-5.48E-01	-5.52E-01	-5.44E-01	4.08E-03
ILE	31	N	453	ILE	31	C	1080	5.30E-01	-6.53E-01	-6.61E-01	-6.45E-01	8.18E-03
ILE	31	N	453	ILE	31	H	1086	3.87E-01	-8.23E-01	-8.32E-01	-8.14E-01	8.74E-03
ILE	31	C	455	GLY	29	O	1064	6.31E-01	-5.04E-01	-5.20E-01	-4.87E-01	1.64E-02
ILE	31	C	455	ALA	30	O	1071	7.79E-01	-3.65E-01	-3.66E-01	-3.64E-01	1.38E-03
ILE	31	C	455	ILE	31	N	1078	5.55E-01	-5.88E-01	-5.91E-01	-5.84E-01	3.45E-03
ILE	31	C	455	ILE	31	O	1081	3.63E-01	-2.33E+00	-2.37E+00	-2.29E+00	4.13E-02
ILE	31	C	455	ILE	32	N	1097	5.75E-01	-5.43E-01	-5.50E-01	-5.36E-01	7.09E-03
ILE	31	C	455	ILE	32	O	1100	7.93E-01	-3.95E-01	-3.98E-01	-3.92E-01	3.08E-03
ILE	31	O	456	GLY	29	C	1063	8.23E-01	-3.78E-01	-3.84E-01	-3.72E-01	6.20E-03
ILE	31	O	456	ALA	30	C	1070	7.83E-01	-4.05E-01	-4.07E-01	-4.03E-01	1.98E-03
ILE	31	O	456	ILE	31	C	1080	6.07E-01	-6.65E-01	-6.71E-01	-6.60E-01	5.57E-03
ILE	31	O	456	ILE	31	H	1086	5.84E-01	-4.17E-01	-4.21E-01	-4.14E-01	3.40E-03
ILE	31	O	456	ILE	32	C	1099	7.96E-01	-3.92E-01	-3.99E-01	-3.85E-01	7.18E-03
ILE	31	H	461	GLY	29	O	1064	5.07E-01	-4.73E-01	-4.89E-01	-4.58E-01	1.56E-02
ILE	31	H	461	ILE	31	N	1078	5.80E-01	-3.08E-01	-3.10E-01	-3.06E-01	1.92E-03
ILE	31	H	461	ILE	31	O	1081	5.15E-01	-5.54E-01	-5.65E-01	-5.44E-01	1.03E-02
ILE	31	HA	462	ILE	31	N	1078	3.51E-01	-5.67E-01	-5.77E-01	-5.57E-01	1.01E-02
ILE	31	HA	462	ILE	31	O	1081	2.44E-01	-2.18E+00	-2.18E+00	-2.18E+00	0.00E+00
ILE	32	N	472	PHE	19	HE1	931	3.47E-01	-4.20E-01	-4.52E-01	-3.88E-01	3.20E-02
ILE	32	N	472	ALA	30	C	1070	6.67E-01	-3.99E-01	-4.01E-01	-3.96E-01	2.51E-03
ILE	32	N	472	ILE	31	C	1080	4.18E-01	-1.17E+00	-1.18E+00	-1.15E+00	1.10E-02
ILE	32	N	472	ILE	31	H	1086	4.79E-01	-4.79E-01	-4.83E-01	-4.76E-01	3.50E-03
ILE	32	N	472	ILE	32	C	1099	5.72E-01	-5.51E-01	-5.68E-01	-5.34E-01	1.72E-02
ILE	32	N	472	ILE	32	HA	1106	3.61E-01	-5.27E-01	-5.54E-01	-4.99E-01	2.74E-02
ILE	32	C	474	ILE	31	N	1078	7.06E-01	-3.56E-01	-3.60E-01	-3.51E-01	4.63E-03
ILE	32	C	474	ILE	31	O	1081	4.23E-01	-1.55E+00	-1.60E+00	-1.50E+00	4.72E-02
ILE	32	C	474	ILE	32	N	1097	5.16E-01	-6.95E-01	-7.05E-01	-6.84E-01	1.05E-02
ILE	32	C	474	ILE	32	O	1100	5.73E-01	-7.57E-01	-7.92E-01	-7.22E-01	3.48E-02
ILE	32	C	474	GLY	33	N	1116	4.87E-01	-6.79E-01	-7.51E-01	-6.07E-01	7.18E-02
ILE	32	C	474	GLY	33	O	1119	5.39E-01	-7.45E-01	-8.51E-01	-6.40E-01	1.06E-01
ILE	32	O	475	LYS	16	C	859	8.95E-01	-4.14E-01	-4.38E-01	-3.90E-01	2.42E-02
ILE	32	O	475	LEU	17	C	881	8.06E-01	-3.89E-01	-4.09E-01	-3.70E-01	1.96E-02
ILE	32	O	475	VAL	18	H	905	7.23E-01	-3.63E-01	-3.81E-01	-3.45E-01	1.77E-02
ILE	32	O	475	ALA	30	C	1070	8.39E-01	-3.60E-01	-3.71E-01	-3.48E-01	1.13E-02
ILE	32	O	475	ILE	31	C	1080	5.09E-01	-1.00E+00	-1.08E+00	-9.23E-01	7.90E-02
ILE	32	O	475	ILE	32	C	1099	4.19E-01	-1.64E+00	-1.84E+00	-1.44E+00	1.97E-01
ILE	32	O	475	ILE	32	H	1105	5.72E-01	-4.42E-01	-4.74E-01	-4.09E-01	3.25E-02
ILE	32	O	475	ILE	32	HA	1106	2.83E-01	-1.53E+00	-1.79E+00	-1.27E+00	2.61E-01
ILE	32	O	475	GLY	33	C	1118	5.36E-01	-9.38E-01	-1.06E+00	-8.11E-01	1.27E-01

ILE	32	O	475	LEU	34	C	1125	7.79E-01	-4.13E-01	-4.35E-01	-3.91E-01	2.21E-02
ILE	32	H	480	ILE	31	N	1078	4.65E-01	-5.14E-01	-5.19E-01	-5.09E-01	4.75E-03
ILE	32	H	480	ILE	31	O	1081	2.04E-01	-7.02E+00	-7.14E+00	-6.89E+00	1.25E-01
ILE	32	H	480	ILE	32	N	1097	3.89E-01	-8.13E-01	-8.29E-01	-7.97E-01	1.62E-02
ILE	32	H	480	ILE	32	O	1100	5.94E-01	-4.02E-01	-4.07E-01	-3.97E-01	5.14E-03
ILE	32	HA	481	ILE	31	O	1081	4.95E-01	-3.22E-01	-3.24E-01	-3.20E-01	2.03E-03
GLY	33	N	491	ILE	31	C	1080	5.55E-01	-5.06E-01	-5.84E-01	-4.28E-01	7.81E-02
GLY	33	N	491	ILE	32	C	1099	5.19E-01	-5.79E-01	-6.41E-01	-5.17E-01	6.19E-02
GLY	33	N	491	ILE	32	HA	1106	3.74E-01	-4.39E-01	-5.67E-01	-3.10E-01	1.28E-01
GLY	33	N	491	GLY	33	C	1118	5.33E-01	-5.50E-01	-5.85E-01	-5.15E-01	3.48E-02
GLY	33	C	493	ILE	31	O	1081	6.92E-01	-5.28E-01	-5.81E-01	-4.75E-01	5.30E-02
GLY	33	C	493	ILE	32	N	1097	7.32E-01	-3.47E-01	-3.87E-01	-3.07E-01	4.00E-02
GLY	33	C	493	ILE	32	O	1100	6.98E-01	-5.39E-01	-6.39E-01	-4.40E-01	9.96E-02
GLY	33	C	493	GLY	33	N	1116	5.56E-01	-4.97E-01	-5.18E-01	-4.75E-01	2.15E-02
GLY	33	C	493	GLY	33	O	1119	4.20E-01	-1.36E+00	-1.50E+00	-1.22E+00	1.42E-01
GLY	33	C	493	LEU	34	N	1123	5.15E-01	-5.62E-01	-5.88E-01	-5.37E-01	2.56E-02
GLY	33	C	493	LEU	34	O	1126	6.81E-01	-4.84E-01	-4.99E-01	-4.68E-01	1.56E-02
GLY	33	C	493	MET	35	N	1142	5.50E-01	-5.43E-01	-5.86E-01	-5.00E-01	4.29E-02
GLY	33	C	493	VAL	36	N	1159	6.78E-01	-3.97E-01	-4.26E-01	-3.69E-01	2.86E-02
GLY	33	O	494	ILE	32	C	1099	7.03E-01	-4.18E-01	-4.74E-01	-3.61E-01	5.67E-02
GLY	33	O	494	GLY	33	C	1118	5.71E-01	-6.39E-01	-6.67E-01	-6.11E-01	2.78E-02
GLY	33	O	494	LEU	34	C	1125	6.42E-01	-4.93E-01	-5.23E-01	-4.63E-01	2.99E-02
GLY	33	H	495	ILE	31	O	1081	4.94E-01	-5.34E-01	-7.03E-01	-3.66E-01	1.68E-01
LEU	34	N	498	GLY	33	C	1118	4.93E-01	-6.28E-01	-6.66E-01	-5.89E-01	3.87E-02
LEU	34	N	498	LEU	34	C	1125	5.17E-01	-5.55E-01	-6.00E-01	-5.11E-01	4.44E-02
LEU	34	C	500	GLY	33	O	1119	5.48E-01	-7.01E-01	-7.66E-01	-6.35E-01	6.55E-02
LEU	34	C	500	LEU	34	N	1123	5.71E-01	-4.38E-01	-4.56E-01	-4.21E-01	1.77E-02
LEU	34	C	500	LEU	34	O	1126	5.93E-01	-6.44E-01	-7.16E-01	-5.73E-01	7.19E-02
LEU	34	C	500	MET	35	N	1142	4.22E-01	-1.06E+00	-1.20E+00	-9.12E-01	1.46E-01
LEU	34	C	500	MET	35	O	1145	7.25E-01	-4.34E-01	-4.67E-01	-4.02E-01	3.22E-02
LEU	34	C	500	VAL	36	N	1159	6.09E-01	-4.91E-01	-5.30E-01	-4.52E-01	3.92E-02
LEU	34	O	501	GLY	33	C	1118	5.44E-01	-8.11E-01	-9.19E-01	-7.02E-01	1.09E-01
LEU	34	O	501	LEU	34	C	1125	3.86E-01	-1.87E+00	-2.10E+00	-1.64E+00	2.31E-01
LEU	34	O	501	LEU	34	HA	1132	3.02E-01	-9.62E-01	-1.21E+00	-7.09E-01	2.53E-01
LEU	34	O	501	MET	35	C	1144	5.23E-01	-9.51E-01	-1.09E+00	-8.09E-01	1.42E-01
LEU	34	O	501	VAL	36	H	1166	4.65E-01	-9.40E-01	-1.10E+00	-7.78E-01	1.62E-01
MET	35	N	517	LEU	34	C	1125	5.71E-01	-5.03E-01	-5.85E-01	-4.20E-01	8.27E-02
MET	35	N	517	MET	35	C	1144	6.46E-01	-3.93E-01	-4.05E-01	-3.81E-01	1.17E-02
MET	35	N	517	MET	35	H	1150	4.07E-01	-5.53E-01	-6.08E-01	-4.99E-01	5.47E-02
MET	35	N	517	VAL	36	H	1166	5.62E-01	-3.89E-01	-4.08E-01	-3.69E-01	1.99E-02
MET	35	C	519	GLY	33	O	1119	6.26E-01	-6.03E-01	-7.43E-01	-4.63E-01	1.40E-01

MET	35	C	519	LEU	34	O	1126	6.22E-01	-6.23E-01	-7.28E-01	-5.17E-01	1.05E-01
MET	35	C	519	MET	35	N	1142	4.19E-01	-1.07E+00	-1.13E+00	-1.02E+00	5.40E-02
MET	35	C	519	MET	35	O	1145	5.86E-01	-6.92E-01	-7.29E-01	-6.56E-01	3.63E-02
MET	35	C	519	VAL	36	N	1159	4.71E-01	-9.18E-01	-9.95E-01	-8.41E-01	7.69E-02
MET	35	C	519	VAL	36	O	1162	5.02E-01	-7.29E-01	-8.29E-01	-6.29E-01	9.99E-02
MET	35	O	520	GLY	33	C	1118	6.87E-01	-5.20E-01	-6.21E-01	-4.20E-01	1.00E-01
MET	35	O	520	LEU	34	C	1125	4.94E-01	-1.03E+00	-1.20E+00	-8.51E-01	1.74E-01
MET	35	O	520	MET	35	C	1144	3.97E-01	-1.78E+00	-1.92E+00	-1.64E+00	1.39E-01
MET	35	O	520	MET	35	H	1150	3.40E-01	-1.51E+00	-2.08E+00	-9.46E-01	5.69E-01
MET	35	O	520	MET	35	HA	1151	2.52E-01	-1.31E+00	-1.42E+00	-1.20E+00	1.12E-01
MET	35	O	520	VAL	36	C	1161	5.07E-01	-7.34E-01	-8.27E-01	-6.41E-01	9.32E-02
MET	35	O	520	VAL	36	CB	1163	5.95E-01	-4.63E-01	-5.40E-01	-3.85E-01	7.75E-02
MET	35	O	520	VAL	36	H	1166	3.58E-01	-2.28E+00	-3.34E+00	-1.22E+00	1.06E+00
MET	35	O	520	GLY	37	C	1177	7.47E-01	-4.12E-01	-4.30E-01	-3.94E-01	1.79E-02
VAL	36	N	534	GLY	33	C	1118	6.90E-01	-3.90E-01	-4.41E-01	-3.39E-01	5.05E-02
VAL	36	N	534	LEU	34	C	1125	5.85E-01	-5.34E-01	-5.82E-01	-4.86E-01	4.78E-02
VAL	36	N	534	MET	35	C	1144	5.32E-01	-6.90E-01	-7.55E-01	-6.26E-01	6.44E-02
VAL	36	N	534	MET	35	H	1150	4.15E-01	-6.17E-01	-7.23E-01	-5.12E-01	1.05E-01
VAL	36	N	534	VAL	36	C	1161	5.60E-01	-4.54E-01	-4.78E-01	-4.30E-01	2.39E-02
VAL	36	N	534	VAL	36	H	1166	4.13E-01	-9.33E-01	-9.83E-01	-8.84E-01	4.97E-02
VAL	36	C	536	VAL	36	N	1159	5.26E-01	-5.26E-01	-5.71E-01	-4.81E-01	4.49E-02
VAL	36	C	536	VAL	36	O	1162	3.72E-01	-1.13E+00	-1.22E+00	-1.04E+00	8.63E-02
VAL	36	C	536	GLY	37	N	1175	5.74E-01	-3.56E-01	-3.70E-01	-3.42E-01	1.40E-02
VAL	36	O	537	VAL	36	C	1161	6.01E-01	-3.49E-01	-3.59E-01	-3.38E-01	1.01E-02
VAL	36	O	537	VAL	36	H	1166	5.87E-01	-3.62E-01	-3.74E-01	-3.49E-01	1.25E-02
VAL	36	CB	538	MET	35	N	1142	5.44E-01	-3.83E-01	-4.29E-01	-3.38E-01	4.53E-02
VAL	36	CB	538	VAL	36	N	1159	4.62E-01	-6.34E-01	-6.89E-01	-5.79E-01	5.47E-02
VAL	36	CB	538	VAL	36	O	1162	3.93E-01	-8.69E-01	-9.61E-01	-7.76E-01	9.27E-02
VAL	36	H	541	MET	35	N	1142	5.37E-01	-4.43E-01	-5.05E-01	-3.82E-01	6.14E-02
VAL	36	H	541	VAL	36	N	1159	5.66E-01	-4.36E-01	-4.54E-01	-4.17E-01	1.82E-02
VAL	36	H	541	VAL	36	O	1162	5.52E-01	-4.19E-01	-4.52E-01	-3.85E-01	3.38E-02
GLY	37	N	550	MET	35	C	1144	5.81E-01	-4.98E-01	-6.06E-01	-3.91E-01	1.07E-01
GLY	37	N	550	VAL	36	C	1161	4.18E-01	-7.70E-01	-8.41E-01	-7.00E-01	7.06E-02
GLY	37	N	550	VAL	36	H	1166	4.86E-01	-5.19E-01	-5.55E-01	-4.83E-01	3.64E-02
GLY	37	N	550	GLY	37	C	1177	4.83E-01	-7.37E-01	-8.77E-01	-5.96E-01	1.41E-01
GLY	37	C	552	VAL	36	N	1159	7.19E-01	-3.54E-01	-3.80E-01	-3.29E-01	2.56E-02
GLY	37	C	552	VAL	36	O	1162	4.68E-01	-8.25E-01	-9.27E-01	-7.22E-01	1.02E-01
GLY	37	C	552	GLY	37	N	1175	5.92E-01	-4.44E-01	-5.01E-01	-3.88E-01	5.65E-02
GLY	37	C	552	GLY	37	O	1178	4.81E-01	-1.11E+00	-1.42E+00	-7.92E-01	3.14E-01
GLY	37	C	552	GLY	38	N	1182	4.99E-01	-6.84E-01	-8.44E-01	-5.25E-01	1.60E-01
GLY	37	C	552	GLY	38	O	1185	7.07E-01	-4.16E-01	-4.56E-01	-3.75E-01	4.02E-02

GLY	37	C	552	VAL	39	N	1189	6.62E-01	-4.18E-01	-4.56E-01	-3.80E-01	3.79E-02
GLY	37	O	553	VAL	36	C	1161	5.94E-01	-4.83E-01	-5.82E-01	-3.84E-01	9.94E-02
GLY	37	O	553	GLY	37	C	1177	5.02E-01	-9.88E-01	-1.28E+00	-6.94E-01	2.93E-01
GLY	37	O	553	GLY	38	C	1184	6.46E-01	-5.43E-01	-7.01E-01	-3.85E-01	1.58E-01
GLY	37	H	554	VAL	36	N	1159	4.35E-01	-4.93E-01	-5.86E-01	-3.99E-01	9.34E-02
GLY	37	H	554	VAL	36	O	1162	2.25E-01	-3.43E+00	-4.23E+00	-2.63E+00	8.04E-01
GLY	37	H	554	GLY	37	N	1175	3.95E-01	-5.02E-01	-5.33E-01	-4.72E-01	3.08E-02
GLY	38	N	557	GLY	37	C	1177	4.97E-01	-6.85E-01	-8.27E-01	-5.44E-01	1.41E-01
GLY	38	N	557	GLY	38	C	1184	5.91E-01	-4.41E-01	-4.80E-01	-4.03E-01	3.84E-02
GLY	38	C	559	VAL	36	O	1162	6.19E-01	-4.54E-01	-5.45E-01	-3.62E-01	9.11E-02
GLY	38	C	559	GLY	37	O	1178	5.30E-01	-9.00E-01	-1.21E+00	-5.89E-01	3.11E-01
GLY	38	C	559	GLY	38	N	1182	4.86E-01	-7.17E-01	-8.54E-01	-5.79E-01	1.37E-01
GLY	38	C	559	GLY	38	O	1185	5.84E-01	-6.06E-01	-6.23E-01	-5.89E-01	1.69E-02
GLY	38	C	559	VAL	39	N	1189	4.52E-01	-9.74E-01	-1.01E+00	-9.34E-01	3.98E-02
GLY	38	C	559	VAL	39	O	1192	4.97E-01	-7.04E-01	-7.52E-01	-6.55E-01	4.84E-02
GLY	38	C	559	VAL	40	N	1205	6.99E-01	-3.70E-01	-3.83E-01	-3.57E-01	1.30E-02
GLY	38	O	560	VAL	36	C	1161	5.98E-01	-4.70E-01	-5.55E-01	-3.84E-01	8.55E-02
GLY	38	O	560	GLY	37	C	1177	4.50E-01	-1.15E+00	-1.31E+00	-9.95E-01	1.60E-01
GLY	38	O	560	GLY	38	C	1184	3.94E-01	-1.58E+00	-1.73E+00	-1.44E+00	1.43E-01
GLY	38	O	560	GLY	38	H	1186	4.26E-01	-1.01E+00	-1.72E+00	-2.89E-01	7.18E-01
GLY	38	O	560	VAL	39	C	1191	5.22E-01	-6.07E-01	-6.56E-01	-5.57E-01	4.96E-02
GLY	38	O	560	VAL	39	CB	1193	4.80E-01	-6.53E-01	-6.98E-01	-6.08E-01	4.49E-02
GLY	38	O	560	VAL	39	H	1196	3.39E-01	-2.00E+00	-2.56E+00	-1.44E+00	5.57E-01
VAL	39	N	564	GLY	37	C	1177	6.46E-01	-4.38E-01	-4.72E-01	-4.03E-01	3.44E-02
VAL	39	N	564	GLY	38	C	1184	5.44E-01	-6.26E-01	-6.41E-01	-6.10E-01	1.54E-02
VAL	39	N	564	VAL	39	C	1191	5.45E-01	-4.82E-01	-5.05E-01	-4.59E-01	2.27E-02
VAL	39	N	564	VAL	39	CB	1193	5.75E-01	-3.78E-01	-3.91E-01	-3.64E-01	1.36E-02
VAL	39	N	564	VAL	39	H	1196	4.09E-01	-9.54E-01	-1.02E+00	-8.92E-01	6.13E-02
VAL	39	C	566	VAL	39	N	1189	5.37E-01	-5.00E-01	-5.26E-01	-4.74E-01	2.62E-02
VAL	39	C	566	VAL	39	O	1192	3.63E-01	-1.20E+00	-1.25E+00	-1.14E+00	5.48E-02
VAL	39	C	566	VAL	40	N	1205	5.77E-01	-4.23E-01	-4.34E-01	-4.11E-01	1.17E-02
VAL	39	C	566	ILE	41	O	1224	7.69E-01	-3.29E-01	-3.44E-01	-3.15E-01	1.48E-02
VAL	39	O	567	VAL	39	C	1191	6.02E-01	-3.48E-01	-3.52E-01	-3.43E-01	4.99E-03
VAL	39	O	567	VAL	39	H	1196	5.80E-01	-3.75E-01	-4.02E-01	-3.47E-01	2.76E-02
VAL	39	CB	568	VAL	39	N	1189	5.09E-01	-5.03E-01	-5.45E-01	-4.61E-01	4.20E-02
VAL	39	CB	568	VAL	39	O	1192	4.23E-01	-7.32E-01	-8.32E-01	-6.31E-01	1.01E-01
VAL	39	H	571	VAL	39	N	1189	5.63E-01	-4.40E-01	-4.51E-01	-4.29E-01	1.13E-02
VAL	39	H	571	VAL	39	O	1192	5.14E-01	-4.91E-01	-5.25E-01	-4.56E-01	3.43E-02
VAL	40	N	580	GLY	38	C	1184	6.34E-01	-4.52E-01	-4.74E-01	-4.30E-01	2.23E-02
VAL	40	N	580	VAL	39	C	1191	4.06E-01	-9.85E-01	-1.02E+00	-9.52E-01	3.24E-02
VAL	40	N	580	VAL	39	CB	1193	5.41E-01	-4.38E-01	-4.78E-01	-3.98E-01	3.99E-02

VAL	40	N	580	VAL	39	H	1196	4.54E-01	-7.44E-01	-8.30E-01	-6.57E-01	8.62E-02
VAL	40	N	580	VAL	40	C	1207	5.57E-01	-4.60E-01	-4.86E-01	-4.34E-01	2.61E-02
VAL	40	N	580	VAL	40	CB	1209	5.40E-01	-4.36E-01	-4.61E-01	-4.12E-01	2.47E-02
VAL	40	N	580	VAL	40	H	1212	5.76E-01	-4.19E-01	-4.25E-01	-4.12E-01	6.53E-03
VAL	40	N	580	ILE	41	C	1223	7.05E-01	-3.58E-01	-3.77E-01	-3.39E-01	1.91E-02
VAL	40	N	580	ILE	41	H	1229	4.53E-01	-5.62E-01	-6.33E-01	-4.91E-01	7.10E-02
VAL	40	C	582	VAL	39	O	1192	4.11E-01	-8.70E-01	-9.57E-01	-7.84E-01	8.64E-02
VAL	40	C	582	VAL	40	N	1205	5.21E-01	-5.34E-01	-5.57E-01	-5.10E-01	2.40E-02
VAL	40	C	582	VAL	40	O	1208	6.01E-01	-3.48E-01	-3.55E-01	-3.41E-01	6.84E-03
VAL	40	C	582	ILE	41	N	1221	4.08E-01	-9.74E-01	-1.02E+00	-9.32E-01	4.21E-02
VAL	40	C	582	ILE	41	O	1224	4.30E-01	-1.19E+00	-1.30E+00	-1.07E+00	1.16E-01
VAL	40	O	583	LYS	28	C	1041	8.00E-01	-3.24E-01	-3.30E-01	-3.17E-01	6.20E-03
VAL	40	O	583	VAL	39	C	1191	4.31E-01	-7.74E-01	-8.57E-01	-6.90E-01	8.36E-02
VAL	40	O	583	VAL	40	C	1207	3.59E-01	-1.23E+00	-1.24E+00	-1.21E+00	1.97E-02
VAL	40	O	583	VAL	40	CB	1209	4.26E-01	-6.95E-01	-7.33E-01	-6.56E-01	3.84E-02
VAL	40	O	583	VAL	40	H	1212	5.13E-01	-4.91E-01	-5.23E-01	-4.60E-01	3.14E-02
VAL	40	O	583	ILE	41	C	1223	4.15E-01	-1.09E+00	-1.24E+00	-9.47E-01	1.46E-01
VAL	40	O	583	ILE	41	H	1229	1.96E-01	-5.24E+00	-5.59E+00	-4.88E+00	3.54E-01
VAL	40	CB	584	VAL	39	O	1192	4.14E-01	-7.88E-01	-9.51E-01	-6.25E-01	1.63E-01
VAL	40	CB	584	VAL	40	N	1205	5.39E-01	-4.38E-01	-4.66E-01	-4.10E-01	2.78E-02
VAL	40	CB	584	ILE	41	N	1221	5.38E-01	-4.40E-01	-4.65E-01	-4.15E-01	2.50E-02
VAL	40	CB	584	ILE	41	O	1224	6.00E-01	-4.77E-01	-5.08E-01	-4.45E-01	3.16E-02
VAL	40	H	587	GLY	38	O	1185	6.45E-01	-3.72E-01	-3.89E-01	-3.56E-01	1.66E-02
VAL	40	H	587	VAL	39	N	1189	4.36E-01	-8.18E-01	-8.96E-01	-7.39E-01	7.85E-02
VAL	40	H	587	VAL	39	O	1192	1.96E-01	-6.96E+00	-7.28E+00	-6.63E+00	3.27E-01
VAL	40	H	587	VAL	40	N	1205	3.88E-01	-1.10E+00	-1.14E+00	-1.05E+00	4.46E-02
VAL	40	H	587	ILE	41	N	1221	4.76E-01	-6.62E-01	-7.36E-01	-5.88E-01	7.41E-02
VAL	40	H	587	ILE	41	O	1224	6.31E-01	-4.77E-01	-5.07E-01	-4.47E-01	3.01E-02
ILE	41	N	596	LYS	28	C	1041	8.05E-01	-3.57E-01	-3.69E-01	-3.46E-01	1.13E-02
ILE	41	N	596	VAL	39	C	1191	6.25E-01	-3.59E-01	-3.76E-01	-3.41E-01	1.73E-02
ILE	41	N	596	VAL	40	C	1207	5.74E-01	-4.29E-01	-4.34E-01	-4.25E-01	4.34E-03
ILE	41	N	596	ILE	41	C	1223	5.24E-01	-6.70E-01	-6.91E-01	-6.49E-01	2.06E-02
ILE	41	N	596	ILE	41	H	1229	3.85E-01	-8.33E-01	-8.44E-01	-8.21E-01	1.15E-02
ILE	41	C	598	LYS	28	O	1042	6.35E-01	-5.52E-01	-5.74E-01	-5.30E-01	2.18E-02
ILE	41	C	598	ILE	41	N	1221	5.54E-01	-5.91E-01	-5.98E-01	-5.84E-01	6.88E-03
ILE	41	C	598	ILE	41	O	1224	3.59E-01	-2.39E+00	-2.44E+00	-2.34E+00	5.08E-02
ILE	41	C	598	ALA	42	N	1240	5.72E-01	-4.93E-01	-5.00E-01	-4.86E-01	7.22E-03
ILE	41	C	598	ALA	42	O	1243	6.74E-01	-4.85E-01	-5.19E-01	-4.51E-01	3.37E-02
ILE	41	O	599	LYS	28	C	1041	8.14E-01	-4.82E-01	-5.02E-01	-4.63E-01	1.95E-02
ILE	41	O	599	VAL	40	C	1207	7.81E-01	-3.19E-01	-3.21E-01	-3.16E-01	2.50E-03
ILE	41	O	599	ILE	41	C	1223	6.01E-01	-6.78E-01	-6.88E-01	-6.69E-01	9.50E-03

ILE	41	O	599	ILE	41	H	1229	5.88E-01	-4.12E-01	-4.22E-01	-4.03E-01	9.29E-03
ILE	41	O	599	ALA	42	C	1242	6.72E-01	-5.43E-01	-5.71E-01	-5.14E-01	2.86E-02
ILE	41	H	604	ILE	41	N	1221	5.76E-01	-3.13E-01	-3.19E-01	-3.08E-01	5.66E-03
ILE	41	H	604	ILE	41	O	1224	5.14E-01	-5.57E-01	-5.69E-01	-5.44E-01	1.24E-02
ILE	41	HA	605	ILE	41	N	1221	3.55E-01	-5.49E-01	-5.73E-01	-5.24E-01	2.48E-02
ILE	41	HA	605	ILE	41	O	1224	2.45E-01	-2.16E+00	-2.19E+00	-2.12E+00	3.56E-02
ALA	42	N	615	LYS	28	C	1041	7.00E-01	-4.15E-01	-4.29E-01	-4.01E-01	1.43E-02
ALA	42	N	615	ILE	41	C	1223	4.10E-01	-1.10E+00	-1.12E+00	-1.08E+00	2.36E-02
ALA	42	N	615	ILE	41	H	1229	4.80E-01	-4.30E-01	-4.45E-01	-4.14E-01	1.57E-02
ALA	42	N	615	ALA	42	C	1242	4.52E-01	-8.79E-01	-9.67E-01	-7.90E-01	8.82E-02
ALA	42	C	617	LYS	28	O	1042	6.42E-01	-5.42E-01	-5.78E-01	-5.07E-01	3.52E-02
ALA	42	C	617	ILE	41	O	1224	4.82E-01	-1.13E+00	-1.20E+00	-1.06E+00	7.12E-02
ALA	42	C	617	ALA	42	N	1240	6.13E-01	-4.28E-01	-4.51E-01	-4.05E-01	2.26E-02
ALA	42	C	617	ALA	42	O	1243	5.40E-01	-7.84E-01	-8.50E-01	-7.19E-01	6.53E-02
ALA	42	O	618	LYS	28	C	1041	7.39E-01	-5.23E-01	-5.77E-01	-4.68E-01	5.45E-02
ALA	42	O	618	ILE	41	C	1223	6.10E-01	-6.09E-01	-7.00E-01	-5.19E-01	9.04E-02
ALA	42	O	618	ALA	42	C	1242	4.44E-01	-1.27E+00	-1.47E+00	-1.08E+00	1.94E-01
ALA	42	CB	619	ILE	41	C	1223	4.78E-01	-4.27E-01	-4.50E-01	-4.05E-01	2.27E-02
ALA	42	CB	619	ALA	42	C	1242	3.89E-01	-7.77E-01	-9.24E-01	-6.29E-01	1.48E-01
ALA	42	H	620	ILE	41	N	1221	4.59E-01	-4.76E-01	-4.85E-01	-4.66E-01	9.23E-03
ALA	42	H	620	ILE	41	O	1224	1.98E-01	-6.92E+00	-7.19E+00	-6.65E+00	2.70E-01
ALA	42	H	620	ALA	42	N	1240	3.85E-01	-6.71E-01	-6.85E-01	-6.57E-01	1.38E-02
ALA	42	H	620	ALA	42	O	1243	4.86E-01	-5.22E-01	-5.80E-01	-4.64E-01	5.79E-02

Supplementary Table 6b: Mapping results for A β 42's (PDB ID: 2NAO) short range (1:2) dominant atom-atom Lennard-Jones interactions across ensemble structures. Columns for each chain correspond to: residue abbreviation, residue number in peptide sequence, atom identity (IUPAC naming convention) and atom number in PDB file. Energy in kT , distance in nm . Mapping analysis began on the 11th residue for both isoforms because original structure data for A β 42 begins with the 11th residue.

Chain 1				Chain 2				Average Distance	Average L-J Values	Lower 95% Confidence Interval Bound	Upper 95% Confidence Interval Bound	Margin of Error
HIS	14	CA	199	HIS	14	O	826	4.19E-01	-1.54E-01	-1.71E-01	-1.37E-01	1.70E-02
HIS	14	C	200	HIS	14	O	826	3.86E-01	-1.88E-01	-1.96E-01	-1.79E-01	8.81E-03
GLN	15	N	215	HIS	14	C	825	3.89E-01	-1.87E-01	-1.90E-01	-1.84E-01	2.82E-03
GLN	15	C	217	LYS	16	N	857	4.12E-01	-1.57E-01	-1.62E-01	-1.52E-01	5.08E-03
GLN	15	O	218	HIS	14	C	825	3.84E-01	-1.88E-01	-2.07E-01	-1.69E-01	1.90E-02
GLN	15	O	218	GLN	15	N	840	4.19E-01	-1.72E-01	-1.88E-01	-1.56E-01	1.59E-02
GLN	15	O	218	GLN	15	CA	841	3.70E-01	-2.31E-01	-2.42E-01	-2.21E-01	1.05E-02
GLN	15	O	218	GLN	15	C	842	3.77E-01	-2.01E-01	-2.06E-01	-1.95E-01	5.70E-03
GLN	15	O	218	LYS	16	CA	858	3.80E-01	-2.20E-01	-2.29E-01	-2.11E-01	9.28E-03
GLN	15	O	218	LYS	16	O	860	3.97E-01	-1.99E-01	-2.34E-01	-1.65E-01	3.41E-02
GLN	15	CB	219	HIS	14	C	825	4.15E-01	-1.33E-01	-1.42E-01	-1.23E-01	9.21E-03
GLN	15	CB	219	GLN	15	CA	841	4.18E-01	-1.46E-01	-1.50E-01	-1.42E-01	3.99E-03
GLN	15	CG	220	HIS	14	O	826	4.18E-01	-1.55E-01	-1.81E-01	-1.30E-01	2.58E-02
LYS	16	CA	233	LYS	16	O	860	4.04E-01	-1.79E-01	-1.98E-01	-1.60E-01	1.88E-02
LYS	16	C	234	LYS	16	O	860	3.86E-01	-1.87E-01	-1.90E-01	-1.84E-01	2.54E-03
LEU	17	N	254	LYS	16	C	859	4.02E-01	-1.71E-01	-1.82E-01	-1.60E-01	1.09E-02
LEU	17	C	256	VAL	18	N	898	4.21E-01	-1.45E-01	-1.47E-01	-1.43E-01	2.18E-03
LEU	17	C	256	VAL	18	O	901	3.84E-01	-1.86E-01	-2.03E-01	-1.69E-01	1.70E-02
LEU	17	O	257	LEU	17	CA	880	3.74E-01	-2.21E-01	-2.35E-01	-2.06E-01	1.45E-02
LEU	17	O	257	LEU	17	C	881	3.84E-01	-1.90E-01	-1.98E-01	-1.83E-01	7.42E-03
LEU	17	O	257	VAL	18	CA	899	3.86E-01	-2.09E-01	-2.23E-01	-1.96E-01	1.32E-02
LEU	17	O	257	VAL	18	C	900	3.73E-01	-1.94E-01	-2.05E-01	-1.83E-01	1.11E-02
LEU	17	CB	258	LEU	17	CA	880	4.33E-01	-1.28E-01	-1.35E-01	-1.21E-01	7.25E-03
LEU	17	CB	258	LEU	17	CG	884	4.23E-01	-1.40E-01	-1.50E-01	-1.30E-01	1.02E-02
LEU	17	CB	258	LEU	17	CD1	885	3.78E-01	-1.68E-01	-1.75E-01	-1.60E-01	7.58E-03
LEU	17	CG	259	LEU	17	CD1	885	4.22E-01	-1.42E-01	-1.46E-01	-1.37E-01	4.84E-03
LEU	17	CD2	261	LEU	17	CG	884	4.04E-01	-1.61E-01	-1.68E-01	-1.53E-01	7.52E-03
VAL	18	N	273	VAL	18	O	901	4.03E-01	-2.06E-01	-2.29E-01	-1.83E-01	2.31E-02
VAL	18	CA	274	VAL	18	C	900	4.26E-01	-1.20E-01	-1.27E-01	-1.14E-01	6.83E-03
VAL	18	C	275	VAL	18	O	901	4.18E-01	-1.38E-01	-1.51E-01	-1.25E-01	1.32E-02
PHE	19	N	289	PHE	19	CA	915	4.45E-01	-1.28E-01	-1.35E-01	-1.20E-01	7.68E-03
PHE	19	CB	293	PHE	19	CG	919	4.28E-01	-1.18E-01	-1.24E-01	-1.13E-01	5.44E-03
PHE	19	CB	293	PHE	19	CD1	920	4.18E-01	-1.29E-01	-1.40E-01	-1.19E-01	1.03E-02

PHE	19	CB	293	PHE	19	CE1	922	3.93E-01	-1.40E-01	-1.48E-01	-1.32E-01	7.84E-03
PHE	20	CZ	319	PHE	19	CE2	923	4.10E-01	-1.22E-01	-1.29E-01	-1.16E-01	6.20E-03
ASP	23	CA	355	ASP	23	O	982	3.86E-01	-1.81E-01	-2.07E-01	-1.56E-01	2.56E-02
VAL	24	N	366	ASP	23	O	982	4.09E-01	-1.96E-01	-2.40E-01	-1.53E-01	4.34E-02
GLY	25	O	385	GLY	25	C	1009	4.15E-01	-1.41E-01	-1.49E-01	-1.33E-01	7.98E-03
GLY	25	O	385	SER	26	N	1014	3.94E-01	-2.25E-01	-2.52E-01	-1.98E-01	2.67E-02
SER	26	CA	390	SER	26	O	1017	4.26E-01	-1.41E-01	-1.49E-01	-1.32E-01	8.23E-03
SER	26	C	391	SER	26	O	1017	3.99E-01	-1.67E-01	-1.70E-01	-1.63E-01	3.20E-03
ASN	27	N	400	SER	26	C	1016	4.05E-01	-1.66E-01	-1.69E-01	-1.63E-01	3.23E-03
ASN	27	CA	401	SER	26	O	1017	3.36E-01	-1.84E-01	-2.12E-01	-1.56E-01	2.81E-02
ASN	27	C	402	SER	26	O	1017	3.85E-01	-1.88E-01	-2.01E-01	-1.75E-01	1.30E-02
ASN	27	C	402	LYS	28	N	1039	3.89E-01	-1.87E-01	-1.89E-01	-1.84E-01	2.72E-03
ASN	27	C	402	LYS	28	O	1042	3.86E-01	-1.78E-01	-1.98E-01	-1.59E-01	1.95E-02
ASN	27	O	403	SER	26	O	1017	3.62E-01	-2.85E-01	-3.10E-01	-2.60E-01	2.52E-02
ASN	27	O	403	ASN	27	CA	1026	4.29E-01	-1.38E-01	-1.46E-01	-1.29E-01	8.38E-03
ASN	27	O	403	ASN	27	C	1027	3.90E-01	-1.81E-01	-1.84E-01	-1.79E-01	2.68E-03
ASN	27	O	403	GLY	29	N	1061	4.01E-01	-2.10E-01	-2.41E-01	-1.79E-01	3.14E-02
ASN	27	CB	404	SER	26	C	1016	4.09E-01	-1.39E-01	-1.45E-01	-1.32E-01	6.76E-03
ASN	27	CB	404	ASN	27	CA	1026	4.05E-01	-1.61E-01	-1.64E-01	-1.59E-01	2.60E-03
ASN	27	CB	404	LYS	28	N	1039	4.15E-01	-1.72E-01	-1.85E-01	-1.60E-01	1.24E-02
ASN	27	CG	405	SER	26	C	1016	3.85E-01	-1.36E-01	-1.39E-01	-1.32E-01	3.57E-03
ASN	27	CG	405	ASN	27	CA	1026	4.24E-01	-1.23E-01	-1.30E-01	-1.15E-01	7.61E-03
LYS	28	N	414	LYS	28	O	1042	4.14E-01	-1.85E-01	-2.12E-01	-1.57E-01	2.78E-02
LYS	28	CA	415	LYS	28	O	1042	3.49E-01	-2.17E-01	-2.34E-01	-2.00E-01	1.69E-02
LYS	28	C	416	LYS	28	O	1042	3.75E-01	-2.03E-01	-2.08E-01	-1.97E-01	5.65E-03
LYS	28	CD	420	LYS	28	CB	1043	3.96E-01	-1.68E-01	-1.75E-01	-1.62E-01	6.47E-03
GLY	29	N	436	GLY	29	CA	1062	4.49E-01	-1.23E-01	-1.31E-01	-1.14E-01	9.00E-03
GLY	29	CA	437	GLY	29	O	1064	4.20E-01	-1.52E-01	-1.68E-01	-1.35E-01	1.65E-02
GLY	29	C	438	GLY	29	O	1064	3.91E-01	-1.79E-01	-1.91E-01	-1.68E-01	1.13E-02
ALA	30	N	443	GLY	29	C	1063	4.00E-01	-1.72E-01	-1.79E-01	-1.65E-01	6.63E-03
ALA	30	CA	444	PHE	19	CZ	924	4.20E-01	-1.27E-01	-1.33E-01	-1.21E-01	5.78E-03
ALA	30	CA	444	GLY	29	O	1064	3.66E-01	-2.16E-01	-2.34E-01	-1.97E-01	1.83E-02
ALA	30	C	445	ALA	30	CA	1069	4.38E-01	-1.08E-01	-1.10E-01	-1.06E-01	1.96E-03
ALA	30	C	445	ILE	31	N	1078	4.17E-01	-1.50E-01	-1.52E-01	-1.48E-01	1.82E-03
ALA	30	O	446	PHE	19	CE1	922	4.05E-01	-1.58E-01	-1.63E-01	-1.53E-01	5.05E-03
ALA	30	O	446	PHE	19	CE2	923	3.80E-01	-1.93E-01	-2.07E-01	-1.80E-01	1.34E-02
ALA	30	O	446	GLY	29	C	1063	3.53E-01	-2.14E-01	-2.16E-01	-2.11E-01	2.24E-03
ALA	30	O	446	ALA	30	N	1068	3.85E-01	-2.45E-01	-2.54E-01	-2.36E-01	9.08E-03
ALA	30	O	446	ALA	30	C	1070	3.61E-01	-2.17E-01	-2.17E-01	-2.16E-01	5.85E-04
ALA	30	O	446	ALA	30	CB	1072	4.44E-01	-1.16E-01	-1.18E-01	-1.13E-01	2.54E-03
ALA	30	O	446	ILE	31	CA	1079	4.06E-01	-1.74E-01	-1.77E-01	-1.71E-01	3.10E-03

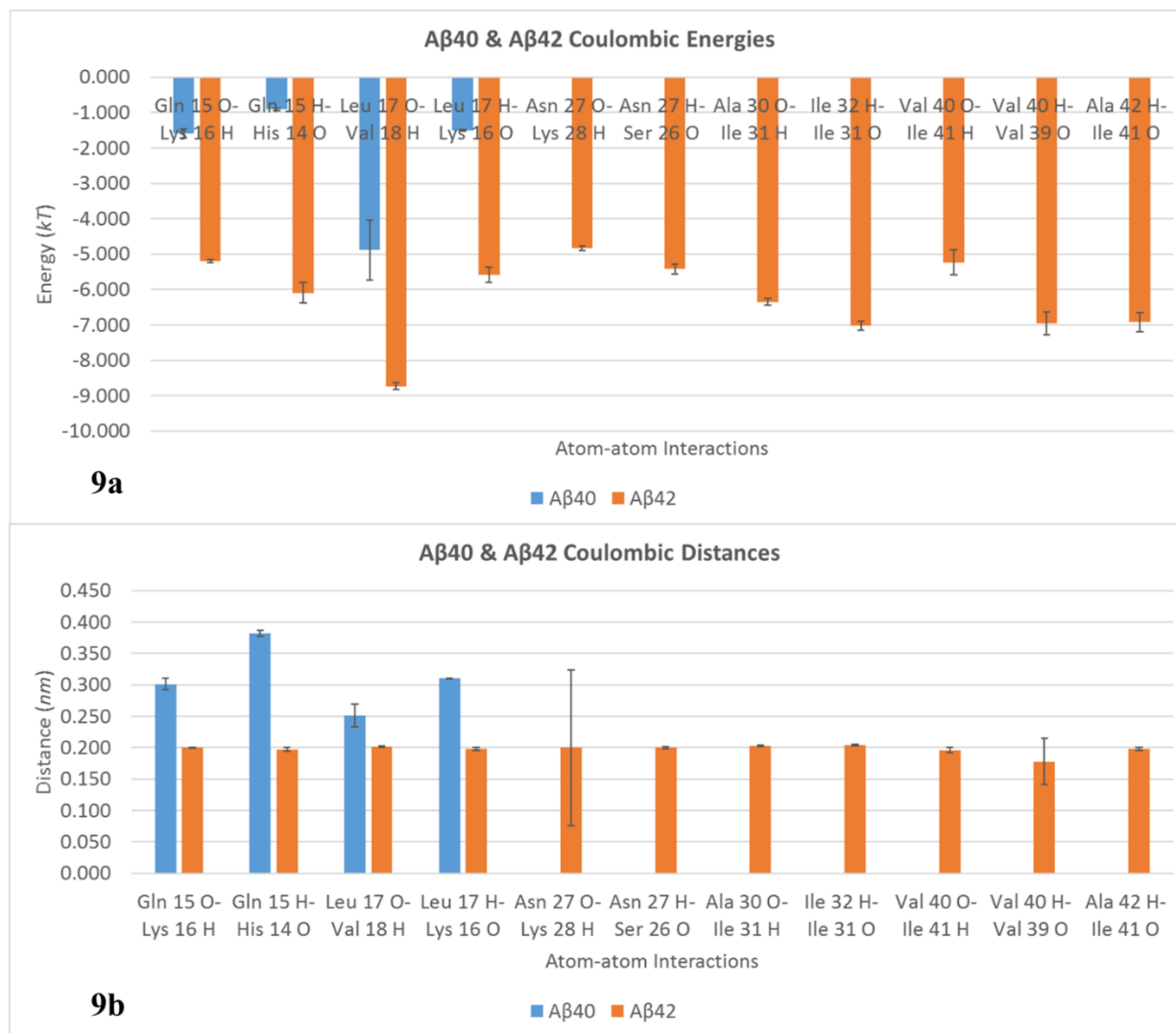
ALA	30	O	446	ILE	31	C	1080	4.33E-01	-1.16E-01	-1.19E-01	-1.13E-01	2.80E-03
ALA	30	O	446	ILE	31	O	1081	3.74E-01	-2.53E-01	-2.60E-01	-2.46E-01	7.27E-03
ALA	30	O	446	ILE	31	CG1	1083	3.98E-01	-1.89E-01	-1.99E-01	-1.80E-01	9.64E-03
ALA	30	CB	447	GLY	29	O	1064	4.09E-01	-1.70E-01	-1.93E-01	-1.46E-01	2.37E-02
ALA	30	CB	447	ALA	30	CA	1069	4.43E-01	-1.16E-01	-1.18E-01	-1.14E-01	1.92E-03
ILE	31	N	453	GLY	29	O	1064	4.36E-01	-1.41E-01	-1.51E-01	-1.30E-01	1.04E-02
ILE	31	N	453	ILE	31	O	1081	4.29E-01	-1.52E-01	-1.58E-01	-1.46E-01	5.94E-03
ILE	31	CA	454	ILE	31	N	1078	4.51E-01	-1.19E-01	-1.22E-01	-1.16E-01	2.91E-03
ILE	31	CA	454	ILE	31	CG1	1083	3.67E-01	-1.64E-01	-1.66E-01	-1.62E-01	2.46E-03
ILE	31	CA	454	ILE	31	CD1	1085	3.92E-01	-1.73E-01	-1.75E-01	-1.70E-01	2.29E-03
ILE	31	C	455	ILE	31	O	1081	3.63E-01	-2.16E-01	-2.17E-01	-2.14E-01	1.51E-03
ILE	31	CB	457	ILE	31	O	1081	4.06E-01	-1.74E-01	-1.82E-01	-1.67E-01	7.53E-03
ILE	31	CG2	459	GLY	29	O	1064	4.03E-01	-1.81E-01	-2.05E-01	-1.57E-01	2.44E-02
ILE	31	CG2	459	ILE	31	CB	1082	4.49E-01	-1.09E-01	-1.11E-01	-1.06E-01	2.43E-03
ILE	31	CG2	459	ILE	31	CD1	1085	3.81E-01	-1.75E-01	-1.78E-01	-1.73E-01	2.49E-03
ILE	32	N	472	ILE	31	C	1080	4.18E-01	-1.49E-01	-1.51E-01	-1.47E-01	2.15E-03
ILE	32	N	472	ILE	31	CG1	1083	4.60E-01	-1.09E-01	-1.11E-01	-1.06E-01	2.24E-03
ILE	32	N	472	ILE	31	CD1	1085	4.16E-01	-1.71E-01	-1.77E-01	-1.66E-01	5.25E-03
ILE	32	CA	473	ILE	31	O	1081	4.07E-01	-1.74E-01	-1.76E-01	-1.71E-01	2.47E-03
ILE	32	C	474	ILE	31	O	1081	4.23E-01	-1.29E-01	-1.36E-01	-1.22E-01	6.96E-03
ILE	32	C	474	ILE	32	CA	1098	4.23E-01	-1.24E-01	-1.28E-01	-1.21E-01	3.29E-03
ILE	32	O	475	ILE	32	CA	1098	3.69E-01	-2.17E-01	-2.45E-01	-1.88E-01	2.85E-02
ILE	32	O	475	ILE	32	CB	1101	3.88E-01	-2.05E-01	-2.29E-01	-1.80E-01	2.41E-02
ILE	32	O	475	ILE	32	CD1	1104	3.99E-01	-1.86E-01	-2.09E-01	-1.62E-01	2.32E-02
ILE	32	CG2	478	PHE	19	CD1	920	4.01E-01	-1.44E-01	-1.50E-01	-1.38E-01	5.90E-03
ILE	32	CG2	478	ILE	31	O	1081	3.92E-01	-2.00E-01	-2.19E-01	-1.82E-01	1.88E-02
GLY	33	CA	492	GLY	33	N	1116	4.30E-01	-1.49E-01	-1.56E-01	-1.41E-01	7.72E-03
MET	35	C	519	MET	35	N	1142	4.19E-01	-1.47E-01	-1.58E-01	-1.36E-01	1.06E-02
MET	35	C	519	MET	35	CA	1143	4.14E-01	-1.31E-01	-1.41E-01	-1.21E-01	9.75E-03
MET	35	O	520	MET	35	C	1144	3.97E-01	-1.69E-01	-1.85E-01	-1.53E-01	1.64E-02
MET	35	SD	523	MET	35	SD	1148	4.87E-01	-2.13E-01	-2.29E-01	-1.96E-01	1.68E-02
VAL	36	CA	535	VAL	36	N	1159	4.26E-01	-1.56E-01	-1.72E-01	-1.39E-01	1.65E-02
VAL	36	C	536	VAL	36	O	1162	3.72E-01	-2.04E-01	-2.23E-01	-1.86E-01	1.85E-02
VAL	36	CB	538	VAL	36	O	1162	3.93E-01	-1.95E-01	-2.16E-01	-1.74E-01	2.12E-02
GLY	38	O	560	GLY	38	C	1184	3.94E-01	-1.73E-01	-1.90E-01	-1.55E-01	1.70E-02
GLY	38	O	560	VAL	39	N	1189	3.80E-01	-2.41E-01	-2.67E-01	-2.16E-01	2.54E-02
VAL	39	CA	565	VAL	39	N	1189	4.43E-01	-1.31E-01	-1.43E-01	-1.19E-01	1.21E-02
VAL	39	C	566	VAL	39	O	1192	3.63E-01	-2.12E-01	-2.16E-01	-2.08E-01	4.03E-03
VAL	40	N	580	VAL	39	C	1191	4.06E-01	-1.65E-01	-1.71E-01	-1.59E-01	6.27E-03
VAL	40	CA	581	VAL	39	O	1192	3.84E-01	-2.01E-01	-2.13E-01	-1.88E-01	1.21E-02
VAL	40	C	582	VAL	39	O	1192	4.11E-01	-1.47E-01	-1.65E-01	-1.29E-01	1.84E-02

VAL	40	C	582	ILE	41	N	1221	4.08E-01	-1.62E-01	-1.69E-01	-1.54E-01	7.75E-03
VAL	40	O	583	VAL	39	O	1192	3.61E-01	-2.71E-01	-3.05E-01	-2.37E-01	3.41E-02
VAL	40	O	583	VAL	40	CA	1206	3.36E-01	-1.68E-01	-1.96E-01	-1.41E-01	2.74E-02
VAL	40	O	583	VAL	40	C	1207	3.59E-01	-2.17E-01	-2.18E-01	-2.17E-01	5.58E-04
VAL	40	O	583	VAL	40	CB	1209	4.26E-01	-1.42E-01	-1.56E-01	-1.29E-01	1.38E-02
VAL	40	O	583	ILE	41	CA	1222	3.92E-01	-1.98E-01	-2.12E-01	-1.83E-01	1.42E-02
VAL	40	O	583	ILE	41	C	1223	4.15E-01	-1.38E-01	-1.57E-01	-1.20E-01	1.82E-02
ILE	41	N	596	ILE	41	O	1224	4.26E-01	-1.58E-01	-1.69E-01	-1.46E-01	1.18E-02
ILE	41	CA	597	ILE	41	O	1224	3.33E-01	-1.74E-01	-1.94E-01	-1.55E-01	1.98E-02
ILE	41	C	598	ILE	41	O	1224	3.59E-01	-2.17E-01	-2.18E-01	-2.16E-01	7.57E-04
ILE	41	CB	600	ILE	41	O	1224	4.21E-01	-1.51E-01	-1.67E-01	-1.35E-01	1.59E-02
ILE	41	CG2	602	LYS	28	O	1042	3.67E-01	-2.33E-01	-2.41E-01	-2.25E-01	7.73E-03
ILE	41	CG2	602	ILE	41	O	1224	3.97E-01	-1.91E-01	-2.18E-01	-1.65E-01	2.68E-02
ILE	41	CG2	602	ILE	41	CB	1225	4.39E-01	-1.21E-01	-1.29E-01	-1.12E-01	8.10E-03
ALA	42	N	615	ILE	41	C	1223	4.10E-01	-1.60E-01	-1.65E-01	-1.56E-01	4.55E-03
ALA	42	N	615	ALA	42	CA	1241	4.53E-01	-1.17E-01	-1.21E-01	-1.12E-01	4.61E-03
ALA	42	CA	616	ILE	41	O	1224	3.95E-01	-1.95E-01	-2.02E-01	-1.87E-01	7.58E-03
ALA	42	CB	619	ILE	41	O	1224	3.89E-01	-2.05E-01	-2.22E-01	-1.88E-01	1.69E-02
ALA	42	CB	619	ALA	42	CA	1241	3.91E-01	-1.63E-01	-1.75E-01	-1.52E-01	1.16E-02

Supplementary Table 7: Mapping results for A β 42's (PDB ID: 2NAO) long range (1:3) dominant atom-atom Coulombic interactions across ensemble structures. Columns for each chain correspond to: residue abbreviation, residue number in peptide sequence, atom identity (IUPAC naming convention) and atom number in PDB file. Energy in kT , distance in nm . Mapping analysis began on the 11th residue for both isoforms because original structure data for A β 42 begins with the 11th residue.

Chain 1				Chain 2				Average Distance	Average Coulombic Values	Lower 95% Confidence Interval Bound	Upper 95% Confidence Interval Bound	Margin of Error
ALA	2	C	15	GLU	3	O	1276	8.54E-01	-3.33E-01	-3.40E-01	-3.26E-01	6.72E-03
ALA	2	O	16	GLU	3	CD	1279	8.97E-01	-3.91E-01	-4.23E-01	-3.59E-01	3.21E-02
PHE	4	C	40	GLU	3	O	1276	8.34E-01	-3.33E-01	-3.40E-01	-3.27E-01	6.82E-03
PHE	4	O	41	ARG	5	C	1310	8.32E-01	-3.81E-01	-3.89E-01	-3.73E-01	7.97E-03
ARG	5	C	60	ARG	5	O	1311	9.04E-01	-3.79E-01	-3.80E-01	-3.77E-01	1.81E-03
HIS	6	N	82	ARG	5	C	1310	9.18E-01	-3.37E-01	-3.39E-01	-3.36E-01	1.63E-03
HIS	6	C	84	ARG	5	O	1311	8.18E-01	-4.07E-01	-4.25E-01	-3.90E-01	1.75E-02
HIS	6	O	85	ARG	5	C	1310	8.57E-01	-3.80E-01	-3.97E-01	-3.63E-01	1.72E-02
HIS	6	O	85	HIS	6	C	1334	9.11E-01	-3.11E-01	-3.13E-01	-3.08E-01	2.40E-03
HIS	14	C	200	HIS	14	O	1451	8.75E-01	-3.32E-01	-3.38E-01	-3.25E-01	6.43E-03
GLN	15	O	218	HIS	14	C	1450	7.77E-01	-4.35E-01	-4.49E-01	-4.21E-01	1.41E-02
GLN	15	O	218	LYS	16	C	1484	8.48E-01	-4.09E-01	-4.14E-01	-4.03E-01	5.26E-03
GLN	15	CD	221	HIS	14	O	1451	7.68E-01	-4.33E-01	-4.85E-01	-3.81E-01	5.18E-02
LYS	16	C	234	LYS	16	O	1485	8.80E-01	-3.83E-01	-3.87E-01	-3.79E-01	4.14E-03
LEU	17	C	256	LYS	16	O	1485	7.90E-01	-3.66E-01	-3.88E-01	-3.45E-01	2.14E-02
LEU	17	O	257	LYS	16	C	1484	8.09E-01	-4.42E-01	-4.69E-01	-4.14E-01	2.74E-02
LEU	17	O	257	VAL	18	H	1530	7.00E-01	-3.46E-01	-3.51E-01	-3.41E-01	5.25E-03
ASN	27	C	402	SER	26	O	1642	8.24E-01	-3.75E-01	-3.82E-01	-3.69E-01	6.64E-03
ASN	27	C	402	LYS	28	O	1667	7.57E-01	-4.24E-01	-4.38E-01	-4.10E-01	1.38E-02
ASN	27	O	403	LYS	28	C	1666	7.25E-01	-5.01E-01	-5.13E-01	-4.90E-01	1.18E-02
ASN	27	CG	405	SER	26	O	1642	7.07E-01	-4.70E-01	-4.80E-01	-4.60E-01	9.73E-03
ASN	27	ND2	407	GLY	25	C	1634	8.51E-01	-4.63E-01	-5.12E-01	-4.14E-01	4.87E-02
ASN	27	ND2	407	SER	26	C	1641	7.84E-01	-4.48E-01	-5.00E-01	-3.96E-01	5.21E-02
ASN	27	ND2	407	LYS	28	C	1666	9.35E-01	-4.88E-01	-5.21E-01	-4.56E-01	3.28E-02
LYS	28	C	416	LYS	28	O	1667	8.50E-01	-4.06E-01	-4.09E-01	-4.02E-01	3.20E-03
ALA	30	C	445	GLY	29	O	1689	7.48E-01	-3.61E-01	-3.68E-01	-3.55E-01	6.83E-03
ALA	30	C	445	ILE	31	O	1706	8.30E-01	-3.66E-01	-3.69E-01	-3.62E-01	3.76E-03
ALA	30	O	446	LYS	28	C	1666	9.22E-01	-3.51E-01	-3.61E-01	-3.41E-01	9.87E-03
ALA	30	O	446	GLY	29	C	1688	7.42E-01	-4.08E-01	-4.11E-01	-4.04E-01	3.94E-03
ALA	30	O	446	ALA	30	C	1695	8.42E-01	-3.19E-01	-3.21E-01	-3.17E-01	1.73E-03
ALA	30	O	446	ILE	31	C	1705	8.25E-01	-3.30E-01	-3.33E-01	-3.27E-01	2.64E-03
ILE	31	C	455	ILE	31	O	1706	8.47E-01	-3.53E-01	-3.56E-01	-3.49E-01	3.49E-03

ILE	32	C	474	ILE	31	O	1706	8.11E-01	-3.80E-01	-3.82E-01	-3.77E-01	2.81E-03
MET	35	O	520	MET	35	C	1769	8.77E-01	-3.20E-01	-3.26E-01	-3.14E-01	6.36E-03
ILE	41	C	598	ILE	41	O	1849	8.36E-01	-3.61E-01	-3.65E-01	-3.56E-01	4.59E-03
ALA	42	C	617	ILE	41	O	1849	9.02E-01	-3.19E-01	-3.27E-01	-3.11E-01	8.02E-03



Supplementary Figure 9a & 9b: Atom-atom interactions imparting exceptionally strong hydrogen bonding energies in the 1:2 configuration of Aβ42 (PDB ID: 2NAO by Walti et al.) compared to Aβ40 (Aβ40 PDB ID: 2M4J by Lu et al.; Figure 9a) and their respective atom-atom interaction distances (Figure 9b). 95% confidence interval error bars included for analysis across all ensemble members. The last seven interactions were not observed in Aβ40. Interaction partners are presented as the residue, residue number in the sequence and the residue's atom of one chain (chain A for both strains) interacting with its partner atom in the 1:2 configuration (on the D-chain in Aβ40 or on the B-chain in Aβ42).

Supplementary Table 8: Ramachandran angle data for A β 40 and A β 42 for chains A-D (A β 40, PDB ID: 2M4J) and chains A-B (A β 42, PDB ID: 2NAO) for the 1:2 interaction configuration across ensemble structures. Data shown starts with residue 11 since structure data for previous A β 42 structure, 2MXU, begins at residue 11.

	A β 40				A β 42			
	Chain A		Chain D		Chain A		Chain B	
	ϕ	ψ	ϕ	ψ	ϕ	ψ	ϕ	ψ
GLU 11	-	152.910 \pm 0.711	-	151.350 \pm 0.487	-	-4.240 \pm 81.181	-	72.450 \pm 59.949
VAL 12	-153.140 \pm 0.201	128.500 \pm 0.357	-149.530 \pm 0.042	130.000 \pm 0.072	-93.290 \pm 55.607	113.060 \pm 35.490	-116.130 \pm 22.275	117.79 \pm 45.136
HIS 13	-135.180 \pm 0.296	146.43 \pm 0.743	-129.880 \pm 0.120	149.470 \pm 0.774	-116.280 \pm 29.775	-19.750 \pm 91.517	-50.350 \pm 61.484	81.920 \pm 64.146
HIS 14	-165.320 \pm 0.569	97.570 \pm 0.373	-165.060 \pm 0.128	104.570 \pm 0.113	-84.090 \pm 52.149	-57.370 \pm 75.291	-128.220 \pm 19.676	-31.780 \pm 46.998
GLN 15	-107.590 \pm 2.008	-173.870 \pm 0.751	-111.070 \pm 2.030	-176.020 \pm 0.175	-107.820 \pm 6.268	107.650 \pm 3.996	-108.000 \pm 6.295	107.510 \pm 3.976
LYS 16	-166.350 \pm 1.700	97.950 \pm 0.938	-162.970 \pm 1.638	105.720 \pm 0.414	-115.340 \pm 2.808	108.290 \pm 6.669	-115.170 \pm 2.661	107.720 \pm 6.858
LEU 17	-117.790 \pm 5.123	158.580 \pm 2.486	-124.310 \pm 5.075	156.280 \pm 2.852	-110.710 \pm 5.090	102.140 \pm 2.852	-111.320 \pm 4.949	101.870 \pm 2.856
VAL 18	-120.610 \pm 9.229	124.710 \pm 2.477	-112.980 \pm 11.974	129.400 \pm 2.469	-145.400 \pm 6.726	57.450 \pm 99.285	-145.160 \pm 6.407	57.160 \pm 99.162
PHE 19	-109.630 \pm 16.980	133.770 \pm 10.920	-110.030 \pm 20.201	133.850 \pm 7.521	-123.310 \pm 13.684	34.390 \pm 63.122	-123.000 \pm 13.958	33.890 \pm 62.975
PHE 20	-13.800 \pm 67.407	34.610 \pm 39.682	-12.140 \pm 67.546	30.070 \pm 41.404	-50.620 \pm 62.655	51.240 \pm 95.121	-50.790 \pm 62.556	50.620 \pm 95.154
ALA 21	-67.680 \pm 12.282	-27.670 \pm 50.357	-68.800 \pm 13.231	-22.500 \pm 50.612	-164.370 \pm 12.877	2.730 \pm 28.591	-164.770 \pm 13.002	2.540 \pm 28.334
GLU 22	-99.030 \pm 13.950	117.940 \pm 17.139	-102.000 \pm 14.163	120.760 \pm 16.175	-83.830 \pm 87.209	-55.680 \pm 65.302	-84.460 \pm 87.238	-55.520 \pm 65.156
ASP 23	-153.20 \pm 5.623	137.940 \pm 1.318	-148.460 \pm 3.594	139.130 \pm 1.409	-67.700 \pm 62.877	102.250 \pm 18.593	-67.680 \pm 62.879	102.520 \pm 18.424
VAL 24	-67.650 \pm 8.347	79.540 \pm 83.862	-70.530 \pm 8.460	80.410 \pm 85.689	-111.600 \pm 13.845	66.450 \pm 87.869	-111.540 \pm 13.905	30.280 \pm 95.969
GLY 25	-114.140 \pm 3.094	50.210 \pm 2.290	-114.730 \pm 2.429	54.310 \pm 3.261	-58.600 \pm 39.646	-96.630 \pm 12.439	-58.700 \pm 39.501	-96.650 \pm 12.330
SER 26	-67.480 \pm 6.196	-79.970 \pm 87.939	-61.550 \pm 4.009	-83.240 \pm 87.483	-119.940 \pm 9.193	134.660 \pm 4.032	-120.500 \pm 9.244	133.710 \pm 3.919
ASN 27	-69.580 \pm 1.699	86.480 \pm 5.961	-69.260 \pm 3.501	91.230 \pm 4.565	-95.740 \pm 2.109	86.080 \pm 3.222	-95.780 \pm 2.151	86.650 \pm 3.217
LYS 28	-82.690 \pm 5.998	135.220 \pm 7.876	-87.910 \pm 5.247	137.660 \pm 8.087	-107.230 \pm 4.571	74.870 \pm 9.705	-107.790 \pm 4.589	75.250 \pm 9.670
GLY 29	-62.690 \pm 0.809	-153.170 \pm 10.428	-60.700 \pm 2.630	-151.460 \pm 9.486	115.200 \pm 10.074	38.470 \pm 4.640	114.800 \pm 10.144	37.910 \pm 4.824
ALA 30	-104.030 \pm 6.560	122.180 \pm 4.709	-105.320 \pm 5.670	123.850 \pm 5.584	-85.960 \pm 5.934	109.160 \pm 3.274	-87.170 \pm 6.321	109.000 \pm 2.977
ILE 31	-100.480 \pm 8.486	130.830 \pm 4.794	-103.190 \pm 8.379	137.610 \pm 3.972	-134.990 \pm 2.373	134.630 \pm 1.413	-134.880 \pm 2.296	134.760 \pm 1.463
ILE 32	-147.380 \pm 4.687	-78.070 \pm 95.222	-152.980 \pm 5.812	-77.810 \pm 96.409	-146.220 \pm 2.943	76.470 \pm 11.805	-146.440 \pm 2.902	75.930 \pm 11.898
GLY 33	63.670 \pm 0.773	21.120 \pm 16.942	63.990 \pm 0.473	20.500 \pm 16.506	-129.870 \pm 15.586	83.040 \pm 66.649	-129.870 \pm 15.317	83.050 \pm 66.889
LEU 34	-83.930 \pm 8.423	126.710 \pm 3.472	-84.830 \pm 7.589	134.400 \pm 2.025	-98.330 \pm 27.120	119.26 \pm 19.960	-98.540 \pm 27.052	119.300 \pm 20.052
MET 35	-159.790 \pm 2.975	150.550 \pm 3.927	-157.400 \pm 0.722	160.480 \pm 2.626	75.600 \pm 22.512	49.090 \pm 13.019	75.480 \pm 22.453	49.030 \pm 13.049
VAL 36	-154.990 \pm 2.092	160.240 \pm 4.458	-163.110 \pm 1.703	161.350 \pm 2.732	-99.820 \pm 18.036	136.710 \pm 11.130	-99.780 \pm 18.086	136.680 \pm 11.262
GLY 37	55.960 \pm 0.472	69.450 \pm 2.115	60.710 \pm 0.370	64.440 \pm 0.783	-88.700 \pm 16.855	-43.430 \pm 71.753	-88.560 \pm 16.874	-43.380 \pm 71.808
GLY 38	152.790 \pm 7.822	7.410 \pm 109.716	150.820 \pm 7.315	8.980 \pm 110.119	-8.570 \pm 65.125	150.790 \pm 14.656	-8.720 \pm 65.157	150.540 \pm 14.674
VAL 39	-122.680 \pm 5.114	153.420 \pm 4.657	-123.450 \pm 4.172	151.310 \pm 3.842	-163.010 \pm 13.144	133.610 \pm 6.114	-163.140 \pm 13.185	133.530 \pm 6.077
VAL 40	65.280 \pm 0.705	-	73.420 \pm 1.158	-	-127.460 \pm 4.471	120.360 \pm 6.579	-127.240 \pm 4.432	120.490 \pm 6.625
ILE 41	-	-	-	-	-126.180 \pm 6.807	129.900 \pm 2.870	-125.960 \pm 6.786	129.880 \pm 2.861

ALA 42

-

-

|

-

-

|

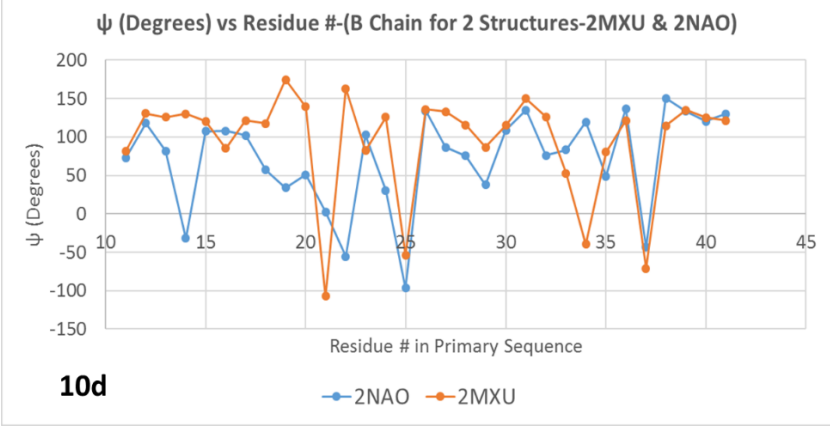
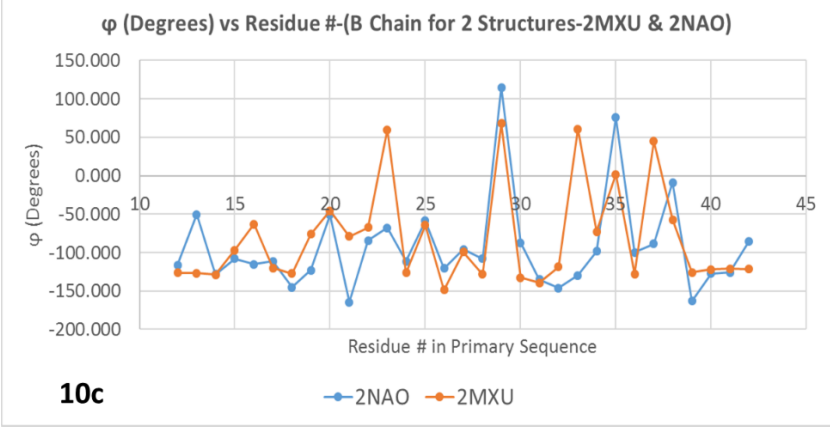
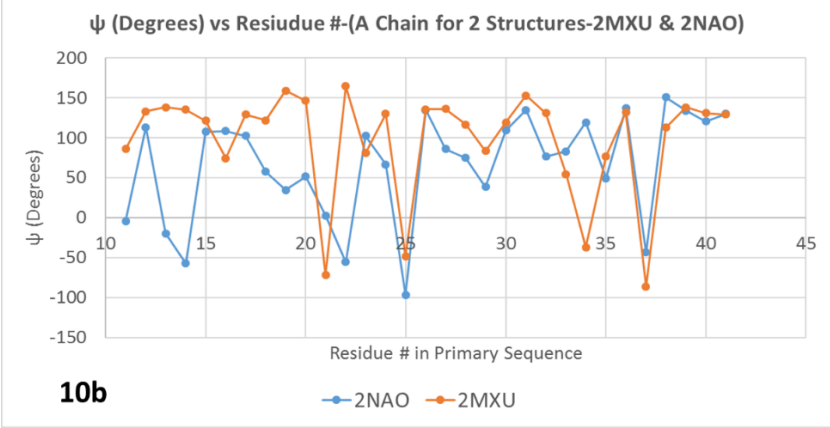
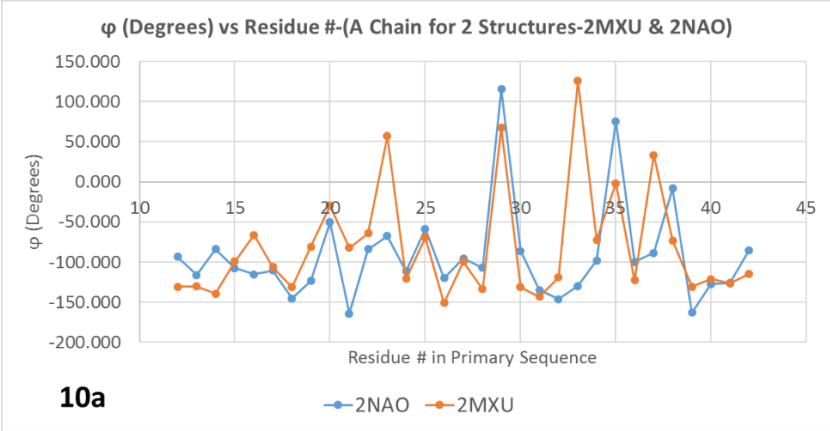
-85.260 ± 6.248

-

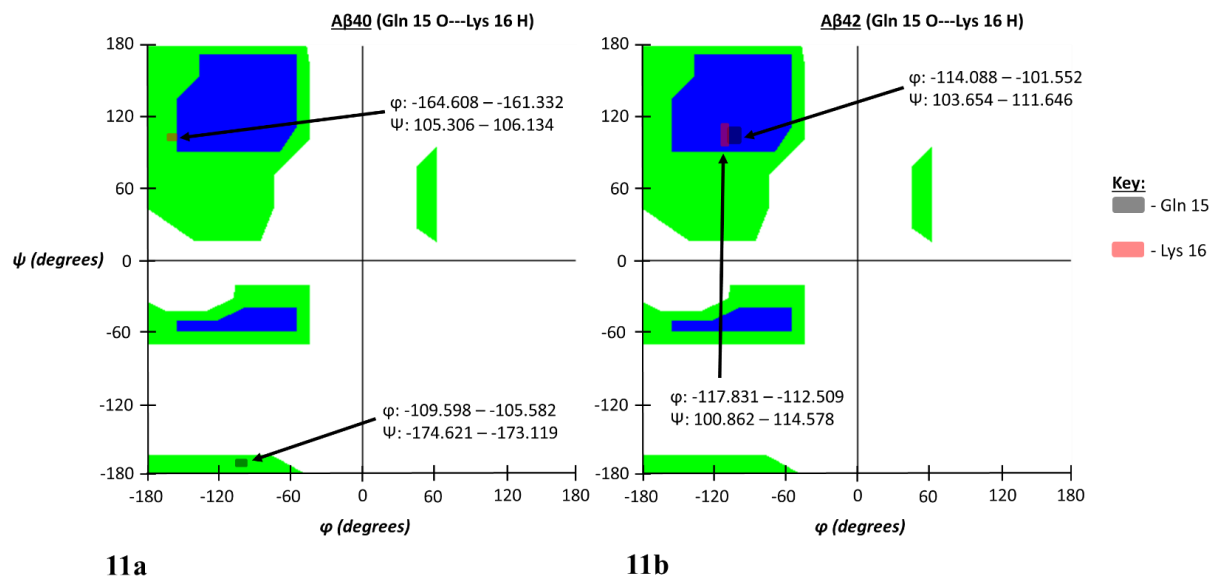
|

-85.240 ± 6.240

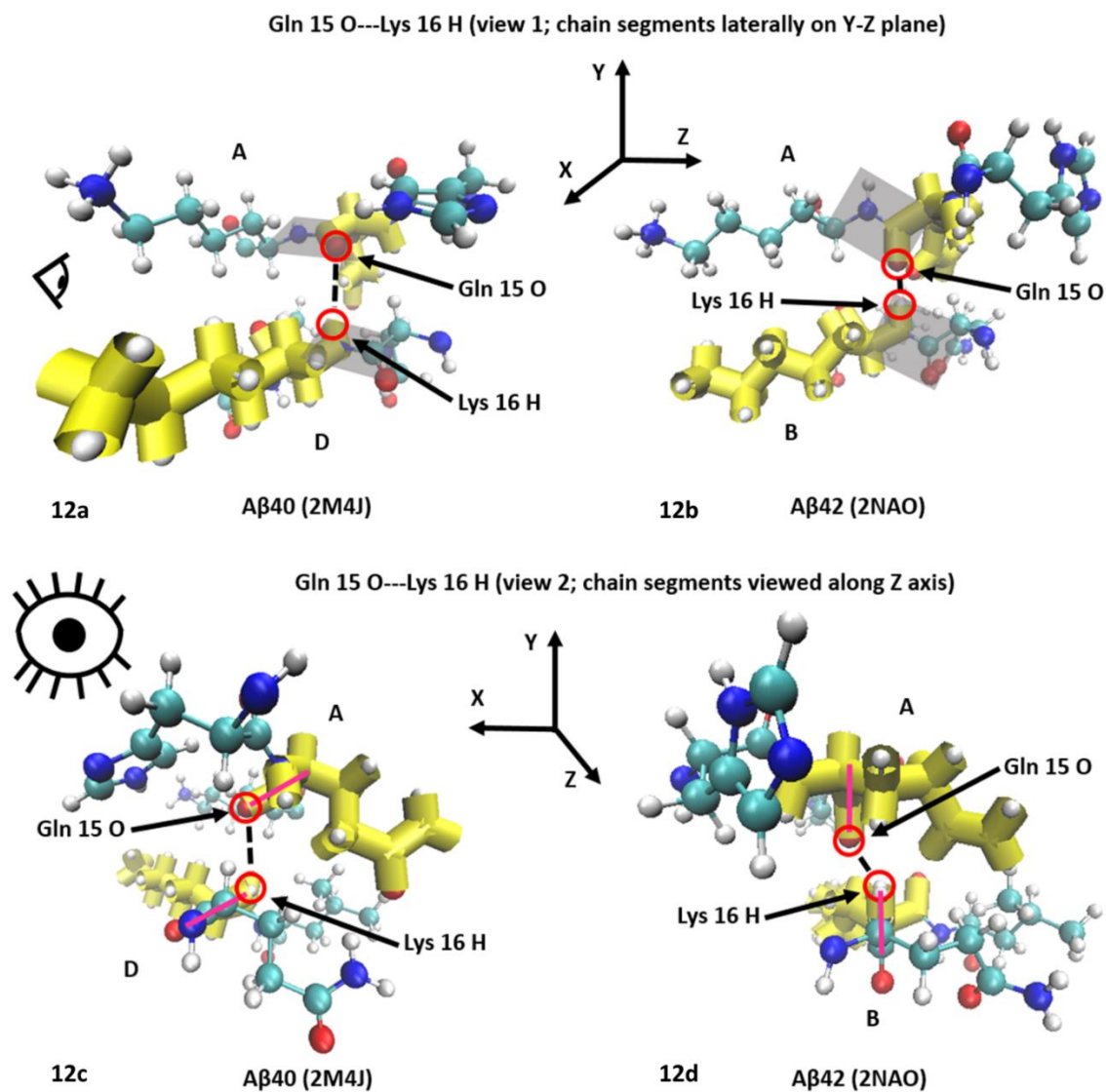
-



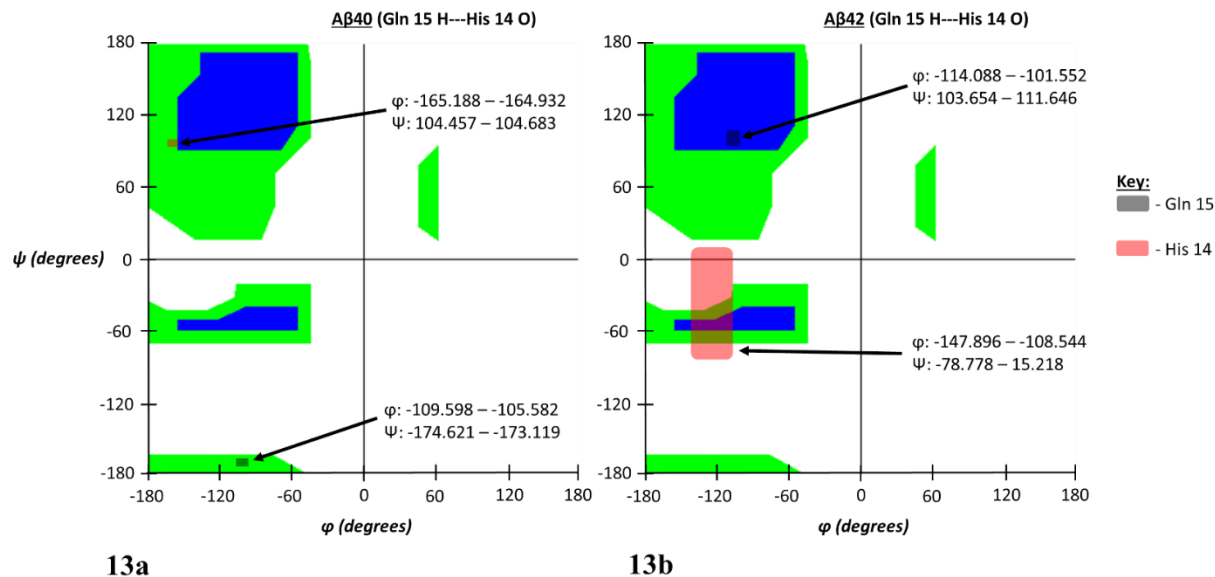
Supplementary Figure 10a-10d: Ramachandran angle profiles for A β 2 structures 2MXU and 2NAO featured as stacked curves for φ and ψ angle value distribution comparison.



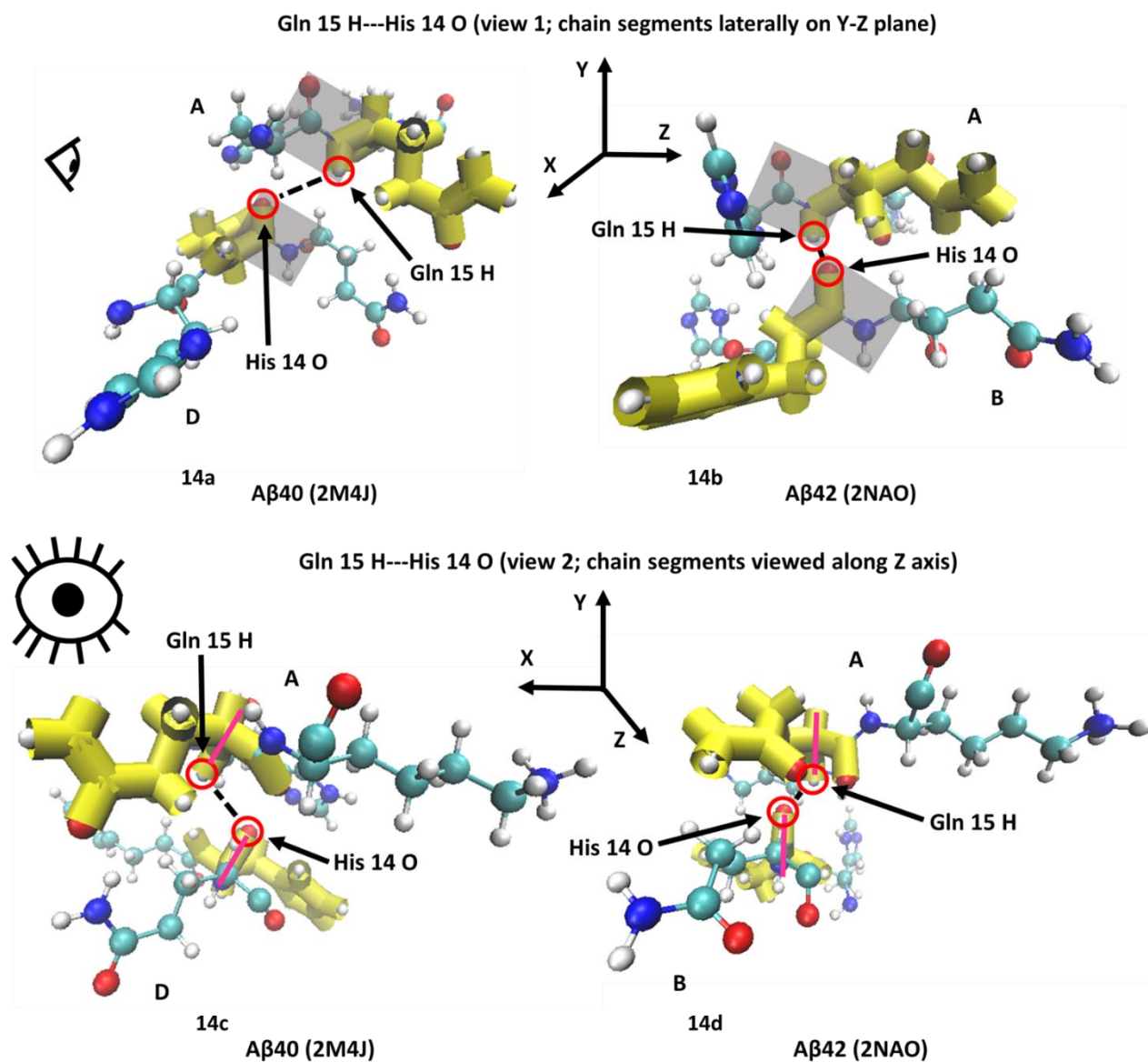
Supplementary Figure 11a-11b: Ramachandran angle profiles for an exceptionally strong atom-atom interaction (Gln 15 O interacting with Lys 16 H) for A β 40 (PDB ID: 2M4J, 11a) and A β 42 (PDB ID: 2NAO, 11b). Ranges for φ and ψ correspond to data spread according to 95% confidence interval analysis for all ensemble members as previously described. As stated before, the first atom is from the A chain of both isoforms and the second corresponds to the partner atom on the appropriate 1:2 interaction chain configuration. Note the acquisition of β -sheet secondary structure for Gln 15 and the more well-defined β -sheet Ramachandran angle values for Lys 16 in A β 42 compared to A β 40.



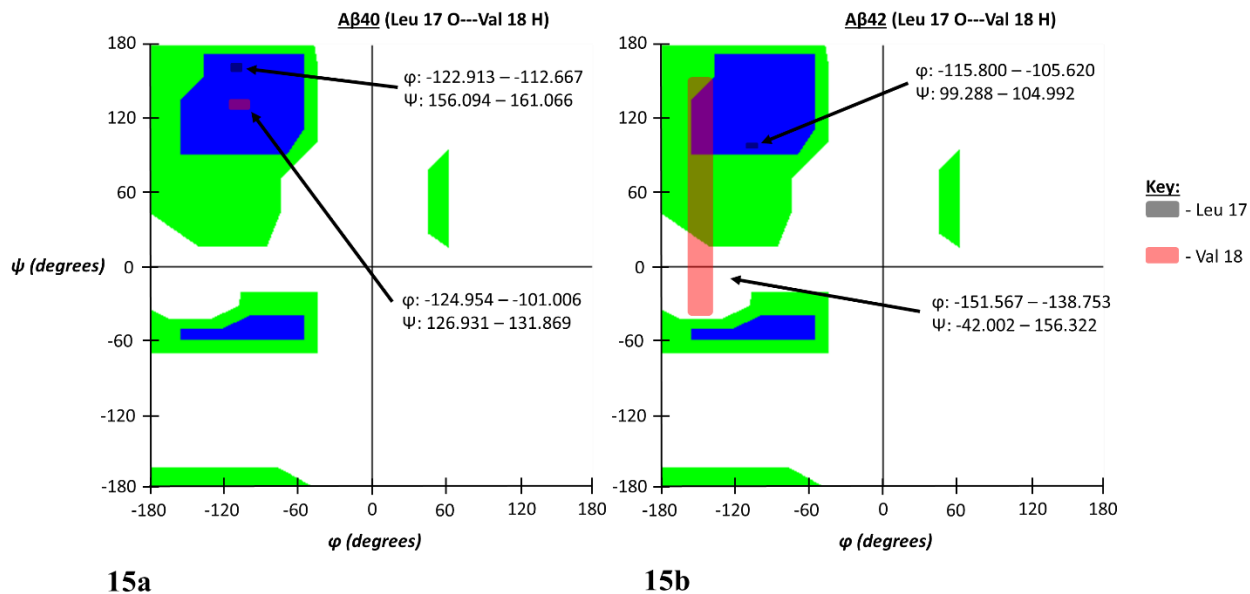
Supplementary Figure 12a-12d: Molecule representations of peptide plane alignment for Aβ40 (12a & 12c) and Aβ42 (12b & 12d). Aβ42 structure here is 2NAO. Shaded parallelograms in Figures 12a and 12b are the peptide planes for the residues whose atoms are participating in the hydrogen bonding. Figures 12c and 12d correspond to a view down the peptide bonds showing the peptide plane profile orientation in magenta. Eye icons indicate view perspective.



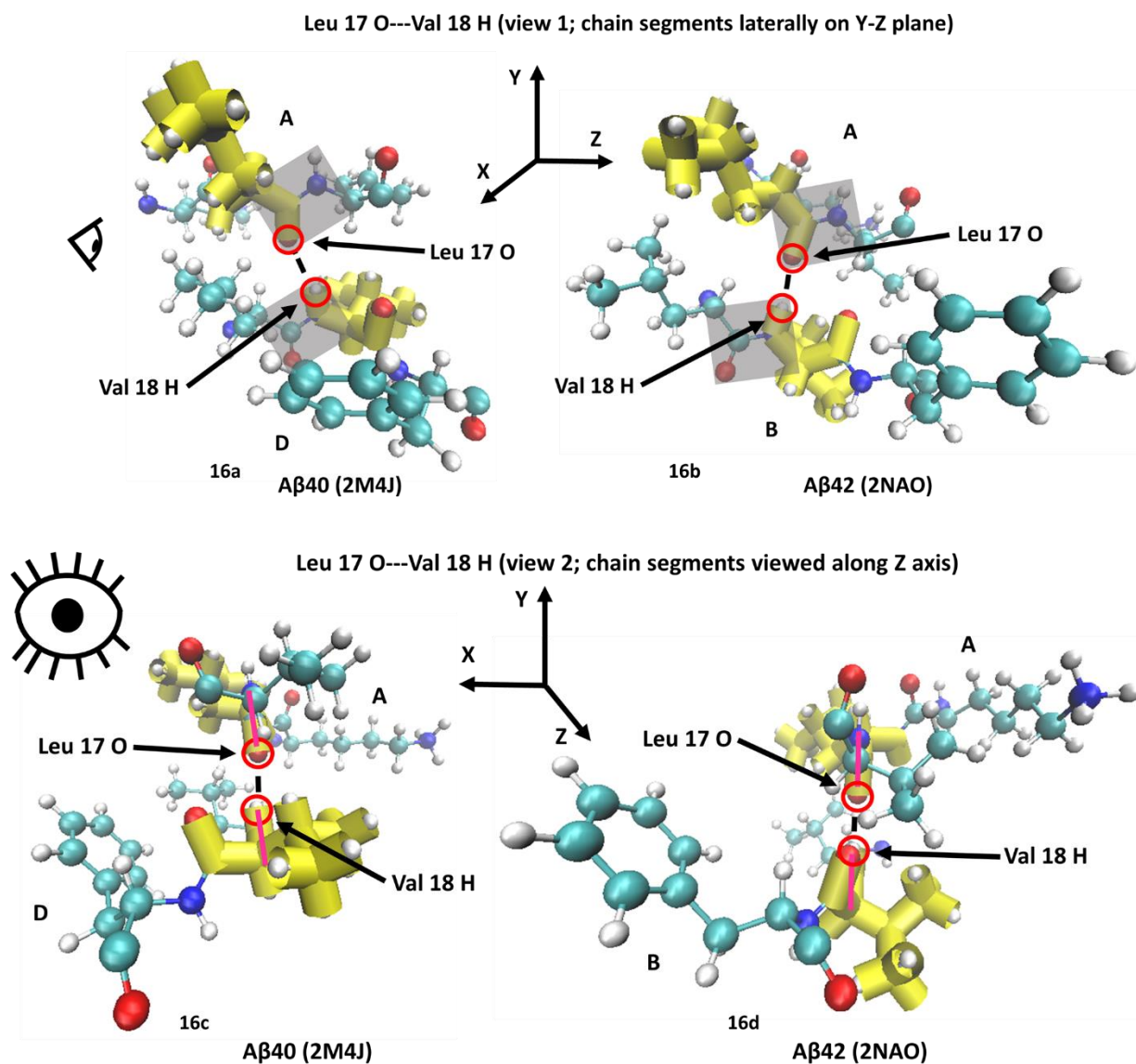
Supplementary Figure 13a-13b: Ramachandran angle profiles for an exceptionally strong atom-atom interaction (Gln 15 H interacting with His 14 O) for A β 40 (PDB ID: 2M4J, 13a) and A β 42 (PDB ID: 2NAO, 13b). Ranges for ϕ and ψ correspond to data spread according to 95% confidence interval analysis for all ensemble members as previously described. As stated before, the first atom is from the A chain of both isoforms and the second corresponds to the partner atom on the appropriate 1:2 interaction chain configuration. Note the acquisition of β -sheet secondary structure for Gln 15 and the acquisition of right-handed α -helix Ramachandran angle values for His 14 in A β 42 compared to A β 40.



Supplementary Figure 14a-14d: Molecule representations of peptide plane alignment for Aβ40 (14a & 14c) and Aβ42 (14b & 14d). Aβ42 structure here is 2NAO. Shaded parallelograms in Figures 14a and 14b are the peptide planes for the residues whose atoms are participating in the hydrogen bonding. Figures 14c and 14d correspond to a view down the peptide bonds showing the peptide plane profile orientation in magenta. Eye icons indicate view perspective.



Supplementary Figure 15a-15b: Ramachandran angle profiles for an exceptionally strong atom-atom interaction (Leu 17 O interacting with Val 18 H) for Aβ40 (PDB ID: 2M4J, 15a) and Aβ42 (PDB ID: 2NAO, 15b). Ranges for ϕ and ψ correspond to data spread according to 95% confidence interval analysis for all ensemble members as previously described. As stated before, the first atom is from the A chain of both isoforms and the second corresponds to the partner atom on the appropriate 1:2 interaction chain configuration. Note the retention of β -sheet secondary structure for Leu 17 and the broader range of Ramachandran angle values for Val 18 in Aβ42 compared to Aβ40.



Supplementary Figure 16a-16d: Molecule representations of peptide plane alignment for Aβ40 (16a & 16c) and Aβ42 (16b & 16d). Aβ42 structure here is 2NAO. Shaded parallelograms in Figures 16a and 16b are the peptide planes for the residues whose atoms are participating in the hydrogen bonding. Figures 16c and 16d correspond to a view down the peptide bonds showing the peptide plane profile orientation in magenta. Eye icons indicate view perspective.

Supplementary Table 9a: Mapping results for Aβ42's (PDB ID: 5KK3 by Colvin et al.) short range (1:2) dominant atom-atom Coulombic interactions across ensemble structures. Columns for each chain correspond to: residue abbreviation, residue number in peptide sequence, atom identity (IUPAC naming convention) and atom number in PDB file. Energy in kT , distance in nm . Mapping analysis began on the 11th residue for both isoforms because original structure data for Aβ42 begins with the 11th residue.

Chain 1				Chain 2				Average Distance	Average Coulombic Values	Lower 95% Confidence Interval Bound	Upper 95% Confidence Interval Bound	Margin of Error
HIS	13	C	34	HIS	13	N	509	6.93E-01	-5.42E-01	-6.46E-01	-4.38E-01	1.04E-01
HIS	13	C	34	HIS	13	O	512	8.04E-01	-3.93E-01	-4.39E-01	-3.48E-01	4.54E-02
HIS	13	C	34	HIS	14	N	526	6.44E-01	-6.08E-01	-7.01E-01	-5.14E-01	9.35E-02
HIS	13	C	34	GLN	15	N	543	7.22E-01	-3.44E-01	-3.66E-01	-3.21E-01	2.22E-02
HIS	13	C	34	GLN	15	O	546	7.36E-01	-4.88E-01	-5.30E-01	-4.45E-01	4.22E-02
HIS	13	O	35	HIS	13	C	511	6.47E-01	-6.49E-01	-8.17E-01	-4.80E-01	1.69E-01
HIS	13	O	35	HIS	14	C	528	7.84E-01	-4.12E-01	-4.62E-01	-3.62E-01	5.00E-02
HIS	14	N	49	HIS	13	C	511	6.47E-01	-5.86E-01	-6.39E-01	-5.32E-01	5.35E-02
HIS	14	N	49	HIS	14	C	528	7.00E-01	-4.94E-01	-5.12E-01	-4.76E-01	1.78E-02
HIS	14	N	49	HIS	14	H	536	5.01E-01	-4.48E-01	-5.13E-01	-3.82E-01	6.55E-02
HIS	14	N	49	GLN	15	H	552	5.32E-01	-4.04E-01	-4.30E-01	-3.78E-01	2.58E-02
HIS	14	C	51	VAL	12	O	496	6.56E-01	-4.37E-01	-4.76E-01	-3.97E-01	3.98E-02
HIS	14	C	51	HIS	13	N	509	5.77E-01	-7.59E-01	-8.56E-01	-6.62E-01	9.71E-02
HIS	14	C	51	HIS	13	O	512	6.03E-01	-6.85E-01	-7.55E-01	-6.15E-01	6.98E-02
HIS	14	C	51	HIS	14	N	526	4.28E-01	-1.54E+00	-1.74E+00	-1.34E+00	2.03E-01
HIS	14	C	51	HIS	14	O	529	6.15E-01	-6.43E-01	-6.59E-01	-6.26E-01	1.67E-02
HIS	14	C	51	HIS	14	ND1	532	6.09E-01	-5.44E-01	-6.21E-01	-4.67E-01	7.70E-02
HIS	14	C	51	GLN	15	N	543	4.07E-01	-1.25E+00	-1.30E+00	-1.20E+00	4.88E-02
HIS	14	C	51	GLN	15	O	546	4.31E-01	-1.65E+00	-1.92E+00	-1.38E+00	2.70E-01
HIS	14	C	51	GLN	15	OE1	550	5.42E-01	-1.55E+00	-2.45E+00	-6.50E-01	9.01E-01
HIS	14	C	51	GLN	15	NE2	551	5.04E-01	-2.33E+00	-3.26E+00	-1.40E+00	9.29E-01
HIS	14	C	51	LYS	16	N	560	6.19E-01	-5.26E-01	-5.60E-01	-4.92E-01	3.39E-02
HIS	14	O	52	VAL	12	C	495	6.17E-01	-4.46E-01	-5.14E-01	-3.79E-01	6.74E-02
HIS	14	O	52	HIS	13	C	511	4.24E-01	-1.61E+00	-1.88E+00	-1.34E+00	2.72E-01
HIS	14	O	52	HIS	14	C	528	3.81E-01	-2.03E+00	-2.16E+00	-1.91E+00	1.24E-01
HIS	14	O	52	HIS	14	CG	531	4.82E-01	-4.90E-01	-5.68E-01	-4.12E-01	7.81E-02
HIS	14	O	52	HIS	14	H	536	2.89E-01	-2.25E+00	-3.03E+00	-1.46E+00	7.84E-01
HIS	14	O	52	GLN	15	C	545	3.99E-01	-1.19E+00	-1.41E+00	-9.82E-01	2.12E-01
HIS	14	O	52	GLN	15	CD	549	4.41E-01	-1.86E+00	-2.55E+00	-1.17E+00	6.87E-01
HIS	14	O	52	GLN	15	H	552	1.97E-01	-6.19E+00	-6.49E+00	-5.89E+00	3.02E-01
HIS	14	O	52	GLN	15	HE21	558	4.47E-01	-1.34E+00	-2.05E+00	-6.23E-01	7.14E-01
HIS	14	O	52	LYS	16	C	562	7.24E-01	-5.15E-01	-5.58E-01	-4.72E-01	4.29E-02
HIS	14	ND1	55	HIS	13	C	511	6.09E-01	-5.44E-01	-6.21E-01	-4.68E-01	7.67E-02
HIS	14	ND1	55	HIS	14	C	528	6.88E-01	-4.24E-01	-4.80E-01	-3.67E-01	5.63E-02
GLN	15	N	66	HIS	13	C	511	6.09E-01	-4.93E-01	-5.53E-01	-4.33E-01	6.01E-02
GLN	15	N	66	HIS	14	C	528	5.92E-01	-5.12E-01	-5.34E-01	-4.90E-01	2.23E-02
GLN	15	N	66	GLN	15	C	545	5.18E-01	-4.37E-01	-4.61E-01	-4.13E-01	2.43E-02
GLN	15	N	66	GLN	15	CD	549	5.25E-01	-7.57E-01	-9.30E-01	-5.83E-01	1.73E-01

GLN	15	N	66	GLN	15	H	552	3.98E-01	-6.04E-01	-6.43E-01	-5.66E-01	3.84E-02
GLN	15	C	68	GLN	15	N	543	5.58E-01	-3.71E-01	-3.97E-01	-3.45E-01	2.63E-02
GLN	15	C	68	GLN	15	O	546	3.63E-01	-1.57E+00	-1.64E+00	-1.49E+00	7.45E-02
GLN	15	C	68	GLN	15	OE1	550	6.41E-01	-4.82E-01	-5.99E-01	-3.65E-01	1.17E-01
GLN	15	C	68	GLN	15	NE2	551	6.12E-01	-7.73E-01	-9.75E-01	-5.71E-01	2.02E-01
GLN	15	C	68	LYS	16	N	560	5.74E-01	-3.89E-01	-4.02E-01	-3.75E-01	1.36E-02
GLN	15	O	69	HIS	13	C	511	7.78E-01	-4.46E-01	-4.99E-01	-3.93E-01	5.30E-02
GLN	15	O	69	HIS	14	C	528	7.86E-01	-4.28E-01	-4.47E-01	-4.08E-01	1.93E-02
GLN	15	O	69	GLN	15	C	545	5.95E-01	-4.66E-01	-4.75E-01	-4.56E-01	9.36E-03
GLN	15	O	69	GLN	15	CD	549	7.02E-01	-5.44E-01	-6.03E-01	-4.84E-01	5.93E-02
GLN	15	O	69	LYS	16	C	562	7.60E-01	-4.97E-01	-5.15E-01	-4.79E-01	1.82E-02
GLN	15	CD	72	GLN	15	O	546	6.44E-01	-6.37E-01	-6.85E-01	-5.88E-01	4.88E-02
GLN	15	CD	72	GLN	15	OE1	550	6.39E-01	-8.07E-01	-1.03E+00	-5.86E-01	2.21E-01
GLN	15	CD	72	GLN	15	NE2	551	5.87E-01	-1.48E+00	-1.95E+00	-1.01E+00	4.66E-01
GLN	15	OE1	73	HIS	14	C	528	9.22E-01	-3.66E-01	-3.94E-01	-3.38E-01	2.85E-02
GLN	15	OE1	73	GLN	15	CD	549	6.66E-01	-7.14E-01	-8.69E-01	-5.59E-01	1.55E-01
GLN	15	NE2	74	HIS	14	C	528	8.91E-01	-5.51E-01	-6.05E-01	-4.97E-01	5.39E-02
GLN	15	NE2	74	GLN	15	C	545	7.68E-01	-4.51E-01	-5.02E-01	-4.00E-01	5.11E-02
GLN	15	NE2	74	GLN	15	CD	549	6.49E-01	-1.04E+00	-1.26E+00	-8.30E-01	2.13E-01
GLN	15	NE2	74	GLN	15	HE21	558	6.13E-01	-9.28E-01	-1.33E+00	-5.29E-01	3.99E-01
GLN	15	NE2	74	GLN	15	HE22	559	6.18E-01	-1.11E+00	-1.72E+00	-5.00E-01	6.10E-01
GLN	15	H	75	GLN	15	O	546	5.22E-01	-4.54E-01	-4.92E-01	-4.17E-01	3.75E-02
GLN	15	HA	76	GLN	15	O	546	2.63E-01	-1.49E+00	-1.74E+00	-1.23E+00	2.57E-01
GLN	15	HE21	81	GLN	15	NE2	551	5.92E-01	-1.18E+00	-1.82E+00	-5.53E-01	6.32E-01
GLN	15	HE22	82	GLN	15	NE2	551	6.84E-01	-6.49E-01	-8.61E-01	-4.37E-01	2.12E-01
LYS	16	N	83	HIS	13	C	511	6.86E-01	-4.35E-01	-4.86E-01	-3.85E-01	5.05E-02
LYS	16	N	83	HIS	14	C	528	6.58E-01	-4.63E-01	-4.88E-01	-4.38E-01	2.53E-02
LYS	16	N	83	GLN	15	C	545	4.06E-01	-8.99E-01	-9.37E-01	-8.60E-01	3.86E-02
LYS	16	N	83	GLN	15	CD	549	6.16E-01	-5.55E-01	-6.45E-01	-4.65E-01	9.01E-02
LYS	16	N	83	GLN	15	H	552	4.98E-01	-3.97E-01	-4.45E-01	-3.48E-01	4.87E-02
LYS	16	N	83	LYS	16	C	562	5.39E-01	-7.81E-01	-8.32E-01	-7.30E-01	5.09E-02
LYS	16	N	83	LEU	17	C	584	6.67E-01	-3.93E-01	-4.24E-01	-3.62E-01	3.10E-02
LYS	16	N	83	LEU	17	H	590	4.24E-01	-5.17E-01	-5.95E-01	-4.40E-01	7.74E-02
LYS	16	C	85	HIS	14	N	526	8.62E-01	-3.73E-01	-3.90E-01	-3.56E-01	1.71E-02
LYS	16	C	85	HIS	14	O	529	8.82E-01	-3.60E-01	-3.76E-01	-3.44E-01	1.58E-02
LYS	16	C	85	GLN	15	N	543	7.19E-01	-3.79E-01	-4.05E-01	-3.53E-01	2.64E-02
LYS	16	C	85	GLN	15	O	546	4.24E-01	-1.84E+00	-2.11E+00	-1.57E+00	2.68E-01
LYS	16	C	85	GLN	15	OE1	550	8.09E-01	-5.45E-01	-6.97E-01	-3.93E-01	1.52E-01
LYS	16	C	85	GLN	15	NE2	551	8.03E-01	-7.82E-01	-1.01E+00	-5.59E-01	2.24E-01
LYS	16	C	85	LYS	16	N	560	5.47E-01	-7.53E-01	-8.02E-01	-7.03E-01	4.96E-02
LYS	16	C	85	LYS	16	O	563	6.00E-01	-7.91E-01	-8.17E-01	-7.64E-01	2.63E-02

LYS	16	C	85	LEU	17	N	582	3.96E-01	-1.35E+00	-1.42E+00	-1.28E+00	7.06E-02
LYS	16	C	85	LEU	17	O	585	4.21E-01	-1.91E+00	-2.25E+00	-1.57E+00	3.39E-01
LYS	16	C	85	VAL	18	N	601	5.94E-01	-6.52E-01	-7.02E-01	-6.01E-01	5.09E-02
LYS	16	O	86	HIS	14	C	528	7.89E-01	-4.25E-01	-4.55E-01	-3.95E-01	2.98E-02
LYS	16	O	86	GLN	15	C	545	4.63E-01	-8.69E-01	-1.03E+00	-7.08E-01	1.61E-01
LYS	16	O	86	GLN	15	CD	549	7.52E-01	-5.22E-01	-6.79E-01	-3.65E-01	1.57E-01
LYS	16	O	86	LYS	16	C	562	3.74E-01	-2.51E+00	-2.70E+00	-2.31E+00	1.95E-01
LYS	16	O	86	LYS	16	HA	570	3.05E-01	-8.60E-01	-1.08E+00	-6.44E-01	2.16E-01
LYS	16	O	86	LEU	17	C	584	3.78E-01	-2.06E+00	-2.49E+00	-1.63E+00	4.26E-01
LYS	16	O	86	LEU	17	H	590	1.98E-01	-5.64E+00	-5.88E+00	-5.39E+00	2.44E-01
LYS	16	O	86	VAL	18	CB	605	6.30E-01	-3.99E-01	-4.46E-01	-3.52E-01	4.72E-02
LYS	16	O	86	VAL	18	H	608	5.41E-01	-6.12E-01	-6.76E-01	-5.48E-01	6.40E-02
LYS	16	H	92	GLN	15	O	546	2.00E-01	-5.21E+00	-5.22E+00	-5.19E+00	1.78E-02
LYS	16	H	92	GLN	15	NE2	551	5.85E-01	-5.18E-01	-6.81E-01	-3.54E-01	1.63E-01
LYS	16	H	92	LYS	16	N	560	3.93E-01	-5.86E-01	-6.27E-01	-5.45E-01	4.05E-02
LEU	17	N	105	LYS	16	C	562	5.86E-01	-5.25E-01	-5.48E-01	-5.03E-01	2.27E-02
LEU	17	N	105	LEU	17	C	584	5.11E-01	-5.66E-01	-5.98E-01	-5.35E-01	3.15E-02
LEU	17	N	105	LEU	17	H	590	3.98E-01	-4.82E-01	-5.16E-01	-4.48E-01	3.40E-02
LEU	17	C	107	GLN	15	O	546	7.54E-01	-3.99E-01	-4.19E-01	-3.78E-01	2.05E-02
LEU	17	C	107	LYS	16	O	563	7.84E-01	-3.70E-01	-3.83E-01	-3.56E-01	1.37E-02
LEU	17	C	107	LEU	17	N	582	5.65E-01	-4.51E-01	-4.82E-01	-4.20E-01	3.14E-02
LEU	17	C	107	LEU	17	O	585	3.65E-01	-2.09E+00	-2.21E+00	-1.97E+00	1.19E-01
LEU	17	C	107	VAL	18	N	601	5.79E-01	-5.39E-01	-5.54E-01	-5.24E-01	1.46E-02
LEU	17	O	108	LYS	16	C	562	8.03E-01	-4.45E-01	-4.65E-01	-4.25E-01	2.03E-02
LEU	17	O	108	LEU	17	C	584	6.01E-01	-6.17E-01	-6.30E-01	-6.04E-01	1.32E-02
LEU	17	HA	114	LEU	17	O	585	2.65E-01	-1.27E+00	-1.47E+00	-1.08E+00	1.95E-01
VAL	18	N	124	LYS	16	C	562	6.68E-01	-5.08E-01	-5.40E-01	-4.76E-01	3.18E-02
VAL	18	N	124	LEU	17	C	584	4.06E-01	-1.27E+00	-1.32E+00	-1.21E+00	5.61E-02
VAL	18	N	124	LEU	17	H	590	4.89E-01	-3.69E-01	-4.09E-01	-3.28E-01	4.06E-02
VAL	18	N	124	VAL	18	C	603	5.67E-01	-4.42E-01	-4.59E-01	-4.24E-01	1.73E-02
VAL	18	N	124	VAL	18	CB	605	5.53E-01	-4.16E-01	-4.50E-01	-3.81E-01	3.40E-02
VAL	18	N	124	VAL	18	H	608	5.79E-01	-4.13E-01	-4.21E-01	-4.05E-01	8.27E-03
VAL	18	C	126	LEU	17	O	585	4.00E-01	-1.30E+00	-1.47E+00	-1.13E+00	1.67E-01
VAL	18	C	126	VAL	18	N	601	5.28E-01	-5.19E-01	-5.46E-01	-4.91E-01	2.78E-02
VAL	18	C	126	VAL	18	O	604	6.10E-01	-3.37E-01	-3.41E-01	-3.32E-01	4.34E-03
VAL	18	C	126	PHE	19	N	617	4.28E-01	-7.11E-01	-7.53E-01	-6.68E-01	4.23E-02
VAL	18	O	127	LYS	16	C	562	7.67E-01	-3.51E-01	-3.72E-01	-3.31E-01	2.05E-02
VAL	18	O	127	LEU	17	C	584	4.25E-01	-1.03E+00	-1.16E+00	-8.97E-01	1.32E-01
VAL	18	O	127	VAL	18	C	603	3.89E-01	-9.94E-01	-1.04E+00	-9.48E-01	4.55E-02
VAL	18	O	127	VAL	18	CB	605	4.64E-01	-5.83E-01	-6.74E-01	-4.92E-01	9.11E-02

VAL	18	O	127	VAL	18	H	608	5.31E-01	-4.55E-01	-4.83E-01	-4.27E-01	2.81E-02
VAL	18	O	127	PHE	19	C	619	5.08E-01	-6.36E-01	-6.99E-01	-5.73E-01	6.28E-02
VAL	18	O	127	PHE	19	H	628	2.49E-01	-2.01E+00	-2.55E+00	-1.46E+00	5.50E-01
VAL	18	CB	128	LEU	17	O	585	4.26E-01	-9.76E-01	-1.10E+00	-8.55E-01	1.21E-01
VAL	18	CB	128	VAL	18	N	601	5.54E-01	-4.17E-01	-4.62E-01	-3.71E-01	4.51E-02
VAL	18	H	131	LYS	16	O	563	6.65E-01	-3.90E-01	-4.13E-01	-3.66E-01	2.32E-02
VAL	18	H	131	LEU	17	N	582	4.60E-01	-5.68E-01	-6.30E-01	-5.05E-01	6.21E-02
VAL	18	H	131	LEU	17	O	585	1.94E-01	-1.00E+01	-1.09E+01	-9.16E+00	8.87E-01
VAL	18	H	131	VAL	18	N	601	3.93E-01	-1.06E+00	-1.09E+00	-1.02E+00	3.34E-02
VAL	18	H	131	VAL	18	O	604	5.91E-01	-3.57E-01	-3.68E-01	-3.45E-01	1.19E-02
VAL	18	H	131	PHE	19	N	617	4.95E-01	-4.94E-01	-5.36E-01	-4.52E-01	4.24E-02
PHE	19	N	140	LEU	17	C	584	6.21E-01	-3.85E-01	-4.16E-01	-3.55E-01	3.04E-02
PHE	19	N	140	VAL	18	C	603	5.74E-01	-3.54E-01	-3.73E-01	-3.35E-01	1.92E-02
PHE	19	N	140	PHE	19	C	619	6.03E-01	-3.88E-01	-4.01E-01	-3.76E-01	1.23E-02
PHE	19	N	140	PHE	19	H	628	3.97E-01	-4.55E-01	-4.87E-01	-4.23E-01	3.19E-02
PHE	19	C	142	LEU	17	O	585	6.87E-01	-4.52E-01	-4.82E-01	-4.21E-01	3.07E-02
PHE	19	C	142	PHE	19	N	617	4.73E-01	-6.91E-01	-7.63E-01	-6.19E-01	7.17E-02
PHE	19	C	142	PHE	19	O	620	5.58E-01	-7.15E-01	-9.76E-01	-4.54E-01	2.61E-01
PHE	19	C	142	PHE	20	N	637	4.31E-01	-9.14E-01	-1.06E+00	-7.69E-01	1.44E-01
PHE	19	C	142	PHE	20	O	640	4.10E-01	-1.47E+00	-1.85E+00	-1.10E+00	3.74E-01
PHE	19	C	142	ALA	21	N	657	5.70E-01	-5.00E-01	-5.74E-01	-4.27E-01	7.36E-02
PHE	19	O	143	LEU	17	C	584	7.67E-01	-3.48E-01	-3.65E-01	-3.30E-01	1.70E-02
PHE	19	O	143	VAL	18	C	603	5.61E-01	-5.18E-01	-5.76E-01	-4.60E-01	5.79E-02
PHE	19	O	143	PHE	19	C	619	4.09E-01	-1.42E+00	-1.64E+00	-1.19E+00	2.24E-01
PHE	19	O	143	PHE	19	H	628	3.74E-01	-7.72E-01	-9.27E-01	-6.16E-01	1.56E-01
PHE	19	O	143	PHE	20	C	639	4.09E-01	-1.57E+00	-2.02E+00	-1.12E+00	4.49E-01
PHE	19	O	143	ALA	21	C	659	6.56E-01	-4.84E-01	-5.54E-01	-4.15E-01	6.94E-02
PHE	20	N	160	PHE	19	C	619	5.60E-01	-5.01E-01	-6.39E-01	-3.63E-01	1.38E-01
PHE	20	N	160	PHE	20	C	639	4.82E-01	-6.68E-01	-7.54E-01	-5.81E-01	8.66E-02
PHE	20	C	162	PHE	20	N	637	6.10E-01	-3.82E-01	-4.10E-01	-3.55E-01	2.76E-02
PHE	20	C	162	PHE	20	O	640	4.07E-01	-1.36E+00	-1.45E+00	-1.27E+00	9.42E-02
PHE	20	C	162	ALA	21	N	657	5.50E-01	-5.27E-01	-5.72E-01	-4.81E-01	4.50E-02
PHE	20	C	162	ALA	21	O	660	5.40E-01	-9.29E-01	-1.25E+00	-6.04E-01	3.25E-01
PHE	20	C	162	GLU	22	O	670	7.35E-01	-4.41E-01	-5.12E-01	-3.71E-01	7.06E-02
PHE	20	O	163	PHE	20	C	639	6.01E-01	-5.37E-01	-5.60E-01	-5.14E-01	2.29E-02
PHE	20	O	163	ALA	21	C	659	6.69E-01	-4.63E-01	-5.26E-01	-4.00E-01	6.32E-02
PHE	20	HA	172	PHE	20	O	640	2.70E-01	-8.55E-01	-1.02E+00	-6.92E-01	1.63E-01
ALA	21	N	180	PHE	20	C	639	4.71E-01	-7.62E-01	-8.38E-01	-6.86E-01	7.64E-02
ALA	21	N	180	ALA	21	C	659	4.63E-01	-8.71E-01	-1.05E+00	-6.94E-01	1.77E-01
ALA	21	C	182	PHE	20	O	640	5.83E-01	-6.28E-01	-7.29E-01	-5.28E-01	1.00E-01
ALA	21	C	182	ALA	21	N	657	6.34E-01	-4.04E-01	-4.43E-01	-3.66E-01	3.84E-02

ALA	21	C	182	ALA	21	O	660	4.38E-01	-1.44E+00	-1.73E+00	-1.14E+00	2.99E-01
ALA	21	C	182	GLU	22	N	667	5.76E-01	-5.20E-01	-5.82E-01	-4.59E-01	6.18E-02
ALA	21	C	182	GLU	22	O	670	6.53E-01	-6.02E-01	-7.24E-01	-4.80E-01	1.22E-01
ALA	21	C	182	GLU	22	OE1	674	8.03E-01	-5.46E-01	-6.47E-01	-4.45E-01	1.01E-01
ALA	21	C	182	GLU	22	OE2	675	8.33E-01	-5.23E-01	-6.29E-01	-4.17E-01	1.06E-01
ALA	21	C	182	ASP	23	N	682	7.05E-01	-4.55E-01	-5.04E-01	-4.05E-01	4.96E-02
ALA	21	O	183	ALA	21	C	659	5.77E-01	-7.09E-01	-8.50E-01	-5.68E-01	1.41E-01
ALA	21	O	183	GLU	22	CD	673	8.37E-01	-4.43E-01	-4.86E-01	-4.00E-01	4.31E-02
ALA	21	H	185	PHE	20	O	640	3.40E-01	-1.48E+00	-2.04E+00	-9.25E-01	5.57E-01
ALA	21	H	185	ALA	21	N	657	4.20E-01	-5.43E-01	-5.92E-01	-4.94E-01	4.88E-02
ALA	21	H	185	ALA	21	O	660	3.57E-01	-2.22E+00	-3.72E+00	-7.28E-01	1.49E+00
GLU	22	N	190	PHE	20	C	639	6.34E-01	-4.14E-01	-4.70E-01	-3.58E-01	5.61E-02
GLU	22	N	190	ALA	21	C	659	4.59E-01	-9.01E-01	-1.03E+00	-7.76E-01	1.25E-01
GLU	22	N	190	GLU	22	C	669	5.42E-01	-5.10E-01	-5.98E-01	-4.22E-01	8.78E-02
GLU	22	N	190	GLU	22	CD	673	7.18E-01	-4.75E-01	-5.77E-01	-3.72E-01	1.03E-01
GLU	22	C	192	ALA	21	O	660	5.30E-01	-7.40E-01	-8.85E-01	-5.94E-01	1.46E-01
GLU	22	C	192	GLU	22	N	667	5.76E-01	-4.36E-01	-4.96E-01	-3.76E-01	6.04E-02
GLU	22	C	192	GLU	22	O	670	5.21E-01	-7.91E-01	-9.26E-01	-6.57E-01	1.35E-01
GLU	22	C	192	GLU	22	OE1	674	7.54E-01	-5.44E-01	-7.08E-01	-3.81E-01	1.63E-01
GLU	22	C	192	GLU	22	OE2	675	7.62E-01	-5.58E-01	-7.57E-01	-3.60E-01	1.99E-01
GLU	22	C	192	ASP	23	N	682	5.08E-01	-7.55E-01	-8.32E-01	-6.77E-01	7.76E-02
GLU	22	C	192	ASP	23	OD1	688	7.01E-01	-5.65E-01	-7.98E-01	-3.32E-01	2.33E-01
GLU	22	C	192	ASP	23	OD2	689	6.94E-01	-5.09E-01	-5.70E-01	-4.47E-01	6.16E-02
GLU	22	O	193	PHE	20	C	639	7.34E-01	-4.26E-01	-4.61E-01	-3.90E-01	3.51E-02
GLU	22	O	193	ALA	21	C	659	5.73E-01	-8.36E-01	-1.08E+00	-5.92E-01	2.44E-01
GLU	22	O	193	GLU	22	C	669	5.02E-01	-9.13E-01	-1.17E+00	-6.57E-01	2.56E-01
GLU	22	O	193	GLU	22	CD	673	7.74E-01	-6.94E-01	-9.71E-01	-4.17E-01	2.77E-01
GLU	22	O	193	ASP	23	C	684	6.29E-01	-4.77E-01	-5.36E-01	-4.18E-01	5.94E-02
GLU	22	O	193	ASP	23	CG	687	6.87E-01	-6.64E-01	-7.37E-01	-5.90E-01	7.40E-02
GLU	22	O	193	VAL	24	H	701	5.43E-01	-6.74E-01	-7.94E-01	-5.54E-01	1.20E-01
GLU	22	CD	196	ALA	21	O	660	5.03E-01	-2.14E+00	-3.21E+00	-1.06E+00	1.07E+00
GLU	22	CD	196	GLU	22	OE1	674	6.04E-01	-1.64E+00	-2.23E+00	-1.05E+00	5.92E-01
GLU	22	CD	196	GLU	22	OE2	675	6.23E-01	-1.35E+00	-1.72E+00	-9.77E-01	3.69E-01
GLU	22	CD	196	ASP	23	N	682	6.16E-01	-1.12E+00	-1.50E+00	-7.46E-01	3.75E-01
GLU	22	OE1	197	ALA	21	C	659	6.20E-01	-1.42E+00	-2.15E+00	-7.00E-01	7.23E-01
GLU	22	OE1	197	GLU	22	CD	673	6.05E-01	-1.60E+00	-2.21E+00	-9.88E-01	6.13E-01
GLU	22	OE2	198	ALA	21	C	659	6.08E-01	-1.27E+00	-1.78E+00	-7.64E-01	5.09E-01
GLU	22	OE2	198	GLU	22	CD	673	6.41E-01	-1.52E+00	-2.17E+00	-8.70E-01	6.48E-01
GLU	22	H	199	GLU	22	O	670	5.01E-01	-6.38E-01	-8.38E-01	-4.38E-01	2.00E-01
ASP	23	N	205	ALA	21	C	659	6.62E-01	-5.11E-01	-5.65E-01	-4.57E-01	5.39E-02
ASP	23	N	205	GLU	22	C	669	5.34E-01	-6.76E-01	-7.67E-01	-5.85E-01	9.11E-02

ASP	23	N	205	GLU	22	CD	673	7.48E-01	-5.70E-01	-6.72E-01	-4.68E-01	1.02E-01
ASP	23	N	205	ASP	23	C	684	6.30E-01	-4.40E-01	-4.81E-01	-3.98E-01	4.19E-02
ASP	23	N	205	ASP	23	CG	687	6.09E-01	-8.69E-01	-1.13E+00	-6.07E-01	2.62E-01
ASP	23	N	205	ASP	23	H	690	5.07E-01	-5.45E-01	-6.66E-01	-4.24E-01	1.21E-01
ASP	23	N	205	VAL	24	H	701	5.51E-01	-5.81E-01	-6.29E-01	-5.32E-01	4.86E-02
ASP	23	C	207	GLU	22	O	670	5.27E-01	-7.83E-01	-1.05E+00	-5.18E-01	2.66E-01
ASP	23	C	207	ASP	23	N	682	4.75E-01	-8.94E-01	-1.11E+00	-6.78E-01	2.16E-01
ASP	23	C	207	ASP	23	O	685	6.21E-01	-3.99E-01	-4.06E-01	-3.92E-01	6.94E-03
ASP	23	C	207	ASP	23	OD1	688	5.84E-01	-8.12E-01	-1.15E+00	-4.70E-01	3.42E-01
ASP	23	C	207	ASP	23	OD2	689	5.77E-01	-7.70E-01	-1.00E+00	-5.38E-01	2.32E-01
ASP	23	C	207	VAL	24	N	694	4.58E-01	-7.24E-01	-7.62E-01	-6.85E-01	3.88E-02
ASP	23	C	207	VAL	24	O	697	5.21E-01	-4.86E-01	-5.37E-01	-4.35E-01	5.12E-02
ASP	23	O	208	GLU	22	C	669	4.26E-01	-1.16E+00	-1.47E+00	-8.42E-01	3.13E-01
ASP	23	O	208	GLU	22	CD	673	7.57E-01	-4.94E-01	-5.70E-01	-4.18E-01	7.59E-02
ASP	23	O	208	ASP	23	C	684	3.87E-01	-1.23E+00	-1.28E+00	-1.18E+00	4.92E-02
ASP	23	O	208	ASP	23	CG	687	4.57E-01	-1.54E+00	-2.07E+00	-1.01E+00	5.30E-01
ASP	23	O	208	ASP	23	H	690	4.03E-01	-1.52E+00	-2.53E+00	-5.17E-01	1.00E+00
ASP	23	O	208	ASP	23	HA	691	2.59E-01	-7.42E-01	-8.51E-01	-6.33E-01	1.09E-01
ASP	23	O	208	VAL	24	C	696	5.14E-01	-6.23E-01	-6.83E-01	-5.64E-01	5.92E-02
ASP	23	O	208	VAL	24	CB	698	5.16E-01	-5.50E-01	-6.17E-01	-4.82E-01	6.73E-02
ASP	23	O	208	VAL	24	H	701	2.76E-01	-3.32E+00	-3.84E+00	-2.80E+00	5.22E-01
ASP	23	CG	210	GLU	22	O	670	7.38E-01	-5.93E-01	-6.80E-01	-5.05E-01	8.74E-02
ASP	23	CG	210	ASP	23	N	682	6.29E-01	-9.18E-01	-1.28E+00	-5.58E-01	3.60E-01
ASP	23	CG	210	ASP	23	O	685	8.26E-01	-4.09E-01	-4.73E-01	-3.44E-01	6.47E-02
ASP	23	CG	210	ASP	23	OD1	688	6.05E-01	-1.32E+00	-1.79E+00	-8.52E-01	4.71E-01
ASP	23	CG	210	ASP	23	OD2	689	5.92E-01	-1.52E+00	-2.08E+00	-9.60E-01	5.60E-01
ASP	23	CG	210	VAL	24	N	694	7.17E-01	-4.82E-01	-5.71E-01	-3.92E-01	8.95E-02
ASP	23	OD1	211	GLU	22	C	669	7.39E-01	-4.68E-01	-5.53E-01	-3.84E-01	8.44E-02
ASP	23	OD1	211	ASP	23	CG	687	6.30E-01	-1.09E+00	-1.35E+00	-8.19E-01	2.68E-01
ASP	23	OD1	211	VAL	24	H	701	6.93E-01	-5.43E-01	-7.27E-01	-3.60E-01	1.84E-01
ASP	23	OD2	212	ASP	23	CG	687	6.10E-01	-1.57E+00	-2.53E+00	-6.08E-01	9.59E-01
ASP	23	OD2	212	VAL	24	H	701	6.95E-01	-4.95E-01	-5.95E-01	-3.95E-01	1.00E-01
ASP	23	H	213	ASP	23	N	682	5.22E-01	-4.94E-01	-5.67E-01	-4.21E-01	7.27E-02
VAL	24	N	217	ASP	23	C	684	5.68E-01	-4.35E-01	-4.52E-01	-4.18E-01	1.69E-02
VAL	24	N	217	ASP	23	CG	687	6.41E-01	-5.95E-01	-6.97E-01	-4.94E-01	1.01E-01
VAL	24	N	217	VAL	24	C	696	5.85E-01	-4.12E-01	-4.36E-01	-3.89E-01	2.36E-02
VAL	24	N	217	VAL	24	H	701	4.03E-01	-9.98E-01	-1.07E+00	-9.22E-01	7.50E-02
VAL	24	C	219	ASP	23	OD2	689	7.61E-01	-4.12E-01	-4.76E-01	-3.48E-01	6.37E-02
VAL	24	C	219	VAL	24	N	694	5.13E-01	-5.58E-01	-6.07E-01	-5.10E-01	4.86E-02
VAL	24	C	219	VAL	24	O	697	3.85E-01	-1.03E+00	-1.11E+00	-9.49E-01	8.31E-02
VAL	24	C	219	GLY	25	O	713	5.30E-01	-5.85E-01	-6.29E-01	-5.41E-01	4.36E-02

VAL	24	O	220	VAL	24	C	696	6.02E-01	-3.48E-01	-3.60E-01	-3.36E-01	1.20E-02
VAL	24	O	220	VAL	24	H	701	5.40E-01	-4.41E-01	-4.83E-01	-3.99E-01	4.20E-02
VAL	24	O	220	GLY	25	C	712	6.93E-01	-3.40E-01	-3.54E-01	-3.25E-01	1.45E-02
VAL	24	CB	221	VAL	24	N	694	5.06E-01	-5.17E-01	-5.74E-01	-4.60E-01	5.72E-02
VAL	24	CB	221	VAL	24	O	697	4.68E-01	-6.02E-01	-7.36E-01	-4.67E-01	1.35E-01
VAL	24	H	224	ASP	23	N	682	6.61E-01	-4.04E-01	-4.61E-01	-3.46E-01	5.75E-02
VAL	24	H	224	ASP	23	OD2	689	7.47E-01	-4.26E-01	-5.08E-01	-3.45E-01	8.16E-02
VAL	24	H	224	VAL	24	N	694	5.91E-01	-3.97E-01	-4.11E-01	-3.82E-01	1.48E-02
GLY	25	N	233	VAL	24	C	696	4.07E-01	-8.31E-01	-9.21E-01	-7.41E-01	8.96E-02
GLY	25	N	233	VAL	24	H	701	4.19E-01	-7.72E-01	-8.85E-01	-6.60E-01	1.13E-01
GLY	25	N	233	GLY	25	C	712	4.86E-01	-6.85E-01	-7.40E-01	-6.31E-01	5.45E-02
GLY	25	C	235	VAL	24	N	694	7.01E-01	-3.73E-01	-4.02E-01	-3.44E-01	2.91E-02
GLY	25	C	235	VAL	24	O	697	4.63E-01	-8.45E-01	-9.44E-01	-7.46E-01	9.88E-02
GLY	25	C	235	GLY	25	N	710	5.97E-01	-4.26E-01	-4.47E-01	-4.05E-01	2.07E-02
GLY	25	C	235	GLY	25	O	713	3.69E-01	-1.88E+00	-2.00E+00	-1.75E+00	1.26E-01
GLY	25	C	235	SER	26	N	717	5.85E-01	-6.43E-01	-6.68E-01	-6.17E-01	2.56E-02
GLY	25	C	235	SER	26	O	720	7.95E-01	-3.77E-01	-3.92E-01	-3.62E-01	1.51E-02
GLY	25	C	235	SER	26	OG	722	7.08E-01	-5.24E-01	-5.75E-01	-4.72E-01	5.15E-02
GLY	25	C	235	ASN	27	N	728	6.33E-01	-4.35E-01	-4.66E-01	-4.03E-01	3.14E-02
GLY	25	C	235	ASN	27	O	731	7.46E-01	-3.83E-01	-4.02E-01	-3.63E-01	1.94E-02
GLY	25	C	235	ASN	27	ND2	735	8.78E-01	-4.35E-01	-4.70E-01	-3.99E-01	3.51E-02
GLY	25	O	236	GLY	25	C	712	5.95E-01	-5.82E-01	-6.01E-01	-5.62E-01	1.96E-02
GLY	25	H	237	VAL	24	N	694	4.08E-01	-6.02E-01	-7.37E-01	-4.67E-01	1.35E-01
GLY	25	H	237	VAL	24	O	697	2.22E-01	-3.32E+00	-4.13E+00	-2.50E+00	8.10E-01
GLY	25	H	237	GLY	25	N	710	4.10E-01	-4.62E-01	-5.06E-01	-4.18E-01	4.39E-02
GLY	25	H	237	GLY	25	O	713	3.70E-01	-8.55E-01	-1.02E+00	-6.85E-01	1.70E-01
SER	26	N	240	VAL	24	C	696	5.21E-01	-6.45E-01	-6.89E-01	-6.01E-01	4.42E-02
SER	26	N	240	VAL	24	H	701	6.49E-01	-3.93E-01	-4.13E-01	-3.73E-01	2.02E-02
SER	26	N	240	GLY	25	C	712	3.97E-01	-1.64E+00	-1.71E+00	-1.57E+00	7.08E-02
SER	26	N	240	SER	26	C	719	5.51E-01	-6.13E-01	-6.53E-01	-5.73E-01	3.98E-02
SER	26	N	240	SER	26	H	723	5.76E-01	-3.95E-01	-4.10E-01	-3.81E-01	1.46E-02
SER	26	N	240	SER	26	HA	724	3.90E-01	-4.22E-01	-4.59E-01	-3.85E-01	3.67E-02
SER	26	N	240	SER	26	HG	727	6.17E-01	-4.59E-01	-5.28E-01	-3.91E-01	6.84E-02
SER	26	N	240	ASN	27	C	730	6.66E-01	-5.26E-01	-5.66E-01	-4.86E-01	3.99E-02
SER	26	N	240	ASN	27	CG	733	7.16E-01	-4.33E-01	-4.70E-01	-3.96E-01	3.70E-02
SER	26	N	240	ASN	27	H	736	4.14E-01	-6.62E-01	-7.60E-01	-5.65E-01	9.74E-02
SER	26	CA	241	GLY	25	O	713	3.53E-01	-4.32E-01	-4.68E-01	-3.96E-01	3.59E-02
SER	26	C	242	GLY	25	O	713	3.98E-01	-1.29E+00	-1.40E+00	-1.18E+00	1.13E-01
SER	26	C	242	SER	26	N	717	5.29E-01	-6.75E-01	-7.29E-01	-6.20E-01	5.42E-02
SER	26	C	242	SER	26	O	720	5.97E-01	-5.48E-01	-5.59E-01	-5.38E-01	1.05E-02
SER	26	C	242	SER	26	OG	722	5.98E-01	-6.11E-01	-6.66E-01	-5.56E-01	5.50E-02

SER	26	C	242	ASN	27	N	728	3.91E-01	-1.13E+00	-1.16E+00	-1.09E+00	3.88E-02
SER	26	C	242	ASN	27	O	731	4.05E-01	-1.27E+00	-1.41E+00	-1.14E+00	1.35E-01
SER	26	C	242	ASN	27	OD1	734	6.19E-01	-5.24E-01	-6.99E-01	-3.50E-01	1.75E-01
SER	26	C	242	ASN	27	ND2	735	6.24E-01	-6.99E-01	-7.96E-01	-6.03E-01	9.66E-02
SER	26	C	242	LYS	28	N	742	5.95E-01	-4.19E-01	-4.48E-01	-3.89E-01	2.96E-02
SER	26	O	243	VAL	24	C	696	6.34E-01	-4.52E-01	-4.89E-01	-4.16E-01	3.62E-02
SER	26	O	243	GLY	25	C	712	4.59E-01	-1.24E+00	-1.37E+00	-1.10E+00	1.36E-01
SER	26	O	243	SER	26	C	719	3.74E-01	-1.72E+00	-1.85E+00	-1.58E+00	1.31E-01
SER	26	O	243	SER	26	H	723	5.52E-01	-4.76E-01	-5.29E-01	-4.23E-01	5.29E-02
SER	26	O	243	SER	26	HA	724	3.03E-01	-1.01E+00	-1.29E+00	-7.44E-01	2.71E-01
SER	26	O	243	SER	26	HG	727	5.38E-01	-7.07E-01	-8.64E-01	-5.49E-01	1.57E-01
SER	26	O	243	ASN	27	C	730	3.63E-01	-2.46E+00	-2.84E+00	-2.07E+00	3.86E-01
SER	26	O	243	ASN	27	CG	733	4.88E-01	-1.10E+00	-1.28E+00	-9.16E-01	1.83E-01
SER	26	O	243	ASN	27	H	736	1.95E-01	-5.94E+00	-6.40E+00	-5.49E+00	4.55E-01
SER	26	O	243	ASN	27	HD21	740	5.36E-01	-5.49E-01	-6.53E-01	-4.45E-01	1.04E-01
SER	26	O	243	LYS	28	C	744	6.91E-01	-6.15E-01	-6.54E-01	-5.77E-01	3.86E-02
SER	26	CB	244	GLY	25	O	713	3.44E-01	-5.91E-01	-6.74E-01	-5.08E-01	8.28E-02
SER	26	OG	245	GLY	25	C	712	5.27E-01	-1.08E+00	-1.40E+00	-7.66E-01	3.16E-01
SER	26	OG	245	SER	26	C	719	5.94E-01	-6.21E-01	-6.81E-01	-5.62E-01	5.96E-02
SER	26	OG	245	SER	26	HA	724	4.07E-01	-4.66E-01	-5.54E-01	-3.79E-01	8.74E-02
SER	26	OG	245	SER	26	HG	727	4.94E-01	-1.00E+00	-1.34E+00	-6.58E-01	3.43E-01
SER	26	OG	245	ASN	27	C	730	6.93E-01	-5.99E-01	-7.03E-01	-4.95E-01	1.04E-01
SER	26	OG	245	ASN	27	CG	733	8.57E-01	-3.72E-01	-4.04E-01	-3.41E-01	3.14E-02
SER	26	OG	245	ASN	27	H	736	4.97E-01	-5.13E-01	-6.10E-01	-4.15E-01	9.76E-02
SER	26	H	246	VAL	24	O	697	3.68E-01	-9.19E-01	-1.05E+00	-7.84E-01	1.34E-01
SER	26	H	246	GLY	25	N	710	4.48E-01	-4.95E-01	-5.31E-01	-4.59E-01	3.59E-02
SER	26	H	246	GLY	25	O	713	1.99E-01	-6.59E+00	-6.78E+00	-6.39E+00	1.92E-01
SER	26	H	246	SER	26	N	717	4.03E-01	-9.40E-01	-1.01E+00	-8.74E-01	6.55E-02
SER	26	H	246	SER	26	O	720	6.01E-01	-3.89E-01	-4.16E-01	-3.61E-01	2.75E-02
SER	26	H	246	SER	26	OG	722	5.59E-01	-5.16E-01	-5.87E-01	-4.44E-01	7.19E-02
SER	26	H	246	ASN	27	N	728	4.47E-01	-5.87E-01	-6.71E-01	-5.02E-01	8.47E-02
SER	26	HG	250	GLY	25	O	713	4.65E-01	-9.28E-01	-1.24E+00	-6.14E-01	3.14E-01
SER	26	HG	250	SER	26	N	717	5.90E-01	-5.31E-01	-6.62E-01	-4.00E-01	1.31E-01
SER	26	HG	250	SER	26	OG	722	5.11E-01	-9.42E-01	-1.24E+00	-6.46E-01	2.97E-01
ASN	27	N	251	GLY	25	C	712	6.02E-01	-4.83E-01	-5.12E-01	-4.54E-01	2.88E-02
ASN	27	N	251	SER	26	C	719	5.82E-01	-4.30E-01	-4.51E-01	-4.09E-01	2.09E-02
ASN	27	N	251	ASN	27	C	730	5.17E-01	-7.22E-01	-7.65E-01	-6.78E-01	4.32E-02
ASN	27	N	251	ASN	27	CG	733	5.70E-01	-5.61E-01	-6.40E-01	-4.82E-01	7.88E-02
ASN	27	N	251	ASN	27	H	736	3.89E-01	-6.06E-01	-6.52E-01	-5.59E-01	4.65E-02
ASN	27	C	253	GLY	25	O	713	7.17E-01	-4.25E-01	-4.43E-01	-4.07E-01	1.78E-02
ASN	27	C	253	SER	26	N	717	8.13E-01	-3.59E-01	-3.75E-01	-3.43E-01	1.57E-02

ASN	27	C	253	SER	26	O	720	7.77E-01	-4.17E-01	-4.29E-01	-4.05E-01	1.19E-02
ASN	27	C	253	SER	26	OG	722	8.58E-01	-3.90E-01	-4.15E-01	-3.65E-01	2.51E-02
ASN	27	C	253	ASN	27	N	728	5.63E-01	-5.92E-01	-6.22E-01	-5.61E-01	3.05E-02
ASN	27	C	253	ASN	27	O	731	3.72E-01	-2.01E+00	-2.16E+00	-1.86E+00	1.48E-01
ASN	27	C	253	ASN	27	OD1	734	5.99E-01	-7.57E-01	-1.02E+00	-4.93E-01	2.64E-01
ASN	27	C	253	ASN	27	ND2	735	5.83E-01	-1.14E+00	-1.45E+00	-8.31E-01	3.12E-01
ASN	27	C	253	LYS	28	N	742	5.90E-01	-5.41E-01	-5.61E-01	-5.21E-01	2.00E-02
ASN	27	C	253	LYS	28	O	745	8.07E-01	-3.78E-01	-3.89E-01	-3.67E-01	1.11E-02
ASN	27	C	253	GLY	29	N	764	6.70E-01	-3.57E-01	-3.78E-01	-3.37E-01	2.04E-02
ASN	27	O	254	ASN	27	C	730	6.05E-01	-6.14E-01	-6.32E-01	-5.95E-01	1.82E-02
ASN	27	O	254	ASN	27	CG	733	6.70E-01	-4.84E-01	-5.42E-01	-4.26E-01	5.80E-02
ASN	27	O	254	LYS	28	C	744	7.92E-01	-4.27E-01	-4.38E-01	-4.15E-01	1.16E-02
ASN	27	CG	256	GLY	25	O	713	7.50E-01	-3.71E-01	-3.92E-01	-3.50E-01	2.12E-02
ASN	27	CG	256	ASN	27	N	728	6.61E-01	-4.17E-01	-4.81E-01	-3.52E-01	6.49E-02
ASN	27	CG	256	ASN	27	O	731	5.52E-01	-7.96E-01	-1.01E+00	-5.87E-01	2.09E-01
ASN	27	CG	256	ASN	27	OD1	734	6.19E-01	-7.73E-01	-1.17E+00	-3.72E-01	4.01E-01
ASN	27	CG	256	ASN	27	ND2	735	5.75E-01	-1.33E+00	-1.92E+00	-7.39E-01	5.92E-01
ASN	27	OD1	257	ASN	27	C	730	6.49E-01	-6.65E-01	-9.26E-01	-4.03E-01	2.61E-01
ASN	27	OD1	257	ASN	27	CG	733	6.00E-01	-1.01E+00	-1.60E+00	-4.22E-01	5.89E-01
ASN	27	ND2	258	GLY	25	C	712	8.89E-01	-4.29E-01	-4.73E-01	-3.84E-01	4.46E-02
ASN	27	ND2	258	SER	26	C	719	8.57E-01	-3.86E-01	-4.46E-01	-3.26E-01	5.97E-02
ASN	27	ND2	258	ASN	27	C	730	7.11E-01	-7.40E-01	-9.60E-01	-5.20E-01	2.20E-01
ASN	27	ND2	258	ASN	27	CG	733	6.27E-01	-9.74E-01	-1.31E+00	-6.37E-01	3.37E-01
LYS	28	N	265	SER	26	C	719	6.53E-01	-3.43E-01	-3.62E-01	-3.24E-01	1.88E-02
LYS	28	N	265	ASN	27	C	730	4.09E-01	-1.29E+00	-1.34E+00	-1.24E+00	4.70E-02
LYS	28	N	265	ASN	27	CG	733	5.29E-01	-6.90E-01	-8.14E-01	-5.66E-01	1.24E-01
LYS	28	N	265	LYS	28	C	744	5.78E-01	-6.65E-01	-6.92E-01	-6.37E-01	2.80E-02
LYS	28	N	265	GLY	29	C	766	7.14E-01	-3.46E-01	-3.64E-01	-3.29E-01	1.73E-02
LYS	28	C	267	SER	26	O	720	8.54E-01	-4.17E-01	-4.39E-01	-3.96E-01	2.12E-02
LYS	28	C	267	ASN	27	N	728	6.88E-01	-4.58E-01	-4.87E-01	-4.29E-01	2.90E-02
LYS	28	C	267	ASN	27	O	731	3.93E-01	-2.09E+00	-2.40E+00	-1.79E+00	3.04E-01
LYS	28	C	267	ASN	27	OD1	734	6.44E-01	-7.44E-01	-9.70E-01	-5.19E-01	2.25E-01
LYS	28	C	267	ASN	27	ND2	735	6.27E-01	-1.11E+00	-1.37E+00	-8.49E-01	2.62E-01
LYS	28	C	267	LYS	28	N	742	5.20E-01	-8.46E-01	-8.91E-01	-8.01E-01	4.47E-02
LYS	28	C	267	LYS	28	O	745	6.07E-01	-7.69E-01	-7.81E-01	-7.56E-01	1.24E-02
LYS	28	C	267	GLY	29	N	764	4.21E-01	-1.22E+00	-1.28E+00	-1.15E+00	6.66E-02
LYS	28	C	267	GLY	29	O	767	6.83E-01	-5.49E-01	-5.72E-01	-5.25E-01	2.38E-02
LYS	28	C	267	ALA	30	N	771	5.54E-01	-6.81E-01	-7.21E-01	-6.41E-01	4.03E-02
LYS	28	C	267	ALA	30	O	774	6.91E-01	-5.87E-01	-6.24E-01	-5.51E-01	3.68E-02
LYS	28	C	267	ILE	31	N	781	8.40E-01	-3.32E-01	-3.45E-01	-3.19E-01	1.28E-02
LYS	28	C	267	ALA	42	O	946	8.36E-01	-4.19E-01	-4.57E-01	-3.81E-01	3.80E-02

LYS	28	O	268	SER	26	C	719	7.44E-01	-3.43E-01	-3.59E-01	-3.27E-01	1.61E-02
LYS	28	O	268	ASN	27	C	730	4.18E-01	-1.61E+00	-1.77E+00	-1.44E+00	1.67E-01
LYS	28	O	268	ASN	27	CG	733	5.70E-01	-7.52E-01	-8.89E-01	-6.15E-01	1.37E-01
LYS	28	O	268	LYS	28	C	744	3.73E-01	-2.50E+00	-2.61E+00	-2.38E+00	1.18E-01
LYS	28	O	268	LYS	28	H	751	5.15E-01	-3.87E-01	-4.06E-01	-3.67E-01	2.00E-02
LYS	28	O	268	LYS	28	HA	752	2.56E-01	-1.30E+00	-1.42E+00	-1.18E+00	1.20E-01
LYS	28	O	268	GLY	29	C	766	4.87E-01	-1.03E+00	-1.12E+00	-9.40E-01	9.12E-02
LYS	28	O	268	GLY	29	H	768	2.23E-01	-3.99E+00	-4.67E+00	-3.30E+00	6.83E-01
LYS	28	O	268	ALA	30	C	773	6.76E-01	-4.91E-01	-5.32E-01	-4.51E-01	4.05E-02
LYS	28	O	268	ALA	30	H	776	4.23E-01	-7.73E-01	-9.24E-01	-6.22E-01	1.51E-01
LYS	28	H	274	ASN	27	N	728	4.50E-01	-4.16E-01	-4.65E-01	-3.67E-01	4.90E-02
LYS	28	H	274	ASN	27	O	731	1.99E-01	-4.89E+00	-4.97E+00	-4.81E+00	7.63E-02
LYS	28	H	274	ASN	27	ND2	735	4.81E-01	-8.12E-01	-1.14E+00	-4.85E-01	3.27E-01
LYS	28	H	274	LYS	28	N	742	4.05E-01	-5.40E-01	-5.64E-01	-5.16E-01	2.40E-02
GLY	29	N	287	ASN	27	C	730	6.05E-01	-4.43E-01	-4.80E-01	-4.06E-01	3.69E-02
GLY	29	N	287	LYS	28	C	744	5.70E-01	-5.86E-01	-6.00E-01	-5.73E-01	1.36E-02
GLY	29	N	287	GLY	29	C	766	6.00E-01	-4.21E-01	-4.36E-01	-4.05E-01	1.59E-02
GLY	29	N	287	GLY	29	H	768	3.92E-01	-5.15E-01	-5.46E-01	-4.83E-01	3.16E-02
GLY	29	N	287	ALA	30	H	776	4.71E-01	-3.72E-01	-3.98E-01	-3.47E-01	2.56E-02
GLY	29	C	289	ASN	27	O	731	6.07E-01	-5.84E-01	-6.38E-01	-5.30E-01	5.41E-02
GLY	29	C	289	ASN	27	ND2	735	6.54E-01	-7.98E-01	-9.55E-01	-6.41E-01	1.57E-01
GLY	29	C	289	LYS	28	N	742	6.78E-01	-3.84E-01	-4.09E-01	-3.59E-01	2.50E-02
GLY	29	C	289	LYS	28	O	745	6.67E-01	-5.10E-01	-5.34E-01	-4.85E-01	2.44E-02
GLY	29	C	289	GLY	29	N	764	4.57E-01	-7.95E-01	-8.54E-01	-7.37E-01	5.89E-02
GLY	29	C	289	GLY	29	O	767	5.82E-01	-6.10E-01	-6.21E-01	-6.00E-01	1.08E-02
GLY	29	C	289	ALA	30	N	771	3.80E-01	-1.37E+00	-1.43E+00	-1.31E+00	5.73E-02
GLY	29	C	289	ALA	30	O	774	3.99E-01	-1.72E+00	-1.98E+00	-1.46E+00	2.56E-01
GLY	29	C	289	ALA	30	CB	775	4.55E-01	-4.98E-01	-5.39E-01	-4.56E-01	4.20E-02
GLY	29	C	289	ILE	31	N	781	5.75E-01	-5.59E-01	-5.95E-01	-5.23E-01	3.61E-02
GLY	29	C	289	ILE	31	O	784	8.55E-01	-3.56E-01	-3.68E-01	-3.43E-01	1.26E-02
GLY	29	O	290	ASN	27	C	730	6.40E-01	-5.58E-01	-6.47E-01	-4.68E-01	8.97E-02
GLY	29	O	290	LYS	28	C	744	5.18E-01	-1.03E+00	-1.17E+00	-8.88E-01	1.41E-01
GLY	29	O	290	GLY	29	C	766	3.68E-01	-1.88E+00	-2.01E+00	-1.76E+00	1.26E-01
GLY	29	O	290	GLY	29	H	768	3.55E-01	-1.01E+00	-1.28E+00	-7.45E-01	2.65E-01
GLY	29	O	290	ALA	30	C	773	3.62E-01	-2.05E+00	-2.43E+00	-1.66E+00	3.83E-01
GLY	29	O	290	ALA	30	H	776	1.93E-01	-6.21E+00	-6.69E+00	-5.72E+00	4.85E-01
GLY	29	O	290	ILE	31	C	783	6.89E-01	-4.29E-01	-4.68E-01	-3.90E-01	3.92E-02
GLY	29	O	290	ILE	31	H	789	5.30E-01	-4.35E-01	-4.79E-01	-3.91E-01	4.39E-02
ALA	30	N	294	LYS	28	C	744	6.86E-01	-4.32E-01	-4.47E-01	-4.16E-01	1.55E-02
ALA	30	N	294	GLY	29	C	766	5.67E-01	-5.15E-01	-5.32E-01	-4.98E-01	1.70E-02
ALA	30	N	294	ALA	30	C	773	4.93E-01	-6.99E-01	-7.23E-01	-6.75E-01	2.41E-02

ALA	30	N	294	ALA	30	H	776	3.83E-01	-6.87E-01	-7.41E-01	-6.33E-01	5.37E-02
ALA	30	C	296	ASN	27	ND2	735	8.17E-01	-4.93E-01	-5.55E-01	-4.31E-01	6.22E-02
ALA	30	C	296	GLY	29	O	767	7.81E-01	-3.34E-01	-3.43E-01	-3.25E-01	8.70E-03
ALA	30	C	296	ALA	30	N	771	5.65E-01	-5.11E-01	-5.36E-01	-4.87E-01	2.46E-02
ALA	30	C	296	ALA	30	O	774	3.56E-01	-2.20E+00	-2.25E+00	-2.15E+00	5.11E-02
ALA	30	C	296	ILE	31	N	781	5.68E-01	-5.59E-01	-5.68E-01	-5.49E-01	9.42E-03
ALA	30	C	296	ILE	31	O	784	7.79E-01	-4.09E-01	-4.16E-01	-4.02E-01	6.73E-03
ALA	30	C	296	ILE	32	N	800	6.57E-01	-4.11E-01	-4.17E-01	-4.04E-01	6.28E-03
ALA	30	C	296	ILE	32	O	803	7.83E-01	-4.05E-01	-4.14E-01	-3.96E-01	8.98E-03
ALA	30	O	297	GLY	29	C	766	7.97E-01	-3.59E-01	-3.70E-01	-3.47E-01	1.12E-02
ALA	30	O	297	ALA	30	C	773	5.96E-01	-6.21E-01	-6.30E-01	-6.12E-01	9.00E-03
ALA	30	O	297	ILE	31	C	783	7.75E-01	-3.68E-01	-3.73E-01	-3.64E-01	4.58E-03
ALA	30	CB	298	ALA	30	C	773	5.23E-01	-3.45E-01	-3.64E-01	-3.26E-01	1.91E-02
ALA	30	H	299	ALA	30	O	774	4.96E-01	-4.85E-01	-5.04E-01	-4.66E-01	1.90E-02
ALA	30	HA	300	ALA	30	O	774	2.43E-01	-1.38E+00	-1.42E+00	-1.34E+00	3.92E-02
ILE	31	N	304	GLY	29	C	766	6.73E-01	-4.00E-01	-4.16E-01	-3.84E-01	1.61E-02
ILE	31	N	304	ALA	30	C	773	4.07E-01	-1.25E+00	-1.29E+00	-1.20E+00	4.21E-02
ILE	31	N	304	ALA	30	H	776	4.96E-01	-3.99E-01	-4.30E-01	-3.68E-01	3.07E-02
ILE	31	N	304	ILE	31	C	783	5.52E-01	-5.94E-01	-6.06E-01	-5.83E-01	1.14E-02
ILE	31	N	304	ILE	31	H	789	5.75E-01	-3.14E-01	-3.19E-01	-3.08E-01	5.34E-03
ILE	31	N	304	ILE	31	HA	790	3.56E-01	-5.44E-01	-5.66E-01	-5.22E-01	2.20E-02
ILE	31	N	304	ILE	32	C	802	7.09E-01	-3.54E-01	-3.59E-01	-3.49E-01	5.03E-03
ILE	31	N	304	ILE	32	H	808	4.56E-01	-5.42E-01	-5.50E-01	-5.33E-01	8.55E-03
ILE	31	C	306	ALA	30	O	774	4.15E-01	-1.47E+00	-1.58E+00	-1.36E+00	1.08E-01
ILE	31	C	306	ILE	31	N	781	5.30E-01	-6.52E-01	-6.69E-01	-6.35E-01	1.69E-02
ILE	31	C	306	ILE	31	O	784	6.07E-01	-6.65E-01	-6.75E-01	-6.55E-01	1.02E-02
ILE	31	C	306	ILE	32	N	800	4.14E-01	-1.19E+00	-1.21E+00	-1.17E+00	2.08E-02
ILE	31	C	306	ILE	32	O	803	4.43E-01	-1.38E+00	-1.45E+00	-1.32E+00	6.43E-02
ILE	31	C	306	GLY	33	N	819	6.42E-01	-3.57E-01	-3.63E-01	-3.51E-01	6.17E-03
ILE	31	O	307	GLY	29	C	766	7.75E-01	-4.21E-01	-4.36E-01	-4.06E-01	1.48E-02
ILE	31	O	307	ALA	30	C	773	4.32E-01	-1.48E+00	-1.56E+00	-1.39E+00	8.45E-02
ILE	31	O	307	ILE	31	C	783	3.65E-01	-2.30E+00	-2.36E+00	-2.23E+00	6.40E-02
ILE	31	O	307	ILE	31	H	789	5.22E-01	-5.38E-01	-5.52E-01	-5.24E-01	1.38E-02
ILE	31	O	307	ILE	31	HA	790	2.47E-01	-2.12E+00	-2.21E+00	-2.03E+00	9.39E-02
ILE	31	O	307	ILE	32	C	802	4.27E-01	-1.52E+00	-1.59E+00	-1.45E+00	6.51E-02
ILE	31	O	307	ILE	32	H	808	2.00E-01	-7.47E+00	-7.58E+00	-7.36E+00	1.13E-01
ILE	31	O	307	ILE	32	HA	809	4.89E-01	-3.31E-01	-3.38E-01	-3.24E-01	6.52E-03
ILE	31	O	307	GLY	33	C	821	7.74E-01	-4.21E-01	-4.31E-01	-4.11E-01	9.57E-03
ILE	31	H	312	ALA	30	N	771	4.70E-01	-4.54E-01	-4.85E-01	-4.23E-01	3.13E-02
ILE	31	H	312	ALA	30	O	774	1.94E-01	-7.42E+00	-8.06E+00	-6.78E+00	6.40E-01
ILE	31	H	312	ILE	31	N	781	3.86E-01	-8.32E-01	-8.55E-01	-8.09E-01	2.26E-02

ILE	31	H	312	ILE	31	O	784	5.82E-01	-4.21E-01	-4.31E-01	-4.11E-01	1.02E-02
ILE	31	H	312	ILE	32	N	800	4.69E-01	-5.06E-01	-5.16E-01	-4.95E-01	1.01E-02
ILE	31	H	312	ILE	32	O	803	6.31E-01	-3.55E-01	-3.62E-01	-3.47E-01	7.74E-03
ILE	32	N	323	ALA	30	C	773	6.38E-01	-4.38E-01	-4.51E-01	-4.24E-01	1.38E-02
ILE	32	N	323	ILE	31	C	783	5.77E-01	-5.39E-01	-5.46E-01	-5.31E-01	7.33E-03
ILE	32	N	323	ILE	32	C	802	5.29E-01	-6.56E-01	-6.66E-01	-6.45E-01	1.10E-02
ILE	32	N	323	ILE	32	H	808	3.90E-01	-8.07E-01	-8.24E-01	-7.90E-01	1.66E-02
ILE	32	C	325	ALA	30	O	774	7.51E-01	-3.91E-01	-4.04E-01	-3.78E-01	1.28E-02
ILE	32	C	325	ILE	31	O	784	7.76E-01	-4.11E-01	-4.17E-01	-4.05E-01	5.98E-03
ILE	32	C	325	ILE	32	N	800	5.55E-01	-5.88E-01	-6.00E-01	-5.77E-01	1.16E-02
ILE	32	C	325	ILE	32	O	803	3.61E-01	-2.36E+00	-2.42E+00	-2.30E+00	6.08E-02
ILE	32	C	325	GLY	33	N	819	5.74E-01	-4.52E-01	-4.59E-01	-4.45E-01	6.87E-03
ILE	32	C	325	GLY	33	O	822	7.98E-01	-3.21E-01	-3.25E-01	-3.16E-01	4.11E-03
ILE	32	O	326	ILE	31	C	783	7.86E-01	-4.01E-01	-4.07E-01	-3.95E-01	5.64E-03
ILE	32	O	326	ILE	32	C	802	6.05E-01	-6.70E-01	-6.79E-01	-6.61E-01	8.55E-03
ILE	32	O	326	ILE	32	H	808	5.91E-01	-4.07E-01	-4.14E-01	-4.00E-01	7.27E-03
ILE	32	O	326	GLY	33	C	821	8.14E-01	-3.85E-01	-3.90E-01	-3.80E-01	4.95E-03
ILE	32	H	331	ALA	30	O	774	6.00E-01	-3.54E-01	-3.69E-01	-3.38E-01	1.55E-02
ILE	32	H	331	ILE	32	O	803	5.19E-01	-5.46E-01	-5.58E-01	-5.33E-01	1.21E-02
ILE	32	HA	332	ILE	32	N	800	3.56E-01	-5.44E-01	-5.63E-01	-5.25E-01	1.88E-02
ILE	32	HA	332	ILE	32	O	803	2.45E-01	-2.17E+00	-2.19E+00	-2.16E+00	1.57E-02
GLY	33	N	342	ILE	31	C	783	6.52E-01	-3.46E-01	-3.55E-01	-3.37E-01	9.21E-03
GLY	33	N	342	ILE	32	C	802	4.13E-01	-9.95E-01	-1.02E+00	-9.71E-01	2.42E-02
GLY	33	N	342	ILE	32	H	808	4.71E-01	-4.14E-01	-4.26E-01	-4.02E-01	1.20E-02
GLY	33	N	342	GLY	33	C	821	5.92E-01	-4.33E-01	-4.41E-01	-4.24E-01	8.50E-03
GLY	33	C	344	ILE	31	O	784	8.59E-01	-3.52E-01	-3.62E-01	-3.43E-01	9.53E-03
GLY	33	C	344	ILE	32	N	800	6.77E-01	-3.95E-01	-4.04E-01	-3.86E-01	8.86E-03
GLY	33	C	344	ILE	32	O	803	4.00E-01	-1.84E+00	-1.92E+00	-1.76E+00	8.07E-02
GLY	33	C	344	GLY	33	N	819	4.91E-01	-6.61E-01	-6.77E-01	-6.44E-01	1.67E-02
GLY	33	C	344	GLY	33	CA	820	3.92E-01	-4.02E-01	-4.16E-01	-3.89E-01	1.34E-02
GLY	33	C	344	GLY	33	O	822	5.91E-01	-5.92E-01	-6.11E-01	-5.73E-01	1.89E-02
GLY	33	C	344	LEU	34	N	826	4.87E-01	-6.40E-01	-6.63E-01	-6.18E-01	2.26E-02
GLY	33	C	344	LEU	34	O	829	7.35E-01	-4.30E-01	-4.95E-01	-3.65E-01	6.50E-02
GLY	33	C	344	MET	35	O	848	5.93E-01	-6.81E-01	-7.73E-01	-5.90E-01	9.15E-02
GLY	33	C	344	VAL	36	N	862	6.76E-01	-4.02E-01	-4.41E-01	-3.64E-01	3.82E-02
GLY	33	O	345	ILE	31	C	783	7.26E-01	-3.82E-01	-3.95E-01	-3.69E-01	1.32E-02
GLY	33	O	345	ILE	32	C	802	4.21E-01	-1.30E+00	-1.36E+00	-1.24E+00	6.46E-02
GLY	33	O	345	ILE	32	H	808	5.96E-01	-3.30E-01	-3.42E-01	-3.17E-01	1.29E-02
GLY	33	O	345	GLY	33	C	821	3.94E-01	-1.57E+00	-1.63E+00	-1.51E+00	6.23E-02
GLY	33	O	345	GLY	33	H	823	4.95E-01	-3.86E-01	-3.98E-01	-3.73E-01	1.24E-02
GLY	33	O	345	GLY	33	HA2	824	2.67E-01	-7.53E-01	-8.84E-01	-6.21E-01	1.31E-01

GLY	33	O	345	LEU	34	C	828	5.70E-01	-6.32E-01	-6.53E-01	-6.11E-01	2.08E-02
GLY	33	O	345	LEU	34	H	834	3.59E-01	-9.68E-01	-1.15E+00	-7.84E-01	1.84E-01
GLY	33	O	345	MET	35	C	847	5.67E-01	-7.11E-01	-8.32E-01	-5.90E-01	1.21E-01
GLY	33	H	346	ILE	32	N	800	4.50E-01	-4.31E-01	-4.47E-01	-4.15E-01	1.61E-02
GLY	33	H	346	ILE	32	O	803	1.98E-01	-5.98E+00	-6.37E+00	-5.59E+00	3.88E-01
GLY	33	H	346	GLY	33	N	819	3.87E-01	-5.27E-01	-5.41E-01	-5.13E-01	1.40E-02
LEU	34	N	349	ILE	32	C	802	5.83E-01	-4.17E-01	-4.40E-01	-3.95E-01	2.27E-02
LEU	34	N	349	GLY	33	C	821	5.27E-01	-5.34E-01	-5.54E-01	-5.13E-01	2.07E-02
LEU	34	N	349	LEU	34	C	828	6.38E-01	-3.45E-01	-3.54E-01	-3.36E-01	9.10E-03
LEU	34	N	349	LEU	34	H	834	4.23E-01	-4.10E-01	-4.30E-01	-3.90E-01	2.01E-02
LEU	34	C	351	ILE	32	O	803	6.53E-01	-5.80E-01	-6.12E-01	-5.47E-01	3.24E-02
LEU	34	C	351	GLY	33	N	819	6.47E-01	-3.55E-01	-3.73E-01	-3.37E-01	1.80E-02
LEU	34	C	351	GLY	33	O	822	5.99E-01	-5.69E-01	-6.03E-01	-5.35E-01	3.43E-02
LEU	34	C	351	LEU	34	N	826	4.52E-01	-7.64E-01	-8.20E-01	-7.09E-01	5.56E-02
LEU	34	C	351	LEU	34	O	829	5.83E-01	-7.23E-01	-9.49E-01	-4.97E-01	2.26E-01
LEU	34	C	351	MET	35	N	845	4.17E-01	-1.11E+00	-1.27E+00	-9.57E-01	1.56E-01
LEU	34	C	351	MET	35	O	848	3.92E-01	-1.96E+00	-2.37E+00	-1.56E+00	4.01E-01
LEU	34	C	351	VAL	36	N	862	5.41E-01	-6.47E-01	-7.26E-01	-5.68E-01	7.93E-02
LEU	34	O	352	ILE	32	C	802	7.21E-01	-4.27E-01	-4.54E-01	-4.00E-01	2.67E-02
LEU	34	O	352	GLY	33	C	821	4.80E-01	-1.10E+00	-1.26E+00	-9.41E-01	1.59E-01
LEU	34	O	352	LEU	34	C	828	4.14E-01	-1.61E+00	-1.83E+00	-1.38E+00	2.25E-01
LEU	34	O	352	LEU	34	H	834	3.83E-01	-9.80E-01	-1.30E+00	-6.64E-01	3.16E-01
LEU	34	O	352	MET	35	C	847	3.66E-01	-2.75E+00	-3.41E+00	-2.08E+00	6.65E-01
LEU	34	H	357	ILE	32	O	803	5.59E-01	-3.70E-01	-4.00E-01	-3.41E-01	2.93E-02
LEU	34	HA	358	LEU	34	N	826	3.17E-01	-4.74E-01	-5.17E-01	-4.30E-01	4.37E-02
MET	35	N	368	GLY	33	C	821	6.07E-01	-4.48E-01	-5.16E-01	-3.79E-01	6.86E-02
MET	35	N	368	LEU	34	C	828	5.89E-01	-5.01E-01	-6.57E-01	-3.44E-01	1.57E-01
MET	35	N	368	MET	35	C	847	4.79E-01	-7.70E-01	-8.09E-01	-7.31E-01	3.89E-02
MET	35	C	370	ILE	32	O	803	8.30E-01	-3.87E-01	-4.04E-01	-3.69E-01	1.77E-02
MET	35	C	370	LEU	34	O	829	7.80E-01	-4.58E-01	-6.61E-01	-2.55E-01	2.03E-01
MET	35	C	370	MET	35	N	845	6.19E-01	-4.29E-01	-4.39E-01	-4.19E-01	1.00E-02
MET	35	C	370	MET	35	O	848	3.82E-01	-1.98E+00	-2.15E+00	-1.81E+00	1.69E-01
MET	35	C	370	VAL	36	N	862	5.71E-01	-5.81E-01	-5.97E-01	-5.65E-01	1.57E-02
MET	35	O	371	LEU	34	C	828	8.37E-01	-3.37E-01	-3.74E-01	-3.01E-01	3.67E-02
MET	35	O	371	MET	35	C	847	6.02E-01	-6.53E-01	-6.78E-01	-6.29E-01	2.44E-02
MET	35	H	376	MET	35	O	848	4.76E-01	-5.33E-01	-5.89E-01	-4.77E-01	5.62E-02
MET	35	HA	377	MET	35	O	848	2.52E-01	-1.30E+00	-1.42E+00	-1.18E+00	1.19E-01
VAL	36	N	385	GLY	33	C	821	6.91E-01	-3.84E-01	-4.20E-01	-3.49E-01	3.57E-02
VAL	36	N	385	LEU	34	C	828	6.95E-01	-3.79E-01	-4.34E-01	-3.25E-01	5.46E-02
VAL	36	N	385	MET	35	C	847	4.54E-01	-9.92E-01	-1.02E+00	-9.67E-01	2.53E-02
VAL	36	N	385	VAL	36	C	864	5.87E-01	-4.08E-01	-4.18E-01	-3.97E-01	1.05E-02

VAL	36	N	385	VAL	36	CB	866	4.83E-01	-5.64E-01	-5.91E-01	-5.37E-01	2.74E-02
VAL	36	N	385	VAL	36	H	869	5.98E-01	-3.86E-01	-3.99E-01	-3.73E-01	1.32E-02
VAL	36	C	387	MET	35	O	848	4.42E-01	-9.99E-01	-1.05E+00	-9.47E-01	5.24E-02
VAL	36	C	387	VAL	36	N	862	5.26E-01	-5.21E-01	-5.34E-01	-5.07E-01	1.37E-02
VAL	36	C	387	VAL	36	O	865	6.12E-01	-3.36E-01	-3.45E-01	-3.27E-01	9.18E-03
VAL	36	C	387	GLY	37	N	878	4.57E-01	-6.08E-01	-6.46E-01	-5.71E-01	3.77E-02
VAL	36	C	387	GLY	37	O	881	5.03E-01	-6.58E-01	-7.06E-01	-6.11E-01	4.75E-02
VAL	36	C	387	GLY	38	O	888	6.69E-01	-3.54E-01	-3.76E-01	-3.32E-01	2.19E-02
VAL	36	O	388	MET	35	C	847	4.52E-01	-9.07E-01	-9.51E-01	-8.63E-01	4.35E-02
VAL	36	O	388	VAL	36	C	864	3.87E-01	-1.01E+00	-1.05E+00	-9.66E-01	4.14E-02
VAL	36	O	388	VAL	36	CB	866	3.24E-01	-1.49E+00	-1.70E+00	-1.28E+00	2.06E-01
VAL	36	O	388	VAL	36	H	869	5.16E-01	-4.83E-01	-4.99E-01	-4.67E-01	1.57E-02
VAL	36	O	388	GLY	37	C	880	5.08E-01	-6.66E-01	-7.14E-01	-6.18E-01	4.82E-02
VAL	36	O	388	GLY	37	H	882	2.87E-01	-1.44E+00	-1.77E+00	-1.11E+00	3.33E-01
VAL	36	O	388	GLY	38	C	887	6.76E-01	-3.57E-01	-3.76E-01	-3.38E-01	1.94E-02
VAL	36	CB	389	MET	35	O	848	5.55E-01	-5.18E-01	-5.54E-01	-4.82E-01	3.61E-02
VAL	36	H	392	ILE	32	O	803	6.82E-01	-4.08E-01	-4.28E-01	-3.87E-01	2.10E-02
VAL	36	H	392	LEU	34	O	829	6.66E-01	-4.73E-01	-7.19E-01	-2.27E-01	2.46E-01
VAL	36	H	392	MET	35	N	845	5.20E-01	-4.62E-01	-4.78E-01	-4.46E-01	1.64E-02
VAL	36	H	392	MET	35	O	848	2.90E-01	-3.34E+00	-4.11E+00	-2.58E+00	7.68E-01
VAL	36	H	392	VAL	36	N	862	4.29E-01	-8.48E-01	-9.03E-01	-7.93E-01	5.49E-02
VAL	36	H	392	GLY	37	N	878	5.57E-01	-3.77E-01	-4.01E-01	-3.53E-01	2.38E-02
GLY	37	N	401	MET	35	C	847	6.23E-01	-4.03E-01	-4.30E-01	-3.77E-01	2.67E-02
GLY	37	N	401	VAL	36	C	864	5.52E-01	-3.89E-01	-4.06E-01	-3.72E-01	1.70E-02
GLY	37	N	401	GLY	37	C	880	5.66E-01	-4.79E-01	-5.03E-01	-4.55E-01	2.38E-02
GLY	37	N	401	GLY	37	H	882	3.98E-01	-4.95E-01	-5.32E-01	-4.58E-01	3.71E-02
GLY	37	C	403	MET	35	O	848	7.32E-01	-4.28E-01	-4.50E-01	-4.06E-01	2.21E-02
GLY	37	C	403	GLY	37	N	878	5.15E-01	-5.95E-01	-6.28E-01	-5.61E-01	3.37E-02
GLY	37	C	403	GLY	37	O	881	3.66E-01	-1.92E+00	-2.05E+00	-1.79E+00	1.31E-01
GLY	37	C	403	GLY	38	N	885	5.74E-01	-4.64E-01	-4.83E-01	-4.45E-01	1.89E-02
GLY	37	C	403	GLY	38	O	888	4.63E-01	-1.05E+00	-1.12E+00	-9.70E-01	7.71E-02
GLY	37	C	403	VAL	39	N	892	6.72E-01	-4.00E-01	-4.14E-01	-3.86E-01	1.41E-02
GLY	37	O	404	GLY	37	C	880	5.96E-01	-5.82E-01	-6.06E-01	-5.58E-01	2.43E-02
GLY	37	O	404	GLY	38	C	887	6.50E-01	-4.84E-01	-5.01E-01	-4.67E-01	1.72E-02
GLY	37	HA2	406	GLY	37	O	881	2.75E-01	-6.70E-01	-7.52E-01	-5.88E-01	8.23E-02
GLY	38	N	408	GLY	37	C	880	4.06E-01	-1.07E+00	-1.14E+00	-1.00E+00	7.05E-02
GLY	38	N	408	GLY	37	H	882	4.39E-01	-3.90E-01	-4.35E-01	-3.44E-01	4.52E-02
GLY	38	N	408	GLY	38	C	887	4.41E-01	-8.69E-01	-9.36E-01	-8.02E-01	6.68E-02
GLY	38	C	410	GLY	37	O	881	4.65E-01	-1.04E+00	-1.12E+00	-9.59E-01	8.06E-02
GLY	38	C	410	GLY	38	N	885	6.25E-01	-3.86E-01	-3.97E-01	-3.75E-01	1.06E-02
GLY	38	C	410	GLY	38	O	888	3.60E-01	-2.00E+00	-2.14E+00	-1.86E+00	1.43E-01

GLY	38	C	410	VAL	39	N	892	5.72E-01	-5.63E-01	-5.85E-01	-5.40E-01	2.24E-02
GLY	38	C	410	VAL	40	N	908	6.54E-01	-4.24E-01	-4.38E-01	-4.09E-01	1.47E-02
GLY	38	O	411	GLY	37	C	880	6.90E-01	-4.30E-01	-4.47E-01	-4.14E-01	1.66E-02
GLY	38	O	411	GLY	38	C	887	6.00E-01	-5.72E-01	-5.92E-01	-5.52E-01	1.98E-02
GLY	38	O	411	VAL	40	H	915	6.51E-01	-3.67E-01	-3.89E-01	-3.45E-01	2.22E-02
GLY	38	H	412	GLY	37	N	878	4.24E-01	-4.24E-01	-4.71E-01	-3.78E-01	4.68E-02
GLY	38	H	412	GLY	37	O	881	2.04E-01	-4.68E+00	-5.36E+00	-3.99E+00	6.85E-01
GLY	38	H	412	GLY	38	N	885	3.95E-01	-5.02E-01	-5.32E-01	-4.71E-01	3.10E-02
GLY	38	H	412	GLY	38	O	888	3.00E-01	-1.53E+00	-1.82E+00	-1.25E+00	2.85E-01
VAL	39	N	415	GLY	37	C	880	5.52E-01	-6.09E-01	-6.36E-01	-5.81E-01	2.75E-02
VAL	39	N	415	GLY	38	C	887	4.09E-01	-1.26E+00	-1.30E+00	-1.21E+00	4.46E-02
VAL	39	N	415	VAL	39	C	894	5.53E-01	-4.65E-01	-4.83E-01	-4.48E-01	1.77E-02
VAL	39	N	415	VAL	39	CB	896	5.21E-01	-4.76E-01	-5.12E-01	-4.39E-01	3.67E-02
VAL	39	N	415	VAL	39	H	899	5.75E-01	-4.20E-01	-4.30E-01	-4.09E-01	1.04E-02
VAL	39	N	415	VAL	40	H	915	4.56E-01	-7.21E-01	-7.42E-01	-7.00E-01	2.07E-02
VAL	39	C	417	GLY	37	O	881	6.45E-01	-3.79E-01	-3.96E-01	-3.62E-01	1.72E-02
VAL	39	C	417	GLY	38	O	888	4.20E-01	-1.03E+00	-1.11E+00	-9.50E-01	7.82E-02
VAL	39	C	417	VAL	39	N	892	5.22E-01	-5.31E-01	-5.56E-01	-5.06E-01	2.52E-02
VAL	39	C	417	VAL	39	O	895	6.01E-01	-3.49E-01	-3.57E-01	-3.41E-01	8.04E-03
VAL	39	C	417	VAL	40	N	908	4.09E-01	-9.66E-01	-9.98E-01	-9.34E-01	3.19E-02
VAL	39	C	417	VAL	40	O	911	4.41E-01	-7.20E-01	-7.44E-01	-6.95E-01	2.40E-02
VAL	39	C	417	ILE	41	N	924	6.39E-01	-3.41E-01	-3.48E-01	-3.35E-01	6.82E-03
VAL	39	O	418	GLY	37	C	880	6.85E-01	-3.47E-01	-3.57E-01	-3.37E-01	9.78E-03
VAL	39	O	418	GLY	38	C	887	4.34E-01	-9.82E-01	-1.06E+00	-9.05E-01	7.69E-02
VAL	39	O	418	VAL	39	C	894	3.63E-01	-1.19E+00	-1.22E+00	-1.16E+00	3.28E-02
VAL	39	O	418	VAL	39	CB	896	4.28E-01	-6.89E-01	-7.34E-01	-6.43E-01	4.52E-02
VAL	39	O	418	VAL	39	H	899	5.13E-01	-4.91E-01	-5.17E-01	-4.64E-01	2.69E-02
VAL	39	O	418	VAL	40	C	910	4.29E-01	-7.72E-01	-8.07E-01	-7.36E-01	3.60E-02
VAL	39	O	418	VAL	40	CB	912	4.29E-01	-6.81E-01	-7.13E-01	-6.49E-01	3.16E-02
VAL	39	O	418	VAL	40	H	915	2.00E-01	-6.57E+00	-6.65E+00	-6.50E+00	7.33E-02
VAL	39	CB	419	GLY	37	O	881	5.67E-01	-4.42E-01	-4.67E-01	-4.17E-01	2.52E-02
VAL	39	CB	419	GLY	38	O	888	4.25E-01	-9.14E-01	-1.08E+00	-7.43E-01	1.70E-01
VAL	39	CB	419	VAL	39	N	892	5.42E-01	-4.37E-01	-4.81E-01	-3.93E-01	4.41E-02
VAL	39	CB	419	VAL	40	N	908	5.33E-01	-4.49E-01	-4.77E-01	-4.21E-01	2.83E-02
VAL	39	H	422	GLY	37	O	881	3.79E-01	-1.34E+00	-1.50E+00	-1.19E+00	1.58E-01
VAL	39	H	422	GLY	38	N	885	4.99E-01	-4.84E-01	-5.13E-01	-4.55E-01	2.92E-02
VAL	39	H	422	GLY	38	O	888	1.98E-01	-8.53E+00	-9.01E+00	-8.05E+00	4.80E-01
VAL	39	H	422	VAL	39	N	892	3.88E-01	-1.09E+00	-1.15E+00	-1.04E+00	5.55E-02
VAL	39	H	422	VAL	39	O	895	5.94E-01	-3.53E-01	-3.73E-01	-3.34E-01	1.95E-02
VAL	39	H	422	VAL	40	N	908	4.85E-01	-6.27E-01	-6.67E-01	-5.86E-01	4.04E-02
VAL	40	N	431	GLY	38	C	887	6.35E-01	-4.50E-01	-4.69E-01	-4.31E-01	1.91E-02

VAL	40	N	431	VAL	39	C	894	5.71E-01	-4.34E-01	-4.47E-01	-4.21E-01	1.30E-02
VAL	40	N	431	VAL	40	C	910	5.27E-01	-5.18E-01	-5.33E-01	-5.04E-01	1.43E-02
VAL	40	N	431	VAL	40	CB	912	5.55E-01	-4.08E-01	-4.15E-01	-4.01E-01	7.35E-03
VAL	40	N	431	VAL	40	H	915	3.84E-01	-1.13E+00	-1.18E+00	-1.07E+00	5.45E-02
VAL	40	C	433	VAL	40	N	908	5.55E-01	-4.61E-01	-4.69E-01	-4.53E-01	7.81E-03
VAL	40	C	433	VAL	40	O	911	3.65E-01	-1.17E+00	-1.22E+00	-1.13E+00	4.58E-02
VAL	40	C	433	ILE	41	N	924	5.81E-01	-4.18E-01	-4.29E-01	-4.07E-01	1.15E-02
VAL	40	O	434	VAL	40	C	910	6.08E-01	-3.40E-01	-3.46E-01	-3.34E-01	5.67E-03
VAL	40	O	434	VAL	40	H	915	5.89E-01	-3.59E-01	-3.64E-01	-3.53E-01	5.90E-03
VAL	40	CB	435	VAL	40	N	908	5.29E-01	-4.54E-01	-4.66E-01	-4.42E-01	1.19E-02
VAL	40	CB	435	VAL	40	O	911	4.31E-01	-6.75E-01	-7.09E-01	-6.40E-01	3.47E-02
VAL	40	H	438	GLY	38	O	888	6.02E-01	-4.31E-01	-4.53E-01	-4.08E-01	2.26E-02
VAL	40	H	438	VAL	40	N	908	5.73E-01	-4.22E-01	-4.35E-01	-4.10E-01	1.28E-02
VAL	40	H	438	VAL	40	O	911	5.14E-01	-4.88E-01	-5.09E-01	-4.66E-01	2.18E-02
ILE	41	N	447	VAL	39	C	894	6.59E-01	-3.20E-01	-3.27E-01	-3.14E-01	6.31E-03
ILE	41	N	447	VAL	40	C	910	4.15E-01	-9.34E-01	-9.57E-01	-9.11E-01	2.29E-02
ILE	41	N	447	VAL	40	CB	912	5.41E-01	-4.32E-01	-4.41E-01	-4.22E-01	9.41E-03
ILE	41	N	447	VAL	40	H	915	4.78E-01	-6.44E-01	-6.59E-01	-6.29E-01	1.53E-02
ILE	41	N	447	ILE	41	C	926	5.61E-01	-5.77E-01	-6.12E-01	-5.42E-01	3.53E-02
ILE	41	N	447	ILE	41	HA	933	3.66E-01	-5.13E-01	-5.63E-01	-4.64E-01	4.95E-02
ILE	41	N	447	ALA	42	H	949	4.82E-01	-4.33E-01	-4.85E-01	-3.81E-01	5.19E-02
ILE	41	C	449	VAL	40	N	908	7.07E-01	-3.55E-01	-3.65E-01	-3.44E-01	1.01E-02
ILE	41	C	449	VAL	40	O	911	4.21E-01	-1.04E+00	-1.11E+00	-9.66E-01	7.01E-02
ILE	41	C	449	ILE	41	N	924	5.31E-01	-6.52E-01	-6.79E-01	-6.24E-01	2.73E-02
ILE	41	C	449	ILE	41	O	927	6.06E-01	-6.69E-01	-6.84E-01	-6.53E-01	1.54E-02
ILE	41	C	449	ALA	42	N	943	4.24E-01	-1.02E+00	-1.09E+00	-9.43E-01	7.56E-02
ILE	41	C	449	ALA	42	O	946	6.19E-01	-5.76E-01	-6.18E-01	-5.34E-01	4.20E-02
ILE	41	C	449	ALA	42	CB	947	4.76E-01	-4.46E-01	-5.17E-01	-3.76E-01	7.07E-02
ILE	41	C	449	ALA	42	OXT	948	7.23E-01	-4.22E-01	-4.46E-01	-3.97E-01	2.49E-02
ILE	41	O	450	LYS	28	C	744	7.79E-01	-5.24E-01	-5.57E-01	-4.91E-01	3.28E-02
ILE	41	O	450	GLY	29	C	766	7.96E-01	-4.03E-01	-4.26E-01	-3.80E-01	2.33E-02
ILE	41	O	450	VAL	39	C	894	7.67E-01	-3.31E-01	-3.44E-01	-3.17E-01	1.35E-02
ILE	41	O	450	VAL	40	C	910	4.31E-01	-1.18E+00	-1.29E+00	-1.07E+00	1.13E-01
ILE	41	O	450	VAL	40	CB	912	5.79E-01	-5.13E-01	-5.41E-01	-4.86E-01	2.78E-02
ILE	41	O	450	VAL	40	H	915	6.23E-01	-4.90E-01	-5.17E-01	-4.63E-01	2.70E-02
ILE	41	O	450	ILE	41	C	926	3.83E-01	-2.01E+00	-2.10E+00	-1.93E+00	8.30E-02
ILE	41	O	450	ILE	41	H	932	5.24E-01	-5.37E-01	-5.69E-01	-5.04E-01	3.23E-02
ILE	41	O	450	ILE	41	HA	933	2.67E-01	-1.78E+00	-2.09E+00	-1.47E+00	3.10E-01
ILE	41	O	450	ALA	42	C	945	5.36E-01	-8.91E-01	-9.74E-01	-8.09E-01	8.28E-02
ILE	41	O	450	ALA	42	H	949	2.49E-01	-3.67E+00	-4.27E+00	-3.07E+00	6.03E-01
ILE	41	H	455	VAL	40	N	908	4.58E-01	-5.35E-01	-5.49E-01	-5.20E-01	1.50E-02

ILE	41	H	455	VAL	40	O	911	1.99E-01	-5.00E+00	-5.26E+00	-4.74E+00	2.58E-01
ILE	41	H	455	ILE	41	N	924	3.93E-01	-7.92E-01	-8.29E-01	-7.54E-01	3.74E-02
ILE	41	H	455	ILE	41	O	927	5.85E-01	-4.18E-01	-4.39E-01	-3.97E-01	2.09E-02
ILE	41	H	455	ALA	42	N	943	4.91E-01	-4.13E-01	-4.55E-01	-3.71E-01	4.20E-02
ALA	42	N	466	ILE	41	C	926	5.69E-01	-5.01E-01	-5.21E-01	-4.80E-01	2.01E-02
ALA	42	N	466	ALA	42	C	945	6.34E-01	-3.98E-01	-4.14E-01	-3.82E-01	1.60E-02
ALA	42	N	466	ALA	42	H	949	3.89E-01	-6.52E-01	-6.88E-01	-6.16E-01	3.57E-02
ALA	42	C	468	LYS	28	O	745	6.93E-01	-4.79E-01	-5.45E-01	-4.12E-01	6.70E-02
ALA	42	C	468	LYS	28	NZ	750	4.15E-01	-7.75E-01	-1.01E+00	-5.35E-01	2.39E-01
ALA	42	C	468	GLY	29	N	764	6.12E-01	-4.04E-01	-4.47E-01	-3.61E-01	4.30E-02
ALA	42	C	468	ILE	41	O	927	6.41E-01	-5.99E-01	-6.33E-01	-5.65E-01	3.42E-02
ALA	42	C	468	ALA	42	N	943	4.18E-01	-1.07E+00	-1.18E+00	-9.55E-01	1.15E-01
ALA	42	C	468	ALA	42	O	946	4.55E-01	-1.18E+00	-1.29E+00	-1.06E+00	1.17E-01
ALA	42	C	468	ALA	42	CB	947	3.43E-01	-1.03E+00	-1.16E+00	-9.09E-01	1.24E-01
ALA	42	C	468	ALA	42	OXT	948	5.77E-01	-6.69E-01	-7.11E-01	-6.28E-01	4.15E-02
ALA	42	O	469	LYS	28	C	744	6.05E-01	-8.08E-01	-9.41E-01	-6.74E-01	1.34E-01
ALA	42	O	469	LYS	28	HZ1	761	4.71E-01	-6.22E-01	-7.91E-01	-4.53E-01	1.69E-01
ALA	42	O	469	LYS	28	HZ2	762	4.10E-01	-1.10E+00	-1.66E+00	-5.36E-01	5.62E-01
ALA	42	O	469	LYS	28	HZ3	763	4.11E-01	-1.17E+00	-1.63E+00	-7.05E-01	4.64E-01
ALA	42	O	469	ILE	41	C	926	6.08E-01	-6.22E-01	-7.24E-01	-5.20E-01	1.02E-01
ALA	42	O	469	ALA	42	C	945	5.33E-01	-8.05E-01	-8.72E-01	-7.39E-01	6.66E-02
ALA	42	O	469	ALA	42	H	949	4.18E-01	-8.53E-01	-1.12E+00	-5.87E-01	2.66E-01
ALA	42	OXT	471	LYS	28	C	744	6.09E-01	-7.84E-01	-9.01E-01	-6.68E-01	1.16E-01
ALA	42	OXT	471	LYS	28	HZ1	761	3.97E-01	-1.20E+00	-1.75E+00	-6.59E-01	5.44E-01
ALA	42	OXT	471	LYS	28	HZ2	762	3.58E-01	-1.76E+00	-2.90E+00	-6.19E-01	1.14E+00
ALA	42	OXT	471	LYS	28	HZ3	763	3.42E-01	-2.88E+00	-4.75E+00	-1.01E+00	1.87E+00
ALA	42	OXT	471	ILE	41	C	926	4.80E-01	-1.06E+00	-1.22E+00	-8.98E-01	1.61E-01
ALA	42	OXT	471	ALA	42	C	945	3.78E-01	-1.95E+00	-2.26E+00	-1.64E+00	3.13E-01
ALA	42	OXT	471	ALA	42	H	949	2.96E-01	-2.23E+00	-2.86E+00	-1.59E+00	6.37E-01
ALA	42	OXT	471	ALA	42	HB2	952	2.74E-01	-6.61E-01	-7.78E-01	-5.43E-01	1.17E-01

Supplementary Table 9b: Mapping results for A β 42's (PDB ID: 5KK3) short range (1:2) dominant atom-atom Lennard-Jones interactions across ensemble structures. Columns for each chain correspond to: residue abbreviation, residue number in peptide sequence, atom identity (IUPAC naming convention) and atom number in PDB file. Energy in kT , distance in nm . Mapping analysis began on the 11th residue for both isoforms because original structure data for A β 42 begins with the 11th residue.

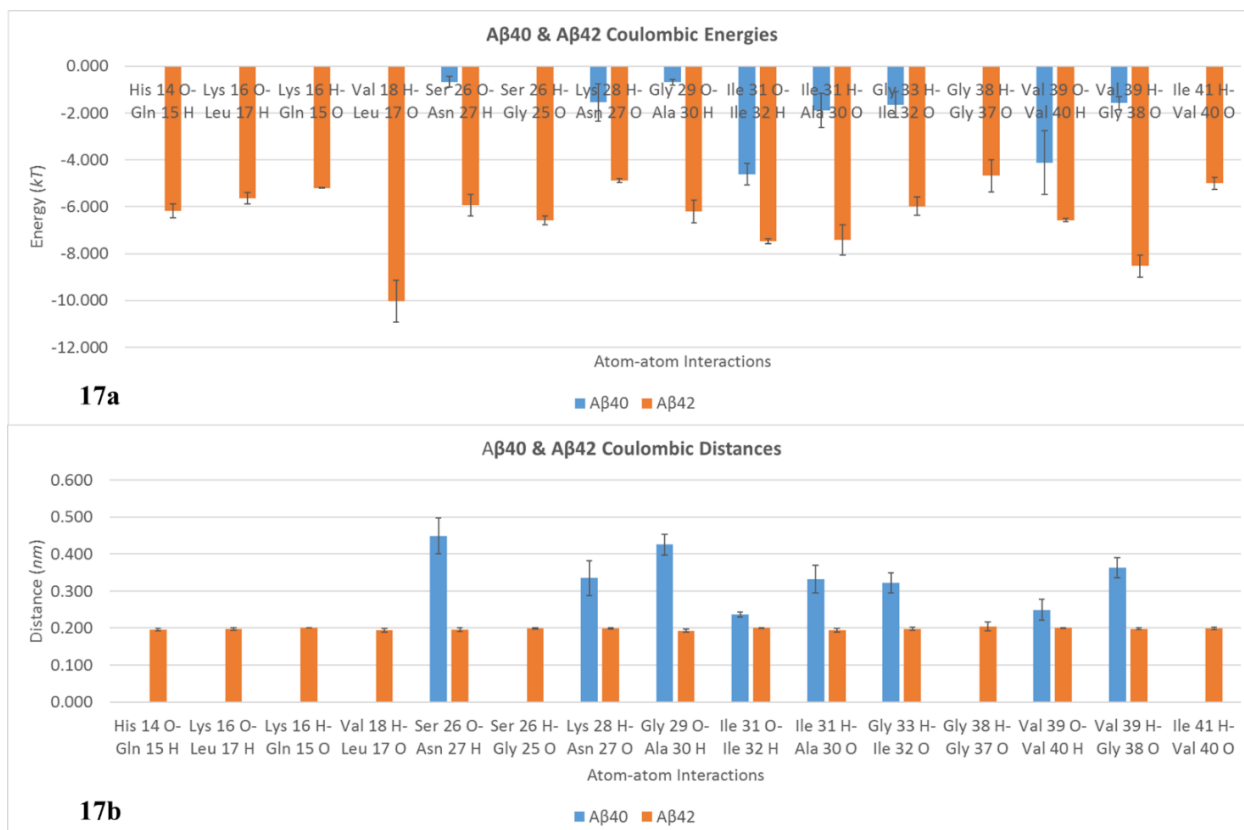
Chain 1				Chain 2				Average Distance	Average L-J Values	Lower 95% Confidence Interval Bound	Upper 95% Confidence Interval Bound	Margin of Error
HIS	14	C	51	GLN	15	N	543	4.07E-01	-1.64E-01	-1.71E-01	-1.57E-01	6.86E-03
HIS	14	O	52	HIS	14	CA	527	3.83E-01	-1.97E-01	-2.19E-01	-1.75E-01	2.21E-02
HIS	14	O	52	HIS	14	C	528	3.81E-01	-1.93E-01	-2.04E-01	-1.82E-01	1.11E-02
HIS	14	O	52	GLN	15	CA	544	3.67E-01	-2.16E-01	-2.30E-01	-2.02E-01	1.40E-02
HIS	14	O	52	GLN	15	CB	547	3.72E-01	-2.04E-01	-2.32E-01	-1.76E-01	2.78E-02
GLN	15	CA	67	GLN	15	CB	547	4.14E-01	-1.47E-01	-1.63E-01	-1.32E-01	1.53E-02
GLN	15	C	68	GLN	15	O	546	3.63E-01	-2.12E-01	-2.17E-01	-2.08E-01	4.46E-03
LYS	16	N	83	GLN	15	C	545	4.06E-01	-1.65E-01	-1.72E-01	-1.58E-01	7.01E-03
LYS	16	CA	84	GLN	15	O	546	3.85E-01	-1.92E-01	-2.12E-01	-1.73E-01	1.97E-02
LYS	16	C	85	LEU	17	N	582	3.96E-01	-1.76E-01	-1.84E-01	-1.68E-01	7.90E-03
LYS	16	O	86	LYS	16	CA	561	3.84E-01	-1.90E-01	-2.20E-01	-1.61E-01	2.96E-02
LYS	16	O	86	LYS	16	C	562	3.74E-01	-1.98E-01	-2.07E-01	-1.89E-01	9.39E-03
LEU	17	CA	106	LEU	17	CB	586	4.18E-01	-1.45E-01	-1.58E-01	-1.32E-01	1.31E-02
LEU	17	C	107	LEU	17	O	585	3.65E-01	-2.10E-01	-2.17E-01	-2.03E-01	6.95E-03
VAL	18	N	124	LEU	17	C	584	4.06E-01	-1.65E-01	-1.73E-01	-1.57E-01	7.93E-03
VAL	18	CA	125	LEU	17	O	585	3.84E-01	-2.10E-01	-2.24E-01	-1.95E-01	1.43E-02
VAL	18	C	126	LEU	17	O	585	4.00E-01	-1.61E-01	-1.84E-01	-1.38E-01	2.27E-02
VAL	18	O	127	VAL	18	CA	602	3.65E-01	-2.11E-01	-2.29E-01	-1.92E-01	1.86E-02
VAL	18	O	127	VAL	18	C	603	3.89E-01	-1.82E-01	-1.91E-01	-1.73E-01	8.70E-03
ASP	23	O	208	ASP	23	C	684	3.87E-01	-1.85E-01	-1.94E-01	-1.76E-01	9.26E-03
ASP	23	O	208	VAL	24	N	694	3.55E-01	-2.83E-01	-3.06E-01	-2.60E-01	2.31E-02
VAL	24	C	219	VAL	24	O	697	3.85E-01	-1.87E-01	-2.03E-01	-1.71E-01	1.63E-02
GLY	25	N	233	VAL	24	C	696	4.07E-01	-1.60E-01	-1.78E-01	-1.42E-01	1.77E-02
GLY	25	N	233	GLY	25	O	713	4.10E-01	-1.93E-01	-2.24E-01	-1.61E-01	3.14E-02
GLY	25	CA	234	GLY	25	O	713	3.79E-01	-2.01E-01	-2.24E-01	-1.78E-01	2.33E-02
GLY	25	C	235	GLY	25	O	713	3.69E-01	-2.03E-01	-2.10E-01	-1.96E-01	7.12E-03
SER	26	N	240	GLY	25	C	712	3.97E-01	-1.77E-01	-1.84E-01	-1.69E-01	7.75E-03
SER	26	CA	241	GLY	25	O	713	3.53E-01	-2.19E-01	-2.37E-01	-2.02E-01	1.76E-02
SER	26	C	242	ASN	27	N	728	3.91E-01	-1.84E-01	-1.89E-01	-1.78E-01	5.54E-03
SER	26	O	243	SER	26	CA	718	3.83E-01	-1.83E-01	-2.10E-01	-1.56E-01	2.72E-02
SER	26	O	243	SER	26	C	719	3.74E-01	-1.99E-01	-2.10E-01	-1.88E-01	1.10E-02
SER	26	CB	244	SER	26	CA	718	4.15E-01	-1.49E-01	-1.62E-01	-1.36E-01	1.30E-02
ASN	27	CA	252	ASN	27	O	731	3.63E-01	-1.74E-01	-2.04E-01	-1.44E-01	3.01E-02

ASN	27	C	253	ASN	27	O	731	3.72E-01	-2.01E-01	-2.10E-01	-1.93E-01	8.40E-03
LYS	28	N	265	ASN	27	C	730	4.09E-01	-1.61E-01	-1.68E-01	-1.53E-01	7.38E-03
LYS	28	CA	266	ASN	27	O	731	3.77E-01	-1.97E-01	-2.18E-01	-1.76E-01	2.09E-02
LYS	28	C	267	ASN	27	O	731	3.93E-01	-1.64E-01	-1.81E-01	-1.48E-01	1.66E-02
LYS	28	C	267	GLY	29	N	764	4.21E-01	-1.45E-01	-1.57E-01	-1.33E-01	1.20E-02
LYS	28	O	268	LYS	28	N	742	4.25E-01	-1.61E-01	-1.81E-01	-1.41E-01	2.02E-02
LYS	28	O	268	LYS	28	CA	743	3.46E-01	-2.14E-01	-2.35E-01	-1.93E-01	2.11E-02
LYS	28	O	268	LYS	28	C	744	3.73E-01	-2.04E-01	-2.11E-01	-1.96E-01	7.33E-03
LYS	28	O	268	GLY	29	CA	765	4.11E-01	-1.68E-01	-1.94E-01	-1.43E-01	2.54E-02
GLY	29	CA	288	GLY	29	N	764	4.41E-01	-1.34E-01	-1.47E-01	-1.20E-01	1.32E-02
GLY	29	C	289	ALA	30	N	771	3.80E-01	-1.91E-01	-1.96E-01	-1.87E-01	4.46E-03
GLY	29	O	290	GLY	29	N	764	4.00E-01	-2.11E-01	-2.58E-01	-1.63E-01	4.79E-02
GLY	29	O	290	GLY	29	CA	765	3.81E-01	-1.95E-01	-2.17E-01	-1.72E-01	2.22E-02
GLY	29	O	290	GLY	29	C	766	3.68E-01	-2.05E-01	-2.12E-01	-1.98E-01	6.90E-03
ALA	30	N	294	ALA	30	O	774	4.06E-01	-1.98E-01	-2.20E-01	-1.75E-01	2.23E-02
ALA	30	CA	295	ALA	30	C	773	4.30E-01	-1.16E-01	-1.20E-01	-1.11E-01	4.42E-03
ALA	30	CA	295	ALA	30	CB	775	4.29E-01	-1.32E-01	-1.44E-01	-1.21E-01	1.16E-02
ALA	30	C	296	ALA	30	O	774	3.56E-01	-2.17E-01	-2.18E-01	-2.15E-01	1.65E-03
ALA	30	CB	298	ALA	30	O	774	4.29E-01	-1.38E-01	-1.56E-01	-1.20E-01	1.84E-02
ILE	31	N	304	ALA	30	C	773	4.07E-01	-1.64E-01	-1.70E-01	-1.57E-01	6.62E-03
ILE	31	N	304	ILE	31	CA	782	4.57E-01	-1.12E-01	-1.18E-01	-1.07E-01	5.47E-03
ILE	31	CA	305	ALA	30	O	774	3.94E-01	-1.97E-01	-2.09E-01	-1.84E-01	1.28E-02
ILE	31	C	306	ALA	30	O	774	4.15E-01	-1.41E-01	-1.57E-01	-1.26E-01	1.56E-02
ILE	31	C	306	ILE	32	N	800	4.14E-01	-1.54E-01	-1.58E-01	-1.50E-01	3.82E-03
ILE	31	O	307	ALA	30	O	774	3.56E-01	-2.88E-01	-3.09E-01	-2.66E-01	2.11E-02
ILE	31	O	307	ILE	31	N	781	4.32E-01	-1.47E-01	-1.58E-01	-1.37E-01	1.03E-02
ILE	31	O	307	ILE	31	CA	782	3.40E-01	-2.07E-01	-2.24E-01	-1.90E-01	1.68E-02
ILE	31	O	307	ILE	31	C	783	3.65E-01	-2.14E-01	-2.16E-01	-2.11E-01	2.43E-03
ILE	31	O	307	ILE	31	CB	785	4.28E-01	-1.38E-01	-1.47E-01	-1.29E-01	8.99E-03
ILE	31	O	307	ILE	32	CA	801	3.97E-01	-1.91E-01	-1.99E-01	-1.83E-01	8.17E-03
ILE	31	O	307	ILE	32	C	802	4.27E-01	-1.24E-01	-1.34E-01	-1.15E-01	9.30E-03
ILE	31	O	307	ILE	32	O	803	3.75E-01	-2.51E-01	-2.74E-01	-2.27E-01	2.39E-02
ILE	31	O	307	ILE	32	CB	804	4.29E-01	-1.36E-01	-1.47E-01	-1.26E-01	1.05E-02
ILE	32	N	323	ILE	32	O	803	4.32E-01	-1.47E-01	-1.55E-01	-1.38E-01	8.72E-03
ILE	32	C	325	ILE	32	O	803	3.61E-01	-2.16E-01	-2.17E-01	-2.15E-01	1.29E-03
ILE	32	CB	327	ILE	32	O	803	4.09E-01	-1.69E-01	-1.81E-01	-1.58E-01	1.16E-02
GLY	33	N	342	ILE	32	C	802	4.13E-01	-1.55E-01	-1.60E-01	-1.51E-01	4.76E-03
GLY	33	N	342	GLY	33	CA	820	4.53E-01	-1.18E-01	-1.24E-01	-1.12E-01	6.00E-03
GLY	33	CA	343	ILE	32	O	803	4.00E-01	-1.85E-01	-1.93E-01	-1.77E-01	8.21E-03
GLY	33	C	344	ILE	32	O	803	4.00E-01	-1.65E-01	-1.75E-01	-1.55E-01	9.72E-03
GLY	33	C	344	GLY	33	CA	820	3.92E-01	-1.53E-01	-1.54E-01	-1.51E-01	1.84E-03

GLY	33	O	345	ILE	32	C	802	4.21E-01	-1.34E-01	-1.45E-01	-1.22E-01	1.12E-02
GLY	33	O	345	ILE	32	O	803	3.53E-01	-3.04E-01	-3.23E-01	-2.84E-01	1.95E-02
GLY	33	O	345	GLY	33	N	819	4.07E-01	-1.96E-01	-2.10E-01	-1.82E-01	1.39E-02
GLY	33	O	345	GLY	33	C	821	3.94E-01	-1.75E-01	-1.84E-01	-1.67E-01	8.63E-03
GLY	33	O	345	LEU	34	N	826	4.08E-01	-1.96E-01	-2.23E-01	-1.69E-01	2.69E-02
LEU	34	CA	350	LEU	34	N	826	4.17E-01	-1.68E-01	-1.82E-01	-1.55E-01	1.37E-02
MET	35	C	370	MET	35	O	848	3.82E-01	-1.91E-01	-2.08E-01	-1.74E-01	1.72E-02
VAL	36	N	385	MET	35	O	848	3.51E-01	-2.67E-01	-2.92E-01	-2.41E-01	2.54E-02
VAL	36	C	387	VAL	36	CA	863	4.25E-01	-1.22E-01	-1.28E-01	-1.16E-01	6.23E-03
VAL	36	O	388	MET	35	O	848	3.88E-01	-2.18E-01	-2.43E-01	-1.92E-01	2.56E-02
VAL	36	O	388	VAL	36	N	862	4.30E-01	-1.51E-01	-1.62E-01	-1.39E-01	1.19E-02
VAL	36	O	388	VAL	36	C	864	3.87E-01	-1.85E-01	-1.94E-01	-1.77E-01	8.24E-03
GLY	37	CA	402	GLY	37	N	878	4.17E-01	-1.69E-01	-1.84E-01	-1.55E-01	1.44E-02
GLY	37	CA	402	GLY	37	O	881	3.53E-01	-2.09E-01	-2.44E-01	-1.75E-01	3.46E-02
GLY	37	C	403	GLY	37	O	881	3.66E-01	-2.06E-01	-2.12E-01	-1.99E-01	6.62E-03
GLY	38	N	408	GLY	37	C	880	4.06E-01	-1.65E-01	-1.78E-01	-1.51E-01	1.38E-02
GLY	38	CA	409	GLY	37	O	881	3.85E-01	-2.06E-01	-2.27E-01	-1.85E-01	2.11E-02
GLY	38	C	410	GLY	38	O	888	3.60E-01	-2.06E-01	-2.12E-01	-2.00E-01	5.93E-03
VAL	39	N	415	GLY	38	C	887	4.09E-01	-1.61E-01	-1.68E-01	-1.54E-01	6.93E-03
VAL	39	CA	416	GLY	38	O	888	3.91E-01	-1.95E-01	-2.07E-01	-1.83E-01	1.16E-02
VAL	39	C	417	GLY	38	O	888	4.20E-01	-1.35E-01	-1.51E-01	-1.18E-01	1.65E-02
VAL	39	C	417	VAL	40	N	908	4.09E-01	-1.61E-01	-1.68E-01	-1.54E-01	6.78E-03
VAL	39	O	418	GLY	38	O	888	3.66E-01	-2.71E-01	-2.99E-01	-2.43E-01	2.76E-02
VAL	39	O	418	VAL	39	N	892	4.27E-01	-1.56E-01	-1.73E-01	-1.38E-01	1.74E-02
VAL	39	O	418	VAL	39	CA	893	3.38E-01	-1.91E-01	-2.21E-01	-1.60E-01	3.02E-02
VAL	39	O	418	VAL	39	C	894	3.63E-01	-2.15E-01	-2.17E-01	-2.12E-01	2.27E-03
VAL	39	O	418	VAL	39	CB	896	4.28E-01	-1.40E-01	-1.56E-01	-1.24E-01	1.61E-02
VAL	39	O	418	VAL	40	CA	909	3.97E-01	-1.91E-01	-1.95E-01	-1.86E-01	4.69E-03
VAL	39	O	418	VAL	40	O	911	3.77E-01	-2.45E-01	-2.69E-01	-2.21E-01	2.41E-02
VAL	39	O	418	VAL	40	CB	912	4.29E-01	-1.37E-01	-1.48E-01	-1.26E-01	1.11E-02
VAL	40	N	431	VAL	40	O	911	4.31E-01	-1.50E-01	-1.62E-01	-1.37E-01	1.22E-02
VAL	40	CA	432	VAL	40	O	911	3.40E-01	-1.97E-01	-2.27E-01	-1.67E-01	3.01E-02
VAL	40	C	433	VAL	40	O	911	3.65E-01	-2.12E-01	-2.15E-01	-2.09E-01	3.45E-03
VAL	40	CG2	437	VAL	40	O	911	4.19E-01	-1.53E-01	-1.71E-01	-1.36E-01	1.72E-02
ILE	41	N	447	VAL	40	C	910	4.15E-01	-1.53E-01	-1.58E-01	-1.48E-01	5.11E-03
ILE	41	CA	448	VAL	40	O	911	3.97E-01	-1.92E-01	-1.98E-01	-1.86E-01	5.94E-03
ILE	41	C	449	ALA	42	N	943	4.24E-01	-1.41E-01	-1.56E-01	-1.26E-01	1.49E-02
ILE	41	O	450	VAL	40	O	911	3.57E-01	-2.73E-01	-3.02E-01	-2.43E-01	2.98E-02
ILE	41	O	450	ILE	41	CA	925	3.58E-01	-2.10E-01	-2.26E-01	-1.94E-01	1.57E-02
ILE	41	O	450	ILE	41	C	926	3.83E-01	-1.92E-01	-2.00E-01	-1.83E-01	8.67E-03

Supplementary Table 10: Mapping results for A β 42's (PDB ID: 5KK3) long range (1:3) dominant atom-atom Coulombic interactions across ensemble structures. Columns for each chain correspond to: residue abbreviation, residue number in peptide sequence, atom identity (IUPAC naming convention) and atom number in PDB file. Energy in kT , distance in nm . Mapping analysis began on the 11th residue for both isoforms because original structure data for A β 42 begins with the 11th residue.

Chain 1				Chain 2				Average Distance	Average Coulombic Values	Lower 95% Confidence Interval Bound	Upper 95% Confidence Interval Bound	Margin of Error
HIS	14	C	51	GLN	15	O	1023	8.04E-01	-4.09E-01	-4.21E-01	-3.98E-01	1.16E-02
HIS	14	O	52	HIS	14	C	1005	8.54E-01	-3.46E-01	-3.56E-01	-3.36E-01	1.01E-02
LYS	16	C	85	GLN	15	O	1023	8.32E-01	-4.23E-01	-4.36E-01	-4.09E-01	1.33E-02
LYS	16	C	85	LEU	17	O	1062	7.80E-01	-4.69E-01	-4.89E-01	-4.49E-01	1.95E-02
LYS	16	O	86	LYS	16	C	1039	8.59E-01	-3.98E-01	-4.08E-01	-3.89E-01	9.31E-03
LYS	16	O	86	LEU	17	C	1061	7.64E-01	-3.88E-01	-4.02E-01	-3.73E-01	1.43E-02
LEU	17	C	107	LEU	17	O	1062	8.42E-01	-3.23E-01	-3.28E-01	-3.18E-01	5.25E-03
VAL	18	H	131	LEU	17	O	1062	6.70E-01	-3.78E-01	-3.83E-01	-3.72E-01	5.50E-03
SER	26	O	243	ASN	27	C	1207	7.71E-01	-4.23E-01	-4.35E-01	-4.11E-01	1.21E-02
LYS	28	C	267	ASN	27	O	1208	7.99E-01	-4.21E-01	-4.40E-01	-4.02E-01	1.89E-02
LYS	28	C	267	ALA	30	O	1251	9.49E-01	-3.36E-01	-3.48E-01	-3.24E-01	1.21E-02
LYS	28	O	268	ASN	27	C	1207	8.13E-01	-3.74E-01	-3.90E-01	-3.57E-01	1.66E-02
LYS	28	O	268	LYS	28	C	1221	8.47E-01	-4.09E-01	-4.19E-01	-3.98E-01	1.06E-02
GLY	29	C	289	ALA	30	O	1251	7.56E-01	-3.95E-01	-4.14E-01	-3.76E-01	1.89E-02
GLY	29	O	290	LYS	28	C	1221	9.16E-01	-3.25E-01	-3.31E-01	-3.19E-01	5.87E-03
GLY	29	O	290	ALA	30	C	1250	7.48E-01	-3.63E-01	-3.79E-01	-3.46E-01	1.65E-02
ALA	30	C	296	ALA	30	O	1251	8.29E-01	-3.27E-01	-3.30E-01	-3.24E-01	2.83E-03
ILE	31	C	306	ALA	30	O	1251	8.11E-01	-3.40E-01	-3.46E-01	-3.34E-01	5.92E-03
ILE	31	C	306	ILE	32	O	1280	8.34E-01	-3.62E-01	-3.68E-01	-3.56E-01	5.70E-03
ILE	31	O	307	ALA	30	C	1250	8.18E-01	-3.75E-01	-3.81E-01	-3.69E-01	6.06E-03
ILE	31	O	307	ILE	31	C	1260	8.45E-01	-3.54E-01	-3.59E-01	-3.48E-01	5.42E-03
ILE	31	O	307	ILE	32	C	1279	8.24E-01	-3.69E-01	-3.76E-01	-3.62E-01	6.99E-03
ILE	31	O	307	ILE	32	H	1285	6.71E-01	-3.12E-01	-3.18E-01	-3.06E-01	5.90E-03
ILE	32	C	325	ILE	32	O	1280	8.49E-01	-3.51E-01	-3.54E-01	-3.48E-01	3.25E-03
GLY	33	C	344	ILE	32	O	1280	7.77E-01	-4.19E-01	-4.27E-01	-4.10E-01	8.08E-03
GLY	33	O	345	ILE	32	C	1279	7.97E-01	-3.21E-01	-3.27E-01	-3.15E-01	6.02E-03
LEU	34	C	351	ILE	32	O	1280	8.82E-01	-3.33E-01	-3.45E-01	-3.21E-01	1.20E-02
MET	35	C	370	MET	35	O	1325	8.68E-01	-3.26E-01	-3.31E-01	-3.20E-01	5.76E-03
VAL	39	H	422	GLY	38	O	1365	6.61E-01	-3.54E-01	-3.59E-01	-3.48E-01	5.80E-03
ILE	41	O	450	ILE	41	C	1403	8.56E-01	-3.47E-01	-3.54E-01	-3.39E-01	7.44E-03
ALA	42	OXT	471	LYS	28	C	1221	8.73E-01	-3.87E-01	-4.14E-01	-3.59E-01	2.73E-02
ALA	42	OXT	471	ALA	42	C	1422	8.28E-01	-3.30E-01	-3.44E-01	-3.16E-01	1.36E-02

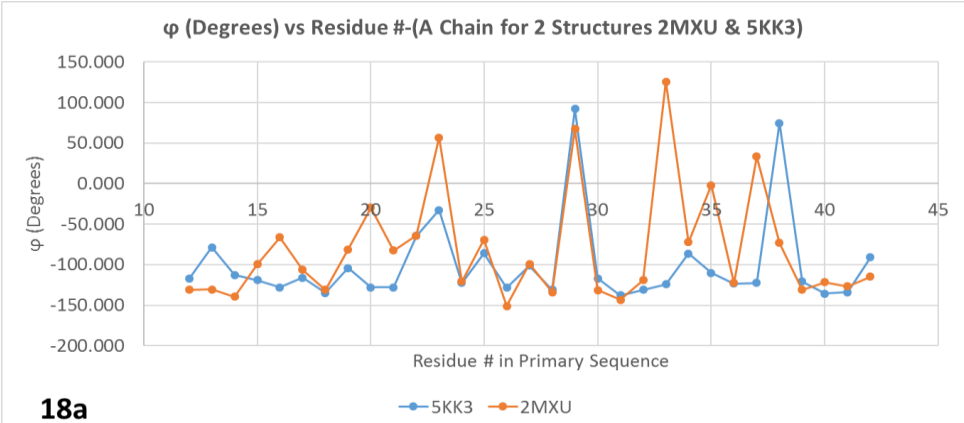


Supplementary Figure 17a & 17b: Atom-atom interactions imparting exceptionally strong hydrogen bonding energies in the 1:2 configuration of Aβ42 (PDB ID: 5KK3 by Colvin et al.) compared to Aβ40 (Aβ40 PDB ID: 2M4J by Lu et al.; Figure 17a) and their respective atom-atom interaction distances (Figure 17b). 95% confidence interval error bars included for analysis across all ensemble members. The first four, sixth, twelfth and fifteenth interactions were not observed in Aβ40. Interaction partners are presented as the residue, residue number in the sequence and the residue's atom of one chain (chain A for both strains) interacting with its partner atom in the 1:2 configuration (on the D-chain in Aβ40 or on the B-chain in Aβ42).

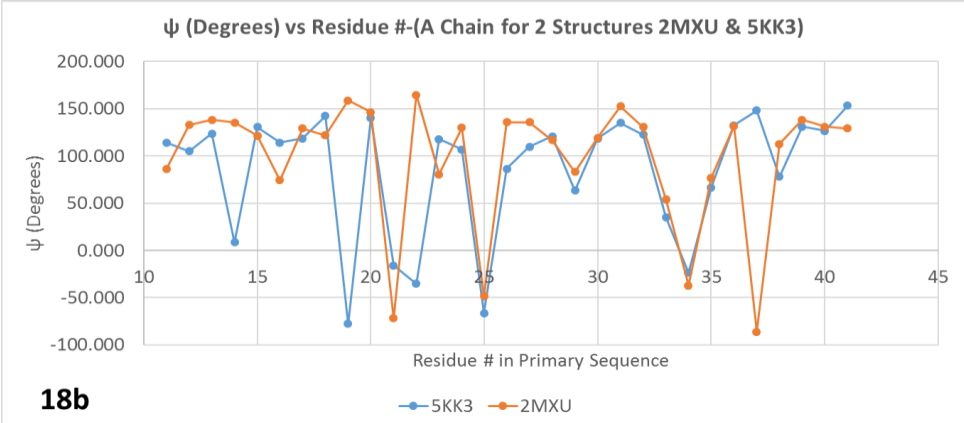
Supplementary Table 11: Ramachandran angle data for A β 40 and A β 42 for chains A-D (A β 40, PDB ID: 2M4J) and chains A-B (A β 42, PDB ID: 5KK3) for the 1:2 interaction configuration across ensemble structures. Data shown starts with residue 11 since structure data for previous A β 42 structure, 2MXU, begins at residue 11.

	A β 40				A β 42			
	Chain A		Chain B		Chain A		Chain B	
	ϕ	ψ	ϕ	ψ	ϕ	ψ	ϕ	ψ
GLU 11	-	152.910 \pm 0.711	-	151.350 \pm 0.487	-	113.950 \pm 24.475	-	118.180 \pm 26.974
VAL 12	-153.140 \pm 0.201	128.500 \pm 0.357	-149.530 \pm 0.042	130.000 \pm 0.072	-117.590 \pm 15.591	105.140 \pm 39.660	-74.540 \pm 45.725	119.550 \pm 16.091
HIS 13	-135.180 \pm 0.296	146.43 \pm 0.743	-129.880 \pm 0.120	149.470 \pm 0.774	-78.850 \pm 34.257	123.440 \pm 19.662	-129.740 \pm 12.850	59.500 \pm 80.411
HIS 14	-165.320 \pm 0.569	97.570 \pm 0.373	-165.060 \pm 0.128	104.570 \pm 0.113	-112.800 \pm 6.861	8.490 \pm 26.078	-82.530 \pm 21.870	-54.480 \pm 5.829
GLN 15	-107.590 \pm 2.008	-173.870 \pm 0.751	-111.070 \pm 2.030	-176.020 \pm 0.175	-118.940 \pm 9.519	130.480 \pm 7.559	-108.380 \pm 7.944	111.720 \pm 8.560
LYS 16	-166.350 \pm 1.700	97.950 \pm 0.938	-162.970 \pm 1.638	105.720 \pm 0.414	-127.990 \pm 7.067	113.950 \pm 11.660	-114.180 \pm 9.841	123.630 \pm 10.138
LEU 17	-117.790 \pm 5.123	158.580 \pm 2.486	-124.310 \pm 5.075	156.280 \pm 2.852	-116.130 \pm 10.380	118.390 \pm 10.395	-127.340 \pm 9.539	99.810 \pm 9.019
VAL 18	-120.610 \pm 9.229	124.710 \pm 2.477	-112.980 \pm 11.974	129.400 \pm 2.469	-134.660 \pm 8.727	142.220 \pm 15.893	-119.870 \pm 10.688	136.880 \pm 6.200
PHE 19	-109.630 \pm 16.980	133.770 \pm 10.920	-110.030 \pm 20.201	133.850 \pm 7.521	-104.300 \pm 12.827	-77.600 \pm 32.583	-106.340 \pm 10.302	-7.690 \pm 50.073
PHE 20	-13.800 \pm 67.407	34.610 \pm 39.682	-12.140 \pm 67.546	30.070 \pm 41.404	-128.200 \pm 27.892	140.560 \pm 11.197	-121.350 \pm 45.654	126.910 \pm 23.841
ALA 21	-67.680 \pm 12.282	-27.670 \pm 50.357	-68.800 \pm 13.231	-22.500 \pm 50.612	-128.210 \pm 16.614	-16.030 \pm 46.343	-116.740 \pm 14.870	-20.670 \pm 44.007
GLU 22	-99.030 \pm 13.950	117.940 \pm 17.139	-102.000 \pm 14.163	120.760 \pm 16.175	-64.540 \pm 83.952	-35.430 \pm 110.939	-133.080 \pm 27.921	0.990 \pm 116.055
ASP 23	-148.460 \pm 153.20 \pm 5.623	137.940 \pm 1.318	-70.530 \pm 3.594	139.130 \pm 1.409	-32.560 \pm 37.678	117.750 \pm 30.390	-33.530 \pm 38.003	120.640 \pm 27.232
VAL 24	-70.530 \pm 8.460	79.540 \pm 83.862	-114.730 \pm 8.460	80.410 \pm 85.689	-122.630 \pm 14.464	106.980 \pm 63.638	-127.010 \pm 14.332	148.350 \pm 7.323
GLY 25	-114.140 \pm 3.094	50.210 \pm 2.290	-114.730 \pm 2.429	54.310 \pm 3.261	-85.780 \pm 16.278	-66.280 \pm 8.731	-89.550 \pm 7.702	-81.750 \pm 13.291
SER 26	-61.550 \pm 79.970 \pm 6.196	87.939	-61.550 \pm 4.009	87.483	-128.270 \pm 4.435	86.420 \pm 7.203	-114.350 \pm 10.789	101.550 \pm 6.123
ASN 27	-69.260 \pm 69.580 \pm 1.699	86.480 \pm 5.961	-69.260 \pm 3.501	91.230 \pm 4.565	-101.220 \pm 5.073	109.860 \pm 7.732	-109.390 \pm 13.988	111.960 \pm 7.995
LYS 28	-87.910 \pm 82.690 \pm 5.998	135.220 \pm 7.876	-87.910 \pm 5.247	137.660 \pm 8.087	-130.940 \pm 13.604	120.640 \pm 13.235	-124.450 \pm 3.264	111.820 \pm 13.668
GLY 29	-60.700 \pm 62.690 \pm 0.809	-153.170 \pm 10.428	-60.700 \pm 2.630	-151.460 \pm 9.486	92.140 \pm 12.896	63.310 \pm 17.138	88.190 \pm 13.707	87.240 \pm 10.903
ALA 30	-105.320 \pm 104.030 \pm 6.560	122.180 \pm 4.709	-105.320 \pm 5.670	123.850 \pm 5.584	-117.120 \pm 13.986	118.410 \pm 7.073	-130.790 \pm 9.981	104.290 \pm 7.173
ILE 31	-103.190 \pm 100.480 \pm 8.486	130.830 \pm 4.794	-103.190 \pm 8.379	137.610 \pm 3.972	-137.680 \pm 6.799	135.100 \pm 5.109	-121.360 \pm 4.968	129.090 \pm 4.516
ILE 32	-152.980 \pm 147.380 \pm 4.687	-78.070 \pm 95.222	-152.980 \pm 5.812	-77.810 \pm 96.409	-131.210 \pm 1.822	122.630 \pm 2.354	-130.630 \pm 5.027	125.050 \pm 2.517
GLY 33	-124.010 \pm 63.670 \pm 0.773	21.120 \pm 16.942	-124.010 \pm 66.107	20.500 \pm 16.506	-124.010 \pm 66.107	35.360 \pm 88.241	-31.520 \pm 109.187	102.960 \pm 59.067
LEU 34	-86.200 \pm 83.930 \pm 8.423	126.710 \pm 3.472	-86.200 \pm 7.589	134.400 \pm 2.025	-86.200 \pm 18.673	-23.550 \pm 34.074	-70.750 \pm 13.752	-36.400 \pm 40.085
MET 35	-110.360 \pm 159.790 \pm 2.975	150.550 \pm 3.927	-110.360 \pm 0.722	160.480 \pm 2.626	-110.360 \pm 37.379	66.660 \pm 10.096	-93.770 \pm 36.336	83.650 \pm 13.953
VAL 36	-123.330 \pm 154.990 \pm 2.092	160.240 \pm 4.458	-123.330 \pm 1.703	161.350 \pm 2.732	-123.330 \pm 11.305	132.270 \pm 9.093	-129.770 \pm 12.213	110.210 \pm 64.154
GLY 37	-122.380 \pm 55.960 \pm 0.472	69.450 \pm 2.115	-122.380 \pm 7.188	64.440 \pm 0.783	-122.380 \pm 7.188	148.270 \pm 13.632	-137.310 \pm 14.763	152.790 \pm 9.917
GLY 38	-124.010 \pm 152.790 \pm 7.822	7.410 \pm 109.716	-124.010 \pm 74.770 \pm 12.909	8.980 \pm 110.119	-124.010 \pm 74.770 \pm 12.909	77.900 \pm 10.721	58.260 \pm 6.782	87.890 \pm 3.666
VAL 39	-131.210 \pm 122.680 \pm 5.114	153.420 \pm 4.657	-131.210 \pm 11.464	151.310 \pm 3.842	-131.210 \pm 11.464	131.010 \pm 7.715	-131.910 \pm 4.738	125.820 \pm 6.784
VAL 40	-135.520 \pm 65.280 \pm 0.705	-	-135.520 \pm 7.355	-	-135.520 \pm 7.355	126.520 \pm 3.370	-126.600 \pm 5.845	126.520 \pm 2.514

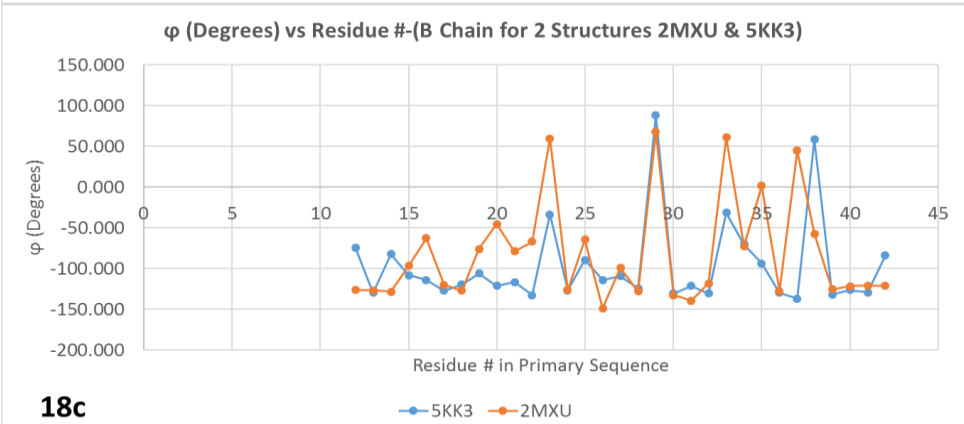
<i>ILE 41</i>	-	-		-	-		-134.050 ± 6.343	153.130 ± 7.317		-129.660 ± 5.408	141.560 ± 4.078
<i>ALA 42</i>	-	-		-	-		-91.080 ± 5.953	-		-84.130 ± 2.845	-



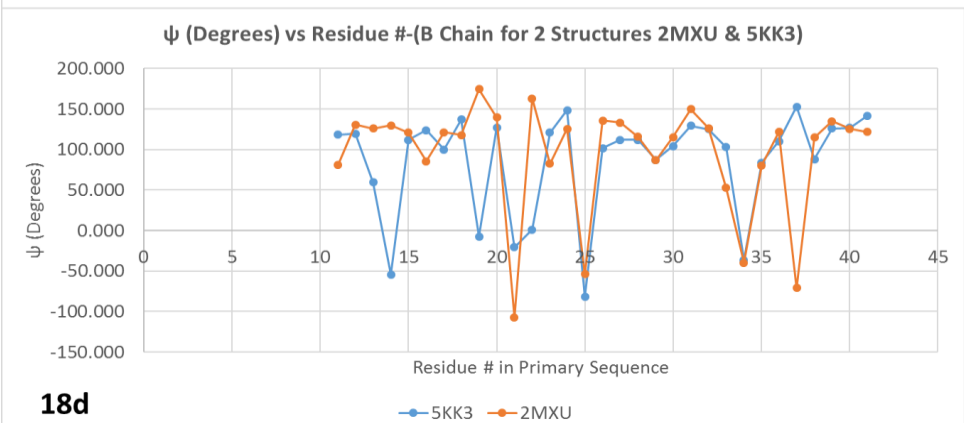
18a



18b

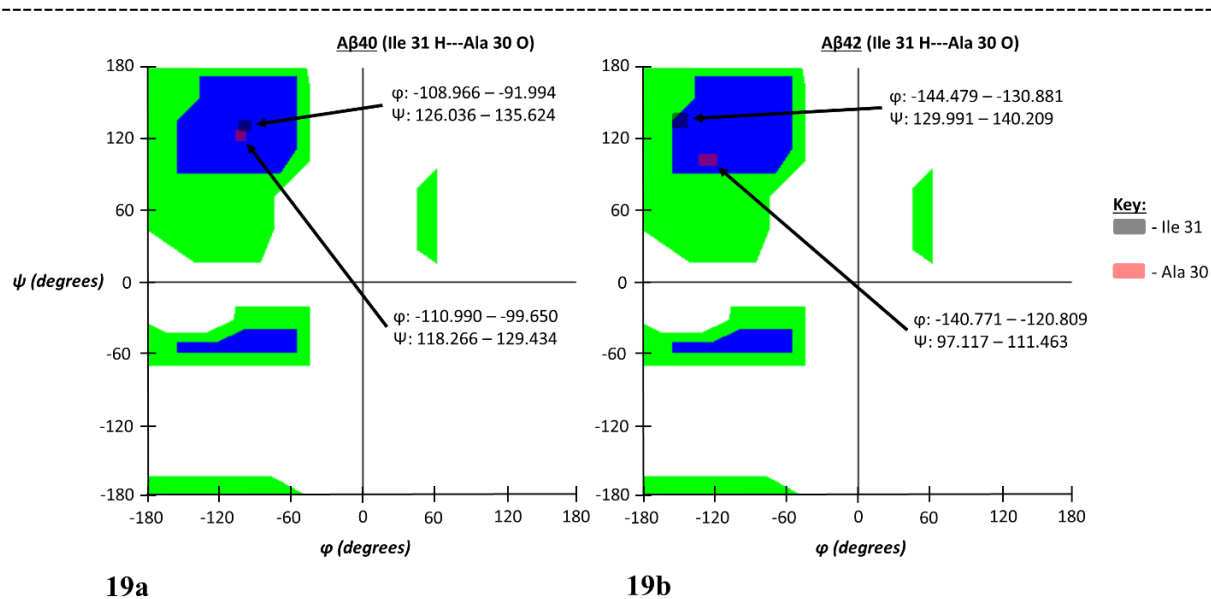


18c

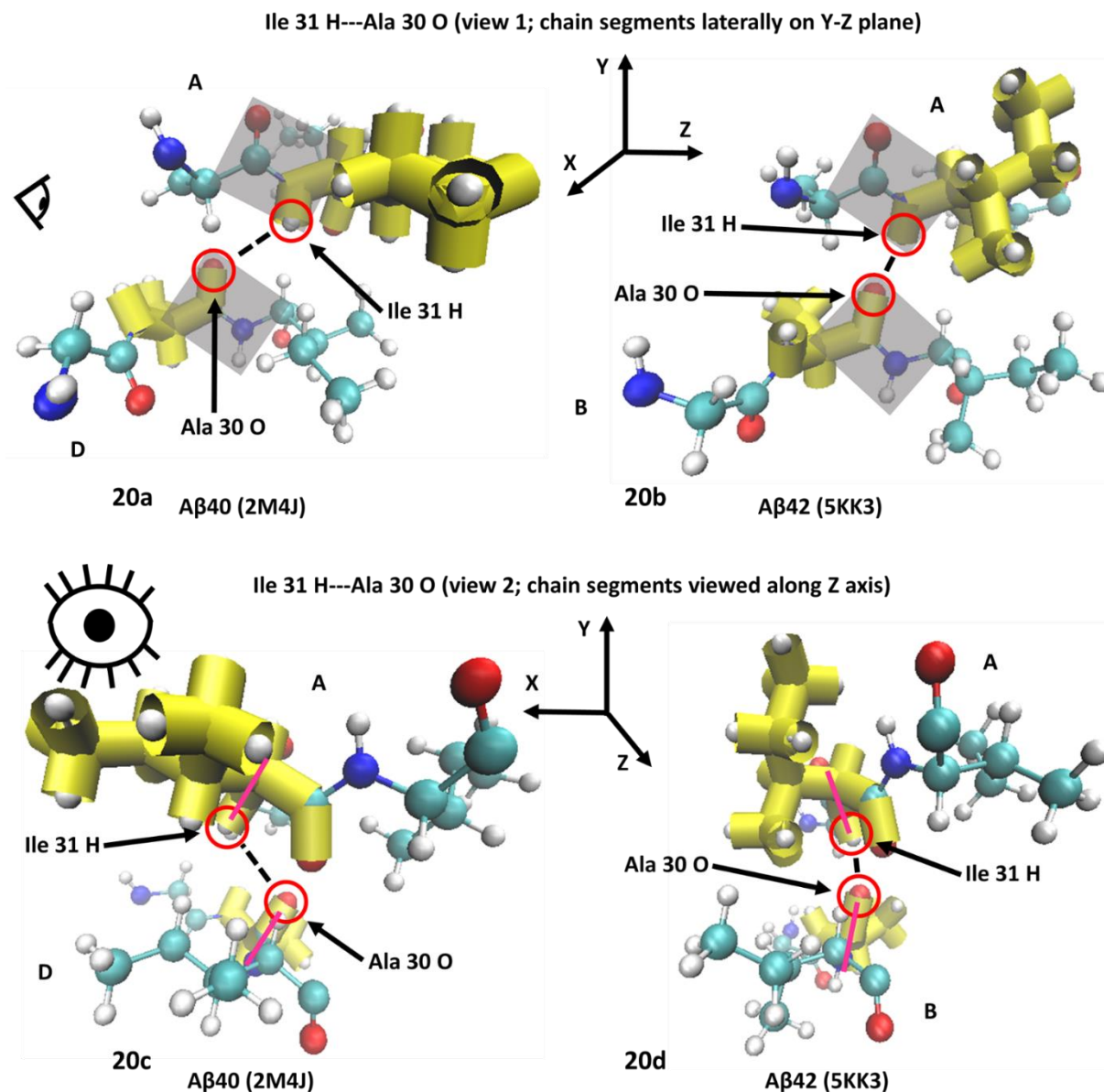


18d

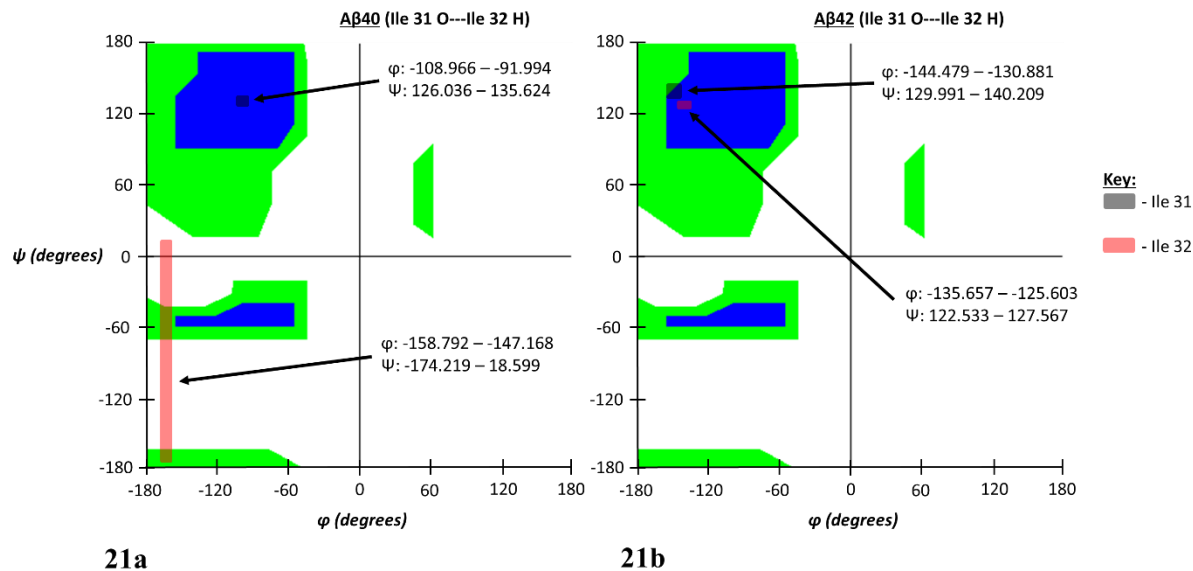
Supplementary Figure 18a-18d: Ramachandran angle profiles for A β 2 structures 2MXU and 5KK3 featured as stacked curves for ϕ and ψ angle value distribution comparison.



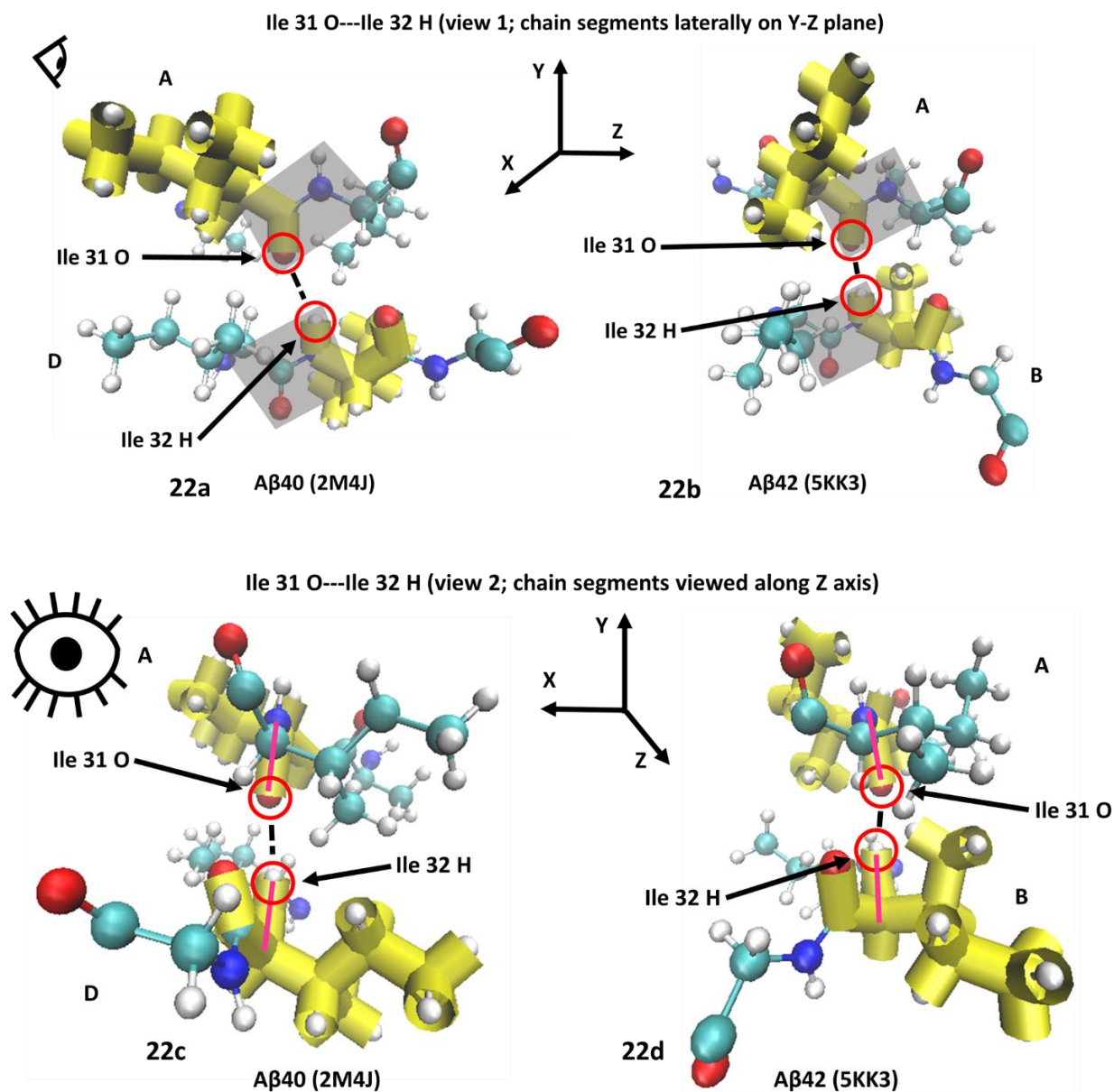
Supplementary Figure 19a-19b: Ramachandran angle profiles for an exceptionally strong atom-atom interaction (Ile 31 H interacting with Ala 30 O) for A β 40 (PDB ID: 2M4J, 19a) and A β 42 (PDB ID: 5KK3, 19b). Ranges for ϕ and ψ correspond to data spread according to 95% confidence interval analysis for all ensemble members as previously described. As stated before, the first atom is from the A chain of both isoforms and the second corresponds to the partner atom on the appropriate 1:2 interaction chain configuration. Note the retention of β -sheet secondary structure for both residues.



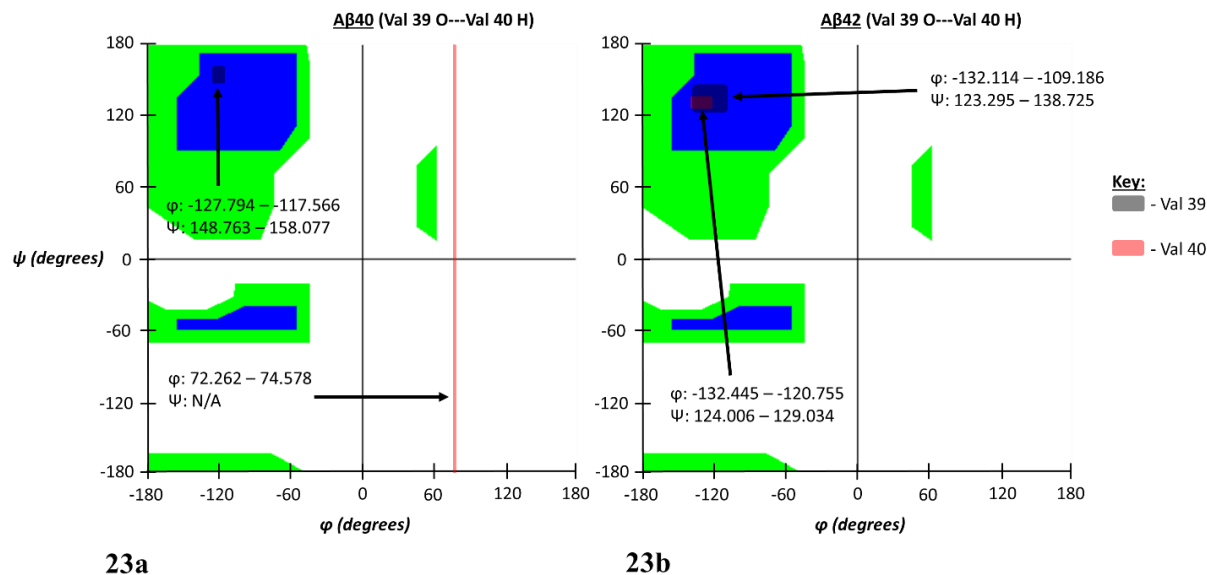
Supplementary Figure 20a-20d: Molecule representations of peptide plane alignment for Aβ40 (20a & 20c) and Aβ42 (20b & 20d). Aβ42 structure here is 5KK3. Shaded parallelograms in Figures 20a and 20b are the peptide planes for the residues whose atoms are participating in the hydrogen bonding. Figures 20c and 20d correspond to a view down the peptide bonds showing the peptide plane profile orientation in magenta. Eye icons indicate view perspective.



Supplementary Figure 21a-21b: Ramachandran angle profiles for an exceptionally strong atom-atom interaction (Ile 31 O interacting with Ile 32 H) for Aβ40 (PDB ID: 2M4J, 21a) and Aβ42 (PDB ID: 5KK3, 21b). Ranges for ϕ and ψ correspond to data spread according to 95% confidence interval analysis for all ensemble members as previously described. As stated before, the first atom is from the A chain of both isoforms and the second corresponds to the partner atom on the appropriate 1:2 interaction chain configuration. Note the retention of β -sheet secondary structure for Ile 31 and the acquisition of β -sheet structure for Ile 32 in Aβ42 compared to Aβ40.

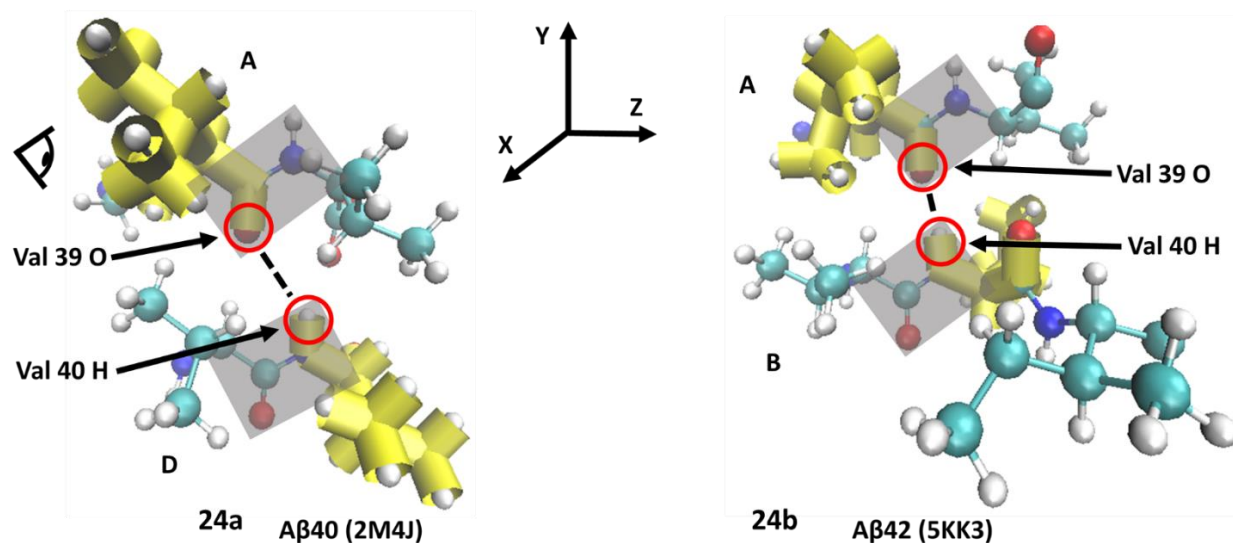


Supplementary Figure 22a-22d: Molecule representations of peptide plane alignment for Aβ40 (22a & 22c) and Aβ42 (22b & 22d). Aβ42 structure here is 5KK3. Shaded parallelograms in Figures 22a and 22b are the peptide planes for the residues whose atoms are participating in the hydrogen bonding. Figures 22c and 22d correspond to a view down the peptide bonds showing the peptide plane profile orientation in magenta. Eye icons indicate view perspective.

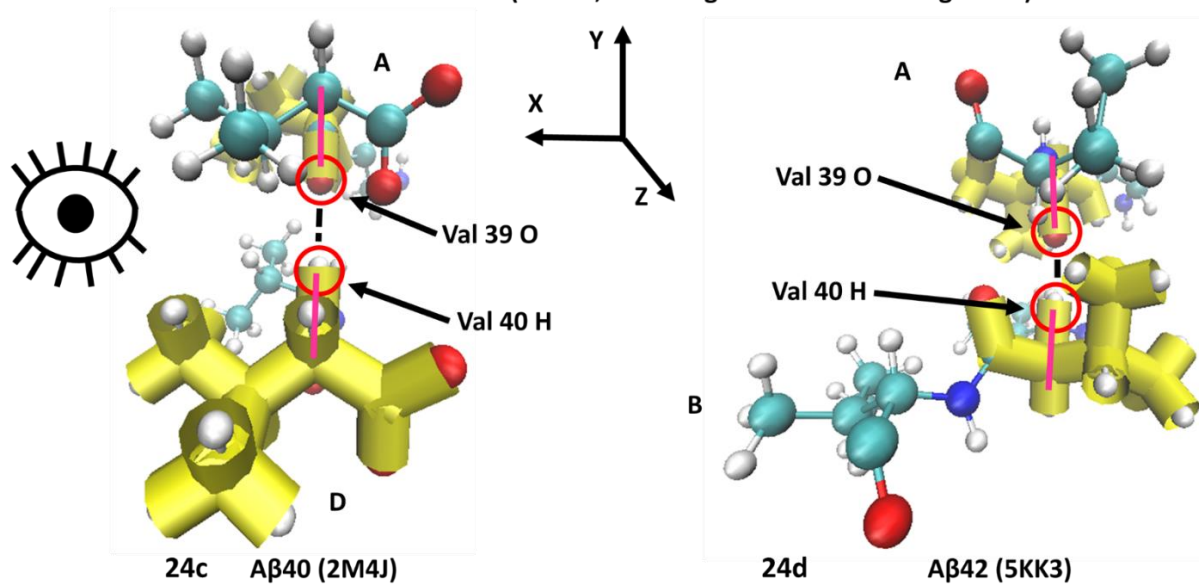


Supplementary Figure 23a-23b: Ramachandran angle profiles for an exceptionally strong atom-atom interaction (Val 39 O interacting with Val 40 H) for Aβ40 (PDB ID: 2M4J, 23a) and Aβ42 (PDB ID: 5KK3, 23b). Ranges for ϕ and ψ correspond to data spread according to 95% confidence interval analysis for all ensemble members as previously described. As stated before, the first atom is from the A chain of both isoforms and the second corresponds to the partner atom on the appropriate 1:2 interaction chain configuration. Note the retention of β -sheet secondary structure for Val 39 and the acquisition of β -sheet structure for Val 40.

Val 39 O---Val 40 H (view 1; chain segments laterally on Y-Z plane)



Val 39 O---Val 40 H (view 2; chain segments viewed along Z axis)



Supplementary Figure 24a-24d: Molecule representations of peptide plane alignment for Aβ40 (24a & 24c) and Aβ42 (24b & 24d). Aβ42 structure here is 5KK3. Shaded parallelograms in Figures 24a and 24b are the peptide planes for the residues whose atoms are participating in the hydrogen bonding. Figures 24c and 24d correspond to a view down the peptide bonds showing the peptide plane profile orientation in magenta. Eye icons indicate view perspective.

Appendix E:

NAMD Simulation Protocol

Prepared by: Oscar Bastidas, 1-24-2017

Prepping files for before beginning:

* *.pdb file-IF FROM NMR:

- Make a *.pdb file of **JUST ONE NMR model/snapshot of only the protein** by copying the 1st model only (of only the protein) from the original NMR *.pdb file and pasting it into a blank text document. Save this new file as a text file format and append the characters “.pdb” manually at the end of the name as part of the name you give it. You need this new *.pdb file for the next step.
- Next, open this new *.pdb file that you just created in DS-Viewer Pro and from the “Tools” menu, select “Hydrogens” and then “Remove.” **This will delete all hydrogens determined by NMR.** From the “File” menu, go to “Save As...” and save this file as a *.pdb file using the “Save as type:” drop down menu. You now have a new *.pdb structure file.
- Next open this new *.pdb file in your text editor and do a “Find and replace” changing HIS to HSE. Then, do a “Find and replace” for CD1 ILE changing it to CD ILE (note the different number of spaces between them). Save this file to save these updates. **This now becomes your working *.pdb file from which you’ll work from. Be sure this working *.pdb file ONLY contains the protein.**

* *.pdb file-IF FROM CRYSTAL:

- Open the *.pdb file in your text editor and do a “Find and replace” changing HIS to HSE. Then, do a “Find and replace” changing CD1 ILE to CD ILE (note how CD ILE has 2 spaces between them-this is important). Save this file to save these updates. **This now becomes your working *.pdb file from which you’ll work from. Be sure this working *.pdb file ONLY contains the protein.**

* *.conf file:

- Make sure that the following variables reflect a total simulation time, timestep and snap-shot writing frequency that you want for your simulation: run (total number of timesteps to run, hence total simulation time), timestep (the timestep frequency of the simulation given; the units of the number you specify will be that number of femtoseconds per timestep) and dcdfreq (the number of timesteps that will elapse in between writing a snapshot structure).
- Be sure that under the section marked “#Output” the variables “binaryoutput” and “binaryrestart” are both set to “no” without quotation marks on the “no.” If these variables do not appear, write them in and set their values manually.
- Finally, make sure that under the “Adjustable Paramaters” section, the variables “structure” and “coordinates” have the name of the working *.pdb file followed by the characters “_wb.psf” and “_wb.pdb” respectively. NO SPACES FOR THESE NAMES! Under the variable section marked “set outputname,” be sure that the name is also the name of the working *.pdb file as before and this time, the name continues with “_wb_eq” and again, no spaces here.

- You can set the temperature you desire with the “set temperature” variable. Whatever number you put in will be understood to be in Kelvin.

- Note the three variables and their values circled below:

```
cdn_wb_eq.conf
88 outputName          $outputname
89
90 restartfreq         500      ;# 500steps = every 1ps
91 dcdfreq             500
92 xstFreq             250
93 outputEnergies     100
94 outputPressure     100
95 binaryoutput       no
96 binaryrestart      no
```

Note the relationship in magnitude between these three variables’ values: “restartfreq” and “dcdfreq” should be the same value and “xstFreq” should be roughly half of “restartfreq”/“dcdfreq.”

-When changing these values to correspond to different time intervals of output trajectory snapshots or different run times, make sure that the digit growth proceeds to the right; ensure that the numbers are “left justified” so that any additional digits that reflect increased orders of magnitude are simply appended to the right of the circled values above.

- This same principle applies to the “run” variable should its value should it be altered:

```
111 run 5000
```

***NOTE: NEVER, EVER, EVER, EVER, EVER CHANGE THE “timestep” VARIABLE:**

```
41 # Integrator Parameters
42 timestep             2.0    ;# 2fs/step
```

LEAVE IT AT “2.0” OR YOUR SIMULATION WILL NOT WORK!

! There are two more edits to the *.conf file that will be carried out later just prior to executing the simulation that depend on calculations that haven’t yet been carried out at this step.

Water Box Simulation for 2 Chain Systems:

! Recommended text editor is Notepad++

* Files needed in working directory:

1) *.pdb (protein structure input)-IF from crystal, MUST EDIT for HIS & ILE CD1 name changes (see above); IF from NMR, MUST EDIT for 1 model, delete hydrogens and HIS & ILE CD1 name changes (see above)

2) *.conf (instructions for simulation)-MUST EDIT to account for file names, timestep, binaryoutput, etc... (see above)

- 3) top...*.inp (forcefield parameters)-NO NEED TO TOUCH
- 4) par...*.inp (forcefield parameters)-NO NEED TO TOUCH

! Establish your working directory containing the above files using VMD's command prompt

- Load your working *.pdb structure into VMD viewer ("File" -> "New Molecule"...). Click "Browse" to select the *.pdb file and click "Load" to actually load it into the VMD viewer.
- In VMD Main window, from the "Extensions" menu, select "Tk Console" and in the resulting window, type:

```
set NAME [atomselect top protein]
$NAME writepdb NAMEp.pdb
```

- ! Replace the word "NAME" with the name of the working *.pdb file.
- ! Hit the return key after each command
- ! NEW FILE CREATED: NAMEp.pdb → this will now appear in your working directory automatically.

- Delete current displayed molecule from VMD viewer
- Load NAMEp.pdb that you just created into VMD viewer. Then in the VMD Main window, click the molecule name just loaded so that it is hi-lighted.
- Still in the VMD Main window, click on the "Extensions" menu, select "Modeling," then "Automatic PSF Builder." A new window will pop up.
- In the panel marked "Step 1: Input and Output Files," in the white box marked "Topology files," click on the first topology file so that it is hi-lighted and then click the button marked "Delete." Delete the remaining topology files in like manner until none remain, then click the button marked "Add" and (you should be in your working directory) select the top...*.inp file and open it. It, alone, should now appear in the "Topology files" white box. Click "Load input files."
- In the next panel marked "Step 2: Selections to include in PSF/PDB," select the "Everything" radio button if it is not already selected and then click "Guess and split chains using current selections."
- In the next panel marked "Step 3: Segments Identified," click "Create chains." A dialogue box will pop up, click "OK." Another dialogue box will pop up, click "OK."
- In the next panel marked "Step 4: Patches," click "Apply patches and finish PSF/PDB." A dialogue box will pop up, click "OK." You may now close the "Automatic PSF Builder" window.
- Now, in the Tk Console window, type:

```
package require solvate
solvate NAMEp_autopsf.psf NAMEp_autopsf.pdb -t 9 -o NAME_wb
```

- In the VMD Main window, delete all of the molecule items that appear listed in the white box section (individually click an item to hi-light it, then right click and select "Delete Molecule").
- In the VMD Main window, load NAME_wb.psf

- Next, load NAME_wb.pdb and you will now see your protein immersed in a water box in the viewer window.
- In Tk Console, type:

```
set everyone [atomselect top all]
measure minmax $everyone
```

- Write down the 2 sets of 3 numbers that now appear in Tk Console as output. The first set of 3 numbers are the minima of the x, y and z coordinates respectively and the second set of 3 numbers are the maxima of the x, y and z coordinates respectively.
- Do the following calculations and write the results: $(x_{\max} + x_{\min})/2$, $(y_{\max} + y_{\min})/2$, $(z_{\max} + z_{\min})/2$ → the resultant 3 numbers are the coordinates for the center of your water box.
- Do the following calculations and write the results: $x_{\max} - x_{\min}$, $y_{\max} - y_{\min}$, $z_{\max} - z_{\min}$ → the resultant 3 numbers are the size of your water box.
- Open the *.conf file and in the section marked “Periodic Boundary Conditions,” you will see 3 headings labeled “cellBasisVector”1-3. For data row labeled “cellBasisVector1,” replace the non-zero number with the results of the calculation $x_{\max} - x_{\min}$. For the data row labeled “cellBasisVector2,” replace the non-zero number with the results of the calculation $y_{\max} - y_{\min}$. For the data row labeled “cellBasisVector3,” replace the non-zero number with the results of the calculation $z_{\max} - z_{\min}$. For the data row labeled “cellOrigin,” replace the first number with the results of the calculation $(x_{\max} + x_{\min})/2$, replace the second number with the results of the calculation $(y_{\max} + y_{\min})/2$ and replace the third number with the results of the calculation $(z_{\max} + z_{\min})/2$. Save the *.conf file.
- In the VMD command prompt window, type “dir” (without the quotes) to establish that you are still in your working directory.
- Finally, run your simulation by typing in the VMD command prompt:

```
namd2 NAME_wb_eq.conf > NAME_wb_eq.log &
```

! Hit the return key to execute this command to run NAMD
 ! TARGET OUTPUT FILES: *.dcd and *.coor (NOT *.restart.coor) → When **BOTH** of these files are present in your working directory, the simulation is finished.

*** BE PATIENT AND WAIT ***

Water Box Simulation for 1 Chain Systems:

! Recommended text editor is Notepad++

* Files needed in working directory:

- 1) *.pdb (protein structure input)-IF from crystal, MUST EDIT for HIS & ILE CD1 name changes (see above); IF from NMR, MUST EDIT for 1 model, delete hydrogens and HIS & ILE CD1 name changes (see above)
- 2) *.pgn (script to make psf & pdb w/hydrogen & w/o water)-MUST EDIT to account for file names
- 3) *.conf (instructions for simulation)-MUST EDIT to account for file names, timestep, binaryoutput, etc... (see above)
- 4) top...*.inp (forcefield parameters)-NO NEED TO TOUCH

5) par...*.inp (forcefield parameters)-NO NEED TO TOUCH

! Establish your working directory containing the above files using VMD's command prompt

- Load your working *.pdb structure into VMD viewer ("File" -> "New Molecule"...). Click "Browse" to select the *.pdb file and click "Load" to actually load it into the VMD viewer.
- In VMD Main window, from the "Extensions" menu, select "Tk Console" and in the resulting window, type:

```
set NAME [atomselect top protein]
NAME writepdb NAMEp.pdb
```

! Replace the word "NAME" with the name of the working *.pdb file.

! Hit the return key after each command

! NEW FILE CREATED: NAMEp.pdb → this will now appear in your working directory automatically.

- Delete current displayed molecule from VMD viewer.
- In Tk Console window,

```
source NAME.pgn
```

! NEW FILES CREATED: NAME.pdb & NAME.psf

- In Tk Console, type:

```
package require solvate
solvate NAME.psf NAME.pdb -t 5 -o NAME_wb
```

! NEW FILES CREATED: NAME_wb.txt, NAME_wb.pdb, NAME_wb.psf

- In VMD Main window, delete any molecules loaded and then load NAME_wb.psf
- In same file browser window, load NAME_wb.pdb, look at it in visualizer window & note box of water encasing our protein.

- In Tk Console, type:

```
set everyone [atomselect top all]
measure minmax $everyone
```

- Write down the 2 sets of 3 numbers that now appear in Tk Console as output. The first set of 3 numbers are the minima of the x, y and z coordinates respectively and the second set of 3 numbers are the maxima of the x, y and z coordinates respectively.

- Do the following calculations and write the results: $(x_{\max} + x_{\min})/2$, $(y_{\max} + y_{\min})/2$, $(z_{\max} + z_{\min})/2$ → the resultant 3 numbers are the coordinates for the center of your water box.

- Do the following calculations and write the results: $x_{\max} - x_{\min}$, $y_{\max} - y_{\min}$, $z_{\max} - z_{\min}$ → the resultant 3 numbers are the size of your water box.

- Open the *.conf file and in the section marked “Periodic Boundary Conditions,” you will see 3 headings labeled “cellBasisVector”1-3. For data row labeled “cellBasisVector1,” replace the non-zero number with the results of the calculation $x_{\max} - x_{\min}$. For the data row labeled “cellBasisVector2,” replace the non-zero number with the results of the calculation $y_{\max} - y_{\min}$. For the data row labeled “cellBasisVector3,” replace the non-zero number with the results of the calculation $z_{\max} - z_{\min}$. For the data row labeled “cellOrigin,” replace the first number with the results of the calculation $(x_{\max} + x_{\min})/2$, replace the second number with the results of the calculation $(y_{\max} + y_{\min})/2$ and replace the third number with the results of the calculation $(z_{\max} + z_{\min})/2$. Save the *.conf file.
- In the VMD command prompt window, type “dir” (without the quotes) to establish that you are still in your working directory.
- Finally, run your simulation by typing in the VMD command prompt:

```
namd2 NAME_wb_eq.conf > NAME_wb_eq.log &
```

! Hit the return key to execute this command to run NAMD
 ! TARGET OUTPUT FILES: *.dcd and *.coor (NOT *.restart.coor) → When **BOTH** of these files are present in your working directory, the simulation is finished.

*** BE PATIENT AND WAIT ***

Getting ensemble of 10 dynamic snapshots:

- Load NAME_wb.psf to VMD
- Next, load NAME_wb_eq.dcd
- Click the molecule in the VMD Main window to hi-light it
- From “File” menu, select “Save coordinates.”
- From the drop-down menu marked “Selected atoms,” select “all.”
- Give the file a name with “.pdb” as part of the extension and save it to a proper location. **You now have an ensemble *.pdb file of 10 snapshots with water molecules (lots of them) and improperly labeled histidine residues.**

Getting rid of water and re-name HSE* to HIS:

- Open the ensemble *.pdb file in the text editor and do a “Find and Replace” of HSE to HIS (for a 1 chain system) **AND** do a “Find and Replace” of HSD to HIS as this may be how HIS is sometimes abbreviated by NAMD.
- Delete all “END” text in the ensemble *.pdb file.
- Save this new version of the ensemble *.pdb file.
- Making sure no other structures or files are loaded in the VMD Main window, load this new version of the ensemble *.pdb file (i.e. without “END”) into the VMD Main window so that the ensemble encased in a box of water becomes visible in the VMD molecule viewer window.
- In Tk Console type:

```
set selection [atomselect top “not water”]  
$selection writpdb NEWNAME.pdb
```

! NEW FILE CREATED: NEWNAME.pdb

! This new *.pdb ensemble file, NEWNAME.pdb, contains no water molecules, HIS instead of HSE or HSD, and of course, well-placed hydrogen atoms.

- Open this *.pdb file in the text editor and delete the entire line beginning with the text “CRYST” if present. Save the file.

*** NEWNAME.pdb is the ensemble ready for processing in Open-Contact as done before ***

Appendix F:

Extended Literature Review: The Blood Brain Barrier (BBB)

An important and challenging aspect to consider when desiring to target amyloid diseases of the brain (specifically such as Alzheimer's disease) is in having the pharmaceutical species cross the blood brain barrier (BBB). The brain receives its nutrient flux from the blood across capillaries within the parenchyma of the brain [1, 2]. This barrier of cerebral parenchymal capillaries that separate the circulating blood from the brain extracellular fluid is what is known as the BBB and constitutes a very selective mode of entry for chemical species and nutrients [1]. The BBB is formed by brain endothelial cells which are connected by tight cellular junctions that provide a high transendothelial electrical resistance of 1500-2000 $\Omega \text{ cm}^2$ and decreased paracellular permeability [3]. This is in contrast to the 3-30 $\Omega \text{ cm}^2$ in peripheral vessels [3]. Additional physical characteristics of the BBB include a low number of vesicles (indicating reduced vesicular transport) and the ensheathment by astrocytic end-feet which provides autocrine factors to maintain BBB function [4]. A schematic illustration of the BBB is shown below in Figure 17.

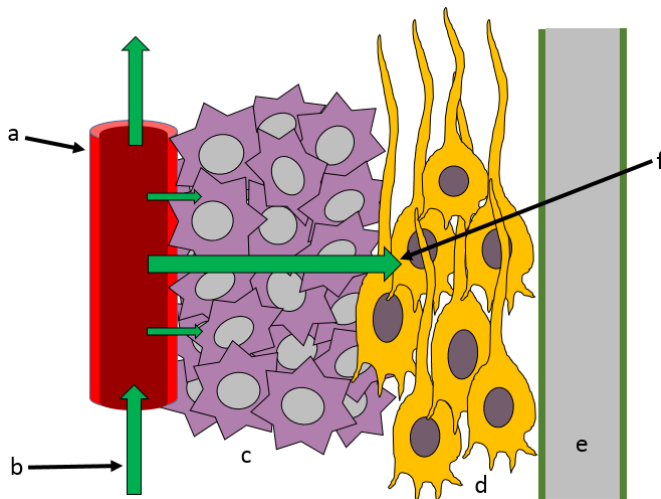


Figure 17: Schematic illustration of the blood-brain barrier (BBB). Item (a) is a brain capillary, (b) is the direction of blood flow, (c) are astrocyte cells, (d) are neurons, (e) is cerebral spinal fluid and (f) is the specific diffusion of water, oxygen and glucose to the astrocytes and neurons.

The BBB also acts as a metabolic barrier possessing a number of proteolytic enzymes including aminopeptidase A, and aminopeptidase M and angiotensin-converting enzyme [4]. Chemical species that can readily cross the BBB typically have molecular weights lower than 400 Da and less than 8 hydrogen bonds [4]. Thus the combined forces of physical tight junctions, an increased electrical resistance and proteolytic enzymes leads to a system that seems virtually impenetrable and is indeed difficult to breach for a successful drug delivery. Common methods to cross the BBB include subjecting the drug warhead to a lipid-mediated transport molecule, improving metabolic stability, masking enzyme cleavage sites and conjugating the drug warhead to a peptide carrier [4]. Actual administration of the drug is typically invasive involving intrathecal delivery or injection into the cerebral spinal fluid [2].

Extended Literature Review: Special Considerations and Challenges Associated with Peptide Drugs

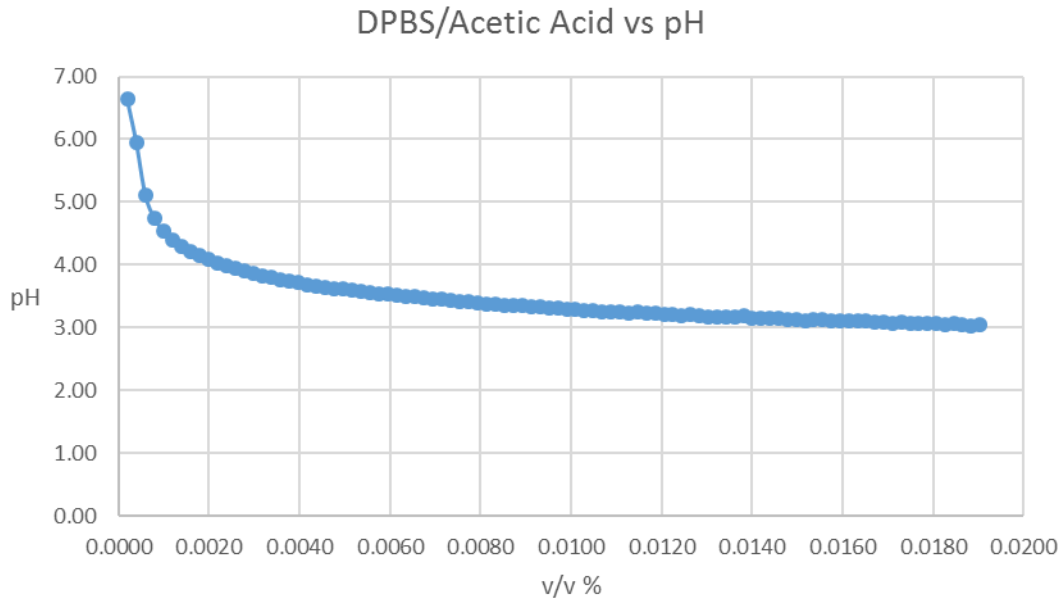
Peptide therapeutics presently represents one of the fastest growing segments of the pharmaceutical industry and they often include efficient delivery platforms and attractive pharmacokinetic profiles [5]. There are a number of unique considerations and challenges associated with using peptides as drugs that ultimately revolve around drug delivery to target organs and the protection of the peptide warhead from biological degradation. Facets that must thus be considered include, for example, extracellular versus intracellular delivery of proteins, agonist versus antagonist actions, solubility, specificity, residue length, nature of binding forces and strength and structural stability and dynamics [6]. An example of drug delivery considerations is the strategy by which the peptide drug will be introduced into the cells of target organs. Identifying these specifications will then dictate potential strategies to maximize the effects of the desired pharmacology. Peptide drugs designed for intracellular targets can employ, for example, the use of cell penetrating peptides (CPPs) and genetic fusion of the target protein to protein transduction domains (PTDs) [7]. Challenges associated with these methods are the inefficient escape of the peptide payload from the endosome to the cytosol resulting in the drug cargoes being sequestered in intra-cellular vesicles [8, 9]. Additionally, nanomaterials such as carbon nanotubes, liposomes, gold nanoparticles, cationic lipid formulations and mesoporous silica

particles have also been used with success to improve in intra-cellular delivery, long circulation time and tumor targeting [10-12]. The use of D-amino acid-based peptide drugs has also provided successful proteolytic-defying properties to provide protection from enzyme-based *in vivo* metabolic processes which selectively favor L-amino acid bio-molecules [13].

References:

- (1) Engelhardt B, Liebner S. Novel insights into the development and maintenance of the blood–brain barrier. *Cell Tissue Res* 2014;355(3):687-699.
- (2) Pardridge WM. Drug transport across the blood–brain barrier. *Journal of cerebral blood flow & metabolism* 2012;32(11):1959-1972.
- (3) Huber JD, Egleton RD, Davis TP. Molecular physiology and pathophysiology of tight junctions in the blood–brain barrier. *Trends Neurosci* 2001;24(12):719-725.
- (4) Egleton RD, Davis TP. Development of neuropeptide drugs that cross the blood-brain barrier. *NeuroRx* 2005;2(1):44-53.
- (5) McGregor, Duncan Patrick. "Discovering and Improving Novel Peptide Therapeutics." *Current opinion in pharmacology* 8.5 (2008): 616-9.
- (6) Groner, B. editor. *Peptides as drugs*. Weinheim: Wiley-VCH; 2009.
- (7) Sawant, Rupa, and Vladimir Torchilin. "Intracellular Transduction using Cell-Penetrating Peptides." *Molecular BioSystems* 6.4 (2010): 628-40.
- (8) Patel, Leena N., Jennica L. Zaro, and Wei-Chiang Shen. "Cell Penetrating Peptides: Intracellular Pathways and Pharmaceutical Perspectives." *Pharmaceutical research* 24.11 (2007): 1977-92.
- (9) Green, Isabelle, et al. "Protein Transduction Domains: Are they Delivering?" *Trends in pharmacological sciences* 24.5 (2003): 213-5.
- (10) Gu, Zhen, et al. "Tailoring Nanocarriers for Intracellular Protein Delivery." *Chemical Society Reviews* 40.7 (2011): 3638-55.
- (11) Du, Juanjuan, et al. "Synthetic Nanocarriers for Intracellular Protein Delivery." *Current Drug Metabolism* 13.1 (2012): 82-92.
- (12) Chatin, Benoît, et al. "Liposome-Based Formulation for Intracellular Delivery of Functional Proteins." *Molecular Therapy—Nucleic Acids* 4.6 (2015): e244.
- (13) H Peters, Michael. "Targeting HIV-1 Envelope Proteins using a Fragment Discovery all-Atom Computational Algorithm." *Current Enzyme Inhibition* 13.1 (2017): 20-6.

Appendix G: DPBS and Acetic Acid pH Dependency Data



DPBS/Acetic Acid v/v%	pH
0.0002	6.64
0.0004	5.95
0.0006	5.11
0.0008	4.74
0.0010	4.54
0.0012	4.40
0.0014	4.30
0.0016	4.22
0.0018	4.15
0.0020	4.08
0.0022	4.03
0.0024	3.98
0.0026	3.94
0.0028	3.90
0.0030	3.86
0.0032	3.83
0.0034	3.80
0.0036	3.77
0.0038	3.74
0.0040	3.72
0.0042	3.69

0.0044	3.67
0.0046	3.65
0.0048	3.63
0.0050	3.61
0.0052	3.59
0.0054	3.57
0.0056	3.56
0.0058	3.54
0.0060	3.53
0.0062	3.51
0.0064	3.49
0.0066	3.49
0.0068	3.47
0.0070	3.46
0.0071	3.45
0.0073	3.43
0.0075	3.42
0.0077	3.41
0.0079	3.39
0.0081	3.38
0.0083	3.38
0.0085	3.36
0.0087	3.36
0.0089	3.35
0.0091	3.34
0.0093	3.33
0.0095	3.32
0.0097	3.31
0.0099	3.30
0.0101	3.29
0.0103	3.28
0.0105	3.27
0.0107	3.26
0.0109	3.26
0.0111	3.25
0.0113	3.24
0.0115	3.25
0.0117	3.23
0.0119	3.23
0.0121	3.22
0.0122	3.22
0.0124	3.20
0.0126	3.21

0.0128	3.20
0.0130	3.18
0.0132	3.18
0.0134	3.18
0.0136	3.17
0.0138	3.19
0.0140	3.15
0.0142	3.16
0.0144	3.16
0.0146	3.15
0.0148	3.13
0.0150	3.13
0.0152	3.11
0.0154	3.13
0.0156	3.12
0.0157	3.11
0.0159	3.10
0.0161	3.10
0.0163	3.10
0.0165	3.10
0.0167	3.08
0.0169	3.08
0.0171	3.07
0.0173	3.08
0.0175	3.06
0.0177	3.07
0.0179	3.06
0.0181	3.06
0.0183	3.04
0.0185	3.06
0.0186	3.05
0.0188	3.03
0.0190	3.04

Vita

Oscar Herminio Bastidas was born on June 27, 1987, in Arlington, Virginia, and is an American citizen. He received his Bachelor of Science from Virginia Commonwealth University, Richmond, Virginia in 2011. He received his Master of Science from Virginia Commonwealth University, Richmond, Virginia in 2014. He also received his Doctorate in Philosophy from Virginia Commonwealth University, Richmond Virginia in 2017. As a graduate student, Oscar has worked managing a variety of research projects as well as being heavily involved in pedagogical roles with students in instructional laboratory settings.

Publications and Intellectual Properties:

Publication: Bastidas, Oscar H., et al. "Few Ramachandran Angle Changes Provide Interaction Strength Increase in A β 42 versus A β 40 Amyloid Fibrils." Scientific reports 6 (2016).

Provisional Patent: O. Bastidas and M.H. Peters, Preliminary Patent Application No. PET-17-054, Virginia Commonwealth University, April 2017.